Development of a Novel Strategy for Targeted Delivery of siRNA to B lymphocytes

By

Hawzheen Aziz Muhammad

A thesis submitted to the University of London for the degree of Doctor of Philosophy in the Faculty of Medicine

January 2014

Bone and Joint Research Unit
William Harvey Research Institute
Barts and The London School of Medicine and Dentistry
Queen Mary University of London

Declaration:

This is to certify that:

(i) the thesis comprises only my original work towards the PhD.

(ii) due acknowledgment has been made in the text to all other materials used.

I attest that I have exercised reasonable care to ensure that the work is original, and does not to the best of my knowledge break any UK law, infringe any third party's copyright or other intellectual Property Right, or contain any confidential material.

I accept that the college has the right to use plagiarism detection software to check the electronic version of the thesis.

I confirm that this thesis has not been previously submitted for the award of a degree by this or any other university.

The author

Hawzheen Aziz Muhammad

The author:

PhD, Gene Therapy of Cancer – present
Queen Mary University of London, London, UK

Technician Diploma, Community Health (1997) – graduation rank: 1st of class
Technical Medical Institute of Sulaimani, Sulaimani, IRAQ

BSc, Microbiology (2001) – graduation rank: 2nd of class
Salahaddin University, Erbil, IRAQ

MSc, Cell Biology (2007) – graduation rank: 1st of class
Sulaimani University, Sulaimani, IRAQ

Acknowledgments

Firstly, I would like to extend my sincere thanks to Mr Yousef Jameel, for sponsoring the program of my PhD studies at University of London. The Yousef Jameel Scholarship has given me the opportunity to realise my dreams of carrying out world-class research at the University of London in the field of “Molecular Targeting of Cancer Cells for Apoptosis”. I would like to express my greatest gratitude for this opportunity to achieve my ambitions towards the advancement of science and medicine. I would also like to offer my deepest gratitude for the gallant efforts made by Mr Christian Hoffmann, the manager of the scholarship program who enabled me to take up the scholarship. His advice, communications, and time spent in arranging the scholarship and related aspects have been absolutely invaluable.

My special thanks also go to Professor Rizgar A. Mageed and Dr David J Gould, my supervisors. I am grateful that I could have so many valuable discussions with them, and also for them helping me to learn the necessary techniques to carry out my research.

I would like to thank my mentor, Professor Yuti Chernajovsky, for supporting me during these past four years. We have shared many insightful discussions about the research.

I would also like to acknowledge my department members for their support. I must express my special gratitude to Dr Lisa Mullen, for her continued support and encouragement. Special thanks to Mrs Gill Adams for her assistance with proofreading of the thesis.

My special thanks to Miss Jacqui Frith for all the paperwork, her continuous advice and support and caring.

Special thanks to Dr Ira H Pastan at the National Cancer Institute for providing me with the DNA constructs to finish part of my PhD study work.

I would also like to thank Dr John F Marshall at the Barts Cancer Institute for his support.

My completion of this project could not have been accomplished without the support of my parents, sisters and brothers.

I will forever be thankful to my former college advisor, Professor Tariq A.G. Aziz, the head of Medical Microbiology department at the School of Medicine in IRAQ, not only for providing me the opportunity to undertake this study, but also for seeking the funding to support the financial requirements of my PhD study at the University of London.

Hawzheen Aziz Muhammad

Abstract

This study describes “proof of concept” experiments for development of a novel therapy to target B cells in pathological settings such as cancer and inflammation. Targeted biological therapies including monoclonal antibodies (mAbs) have revolutionised medicine, thus biological therapies are increasingly used in the treatment of patients with a range of diseases including cancer. However, despite significant progress in the treatment modalities, haematological malignancies remain a leading cause of cancer related mortality. Though RNA interference (RNAi) is a promising strategy for cancer gene therapy, targeted delivery of siRNAs into cells is a key challenge to their therapeutic application. One approach to target intracellular delivery could be to harness cell surface receptors that are internalised upon ligation by mAb. Thus, single-chain fragment of variable regions (scFv) mediated siRNA delivery into diseased B cells via cell surface receptors is a promising strategy. The approach involves generating an engineered scFv-protamine fusion protein to deliver siRNA specifically to B cells via CD22. For this purpose, gene constructs that combine the V_H and V_L of mAb (Cy34.1.2) targeting mouse CD22 and HA22, a scFv that targets human CD22, were fused to a truncated protamine peptide. Gene constructs have been produced for the expression of fusion proteins using a range of expression systems. HA22 fusion protein was expressed as secretable protein in serum-free cultures of mammalian cells. The protein was shown to retain specificity of binding to CD22 on B cells with subsequent internalisation and was also able to deliver fluorescently-labelled siRNA into B cells. The feasibility of harnessing protamine peptide for siRNA delivery was verified in tumour cells expressing $\alpha v\beta 6$ integrin using the A20FMDV2-protamine peptide. Furthermore, siRNAs to *MCL1* and *PLK1* genes delivered with HA22 fusion protein to malignant B cells induced apoptosis. This study demonstrates the potential for systemic, cell-type specific, antibody-mediated siRNA delivery.

Table of contents:

List of figures:

Chapter 4:

List of tables:

Abbreviations

2'-F:	2'-fluoro
2-ME:	2-mercaptoethanol
2'-OMe:	2'-methoxy
3'-UTR:	3'-untranslated region
Abl:	Ableson tyrosine kinase gene
AcMNPV:	*Autographa californica* multinucleocapsid NPV
ADCC:	Antibody-Dependent Cell-mediated Cytotoxicity
Ad5:	Adenovirus type5
Ago-2:	Argonaute 2
Ahx:	Aminohexanoic acid
AIF:	Apoptosis-Inducing Factor
ALL:	Acute Lymphoblastic Leukaemia
AML:	Acute Myeloid Leukaemia
Antagomirs:	Anti-miRNA oligonucleotides
APCs:	Antigen-Presenting Cells
Arg:	L-arginine
ASO:	Antisense DNA Oligonucletides
BAX:	Bcl-2 associated X protein
BAK:	Bcl-2 homologous antagonist killer
BAD:	Bcl-2 associated death promoter
BCL2:	B cell leukaemia/lymphoma 2
BCL-XL:	B cell leukaemia/lymphoma extra large
BCL-W:	Bcl-2 like protein 2
Bcr:	Break point cluster
BCR:	B Cell Receptor
BCA:	Bicinchoninic Acid
BID:	BH3 interacting-domain death agonist
BIM:	Bcl-2 interacting mediator of cell death
BHK:	Baby Hamster Kidney cells
BLAST:	Basic Local Alignment Search Tool
BMF:	Bcl-2 modifying factor
BSA:	Bovine Serum Albumin
BV:	Baculoviruses
CARDs:	Caspase Recruitment Domains
CDE/CHR:	Cell cycle-Dependent Element/Cell cycle gene Homology Region
CD22:	Cluster of Differentiation 22
CDRs:	Complementarity Determining Regions
CHO:	Chinese Hamster Ovary cells
CLSM:	Confocal Laser Scanning Microscopy
CLL:	Chronic Lymphocytic Leukaemia
cSLN:	cationic Solid Lipid Nanoparticles
CML:	Chronic Myelogenous Leukaemia
Cγ cDNA:	PCR product of V_H and C_H1gamma region
Cκ cDNA:	PCR product of V_L and C_H1 kappa region
Cyt *c*:	Cytochrome *c*
DAPI:	4′,6-Diamidino-2-phenylindole dihydrochloride
DD:	Death Domain
DED:	Death Effector Domain
DGCR8:	DiGeorge syndrome Critical Region Gene 8
DISC:	Death-Inducing Signaling Complex
DLBCL:	Diffuse Large B Cell Lymphoma
DMEM:	Dulbecco's Modified Eagle Medium

DOPE: Dioleoyl phosphatidylethanolamine
dsRNA: double stranded RNA

eIF2: Eukaryotic translation Initiation Factor 2
EBV: Epstein-Barr virus
ECM: Extracellular Matrix
EDEM: ER-Degradation Enhancing α-Mannosidase-like protein
EDTA: Ethylene Diamine Tetraacetic Acid
EGF: Epidermal Growth Factor
ERK: Extracellular signal-Regulated Kinase
ErbB2: v-erb-b2 avian erythroblastic leukaemia viral oncogene homolog 2,
ERAD: Endoplasmic Reticulum-Associated Degradation
EMSA: Electrophoretic Mobility gel Shift Assay
EtBr: Ethidium Bromide
E. coli: *Escherichia coli*

Fab: Fragment antigen-binding
FACS: Fluorescence Activated Cell Sorting
Fc: Fragment crystallisable region
FMD: Foot-and-Mouth-Disease virus
FPLC: Fast Protein Liquid Chromatography
FWR: Framework

$(Gly_4Ser)_3$: Glycine-Serine peptide linker
GC: Germinal Centre
GDP: Guanosine-5'-Diphosphate
GTP: Guanosine-5'-Triphosphate
G2: Gap 2 phase
Glu: L-glutamine
GFP: Green Fluorescent Protein
GM CSF: Granulocyte-Macrophage Colony-Stimulating Factor
GSSH: reduced glutathione
GSSG: oxidized glutathione
Grb2: Growth factor receptor-bound protein 2

HI-FBS: Heat-Inactivated Foetal Bovine Serum
HEPES: 4-(2-hydroxyethyl)-piperazine-1-ethanesulfonic acid
HA: Haemagglutinin A epitope
HBS: HEPES-Buffered Saline
HEK293: Human Embryonic Kidney cells
HUVEC: Human Umbilical Vein Endothelial Cells
HSC: Haematopoietic Stem Cells
HCL: Hairy Cell Leukaemia
HGFR: Hepatocyte Growth Factor Receptor
HAX-1: HS1-associated protein X-1
HIV: Human Immunodeficiency Virus
HPLC: High-Performance Liquid Chromatography

ID: Idiotype
Ig: Immunoglobulin
IgVH: mutational status of the Ig V_H gene locus
IMAC: Immobilized Metal Affinity Chromatography
IPTG: isopropyl-β-D-galactoside
ITAM: Immunoreceptor Tyrosine-based Activation Motif
ITIM: Immunoreceptor Tyrosine Inhibitory Motif

KLH: Keyhole Limpet Haemocyanin
K-RAS: Kirsten rat sarcoma viral oncogene homolog

KGM: Keratinocyte Growth Medium

LAP: Latency Associated Peptide
LB: Luria-Bertani
LFA-1: integrin Lymphocyte Function-associated Antigen-1
LNP: Lipid Nanoparticles

mAb: monoclonal antibody
miRNA: microRNA
MDR1: Multi-Drug Resistance protein 1
MCL1: Myeloid leukaemia cell differentiation protein-1
M: Mitotic phase
MCS: Multiple Cloning Site
MPa: Megapascal
Met-$tRNA_i^{Met}$: Methionyl initiator transfer RNA
MMP9: Matrix Metalloproteinase-9

NSCLC: Non-Small Cell Lung Cancer
NPC1: Niemann-Pick type C1
NS0: mouse myeloma cells
NTC: No-Template Control
Ni-NTA: Nickel-Nitrilotriacetic Acid
ncRNAs: non-coding RNAs
Noxa: phorbol-12-myristate-13-acetate-induced protein 1

ODN: Oligodeoxynucleotides
OMI/Htr2A: HtrA serine peptidase 2
OSCC: Oral Squamous Cell Carcinoma

PBS: Phosphate-Buffered Saline
PCR: Polymerase Chain Reaction
PE38: *Pseudomonas* exotoxin A
PEI: Polyethylenimine
PES: Polyethersulfone
PLK1: Polo-Like Kinase-1
Pfu: *Pyrococcus furiosus*
pelB: pectate lyase B
PTD: Protein Transduction Domain
PVDF: Polyvinylidene Fluoride

qRT-PCR: quantitative real-time PCR

Ran: Ras-related nuclear protein
RGD: arginine-glycine-aspartate
RNAi: RNA interference
RISC: RNA-Induced Silencing Complex
RPMI: Roswell Park Memorial Institute medium

scFv: single-chain Fragment of variable regions
SDS PAGE: Sodium Dodecyl Sulphate Polyacrylamide Gel Electrophoresis
siRNA: small interfering RNA
Siglec-2: Sialic acid binding Ig-like lectin 2
SHIP-1: SH2-domain containing inositol 5-phosphatase-1
SLE: Systemic Lupus Erythematosus
shRNA: short hairpin RNA
Smac/Diablo: Second mitochondria-derived activator of caspases/ Diablo homolog
S: Synthesis phase

TAT-PTD:	Trans-Activator of Transcription-Protein Transduction Domain
Taq:	*Thermus aquaticus*
TCA:	Trichloroacetic Acid
TCR:	T Cell Receptor
TdT:	Terminal deoxynucleotidyl Transferase
TE:	Tris-EDTA
TFP:	Tetrafluorophenyl
TGFβ:	Transforming Growth Factor β
TLR:	Toll-like receptor
TNF:	Tumour Necrosis Factor
TRBP:	HIV-1 transactivating response (TAR) RNA-binding protein
TRBP:	Transactivation responsive RNA-binding protein
UPR:	Unfolded Protein Response
VP1:	Viral coat Protein-1
$V_{H:}$	Variable region of the heavy chain
V_L1:	PCR reverse primer with *Nhe*I site for amplification of V_L genes in scFv-protamine-His6
V_L2:	PCR reverse primer with *EcoR*I site for amplification of V_L genes in scFv-His6
X-Gal:	bromo-chloro-indolyl-galactopyranoside
ZAP-70:	ζ-chain (zeta-chain) associated protein kinase 70

Chapter One

Introduction and reviews of the literature

1.1. Introduction:

Targeted therapies, which include monoclonal antibodies (mAbs) and small molecule inhibitors, have significantly changed treatment of diseases including many types of cancer and chronic inflammatory diseases. These therapies act on specific targets that are selected to maximise efficacy of treatment while minimising side effects and damage to normal cells and tissues. In contrast, standard pharmaceutical therapies affect all cells and are usually associated with adverse effects including damage to normal healthy cells (1). One example of such benefits can be seen with gene therapy. Thus, using this mode of therapy, high and long-term concentrations of therapeutic molecules can be achieved locally by targeted delivery to the desired tissue or organ while systemic levels are minimised with minimal adverse effects (2).

The study described in this thesis was conceived to develop a novel approach for targeting aberrant B lymphocytes in diseases with a focus on how to change the fate of cells especially malignant B cells. Whilst the approach would be highly beneficial in the treatment of a wide range of diseases including chronic inflammatory diseases and cancer, an immediate outcome of such treatment could best be seen in cancer.

Cancer is a complex and potentially fatal disease that is considered a major world-wide public health problem. It starts because of out-of-control growth of abnormal cells due to genetic aberrations and environmental factors. Today, millions of people are living with cancer or have had cancer. Unfortunately, there is no curative treatment once a cancer had spread and some interventions might even be more harmful. Despite improved understanding of cancer biology and ability to devise more specific therapeutics, cancer treatment has gone through a slow process of development (3, 4).

Treatment of early-stage cancers can mostly be successful. Unfortunately, however, most solid tumours and haematological malignancies remain asymptomatic until they advance to invade surrounding tissues and/or metastasize to distant tissues. Thus at this advanced stage of the disease, cancers frequently become fatal (5).

Systemic cytotoxic chemotherapies and radiotherapies which mostly provide minimal survival benefits in most advance stage cancers are non-specific therapies that may destroy normal healthy tissues in addition to the cancer cells. In addition, several factors such as resistance to therapy, severe side effects and toxicities limit the benefits of these generalised therapies (6-8). Therefore, there is an unmet need to develop novel therapeutics particularly targeted therapies with low toxicities, or personalised cancer therapies for individual patients with unique “cancer signatures” (9, 10). Analyses of the whole-genome sequences of cancers allow the identification of signatures of different mutational processes, “cancer signatures”. Therefore, each signature is defined as the imprint left on the cancer genome by one or more mutational process (9).

The rapid progression seen in the treatment of cancer, in particular haematological malignancies, demonstrates the great success in development of targeted therapies (11, 12). Haematological malignancies are a complex group of neoplastic diseases of bone marrow derived cells. Patients with haematological malignancies have high rates of morbidity and mortality and are at high risk of thrombotic or haemorrhagic complications in spite of the adverse effects associated with current therapies. The main groups of these cancers are acute and chronic leukaemias, Hodgkin and non-Hodgkin lymphomas and myeloma (13).

The range of therapeutic options including single and combination chemotherapy, radiotherapy and bone marrow transplantation each have a role in the management of individual patients with haematological malignancy. Nevertheless, in spite of progress in these treatment modalities there are still unmet needs for further innovative therapies. This is especially true for patients with more aggressive forms of such diseases, for those who relapse or are resistant to treatment and those who develop serious side effects (13).

Targeted therapies using mAbs represent a viable therapeutic approach for many diseases including cancer. Furthermore, targeted therapies using mAbs have the potential for decreased toxicity, suggesting these agents could lead to improved cancer therapy (14).

The concept of targeted therapy was first described by Paul Ehrlich, the founder of chemotherapy. His postulation of creating “magic bullets” to treat human diseases has led to development of molecularly-targeted cancer therapeutics. Hence, targeted therapy is defined as using a drug with a focused mechanism that specifically acts on a well-defined target or biologic pathway that, when inactivated, causes regression or destruction of the disease process (15).

Despite the progress made towards treatment modalities, cancer remains an incurable disease and the introduction of new therapeutic strategies is needed. There is a need, therefore, for research to focus on the development of new therapeutic strategies to target molecular pathologic mechanisms. In this respect, the study described in this thesis was conceived to benefit from internalising membrane receptors, in this case CD22, for the delivery of therapy. This aim was to develop conjugated antibody fragments for anti-CD22 mAb for the delivery of therapeutic agents.

1.2. Strategies for targeted delivery:

1.2.1. Monoclonal antibodies (mAbs) as targeting therapeutics:

Antibodies, or immunoglobulins (Igs), are glycoproteins of molecular weight of 150-900 kDa that are generated in all mammals. Ig synthesis is the defining property of B lymphocytes and plasma cells. Resting B lymphocytes produce only small amounts of Igs that are mainly inserted in the cell membrane. These membrane-bound Abs capture antigens for which they are specific for further processing. However, end-stage differentiated B lymphocytes, plasma cells, which show very limited mitotic activity, are specialised to produce and secrete copious amounts of Igs. Free Igs that exist in body fluids have functions such as agglutination, opsonisation, neutralisation, immobilisation of bacteria and their toxins, complement activation, mucosal protection, antibody-dependent cell-mediated cytotoxicity (ADCC) and conferring immunity to the foetus (16). A schematic cartoon representing antibody structure is shown in Figure 1.

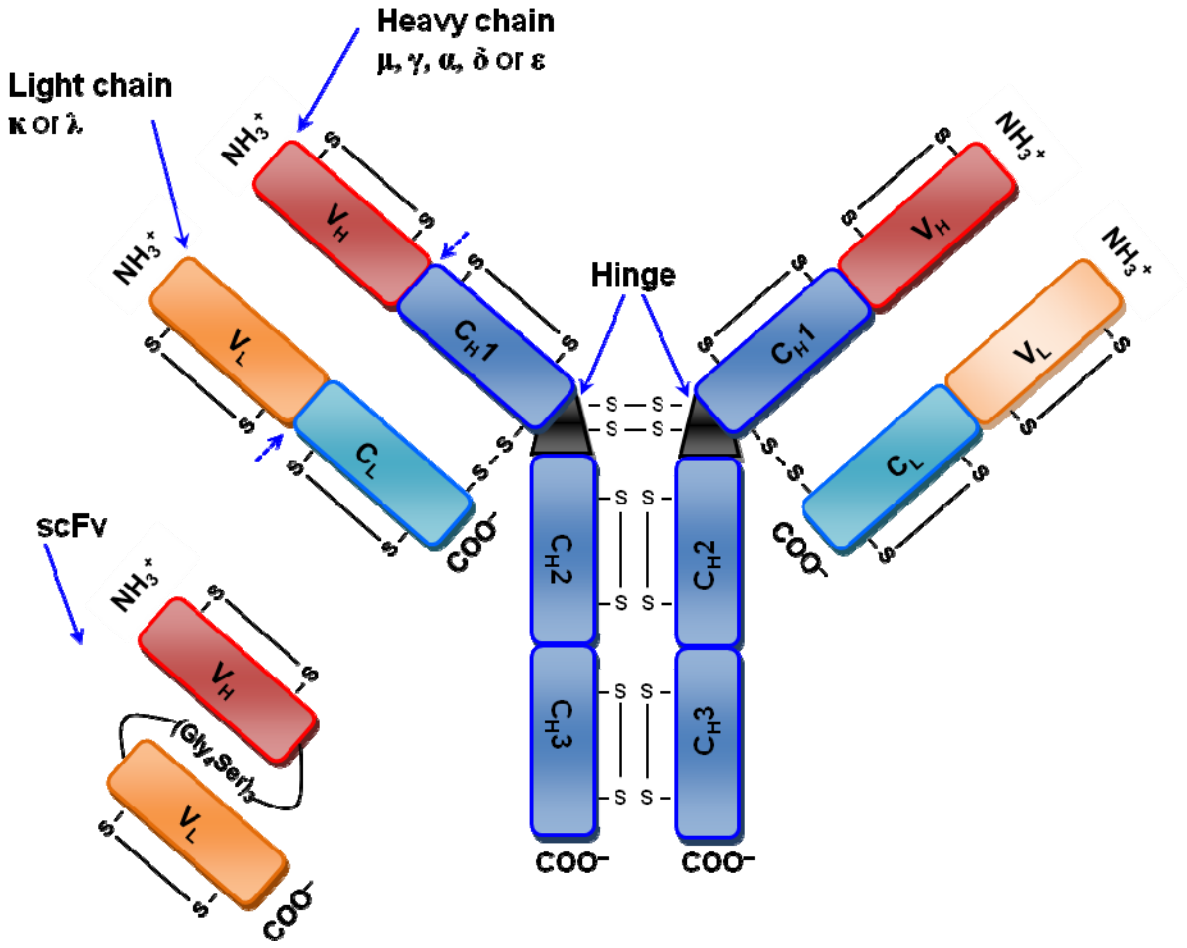

Figure 1: A cartoon depicting the basic structure of an antibody molecule. Ig molecules consist of two light chains, each of molecular weight of ~25 kDa and two heavy chains, each of molecular weight ~50 kDa, for IgG and IgD isotypes. These are linked by both disulphide covalent bonds and also non-covalent forces. There are five distinctive classes, or isotypes of Igs which are IgM, IgG, IgA, IgD, and IgE which differ in size as well as amino acid sequences and carbohydrate composition. Light chains exist in two classes, lambda and kappa. Each antibody molecule has either lambda or kappa light chains, not both. Regions concerned with antigen binding are extremely variable between Ab produced by different clones for B cells, whereas in other regions of the molecule, they are relatively constant. Thus, each heavy and each light chain possesses a variable (Fab) and a constant region (Fc). Light chains are attached to heavy chains by disulphide bonds. Smaller antibody fragments such as single-chain fragment of variable regions (scFv) can be engineered by recombinant DNA technology to generate a single V_H-V_L polypeptide antibody fragment. The Figure is adapted and redrawn from reference number 16.

Monoclonal antibodies (mAbs) are molecules of great interest for diagnosis and treatment of diseases. For example, the use of mAbs for therapy is now one of the most successful and important strategies for treating patients, for example patients with solid tumours and haematological malignancies which has achieved considerable success (17-19). The development of therapeutic antibodies for cancer requires understanding of cancer biology, protein engineering techniques and mechanisms of action of the targeting Abs. Observation of antigen expression by tumour cells is the fundamental basis of antibody-based therapy. The characterisation of cell surface antigens that are expressed by human disease-causing cells, including cancer cells, has revealed a broad array of targets that are overexpressed, mutated or selectively expressed compared with normal tissues. Identifying a suitable tumour antigen for treating cancer is a key challenge for antibody-based therapeutics (20). MAbs with increased half-life and reduced immunogenicity were generated through the introduction of genetically engineered Igs and better identification of targets for antibody therapy. Full length mAbs or their recombinant derivatives such as single-chain fragment of variable regions (scFv) now account for the single largest group of biotechnology-derived molecules. Their successful therapeutic applications include prophylaxis, treatment and control of allergic and autoimmune diseases, complications of angioplasty, sepsis, a variety of inflammatory diseases, many viral and bacterial infections, organ transplantation rejections and solid tumours and haematological malignancies (21, 22).

MAb-based therapies bring the promise of increased response rates without excessive toxicity. For instance, engineered antibody fragments such as scFvs have some advantages compared to intact antibodies due to their smaller size, unique and highly specific antigen-binding ability, stability and possibly reduced immunogenicity (20-22). Besides, it is possible to be designed as a bifunctional antibody fragment to work as a cargo/carrier fusion protein such as anti-CD22 scFv that will be the subject of this thesis. It, thus, makes scFv potentially the best candidate for medical, diagnostic and research applications.

1.2.2. Engineering therapeutic antibodies to generate scFv:

The use of single-chain fragment of variable regions (scFv) is a new approach in which an engineered recombinant monovalent portion of a monoclonal antibody of molecular weight 26-28 kDa is used for targeting, or to deliver a therapeutic cargo. Recombinant scFv consists of the Ig variable region binding domains of the heavy (V_H) and light (V_L) chains that are joined together between the C-terminus and the N-terminus with a flexible linker usually 10–25 amino acids in length into a single heterodimer polypeptide chain (23, 24). Therefore, a scFv contains the entire antigen-binding region and hence retains specificity of the parent antibody (25). The most common linker used is the 15-mer peptide glycine-serine $(Gly_4Ser)_3$ and the length of this linker plays a vital role for the state of the soluble scFv. Shorter and longer linkers have been shown to favour the formation of dimers and multimers, respectively (26, 27). The $(Gly_4Ser)_3$ linker should provide adequate flexibility to both V_H and V_L domains, which is the underlying principle followed in the most commonly used linker sequences (28).

scFvs are thought to bind their cognate antigens with affinity similar to that of the parent antibodies (26, 29) if the effect of the bivalency of the parent Ig is taken into consideration. Retaining specificity of the parent antibody combined with their small size has made scFvs attractive candidates for a wide range of applications, including in therapeutics, imaging and diagnostics (30). scFvs are currently in pre-clinical and clinical trials to treat human diseases ranging from heart disease to cancer and also for use in medical imaging (25). In addition, scFvs have shown promise in drug delivery systems and for the targeting of vectors for gene therapy (31, 32).

Various expression systems for scFvs have also been described, including bacteria, fungi, plants, insect and mammalian cells (33-37). Engineering of therapeutic antibodies to create scFvs have a number of advantages. For example, scFvs are less likely to generate an immune response and the smaller size of the fragments enables faster and deeper penetration into tissues impenetrable by full-size mAbs for tumour targeting or therapy (38, 39). In addition, antibody engineering allows for increasing affinity by mutagenesis. However, monovalency and rapid elimination through the kidneys results in lower tumour accumulation of scFvs compared with their parent Abs (40, 41). This makes scFv more suited, perhaps, for imaging purposes than for therapeutic applications for some antibodies. This problem can be solved by forming multivalent scFv variants, which in addition to a larger size have the benefit of higher functional affinity (avidity). This could also prolong retention of the recombinant antibodies within the tumour tissue (42-44).

Today, the generation of scFv has become an established technique for producing functional antigen-binding fragments. Further, bifunctional scFvs can be generated to direct therapeutics to desired cells or tissues. For this purpose, the studies reported in this thesis have examined the potential of linking anti-CD22 scFv to a positively-charged peptide from human protamine (RSQSRSRYYRQRQRSRRRRRR) which has a strong ability to bind small interfering RNA (siRNA) (45) and target these to B cells. The siRNA to be used would be intended to target key signaling molecules, or proteins that are uniquely upregulated in disease settings, for example in malignant B cells.

Protamines are a group of small highly basic arginine-rich proteins that replace histones and non-histone chromosomal proteins in spermatids during vertebrate spermatogenesis. DNA in mature sperm cells is packaged by protamines at a high density which makes them transcriptionally inactive (46, 47). Each protamine/DNA particle is estimated to contain in the order of 50 kb of DNA (48). Therefore, it has been established that the positively-charged guanidinium groups of arginine bind the negatively-charged phosphate groups of siRNA (45).

1.3. B cells and their role in diseases:

B cells, the principal mediators of humoral immunity, arise from haematopoietic stem cells (HSCs) in the bone marrow. Their development proceeds through a series of organised gene expression and selection events in the bone marrow followed by migration to secondary lymphoid organs to become follicular, germinal centre or memory cells (49-52).

The available repertoire of B cells emanates from the generation of an extraordinarily diverse range of clones that differ by the specific structure of their B cell receptor (BCR). The BCR, or membrane Ig, is composed of two identical heavy chains and two identical light chains covalently linked by disulphide bridges. This membrane Ig is associated with two polypeptide chains, the CD79A and CD79B, which contain cytoplasmic immunoreceptor tyrosine-based activation motifs (ITAMs) that help transmit intracellular signaling upon BCR engagement by antigens. The intracellular signaling pathways activated following BCR cross-linking involves a range of tyrosine kinases and phosphatases. Depending on the differentiation and activation status, the B cell might be induced to proliferate, differentiate or undergo apoptosis upon BCR engagement (53).

Production of antibodies by B cells is the key effector function of these cells. However, B cells also carry out various other effector and regulatory functions during the course of an immune response. For example, B cells present antigens to and interact with T cells to modulate cellular and humoral immune responses to pathogens and to autoantigens (54). B lymphocytes can also modulate immune response through the production of cytokines. B lymphocyte responses are normally well-regulated and disruption of these regulatory events due to mutations, oncogenic chromosomal translocations, evasion from apoptosis or uncontrolled proliferation can lead to the aberrant responses and diseases (55). These defective responses can lead to malignancies or autoimmune diseases. Therefore, therapeutic targeting of B cell depletion could be desirable in patients with haematological malignancies or patients with autoimmune inflammatory diseases. In this respect, the last 15 years have seen a substantial increase in the generation and use of B cell depleting, or modulating mAbs that have been used to treat human diseases. Some of the mAbs target membrane proteins including CD20, CD52, CD22 and CD40 receptors (56).

1.4. CD22 receptor:

Development, activation and differentiation of B lymphocytes are complex processes regulated in part by cell surface co-receptors, soluble mediators and by intracellular signaling pathways. An array of cell surface and cytoplasmic proteins also modify intracellular signal transduction through BCR following engagement by antigens. One such B cell-specific surface molecule is CD22, also known as sialic acid binding Ig-like lectin 2 (Siglec-2), that functions as an adhesion molecule, a transducer and modulator of intracellular signaling mediated through the BCR complex (57).

1.4.1. CD22 expression:

Expression of human CD22 (hCD22) is found in the cytoplasm of pro-B and pre-B cells but is expressed on the membrane of IgM^+ B cells at about the same time as IgD is expressed. In lymphoid tissues, hCD22 is expressed by follicular mantle and marginal zone B cells, but only weakly by germinal centre B cells (58). Indeed, the vast majority of IgM^+IgD^+ B cells express CD22 (59, 60). Expression of hCD22 in malignant cells was first reported to be restricted to the cytoplasm in pre-B acute lymphoblastic leukaemia (ALL), with surface expression found only on malignancies corresponding to more mature B cells (61-63). Expression of mouse CD22 (mCD22) was found on all mature B cells including follicular and marginal zone B cells of the spleen, peritoneal B-1 cells and isotype-switched IgA-expressing B cells in Peyer's patches. However, mCD22 expression is lost during B cell differentiation to plasma cells and the molecule is not present on the membrane during the early stages of B cell development and is not expressed on stem cells (64).

1.4.2. CD22 structure and function:

CD22 is a type I membrane protein with molecular weight of ~140 kDa. The extracellular portion of CD22 comprises seven immunoglobulin-like domains (65-69). CD22 is a B cell-restricted glycoprotein involved in cell adhesion and signaling and plays an important role in interactions with other cells by recognising *N*-linked oligosaccharides possessing α2-6-linked sialic acid residues and consequently regulating signaling thresholds (70, 71). CD22 ligands include structurally-diverse sialic acid-bearing glycoproteins, glycolipids and gangliosides expressed by lymphocytes, neutrophils, monocytes and erythrocytes as well as non-haematopoietic cells. Ligands composed of α2,6-linked *N*-glycolylneuraminic acid recognise mCD22 specifically, whereas ligands in the form of *N*-acetylneuraminic acid recognise hCD22 (72-75). Known ligands of CD22 include CD22 itself, all isoforms of CD45, soluble IgM pentamers, haptoglobin, Ly-6 proteins and a variety of other proteins present on leukocyte cell surfaces (76, 77). CD22 is known to modulate B cell activation upon BCR cross-linking with an antigen (78, 79). Furthermore, strong cross-linking of CD22 is known to trigger programmed cell death in B cells (80). The mouse anti-CD22.2 mAb produced by Cy34.1.2 hybridoma (page 55, section 2.2 and page 120, section 3.1) and the anti-human scFv BL22 and HA22 (page 84, section 2.26) were both used in this study to generate recombinant proteins to target mouse and human CD22 receptor respectively. A schematic diagram illustrating the structure and signaling components of CD22 is shown in Figure 2.

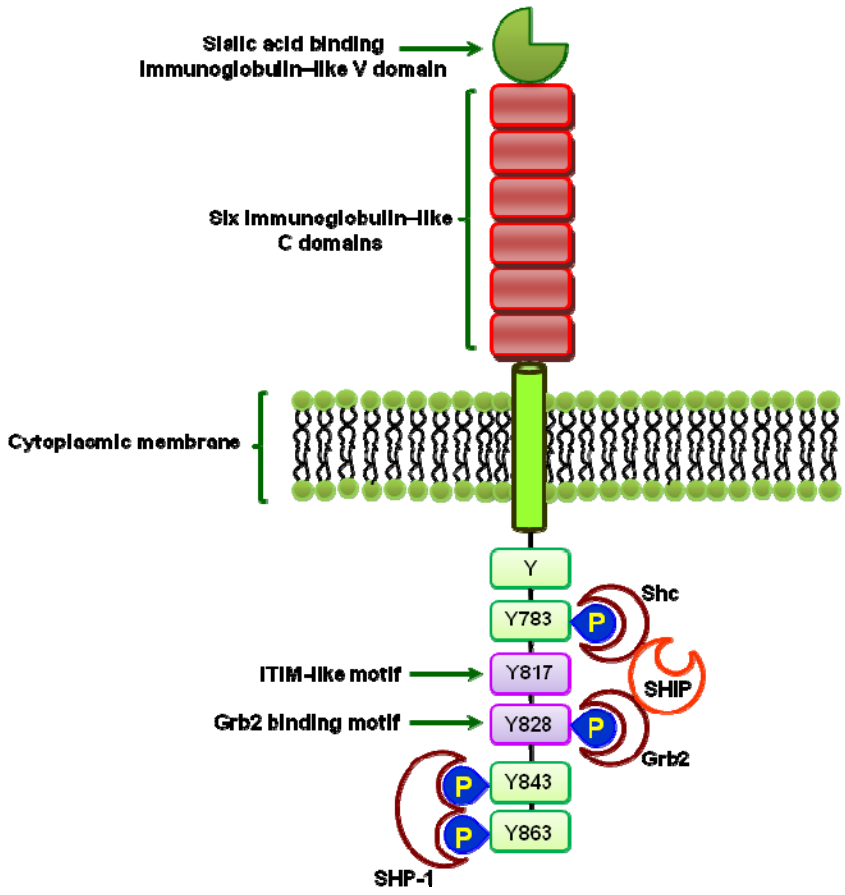

Figure 2: Schematic diagram of domain structure of CD22 in humans and mice. CD22 is a 140 kDa type I transmembrane protein that associates with the BCR both physically and functionally and negatively regulates BCR signaling. Phosphorylation of CD22 occurs rapidly following CD22 or BCR ligation. The cytoplasmic tail of CD22 has six tyrosines that are potential targets for phosphorylation, of which three are found within conventional ITIM motifs (Y783, Y843, Y863) (green boxes), one is part of an ITIM-like motif (Y817) and one is needed for the recruitment of Grb2 (Y828). SHP-1 binds to two phosphorylated ITIMs. SHP-1 interferes with signaling pathways leading to the depletion of calcium stores from the endoplasmic reticulum (ER) and promotes calcium efflux. Shc and Grb2 bind to the indicated tyrosines and form a complex with SHIP. Abbreviations: Grb2: growth factor receptor-bound protein 2; ITIM: immunoreceptor tyrosine inhibitory motif; SHIP-1: SH2-domain containing inositol 5-phosphatase-1. The Figure is adapted and redrawn from reference number 69.

1.4.3. The kinetics of CD22 endocytosis:

Cytoplasmic CD22 represents an internal reservoir for CD22 expression, with cytoplasm-to-surface transport occurring in response to activation or differentiation signals (81). CD22 is also constitutively endocytosed with kinetics of internalisation ($t_{1/2}$) of less than 1 hour by a clathrin-mediated mechanism and degraded with a relatively short half-life after endocytosis from the cell surface (82). The internalisation is then followed by routing of CD22 molecules to an acidic intracellular compartment where degradation ($t_{1/2}$ is ~8 hours) occurs without detectable recycling of the molecule back to the surface (83-92). However, another study has shown that intracellular CD22 rapidly moves to the surface of B cells in a tyrosine kinase-dependent manner following antigen receptor stimulation. Therefore, CD22 can carry cargo between the cell surface and endosomal compartments of B cells (93).

1.4.4. Therapeutic targeting of CD22:

Because most B cells in patients with non-Hodgkin's lymphoma express CD22 that becomes internalised upon ligation, CD22 has been considered a promising target for toxin or radioisotope-mediated immunotherapy (91). A recent study showed that the rapid internalisation of large amounts of anti-CD22 mAb immunotoxin, BL22, bound to CD22 makes CD22 a better therapeutic target than CD19 for immunotoxins to act inside cells (90). Furthermore, restricted expression of CD22 to the surface of B cells is an attractive target in certain haematopoietic malignancies (89). Recently, CD22 was also shown to be expressed on a variety of lung cancer cell lines and a panel of primary patient lung cancer specimens. Interestingly, anti-CD22 mAb HB22.7 displayed cytotoxicity against $CD22^+$ human lung cancer cells and tumour xenograft models. Therefore, aberrant expression of CD22 on various human lung cancer cells is also a potential target for anti-CD22 based therapy of lung cancer that has few tumour specific targets (94). Furthermore, because B cells play an important role in the pathogenesis of many chronic inflammatory diseases, specific B cell directed antibodies are now used in the management of these diseases. Epratuzumab, a humanised anti-CD22 mAb, originally developed for treatment of non-Hodgkin's lymphoma, has been reported to be effective in treatment of systemic lupus erythematosus (SLE) and primary Sjögren's syndrome (95).

1.5. Targeting αvβ6 integrin for therapy:

αvβ6 integrin is a member of a large family of heterodimeric transmembrane receptors that consists of α and β subunits and functions as cell-substratum adhesion and signaling molecules. The integrin family which comprises of at least 24 distinct integrin heterodimers with different functions and ligand binding properties are formed by the combination of 18 α and 8 β subunits (96). A generalised structure of an integrin and its component domains is shown in Figure 3.

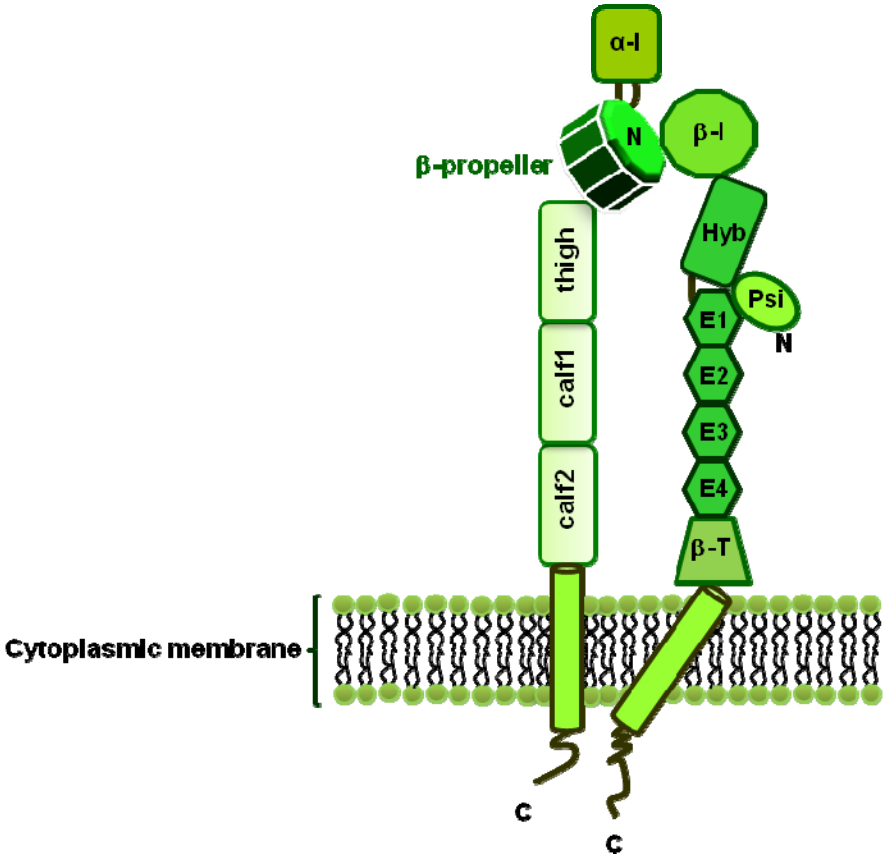

Figure 3: Cartoon representation of integrin structure. The α and β subunits consist of several domains with flexible linkers between them. Each subunit has a single membrane-spanning helix and usually a short unstructured cytoplasmic tail. The α subunit ectodomain consists of α –I domain, a seven-bladed β-propeller, a thigh and two calf domains. The β subunit has seven domains with flexible interconnections. The β-I is inserted in a hybrid (Hyb) domain. The hybrid domain, in turn, is inserted in a plexin-semaphorin-integrin (Psi) domain. These are followed by four cysteines-rich epidermal growth factor (EGF) molecules (E) and a β-tail (β-T) domain. The Figure is adapted and redrawn from reference number 96.

Integrins serve as anchoring molecules that function as bidirectional signaling molecules controlling various cell functions like adhesion, polarity, differentiation, migration, cell division and apoptosis during embryogenesis and in the maintenance of tissue homeostasis under physiological conditions (97, 98). However, in pathology, defective integrin signaling can disrupt these functions resulting in abnormal cell division, migration and adhesion, which are hallmarks of cancer, invasion and metastasis (99, 100).

αvβ6 integrin is an exclusive epithelial cell-specific surface molecule that is a receptor for the extracellular matrix (ECM) proteins fibronectin, vitronectin, tenascin and the latency associated peptide (LAP) of transforming growth factor β (TGFβ). The integrin $\alpha v\beta 6$ functions as an adhesion molecule, a signal transduction molecule and as a modulator of intracellular signaling. During embryogenesis, αvβ6 is expressed at high levels in the developing lung, skin and kidney epithelial tissues but its expression is downregulated in healthy adult epithelial tissues (101, 102).

Expression of $\alpha v\beta 6$ integrin is low or undetectable in normal adult epithelial tissue while during reorganisation of epithelial tissue in development, tissue repair and in neoplasia αvβ6 expression is upregulated to support cell spreading, migration and growth (102). Furthermore, there are circumstances in which $\alpha v\beta 6$ integrin expression is upregulated which include wound healing, development and inflammation (103, 104). Previous studies have shown that ligands such as fibronectin, tenascin, LAP of TGF$\beta 1$ and TGF$\beta 3$ and the viral coat protein-1 (VP1) of the foot-and-mouth-disease (FMD) virus that contain arginine-glycine-aspartate (RGD) motif can bind to $\alpha v\beta 6$ integrin (105-107).

1.5.1. αvβ6 integrin as a therapeutic target for cancer therapy:

The expression of integrins in various cell types that are involved in tumour progression and their ability to crosstalk with growth factor receptors has made them appealing therapeutic targets. Since αvβ6 is not expressed in normal epithelia except under conditions such as wound healing, αvβ6 lends itself to be a very good molecular target for therapy of cancer. Integrin αvβ6 is highly expressed in >95% of oral squamous cell carcinomas (OSCCs) and, hence, has been exploited as an efficient means for imaging, diagnosis and treatment (108).

For therapeutic targeting of αvβ6, panels of mAbs with specificity for human and mouse αvβ6 integrin with high affinity have been generated and studied (109). For example, mAb 10D5 was used for blocking αvβ6 integrin in colon cancer cells and resulted in reducing metastasis through disrupting extracellular signal-regulated kinase (ERK) binding to αvβ6 (110). In another study, blocking αvβ6 with 10D5, resulted in tumour cell apoptosis (111). Furthermore, blocking αvβ6 with mAb 6.3G9 led to growth inhibition of human pharyngeal carcinoma cells both *in vitro* and *in vivo* (112).

A study using peptide A20FMDV2 derived from a protein of FMD virus that mimics the ligand for αvβ6 was successfully used for diagnosis by imaging of αvβ6-expressing tumours and also to deliver chemotherapeutics to the tumour (113). Based on this finding, targeted delivery of therapeutics via integrins can be beneficial for targeting tumour cells. This observation was exploited in the current study by using A20FMDV2-protamine peptide to deliver siRNA to verify specificity and that the protamine peptide did not undermine specificity of the targeted delivery.

1.6. Targeting gene therapy in cancer:

Gene-based therapeutics are defined as the introduction, using a vector or delivery vehicle, of nucleic acids into cells with the intention of altering gene expression to prevent, halt or reverse a pathological process. Somatic cell gene therapy can be carried out through four routes: gene replacement/correction, gene silencing/knockdown, gene addition/augmentation and suicide gene therapy (114). Therefore, gene therapy is a promising treatment option for a number of diseases including inherited single gene disorders, cancer and viral infections. In cancer, for example, targeting of cancer cells with gene therapy has the potential to treat cancer on the basis of its molecular characteristics. Although results from preclinical and clinical trials have been encouraging, many practical obstacles need to be overcome before gene therapy can fulfill its goals in the clinic. One major challenge is directed delivery of the therapeutic gene to target cancer cells (114, 115).

For gene therapy to achieve cell-specific targeted delivery, therapeutic genes can be transferred into target cells by integrating ligands such as mAbs that recognise specific cellular receptors (116-119). Such a delivery strategy also improves the efficiency of gene transfer by enhancing the entry of therapeutic genes into desired cells and reducing uptake by non-target cells. Characteristically, receptor-mediated gene delivery capitalises on the presence of specific cell surface molecules for uptake of the therapeutic genes into cells and represents a particularly appealing approach for targeting to specific cell types *in vitro* and *in vivo*. Such a method utilises a natural mechanism which is receptor-mediated endocytosis (120).

In cancer gene therapy, selective delivery via targeting cell surface receptors is a promising method since many receptors are expressed in a cell type-specific manner, such as mannose receptor (CD206) on tumour-associated macrophages (121), or are highly expressed in malignant cells such as transferrin receptor (122-124). Hence, this study intends to employ anti-CD22 scFv-protamine fusion protein for receptor-mediated gene transfer via CD22 in B cells derived from leukaemias, lymphomas and other diseases in which B cells play a key role. Circulating malignant B cells are readily accessible via blood in most leukaemias whereas in lymphomas, tissue penetration is more challenging. Therefore, an advantage of using scFv over full-size mAbs is their

small size which allows them to extravasate rapidly from blood and penetrate faster and deeper into tissues. Since they lack the constant region of the antibody molecule, they do not bind Fc receptors and, thus, are not retained in tissues such as the liver and the kidneys. Thus, potential side effects are also reduced (38). New anti-cancer targeted therapies that make use of siRNA therapeutics have made treatments more specific and less toxic (125, 126). Recent data from human clinical trials have shown safe and tolerable intravenous administration of siRNA therapeutics in patients with liver metastases secondary to endometrial cancer with significant regression of the tumours (125). Therefore, therapeutic gene silencing is a promising approach for treatment of cancer.

1.7. Cancer therapy using siRNA:

RNA interference (RNAi) is a natural cellular process for post-transcriptional regulation of gene expression. This involves forming double stranded RNA (dsRNA) that suppress the expression of specific genes with complementary nucleotide sequences either by degrading specific mRNA or by blocking mRNA translation. RNAi can be activated exogenously by expressing short hairpin RNA (shRNA) and microRNA (miRNA) duplexes with viral vectors, or by incorporating synthetic siRNAs, double stranded miRNA mimetics and anti-miRNA oligonucleotides (antagomirs) directly into the cell cytoplasm (127-129). Since the discovery of RNAi, its potential application in therapeutics received much attention (130). Targeted post-transcriptional gene silencing by RNAi represents a promising new approach for the inhibition of gene expression *in vitro* and *in vivo*. RNAi has also emerged as a promising new strategy for drug target validation and the study of functional genomics and it is currently being evaluated in clinical trials as a potential therapy for diseases (131-140). RNAi technology can be directed against many cancers using a variety of strategies including the suppression of overexpressed oncogenes, promotion of apoptosis, regulation of the cell cycle, anti-angiogenesis and enhanced efficacy of traditional chemotherapy and radiotherapy. For example, through the use of an RNAi retroviral system targeting Kirsten rat sarcoma virus oncogene homolog (K-RAS) in human pancreatic carcinoma cells, loss of anchorage-independent growth and tumourigenicity were induced (141). Furthermore, RNAi was used to knockdown the multi-drug resistance protein 1 (MDR1) gene product P-glycoprotein, thus, reducing cancer cell multidrug resistance (142).

1.7.1. Mechanism of gene silencing by using RNAi:

miRNAs and siRNAs are ~19-25 nucleotide non-coding RNAs (ncRNAs) capable of regulating gene expression at the transcriptional and translational levels. They are involved in various biological processes such as cell cycle regulation, differentiation, development, metabolism, neuronal patterning, apoptosis and aging (143, 144). Both miRNAs and siRNAs share most of the components of RNAi pathway. In the nucleus of eukaryotic cells, miRNA synthesis begins where an RNA polymerase II transcribes a long, capped and polyadenylated primary precursor (pri-miRNA), which is then cleaved into a hairpin-shaped nucleotide precursor of ~70-100 pre-miRNA by the ribonuclease III Drosha and the double-stranded DNA-binding protein DiGeorge Syndrome Critical Region Gene 8 (DGCR8)/Pasha. Endogenously-synthesised pre-miRNAs then translocate to the cytoplasm through the nuclear export factor, exportin 5/ Ras-related nuclear protein (Ran) guanosine-5'-triphosphate (GTP), where the ribonuclease III Dicer and the double-stranded RNA-binding protein TRBP (HIV-1 transactivating response (TAR) RNA-binding protein) process pre-miRNAs into a 19-25 nucleotide miRNA duplex. In addition, exogenous long double stranded RNAs (dsRNAs) delivered into the cell are cleaved in the cytoplasm by the endoribonuclease III Dicer into short duplex siRNAs. Subsequently, miRNA or siRNA duplex is incorporated into the RNA-induced silencing complex (RISC) and drives the RISC to the target mRNA. RISC contains Argonaute 2 (Ago-2) which cleaves and releases one strand from the dsRNA, resulting in an activated form of RISC with a single-strand RNA (guide siRNA) that directs the specificity of the target mRNA recognition through complementary base pairing. Consequently, translation inhibition may occur through mRNA cleavage and degradation in cases of perfect complementarity to the 3’-untranslated region (3'-UTR) of the target. In this case Ago-2 cleaves the target mRNA between bases 10 and 11 relative to the 5′ end of the siRNA antisense strand, thereby causing mRNA degradation and gene silencing. Alternatively, translation inhibition occurs without mRNA degradation in cases of partial complementarity to the 3'-UTR of the target (145-147). The mechanism of biogenesis of miRNA and gene silencing through RNAi pathway is illustrated in Figure 4.

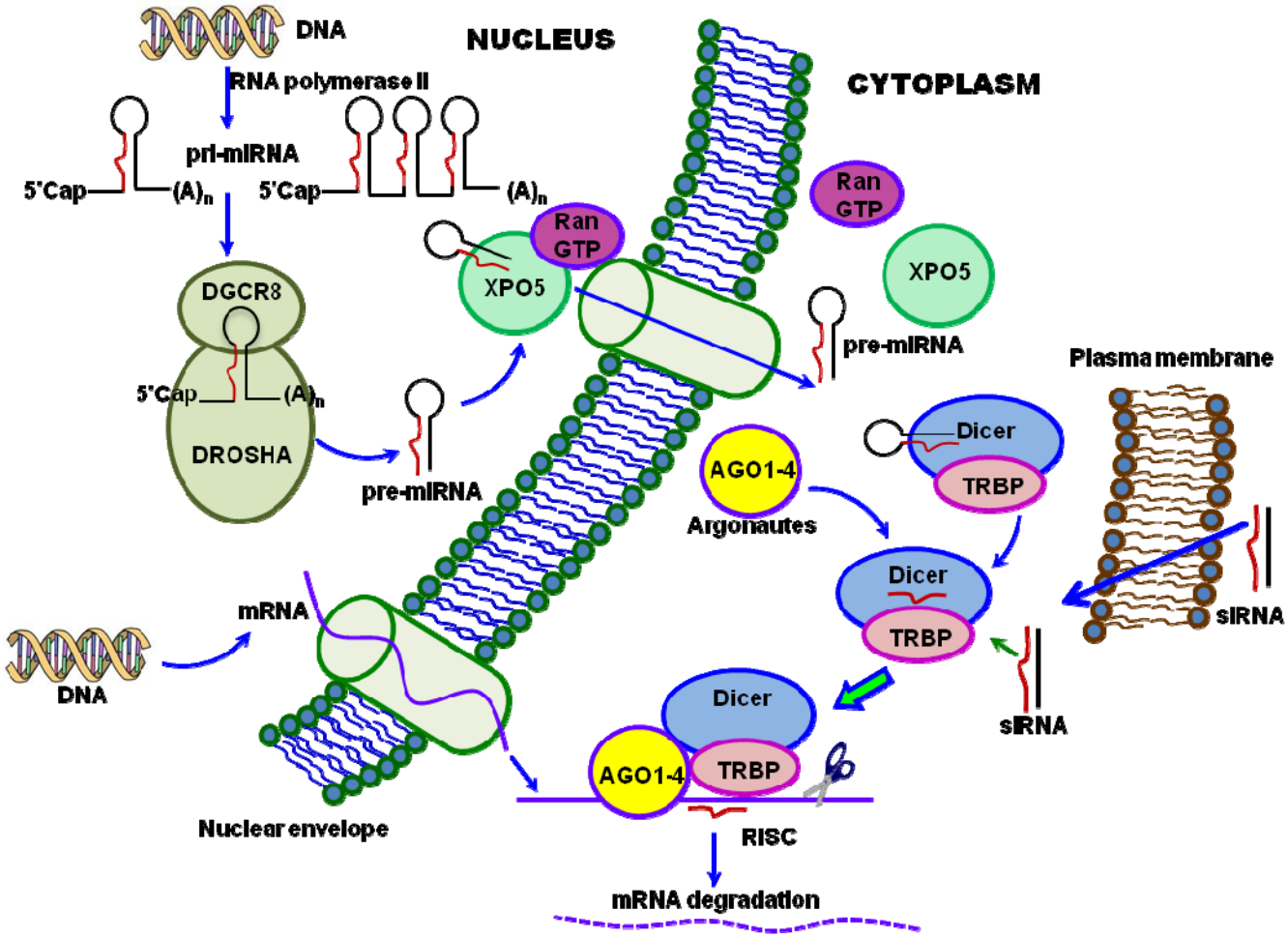

Figure 4: Genes can be regulated post-transcriptionally by miRNAs and siRNAs. miRNA genes are transcribed mainly by RNA polymerase II into an immature form of about 80 nucleotides in length called primary miRNAs (pri-miRNAs) which are capped and polyadenylated. The stem loop structure of the pri-miRNA is recognised in the nucleus by the RNase III enzyme Drosha and its partner DGCR8 and it is further processed to the ~70-nucleotide precursor miRNA (pre-miRNA). The hairpin-shaped pre-miRNA is then transported from the nucleus to the cytoplasm by Ran GTP and exportin-5 (XPO5), where it is loaded by the RNase III enzyme Dicer–TRBP complex and cleaved into a ~22 nucleotide double-stranded miRNA. This duplex is then loaded into the miRNA-associated multiprotein RNA-induced silencing complex (RISC), which includes the Argonaute proteins, and the guide strand (mature single-stranded) miRNA (red) is preferentially retained in this complex. Synthetic siRNA can be directly delivered to cells and enters the RNAi pathway when it assembles with RISC. In this case a transport mechanism such as receptor-mediated delivery introduces the siRNA into cells. The siRNA is recognised by RISC which then mediates cleavage of the target mRNA for gene silencing. The Figure is adapted and redrawn from reference number 145.

It is clear that RNAi can be potent and versatile tools for gene silencing. Therapeutic application of siRNAs in human, however, requires effective delivery to the correct intracellular location to interact with the RNAi machinery within the targeted cell. To achieve these objectives, systemically-administered siRNA must survive in the circulation long enough to reach target tissues, enter the desired cells, escape the endosome and/or delivery packaging and, finally, become incorporated into the RISC. However, the major challenge for the use of siRNA in the clinic as a therapeutic tool remains to be efficient intracellular siRNA delivery to target sites following systemic administration (148-151).

The key to efficacious siRNA application *in vitro* and *in vivo* is overcoming the difficulty of delivering siRNA selectively into target cells. Because of their high molecular weight (~14 kDa) and strong polyanionic nature (~40 negative phosphate charges in their backbone), naked siRNAs cannot easily pass through cell membranes. Thus, delivery systems are required to facilitate access to intracellular sites of action (152). Delivery has, therefore, been one of the major challenges for the application of RNAi technology. Various means of delivery have been developed and tested in murine and non-human primate models, ranging from the injection of naked siRNA into a target organ (153-155) to systemic delivery of the RNA in nanoparticles (156). For most of these approaches, covalent conjugation of siRNAs requires chemical reactions which could be detrimental to the activities or release of the therapeutic siRNA (157). One such delivery approach which will be described in this study in detail is the conjugation of cell-surface receptor targeting mAb fragment and charge interaction with siRNAs.

1.7.2. Delivery methods for therapeutic siRNA:

Under normal physiological conditions, nucleic acids, including siRNA, carry a net negative charge on the sugar-phosphate backbone. In order to enter the cell, siRNA first come into contact with the lipid bilayer of the cell membrane whose head groups are also negatively charged. For this reason most mammalian cells cannot take up siRNA, thus, intravenous injection of naked siRNA often fails to achieve significant silencing effects (152, 158). Therefore, a protocol to promote uptake is required for effective delivery of siRNA as therapeutics. Targeted delivery of siRNAs provides such a mechanism, as well as providing tissue specificity in gene silencing. However, the approach faces many of the same issues of targeted delivery of small molecule drugs, including stability in the blood, target tissue accumulation and penetration, pharmacokinetics and biodistribution. In addition and unlike many small molecule drugs that can passively diffuse into surrounding cells, siRNAs need to be internalised and then delivered to the proper subcellular localisation in the cytosol to achieve effective gene silencing. The commonly used methods to transfer RNAi molecules into cells *in vitro* are electroporation, lipid-based transfection reagents and using nanoparticles. Unfortunately, when employed *in vivo*, these methods are not cell-specific and, thus, limit their utility for delivering RNAi to target specific organs, or specific cell types within that organ (159).

1.7.3. Targeted delivery of siRNA using antibody-protamine fusion proteins:

The clinical success of *in vivo* applications of RNAi hinges on the development of new delivery methods. Therefore, the current study aimed at developing an efficient strategy to deliver siRNAs into desired cells via cell-surface receptors to achieve maximal therapeutic benefits, decrease the amount of siRNA required and avoid nonspecific silencing and toxicity in bystander cells. To achieve this, recombinant proteins were engineered with the positively charged amino acid residues of protamine peptide and anti-CD22 scFv to bind siRNA and deliver into desired cells *in vitro* and, ultimately, *in vivo*. Thereby, a complex between anti-CD22 scFv-protamine targeting proteins and siRNA will be prepared through electrostatic interaction between the positively charged protamine peptides and the negatively charged siRNAs. This assembled complex may obviate the need for aggressive and reagent-wasteful chemical reactions and, possibly, preserve the activities of the targeting moieties. In this regard, a number of studies have

used engineered scFv-protamine fusion proteins for directed delivery of siRNA into cancer cells via receptor-mediated endocytosis (160-162). As a proof of concept, the Fab of mAb F105 with specificity for HIV-1 envelope fused with protamine (F105-P) was used to deliver siRNAs to cells transfected to express HIV envelope glycoprotein gp160. siRNA complexed with the antibody-protamine fusion protein (F105-P) by electrostatic interactions did not require covalent coupling for effective delivery. *gag* siRNA, against HIV gag polyprotein structure, delivered with F105-P fusion protein reduced HIV replication in previously infected $CD4^+$ primary T cells. The proportion of productively infected cells declined from 85% in untreated cultures to 36% when 1 nM of *gag* siRNA was added (160). In addition, the effective delivery of siRNAs was further evaluated in B16 subcutaneous melanoma tumour models *in vivo* expressing HIV gp160 (env). Intravenous or intratumoral injection of F105-P-complexed with siRNAs delivered siRNAs into env^+ tumours but not into normal tissues or env^- tumours. Because this method can also be generalised for other targets, similarly, an anti-ErbB2-protamine fusion protein was used to deliver siRNAs specifically to ErbB2-expressing (v-erb-b2 avian erythroblastic leukaemia viral oncogene homolog 2, $ErbB2^+$) breast cancer cells (160). In another study, it was shown that a scFv-protamine fusion protein targeting the human integrin lymphocyte function-associated antigen-1 (LFA-1) resulted in efficient delivery of siRNAs and cell type-specific gene silencing in primary lymphocytes, monocytes and dendritic cells (161). Furthermore, it was shown that targeted delivery of PLK1 siRNA by the fusion protein anti-ErbB2 scFv-protamine *in vivo* using $Her2^+$ breast cancer models in mice significantly suppressed $Her2^+$ breast cancer growth and metastasis (162).

1.8. Targeted gene therapy for the induction of apoptosis in cancer cells:

A common hallmark of aberrant cells including cancer cells is their ability to evade apoptosis by survival signals, or by defects in cell death signal transduction pathways (163). Therefore, a permanent eradication of neoplastic cells through apoptosis is required for cancer treatment (164). On the basis of this knowledge, an important goal of cancer drug development would be to facilitate apoptosis in neoplastic cells. Consequently, cancer gene therapy represents a somewhat special category for gene therapy because its intended goal is the destruction of the cancer cell rather than its correction or preservation. In this respect, the current study was intended to apply siRNA knockdown of genes in B lymphocytes to evaluate their impact on survival by inducing cell death.

Apoptosis was first described in a landmark paper as a controlled cell deletion mechanism, which plays a complementary but opposite role to mitosis in the regulation of animal cell populations (165). Accordingly, apoptosis was defined as an active, inherently-programmed phenomenon that can be initiated, or inhibited by a variety of environmental stimuli, both physiological and pathological. The structural features of apoptosis comprise nuclear and cytoplasmic condensation and breaking up of the cell into a number of membrane-bound apoptotic bodies. These fragments shed from dying cells are then phagocytosed by neighboring cells, or by phagocytic cells (165). Apoptosis is central to various physiological processes and the maintenance of tissue homeostasis in multicellular organisms (3, 163-165). Even more important is a causative or contributing role of apoptosis to various human diseases, for instance accumulation of cancer cells or failure to eradicate transformed cells. Emerging knowledge about molecular mechanisms of apoptosis dysregulation in cancer has revealed a plethora of potential drug targets and, hence, made it possible to devise novel approaches, which exploit this process to treat cancer (3, 163). Apoptosis-triggering therapeutics comprises of two distinct mechanistic approaches. Pro-apoptotic strategies directly induce apoptosis such as introduction of pro-apoptotic molecules, modulation of anti-apoptotic molecules, or restoration of the function of tumour suppressor genes. Alternatively, permissive strategies modulate survival signaling pathways thereby facilitating the activation of apoptosis such as targeting of oncogenic signaling pathways (166-173).

1.8.1. Pathways and mechanisms of apoptosis:

Several pathways exist for triggering of apoptosis through caspase activation; two have been elucidated in detail and have been the subject of great interest in recent years. Thus, the apoptotic cell is believed to either receive and process extracellular death-inducing signals “extrinsic apoptotic program” or sense and integrate a variety of intracellular signals, “intrinsic apoptotic program” (174).

The intrinsic apoptotic pathway centres on mitochondria. The outer mitochondrial membrane is controlled by counterbalancing pro-apoptotic [Bcl-2 associated X protein (BAX), Bcl-2 homologous antagonist killer (BAK), Bcl-2 associated death promoter (BAD), BH3 interacting-domain death agonist (BID), Bcl-2 interacting mediator of cell death (BIM), Bcl-2 modifying factor (BMF), phorbol-12-myristate-13-acetate-induced protein 1 (Noxa)] and anti-apoptotic [B cell leukaemia/lymphoma 2 (BCL2), B cell leukaemia/lymphoma extra large (BCL-XL), Bcl-2 like protein 2 (BCL-W), myeloid leukaemia cell differentiation protein 1 (MCL1)] members of the Bcl-2 family of proteins (175, 176). BCL2 and other anti-apoptotic proteins are inhibitors of apoptosis acting in large parts by binding to and, thereby, suppressing pro-apoptotic triggering proteins. In most cases of cell death, the point of no return is permeabilisation of the outer mitochondrial membrane to the release of apoptogenic proteins (177). Multiple signals converge on mitochondria, including DNA damage, microtubule disruption and growth-factor deprivation, causing these organelles to release cytochrome *c* (cyt *c*) and other apoptogenic proteins such as second mitochondria-derived activator of caspases/ Diablo homolog (Smac/Diablo), HtrA serine peptidase 2 (OMI/Htr2A) , apoptosis-inducing factor (AIF) and endonuclease G into the cytosol. When cyt *c* binds the caspase-activating protein, apoptotic protease-activating factor 1 (Apaf1), this triggers its oligomerisation into a heptameric complex that binds pro-caspase-9, forming a multiprotein structure known as the “apoptosome” (175, 176). Apaf1 and pro-caspase-9 then bind through their caspase recruitment domains (CARDs), thereby, a cascade of caspases are activated such as caspase-9 which in turn activates downstream effector proteases such as pro-caspase-3. Consequently, proteolytic activities of activated caspases induce the multiple cellular changes associated with the apoptotic program (178, 179).

In contrast, the extrinsic death receptor apoptotic pathway relies on tumour necrosis factor (TNF) family death receptors for triggering apoptosis. These death receptors contain a cytoplasmic death domain (DD), which enables their intracellular interaction with downstream adapter proteins, linking these receptors to specific caspases (180). Upon ligand binding, TNF family receptors oligomerise and their cytoplasmic death domains cluster in the membrane, recruiting caspase-binding adaptor proteins, including the bipartite adapter Fas-associating protein with death domain (FADD) that contains both a death domain (DD) and a death effector domain (DED) (181). The DED of FADD binds DED-containing pro-caspases such as caspases-8 and -10, forming a “death-inducing signaling complex” (DISC) and resulting in caspase activation by an “induced proximity” mechanism (182, 183). The intrinsic and extrinsic pathways of apoptosis are explained in Figure 5.

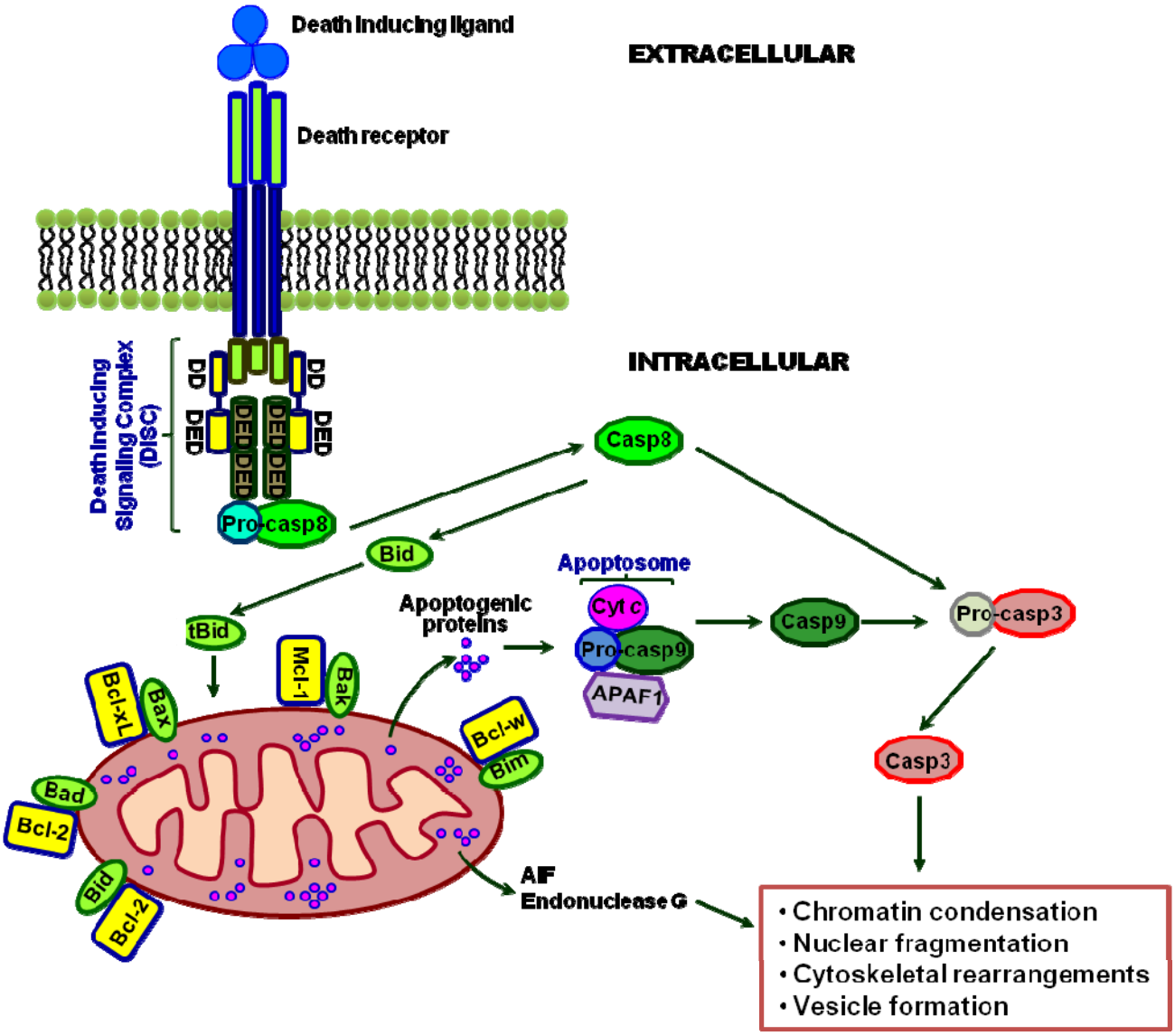

Figure 5: Mechanisms of intrinsic and extrinsic pathways of apoptosis. The intrinsic or mitochondrial pathway of apoptosis is controlled by the Bcl-2 family of pro- and anti-apoptotic proteins. When activated upon receiving a variety of apoptosis-triggering signals, pro-apoptotic proteins oligomerise to produce mitochondrial outer membrane permeabilisation (MOMP), release of apoptogenic proteins and thus activation of caspase-3 and -7. In the extrinsic or death receptor pathway, receptor ligation (TRAIL, CD95L and TNF) triggers the membrane bound death inducing signaling complex (DISC) formation, caspase-8 activation and cell death. The Figure is adapted and redrawn from reference number 176.

Stabilisation of mitochondrial integrity is a key mechanism for both the survival of malignant cells and for resistance to chemotherapy (184, 185). A well-established family of proteins that has a significant impact on mitochondrial integrity by influencing the permeability of the mitochondrial membrane is the BCL2 family. Proteins of the BCL2 family have been identified as key regulators of apoptosis (175, 176). Myeloid cell leukaemia 1 (MCL1), an anti-apoptotic member of the BCL2 family genes, is essential for development, differentiation and survival of human leukaemic lymphocytes and cell lines derived from multiple myeloma (186). *MCL1* was originally identified as an early induction gene during differentiation of myeloid leukaemia cells (186). Previous studies have confirmed that MCL1 requirement is critical for the survival of both normal and malignant B cells (187, 188). MCL1 protein exerts an anti-apoptotic function by binding and sequestering the pro-apoptotic members Bak and Bax that can form pores in the mitochondrial membrane leading to cytochrome *c* (cyt *c*) release into the cytoplasm and, thus, activating downstream caspases. Additionally, MCL1 interacts with several BH3-only pro-apoptotic proteins that act to induce oligomerisation of Bak and Bax (189, 190).

In contrast to BCL2, MCL1 is not only found in mitochondrial membranes but also in the nucleus and cytoplasm (191). Several modes of action have been suggested for the anti-apoptotic activity of MCL1. For example, MCL1 was suggested to block cyto *c* release from mitochondria by interacting with pro-apoptotic members of the BLC2 protein family, for example Bim (192), Bak (193, 194) and NOXA (195). Furthermore, MCL1 was shown to interact with truncated Bid and, thereby, inhibit intrinsic as well as extrinsic apoptotic signaling (196).

The *MCL1* gene has been reported to be overexpressed in many human malignancies, including hepatocelluar carcinoma, CLL, colorectal carcinoma, breast cancer and B cell non-Hodgkin's lymphoma (197-201). More importantly, MCL1 contributes to the resistance of cancer cells to the induction of apoptosis by chemotherapeutic agents, radiation and other agents (202). In transgenic mice, overexpression of MCL1 was shown to promote immortalisation of haematopoietic cells, while in knock-out mice loss of MCL1 resulted in peri-implantation embryonic lethality (203).

In addition to the direct role of anti-apoptotic proteins upregulation in the evasion mechanism of apoptosis in cancer, other mechanisms such as amplification of cell proliferation and survival kinases also negatively regulate apoptotic pathways (204). One of these kinases is the polo-like kinase-1 (PLK1). The polo-like kinases (PLKs) are a family of mitotic serine/threonine protein kinases that are structurally and functionally related (205). Mammalian PLK1 plays a pivotal role in the maturation of centrosomes, entry into M phase, spindle formation and cytokinesis (206, 207). Furthermore, PLK1 was found to contribute to DNA synthesis where it plays a role in pre-replication complex formation (208).

PLK1 gene expression occurs at low levels during the early phase of the cell cycle and is mediated by a repression mechanism involving a promoter element termed cell cycle-dependent element/cell cycle gene homology region (CDE/CHR). However, its levels accumulate throughout DNA synthesis (S) and gap 2 (G2) phases with a sharp increase in enzymatic activity occurring prior to the onset of mitotic (M) phase (209-213). *PLK1* gene is oncogenic and constitutive expression of the enzyme was shown to cause transformation of NIH3T3 cells (214). Additionally, PLK1 is upregulated in many human malignancies and is widely considered to be a potential therapeutic target (207).

Hypothesis:

This study is based on the knowledge that faulty regulations of gene expression and/or intracellular signaling pathways result in defective apoptosis in B lymphocytes including neoplastic transformation in patients with leukaemias and lymphomas.

CD22 is a membrane protein expressed exclusively on B lymphocytes. The working hypothesis of the study is that a scFv of mAb to CD22 can be used to target therapeutic agents to B lymphocytes in disease setting including leukaemias/lymphomas to induce cell death.

A number of the pathogenic lesions in neoplastic B lymphocytes are known to exist. Therefore, the study was intended to target key defect(s) by attaching siRNA specific for the defective target gene to a truncated protamine peptide fused to anti-CD22 scFv for specific delivery to B lymphocytes. In this way, either the survival of defective B lymphocytes or their biology could be altered. Following internalisation of the fusion protein/siRNA complex, the proton sponge phenomenon (pH buffering effect), presumably, causes the release of the cargo from endolysosomal compartment. In this respect, the cationic protamine peptide is expected to have a high pH buffering capability and thus becomes protonated and resists the acidification of endosomes. As a result, protons will be pumped from the cytosol into the endosomes with the attempt to lower the pH. This proton pumping action is followed by passive entry of chloride ions, increasing ionic concentration and, thereby, water moves into the endolysosome. Ultimately, osmotic pressure causes swelling and rupture of endosomes, releasing their contents to the cytosol. Following endosomal escape and un-packaging, siRNA is released and incorporated into the RNAi pathway forming RISC for specific silencing of the target mRNA (215-217). The proposed mechanism involved in the delivery of siRNA to B cells is illustrated in Figure 6.

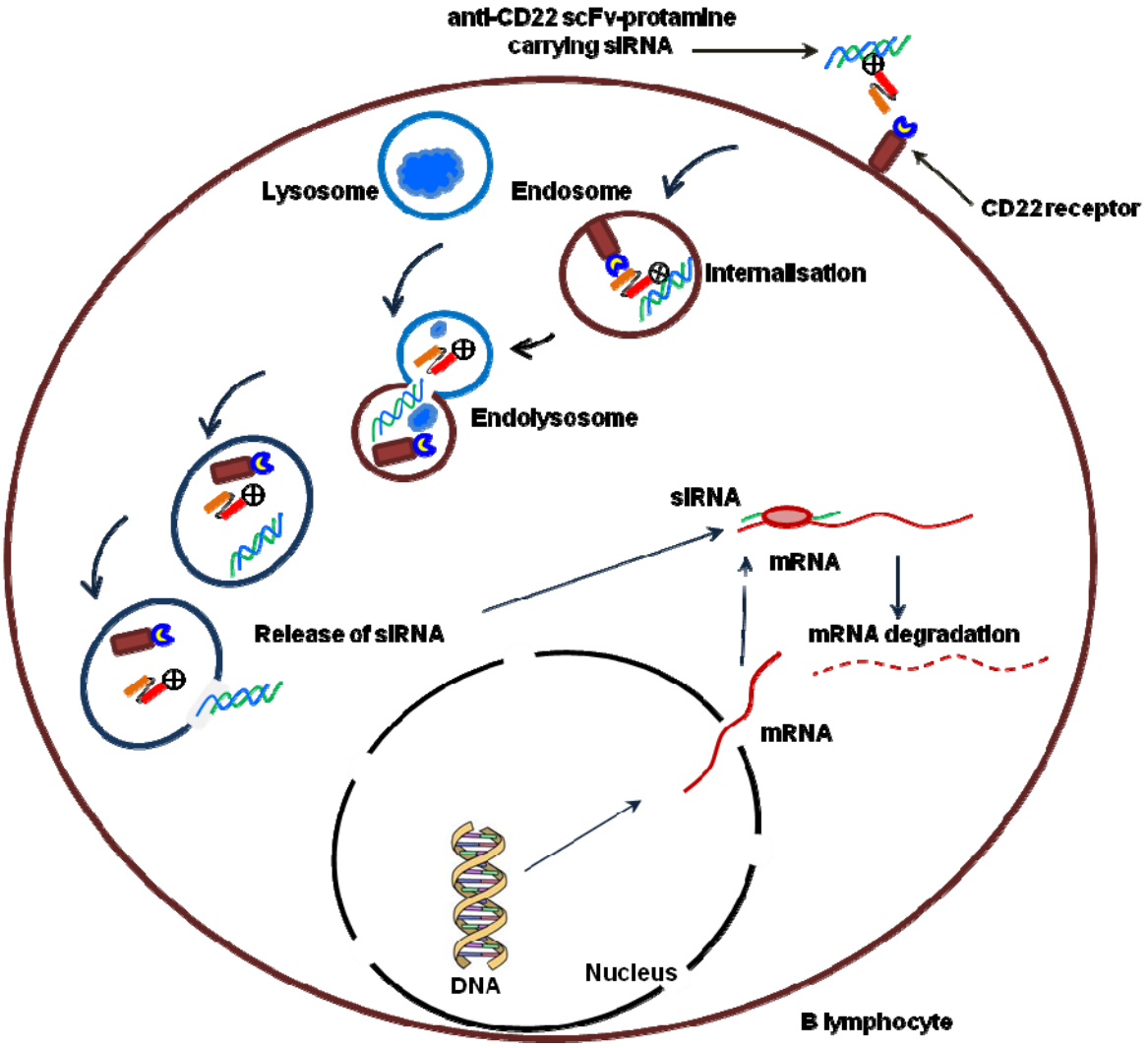

Figure 6: Mechanisms and pathways involved in the delivery of siRNA and targeting selected genes. This delivery system utilises a natural mechanism which is receptor-mediated endocytosis. Anti-CD22 scFv-protamine-His6/siRNA complex specifically binds to and internalises via CD22 receptor. Following internalisation, the endosome fuses with lysosomes forming endolysosome. siRNA is then expected to be released to cytoplasm because of the pH buffering effect of the cationic protamine peptide.

Aims of the Study:

The overall aim of the present study is to provide proof of principle for a novel approach to target and modify the pathophysiology of aberrant B lymphocytes in pathological settings including B cell leukaemias and lymphomas. The approach involves using engineered recombinant scFv of anti-CD22 mAbs and a protamine peptide to attach to and specifically deliver siRNA to target signaling pathways and transcription factors in B lymphocytes.

The study specifically aims to:

1. Identify and use monoclonal anti-CD22 antibodies that would be internalised selectively into B lymphocytes.
2. Generate recombinant anti-CD22 scFv-protamine fusion proteins that retain the ability to bind specifically to and be internalised by B lymphocytes via CD22.
3. Deliver siRNA to target specific genes with critical roles in modulating B lymphocyte functions.
4. Assess the veracity of the selectivity of delivery using truncated protamine peptide fused with recombinant proteins to their intended target cells.

Chapter Two

Materials and Methods

2.1. Cell lines:

2.1.1. Mouse leukaemia B cell line, BCL1-3B3:

The mouse leukaemia B cell line, BCL1-3B3 (kindly provided by Professor M J Glennie; University of Southampton) was cultured in RPMI 1640 (Lonza Group Ltd., Switzerland) with 10% heat-inactivated foetal bovine serum (HI-FBS), 2.0 mM L-glutamine, 100 IU/mL Penicillin and 100 IU/mL Streptomycin, 1.0 mM sodium pyruvate and 0.05 mM 2-mercaptoethanol (2-ME). The cells were maintained in a humidified incubator at 37°C with 5% CO_2.

The mouse leukaemia B cell line, CW13.20-3B3 (clone of BCL1) was purchased from the ATCC (Middlesex, UK) and cultured in RPMI 1640 (ATCC®) which contained 10 mM 4-(2-hydroxyethyl)-piperazine-1-ethanesulfonic acid (HEPES), 1.0 mM sodium pyruvate, 4.5 g/L glucose and 1.5 g/L sodium bicarbonate and supplemented with 2.0 mM L-glutamine, 10% non-heat-inactivated FBS [ATCC®] and 100 IU/mL Penicillin and 100IU/mL Streptomycin [Hybri-Max™, Sigma-Aldrich Inc, Poole, UK] and 0.05 mM 2-ME.

2.1.2. The mouse hybridoma cell line, Cy34.1.2:

The Cy34.1.2 mouse hybridoma line, which produces a mAb to mouse CD22.2, was purchased from the ATCC and grown in DMEM medium supplemented with 10% HI-FBS, 2.0 mM L-glutamine, 100 IU/mL Penicillin, 100 IU/mL Streptomycin. The cells were cultured in a humidified incubator at 37°C with 5% CO_2 in the air.

2.1.3. SF9 insect cell line:

The SF9 insect cells (Invitrogen Ltd, Paisley, UK) were grown in the serum-free SF-900 II medium (Invitrogen Ltd) supplemented with 50 IU/mL Penicillin and 50 IU/mL Streptomycin and incubated at 27°C in a humidified incubator with no CO_2.

2.1.4. HighFive insect cell line:

The HighFive insect cells (Invitrogen Ltd) were grown in the serum-free ExpressFive® medium supplemented with 50 IU/mL Penicillin and 50 IU/mL Streptomycin and 20 mM L-glutamine and incubated at 27°C in a humidified incubator.

2.1.5. HEK293T human cell line:

HEK293T human cells were grown in DMEM medium supplemented with 10% HI-FBS, 100 IU/mL Penicillin, 100 IU/mL Streptomycin and 2.0 mM L-glutamine. The cells were cultured in a humidified incubator at 37°C with 10% CO_2.

2.1.6. CHO-S cell line:

The CHO-S Hamster cells (Invitrogen Ltd) adapted to suspension culture were grown in Freestyle CHO-S expression medium supplemented with 8.0 mM L-glutamine and incubated at 37°C humidified 10% CO_2 incubator with rocking at 225 rpm.

2.1.7. HEK293F cell line:

The HEK293F FreeStyle™ 293-F human cells (Invitrogen Ltd), adapted to high density and serum-free suspension culture, were cultured in the FreeStyle™ 293 expression medium in suspension culture at 125 rpm rocking and 8% CO_2 at 37°C.

2.1.8. HF28 RA human follicular lymphoma B cell line:

Human follicular lymphoma HF28 RA (EBV-positive) B cells were kindly provided by Professor Pelkonen (University of Kuopio, Kuopio, Finland). The cells were cultured at 37°C in a humidified incubator with 5% CO_2 in the air in RPMI 1640 medium supplemented with 5% HI-FBS, 2.0 mM L-glutamine, 100 IU/mL Penicillin, 100 IU/mL Streptomycin, 10 mM HEPES buffer, 1.0 mM sodium pyruvate and 2.0 mM 2-ME.

2.1.9. L3/Bcl-2 B cell line:

L3/Bcl-2 cells, Burkitt's lymphoma B cell line L3055 (EBV-negative) which was stably transfected with anti-apoptotic *bcl*-2, were kindly provided by Professor John Gordon (University of Birmingham). The cells were cultured in RPMI 1640 medium supplemented with 10% HI-FBS, 2.0 mM L-glutamine, 100 IU/mL Penicillin and 100 IU/mL Streptomycin. The cells were cultured at 37°C in humidified incubator with 5% CO_2 in the air.

2.1.10. Jurkat T cell line:

Jurkat T cell human leukaemia line was maintained in RPMI 1640 medium supplemented with 10% HI-FBS, 10 mM HEPES, 2.0 mM L-glutamine, 100 IU/mL Penicillin and 100 IU/mL Streptomycin. The cells were maintained at 37°C with 5% CO_2 in the air.

2.1.11. U-937 histiocytic lymphoma cell line:

U-937 human histiocytic lymphoma cells were maintained in RPMI 1640 supplemented with 10% HI-FBS, 2.0 mM L-glutamine and 10.0 mM HEPES, at 37°C in a humidified incubator with 5% CO_2 in the air.

2.1.12. A375Ppuro and A375Ppuroβ6 cell lines:

αvβ6-negative A375Ppuro and αvβ6-positive A375Ppuroβ6 cell lines were generated from the human melanoma cell line A375P, which was infected with pBabe retroviruses encoding Puromycin resistance or, in addition, cDNA for human β6 (218). The cells were grown in DMEM supplemented with 10% HI-FBS and 2.0 mM L-glutamine and maintained in 10% CO_2 and at 37°C.

2.1.13. DX3Ppuro and DX3Ppuroβ6 cell lines:

αvβ6-negative DX3Ppuro and αvβ6-positive DX3Ppuroβ6 cell lines (113) were cultured in DMEM supplemented with 10% HI-FBS and 4.0 mM L-glutamine. The cells were maintained in 10% CO_2 and at 37°C.

A375Ppuro, A375Ppuroβ6, DX3Ppuro, DX3Ppuroβ6 and VB6 cell lines were kindly provided by Dr. John F Marshall (Barts Cancer Institute, Queen Mary University of London).

2.1.14. The VB6 human cell line:

VB6 is a keratinocyte oral squamous cell carcinoma-derived cell line transfected to express integrin αvβ6. The cell line was established by retroviral transfection of the αvβ5 expressing human V3 cell line (engineered from the αv-negative H357 OSCC line transfected with αv cDNA) with β6 cDNA for constitutive high expression of the αvβ6 heterodimer (218). The cells were maintained in complete keratinocyte growth medium (KGM) which is composed of Minimum Essential Medium-α base medium (MEM-α) supplemented with 10% HI-FBS, 10 ng/mL epidermal growth factor (EGF), 0.4 µg/mL hydrocortisone, 5.0 µg/mL insulin, 18 mM adenine, 3.0 mM L-glutamine and 1.0 x 10^{-10} M cholera toxin (Sigma-Aldrich Inc). The cells grow as adherent monolayers and were kept in an incubator with 10% CO_2 at 37°C.

2.2. Production and purification of anti-CD22.2 mAb:

The mouse Cy34.1.2 hybridoma cell line was cultured in complete DMEM medium and supernatant collected for purification of the mAb. The mouse anti-mouse CD22.2 mAb produced by Cy34.1.2 was then purified by affinity chromatography using PROSEP-G column (a protein G column; Millipore, Billerica, USA). The column was initially prepared by passing 5x column volumes of freshly prepared 6 M guanidine HCl and then regenerated with 10x column volumes of HCl pH 1.5 (0.0316M) followed by 5x column volumes of phosphate-buffered saline (PBS) pH 7.4. The supernatant was filtered through a 0.2 µm filter to remove cell debris before loading onto the column followed by washing with 5x column volumes of 2x PBS containing 0.02% NaN_3. mAb bound to PROSEP-G beads was then eluted with 3 M potassium thiocyanate (KSCN) in PBS followed by 2x column volumes of PBS. Optical density values of the collected elution fractions were determined using a Nanodrop spectrophotometer (Thermo Fisher Scientific Inc., Warrington, UK) and aliquots with purified mAbs dialysed extensively against PBS using a 2-18/32" dialysis membrane (Medicell International Ltd, London, UK) for 48 hours at 4^{o}C. Purity of the isolated mAb was determined by electrophoresis using a pre-cast NuPAGE Novex Bis Tris Mini Gel (Invitrogen Ltd) under non-reducing and reducing conditions.

2.3. Conjugation of purified anti-mouse CD22.2 mAb with AlexaFluor®488:

The purified anti-mouse CD22.2 mAb was conjugated with AlexaFluor®488 fluorochrome dye using AlexaFluor®488 Monoclonal Antibody Labeling kit (Invitrogen Ltd). The conjugated mAb was tested against BCL1-3B3 cells to assess reactivity of the antibody with CD22.2 molecules on mouse B cells. The degree of labeling was determined according the manufacturer's instructions:

A small amount of the purified conjugated antibody was diluted (1:2) in PBS and absorbance measured at both 280 nm (A_{280}) and 494 nm (A_{494}). The concentration of protein in the sample was calculated using the following equation:

Protein concentration (M) = [A_{280} – (A_{494} x 0.11)] x dilution factor / 203,000

Where 203,000 is the molar extinction coefficient in $cm^{-1}M^{-1}$ of IgG at 280 nm and 0.11 is a correction factor for the fluorophore's contribution to the absorbance at 280 nm.

Concentration of the protein at 280 nm (A_{280}) = 4.82 mg/mL

Dilution: 2x

Absorbance at 280 nm (A_{280}) = 0.031

Absorbance at 494 nm (A_{494}) = 0.001

Protein concentration (M) = 1.52×10^{-7}

Calculating the degree of labeling:

Moles dye per mole protein = A_{494} x dilution factor / 71,000 x protein concentration (M)

Where 71,000 $cm^{-1}M^{-1}$ is the approximate molar extinction coefficient of the AlexaFluor®488 dye at 494 nm. For IgGs, the labeling with 4–9 moles of AlexaFluor®488 dye per mole of antibody is optimal. Based on these calculations, the degree of labeling of the mAb was 0.9266 moles dye per mole protein.

2.4. Detection of CD22.2 on B lymphocytes by flow cytometry:

BCL1-3B3 cells were stained for fluorescence activated cell sorting (FACS) analysis using the purified AlexaFluor®488 labeled anti-CD22.2 and PE labeled anti-mouse CD19 (BD Biosciences, Oxford, UK). The cells were washed in ice-cold staining buffer (PBS containing 0.1% NaN_3 and 2% FBS) and pellets resuspended in ice-cold staining buffer and their number adjusted to 0.5-1 x 10^7 cells/mL. The stained cells were incubated for 20 minutes on ice, washed 3 times and resuspended in ice-cold staining buffer. The stained cells were analysed using a FACS Calibur flow cytometer (BD Biosciences) by gating on live cells with the forward and side scatter properties of lymphocytes. Mouse $IgG_1\kappa$ isotype control conjugated with FITC (BD Biosciences) was used as a control for background staining.

2.5. Analysis of CD22.2 mAb internalisation on B cells by Confocal Laser Scanning Microscopy (CLSM):

BCL1-3B3 cells (10^5 cells) were stained with AlexaFluor®488 anti-CD22.2 in RPMI medium on ice for 30 minutes. The cells were then incubated for various time points (0, 30 and 60 minutes) at 37°C and then the reactions stopped by adding cold medium followed by centrifugation at 4°C and washing of the cells. Simultaneously, cells were also stained in separate tubes with AlexaFluor®488 isotype control. All stained cells were washed once with ice-cold staining buffer (5% FBS in PBS) and then incubated with proteinase K (VWR International Ltd, Soulbury, UK) (50 μL of ice-cold PBS containing 2 mg/mL proteinase K final concentration) on ice for 30 minutes (219). The cells were then washed 2x with PBS and fixed in 2% PFA in PBS for 20 minutes on ice. The cells were then stained with 4′,6-Diamidino-2-phenylindole dihydrochloride (DAPI, 1:5000) for 5 minutes at 4°C and washed 2x with PBS, resuspended in 50 μL PBS, mounted on poly-L-lysine coated slides using Dako fluorescent mounting medium (Dako UK Ltd, Cambridge, UK) and examined by an LSM 510 confocal microscope.

2.6. Polymerase chain reaction (PCR) amplification:

For PCR amplification using *Thermus aquaticus* (*Taq*) DNA polymerase (Promega, Southampton, UK), a PCR mastermix (94 μL) was prepared by combining 5x GoTaq® Flexi Buffer 20 μL, $MgCl_2$ (25 mM) 6 μL, dNTPs (Invitrogen Ltd) (10 mM) 2 μL, forward primer (Sigma-Aldrich Inc) (10 mM) 5 μL, reverse primer (Sigma-Aldrich Inc) (10 mM) 5 μL, dH_2O 55 μL and 2 units (1 μL) of GoTaq® Flexi DNA Polymerase. From the cDNA of either the V_H, or Vκ genes about 20 ng were then added to the mastermix. For other PCR reactions, about 20 ng template DNA was added to the mastermix accordingly.

For PCR amplification using *Pfu* polymerase (Promega), a PCR mastermix was prepared by mixing *Pfu* DNA polymerase 10x reaction Buffer (200 mM Tris-HCl, 100 mM KCl, 100 mM $(NH4)_2SO_4$, 20 mM $MgSO_4$, 1.0% Triton® X-100, 1 mg/mL nuclease-free BSA, pH 8.8) 5 μL, dNTP mix, 10 mM each: 1 μL, upstream primer (10 μM): 1 μL, downstream primer (10 μM): 1 μL, 2 units/μL of *Pyrococcus furiosus* (*Pfu*) DNA polymerase: 0.5 μL and dH_2O to final volume of 50 μL. Approximately 20 ng of plasmid DNA template was added to the mastermix.

All the primer sequences are detailed in the Appendix. GoTaq® and *Pfu* polymerase PCR kits were all from Promega.

From the PCR reaction, 5 μL was mixed with 4 μL of dH_2O and 1 μL of 10x bromophenol blue loading dye (3.9 mL glycerol in TAE buffer, 0.025 g bromophenol blue, 0.025 g xylene cyanol and dH_2O to 10 mL total volume) and was separated on 1% agarose gel with 0.5x TAE buffer (0.02 M Tris-acetate, 0.5 mM EDTA, pH 8.0) at 120 V for 40 minutes. 1k Plus DNA ladder (Invitrogen Ltd) was run alongside samples. Ethidium bromide (Sigma-Aldrich Inc) or SyberSafe stain (Invitrogen Ltd) at 1 μg final concentration was incorporated in 1% agarose gel to visualise DNA under UV light and image was captured using a gel documentation system (Uvitec Ltd, Cambridge, UK).

2.7. RNA extraction, cDNA synthesis, poly-G-tailing and amplification of immunoglobulin V_H and V_L genes:

Total RNA was extracted using the RNAqueous®-4PCR Kit (Applied Biosystems, Warrington, UK). Cy34.1.2 hybridoma cells (1 x 10^6 cells) were pelleted by centrifugation at 1200 rpm for 5 minutes at 4°C and then lysed with 500 μL of Lysis/Binding solution. The cell lysate was clarified by centrifugation and an equal volume of 64% ethanol was added. The lysate/ethanol mixture was applied to the filter cartridge and centrifuged at 10,000 rpm for 1 minute at room temperature. The flow-through was discarded and the cartridge washed with 700 μL of Wash Solution #1 (containing guanidinium thiocyanate) and centrifuged at 10,000 rpm for 1 minute at room temperature. The cartridge was then washed twice with 500 μL Wash Solution #2/3 and put in a fresh collection tube and RNA eluted with 50 μL pre-heated (70°C) Elution Solution and centrifuged at 14,000 rpm for 30 seconds at room temperature. To each 9 μL RNA solution, 1 μL of 10x DNase I buffer (100 mM Tris, 25 mM $MgCl_2$ and 1 mM $CaCl_2$) and 1 μL of DNase I (RNase-free) were added and incubated at 37°C for 30 minutes. To precipitate the DNase I, 1 μL of the slurry DNase inactivation reagent was added to the RNA solution, incubated at room temperature for 2 minutes and centrifuged at 10,000 *g* for 1 minute. Purity of the RNA was assessed by measuring the A_{260}/A_{280} ratio using a Nanodrop spectrophotometer. Agarose gel electrophoresis was carried out to verify integrity of the RNA and to observe the 28S and 16S rRNA bands. Then, cDNA for both V_H and V_L were synthesised using High Capacity cDNA Reverse Transcription Kit (Applied Biosystems) [10x Reverse Transcriptase buffer 2 μL, 25x dNTP Mix (100 mM) 0.8 μL, Cγ1 or Cκ1 primer (10 mM) 2 μL, Reverse Transcriptase (50 U/μL) 1 μL, RNase inhibitor 1 μL, nuclease-free H_2O 3.2 μL and total RNA (1.0 μg/μL) 10 μL (20 μL total reaction volume)]. The Cγ1 and Cκ1 primers within the 5' end of the constant regions of mouse γ1 and κ chains were designed based on the IMGT® database, the international ImMunoGeneTics information system® (http://www.imgt.org/). The primer designed for mouse γ1 for the cDNA was called Cγ1: 5'AGTTAGTTTGGGCAGCAGAT3', and that for the κ chain was Cκ1: 5'GTAGAAGTTGTTCAAGAAGCACAC3'. The cDNA synthesis reaction [step 1: 25°C for 10 minutes, step 2: 37°C for 120 minutes and step 3: 85°C for 5 minutes] was performed in a thermal cycler (MJ Research PTC-200 Peltier Thermal Cycler, Global Medical Instrumentation Inc, California, USA) for 1 hour at 37°C using total RNA. The

inactivation reaction was carried out at 70°C for 10 minutes. cDNA was purified using the PureLink PCR Purification Kit (Invitrogen Ltd). cDNA was poly guanine-tailed at the 5' end using the enzyme terminal deoxynucleotidyl transferase (TdT, Promega) [terminal transferase 5x buffer 8 μL, cDNA (1 ng/μL) 25 μL, dGTP (20 mM) 2 μL, TdT (30 units) 1 μL and H_2O 4 μL]. The poly-G tailing reaction was carried out at 37°C for 60 minutes and the reaction stopped by heating at 70°C for 10 minutes. Tailed cDNA was purified using PureLink PCR Purification Kit (Invitrogen Ltd) and amplified by anchored PCR. The anchored PCR was carried out using a poly-(C) primer with a restriction site complementary to the poly-(G) tail (anchor primer: 5'ACGAATTCTAGAGTCGACCCCCCCCCCCCCC3') together with a primer complementary to mouse γ1 constant region upstream of the Cγ1 site used for the cDNA synthesis (nested primer Cγ2, 5'GCCAGTGGATAGACAGAT3'). The nested primer for the κ light chain was upstream of the cDNA primer Cκ1 site (Cκ2, 5'AGATGTTAACTGCTCACTGGAT3'). All primers were desalted and purchased from Sigma-Aldrich Inc. The poly-(C) primer was allowed to extend for 15 minutes at 70°C before adding the nested primers Cγ2 or Cκ2. The PCRs were performed using GoTaq® polymerase. From the poly-G-tailed cDNA of either the V_H or Vκ, 2 μL was then added to the mastermix. The PCRs were carried out using the following conditions: denaturation at 95°C for 30 seconds, annealing at 62.9°C for 30 seconds, extension at 72°C for 1 minute and heated lid at 110°C (G-Storm thermal cycler, Gene Technologies Ltd, Somerton, UK). The PCR products were analysed on 1% agarose gels and purified by gel extraction using the PureLink Quick Gel Extraction Kit (Invitrogen Ltd) and the recovered poly-G-tailed cDNA used for TA cloning.

2.8. Plasmid DNA mini-preparation:

Mini-preparations of plasmid DNA were carried out using a PureLink Quick Plasmid Miniprep Kit (Invitrogen Ltd) according to the manufacturer's instructions. Transformed colonies of DH5α *Escherichia coli* (*E. coli*) bacteria were picked and cultured in 5 mL Luria-Bertani (LB) broth with 5 μL Carbenicillin (100 mg/mL) overnight at 37°C. Next day, 1.5 mL of bacterial cultures were centrifuged at 12,000 *g* for 4 minutes at room temperature and cell pellets resuspended in resuspension buffer with RNase A and lysed with lysis buffer for 5 minutes. The lysates were centrifuged at 12,000 *g* for 10

minutes at room temperature to remove debris and proteins precipitated from the lysates using precipitation buffer. The supernatant was loaded onto spin columns, centrifuged at 12000 *g* for 1 minute at room temperature and columns washed with wash buffer containing ethanol. The columns were centrifuged at 12,000 *g* for 1 minute at room temperature and plasmid DNA eluted with 75 µL pre-heated (70°C) Tris-EDTA (TE) pH 8.0 buffer. The extracted plasmid DNA was analysed by restriction digestion and sequencing.

2.9. Plasmid DNA maxi-preparation:

Maxi-preparations were carried out using PureLink™ HiPure Plasmid DNA Purification Kits (Invitrogen Ltd) according to the manufacturer's instructions. To expand the plasmid DNA from transformants, 250 mL bacterial culture from the transformed DH5α *E. coli* in LB broth medium with Carbenicillin (100 mg/mL) overnight at 37°C was used. Next day, the bacterial culture was centrifuged at 5,000 *g* for 10 minutes at 4°C and the cell pellet resuspended in resuspension buffer (R3) containing RNase A until homogeneous and lysed with lysis buffer (L7) for 5 minutes at room temperature with gentle mixing. The lysates were precipitated with the precipitation buffer (N3) and mixed immediately until the mixture was homogeneous then centrifuged at 5,000 *g* for 30 minutes at 4°C to clarify the lysates from debris and proteins precipitated from the lysates using precipitation buffer. The supernatant was carefully removed and loaded onto the equilibrated column (HiPure Maxi Column was pre-equilibrated with 30 mL Equilibration Buffer (EQ1)) and the solution allowed to drain by gravity flow. The column was then washed once with 60 mL Wash Buffer (W8) allowing the solution to drain by gravity flow. Next, the plasmid DNA was eluted from the column by adding 15 mL Elution Buffer (E4) and the flow-through collected in a sterile tube. The plasmid DNA was precipitated by adding 10.5 mL isopropanol to the eluate, mixed well and centrifuged at 5,000 *g* for 30 minutes at 4°C. The supernatant was discarded and the DNA pellet washed with 70% ethanol and centrifuged at 5,000 *g* for 30 minutes at 4°C. The supernatant was removed and DNA pellet air-dried and resuspended in 500 µL TE buffer pH 8.0.

2.10. Preparation of competent *Escherichia coli*:

Bacterial glycerol stocks (stored at -80°C) were regrown at 37°C overnight by initiation of 5 mL starter cultures without antibiotics. Next day, a large scale (500 mL) bacterial culture was grown at 37°C (with shaking at 250 rpm), until the OD_{600} reached 0.4-0.6 then centrifuged at 4°C for 10 minutes at 5000 rpm. The supernatant was discarded and bacterial pellet resuspended in ice-cold 0.1 M $MgCl_2$ and centrifuged at 4°C for 10 minutes at 2000 rpm. The supernatant was discarded and bacteria resuspended in ice-cold 0.1 M $CaCl_2$. The bacteria were centrifuged at 2000 rpm for 20 minutes at 4°C. The supernatant was discarded and cells resuspended in ice cold 0.1 M $CaCl_2$ containing 14% glycerol, 100 μL aliquots of competent bacteria were prepared in 1.5 mL pre-chilled Eppendorf tubes on dry ice and were stored at -80°C.

For preparation of competent DH5α *E. coli* and DH10Bac™ *E. coli*, cells were grown in LB broth without Carbenicillin and for HB2151 *E. coli,* cells were grown in 2xTY (16 g tryptone, 10 g yeast extract and 5 g NaCl in 1 litre dH_2O) without Carbenicillin.

2.11. Gel extraction for the purification of DNA:

DNA was extracted using a PureLink® Quick Gel Extraction Kit (Invitrogen Ltd) according to the manufacturer's instructions: the agarose gel containing the desired DNA fragment was excised, weighed and placed into a clean microcentrifuge tube and solubilised with 3 volumes Gel Solubilisation Buffer (L3) on a 50°C hot block for 15 minutes with mixing. After the gel slice was dissolved, the mixture was loaded onto a Quick Gel Extraction Column inside a wash tube and centrifuged at 12,000 *g* for 1 minute. Then, 700 µL of Wash Buffer (W1) containing ethanol was added to the column and centrifuged at 12,000 *g* for 1 minute, the flow-through was discarded and the column centrifuged again at maximum speed for 3 minutes to remove residual Wash Buffer and ethanol. The DNA was eluted with 50 µL Elution Buffer (E5) by incubation for 1 minute at room temperature and centrifugation at 12,000 *g* for 1 minute.

2.12. Ligation reactions and bacterial transformation:

PCR products as well as plasmid vectors were digested with appropriate enzymes. Digested fragments were separated on 1% agarose gels according to fragment size with 0.5x TAE. DNA fragments of interest were excised from the gel and purified using the PureLink® Quick Gel Extraction Kit. For the ligation reaction, insert DNA (PCR product or digested DNA fragment) was combined with the vector DNA backbone and ligated at 4°C overnight with T4 DNA ligase (NEB Inc., Ipswich, UK) in a final volume of 20 µL.

The ligation reaction [plasmid DNA, PCR product, 2.0 µL of 10x ligase buffer, 1.0 µL of T4 DNA ligase (400,000 U/mL) and dH_2O to a final volume of 20 µL] was incubated at 4°C overnight. For bacterial transformation, 100 µL of DH5α *E. coli* was thawed on ice and mixed with the ligation reaction and incubated on ice for 30 minutes. The bacteria were then heat-shocked at 42°C on a pre-warmed hot block for 90 seconds and returned immediately onto ice for 2 minutes. Fresh LB medium without antibiotics was added to the transformed bacteria and incubated at 37°C in a shaker incubator (225 rpm) for 2 hours. LB agar plates [10 g Bacto-tryptone, 5 g yeast extract, 10 g NaCl, 15 g agar, 1 L dH_2O. pH 7.5] with Carbenicillin (100 mg/mL) were inoculated with 400 µL of the bacterial cultures and incubated overnight at 37°C. Next day, the plates were checked for bacterial colonies and single colonies selected and expanded for DNA mini-preparations.

2.13. TA cloning and bacterial transformation:

Taq DNA polymerase, which was used to amplify the poly-G tailed cDNA, preferentially adds an adenine to the 3' end of PCR products. The PCR products were cloned into linearised pCR®2.1 vector (Invitrogen Ltd) that has a complementary 3' thymine overhang. The ligation reaction between pCR®2.1 linear plasmid DNA and the Cγ2 or Cκ2 PCR product was performed overnight at 4°C using T4 DNA ligase. Next day, to use blue/white colour screening for recombinants and maintain antibiotic selection, ligated plasmid DNA was transfected into chemically-competent DH5α *E. coli* cells and LB agar plates with Carbenicillin (100 mg/mL) and 40 mg/mL bromo-chloro-indolyl-galactopyranoside (X-Gal) were inoculated with the bacteria and incubated overnight at 37°C. The next day, plates were checked for colonies and white colonies selected and

expanded for mini-DNA preparations. The principle of TA cloning depends on disruption of *lacZ* gene which is illustrated in Figure 7. pCR®2.1 vector uses the *lac* operon which encodes the *β-galactosidase* gene *lacZ*. This enzyme catalyses the breakdown of lactose; it can also degrade X-Gal, which turns blue when it is broken down by β-galactosidase. Colonies that produce β-galactosidase (i.e. the *lacZ* gene is intact or the PCR product is not inserted) turn blue while colonies that do not produce β-galactosidase (i.e. the PCR product inserted into the *lacZ* gene) remain white. Successful ligation of a foreign DNA into *lacZ* abolishes production of functional β-galactosidase (220). V_H- and Vκ-containing plasmid DNAs were digested using *Eco*RI restriction enzyme (NEB Inc.) and the plasmid DNAs sequenced using M13 forward and reverse primers. Part of the TA cloning vector pCR®2.1 sequences showing the *lacZ* gene, unique restriction sites and M13 priming sites are shown in Figure 8.

All the sequencing reactions (Sanger sequencing) were performed at the Genome Centre, Queen Mary University of London.

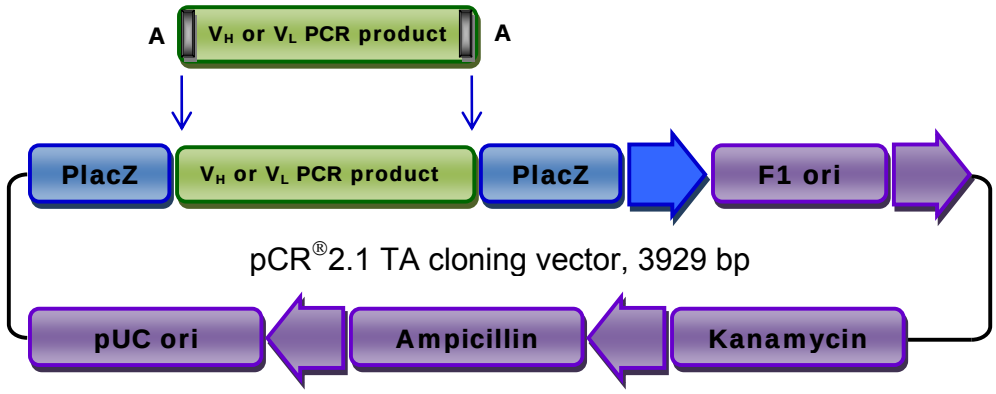

Figure 7: Schematic map of the TA cloning vector pCR®2.1 illustrating the insertion site of a PCR product within the *lacZ* gene. Linearised pCR™2.1 has a 3'-T overhang for direct ligation of *Taq*-amplified PCR products, a versatile polylinker with flanking *Eco*RI sites for easy excision of inserts and M13 forward and reverse primer sites for sequencing. The figure depicts disruption of the *lacZ* gene with insertion of V_H or V_L PCR product in the positive clones. *lacZ*α gene: bases 1-545, M13 reverse priming site: bases 205-221, T7 promoter: bases 362-381, M13 (-20) forward priming site: bases 389-404, f1 origin: bases 546-983, Kanamycin resistance ORF: bases 1317-2111, Apm resistance ORF: bases 2129-2989 and pUC origin: bases 3134-3807.

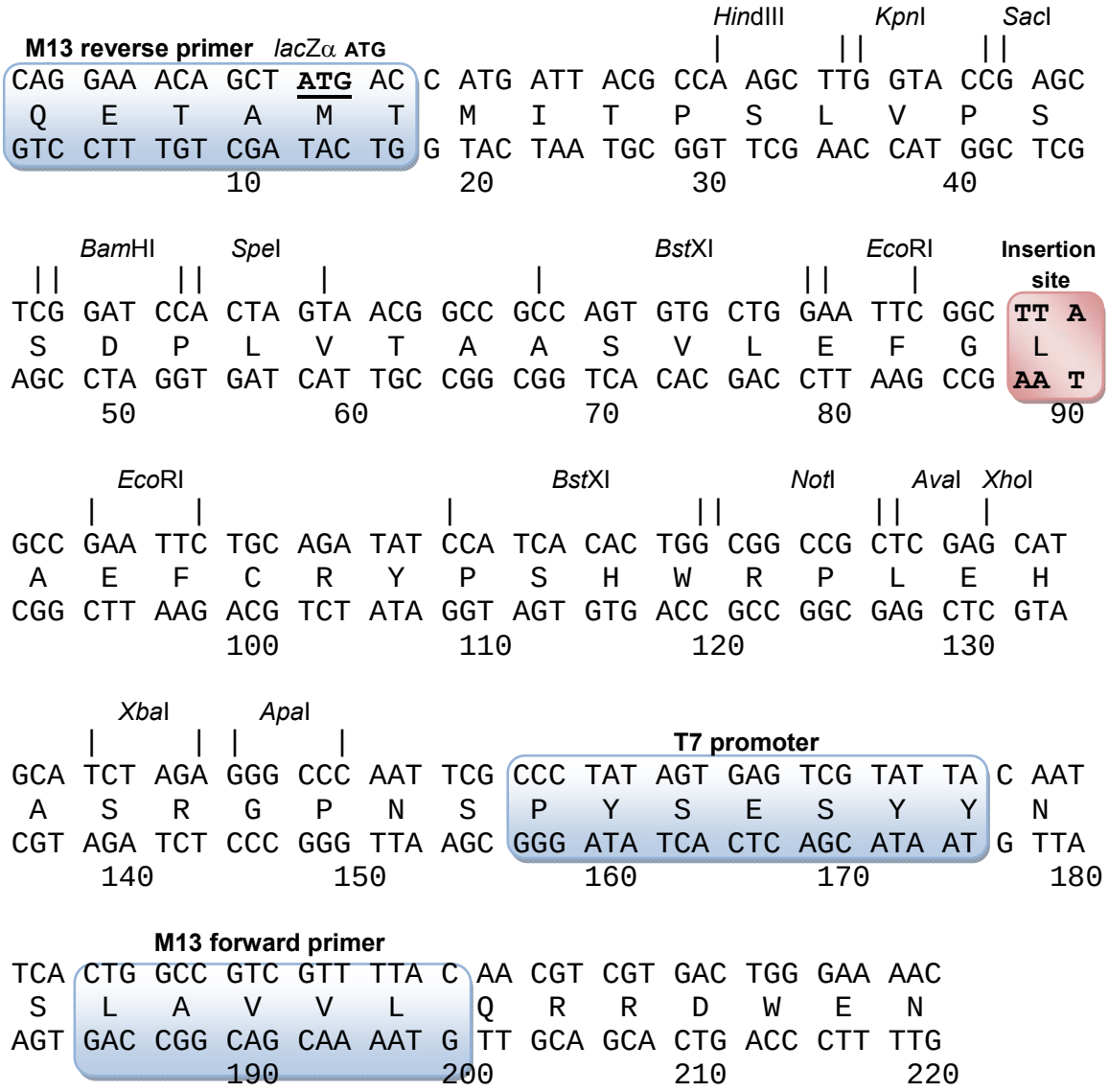

Figure 8: Sequence of pCR®2.1 containing a portion of the *lacZ* gene sequence and unique restriction sites. The insertion site of PCR products is within the *lacZ* gene and M13 forward and reverse priming sites are also indicated.

2.14. Analysis of nucleotide sequences of the V_H and V_L of the Cy34.1.2 mAb:

Nucleotide sequences of the V_H and V_L genes of Cy34.1.2 mAb were analysed by carrying out a Basic Local Alignment Search Tool (BLAST) search in the National Center for Biotechnology Information (http://www.ncbi.nlm.nih.gov/). The leader sequences of the signal peptide at the N-terminal end of the V_H and V_L were determined by analysis of the variable regions of both V_H and V_L genes using a bioinformatics protein hydrophobicity plot (http://www.vivo.colostate.edu/molkit/hydropathy/). The output interface of the bioinformatics tool generated a hydrophobicity plot of the signal peptide. According to the Kyte-Doolittle scale, which constitutes the basis of the analysis for detecting hydrophobic regions in proteins, each amino acid has a specific value and those with a hydrophobic nature have positive values (221).

2.15. Generation of anti-CD22.2 scFv cDNAs:

In order to generate anti-CD22.2 single chain fragment of variable regions (scFv), cDNA was produced from the mRNA of the V_H and V_L of the Cy34.1.2 mAb. The cDNAs were then poly-G tailed at the 5'UTR regions and amplified by PCR. The PCR products were cloned into the pCR®2.1 TA vector (Invitrogen Ltd) and sequenced with M13 forward primer. After obtaining the information about the V_H and V_L genes, specific primers were designed to amplify the cDNA for the V_H and V_L genes incorporating restriction sites to enable cloning of the DNA fragments in-frame into restriction sites within the multiple cloning site (MCS) of the plasmid DNA for expression of recombinant proteins. To obtain the scFv, a sequence encoding the $(Gly_4Ser)_3$ linker was incorporated between the V_H and V_L cDNAs. Two different clones were constructed. The scFv cDNA was fused at its C-terminal end with a hexahistidine purification tag to generate scFv-His6 and the second construct was fused at its C-terminal end with the truncated protamine peptide and a hexahistidine tag to generate scFv-protamine-His6. Both constructs were cloned into the transfer vector pFastBac^{TM}1, a plasmid donor vector constructed so that it can propagate in two different host species.

2.16. Construction and cloning of anti-CD22.2 scFv-His6 and scFv-protamine-His6 into expression vectors using the baculovirus shuttle vector:

For this approach, the Bac-to-Bac® Baculovirus Expression System (Invitrogen Ltd) was used. This expression system is based on site-specific transposition of an expression cassette from a recombinant donor plasmid DNA vector (pFastBac^{TM}1) (Figure 9). This allowed for the generation of an expression construct containing the genes of interest, into a baculovirus shuttle vector (bacmid) propagated in *E. coli*.

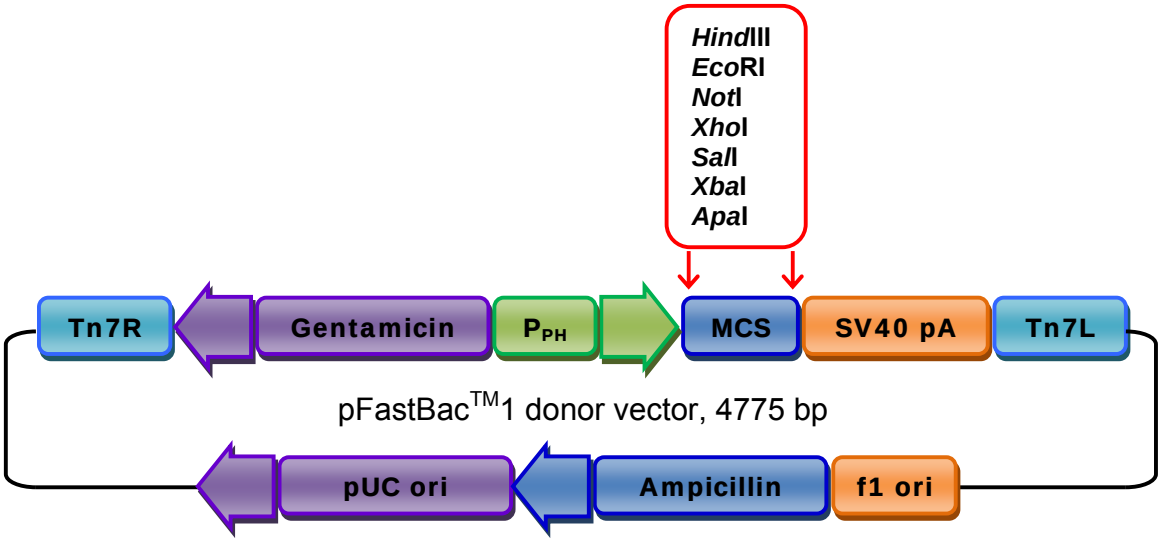

Figure 9: A schematic diagram of the transfer donor vector pFastBac^{TM}1. The figure depicts a donor vector with left and right Tn7 transposable elements which is the basis of site-specific transposition of the expression cassette into the recipient vector during recombination. This vector was previously used to clone mIFNβ-MMP-1-11E scFv in our department with restriction sites *Hind*III, *Eco*RI, *Not*I, *Xho*I, *Sal*I, *Xba*I and *Apa*I in the MCS. The anti-CD22.2 scFv-His6 and scFv-protamine-His6 expression cassettes were cloned into the MCS between *Hind*III and *Apa*I restriction sites. f1 origin: bases 2-457, Ampicillin resistance gene: bases 589-1449, pUC origin: bases 1594-2267, Tn7R: bases 2511-2735, Gentamicin resistance gene: bases 2802-3335 (complementary strand), Polyhedrin promoter (P_{PH}): bases 3904-4032, Multiple cloning site (MCS): bases 4037-4142, SV40 polyadenylation signal: bases 4160-4400 and Tn7L: bases 4429-4594.

2.17. DNA preparation and plasmid manipulation:

The plasmid vector pFastBac^{TM}1 mIFNβ-MMP-1-11E was digested with *Sal*I and *Xba*I restriction enzymes to remove the V_L sequence and was purified by gel extraction to prepare the vector for subcloning of the new V_L DNA sequence. Concomitantly, both V_H and V_L genes of the mAb Cy34.1.2 were amplified by PCR from TA cloned plasmid DNA miniprep using specific primers designed to incorporate the restriction sites in a PCR extension. The V_H primers were: V_H forward primer with *Hind*III restriction site (underlined) and start codon (bold): 5'CAGAAGCTT**ATG**AGATGGAGCTGTATC3'; V_H reverse primer with *Xho*I restriction site (underlined): 5'CGCTCGAGACAAAGTAGAATGAGTAAGT3'. The V_L primers were: a common V_L forward primer with *Sal*I restriction site (underlined): 5'GGCGGGTCGACGGATATTGTGATGACGCAG3' and two different reverse primers: V_L1 reverse primer (V_L1) with an *EcoR*I restriction site (underlined) for construction of anti-CD22.2 scFv-protamine-His6 expression cassette : 5'TCGGAATTCCGGAAGTTCTAGATTTT3' and the second primer V_L2 reverse primer (V_L2) with an *Nhe*I restriction site (underlined) for construction of anti-CD22.2 scFv-His6 expression cassette: 5'TCGGCTAGCCGGAAGTTCTAGATTTT3' (Figure 10). The PCR mastermixes were prepared according to GoTaq® PCR kit. From the cDNA of either the V_H or Vκ genes 6 μL were then added to the mastermix. The PCRs were performed using GoTaq® polymerase in a G-Storm thermal cycler (Gene Technologies Ltd, Somerton, UK) with the conditions described in Table 1.

Table 1: PCR conditions using GoTaq® polymerase to amplify Cy34.1.2 V_H and V_L genes from pCR®2.1 TA cloning vector.

Step	Time	Temperature	Cycles
Start cycle			30x
Denaturation	30 seconds	95°C	30x
Annealing	30 seconds	55°C	
Extension	1 minute	72°C	
Heated lid		110°C	

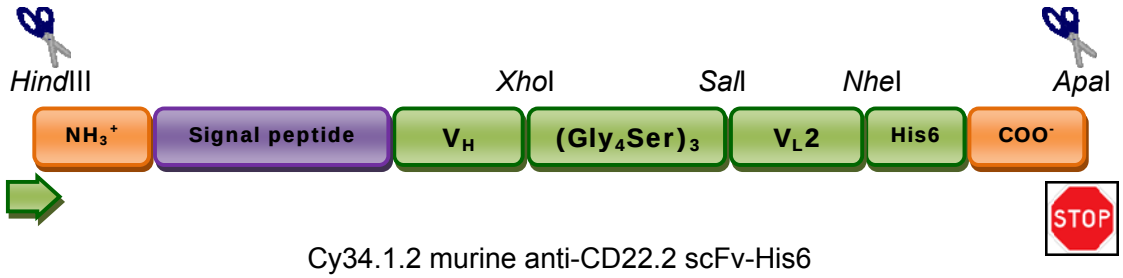

Cy34.1.2 murine anti-CD22.2 scFv-His6

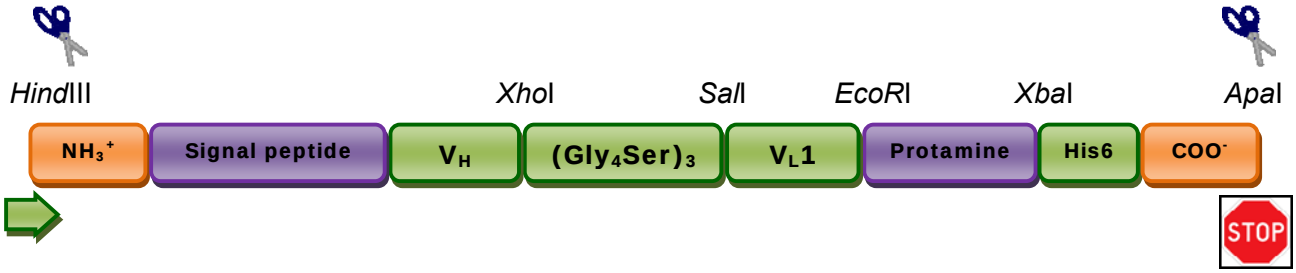

Cy34.1.2 murine anti-CD22.2 scFv-protamine-His6

Figure 10: An illustration of the strategy for the construction of in-frame anti-CD22.2 scFv-His6 and scFv-protamine-His6 expression cassettes. The native signal peptide sequence located at the N-terminus is in-frame with the V_H which is connected with a short glycine-serine linker peptide to the V_L for flexibility and a hexahistidine at the C-terminus followed by a stop codon in scFv-His6 (top). The 75 nucleotide sequence comprising the human truncated protamine domain is cloned in-frame between the V_L and the His-tag sequence in scFv-protamine-His6 construct (bottom).

Amplified V_H and V_L PCR products were purified using the PureLink PCR Purification Kit (Invitrogen Ltd). The V_H DNA was then digested with *Hind*III and *Xho*I restriction enzymes; the V_L1 DNA was digested with *Sal*I and *Eco*RI enzymes and V_L2 DNA was digested with *Sal*I and *Nhe*I enzymes. Later, the digested DNA of V_H, V_L1 and V_L2 were purified from agarose gel using the PureLink Quick Gel Extraction Kit (Invitrogen Ltd) and recovered DNAs used for cloning.

cDNA for the truncated human protamine used to generate anti-CD22.2 scFv-protamine-His6 was composed of nucleotides encoding 21 amino acids: RSQSRSRYYRQRQRSRRRRRR (120). The truncated protamine cDNA was generated by annealing of two overhang HPLC-purified primers (Sigma-Aldrich Inc). An *Eco*RI restriction site was incorporated in the forward protamine oligo sequence and an *Xba*I restriction site was incorporated into the reverse protamine oligo primer. The forward protamine primer sequence: 5'AATTCCGATCACAATCACGATCACGATACTACCGACAACGACAACGATCACGACG

ACGACGACGACGAT3' and the reverse protamine primer sequence: 3'GGCTAGTGTTAGTGCTAGTGCTATGATGGCTGTTGCTGTTGCTAGTGCTGCTGCT GCTGCTGCTAGATC5' were annealed by mixing 10x dilution of each primer stock (100 mM), T4 DNA ligase buffer (10x) and sterile dH_2O. The mixture was boiled for 5 minutes in a waterbath and left to cool. Next, a ligation reaction was set up by overnight incubation at 4°C for cloning of the V_L1 and truncated protamine cDNA into the pFastBac^{TM}1 vector backbone and then the V_H to generate anti-CD22.2 scFv-protamine-His6 construct.

2.18. Construction of anti-CD22.2 scFv-His6 donor vector:

The V_L2 DNA PCR product was cloned into the pFastBac^{TM}1 vector backbone between *Sal*I and *Nhe*I sites. The resulting vector was digested with *Hind*III and *Xho*I, gel purified and used for cloning of V_H DNA sequence (Figure 11). Positive clones were verified by restriction analysis and sequencing using SV40 poly-adenylation (SV40 pA) reverse primer: 5'GAAATTTGTGATGCTATTGC3'.

2.19. Construction of anti-CD22.2 scFv-protamine-His6 donor vector:

The V_L1 DNA PCR product and the annealed protamine cDNA were cloned into the pFastBac^{TM}1 vector backbone. The V_L1 PCR product was cloned between *Sal*I and *EcoR*I sites and the protamine cDNA was cloned between *Eco*RI and *Xba*I sites. Having confirmed that the V_L1 and the truncated protamine sequences were subcloned, the plasmid pFastBac^{TM}1 vector now containing V_L1 and protamine was digested with *Hind*III and *Xho*I enzymes, gel purified and used for subcloning of the V_H sequence (Figure 12).

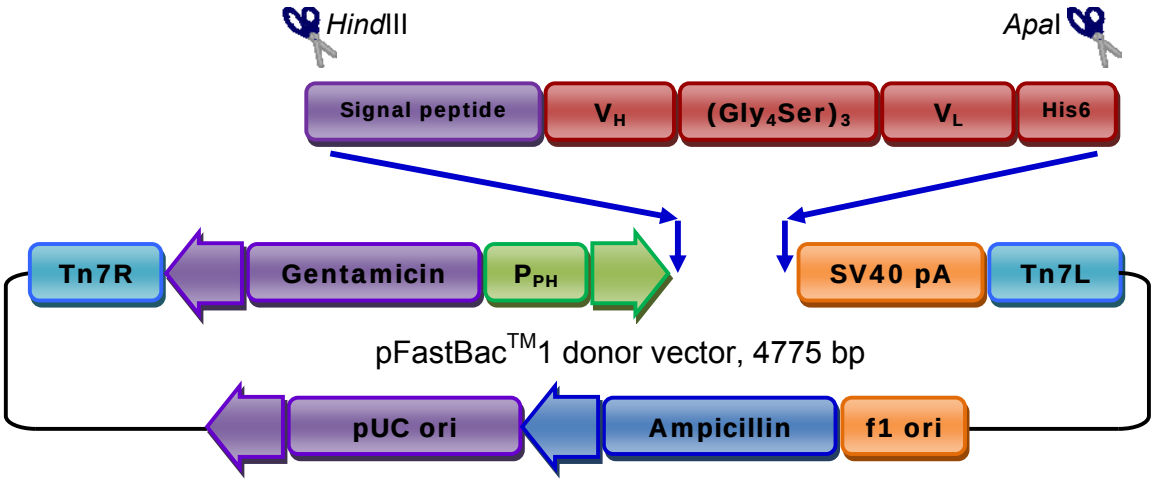

Figure 11: Cloning strategy for the construction of anti-CD22.2 scFv-His6 in pFastBac™ donor vector. The expression cassettes were PCR-amplified and cloned between *Hind*III and *Apa*I sites in the order shown into the backbone of the vector. The donor vector was used later for transposition with the baculovirus shuttle vector by site-specific recombination using Tn7 sites.

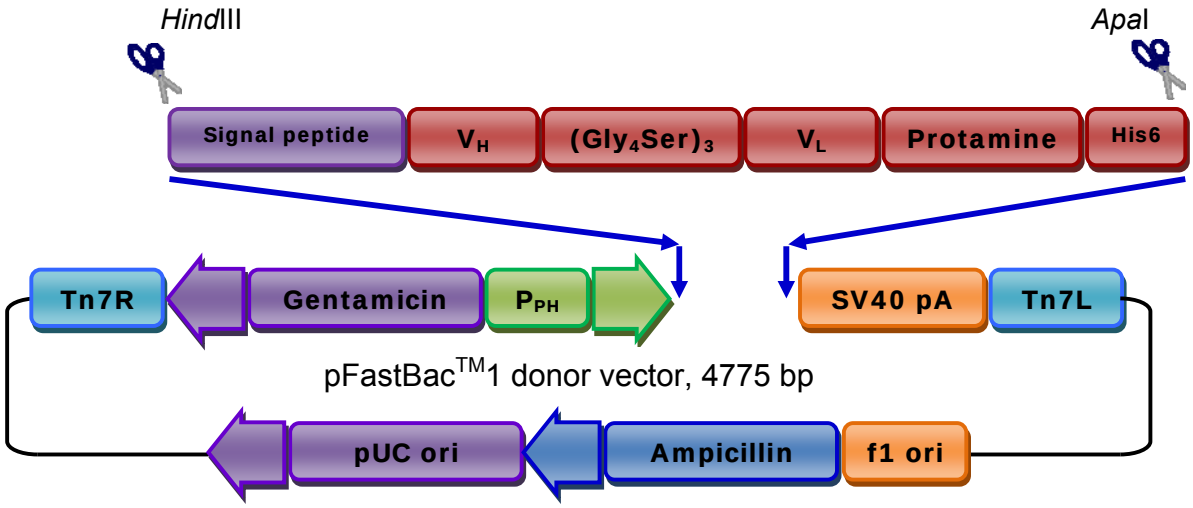

Figure 12: Cloning strategy for the construction of anti-CD22.2 scFv-protamine-His6 in pFastBac™ donor vector. The expression cassettes were PCR-amplified and cloned between *Hind*III and *Apa*I sites in the order shown into the backbone of the vector. The donor vector was used later for transposition with the baculovirus shuttle vector by site-specific recombination using Tn7 sites.

2.20. Generation of recombinant bacmids:

Once the anti-CD22.2 pFastBac^{TM}1 scFv-His6 and scFv-protamine-His6 were generated, purified DNA plasmids of the constructs were used to transform DH10Bac^{TM} *E. coli* for transposition into the baculovirus shuttle vector (bacmid). The process involves site-specific transposition of the expression cassettes from the donor vector to the recipient bacmid. The expression cassettes are flanked by left and right Tn7 transposable elements from the pFastBac^{TM} donor vector which can transpose with the help of a transposase enzyme produced by a helper plasmid to the baculovirus genome which has the mini-*att*Tn7 site. The entire process occurs in the DH10Bac strain of *E. coli* (Figure 13).

Competent DH10Bac™ *E. coli* cells were transformed with 1 ng plasmid DNA pFastBac^{TM}. The cells were heat-shocked for 90 seconds at 42°C and the transformed bacteria grown in 900 µL of LB medium and incubated at 37°C shaker incubator at 225 rpm for 4 hours. For each transformation, 10-fold serial dilutions of the cells (10^{-1}, 10^{-2}, 10^{-3} and 10^{-4}) with LB medium were prepared. Then from each dilution, 100 µL of the bacterial culture were plated on LB agar plates containing 50 µg/mL Kanamycin, 7 µg/mL Gentamicin, 10 µg/mL Tetracycline, 100 µg/mL X-gal and 40 µg/mL isopropyl-β-D-galactoside (IPTG). The plates were incubated for 48 hours at 37°C. Since the transformation depends on blue/white colony selection, the white colonies were picked for analysis to verify the phenotype. Verification was carried out by selecting 10 white colonies and re-streaking them on fresh LB agar plates containing 50 µg/mL Kanamycin, 7 µg/mL Gentamicin, 10 µg/mL Tetracycline, 100 µg/mL X-gal and 40 µg/mL IPTG. The plates were incubated overnight at 37°C. Single colonies were picked for plasmid DNA minipreparation.

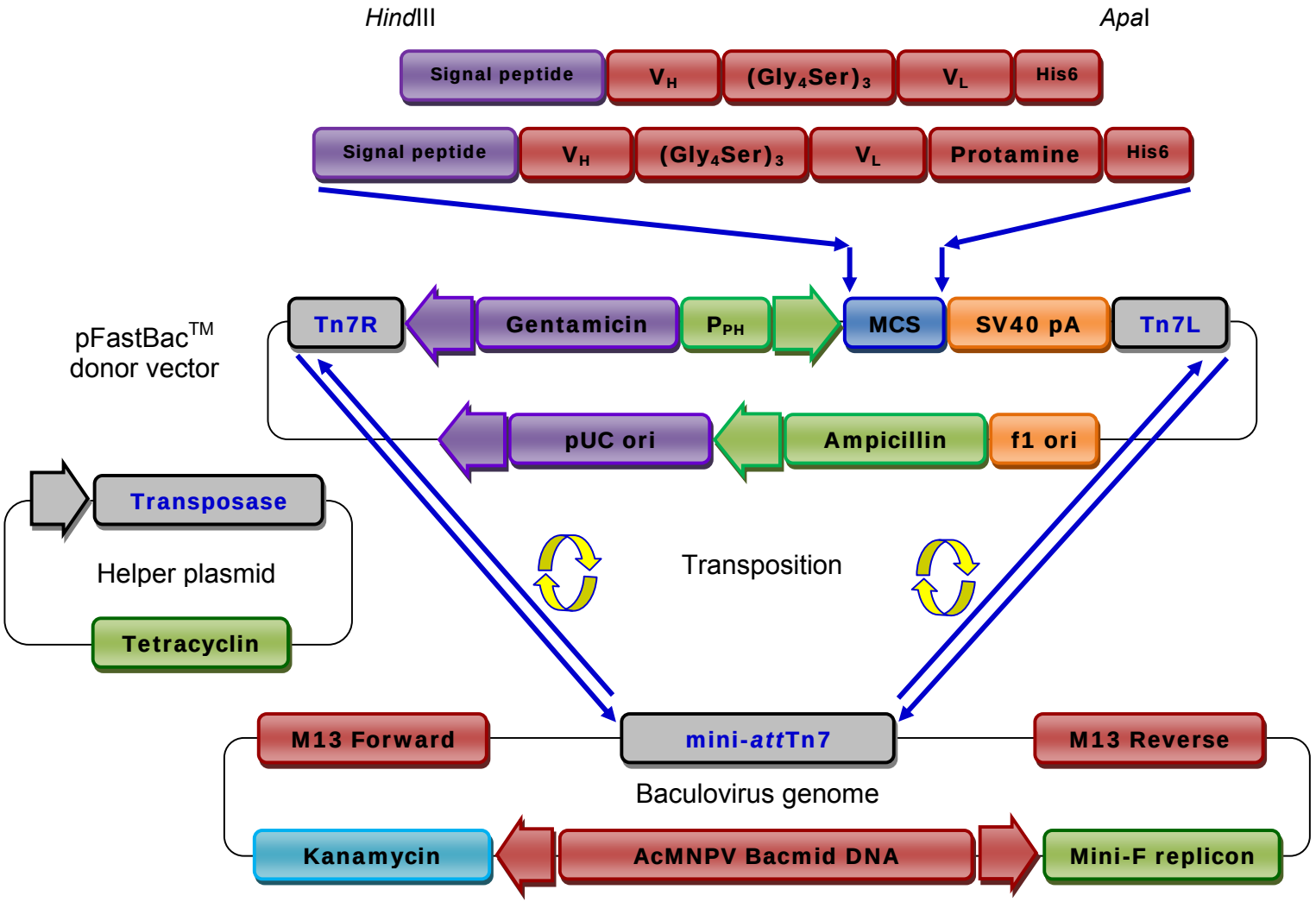

Figure 13: An illustration depicting the process of site-specific recombination of the expression cassettes from a donor vector to a recipient baculovirus vector. The expression cassettes are flanked by 3' and 5' Tn7 transposable elements from the pFastBac™ donor vector which can transpose, with the help of a transposase enzyme produced by a helper plasmid, from the donor vector to the baculovirus genome which has the mini-*att*Tn7 site. The entire process occurs in DH10Bac strain of *E. coli.*

2.21. Analysis of recombinant bacmids:

Recombinant bacmid DNA is greater than 135 kb in size. Since restriction analysis is difficult to perform with DNA of this size, PCR analysis was used to verify the presence of the gene of interest in the recombinant bacmid. The bacmid DNA contains M13 forward and M13 reverse priming sites flanking the mini-*att*Tn7 site within the *lac*Zα-complementation region to facilitate PCR analysis.

The PCRs were performed with M13 forward primer 5'GTTTTCCCAGTCAGAC3' and M13 reverse primer 5'CAGGAAACAGCTATGAC3' using GoTaq® polymerase. The PCRs were carried out using the conditions shown in Table 2. A schematic illustration for the expected PCR products is shown in Figure 39, page 146.

Table 2: PCR conditions to amplify the gene of interest in the recombinant bacmid.

Step	Time	Temperature	Cycles
Initial denaturation	3 minutes	93°C	1x
Denaturation	45 seconds	94°C	30x
Annealing	45 seconds	55°C	
Extension	5 minutes	72°C	
Final extension	7 minutes	72°C	1x
Heated lid		110°C	

2.22. Cloning of anti-CD22.2 scFv-His6 and scFv-protamine-His6 into pcDNA3 vector for expression in mammalian cells:

The baculoviral polyhedrin gene promoter (*polh*) that generally drives gene expression of baculoviruses is not active in mammalian cells; hence for expression of the recombinant proteins in mammalian cells the scFv DNAs were cloned into the pcLuc+ in place of the luciferase gene (Figure 14). Anti-CD22.2 scFv-His6 and scFv-protamine-His6 expression cassettes were PCR-amplified using HindIII forward primer: 5'CCAAAGCTTATGAGATGGAGCTGTATCATT3' and ApaI reverse primer: 5'AGCTCGGGCCCTCAATGGTGGTGGTGATGGTG3'. The PCRs were carried out using the conditions in Table 1. The plasmid pcLuc^{+} (222) was restricted with *Hind*III and *Apa*I enzymes to remove the luciferase gene (*Luc*$^{+}$) and the backbone pcDNA3 used for subcloning of the expression cassettes anti-CD22.2 scFv-His6 and scFv-protamine-His6 restricted with the same enzymes (Figure 15). Positive clones were confirmed by restriction digestion with *Hind*III and *Nde*I and by sequencing.

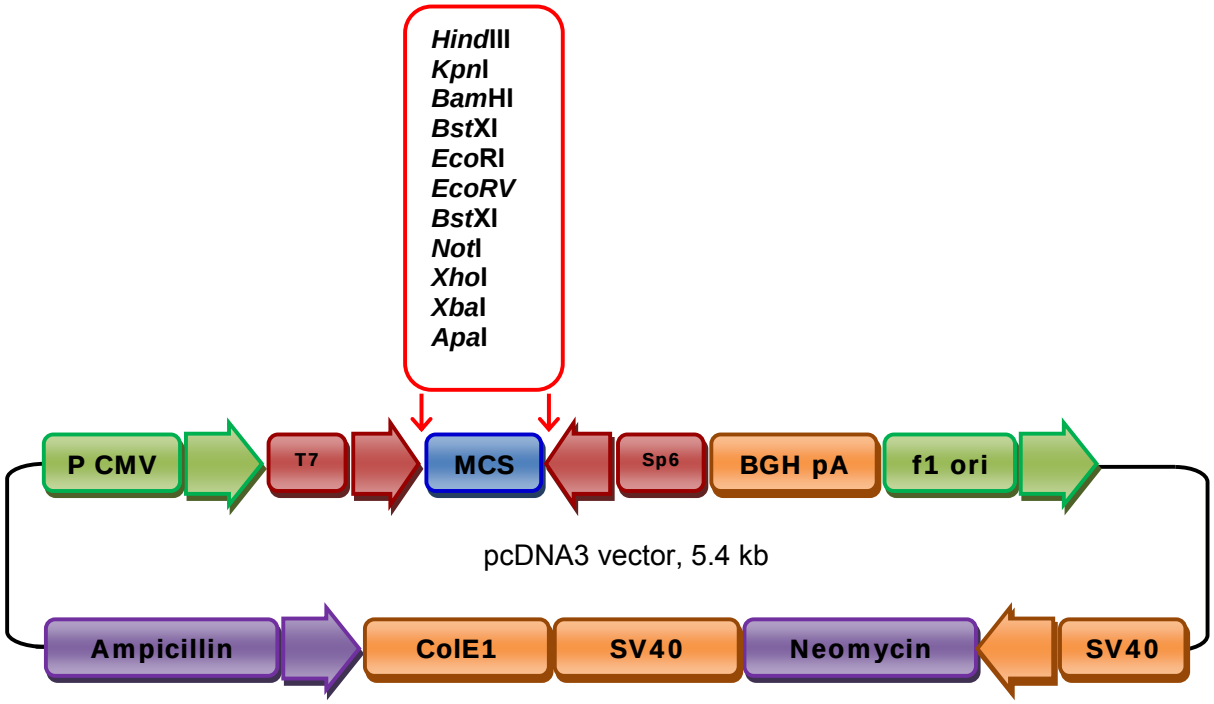

Figure 14: A diagram showing the genetic map of pcDNA3. The anti-CD22.2 scFv-His6 and scFv-protamine-His6 expression cassettes were cloned into the MCS between *Hind*III and *Apa*I restriction sites. CMV promoter: bases 209-863, T7 promoter: bases 864-882, Polylinker: bases 889-994, Sp6 promoter: bases 999-1016, BGH poly A: bases 1018-1249, SV40 promoter: bases 1790-2115, SV40 origin of replication: bases 1984-2069, Neomycin ORF: bases 2151-2945, SV40 poly A: bases 3000-3372, ColE1 origin: bases 3632-4305 and Ampicillin ORF: bases 4450-5310.

Figure 15: Schematic diagrams showing the strategy used for inserting the anti-CD22.2 scFv-His6 (top) and scFv-protamine-His6 (bottom) cDNA into the MCS of pcDNA3 for the construction of the mammalian expression vector. CMV promoter located upstream to the start codon of the V_H gene's native signal peptide drives expression of the recombinant protein. The native signal sequence of the V_H gene was retained to allow secretion of the fusion proteins.

2.23. Cloning of anti-CD22.2 scFv-His6 and scFv-protamine-His6 into the pHEN1 phagemid for expression in bacteria:

Both, the anti-CD22.2 scFv-His6 and scFv-protamine-His6 DNA expression cassettes were PCR-amplified with new primers (pHEN1 forward primer with *Nco*I restriction site (underlined) and the start codon (bold) downstream to the restriction site: 5'GCC**ATG**GCCCAGGTCCAACTGCAGCAGCCT3' and pHEN1 reverse primer with *Not*I restriction site (underlined): 5'GCGGCC GCGGGCCCTCAATGGTGGTGGTGATG3'. The PCRs were performed using GoTaq® polymerase. From either the scFv-His6 or scFv-protamine-His6 cloned into pcDNA3, about 20 ng of the plasmid DNA was used in the PCR. The PCRs were carried out using the conditions in Table1. The PCR products were then cleaned, digested with *Nco*I and *Not*I restriction enzymes and gel purified for cloning into the plasmid vector pHEN1 (223). The pHEN1 phagemid vector (Figure 16) was digested with *Nco*I and *Not*I enzymes. The competent HB2151 *E. coli* cells were transformed with the ligations and positive clones analysed by restriction digestion.

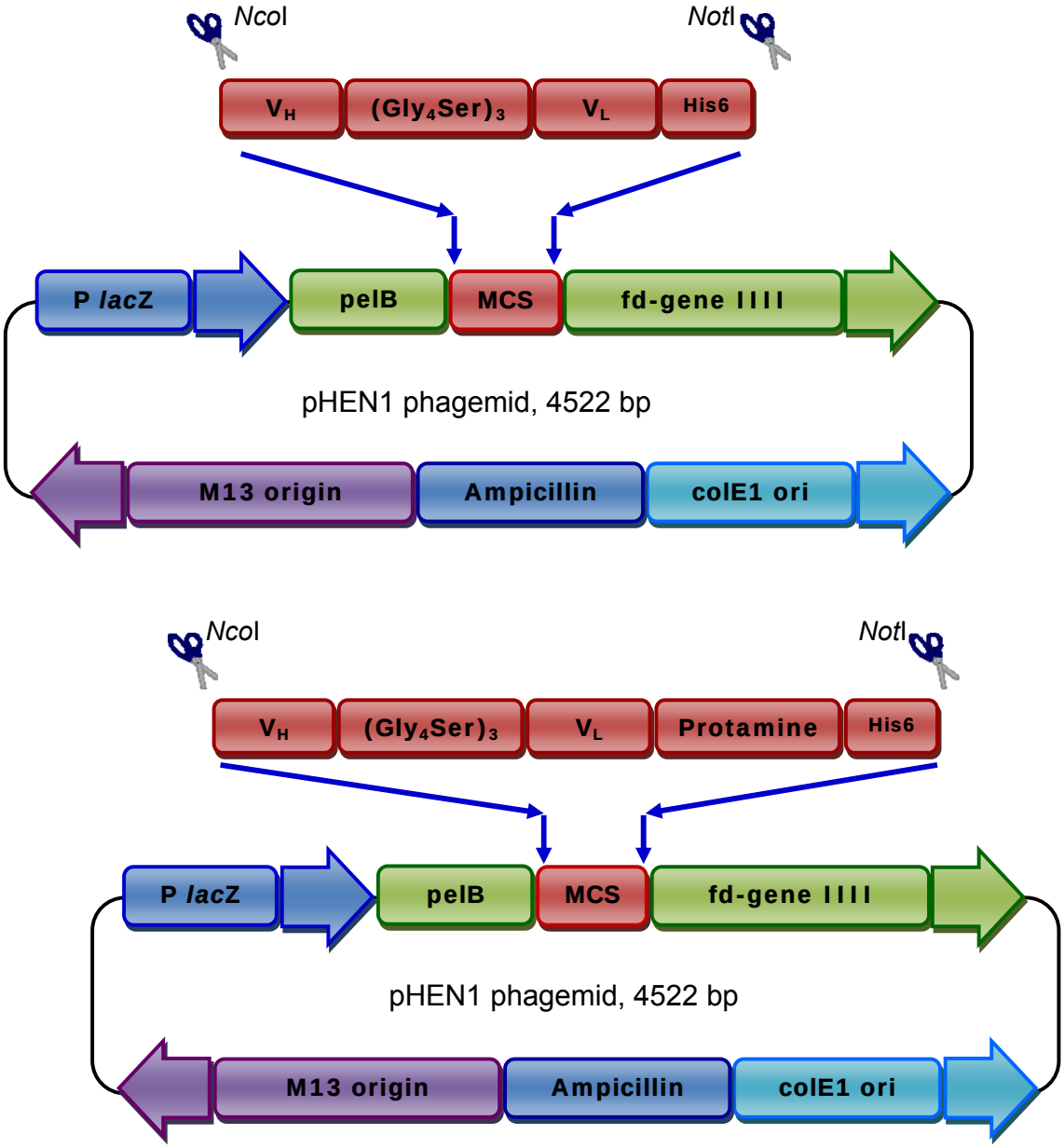

Figure 16: Schematic diagrams showing the genetic map and the strategy for cloning anti-CD22.2 scFv-His6 (top) and scFv-protamine-His6 (bottom) cDNA into pHEN1 phagemid. The phagemid pHEN1 is a derivative of pUC119 plasmid. A pelB signal peptide precedes the multiple cloning site (MCS). The anti-CD22.2 scFv-His6 and scFv-protamine-His6 expression cassettes were cloned into the MCS between *Nco*I and *Not*I restriction sites.

2.24. Cloning of anti-CD22.2 scFv-His6 and scFv-protamine-His6 at the C-terminal region of human latency associated peptide (LAP):

Two antibody constructs without the native signal sequences were cloned downstream of the latency associated peptide (LAP) cDNA of human transforming growth factor beta (TGFβ). A cDNA sequence for the HRV3C cleavage site (LEVLFQGP) was cloned between the scFvs and the LAP to facilitate enzymatic removal of the antibody fragments from the LAP domain for secretion from cells. The cloning process involved PCR amplification of scFv-His6 and scFv-protamine-His6 using 5' sense HPLC-purified HRV3C forward primer with *Bam*HI site (underlined): 5'ATATGGATCCCTCGAGGTTCTCTTTCAGGGACCCCAGGTCCAACTGCAGCAGCCT 3' to incorporate the restriction site for cloning into LAP and the HRV3C cleavage site for enzymatic fragmentation of the protein and a 3' poly-His reverse primer with *Nhe*I site: 5'TGCAGCTAGCGGGCCCTCAATGGTGGTGGTGATG3' to enable cloning into pcDNA3-hLAP vector backbone. The PCRs were performed using GoTaq® polymerase and the PCR conditions in Table 1. The PCR products were checked on an agarose gel and purified by gel extraction. The expression vector pcDNA3-hLAP-MMP-TGFβ was digested with *Bam*HI and *Xba*I restriction enzymes; the PCR products were digested with *Bam*HI and *Nhe*I enzymes. The digested vector backbone and the PCR products were purified by gel extraction and ligated using T4 DNA ligase at 4°C overnight. *Xba*I and *Nhe*I restriction sites have compatible cohesive ends that can restore the open reading frame when digested and ligated together. Positive clones were selected on Carbenicillin (100 mg/mL) LB agar plates and were analysed by restriction digestion (Figure 17). Positive clones were sequenced for their validity using T7 promoter forward primer 5'TAATACGACTCACTATAGGG3', F-LAP forward primer 5'ATTGAGGGCTTTCGCCTTAGC3' and BGH reverse primer 5'TAGAAGGCACAGTCGAGG3'.

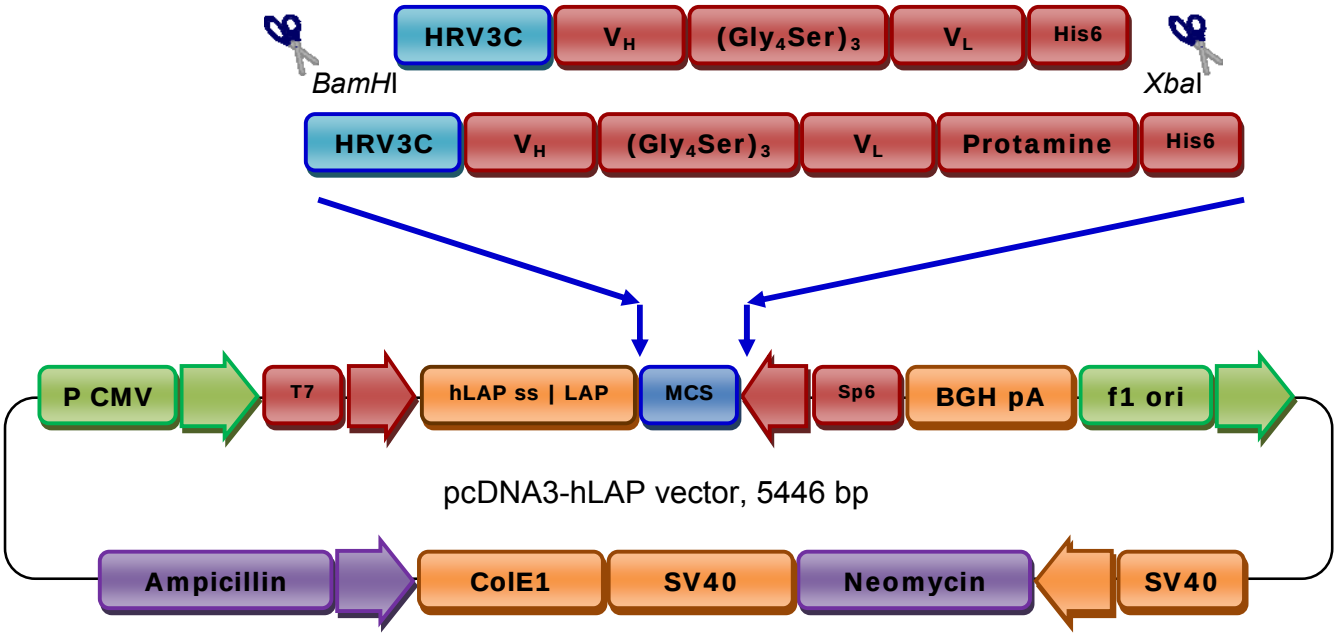

Figure 17: Schematic diagram showing the strategy for cloning of the anti-CD22.2 scFv at the C-terminal region of human LAP with HRV3C cleavage site into pcDNA3. The signal sequence and LAP part from human TGFβ-LAP were cloned upstream of the cloning site in pcDNA3 mammalian expression vector. The expression cassettes of anti-CD22.2 scFv-His6 and scFv-protamine-His6 cDNA were PCR-amplified and cloned without the native signal sequence into the MCS between *Bam*HI and *Xba*I sites.

2.25. Cloning of anti-CD22.2 scFv-protamine-His6 into pDisplay mammalian expression vector using murine Ig kappa chain signal sequence:

Proteins expressed from pDisplay™ vector are fused at the N-terminus to the murine Ig kappa chain leader sequence, which helps direct the protein to the secretory pathway. This has been studied before for several engineered antibodies in mammalian expression systems (224-227). Hence, mouse anti-CD22.2 scFv-protamine-His6 was cloned into pDisplay vector to investigate whether or not the choice of signal peptide may have an impact on the expression/secretion of the recombinant protein (Figure 18).

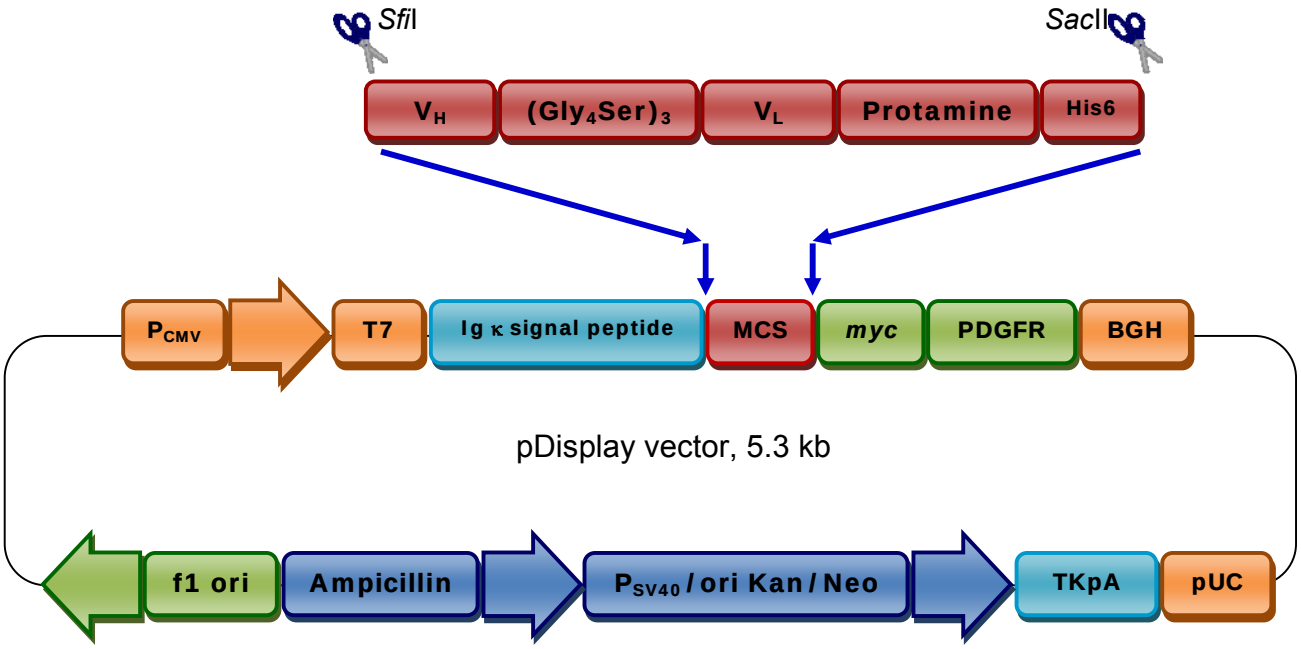

Figure 18: A schematic diagram showing cloning of anti-CD22.2 scFv-protmaine-His6 into modified pDisplay vector for expression in mammalian cells. The PCR-amplified expression cassette without the native signal sequence was cloned between *Sfi*I and *Sac*II sites in the MCS. Proteins expressed from pDisplay were fused at the N-terminus to the murine Ig kappa chain leader sequence to direct the protein to the secretory pathway.

In order to clone the anti-CD22.2 scFv-protamine-His6 into modified pDisplay vector, scFv-protamine-His6 expression cassette was amplified by PCR using Cy34 *Sfi*I forward primer: 5'ATAAGGCCCAGCCGGCCCAGGTCCAACTGCAGCAGCCT3' and Cy34 *Sac*II reverse primer: 5'ATATCCGCGGTTAATGGTGGTGGTGATGGTG3'. The PCRs were performed using *Pfu* DNA polymerase and the PCR conditions in Table 3. The PCR product was then cleaned and digested with *Sfi*I and *Sac*II restriction enzymes followed by gel extraction. The pDisplay mammalian expression vector that was modified to remove an N-terminal tag later, was digested with same restriction enzymes. The modified pDisplay vector was purified by gel extraction. Both PCR product and the vector backbone were ligated in a reaction overnight followed by transformation of DH5α *E. coli* in LB broth. Colonies resulting from the transformants were selected on Carbenicillin (100 mg/mL) LB agar plates and were processed for plasmid minipreparation. Positive clones were confirmed by restriction analysis and sequencing using T7 forward and BGH reverse primers.

Table 3: PCR conditions for amplification of DNA fragments using *Pfu* polymerase.

Step	Time	Temperature	Cycles
Initial denaturation	2 minutes	95°C	1x
Denaturation	30 seconds	95°C	35x
Annealing	30 seconds	59°C	
Extension	2 minutes	72°C	
Final extension	5 minutes	72°C	1x
Heated lid		110°C	

2.26. Obtaining the cDNA for the anti-human CD22 scFv:

cDNAs for the anti-human CD22 was kindly provided by Dr. Ira Pastan (National Cancer Institute; Center for Cancer Research, Bethesda, USA). Two cDNAs, BL22 and HA22, were provided in mammalian expression plasmids pMH112 and pMH113, respectively as described previously (228).

BL22 was generated from anti-CD22 RFB4 IgG-producing hybridoma as described previously (59) and was originally obtained from the Royal Free Hospital School of Medicine, University of London. Briefly, light and heavy genes from RFB4 were used to generate anti-human CD22 scFv by PCR-amplification using specific primers (229). This scFv was cloned into pDisplay vector (named pMH112) and later the *Pseudomonas* exotoxin A (PE38) was fused to anti-CD22 scFv to create RFB4 (scFv)-PE38, or BL22 for B-cell leukaemia/lymphoma/CD22. A mutated form of anti-CD22 named HA22 was generated by site-directed mutations in 3 amino acid residues in CDR3 region of the heavy chain from SSY to THW which increased affinity by ~15-fold. HA22 was then cloned into pDisplay vector and hence called pMH113 (230).

2.27. Preparation of pMH vectors and scFv cDNAs construct for cloning:

Plasmid DNAs, pMH112 and pMH113 which encode BL22 and HA22 respectively, were received in dried formats on Whatman filter papers (500 ng/μL in 10 mM TE buffer, pH 7.0). Upon receipt, the expression plasmids were recovered by cutting areas on the Whatman papers indicated by circles and rehydrating the Whatman paper with DNA in 50 μL of 10 mM TE buffer, pH 7.0 for 10 minutes at room temperature followed by centrifugation at 12,000 rpm for 5 minutes. The recovered plasmids were transformed into DH5α *E. coli* and selected by Carbenicillin resistance using standard procedures. A selected colony was analysed by restriction digestion and sequencing.

2.28. Construction of anti-human CD22 scFv-protamine-His6 in pcDNA6 mammalian expression vector:

The HA22 scFv was amplified by PCR from pMH113 vector with *Eco*RI forward primer (restriction site underlined): 5'GCGGGAATTCATGGAAGTGCAGCTGGTGGAG3' and *Bgl*II reverse primer (restriction site underlined): 5'AGCAGATCTGCTTTCCAGCTTGGTGCCTCCACC3'. Meanwhile, the DNA fragment that encodes truncated protamine-hexahistidine, generated earlier in this study for the mouse antibody constructs, was also amplified by PCR using *Bgl*II forward primer (restriction site underlined): 5'AGCAGATCTCGATCACAATCACGATGA3' and *Nhe*I reverse primer (restriction site underlined): 5'AGCGCTAGCTCAATGGTGGTG GTGATGGTG3'. The PCR mastermixes were prepared for *Pfu* polymerase and the PCR conditions were the same as in Table 3. PCR products of HA22 scFv and protamine-His6 were digested with *Eco*RI and *Nhe*I and purified by gel extraction for ligation with pcDNA6-interleukin-2 signal sequence (pcDNA6|IL2ss) digested with *Eco*RI and *Xba*I enzymes (Figure 19). Plasmid DNA minipreps from obtained clones were analysed by restriction digestion and sequencing.

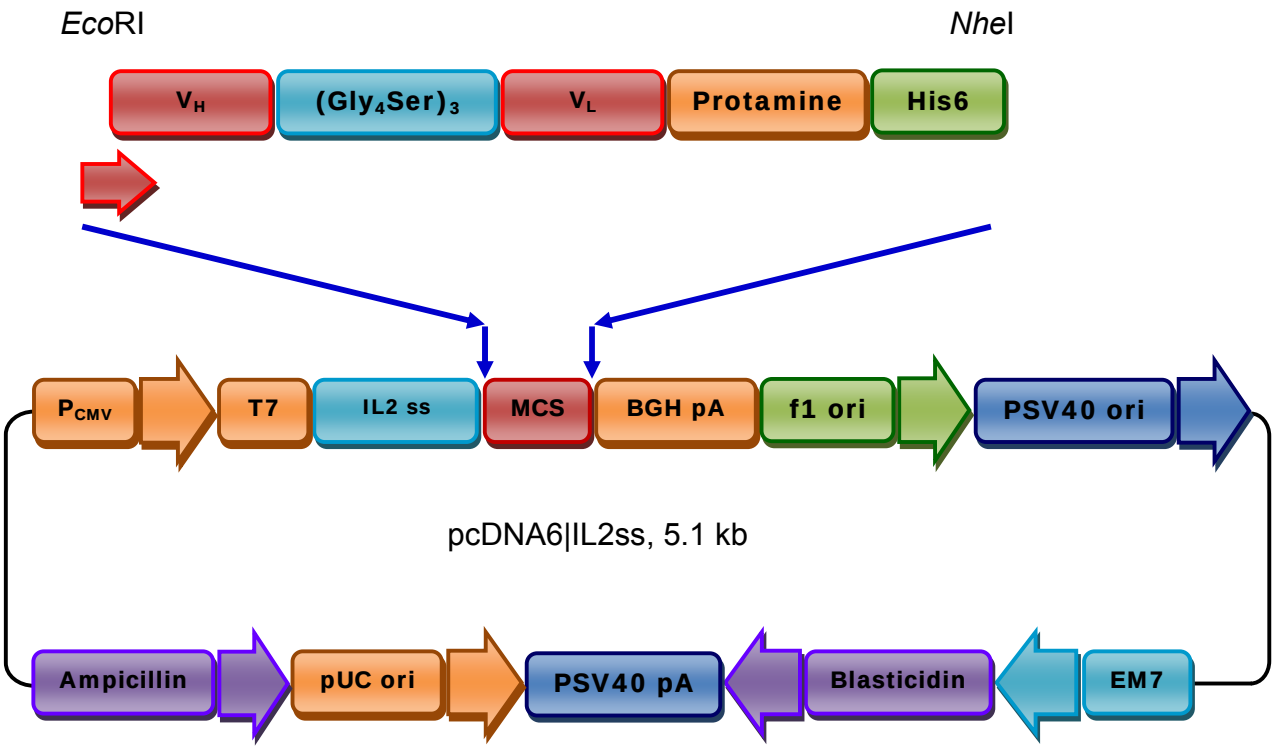

Figure 19: A schematic diagram outlining the strategy for cloning HA22 scFv-protamine-His6 into pcDNA6 with IL2ss. HA22 scFv was PCR-amplified with *Eco*RI forward and *Bgl*II reverse primers. The truncated protamine-hexahistidine was PCR-amplified with *Bgl*II forward and *Nhe*I reverse primers. PCR products were digested with the corresponding enzymes in the restriction sites of the primers. pcDNA6|IL2ss vector was digested with *Eco*RI and *Xba*I enzymes. The three pieces were combined in a ligation reaction to generate the expression vector depicted in the figure.

2.29. Construction of HA22 scFv-protamine-His6 in pDisplay mammalian expression vector:

HA22 scFv-protamine-His6 DNA was also cloned into pDisplay vector which contains the murine Ig kappa chain signal sequence. The expression construct was generated by PCR amplification of HA22 scFv-protamine-His6 from pcDNA6|IL2ss plasmid with *Sfi*I forward primer: 5'GGGGCCCAGCCGGCCATGGAAGTGCAGCTGGTGGAGTCT3' and *Sac*II reverse primer: 5'ATATCCGCGGTTAATGGTGGTGGTGATGGTG3' using *Pfu* polymerase mastermix and conditions. PCR products and pDisplay vector were digested with *Sfi*I and *Sac*II enzymes, purified by gel extraction and used in ligation reaction. DH5α *E. coli* were transformed with the ligation (Figure 20). Bacterial colonies from transformants were expanded for DNA minipreparations and the plasmid DNA minipreps analysed by restriction digestion and sequencing.

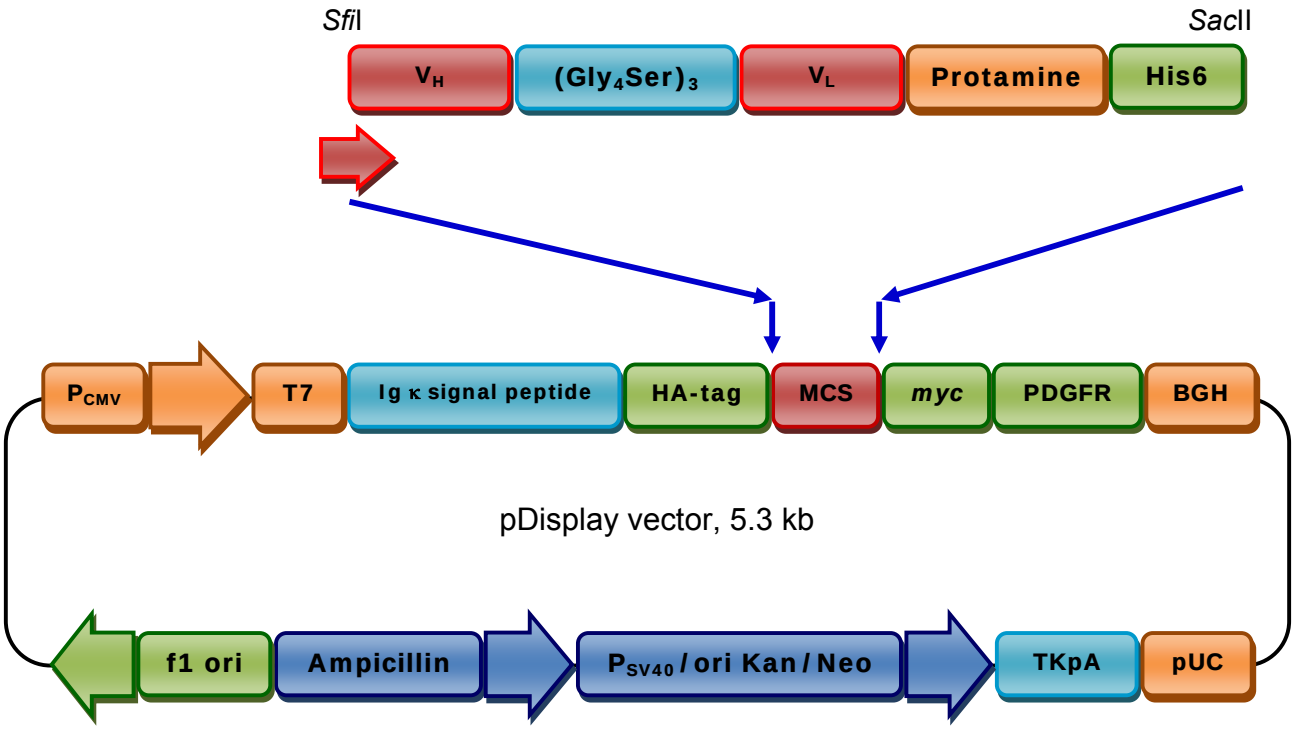

Figure 20: A diagram showing cloning strategy of HA22 scFv-protamine-His6 into pDisplay expression vector. HA22 expression cassette was cloned between *Sfi*I and *Sac*II sites in the MCS.

2.30. Cloning plan to remove the haemagglutinin A epitope (HA tag) from the pDisplay expression vector:

A modified construct of HA22 scFv-protamine-His6 was generated in pDisplay vector. The vector was modified to remove haemagglutinin A epitope tag which was present between the Ig kappa chain signal sequence and the MCS. Therefore, the vector was digested with *Hind*III and *Sfi*I enzymes to release the DNA fragment between *Hind*III and *Sfi*I sites which includes the haemagglutinin A epitope. Next, the region between *Hind*III and end of the leader signal sequence was amplified by PCR using pDisplay-F *Hind*III forward primer: 5'GACCCAAGCTTGGTACCGAGCTCGGATCCA3' and pDisplay-R *Sfi*I reverse primer: 5'TGGATAGGCCGGCTGGGCCCCGTCACCAGTGGAACCTGG3' to retain the Ig kappa chain signal sequence in-frame with the expression cassette. The PCR product was digested with *Hind*III and *Sfi*I enzymes and purified by gel extraction and used in a ligation reaction to clone back into the pDisplay vector which was restricted with the same restriction enzymes. A scheme illustrating the strategy for removal of HA tag is shown in Appendix 6, page 366. Following standard procedures, the resulting clone was confirmed by sequencing from both sides that flank the multiple cloning sites with pMH R-113 reverse 5'GGAGAGTTTCAGGGACCCTCCAGG CTTCACTAA3' and T7 primers. In parallel, HA22 scFv-protamine-His6 DNA expression cassette was PCR-amplified from pcDNA6 construct and digested with *Sfi*I and *Sac*II enzymes. In addition, the modified pDisplay vector was digested with *Sfi*I and *Sac*II enzymes to use in a ligation reaction to combine the expression DNA and the vector into one construct. The generated expression vector was transformed into bacteria and positive clones selected for further analyses by restriction digestion and sequencing. PCR mastermixes and conditions were the same as described for *Pfu* polymerase.

2.31. Expression of anti-CD22.2 scFv-His6 and scFv-protamine-His6 fusion proteins in insect cells using recombinant baculovirus:

The recombinant bacmid DNA for scFv-His6 and scFv-protamine-His6 were used to transfect insect cells to produce recombinant baculovirus and subsequently recombinant fusion proteins. The transfection of insect cells was carried out for 18 days by subsequent propagation of the baculovirus in SF9 insect cells for three rounds and expression of the fusion protein in the HighFive insect cells. The transfection procedure was as follow: in a 6-well cell culture plate, 9 x 10^5 SF9 cells per well were seeded in 2 mL of Sf-900 II SFM growth medium (Invitrogen Ltd) containing 50 IU/mL Penicillin and 50 IU/mL Streptomycin. The cells were allowed to attach to the wells at 27°C for at least 1 hour. For each transfection, bacmid DNA:Cellfectin® Reagent complexes were prepared as follows in 12 x 75 mm sterile tubes: 1 µg of bacmid DNA diluted in 100 µL of unsupplemented Grace's Medium (Invitrogen Ltd). The Cellfectin® Reagent is provided as a 1:1.5 (M/M) liposome formulation of the cationic lipid N, NI, NII, NIII-Tetramethyl-N, NI, NII, NIII-tetrapalmitylspermine (TM-TPS) and dioleoyl phosphatidylethanolamine (DOPE) in membrane-filtered water (Invitrogen Ltd). For transfection, 6 µL of Cellfectin® Reagent was diluted in 100 µL of unsupplemented Grace's Medium. The diluted bacmid DNA and the diluted Cellfectin® Reagent were combined (total volume was 200 µL), mixed gently and incubated for 30 minutes at room temperature after which the volume was increased to 1 mL by addition of 0.8 mL of unsupplemented Grace's Medium. The media from the cells were removed and cells washed once with 2 mL of unsupplemented Grace's Medium. The transfection mixture was added to each of the SF9 cells and incubated at 27°C for 5 hours. Next, the DNA:lipid complexes were removed and 2 mL of complete Sf-900 II SFM growth medium added to the cells and incubated in a 27°C humidified incubator for 120 hours (5 days) when signs of viral infection were seen. Virally-infected insect cells typically display characteristics that can be identified using an inverted phase microscope at 250-400X magnification (Table 4).

Table 4: Phenotypic characteristics of the HighFive insect cells after transfection with the recombinant baculovirus.

Signs of Infection	Phenotype	Description
Early (first 24hours)	Increased cell diameter	A 25-50% increase in cell diameter may be seen
	Increased size of cell nuclei	Nuclei may appear to "fill" the cells
Late (24-72hours)	Cessation of cell growth	Cells appear to stop growing when compared to a cell-only control
	Granular appearance	Signs of viral budding; vesicular appearance to cells
	Detachment	Cells release from the plate or flask
Very Late (>72hours)	Cell lysis	Cells appear lysed and show signs of clearing in the monolayer

Once the transfected cells showed signs of late stage infection, the medium containing viruses from each well was collected and transferred to sterile tubes and centrifuged at 500 *g* for 5 minutes at 4°C to remove cells and large debris. The clarified supernatant was transferred to fresh tubes and this was called the P1 viral stock and stored in 2% HI-FBS at 4°C, protected from light.

Next, the P1 baculoviral stock was propagated to obtain the highest viral titers and optimal protein expression. For amplification of the P1 baculovirus, 4 x 10^6 SF9 cells in a 25 cm^2 flask were cultured in Sf-900 II SFM growth medium containing 50 IU/mL Penicillin and 50 IU/mL Streptomycin and incubated at 27°C for 1 hour to allow cells to attach. After 1 hour, the cells were inspected to verify attachment. From the P1 baculovirus, 0.4 mL was added to each SF9 culture and cells incubated for 5 days in a 27°C humidified incubator. Five days post-infection, the culture medium containing viruses in each flask were harvested to sterile tubes and centrifuged at 500 *g* for 5 minutes at 4°C to remove cells and large debris. The supernatants were transferred to fresh tubes and these were the P2 baculoviral stocks. The P2 baculoviral stock stored in 2% HI-FBS at 4°C, protected from light.

The recombinant baculovirus was further propagated to obtain P3 stock by transfection of 12 x 10^6 pre-attached SF9 cells in a 75 cm^2 flask with 3 mL of P2 virus stock in Sf-900 II SFM growth medium and incubated at 27°C in a humidified incubator for 5 days.

Once the recombinant baculovirus was generated, it was used to infect HighFive insect cells for protein expression. For expression of the recombinant proteins, 2 x 10^7 HighFive insect cells were cultured in 162 cm^2 flasks in ExpressFive growth medium containing 50 IU/mL Penicillin, 50 IU/mL Streptomycin and 20 mM L-glutamine and incubated at 27°C for 1 hour to allow cells to attach. HighFive insect cells were transfected by adding 2.5 mL of the P3 baculovirus to each culture flask containing the cells and incubated at 27°C for 72 hours. Three days post-infection the cultures were harvested and centrifuged at 500 *g* for 5 minutes at 4°C and both the supernatant and the cells analysed by Western blotting for protein expression.

2.32. Expression of anti-CD22.2 scFv-His6 and scFv-protamine-His6 fusion proteins by transient transfection of mammalian HEK293T cells:

For transient transfection with mammalian expression vectors (231), HEK293T cells were grown in complete DMEM growth medium to about 70% confluence. Cells were then washed once with PBS and trypsinised for 5 minutes at 37°C. The cells (1.5 x 10^6) were transferred to a 10 cm cell culture plate in 9 mL fresh medium and grown overnight. For each transfection, the DNA precipitation mixture was prepared in the order shown in Table 5.

Table 5: Transfection of mammalian cells using calcium phosphate method.

Component	Amount
HBS 2x*	500 μL
Sterile Distilled H_2O	To final volume of 1000 μL
Plasmid DNA	20 μg
$CaCl_2$ (2.5M)	50 μL added dropwise with shaking
Total volume	1000 μL

Note:
*** HBS 2x is HEPES-Buffered Saline 2x** (8 g NaCl, 0.2 g Na_2HPO_4-$7H_2O$ and 6.5 g HEPES, 500 mL dH_2O. pH 7.0).
HEPES is zwitterionic organic buffering agent 4-(2-hydroxyethyl)-piperazine-1-ethanesulfonic acid.

The mixture was left at room temperature for 20 minutes. The medium was then removed from the cells and 1 mL of the DNA precipitation mixture added to the plates. The plates were left at room temperature for 30 minutes with occasional tilting. The cells were then supplemented with 9 mL of fresh growth DMEM medium and plates incubated in a 37°C incubator overnight. Next day, the media were removed from the cells and replaced with 4 mL of serum-free DMEM growth medium and incubated at 37°C overnight. Next day, the supernatants were harvested, cells washed with PBS and then removed by scraping and kept for cell lysis and further analysis by Western blotting.

2.33. Expression of anti-CD22.2 scFv-His6 and scFv-protamine-His6 fusion proteins by transient transfection of CHO-S cells:

CHO-S cells were cultured in Freestyle CHO-S expression medium supplemented with 8.0 mM L-glutamine. Transient transfection was performed using 25 kDa linear polyethylenimine (PEI) (Polysciences Inc., Northampton, UK). Stock solutions of PEI were prepared in water at a concentration of 1 mg/mL, pH7.0. CHO-S cells were cultured to a density of 2 x 10^6 cells/mL and transfected with 2.5 μg/mL of DNA. The transfection complex was formed at a DNA:PEI ratio of 1:2 in OPTI-MEM®I Reduced Serum Medium (Invitrogen Ltd) containing 150 mM NaCl, with a 10 minute incubation at room temperature prior to addition to the CHO-S culture. Culture supernatants were collected 3 days after transfection for analysis of protein content by Western blotting.

2.34. Expression of recombinant proteins in bacteria:

The protocol was obtained from previous research work for expression of similar recombinant proteins in bacteria (232). Competent HB2151 *E. coli* bacteria were transformed with maxi-prep DNA from the previously obtained anti-CD22.2 scFv-His6 in pHEN1 phagemid vectors and inoculated into 2xTY agar (containing 1% glucose and 100 μg/mL Carbenicillin) and grown overnight at 37°C. From the overnight grown bacteria (starter culture), 50 mL 2xTY broth (containing 1% glucose and 100 μg/mL Carbenicillin) were cultured at 37°C incubator with shaking at 225 rpm overnight. A large-scale (200 mL) 2xTY (containing 0.1% glucose and 100 μg/mL Carbenicillin) culture was then inoculated with 2 mL of this starter culture and incubated at 30°C with shaking at 225 rpm until the OD_{600} reached 0.8-0.9, then IPTG to a final concentration of 1 mM was added to induce expression of the recombinant protein. The bacteria were grown overnight in a 30°C incubator with shaking at 225 rpm. Next day, the bacteria were pelleted by centrifugation at 5000 rpm for 20 minutes at 4°C. The culture supernatant was kept at 4°C for analysis of secreted recombinant proteins, the pellet was resuspended in 10 mL ice-cold TES buffer (0.2 M Tris-HCl, 0.5 mM EDTA and 0.5 M sucrose), incubated on ice for 30 minutes and centrifuged at 5000 rpm for 20 minutes at 4°C. The supernatant (periplasmic extract) was transferred to a fresh tube and kept at 4°C until analysed. The pellet was lysed with guanidinium lysis buffer (6 M guanidine HCl, 20 mM NaH_2PO_4 and 500 mM NaCl pH 7.8) at room temperature. EDTA-free Protease Inhibitor cocktail 1:20 (Calbiochem, Nottingham, UK) was added during lysis of the cells to inhibit the activity of all proteases. The cell lysate was sonicated on ice with three 5-second pulses at high intensity and then centrifuged at 3,000 *g* for 15 minutes to pellet cellular debris. The supernatant was transferred to a fresh tube and used for purification under denaturing conditions. The culture supernatant, periplasmic extract and the bacterial cell lysate were analysed by SDS PAGE and Western blotting.

2.35. Analysis of recombinant proteins by Sodium Dodecyl Sulphate Polyacrylamide Gel Electrophoresis (SDS PAGE) and Western blotting:

2.35.1. Cell lysis:

Harvested cells were centrifuged at 600 x g for 5 minutes and pellets lysed on ice for 15 minutes by the addition of 100 µL of lysis buffer (50 mM HEPES pH 8.3, 420 mM KCl, 0.1% NP-40, 1 mM EDTA) to each sample with vortexing for 15 seconds. Lysates were clarified by centrifugation at 16,000 *g* at 4°C for 10 minutes to remove cellular debris and clarified lysates were transferred to fresh tubes and stored on ice for immediate use or alternatively stored at –20°C for later use.

2.35.2. SDS PAGE:

The NuPAGE® electrophoresis system (Invitrogen Ltd) was used for SDS PAGE. Each sample (4 volumes) was mixed with one volume of 5x Laemmli buffer (0.313 M Tris-HCl, 10% SDS, 0.05% bromophenol blue and 50% glycerol; pH 6.8) with 10% 2-mercaptoethanol and boiled for 5 minutes for reduced samples, and 10 µL was loaded into each well of a NuPAGE® 4-12 % gradient or 10% precast Bis-Tris gel. All Blue protein ladder (Bio-Rad Laboratories Inc., Hertfordshire, UK) was loaded as a standard protein marker. The gel was run in 1x NuPAGE® MOPS SDS Running Buffer (50 mM MES [2-(*N*-morpholino)-ethanesulfonic acid], 50 mM Tris Base, 0.1% SDS, 1 mM EDTA, pH 7.3) at 150 volts for 80 minutes.

2.35.3. Coomassie blue staining of SDS PAGE gels:

SDS PAGE gels were fixed in a solution of (50% (v/v) ethanol in dH_2O and 10% (v/v) acetic acid) for 30 minutes and then immersed in the staining solution (0.1% (w/v) Coomassie Brilliant Blue (Sigma-Aldrich Inc), 20% (v/v) methanol in dH_2O and 10% (v/v) acetic acid). Gels were incubated on a rotating platform until protein bands became visible. Gels were then washed with several changes of dH_2O and de-stained in the de-staining solution (50% (v/v) methanol in dH_2O and 10% (v/v) acetic acid) with shaking until the background staining reduced and protein bands became visible. Finally, gels were stored in dH_2O, scanned and data saved.

2.35.4. Silver nitrate staining of SDS PAGE gels:

The Silver Stain Plus kit (Bio-Rad Laboratories Incs) was used for silver nitrate staining of SDS PAGE gels. After gel electrophoresis, gels were fixed in the fixative enhancer solution (reagent grade methanol 50% [v/v], reagent grade acetic acid 10% [v/v], fixative enhancer concentrate 10% [v/v] and dH_2O 30% [v/v]) with gentle agitation for 20 minutes at room temperature followed by rinsing twice in 400 mL dH_2O for 10 minutes with gentle agitation. Gels were then stained and developed with the staining and developing solutions (the staining solution was prepared within 5 minutes of use by mixing 35 mL dH_2O with 5 mL silver complex solution [NH_4NO_3 and $AgNO_3$], 5 mL reduction moderator solution [tungstosilicic acid], 5 mL image development reagent [formaldehyde] and, immediately before use, quickly added 50 mL of a room temperature development accelerator solution [Na_2CO_3]). The gels were then stained for approximately 20 minutes at room temperature or until desired staining intensity reached. Once the desired staining was reached, the reaction was stopped by placing the gel in 5% acetic acid for 15 minutes. After stopping the reaction, gels were rinsed with dH_2O for 5 minutes and photographed.

2.35.5. Western blotting:

For Western blotting, polyvinylidene fluoride (PVDF) membranes (GE Healthcare, London, UK), reactivated with reagent grade methanol, were used to transfer proteins and gels were sandwiched between two layers of filter paper and sponges soaked in the NuPAGE® Transfer Buffer (proprietary composition). The inner chamber of the tank was filled with NuPAGE® Transfer Buffer and the outer chamber filled with water for cooling the tank. Proteins were transferred to the PVDF membrane electrophoretically for 2 hours at 30 volts.

2.35.6. Detection of recombinant proteins:

When PVDF membranes were stained with horseradish peroxidase (HRP) conjugated anti-His mAb (Qiagen Ltd, Manchester, UK), membranes were first washed twice with Tris-buffered saline (TBS) buffer (10 mM Tris-HCl, pH 7.5 and 150 mM NaCl) for 10 minutes at room temperature and then incubated for 1 hour in blocking buffer (0.1g Blocking Reagent added to 20 mL 1x blocking buffer, 10% [v/v] Tween-20 added for final concentration of 0.1% [v/v]) (Qiagen Ltd). After blocking, membranes were washed

twice for 10 minutes in TBS-Tween/Triton buffer (20 mM Tris-HCl, pH7.5; 500 mM NaCl; 0.05% [v/v] Tween 20 and 0.2% [v/v] Triton X-100) at room temperature and 10 minutes wash with TBS buffer. The membranes were then incubated in anti-His mAb HRP conjugate (1/2000 in blocking buffer) at room temperature for 1 hour. After staining, the membranes were washed twice in TBS-Tween/Triton buffer for 10 minutes at room temperature and then once with TBS buffer for 10 minutes. The blots were developed using enhanced chemiluminescence (ECL) reagents (GE Healthcare) and exposed to autoradiography using Hyperfilm (GE Healthcare). Films were developed using the SRX-101A tabletop processor (Konica Minolta, USA).

Because of the high background noise with anti-His Ab from Qiagen Ltd, an alternative HRP conjugated anti-His Ab was used to probe His-tagged fusion proteins. Recombinant proteins were separated on 10% SDS PAGE and transferred to PVDF. The PVDF membrane was stained with HRP conjugated anti-His(C-term) mAb from Invitrogen Ltd. After the transfer, membranes were incubated in 10 mL blocking buffer containing 5% non-fat dry milk and 0.05% Tween-20 in PBS with gentle agitation on a rocker platform for 1 hour at room temperature. The membranes were then washed in 20 mL wash buffer (0.05% Tween-20 in PBS) twice for 5 minutes with gentle agitation. The membranes were then stained with the HRP conjugated anti-His(C-term) mAb (1:5000) in blocking buffer and incubated with gentle agitation overnight at 4°C. The membranes were then washed with 20 mL wash buffer twice and bound HRP conjugated mAb revealed with ECL and exposed to autoradiography film and developed.

2.36. Purification of anti-CD22.2 scFv-His6 and scFv-protamine-His6 recombinant proteins under native conditions:

Insect cells were lysed with the Insect Cell Protein Extraction Reagent (I-PER®) (contains a proprietary non-ionic detergent in 130 mM NaCl, 25 mM Tris-HCl; pH 7.5 and a microbial growth inhibitor) (Fisher Scientific Ltd, Leicestershire, UK). The HighFive insect cells were harvested and the total number of cells determined. Cells were collected by centrifugation at 800 *g* for 5 minutes at room temperature and gently resuspended with an equal volume of PBS. The cells were washed twice with PBS and 10 μL of EDTA-free Halt Protease Inhibitor Cocktail (Thermo Fisher Scientific) was added to the I-PER® buffer to produce a 1x final concentration and 1 mL of the later was used to lyse 5 x 10^6 – 2 x 10^7 cells in the washed cell pellet. The cells were resuspended and vortexed for 5 seconds at medium speed and then incubated on ice for 10 minutes and centrifuged at 15,000 *g* for 15 minutes at 4°C. The supernatants containing soluble proteins were carefully transferred to new tubes and used for purification of the recombinant proteins by nickel affinity chromatography. Nickel-nitrilotriacetic acid (Ni-NTA) agarose slurry (50%) in 30% ethanol was resuspended thoroughly and 1.5 mL poured into a sterile tube and pelleted by centrifugation at 800 *g* for 1 minute. The supernatant was gently aspirated and 6 mL sterile distilled water added to resuspend the resin. The resin was then centrifuged at 800 *g* for 1 minute before use. For purification of proteins under normal conditions, the resin was resuspended in 6 mL of native protein binding buffer (50 mM NaH_2PO_4 and 0.5 M NaCl; pH 8.0) and centrifuged at 800 *g* for 1 minute. Washing with native protein binding buffer was repeated three more times and the resin was finally loaded into the purification column. Insect cell lysates prepared under native conditions were added to the purification column and proteins allowed to bind for 60 minutes at 4°C using gentle agitation to keep the resin suspended in the lysate solution. The resin was allowed to settle by gravity and unbound proteins allowed to pass through the column and collected for further analysis. The column was washed with native protein binding buffer and then washed four more times with 8 mL native wash buffer (50 mM NaH_2PO_4 and 0.5 M NaCl with 10 mM imidazole; pH 8.0) and flow-through collected for analysis. The protein was eluted with 5 mL native protein elution buffer (50 mM NaH_2PO_4 and 0.5 M NaCl with 250 mM imidazole; pH 8.0) and 1 mL fractions collected and analysed by Western blotting.

2.37. Purification of anti-CD22.2 scFv-His6 and scFv-protamine-His6 recombinant proteins under denaturing condition:

To purify recombinant protein under denaturing conditions, HighFive insect cell pellets were resuspended in 8 mL guanidinium lysis buffer (6 M guanidine HCl, 20 mM NaH_2PO_4 and 500 mM NaCl; pH 7.8). To inhibit all potential proteolysis, an EDTA-free cocktail of Protease Inhibitors (Calbiochem®) at 1:200 dilution was added during lysis of the cells in guanidinium lysis buffer. The lysate was passed through an 18-gauge needle four times and centrifuged at 3,000 *g* for 15 minutes to remove cellular debris and the supernatant was transferred to a fresh tube. To prepare the purification column, 2 mL of the Ni-NTA agarose was pipetted into a 10 mL purification column. The resin was centrifuged for 1 minute at 800 *g* and supernatant aspirated gently. To wash the nickel beads, 6 mL of sterile dH_2O was added to resuspend the resin then allowed to settle by low speed centrifugation for 1 minute at 800 *g* and the supernatant aspirated. Then, the Ni-NTA agarose column was washed twice with 6 mL of denaturing binding buffer (8 M urea, 20 mM NaH_2PO_4 and 500 mM NaCl; pH 7.8). The resin was resuspended and allowed to settle by low speed centrifugation for 1 minute at 800 *g* and supernatant aspirated. From clarified insect cell lysates, 8 mL was applied to the prepared nickel resin and allowed to bind for 45 minutes at room temperature with gentle agitation on a rotating wheel to keep the resin suspended. The resin was then allowed to settle by gravity and the flow-through collected (unbound fraction). The column was washed twice with 4 mL denaturing binding buffer (8 M urea, 20 mM NaH_2PO_4 and 500 mM NaCl; pH 7.8) and the flow-through collected. Next, the column was washed twice with 4 mL denaturing wash buffer (8 M urea, 20 mM NaH_2PO_4 and 500 mM NaCl; pH 6.0) and the resin allowed to settle again and flow-through collected for analysis. The column was washed twice with 4 mL denaturing wash buffer (8 M urea, 20 mM NaH_2PO_4 and 500 mM NaCl; pH 5.3) for 2 minutes and resin allowed to settle by gravity. The flow through was collected for analysis. The protein was eluted with 3 mL of increasing concentrations of imidazole (10, 25, 50, 100 and 200 mM) in denaturing elution buffer (8 M urea, 20 mM NaH_2PO_4 and 500 mM NaCl; pH 4.0). Proteins in the collected fractions were precipitated with trichloroacetic acid (TCA) for 10 minutes and washed with cold acetone and analysed with SDS PAGE and Western blotting.

2.38. Analysis of recombinant proteins from culture supernatants of insect cells obtained by centrifugal concentration:

The HighFive insect cell supernatants were concentrated using a specialised Immobilized Metal Affinity Chromatography (IMAC) purification device by centrifugation. Culture supernatant (20 mL) was loaded onto 10 kDa molecular weight spin column (Vivapure Metal Chelate Maxi spin column; Vivaproducts, Inc. Littleton, USA) and centrifuged at 5,000 *g* for 2 hours to bring down the final volume to a 1 mL concentrated sample. The concentrated sample was then pipetted out into a clean tube and analysed by SDS PAGE and Western blotting. Precipitates from the concentration process that were lodged in the groove of the column were also collected and subjected to analysis by Western blotting.

2.39. Analysis of recombinant proteins in culture supernatants of insect cells by precipitation with trichloroacetic acid (TCA):

In order to detect recombinant proteins in culture supernatants, all proteins were precipitated with TCA. One volume of cold TCA stock solution (100% w/v) was added to four volumes of culture supernatants from the HighFive insect cell cultures and incubated at 4°C for 10 minutes then centrifuged at 14,000 rpm for 5 minutes. The supernatants from the centrifugation were discarded and pellets washed with 200 μL cold acetone and centrifuged again at 14,000 rpm for 5 minutes. The pellets were left to dry at 95°C on a hot-block. Because of the very strong acidity of TCA, 10 μL of 1 M NaOH was added to the pellet to neutralise the effect of strong acidic pH of TCA. The pellets were then resuspended in 5x Laemmli buffer and analysed by SDS PAGE and Western blotting.

2.40. Dialysis, refolding and ion-exchange chromatography purification of recombinant proteins:

The recombinant proteins anti-CD22.2 scFv-His6 and scFv-protamine-His6 extracted from HighFive cell lysates were bound to nickel affinity chromatography columns and eluted under denaturing conditions with a minor modification (addition of 50 mM L-glutamine to all purification buffers). The eluted recombinant protein fractions were dialysed to remove the urea and the proteins refolded in a refolding buffer (10 mM Tris, 0.4 M L-arginine, 5 mM GSSH [reduced glutathione] and 0.5 mM GSSG [oxidized glutathione] supplemented with 6.0 M, 4.0 M, 2.0 M, 1.0 M and without urea; pH 8.0) over a period of 72 hours. The protocol was modified from a method used for the refolding of similar recombinant proteins (120). The eluted proteins were added to Slide-A-Lyzer® Dialysis Cassettes 10 kDa molecular cutoff (Thermo Scientific) and dialysed against the refolding buffer with decreasing concentrations of 6.0, 4.0 and 2.0 M of urea to prevent aggregation of the proteins. This was carried out at room temperature followed by dialysis against 1.0 M and no urea in the refolding buffer at 4°C for 4 hours in each step. Ultimately, the buffer was exchanged to a fresh refolding buffer and dialysed overnight at 4°C. The protein samples were removed from the Slide-A-Lyzer® Dialysis Cassettes and stored at -20°C.

The next step was to purify the proteins by ion-exchange chromatography and to achieve this, the isoelectric point (PI) of the recombinant proteins anti-CD22.2 scFv-His6 and scFv-protamine-His6 were calculated using the interactive bioinformatic database (http://isoelectric.ovh.org/) which measures the PI according to different scales. The average PI for the scFv-His6 and scFv-protamine-His6 were determined to be 7.268 and 9.665, respectively.

The Q Sepharose™ Fast Flow HiTrap™ column (GE Healthcare) was used for the purification of scFv-His6 protein which has a net negative charge at pH 8.0 and, hence, needed an anion exchange column with positively charged resin. For the purification of the scFv-protamine-His6 protein which has a net positive charge at pH 8.0, SP Sepharose™ Fast Flow HiTrap™ column, a cation exchange column which has a negatively charged resin, was used. The ion-exchange chromatography experiments were carried out at 4°C using fast protein liquid chromatography (FPLC) (Amersham Pharmacia, GE Healthcare) and the UNICORN™ controlled ÄKTA*explorer*™ systems. The columns were first equilibrated with filter-sterilised cold buffer A (10 mM Tris, 0.4 M L-arginine, 5 mM GSSH [reduced glutathione] and 0.5 mM GSSG [oxidized glutathione]; pH 8.0) and then the proteins were diluted 1:2 with fresh refolding buffer and applied onto the equilibrated columns in the FPLC system for binding to the column. Unbound flow-through was collected. Bound proteins were eluted with filter-sterilised cold buffer B with gradient increase in NaCl (10 mM Tris, 0.4 M L-arginine, 5 mM GSSH [reduced glutathione] and 0.5 mM GSSG [oxidized glutathione] and 1 M NaCl; pH 8.0) and 0.5 mL fractions collected by fraction collector (Frac-950, Amersham Pharmacia). The dialysed protein sample, unbound flow-through and eluted fractions were analysed on reducing SDS PAGE gel and by Western blotting.

2.41. Small-scale purification of HA22 scFv-protamine-His6 recombinant fusion protein by nickel affinity chromatography:

To purify proteins under native conditions and optimise the system, small-scale protein purification was carried out to study the effect of no-dialysis versus dialysis on binding of His-tagged recombinant HA22 fusion protein to nickel column. Culture supernatant from HEK293F cells was divided into two equal fractions (20 mL each). One fraction was dialysed against PBS for 48 hours and the other fraction left undialysed. Nickel agarose beads Ni-NTA were used to prepare nickel affinity purification columns. For purification under native conditions, the Ni NTA resin was washed and resuspended in 600 μL of native protein binding buffer (50 mM NaH_2PO_4 and 0.5 M NaCl; pH 8.0) and centrifuged at 800 *g* for 1 minute at room temperature. The resin was then mixed with 800 μL of either undialysed or dialysed culture supernatant and allowed to bind for 90 minutes at 4°C using gentle mixing to keep the resin suspended in the protein solution. The resin/protein mixture was then loaded onto the purification column and allowed to settle by gravity. Unbound proteins passed through the resin and were collected for further analysis. The column was washed with native binding buffer (800 μL) and then washed four more times with 800 μL native wash buffer (50 mM NaH_2PO_4 and 0.5 M NaCl with 20 mM imidazole; pH 8.0) and the flow-through collected for analysis. The fusion protein was then eluted with 2 mL native elution buffer (50 mM NaH_2PO_4 and 0.5 M NaCl with 250 mM imidazole; pH 8.0) and analysed by Western blotting.

2.42. Large-scale purification of HA22 scFv-protamine-His6 by nickel affinity chromatography using FPLC system:

Large-scale cultures of HEK293F cells were transfected using PEI and about 3 litres of culture supernatant collected 3 days post-transfection by centrifugation at 5,000 rpm at 4°C for 10 minutes and frozen at -80°C until processed. All purification steps were performed at 4°C. Recombinant protein was purified using HiTrap 5 mL chelating HP nickel column (Amersham-Phrmacia, GE Healthcare) using an automated FPLC system. The culture supernatant was defrosted slowly at 4°C and filtered using a sterile vacuum filter unit, polyethersulfone (PES) membrane, with a 0.22 µm pore size low protein binding filter. The binding buffer (20 mM NaH_2PO_4 and 0.5 M NaCl; pH 7.4) was used to wash the FPLC tubing and to equilibrate the column with 5 column volumes at a flow rate of 2 mL/minute. The column pressure limit applied was 2.0 megapascal (MPa). The filtered protein sample was loaded directly onto the equilibrated column at 2 mL/minute flow rate over a period of 24 hours and unbound sample washed out and collected for analysis. The column was then washed with 6 column volumes of 20 mM imidazole in the binding buffer and the wash collected for analysis. The bound protein was eluted with 30 mL of the elution buffer (20 mM NaH_2PO_4, 0.5 M NaCl and 250 mM imidazole; pH7.4) and 6 fractions of 5 mL each collected. A further elution was followed with 500 mM imidazole and 3 fractions of 10 mL each collected to ensure that all His-tagged bound proteins had been eluted from the column. The column was then re-equilibrated with 5 column volumes of binding buffer. The sample load, wash and elution fractions were analysed by SDS PAGE and Western blotting. Purity of the protein was determined with Coomassie blue-stained gel. Purified protein fractions were concentrated by centrifugation at 5,000 x g for 30 minutes in 10,000 MWCO Vivaspin spin columns. After centrifugation, the resulting supernatant and the flow through were resolved on SDS PAGE and Western blotting.

2.43. Cation exchange chromatography:

The purified fusion protein obtained from the nickel affinity chromatography was subjected to further purification by cation exchange chromatography using a HiTrap SP FF column. A 1 mL HiTrap pre-packed SP FF (Fast Flow) Sepharose, cation exchanger column was installed on the FPLC system. The protein sample was dialysed against 20 mM Tris-HCl pH 7.5 for 48 hours in Slide-A-Lyzer 10,000 MWCO cassette. The retrieved protein sample was then gently resuspended and centrifuged at 1,200 rpm for 5 minutes at 4°C. Before sample loading, the cation column was equilibrated with 5 column volumes of wash buffer (20 mM Tris-HCl; pH 7.5) and the protein sample supernatant loaded at a 0.5 mL/minute flow rate into the equilibrated column at a column pressure limit of 4.00 MPa. The protein was eluted with a gradient increase of elution buffer (20 mM Tris-HCl and 0.5 M NaCl; pH 7.5) and fractions containing the purified protein identified by SDS PAGE and Western blotting.

2.44. Concentration and PD-10 desalting of the protein:

Eluted fractions of the protein were analysed on Coomassie blue-stained SDS PAGE gels and Western blots to determine purity and proportion of the protein in each fraction. Fractions that contained highly pure protein were pooled and concentrated using 10,000 Da MWCO Vivaspin columns. Concentrated protein fractions were then desalted using pre-packed Sephadex G-25 medium in disposable PD-10 desalting columns to remove imidazole from the protein. The pooled protein fraction was divided to two equal volumes and each one eluted from the PD-10 column with either buffer A (20 mM NaH_2PO_4 and 0.5 M NaCl; pH 7.4) or buffer B (20 mM Tris-HCl and 0.5 M NaCl; pH 7.4). For this purpose, the columns were equilibrated with five washes of 2.5 mL of binding buffer A or buffer B, followed by loading of 2.5 mL of the protein sample and elution with 3.5 mL of the binding buffer. Protein samples before and after PD-10 desalting were resolved by SDS PAGE and Western blotting.

2.45. Determination of protein concentration:

Concentration of purified proteins was determined using bicinchoninic acid protein assay kit (Pierce® BCA Protein Assay, Thermo Scientific) in fractions that were eluted with 500 mM imidazole. To generate a standard curve for measurement of protein concentration, 2-fold serial dilutions of protein samples and bovine serum albumin (BSA) standard (2 mg/mL in 0.9% NaCl and 0.05% NaN_3) were prepared in the binding buffer (20 mM NaH_2PO_4 and 0.5 M NaCl; pH 7.4). From each dilution 25 μL were added in duplicates into each well of a 96-well microplate. Then, 50 μL of Working Reagent (WR, 50:1), prepared by mixing 50 parts of BCA Reagent A (Na_2CO_3, $NaHCO_3$, $C_{20}H_{12}N_2O_4$ [bicinchoninic acid] and $Na_2C_4H_4O_6$ [sodium tartrate] in 0.1 M NaOH) with 1 part of BCA Reagent B (4% $CuSO_4.5H_2O$) were added to each well. The plate was incubated at 37°C for 30 minutes and the absorbance measured at 562 nm using a spectrophotometer. Protein concentration was determined by extrapolation from the linear equation of the standard curve obtained by plotting concentrations of BSA (μg/mL) versus absorbance using Microsoft Excel.

2.46. Optimisation of HA22 fusion protein preservation:

Recombinant protein was subjected to various storing conditions to optimise a method for maximal protein preservation. Fusion protein was, thus, stored either at 4°C, frozen at -80°C or stored in liquid N_2 in 10% glycerol. Under each condition three aliquots were preserved in different buffers (20 mM NaH_2PO_4 and 0.5 M NaCl; pH 7.4), (20 mM NaH_2PO_4 and 0.15 M NaCl; pH 7.4) or (20 mM Tris-HCl and 0.5 M NaCl; pH 7.4). All aliquots were retrieved after 10 days of storage and frozen samples defrosted slowly on ice. Visual observations for precipitate formation were noticed in some of the samples and all were re-analysed on Coomassie blue-stained SDS gels and by Western blotting.

2.47. Labelling of the recombinant protein with AlexaFluor®488:

AlexaFluor®488 dye was selected for labeling the recombinant protein because the die is brighter and more photostable than fluorescein. According to the manufacturer's instructions, the principle of the labeling using AlexaFluor®488 Microscale Protein Labeling Kit depends on the fact that tetrafluorophenyl (TFP) ester moiety in AlexaFluor®488 reactive dye solution reacts efficiently with primary amines of proteins to form stable dye-protein conjugates.

For the labeling reaction, 500 μL of protein solution (200 μg/mL) was transferred to a reaction tube and mixed with 50 μL of sodium bicarbonate (pH 8.3) to give a final concentration of 0.1 M. Meanwhile, the AlexaFluor®488 TFP ester dye was dissolved in its vial immediately before use by addition of 10 μL of dH_2O [11.3 nmol/μL reactive dye stock solution]. The appropriate volume of reactive dye solution was added to the reaction tube containing the pH-adjusted protein and mixed thoroughly by pipetting up and down several times. The reaction mixture was then incubated for 15 minutes at room temperature. The labeled protein was separated from the unbound dye by purification of the conjugated protein using resin gel in a spin column filter. For this purpose, the upper chamber of a spin filter in a collection tube was filled with resuspended resin gel and centrifuged at 16,000 *g* for 15 seconds. This was repeated until about half of the upper chamber was filled with resin gel. When the resin bed was at the correct level, the resin buffer was exchanged with the protein sample buffer (20 mM NaH_2PO_4 and 0.5 M NaCl; pH 7.4). This buffer exchange was carried out through the resin bed several times by brief low-speed centrifugation. After the spin filter was prepared, 50 μL of the conjugate reaction mixture was added onto the center of the resin bed surface. The conjugate was collected by centrifugation at 16,000 *g* for 1 minute. The labeled protein was stored at -20°C protected from light.

2.48. Assessment of the HA22 fusion protein binding to CD22 on B cell lines by flow cytometry:

In order to confirm that the purified HA22 fusion protein has retained its specificity, its binding to a panel of CD22-positive (HF28 RA and L3/Bcl-2) and CD22-negative (Jurkat and U937) cell lines was tested by flow cytometry. Cells grown to about 80% confluency were harvested, washed in ice-cold staining buffer (PBS containing 0.1% NaN_3 and 2% FBS) and chilled on ice. The cells were centrifuged at 1300 rpm for 5 minutes at 4°C and resuspended in ice-cold staining buffer containing Fc blocking agent (10% mouse serum) (233) and incubated on ice for 15 minutes. Resuspended cells were transferred to FACS tubes and their number adjusted to 5 x 10^5 cells /mL in each FACS tube. The cells were washed once with ice-cold staining buffer and stained either with AlexaFluor®488 labelled HA22 fusion protein (2-10 μg/mL) or with unlabelled protein (3 μg/mL) on ice for 1 hour. For unlabelled protein, the fusion protein was mixed with anti-6X His tag® antibody [DyLight®650] (abcam, Cambridge, UK) (1:500) for 20 minutes on ice before they were added to the cells. Before the FACS acquisition, the cells were washed twice and resuspended in ice-cold staining buffer. In order to exclude dead cells from the analysis 2 μL of propidium iodide was added to the FACS tubes and live cells were gated for the analysis. Anti-6X His tag® antibody [DyLight®650] and unstained cells were used as controls.

2.49. Demonstration of binding to and internalisation of the HA22 fusion protein into B cells by confocal microscopy:

For internalisation by confocal microscopy, CD22-negative Jurkat T cells and CD22-positive HF28 RA B cells were cultured at a density of 1 x 10^5 cells/well in 900 μL complete growth medium. After cultivation overnight, the cells were washed with ice-cold PBS containing 2% FBS and chilled on ice. Simultaneously, HA22 fusion protein (10 μg) was mixed with siGLO Red non-specific fluorescently-labeled siRNA (100 nM final concentration) and incubated on ice for 20 minutes (1.8 molecules of HA22 fusion protein:8 molecules of siGLO Red ratio). The cells were then stained with the complex and incubated on ice for 45 minutes. Unbound HA22 protein/siGLO Red was washed off with pre-warmed RPMI-1640 and the cells incubated at 37°C for various time points (15, 30, 45 and 60 minutes). The 0 time point was left on ice. At the end of the indicated time points, cells were kept on ice and washed once with ice-cold staining buffer and then incubated with proteinase K (2 mg/mL proteinase K in PBS) on ice for 30 minutes to remove surface bound molecules. The cells were then washed twice with PBS and fixed in paraformaldehyde (4% in PBS) for 10 minutes and treated with 0.1% Triton X-100 for 5 minutes. The cells were then stained with DAPI (1:5000) for 5 minutes at 4°C and washed twice with PBS. The cells were mounted on poly-L-lysine coated slides using anti-fade mounting medium (6 mL Citifluor anti-fade, 2.4 g Mowiol 4.88 [Calbiochem], 6 mL dH_2O and 12 mL 200 mM Tris-HCl, pH 8.5). Samples were analysed on a Zeiss LSM710 confocal microscope (Zeiss, Welwyn Garden City, UK).

2.50. Gel retardation assay:

siRNA (100 nM) was mixed with various concentrations of either HA22 fusion protein (10–100 μg) or A20FMDV2-protamine peptide (0.2–20 μg) and incubated on ice for 30 minutes. The mixture was then resolved on a 1% agarose gel containing 1 μg SYBER safe and visualised by UV illuminator.

2.51. siRNA for targeted genes:

Synthetic siGENOME SMARTpool siRNAs were obtained from Dharmacon (Thermo Scientific) composed of pools of four duplexes of 19 bp in length with 3' dinucleotide overhangs siRNAs. Cellular pathways and mechanisms that have roles in proliferation and survival were targeted with specific siRNAs. To achieve this, two genes were selected for targeting, *MCL1* and *PLK1*. These genes are known to promote cell proliferation and survival. In addition, *ITGB6* (integrin β6) was targeted to study tumour cell invasion using a specific targeting approach with A20FMDV2-protamine peptide. The specificity of selective binding of A20FMDV2 peptide to αvβ6 integrin has been clearly defined (113).

All of the selected siRNAs are specific for human genes. Control siRNA for the housekeeping gene was siGAPDH (Ambion by Life Technologies Ltd, Paisley, UK) as a positive control. Negative control includes a non-specific scrambled siRNA which is known not to downregulate any gene (Ambion by Life Technologies Ltd). Gene target sequences for the siRNAs are shown in Table 6.

Table 6: Gene designation, mRNA sequence targets and molecular weights of siRNAs.

Gene-specific target siRNA	mRNA target sequence	Mol. Wt. of siRNA (g/mol)
MCL1 gene – 10 noml siRNA		
siGENOME SMARTpool siRNA D-004501-41, MCL1	GCUACGUAGUUCGGGCAAA	13,403.0
siGENOME SMARTpool siRNA D-004501-40, MCL1	GGACCAACUACAAAUUAAU	13,343.0
siGENOME SMARTpool siRNA D-004501-39, MCL1	AGAACGAAUUGAUGUGUAA	13,343.0
siGENOME SMARTpool siRNA D-004501-38, MCL1	CGAAGGAAGUAUCGAAUUU	13,358.0
PLK1 gene – 10 nmol siRNA		
siGENOME SMARTpool siRNA D-003290-05, PLK1	CAACCAAAGUCGAAUAUGA	13,358.0
siGENOME SMARTpool siRNA D-003290-06, PLK1	CAAGAAGAAUGAAUACAGU	13,343.0
siGENOME SMARTpool siRNA D-003290-07, PLK1	GAAGAUGUCCAUGGAAAUA	13,358.0
siGENOME SMARTpool siRNA D-003290-08, PLK1	CAACACGCCUCAUCCUCUA	13,403.0
ITGB6 gene – 10 nmol siRNA		
siGENOME SMARTpool siRNA D-008012-01, ITGB6	GCUAAAGGAUGUCAAUUAA	13,343.0
siGENOME SMARTpool siRNA D-008012-02, ITGB6	GAACGGCUCUUUCCAGUGU	13,403.0
siGENOME SMARTpool siRNA D-008012-03, ITGB6	CAUCUCAGCUUAUGAAGAA	13,358.0
siGENOME SMARTpool siRNA D-008012-05, ITGB6	GCCAACCCUUGCAGUAGUA	13,403.0
Control siRNAs		
siRNA for *GAPDH* gene	Proprietary sequence	
siGLO Red transfection indicator	Proprietary sequence	
Scrambled siRNA (not targeting any known genes)	Proprietary sequence	

2.52. Preparation of siRNA:

Tubes containing siRNA were briefly centrifuged to ensure that all the siRNA content is collected at the bottom of the tube. siRNAs (10 nM) were resuspended in 500 µL of 1x Dharmacon siRNA buffer (20 mM KCl, 6 mM HEPES and 0.2 mM $MgCl_2$; pH 7.5) diluted in sterile nuclease-free H_2O. The solution (resuspended siRNA) was mixed gently and placed on an orbital mixer for 30 minutes at room temperature. The tubes were then centrifuged briefly to collect the solution at the bottom of the tube. A stock of 20 µM of each resuspended siRNA was aliquoted and kept at -80°C. The stocks were diluted in nuclease-free H_2O before use. Resuspension of siRNAs was performed in a sterile hood.

2.53. Cell transfection with siRNA using transfection reagents:

HF28 RA human B cells were grown in complete RPMI 1640 medium without antibiotics. For cell transfection, 100 nM of siRNA was mixed with INTERFERin or jetPRIME™ (Polyplus-transfection, Nottingham, UK) or NeoFX transfection reagent (Ambion by Life Technologies Ltd) according to manufacturer's instructions. Depending on the number of cells, an amount of the transfection reagent was mixed with siRNA and incubated at room temperature for 20 minutes. Before adding the mixture, fresh medium was added to the cells. The cells were incubated at 37°C for 3-5 days and then analysed for gene down regulation by real-time RT-PCR and reduction in protein levels by Western blotting.

2.54. Delivery of siRNA to mRNA of *MCL1* and *PLK1* genes with the HA22 fusion protein to B cells via CD22:

For the delivery of siRNA, cells were grown to about 80% confluency in antibiotic-free complete medium. Before transfection, fresh medium was added to the cells and the number of cells adjusted according to the scale of transfection. HA22 fusion protein (12.5 or 25 µg) was mixed with 100 nM of siRNA in a final volume of 100 µL. Protein/siRNA mixtures were incubated on ice for 30 minutes. The mixtures were then added to cells and incubated at 37°C for 2-5 days before analysis by real-time RT-PCR, Western blotting or cell viability assay. Etoposide was used as a positive cell death-inducing control. A scrambled siRNA was used as a negative control.

2.55. Quantitative real-time PCR experiments:

Quantitative RT-PCR (qRT-PCR) is an established technique for quantifying mRNA levels in biological samples. To perform qRT-PCR experiments, initially the assays were designed to make standards and reference genes for normalisation of data using the qRT-PCR facility (qStandard) at King's College London. Later, qRT-PCR experiments were performed in our laboratory and qRT-PCR plates were read at the Genome Centre, Queen Mary University of London using ABI7900HT Fast system from Applied Biosystems.

2.55.1. RNA extraction:

RNA extraction was performed according to a modified method using the Qiagen RNeasy column kit. According to the manufacturer's information, the kit extracts only RNA molecules that are > 200 nucleotides in length. For adherent cells, the medium was removed and the cells washed once with PBS. For non-adherent or suspension cells, the culture was centrifuged, medium removed and cells washed once in PBS. The cells were then lysed on ice by adding 300 µL of QIAzol (Qiagen Ltd) which preserves the integrity of the RNA. Cell lysates were clarified by centrifugation at 12,000 *g* for 5 minutes at 4°C and the supernatant transferred to a fresh tube and mixed with 200 µL chloroform. The mixture was centrifuged at 12,000 *g* for 10 minutes at 4°C. The aqueous phase was transferred to a fresh tube and 1.5 volumes of 100% ethanol added. The mixture was transferred to an RNeasy spin column placed in a 2 mL collection tube to adsorb RNA onto the silica gel membrane of the spin column and centrifuged at 8,000 *g* for 15 seconds. The flow-through was discarded and unwanted cellular contents (protein, DNA) washed away by adding 700 µL of RW1 buffer to the RNeasy spin column. The column was centrifuged at 8,000 *g* for 15 seconds. The column was then washed twice with 500 µL RPE buffer and the RNA eluted with 50 µL RNase-free H_2O by placing the RNeasy spin column in a fresh 1.5 mL collection tube and centrifugation at 8,000 *g* for 1 minute. Quantity and quality of RNA were determined using a Nanodrop spectrophotometer and agarose gel, respectively. RNA was then stored at -20°C until used.

2.55.2. cDNA synthesis by reverse transcription:

Total RNA isolated with QIAzol was reverse transcribed using a modified method. cDNA was made in triplicates for each sample by adding 1 μg of total RNA into each PCR reaction tubes. Template RNA was thawed on ice and prepared for genomic DNA elimination reaction (1:2 dilutions of 7x gDNA Wipeout Buffer 2 µL, variable amount of template RNA [microliters of total RNA calculated to give 1 µg] and RNase-free H_2O to total volume of 14 µL). Genomic DNA elimination reaction was carried out for 4 minutes at 42°C and then tubes placed immediately on ice. Reverse transcription mastermix was prepared on ice (Quantiscript Reverse Transcriptase containing RNase inhibitor 1 µL, 5x Quantiscript RT Buffer containing Mg^{2+} and dNTPs 4 µL and RT Primer Mix 1 µL). Template RNA (14 µL) from entire genomic DNA elimination reaction was added to each tube containing the reverse transcription mastermix, mixed and kept on ice. cDNA synthesis reaction was carried out by incubation for 15 minutes at 42°C followed by incubation for 3 minutes at 95°C to inactivate the reverse transcriptase. “No-reverse transcription” negative control sample labelled ‘RT negative’ was used to determine if there is any DNA contamination by addition of nuclease-free water to the mastermix without RNA template. Prior to use in qPCR reaction, the cDNA was diluted 10-fold (1:10) with tRNA (10 μg/mL) in a 1.5 mL centrifuge tube. This dilution was repeated for the “RT negative” control as well. tRNA is used simply as a carrier to minimise adsorption of cDNA onto surfaces. The tRNA itself cannot be amplified by PCR. It has also been reported to minimise primer-dimers. Dilution of cDNA ensures that the salts and buffers in the RT enzyme mix are diluted sufficiently to allow the proper conditions such as salt concentrations and pH to be achieved for efficient qRT-PCR. Furthermore, dilution ensures that the concentration of primers (oligo-dT, random primers used in the RT reaction) in the cDNA is reduced and so is less likely to generate any non-specific amplification during PCR (234).

2.55.3. DNA standards of reference genes:

For normalisation of qRT-PCR data, standards for reference genes and genes under investigation were designed and obtained from qStandard (King's College London). The qRT-PCR standards in each vial contained 1 x 10^9 copies of dried DNA standard (amplicon) purified from PCR products. Standards were reconstituted in yeast tRNA (5 μg/mL) dissolved in nuclease-free H_2O. Standards were prepared from the reference genes in 0.5 mL tube by serial dilutions of the 10^7 copies/2 μL down to 10^1 copies/2 μL in tRNA (5 μg/mL). A standard curve was constructed from the dilutions of each reference gene.

2.55.4. Setting up a qRT-PCR assay:

In the first qRT-PCR run, the primers were tested to ensure amplification of only the specific product expected and determine the melting point of the amplicon generated. Although this step could be performed in a normal PCR block, a qPCR machine was used to perform this for two reasons: (a) to check when the product amplifies in real-time and (b) to run a melt curve to check specificity. Simultaneously, the 'RT negative' sample was also subjected to qRT-PCR. This sample should not amplify as there is no DNA in the sample. A mastermix was prepared in a 1.5 mL centrifuge tube by using Brilliant III UltraFast SYBER Green qPCR Master Mix (Agilent Technologies, Berkshire, UK) as shown in Table 7.

Table 7: qRT-PCR mastermix for designed assays to generate the standards.

Reagent	Volume per reaction (μL)
Brilliant III SYBER Green qPCR mix (2x)	5.0
Forward primer (10 μM, 500 nm final)	0.5
Reverse primer (10 μM, 500 nm final	0.5
Nuclease-free H2O	2.0
Total per sample	8.0

From the mastermix, 8 μL was added to each reaction in the PCR tubes containing either 2 μL tRNA for no-template control (NTC), 2 μL of RT negative sample or 2 μL of two diluted cDNA (template) tubes. The final reaction volume was 10 μL per tube. The tubes were capped and run in qPCR machine using the conditions shown in Table 8. To determine primer specificity, size of the PCR products were determined on 2% agarose gels and compared with a 50 bp DNA ladder.

Table 8: Cycling conditions for qPCR for gene standards.

Step	Time	Temperature	Cycles
Activation	3 minutes	95°C	1x
Amplification:			
Denaturation	5 seconds	95°C	
Annealing	1 second	57°C	40x
Extension	1 second	57°C	
Melt		ramp from 65°C to 95°C rising by 1°C per step	

2.55.5. Measurement of gene expression by SYBER Green qRT-PCR:

In the next qRT-PCR run to measure gene expression, a standard curve was constructed by making serial 10-fold dilutions of standards that contains 10^7 copies in 2 μL. The final volume for each qRT-PCR reaction was 10 μL by adding 2 μL of template cDNA, or the diluted standards which contained from 10^7 to 10^1 copies per 2 μL to 8 μL of mastermix. SYBER qPCR kits come as a ready-to-use mix containing *Taq* polymerase enzyme, 10x polymerase buffer, dNTPs, SYBER dye and optimised Mg^{2+}.
qRT-PCR reactions were set up in a 384-well microplate in triplicates including NTC (no-template control) as a negative control (i.e. tRNA only, no cDNA), cDNA (unknown quantity sample, RT reaction) and dilutions of 10^1 to 10^7 gene copy standards of reference genes.

The qRT-PCR mastermix was prepared as shown in Table 7 with the addition of 0.3 μL of diluted (1:50 for a final concentration of 300 nM in the reactions) ROX reference dye (Agilent Technologies). Conditions of the qRT-PCR are shown in Table 9. The plate was then sealed, centrifuged briefly and the qRT-PCR run in an ABI7900HT Fast machine (Applied Biosystems) at the Genome Centre, Queen Mary University of London.

Table 9: qRT-PCR conditions for amplification of target genes.

Cycles	Duration of cycle	Temperature
1	3 minutes	95°C
40	5 seconds	95°C
	15 seconds	60°C

The data analysis software of qPCR machines allows for the generation of a standard curve and the calculation of the number of copies present in each of the unknown cDNA samples. For SYBER Green-based assays, the software can also check the melting temperature of the product generated in every one of the samples; this is called melting analysis.

2.55.6. Targeted and reference genes

Assays were designed to study the expression level of mRNA of genes under investigation using qRT-PCR. The most commonly used housekeeping genes as references for normalisation in qRT-PCR assays and the targeted genes are shown in Table 10.

Table 10: Primer sequences of targeted and reference genes.

Target genes	Forward primer (5' to 3')	Reverse primer (5' to 3')
Myeloid cell leukaemia sequence1 (*MCL1*)	CGGCAGTCGCTGGAGATTATC	TGATGTCCAGTTTCCGAAGCA
Polo-like kinase1 (*PLK1*)	ACTGCCACCTCAGTGACATG	ATCACAGAGCTGATACCCAAGG
Reference genes	Forward primer (5' to 3')	Reverse primer (5' to 3')
β-actin (*ACTB*)	CACCATGTACCCTGGCATT	CCGATCCACACGGAGTA
β-2 microglobulin (*B2M*)	CTCTCTCTTTCTGGCCTGGAG	ACCCAGACACATAGCAATTCAG
Glyceraldehyde-3-phosphate dehydrogenase (*GAPDH*)	TGCACCACCAACTGCTTAGC	GGCATGGACTGTGGTCATGAG
Phosphoglycerate kinase (*PGK1*)	CCTCGTTGACCGAATCACC	AGCAGCCTTAATCCTCTGGT
Transferrin receptor (*TFRC*)	ATCTGAACCAATACAGAGCAGACAT	GAGGAAGTGATACTCCACTCTCAT

Note:
For *MCL1*, *ACTB* and *B2M* genes, assays are designed with intron-flanking primers which amplify genomic DNA if present in the samples.
For *PLK1*, *GAPDH*, *PGK1* and *TFRC* genes, assays are designed with intron-spanning primers. If genomic DNA is present in a sample it should not be amplified. Primers of this assay amplifies mature transcript.

2.56. CellTiter-Glo® luminescent cell viability assay:

The CellTiter-Glo® Luminescent Cell Viability Assay is a method used to determine the number of viable cells in culture. Detection is based on using the luciferase reaction to measure the amount of ATP in viable cells. The amount of ATP in cells correlates with cell viability. Measurement of cell viability indirectly reflects amount of cell death under investigation. In order to measure cell viability in cell death induction experiments, after the incubation period, 100 µL of CellTiter-Glo® reagent was added to cells and incubated at room temperature for 20 minutes. Complete reagent mixing with cells was achieved by centrifugation at 1,200 rpm for 2 minutes at room temperature. The lysates were transferred to opaque-walled multiwell plates and relative light units (RLU) measured in Dynex Technologies MLX 96 Well Plate Luminometer (Dynex Technologies Inc., Sussex, UK).

2.57. Measurement of activated caspase-3 and -7:

The Caspase-Glo® 3/7 luminescent assay measures the activation of the cysteine aspartic acid-specific protease caspase-3 and -7. The assay is based on a luminogenic caspase-3/7 substrate, which contains the tetrapeptide amino acid sequence Asp-Glu-Val-Asp sequence (DEVD) in a reagent optimised for caspase activity, luciferase activity and cell lysis. Accordingly, 50 µL of the Caspase-Glo® 3/7 Reagent was added to cells in each well of a 96-well microtiter plate for cell lysis, cleavage of the DEVD substrate by activated caspase-3 and -7 with release of aminoluciferin. Aminoluciferin would then generate luminescent signal by luciferase activity. Luminescence is proportional to the amount of activated caspase-3 and -7 present in the cells. The lysates were transferred to opaque-walled multiwell plates and the RLU measured in 96 Microplate Luminometer.

2.58. A20FMDV2-protamine peptide:

A 42-mer fluorescence-labeled synthetic peptide with an RGD motif that combines the A20FMDV2 with the truncated protamine domain in a single peptide which is FITC-Ahx-A20FMDV2-protamine (fluorescein isothiocyanate-aminohexanoic acid-NAVPNLRGDLQVLAQKVART-RSQSRSRYYRQRQRSRRRRRR) was obtained from PeptideSynthetics (Hampshire, UK). The peptide, which has a molecular mass of 5566.33 g/mol, was generated *in vitro* using an automatic synthesiser and 10.8 mg of the product purified by reversed phase-HPLC in acetonitrile and H_2O containing 0.1% trifluoroacetic acid and was supplied lyophilised. For the purpose of imaging studies, the peptide was labeled with FITC at the N-terminus.

2.58.1. Resuspension of the peptide:

Lyophilised FITC-Ahx-A20FMDV2-protamine peptide was brought to room temperature and resuspended in 192 μL of 100% DMSO (1.1 g/mL) to give a final stock concentration of 10 mM. The peptide was aliquoted and frozen at -20°C and further diluted with the growth medium before adding it to cells.

2.59. Binding to αvβ6 integrin and internalisation of A20FMDV2-protamine peptide by confocal microscopy:

For internalisation by microscopy, monolayers of αvβ6-negative (A375Ppuro or DX3Ppuro) and αvβ6-positive (A375Ppuroβ6 or DX3Ppuroβ6) cells were plated onto 13 mm diameter coverslips placed in a 4-well plate (Thermo Fisher Scientific Inc.) (2 x 10^4 cells per well) overnight. The cells were washed with chilled DMEM and medium was replaced with ice-cold FITC-Ahx-A20FMDV2-protamine peptide (100 nM peptide/500 μL serum-free DMEM). After 15 minutes incubation on ice, unbound peptide was washed off with pre-warmed DMEM and cells incubated at 37°C for various time points (10, 20, 30, 40, 50 and 60 minutes). For the 0 time point, the cells were left on ice. At the end of the indicated time points, the coverslips were removed, cells fixed in formaldehyde (4% in PBS) for 10 minutes and then treated with 0.1% Triton X-100 for 5 minutes. The cells were washed with PBS and stained with DAPI (1:5000) for 5 minutes. The coverslips were mounted on slides using anti-fade mounting medium. Samples were analysed using a Zeiss LSM710 confocal microscope (Zeiss, Welwyn Garden City, UK).

2.60. Delivery of siGLO Red siRNA with A20FMDV2-protamine peptide:

Monolayers of αvβ6-negative A375Ppuro and αvβ6-positive A375Ppuroβ6 cells were plated onto 13 mm diameter coverslips placed in a 4-well plate (2 x 10^4 cells per well) overnight. Next day, FITC-Ahx-A20FMDV2-protamine peptide was diluted in growth medium to 10 µM and bound with siGLO Red siRNA (10 nM) for 15 minutes on ice. The cells were washed with DMEM, chilled on ice and medium replaced with ice-cold FITC-Ahx-A20FMDV2-protamine/siGLO Red mixture. After 15 minutes on ice, unbound peptide/siRNA was washed off with pre-warmed DMEM and cells were incubated at 37°C for various time points (15, 30, 45 and 60 minutes). The rest of the procedure was as described in the previous section to test for internalisation of the peptide by confocal microscopy.

2.61. Delivery of siRNA for *ITGB6* gene with A20FMDV2-protamine peptide:

Monolayers of only αvβ6-positive VB6 cells were plated in a 12-well plate at a density of 0.1-0.4 x 10^6 cells per well in 1 mL complete growth medium overnight. Next day, cells were washed and medium replaced with fresh DMEM. FITC-Ahx-A20FMDV2-protamine peptide was diluted in growth medium to 100 nM and bound with siRNA for *ITGB6* (10-100 nM) for 15 minutes on ice. The mixture was then added to cells and incubated at 37°C for 3-5 days. Cells were harvested and analysed by Western blotting for ITGB6 protein.

2.62. Statistical analyses:

Data analyses were conducted using the Microsoft Excel 2007 and GraphPad Prism software version 5.00 (GraphPad Software, California, USA). Values are given as mean ± standard error of the mean (SEM) where *n* represents the number of experiments carried out. The significance of difference between two groups at a given time was determined by unpaired Student's *t*-test.

Chapter Three

Construction and Generation of anti-Mouse CD22 scFv Recombinant Proteins

In this chapter, methods for the isolation, fluorescence labeling, binding and internalisation assays by flow cytometry and confocal microscopy of the mouse anti-CD22.2 mAb are presented and discussed. Furthermore, results on the generation of proteins by recombinant DNA technology, analysis, multi-step purification and test for biology of the fusion proteins are presented.

The objective was to identify and use a suitable anti-CD22 mAb in order to generate recombinant anti-CD22 scFv-protamine-His6 fusion protein that retains the ability to bind specifically to and be internalised by mature B cells.

3.1. The Cy34.1.2 hybridoma as a source of anti-CD22.2 mAb:

B cells are known to express an extensive array of surface molecules collectively termed Lyb and Ly antigens. Lyb-8.2, a murine B lymphocyte differentiation glycoprotein, is expressed on pre-B cells and on all mature B lymphocytes. The molecular weight of the protein is 95–105 kDa and its expression is controlled by a locus on chromosome 7. Mouse strains C57BL/6J, C57BL/10J, B10.D2, SJLJ, A.CA, A/J, AL/N, BALB/c, C3H/HeJ, CBA/J, C57L/LJ, C58, RF/J, SWR/J, CE/J, C3H.SW, CBA/N, (CBA/N x BALB/c)F_1 ♂ and ♀ (DBA/2 x BALB/c)F_1 are positive for Lyb-8.2. The Cy34.1.2 hybridoma was generated from DBA/1 mice immunised with spleen cells of B10.D2 mice. The hybridoma secretes non-cytotoxic IgG1 antibody which identifies Lyb-8.2 antigen on B lymphocytes from the strains mentioned above (235).

3.2. Isolation of the anti-CD22.2 mAb from culture supernatants of Cy34.1.2 hybridoma:

The mouse Cy34.1.2 mAb was purified from culture supernatants of the hybridoma using protein G-coated beads (Millipore). Integrity and purity of the purified mAb was assessed on a Coomassie blue-stained SDS-PAGE gel. A sample of the purified mAb was analysed under non-reducing and reducing conditions (Figure 21). The non-reducing gel showed a ~150 kDa band representing the intact IgG. When the purified mAb was analysed under reducing conditions, there were two main bands, ~25 kDa and ~50 kDa bands representing the light and the heavy chains of the mAb, respectively. Minor contaminations of the mAb could also be seen on the gels. A pre-stained protein marker was used to determine the molecular mass of each band. Concentration of the protein at 280 nm (A_{280}) = 4.82 mg/mL.

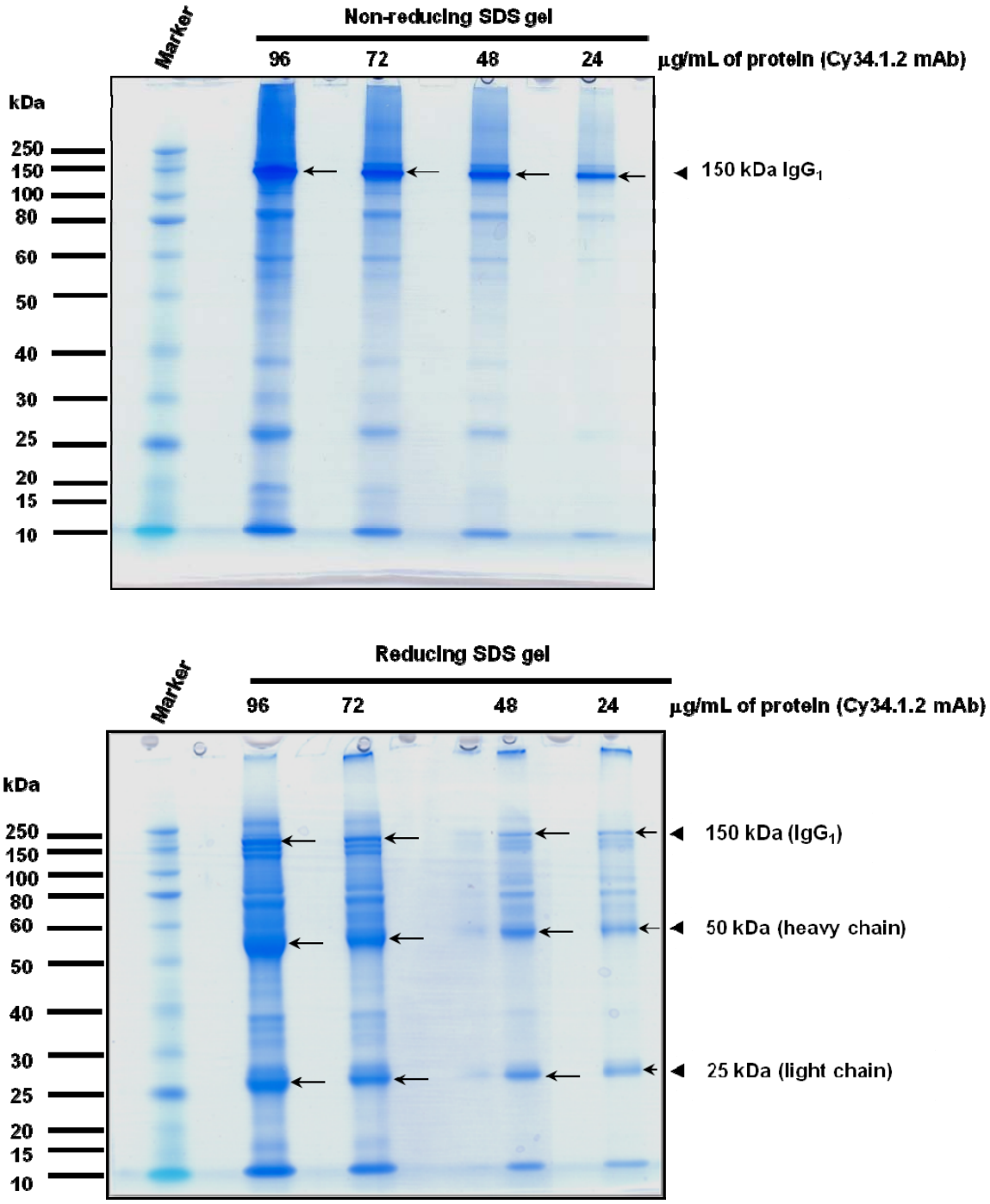

Figure 21: SDS PAGE analysis of affinity purified mAb Cy34.1.2. Approximately 96, 72, 48 and 24 µg/mL of the purified protein were subjected to gel electrophoresis on a 10% pre-cast NuPAGE gel under non-reducing condition (top) or reducing condition (bottom). The proteins were reduced using 2-mercaptoethanol added to the denaturing sample buffer and incubated for 10 minutes at 95°C. Protein bands were visualised by Coomassie brilliant blue staining (SimplyBlue™ SafeStain, Invitrogen). No or minimal contamination with BSA (66.5 kDa) and other protein impurities can be seen.

3.3. Expression of CD22.2 on mouse B cells was detected by flow cytometry:

CD22.2 expression on the mouse B cell line BCL1-3B3 was assessed using two antibodies, the commercial anti-CD22.2 FITC (Cy34.1, BD Biosciences) and the purified Cy34.1.2 mAb that was labelled with AlexaFluor®488 fluorescent dye. The cell line BCL1 is a clone of 13.20-3B3 derived from leukaemic peripheral blood B lymphocytes of BALB/c mice. The binding of anti-CD22.2 mAb was assessed by gating on positive living cells in the forward scatter. The cells were also stained with an isotype control and used as a negative control for background fluorescence staining during the acquisition. The FACS data were analysed using CellQuest software (Figure 22).

Furthermore, binding and the kinetics of internalisation of CD22.2 receptor on BCL1-3B3 B cells was assessed by confocal microscopy using AlexaFluor®488 conjugated anti-CD22.2 mAb. The reason for using AlexaFluor®488 conjugated anti-CD22.2 mAb was to address the problem of rapid photobleaching associated with the use of the commercial FITC labelled anti-CD22.2 mAb (section 3.4, page 124).

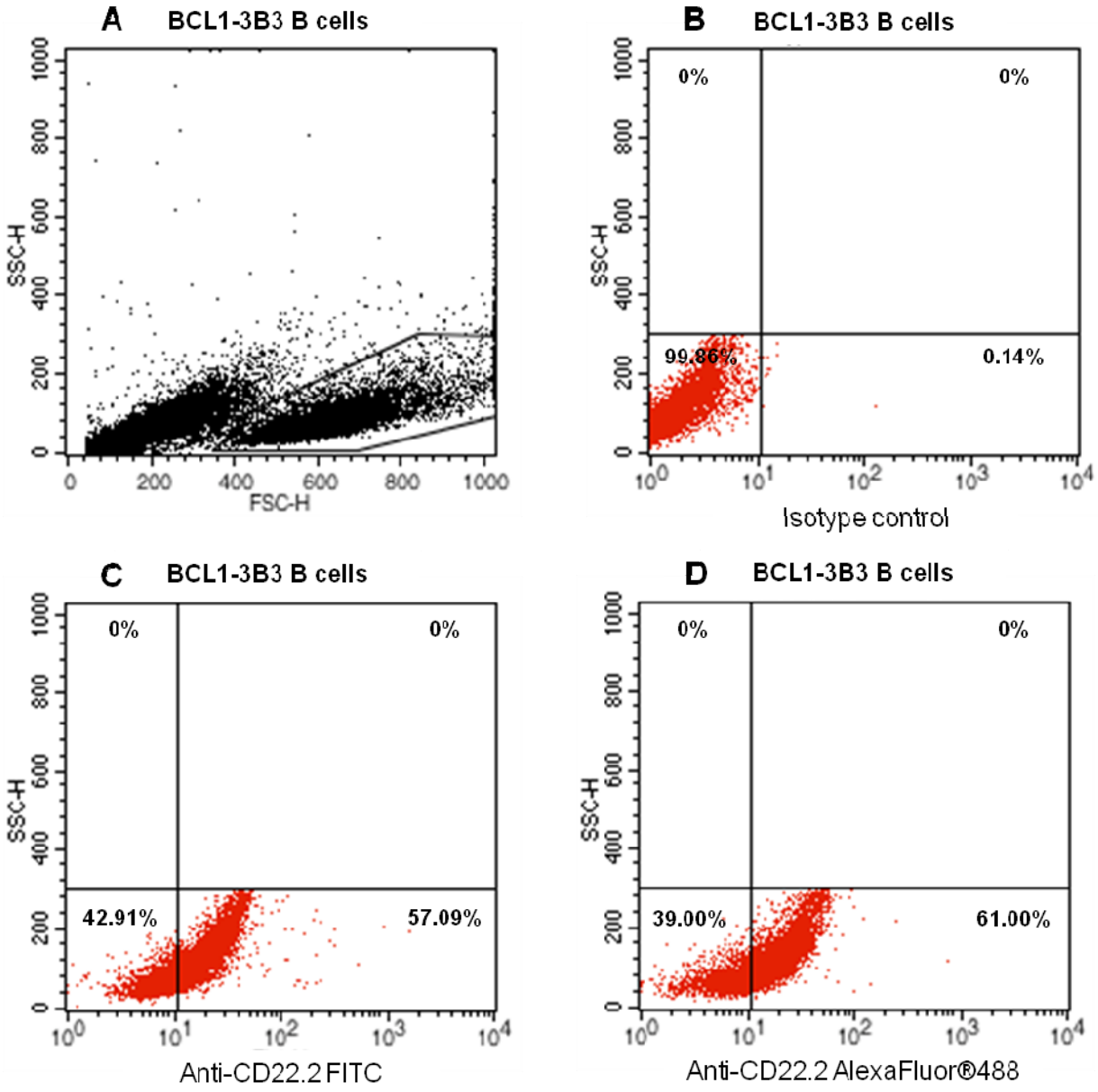

Figure 22: Analysis of murine BCL1-3B3 B cells for CD22.2 expression by flow cytometry. The figure depicts FACS profiles for the BCL1-3B3 cells. Dot plots (A) showing the forward and side scatter for the cells; (B) illustrating cells stained with the isotype control mAb (FITC mouse IgG1 kappa) with fluorescence on the x-axis. CD22.2 staining using anti-CD22.2 Cy34.1 FITC commercial Ab (C) and using AlexaFluor®488-conjugated Cy34.1.2 mAb (D).

3.4. Kinetics of anti-CD22.2 internalisation in B cells by confocal microscopy:

To study the kinetics of internalisation of CD22.2, BCL1-3B3 B cells that were stained with anti-CD22.2 FITC mAb and DAPI blue nuclear stain did not show CD22.2 on cell surface but the blue-stained nuclei of the cells were clearly seen under the microscope (data not shown) when examined by confocal laser scanning microscopy (CLSM). The reason for this could be due to the rapid photobleaching of the FITC fluorophore, which is a recognised problem. Therefore, preventing the fading of fluorescence intensity caused by the excitation light is very important for obtaining stable and accurate images (236).

To address this problem, the purified Cy34.1.2 mAb was conjugated with AlexaFluor®488. The BCL1-3B3 cells were stained with the anti-CD22.2 AlexaFluor®488 conjugated Cy34.1.2 mAb and analysed for expression and kinetics of internalisation of the surface CD22.2 by CLSM. The cells were analysed for CD22.2 internalisation at different time points incubated at 37°C. Demonstration of binding and internalisation by confocal microscopy was thus improved significantly by prevention of photobleaching and fading using AlexaFluor®488 dye. The analysis showed that the anti-CD22.2 was rapidly endocytosed by the cells with clear internalisation visible after 30 minutes. Cells were also stained with DAPI (Figure 23).

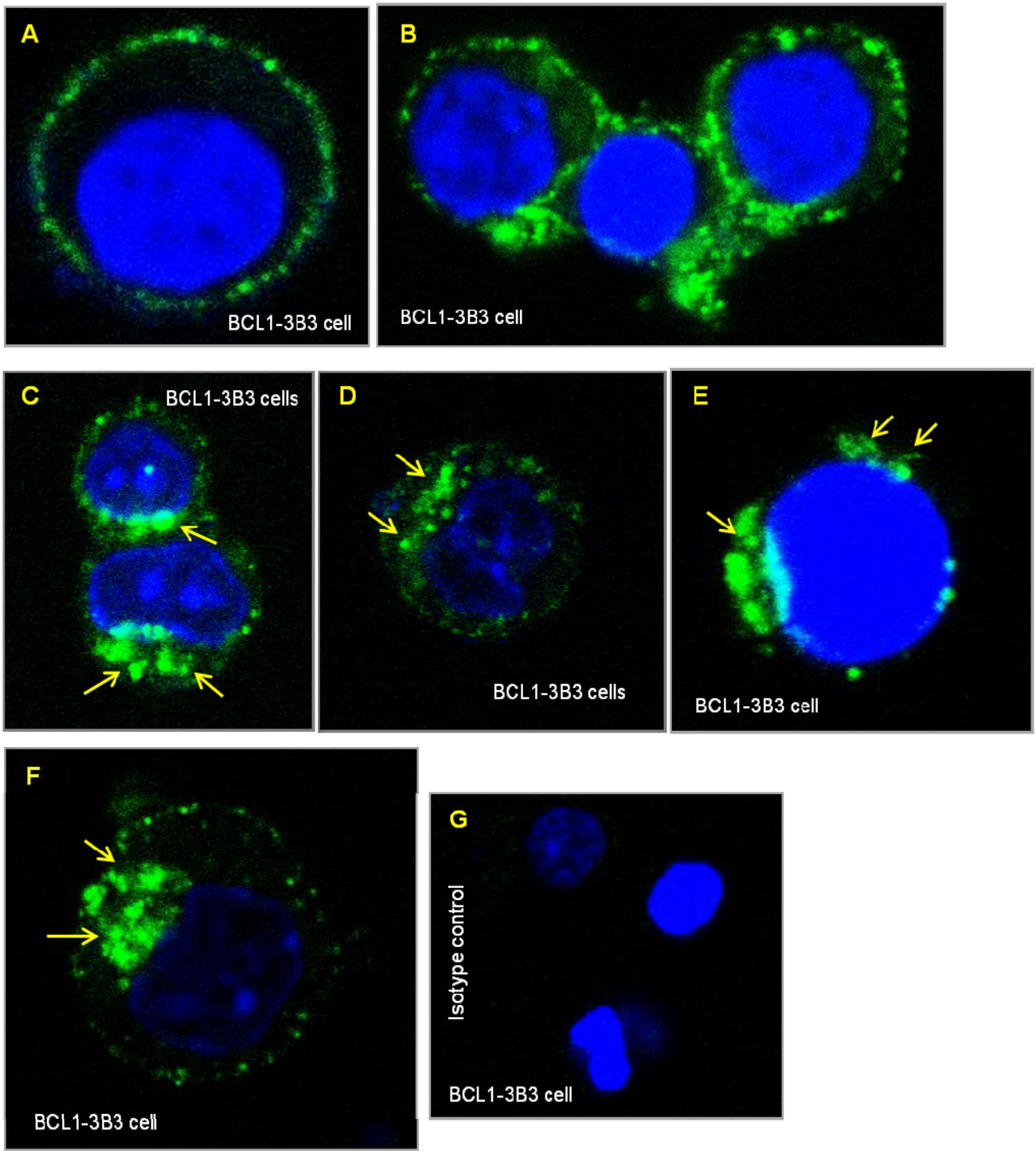

Figure 23: Confocal microscopic analysis of the kinetics of CD22.2 internalisation following Cy34.1.2 AlexaFluor®488 binding. Membrane binding of Cy34.1.2 AlexaFluor®488 to CD22.2 on murine BCL1-3B3 B cells (A and B) at 4°C followed by internalisation into the cell after 30 minutes incubation at 37°C (C and D) and 60 minutes (E and F). CD22.2 internalisation is evident from capping and punctate staining of endocytic vesicles (arrows) visible in cells incubated at 37°C. Cells stained with the isotype control AlexaFluor®488 anti-mouse IgG_1 at 4°C (G). The nuclei are stained with DAPI. Slides were examined with 63x oil immersion lens in LSM 710 Zeiss confocal microscope.

3.5. Quality and integrity of RNA extracted from Cy34.1.2 hybridoma cells assessed on agarose gel:

Isolation of intact RNA is essential for many techniques regardless of the downstream application. The most common method used to assess the quality of total RNA is to run an aliquot of the RNA sample on an agarose gel. Intact total RNA obtained from eukaryotic samples will have clear 28S and 18S rRNA bands. The 28S rRNA band should be approximately twice as intense as the 18S rRNA band. This 2:1 ratio (28S:18S) is a good indication that the RNA is completely intact.

The A_{260}/A_{280} ratio at 1:20 dilution of RNA extracted from the Cy34.1.2 hybridoma cells was 2.08. Analysis of the RNA by electrophoresis showed two bands of 1900 bp and 4800 bp which are rRNA bands of 18S and 28S, respectively (Figure 24). The 28S rRNA band was approximately twice as intense as the 18S rRNA band; this 2:1 ratio indicates intact RNA.

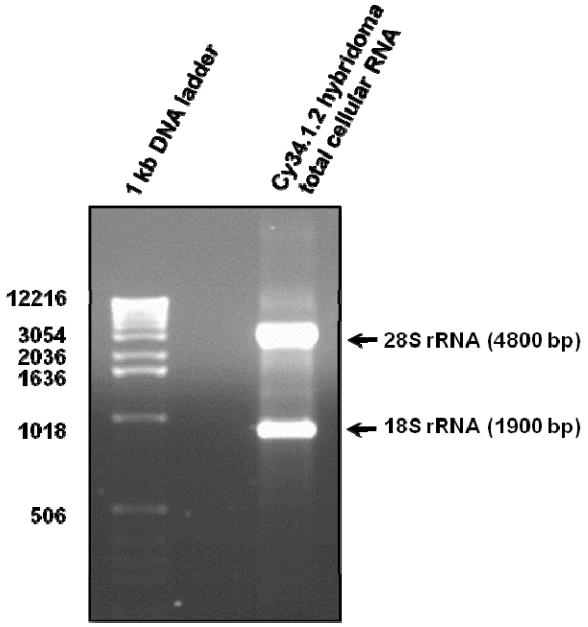

Figure 24: Analysis of quality and integrity of total RNA extracted from Cy34.1.2 hybridoma cells. Total RNA was run on a 1% agarose gel and shows two distinct ribosomal bands corresponding to 18S (1900 bp) and 28S (4800 bp) RNA species.

3.6. Poly-G tailing and amplification of cDNAs for the V_H and V_L genes of Cy34.1.2 mAb by PCR for cloning:

Sequences of the V_H and V_L of the Cy34.1.2 anti-CD22.2 mAb were not known at the start of this study. The family group, to which the V_H and V_L of Cy34.1.4 belong, was unknown and no primers could, therefore, be designed to anneal with the leader sequences of either chain. To amplify the cDNA of the two genes, a sequence composed of guanine bases (poly-G tail) was, therefore, intentionally added to the 5'UTR sequence of the V_H and V_L using the enzyme terminal deoxynucleotidyl transferase (TdT). Amplification of the V_H and V_L genes would then be possible with the aid of a primer specific to the poly-G tail (namely, poly-C primer with a restriction site) and primers that anneal to sequences within the 5' of the C_H1 and C_κ of the mAb. cDNA was made from RNA after concentrating the RNA by precipitation with 0.3 M sodium acetate and ethanol. The newly-synthesised cDNA was extracted with equal volumes of phenol:chloroform and used for the poly-G tailing reaction.

Using commercially-available PCR purification kits, a considerable amount of material was lost during cleaning of the cDNA. To solve this problem, columns packed with sterile Sephadex G-25M were made for this purpose. cDNAs for the V_H and V_L genes were then passed through a size-exclusion column (Sephadex G-25M PD10, GE Healthcare) to remove excess dNTPs, primers and salts from the solution, the enzyme reverse transcriptase and buffer. The filtrates which contained the purified cDNAs were then used in the poly-G tailing reaction. Tailed cDNAs were passed through the Sephadex G-25M size-exclusion column again to remove excess dGTPs, salts in the solution, TdT and the caccodylate buffer and then used for the PCR. The PCR products of both V_H and V_L cDNA were analysed on a 1% agarose gel and DNA bands extracted using PureLink® Quick Gel Extraction Kit. The purified PCR products were used for TA cloning (Figure 25).

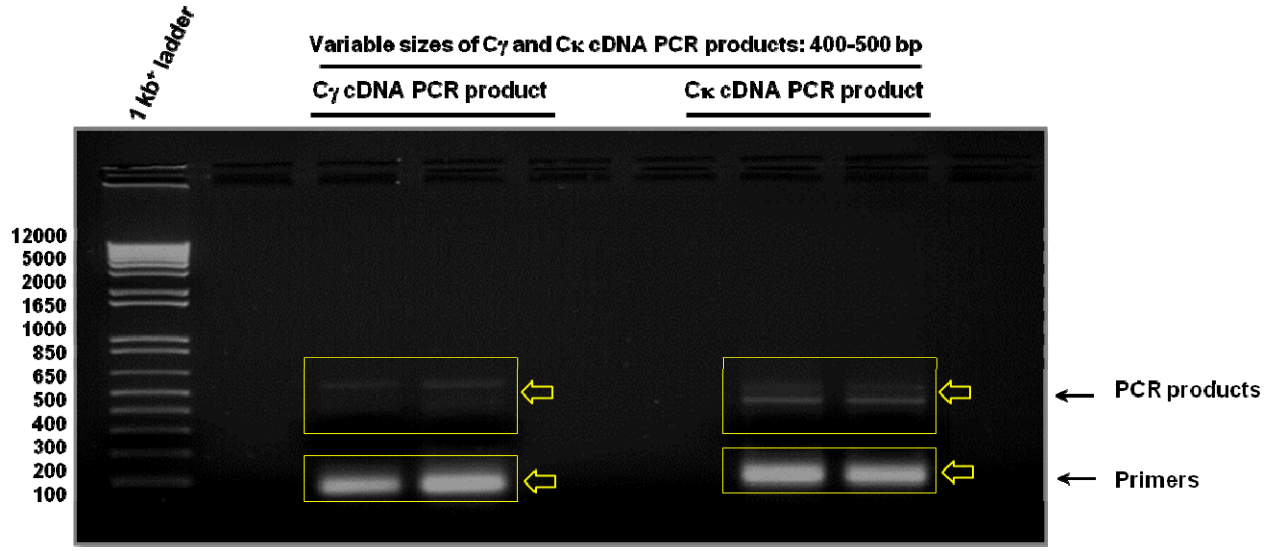

Figure 25: Agarose gel electrophoresis for the analysis of nested PCR products of V_H and V_L genes using primers in the Cγ and Cκ and a primer for the poly-G tail. cDNAs were amplified using internal primers in the Cγ and Cκ and a primer to the poly-G tail.

The predicted size of cDNA for both the V_H and V_L genes would be ~330 bp. Analysis of the products showed multiple bands with slightly different sizes on the agarose gel. The presence of multiple bands is likely to be due to the fact that the length of the added poly-G sequence is inconsistent and results in more G bases added onto the 5'UTR leader sequence of some of the cDNA molecules than others. There was also a low cDNA yield for both the V_H and V_L genes due to the considerable loss of cDNA during the purification process.

3.7. PCR products of V_H and V_L genes of Cy34.1.2 mAb were analysed:

PCR products of the poly-G-tailed cDNA for the V_H and the V_L genes were cloned into the linearised pCR®2.1 TA vector and used to transform DH5α *E. coli* and DNA minipreparations from positive transformants used in sequencing. This was achieved by cloning the PCR product for the V_H and the V_k genes of Cy34.1.2 mAb into the pCR®2.1 plasmid (Figure 26).

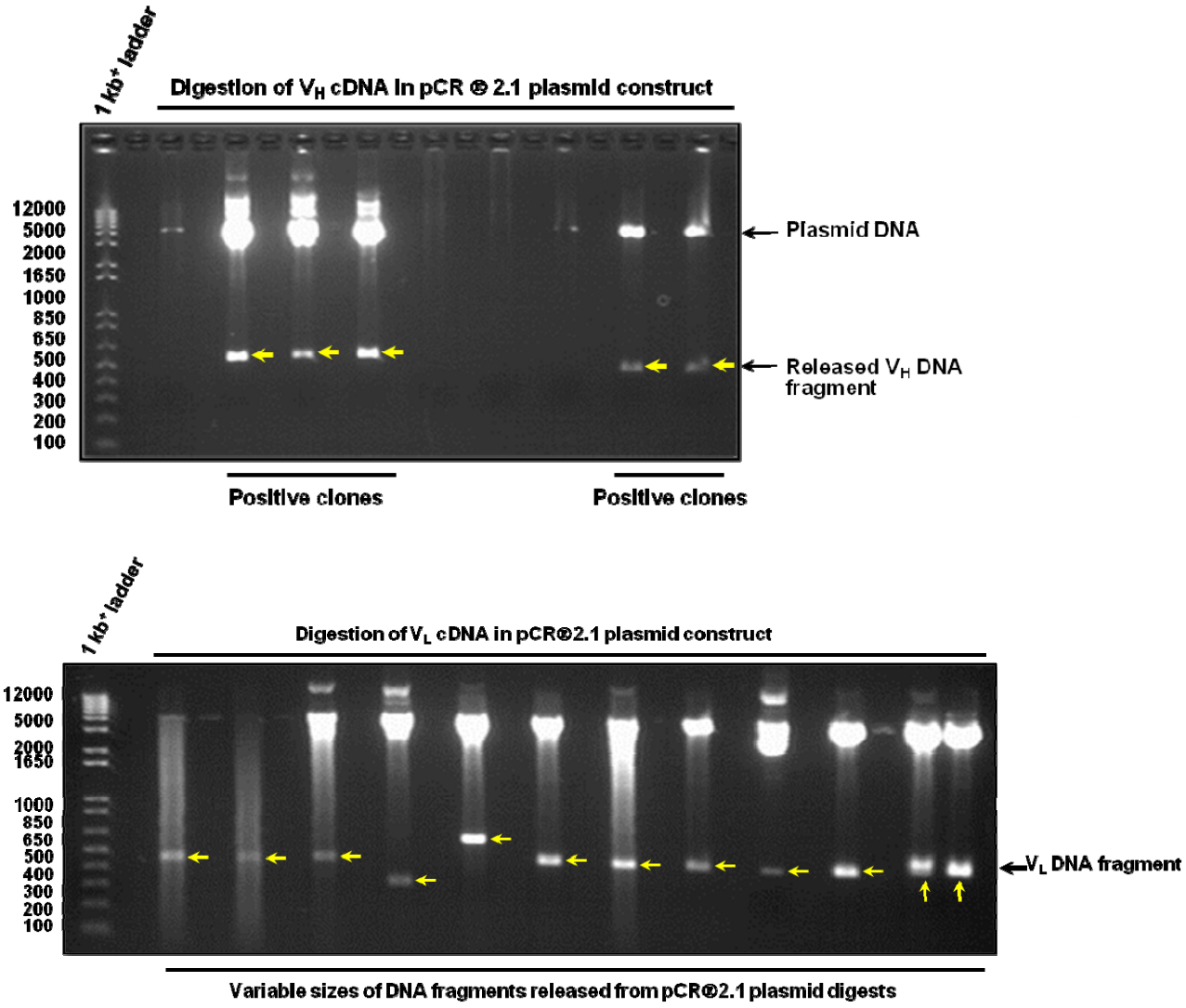

Figure 26: Restriction analysis of pCR®2.1 plasmid DNA constructed with PCR products for the V_H and the V_L genes of Cy34.1.2 mAb. The nested PCR products generated using anchor and internal primers were cloned into the pCR®2.1 plasmid. The resulting pCR®2.1 plasmid construct DNAs were restricted with *Eco*RI to release the V_H (top) and the V_L (bottom) cDNA. Plasmid DNAs with inserted PCR products for the V_H and the V_L genes of Cy34.1.2 mAb were sequenced and analysed by NCBI/BLAST search.

3.8. Determination and analysis of nucleotide sequences of the V_H and V_L of Cy34.1.2 mAb:

Nucleotide sequences of the V_H and V_L genes of Cy34.1.2 were analysed using Basic Local Alignment Search Tool (BLAST) in the National Center for Biotechnology Information (http://www.ncbi.nlm.nih.gov/). BLAST, an algorithm for comparing primary biological sequence information such as amino acids or nucleotides, enables you to compare a query sequence with a library of sequences and identify library sequences that resemble the query sequence above a certain threshold. The database allows specialised IgBLAST (http://www.ncbi.nlm.nih.gov/igblast/) for particular species. The process involved entry of the nucleotide sequence into an interactive program and selection of the species (in this case mouse for Cy34.1.2 mAb V_H and V_L) and the library (KABAT). The database will automatically search and align the query to all available sequences and matches the query sequence with the closest relating germ-line gene families. Accordingly, the IgBLAST searches generated alignments with related germ-line nucleotide sequences and similarity was observed with the IgH-VJ558 V_H1 gene family for the mouse immunoglobulin V_H gene family. The V_L gene family was determined as the Igκ-V24/25 subgroup. Based on the alignments it was then possible to identify the framework (FWR) and the hypervariable regions [complementarity determining regions (CDRs)] of the V_H and V_L genes. In parallel, the sequence of the signal peptide at the N-terminal end of the mAb was determined by analysis of the variable region of both V_H and V_L genes using a bioinformatics protein hydrophobicity plot as described in chapter two. Full length nucleotide sequences of V_H and V_L genes after sequencing from TA cloning vector are shown in Appendix 2, pages 341 and 342 respectively. Results of analyses of the nucleotide sequences and amino acids of the signal peptide are shown in Figure 27. The process of sequence analysis is described in section 2.14, page 67.

Cy34.1.2 V_H gene nucleotide sequence:

```
                |                        Native signal sequence                                 |
               ATG AGA TGG AGC TGT ATC ATT CTC TTC TTG GTA GCA ACA GCT ACA AGT GTC GAC TCC
                M   R   W   S   C   I   I   L   F   L   V   A   T   A   T   S   V   D   S
                |                                FWR1
Rearranged     CAG GTC CAA CTG CAG CAG CCT GGG GCT GAA ATT GTG AGG CCT GGG ACT TCA GTG AAG
a.a             Q   V   Q   L   Q   Q   P   G   A   E   I   V   R   P   G   T   S   V   K
IgH-VJ558 VH1  ... ... ... ... ... ... ... ... ... GAG CTT ... AAG ... ... GCT ... ... ...
a.a.            Q   V   Q   L   Q   Q   P   G   A   E   L   V   K   P   G   A   S   V   K

                                                                | |     CDR1        | |
Rearranged     CTG TCC TGT AAG GCT TCA GGC TAC ACC TTT ACC GAC TAT TGG ATG AAC TGG GTG AAG
a.a             L   S   C   K   A   S   G   Y   T   F   T   D   Y   W   M   N   W   V   K
IgH-VJ558 VH1  ... ... TGC ... ... TCT ... ... ... TTC ACA AGC TAC ... ... CAC ... ... ...
a.a.            L   S   C   K   A   S   G   Y   T   F   T   S   Y   W   M   H   W   V   K

                            FWR2                                | |
Rearranged     CAA AGG CCT GGA CAA GGC CTT GAG TGG TTC GGA GCA ATT GAT CCT TCT GAT AGT TAT
a.a             Q   R   P   G   Q   G   L   E   W   F   G   A   I   D   P   S   D   S   Y
IgH-VJ558 VH1  CAG ... ... ... ... ... ... ... ... ATT ... GAG ... ... ... ... ... ... ...
a.a.            Q   R   P   G   Q   G   L   E   W   I   G   E   I   D   P   S   D   S   Y

                            CDR2                  | |             FWR3
Rearranged     ACT AGG TAC AAT CAA GAG TTC AAG GGC AAG GCC ACA TTG ACT GTA GAC ACA TCC TCC
a.a             T   R   Y   N   Q   E   F   K   G   K   A   T   L   T   V   D   T   S   S
IgH-VJ558 VH1  ... AAC ... ... ... AAG ... ... ... ... ... ... ... ... ... ... AAA ... ...
a.a.            T   N   Y   N   Q   K   F   K   G   K   A   T   L   T   V   D   K   S   S

Rearranged     ACC ACA GCC TAC ATG CAG CTC AGC AGC CTG ACA TCC GAG GAC TCT GCG GTC TAT TTC
 a.a            T   T   A   Y   M   Q   L   S   S   L   T   S   E   D   S   A   V   Y   F
IgH-VJ558 VH1  AGC ... ... ... ... ... ... ... ... ... ... TCT ... ... ... ... ... ... ...
a.a.            S   T   A   Y   M   Q   L   S   S   L   T   S   E   D   S   A   V   Y   F

                      | |             CDR3                  |
Rearranged     TGT GCA AGA TCG GAC TAT ACT TAC TCA TTC TAC TTT
a.a             C   A   R   S   D   Y   T   Y   S   F   Y   F
IgH-VJ558 VH1 ... ... ... ... ... ... ... ... ... ... ... ...JH2
a.a.            C   A   R   S   D   Y   T   Y   S   F   Y   F
```

Cy34.1.2 V_L gene nucleotide sequence:

```
                |                                FWR1
Rearranged     GAT ATT GTG ATG ACG CAG GCT GCA TTC TCC AAT CCA GTC ACT CTT GGA ACA TCA GCT
a.a             D   I   V   M   T   Q   A   A   F   S   N   P   V   T   L   G   T   S   A
Igκ-V24/25     ... ... ... ... ... ... ... ... ... ... ... ... ... ... ... ... ... ... ...
a.a.            D   I   V   M   T   Q   A   A   F   S   N   P   V   T   L   G   T   S   A
                      | |               CDR1                                    | |
Rearranged     TCC ATC TCC TGC AGG TCT AGT AAG AGT CTC CTA CAT AGT AAT GGC ATC ACT TAT TTG
a.a             S   I   S   C   R   S   S   K   S   L   L   H   S   N   G   I   T   Y   L
Igκ-V24/25     ... ... TCT ... AGT ... ... ... ... ... ... ... ... ... ... ... ... ... ...
a.a.            S   I   S   C   S   S   S   K   S   L   L   H   S   N   G   I   T   Y   L
                                              FWR2                                | |
Rearranged     TAT TGG TAT CTG CAG AAG CCA GGC CAG TCT CCT CAG CTC CTG ATT TAT CAG ATG TCC
a.a             Y   W   Y   L   Q   K   P   G   Q   S   P   Q   L   L   I   Y   Q   M   S
Igκ-V24/25     ... ... ... ... ... ... ... ... ... ... ... ... ... ... ATA ... CGG ... ...
a.a.            Y   W   Y   L   Q   K   P   G   Q   S   P   Q   L   L   I   Y   R   M   S
                 CDR2       | |             FWR3
Rearranged     AAC CTT GCC TCA GGA GTC CCA GAC AGG TTC AGT AGC AGT GGG TCA GGA ACT GAT TTC
a.a             N   L   A   S   G   V   P   D   R   F   S   S   S   G   S   G   T   D   F
Igκ-V24/25     ... ... ... ... ... ... ... ... ... ... ... GGC ... ... ... ... ... ... ...
a.a.            N   L   A   S   G   V   P   D   R   F   S   G   S   G   S   G   T   D   F
                                                                                    | |
Rearranged     ACA CTG AGA ATC AGC AGA GTG GAG GCT GAG GAT GTG GGT GTT TAT TAC TGT GCT CAA
a.a             T   L   R   I   S   R   V   E   A   E   D   V   G   V   Y   Y   C   A   Q
Igκ-V24/25     ... ... ... ... ... ... ... ... ... ... ... ... ... ... ... ... ... ... ...
a.a.

                     CDR3       |
Rearranged     AAT CTA GAA CTT CCG
a.a             N   L   E   L   P
Igκ-V24/25 ATG ... ... ... ...
a.a.            M   L   E   L   P
```

Figure 27: Nucleotide sequences of the Cy34.1.2 mAb V_H and V_L genes. The native secretion signal sequence, framework regions (FWRs) and complementarity determining regions (CDRs) are indicated.

3.9. Generation and cloning of Cy34.1.2 anti-CD22.2 scFv-His6 and scFv-protamine-His6 constructs:

The construction and use of a scFv from the Cy34.1.2 mAb to deliver therapeutic molecules, or siRNA/miRNA has a number of potential advantages. These include, at least theoretically, a weak stimulatory effect on B lymphocytes to which it binds, reduction in toxicity and a relatively small molecular size, yet retaining the affinity for binding to the receptor. In addition, antibody engineering using recombinant DNA technology will allow scFv to be equipped with different tags.

One of the key aims of this study is to engineer a fusion protein that combines the ability of anti-CD22 scFv to specifically target disease-causing B lymphocytes and carry therapeutic siRNA with the ability to change fate and biology B lymphocytes. For this purpose, the V_H and V_L chains were fused to a highly positively charged peptide, a truncated domain from human protamine (RSQSRSRYYRQRQRSRRRRRR) which has a known strong ability to bind siRNA and target these to B cells. The siRNA to be used would be intended to target key signaling molecules and proteins that are specifically upregulated in disease settings such as B cell leukaemia/lymphoma and other diseases mediated by B cell abnormalities. Thus to achieve the objective of constructing and generating scFv with the truncated protamine and a histidine purification tag, the PCR products of the poly-G-tailed cDNA for the V_H and the V_L genes were cloned into the linearised pCR®2.1 TA vector and used to transform DH5α *E. coli*, and DNA maxi-preparations from positive transformants used in subcloning procedures to construct the scFv cDNAs.

3.10. Analysis of the plasmid pFastBac^{TM}1 donor vector by restriction digestion in preparation for cloning:

The plasmid pFastBac^{TM}1 donor vector containing mIFNβ-MMP-1-11E scFv-His6 expression cassette (237) was analysed by restriction digestion to assess the feasibility of cloning the V_H and the V_L genes into the multiple cloning site (MCS) (Figures 28 and 29). The vector has left and right Tn7 transposable elements which flank the cloning sites that encompass the expression cassette. This enables the plasmid to donate the DNA fragment flanked by transposons to a recipient vector.

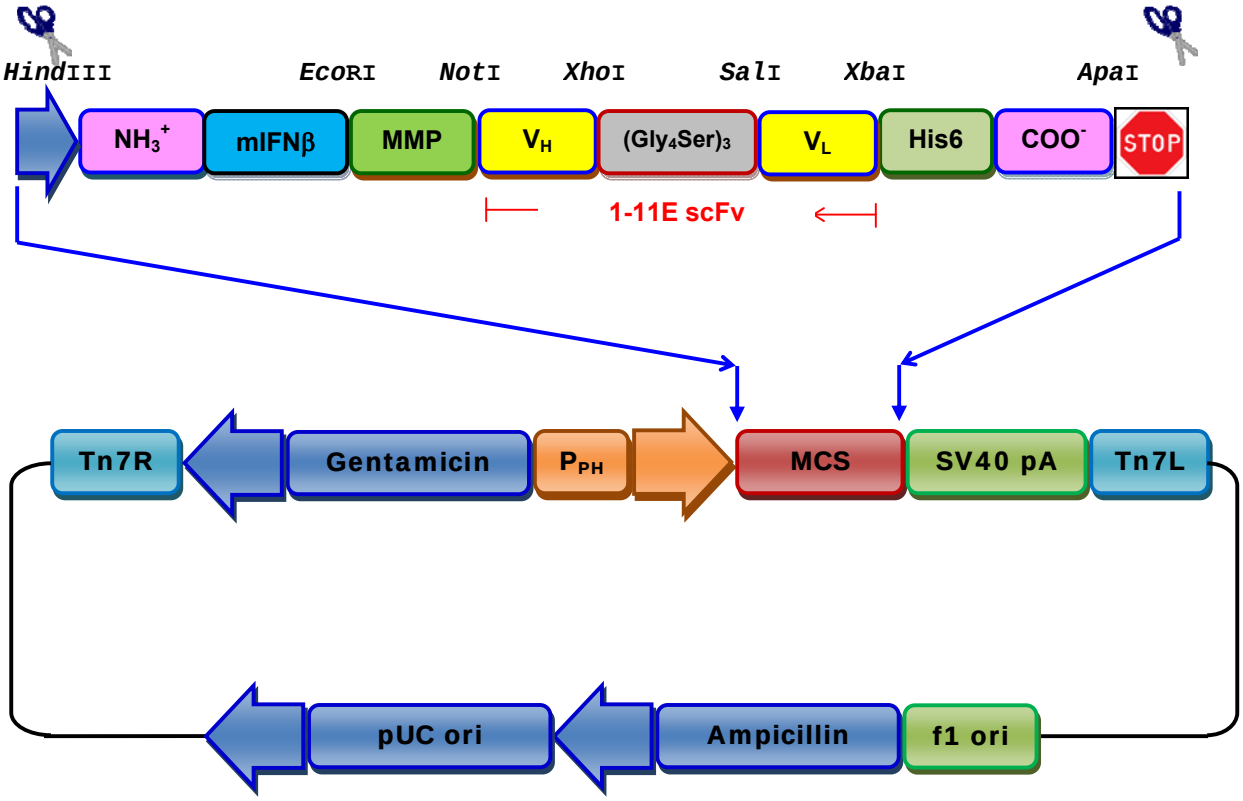

Figure 28: Schematic map of the pFastBac™1 donor vector illustrating the insertion sites of mIFNβ-MMP-1-11E scFv-His6 expression cassette. This construct was used to generate the mouse anti-CD22.2 scFv-His6 and scFv-protamine-His6 constructs using similar restriction sites. Genetic map of the construct is also shown in Appendix 3, page 354.

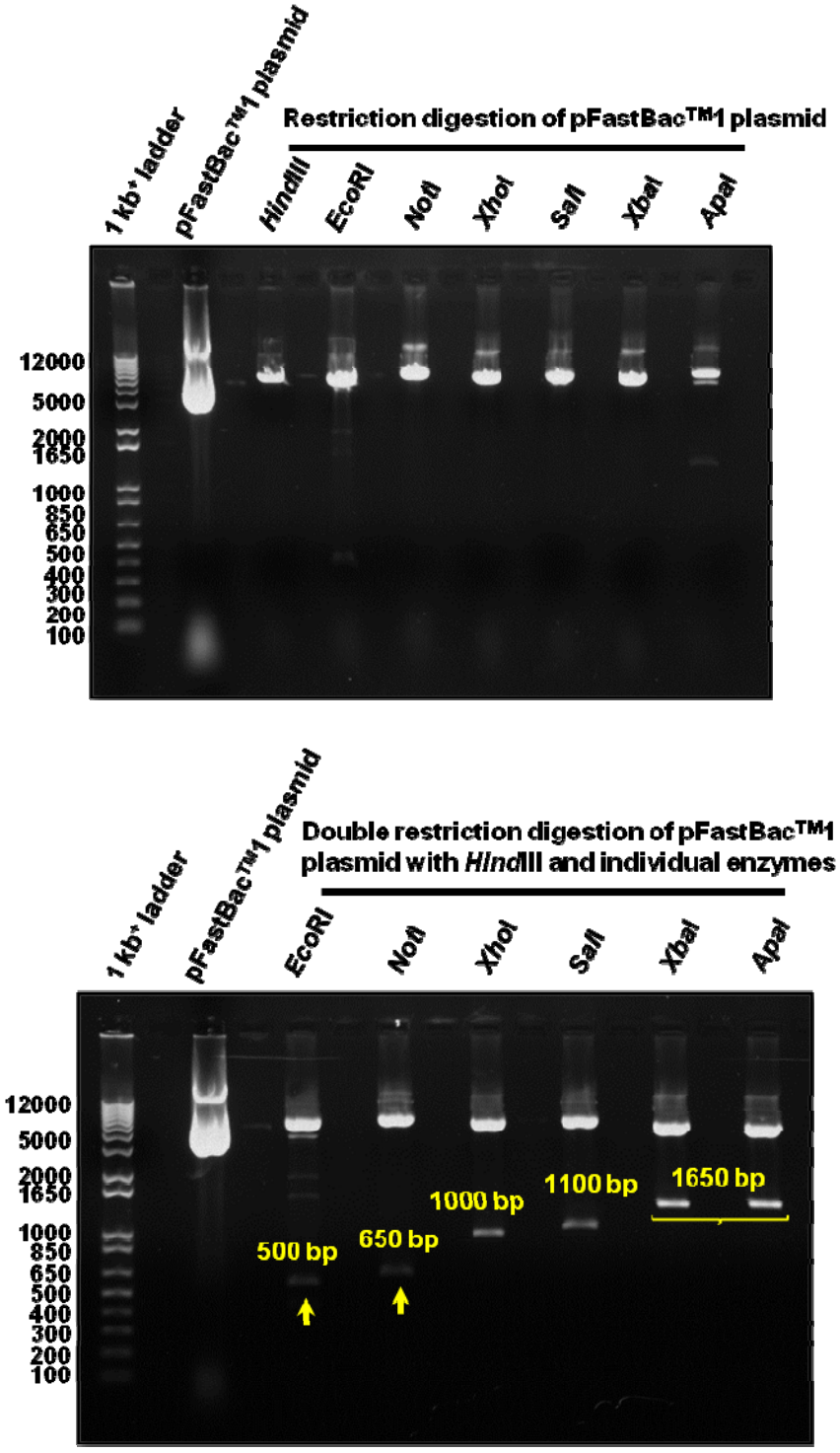

Figure 29: Restriction digestion of the pFastBac™1 plasmid (mIFNβ-MMP-1-11E scFv-His6) to assess suitability for cloning the V_H and the V_L genes of Cy34.1.2 mAb. The pictures depict results of restriction digestion of pFastBac™1 with *Hind*III, *Eco*RI, *Not*I, *Xho*I, *Sal*I, *Xba*I and *Apa*I. Plasmid DNA was digested with individual enzymes to linearise the vector (top), or with *Eco*RI, *Not*I, *Xho*I, *Sal*I, *Xba*I and *Apa*I restriction endonucleases in double restriction digestion reactions with *Hind*III enzyme to release DNA fragments from the vector at MCS (bottom).

3.11. V_H and the V_L gene cDNA amplification by PCR with specific primers for cloning into the pFastBac^{TM}1 donor vector:

The cDNAs for the V_H and the V_L genes of the Cy34.1.2 mAb cDNA cloned into the pCR®2.1 vector were PCR-amplified with specific nested primers internal to the Cγ and Cκ primers used for the first round of PCRs and also primers to anneal to the leader sequence of the V_H and the V_L genes as determined by sequencing. The PCR products were intended for insertion into the MCS of the pFastBac^{TM}1 transfer donor vector.

For the purpose of the experiments to be carried out, two constructs were generated. One construct was to consist of the scFv of the Cy34.1.2 mAb without the protamine peptide using V_L2 reverse primer for PCR amplification of V_L genes and one scFv with the protamine peptide using V_L1 reverse primer for PCR amplification of V_L genes. It was necessary to do this so that the scFv alone would be used as a control for any biological changes induced in the B lymphocytes independent of delivered siRNA. For this purpose the cloning strategy was altered such that for the scFv-His6 construct, PCR-amplified V_L genes using V_L2 reverse primer was cloned followed by the V_H and His6-tag (Figure 10 top, page 70) while for the scFv-protamine-His6 construct the order of cloning was to ligate the V_L genes PCR product using V_L1 reverse primer and the truncated protamine in one reaction and then ligate the V_H into the vector backbone (Figure 10 bottom, page 70). Results of the PCR reactions and restriction digestion of the PCR DNA fragments and the pFastBac^{TM1} vector are shown in Figure 30.

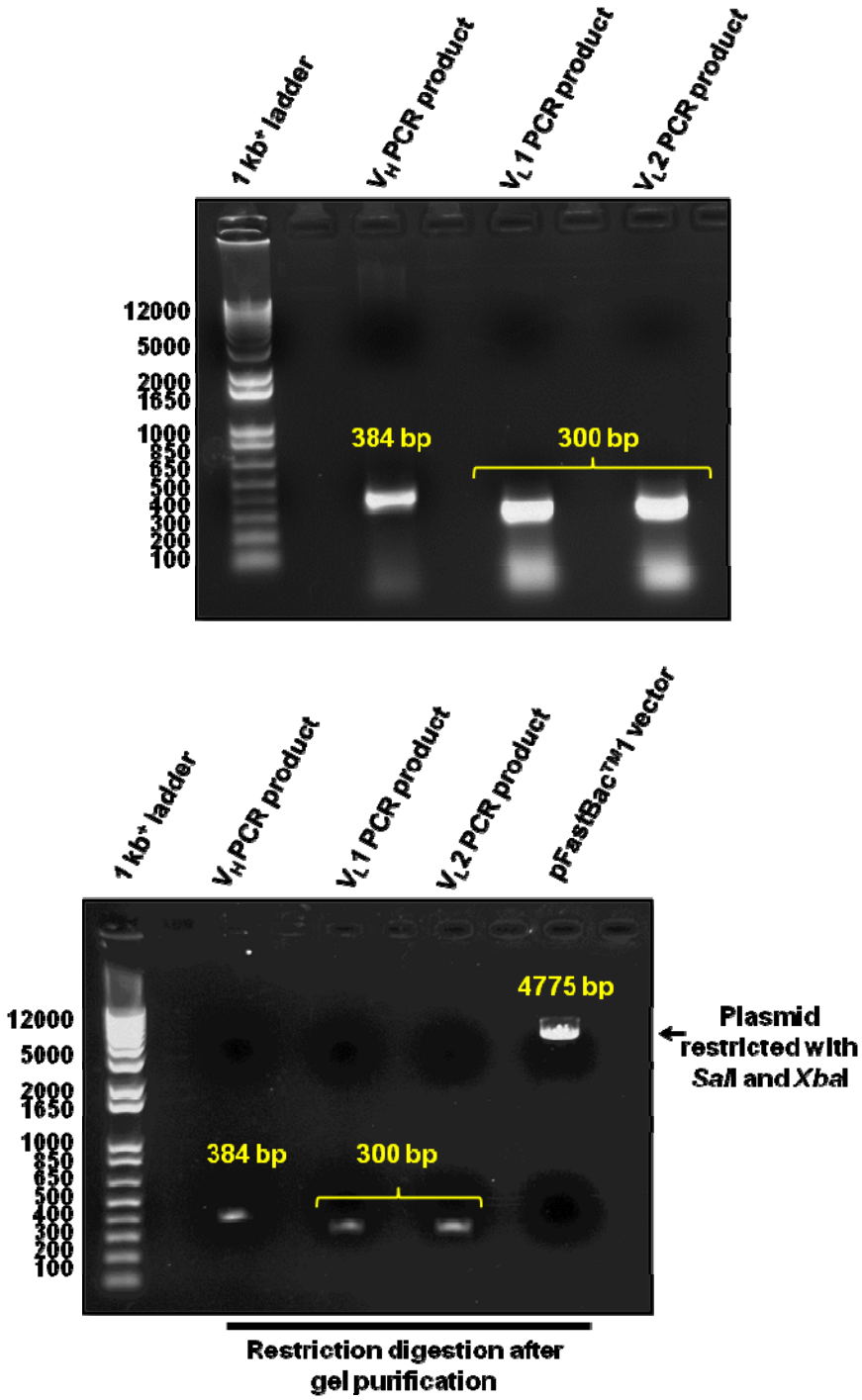

Figure 30: Preparation of PCR products and vector for cloning. PCR products of V_H (384 bp), V_L1 and V_L2 (300 bp) cDNAs are shown (top). The V_H and V_L genes were amplified with primers to incorporate specific restriction sites that enable cloning into the MCS of the pFastBac™1 vector. V_H DNA with *Hind*III and *Xho*I restriction sites, V_L1 DNA with *Eco*RI and *Sal*I restriction sites and V_L2 DNA with *Sal*I and *Nhe*I restriction sites. PCR products and vector (with *Sal*I and *Xba*I) were restricted and purified by gel extraction (bottom).

Schematic illustrations for restriction digestion and cloning process of the pFastBac^{TM}1-IFNβ-MMP-1-11E scFv to replace the V_L and V_H genes of 1-11E scFv with Cy34.1.2 scFv is shown in Figure 31.

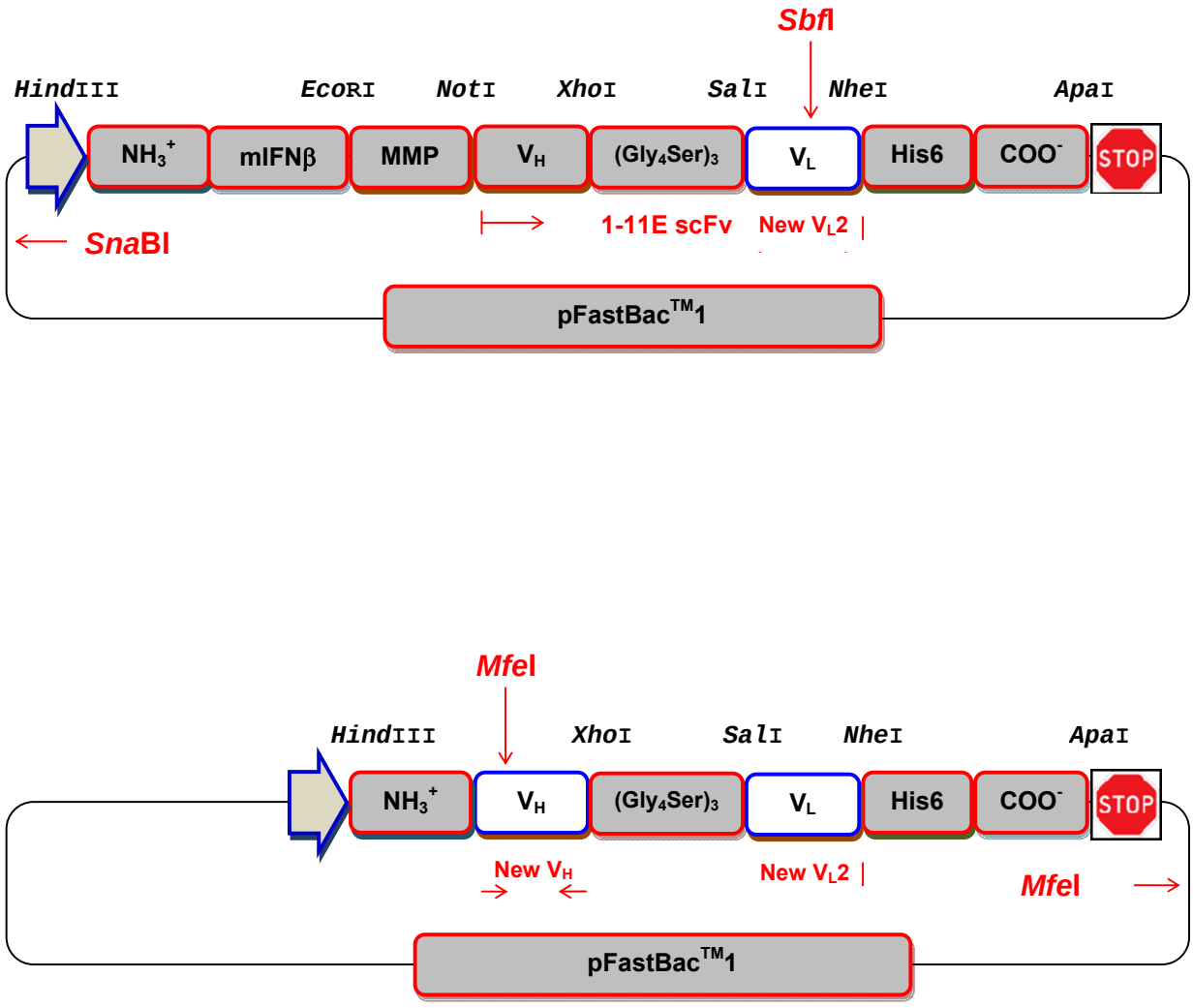

Figure 31: Schematic illustrations showing the cloning process and restriction digestion of the pFastBac^{TM}1-IFNβ-MMP-1-11E vector to generate the scFv-His6. Successful cloning of the Cy34.1.2 V_L is confirmed by restriction digestion of the new construct (pFastBac^{TM}1-V_L2) with *Sbf*I and *Sna*BI enzymes (top). Furthermore, the new Cy34.1.2 scFv-His6 construct (pFastBac^{TM}1-V_H/V_L2-His6) was verified by restriction digestion with MfeI enzyme (bottom).

3.12. Confirmation of the cloning of the V_L2 cDNA into the vector backbone by restriction analysis and sequencing:

Result of analysing V_L2 cloning showed that the cDNA was successfully incorporated into the pFastBac™ plasmid backbone between *Sal*I and *Nhe*I site as indicated by digestion with *Sbf*I and *SnaB*I (Figure 32). This restriction digestion is to confirm generation of pFastBac™1-IFNβ-MMP-1-11E scFv with 1-11E's V_L replaced with Cy34 V_L2 cDNA.

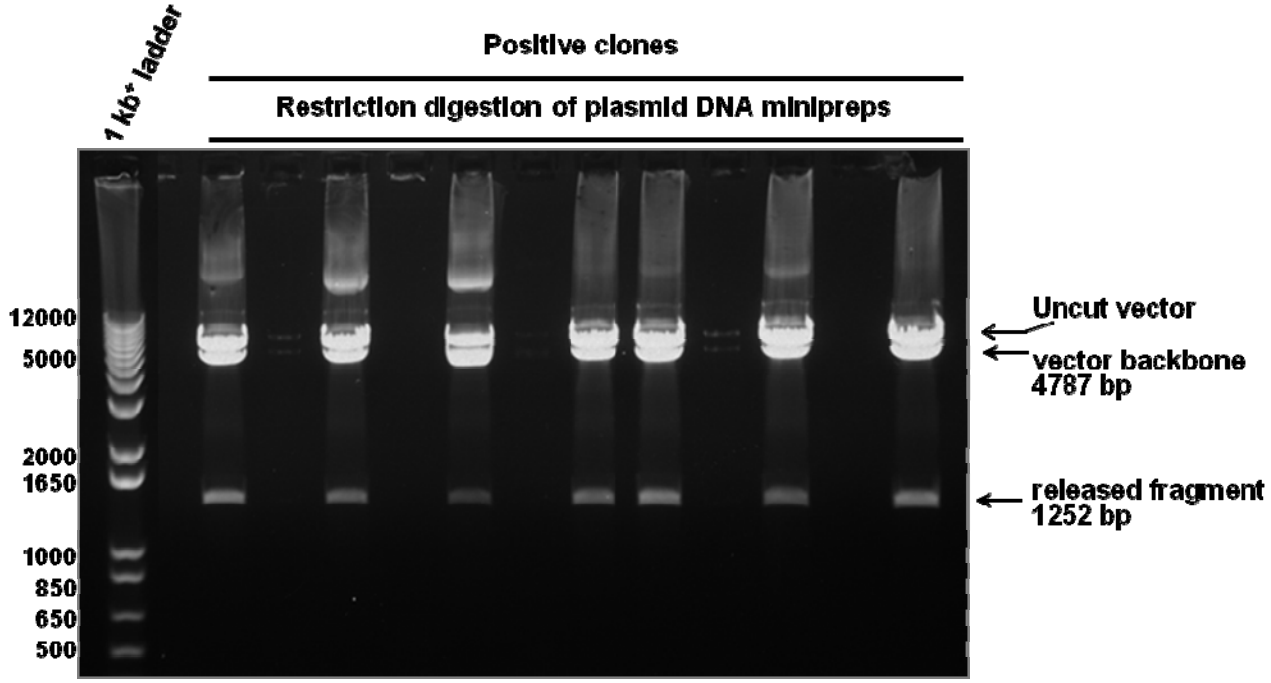

Figure 32: Cloning of V_L2 into the pFastBac™1 plasmid. The gel image shows results of the restriction digestion of the pFastBac™1 vector (after cloning of the V_L2 cDNA; named pFastBac™1-V_L2) with *Sbf*I and *SnaB*I. The *Sbf*I site is unique to the insert V_L cDNA and the *SnaB*I site is located in the vector backbone outside the insert region. Restriction analysis with *Sbf*I and *SnaB*I has, as expected, generated two fragments 4787 bp 1252 bp. All the V_L2 clones analysed were positive for the correct inserts and were further confirmed by sequencing.

Once the insertion of the V_L2 into the plasmid was confirmed, the V_H cDNA was prepared to be ligated into the construct between *Hind*III and *Xho*I in the new plasmid DNA backbone pFastBac™1-V_L2 which was digested with the same restriction enzymes (Figure 33).

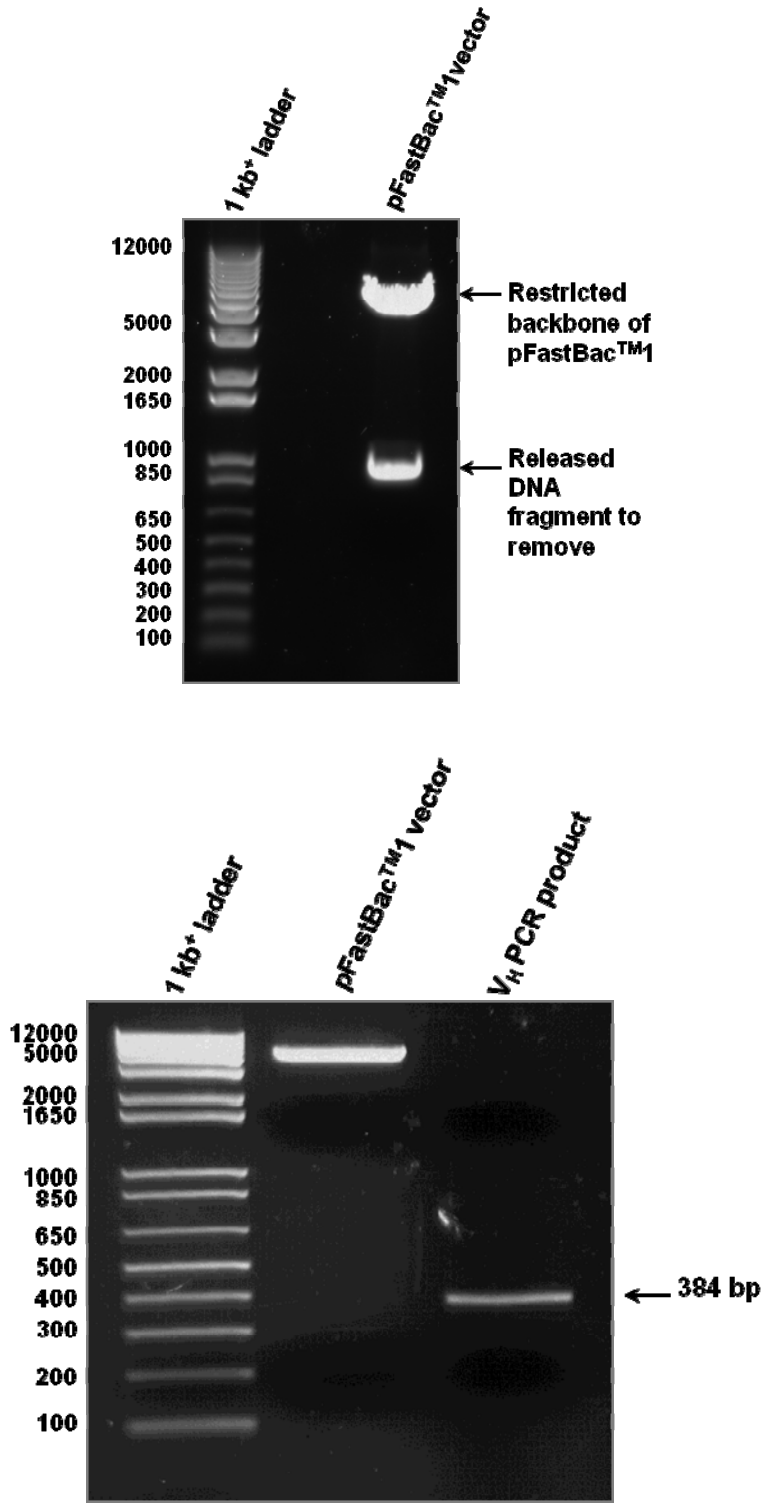

Figure 33: Preparation of the V_L2/pFastBac™1 construct for cloning of the V_H of mAb Cy34.1.2. The top photograph depicts the result of plasmid DNA maxiprep with the V_L2 insert after restriction with *Hind*III and *Xho*I enzymes to prepare it for the cloning of V_H DNA in the next stage. V_L2 construct and the V_H cDNA after restriction digestion and purification by gel extraction (bottom).

3.13. Cloning of in-frame V_H gene cDNA into the FastBac^{TM}1-V_L2 construct:

Once the pFastBac^{TM}1-V_L2 construct was generated the V_H was sub-cloned in between the *Hind*III and *Xho*I sites, colonies analysed by restriction digestion and those with the correct inserts verified by sequencing (Figure 34).

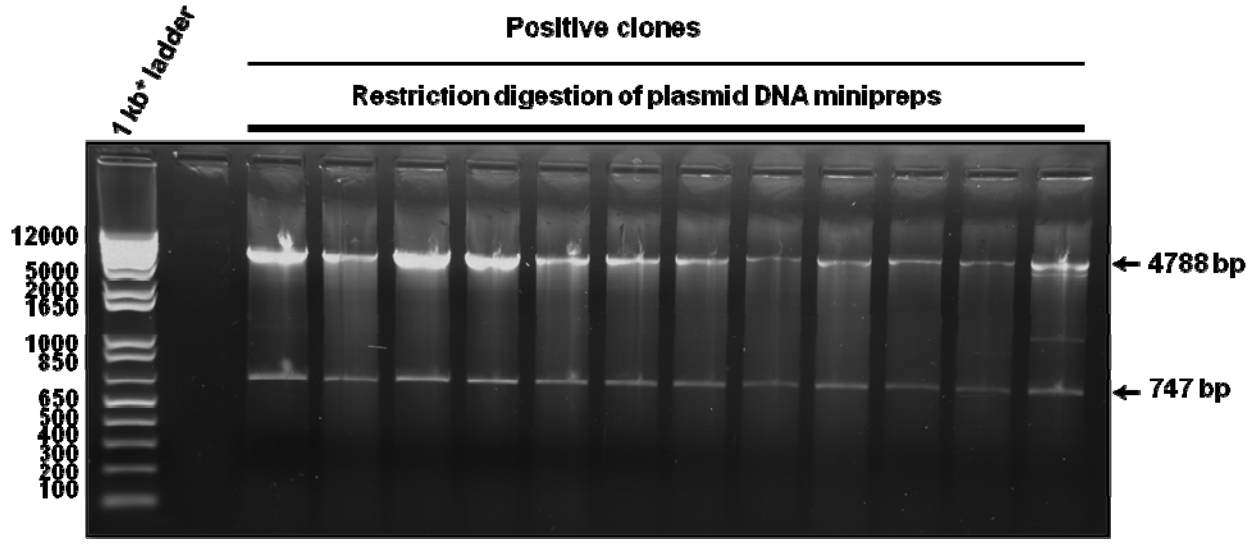

Figure 34: Restriction digestion of plasmid DNA to verify the successful cloning of the V_H of Cy34.1.2 mAb into the V_L2/pFastBac^{TM}1 construct. The image depicts results of restriction digestion of plasmid DNA minipreps with *Mfe*I to verify insertion of the Cy34.1.2 V_H. All the clones had the correct insert as the two expected DNA fragments were generated: 4788 bp against 747 bp.

3.14. Annealing of overhang protamine primers to generate the cDNA for the truncated protamine sequence:

In order to generate the scFv of mAb Cy34.1.2 containing the designated protamine peptide, overhanging primers for the truncated protamine sequence were designed and generated. The HPLC-purified overhanging primers were annealed by incubating equal volumes of 10x dilution of each primer stock (100 mM) with T4 DNA ligase buffer (10x) and sterile distilled water. The mixture has then boiled for 5 minutes and left to anneal gradually overnight. Individual and annealed primers were checked by agarose gel electrophoresis (Figure 35).

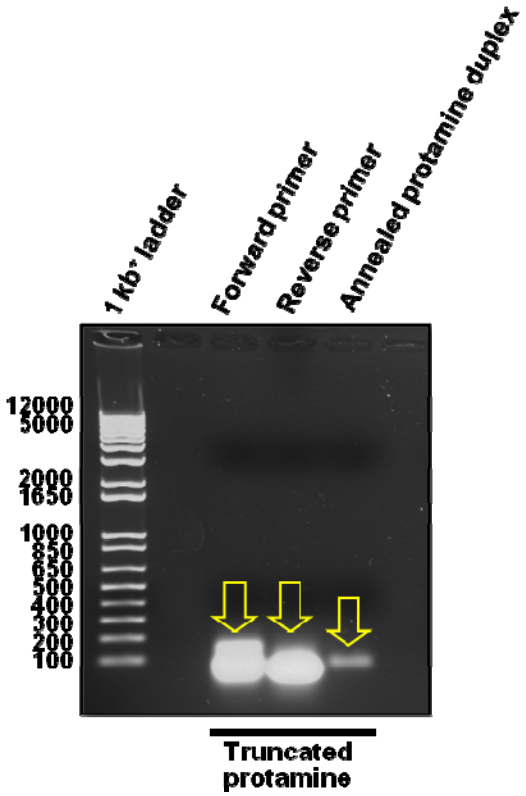


```
  |EcoRI|                                                                                                |XbaI|
5' AA TTC CGA TCA CAA TCA CGA TCA CGA TAC TAC CGA CAA CGA CAA CGA TCA CGA CGA CGA CGA CGA CGA T      3'
          R   S   Q   S   R   S   R   Y   Y   R   Q   R   Q   R   S   R   R   R   R   R   R
3'      G GCT AGT GTT AGT GCT AGT GCT ATG ATG GCT GTT GCT GTT GCT AGT GCT GCT GCT GCT GCT GCT AGA TC 5'
```

Figure 35: Gel electrophoresis of free and annealed primers used for the protamine sequence. The HPLC-purified primers [10 mM] were annealed by incubation with T4 DNA ligase buffer by boiling (5 minutes) and overnight cooling.

Schematic illustrations for restriction digestion and cloning process of the pFastBac^{TM}1-IFNβ-MMP-1-11E scFv to replace the V_L and V_H genes of 1-11E with Cy34.1.2 scFv-protamine is shown in Figure 36.

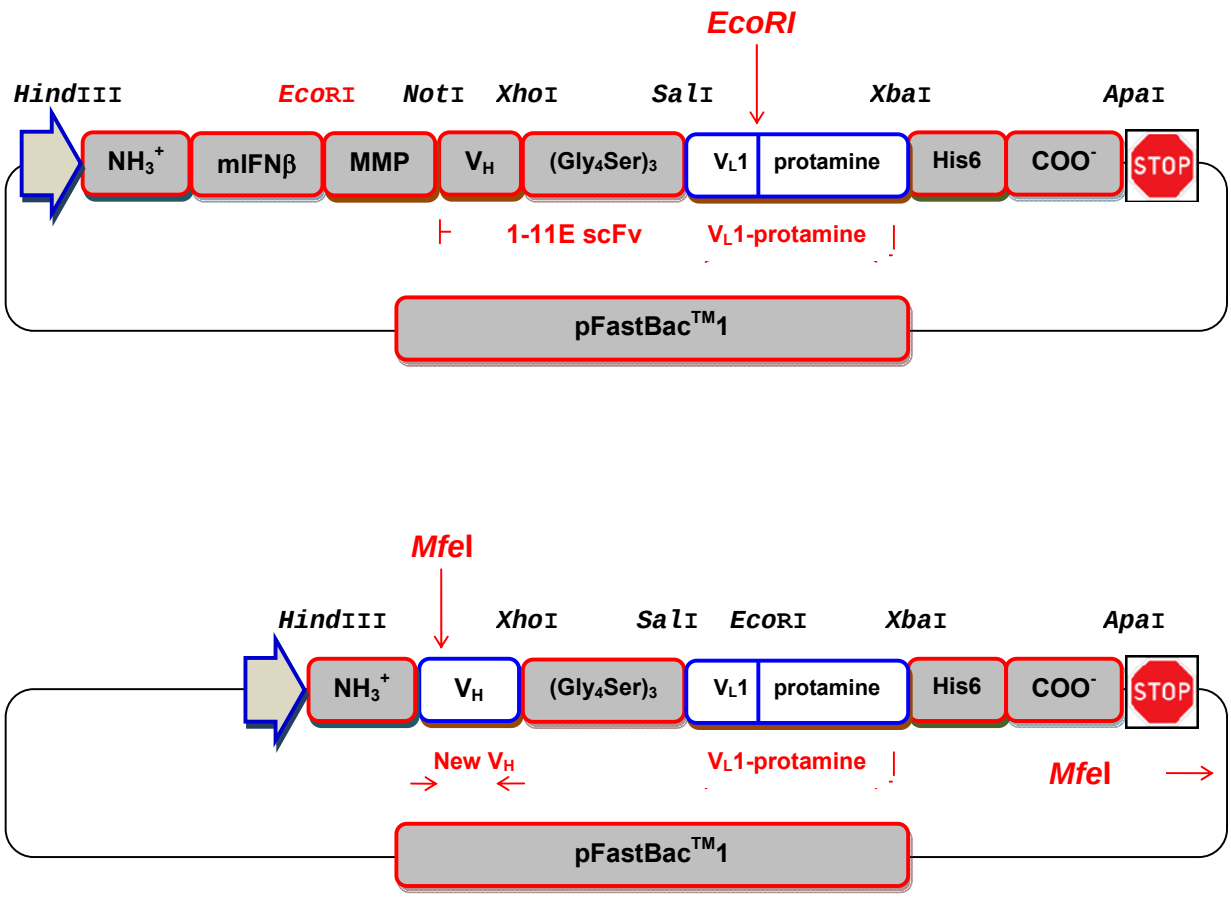

Figure 36: Schematic illustrations showing the cloning process and restriction digestion of the pFastBac^{TM}1-IFNβ-MMP-1-11E vector to generate the scFv-protamine-His6. Successful cloning of the Cy34.1.2 V_L1-protamine is confirmed by restriction digestion of the new construct (pFastBac^{TM}1-V_L1-protamine) with *Eco*RI (top). The new Cy34.1.2 scFv-protamine-His6 construct (pFastBac^{TM}1-V_H/V_L1-protamine-His6) was verified by restriction digestion with MfeI enzyme (bottom).

3.15. Cloning of the V_L1 gene cDNA with protamine peptide DNA:

The V_L1 PCR product and the cDNA for the protamine peptide were ligated between *Sal*I and *Xba*I sites in the plasmid DNA that was restricted using the corresponding enzymes. For this cloning, the plasmid backbone pFastBac^{TM}1 was linearised by digestion with *Sal*I and *Xba*I enzymes. Then, the V_L1 PCR product was digested with *Sal*I and *EcoR*I enzymes so that it can be ligated with the protamine cDNA which has *EcoR*I and *Xba*I overhang restriction sites. Positive clones containing the appropriate inserts were identified by restriction analysis (Figure 37) and confirmed by sequencing.

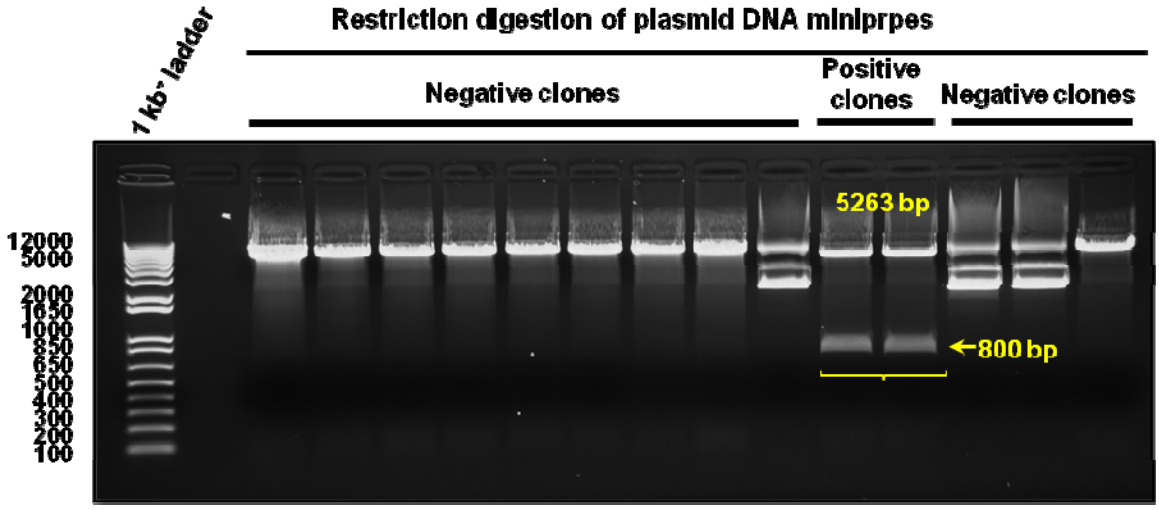

Figure 37: Generation of constructs for V_L1 and protamine peptide. Plasmid DNA minipreps for colonies selected following co-ligation of the V_L1 and protamine gene cDNAs were analysed by restriction digestion. Plasmid DNAs were digested with *Eco*RI which resulted either in linearisation of the vector if the cloning was not successful, or in generation of two fragments of 800 bp and 5263 bp. Colonies containing the appropriate inserts were verified by sequencing.

3.16. Cloning of the V_H gene cDNA into the pFastBac^{TM}1-V_L1-protamine construct:

Once the pFastBac^{TM}1-V_L1-protamine construct was generated, the V_H gene cDNA was sub-cloned in between the *Hind*III and *Xho*I sites and miniprep DNAs from colonies of transformants were analysed by restriction digestion (Figure 38) and those with the correct inserts verified by sequencing.

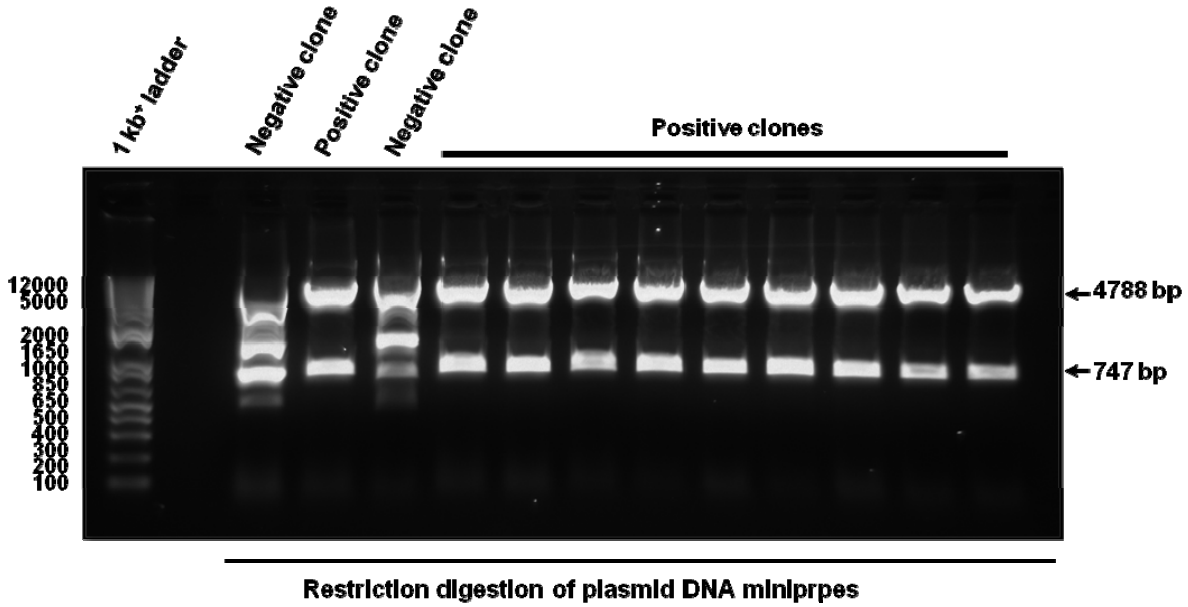

Figure 38: Cloning of the Cy34.1.2 V_H DNA into the pFastBac^{TM}1-V_L1-protamine construct. Plasmid DNA minipreps digested with *Mfe*I resulted in two DNA fragments of 4788 bp and 747 bp in correct clones containing the V_H DNA.

Full sequencing data showing the validity of the in-frame nucleotide sequences for the construction of anti-CD22.2 scFv-His6 and scFv-protamine-His6 pFastBac^{TM}1 donor vectors is shown in Appendix 2, pages 343 and 344 respectively. In addition, the genetic maps with unique restriction sites of both constructs are shown in Appendix 3, pages 355 and 356 respectively.

3.17. Generation of recombinant bacmids for protein expression:

Successful generation of infectious recombinant baculoviruses was accomplished by site-specific transposition of the expression cassettes containing the V_H and V_L genes of the Cy34.1.2 mAb into a baculovirus genome. The transposition was carried out such that the donor plasmid vector with an open reading frame downstream to the promoter region of the polyhedrin gene of the baculovirus shuttle vector (bacmid) propagated in DH10Bac *E. coli*. To achieve protein production, the Bac-to-Bac® Baculovirus Expression System was used.

Since the recombinant bacmid DNA is greater than 135 kb in size, restriction analysis is difficult to perform. Therefore, PCR analysis was used to verify the presence of the genes of interest in the recombinant bacmid. For this purpose, the pUC/M13 forward primer: 5'CCCAGTCACGACGTTGTAAAACG3' and pUC/M13 reverse primer: 5'AGCGGATAACAATTTCACACAGG3' were used to hybridise to sites flanking the mini-*att*Tn7 site within the *lac*Zα-complementation region to facilitate PCR amplification (Figures 39 and 40).

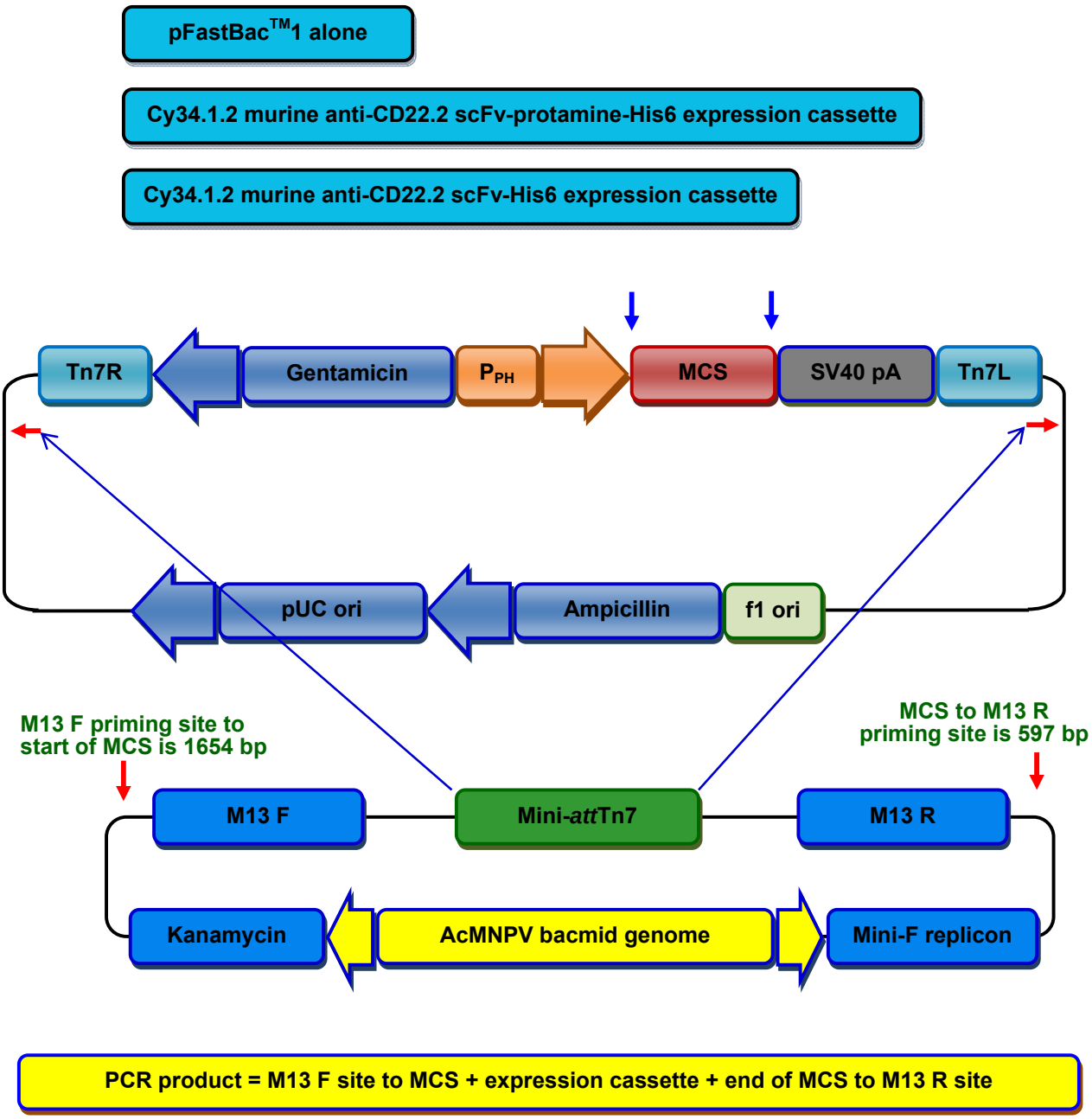

Figure 39: Schematic map illustrating the PCR analysis of recombinant bacmid. The pFastBac™1 donor vector with the gene of interest inserted at MCS is transposed by site-specific recombination with the bacmid genome. The bacmid DNA is >135 kb. Verification of the insertion of the gene of interest is difficult using classical restriction endonuclease digestion analysis. Hence, PCR amplification was used to confirm that the gene of interest has transposed to the bacmid. The pUC/M13 amplification primers were directed at sequences on either side of the mini-*att*Tn7 site within the *lac*Z α-complementation region of the bacmid. If transposition has occurred, the PCR product produced by these primers would be 2,300 bp plus the size of the insert.

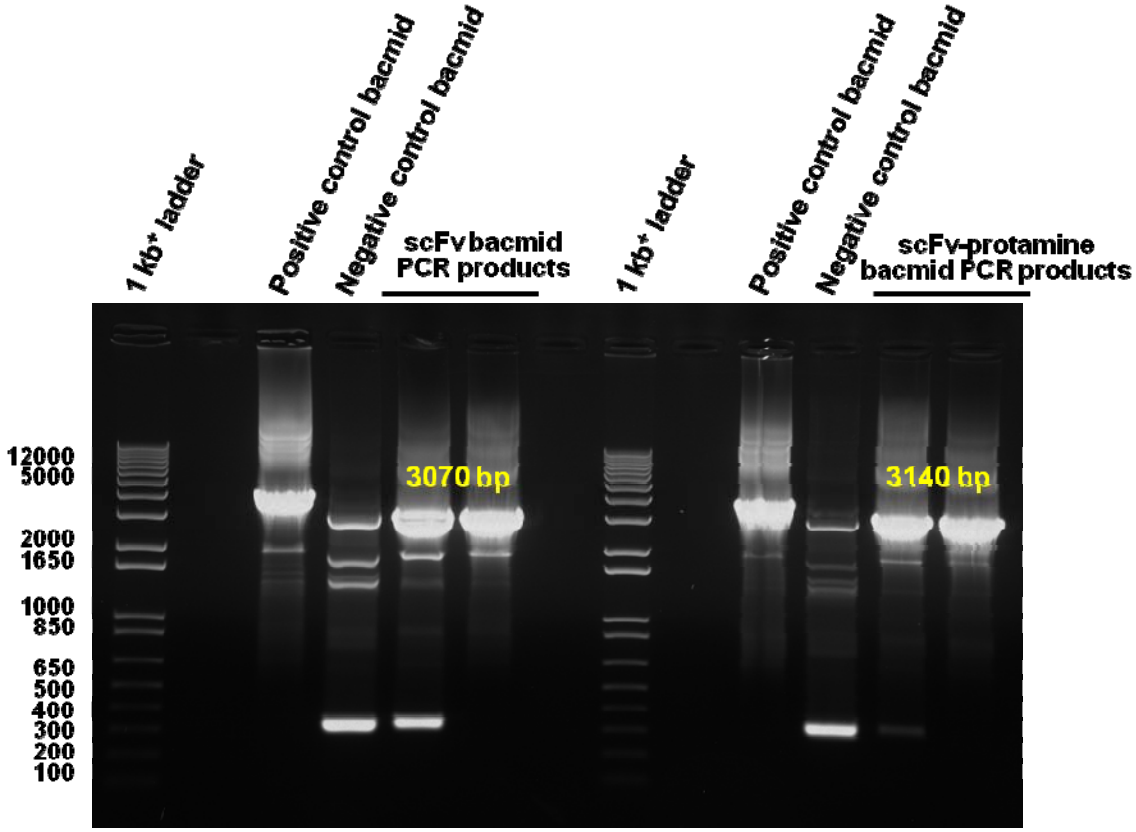

Figure 40: Assessment of recombinant baculoviruses by PCR. M13 forward and reverse primers were used to amplify from the M13F priming site which is 1654 bp upstream to the MCS and M13R priming site which is 597 bp downstream to the MCS. Expected sizes for the PCR products: pFastBac™1 alone, ~300 bp; Bacmid transposed with pFastBac™1, ~2300 bp + size of genes of insert (770 bp for scFv-His6 and 840 bp for scFv-protamine-His6). The PCR products were also verified with three sequencing primers (M13 F, P_{PH} F and SV40 pA R primers).

When incorporation of genes of interest into the recombinant bacmids was established, the PCR products from the bacmid DNA were further analysed by restriction digestion to confirm release of the scFv-His6 and scFv-protamine-His6 expression cassettes and this was verified by agarose gel electrophoresis (Figure 41). A schematic illustration explaining the PCR amplification to confirm generation of the recombinant baculoviruses is shown in Figure 39, page 146.

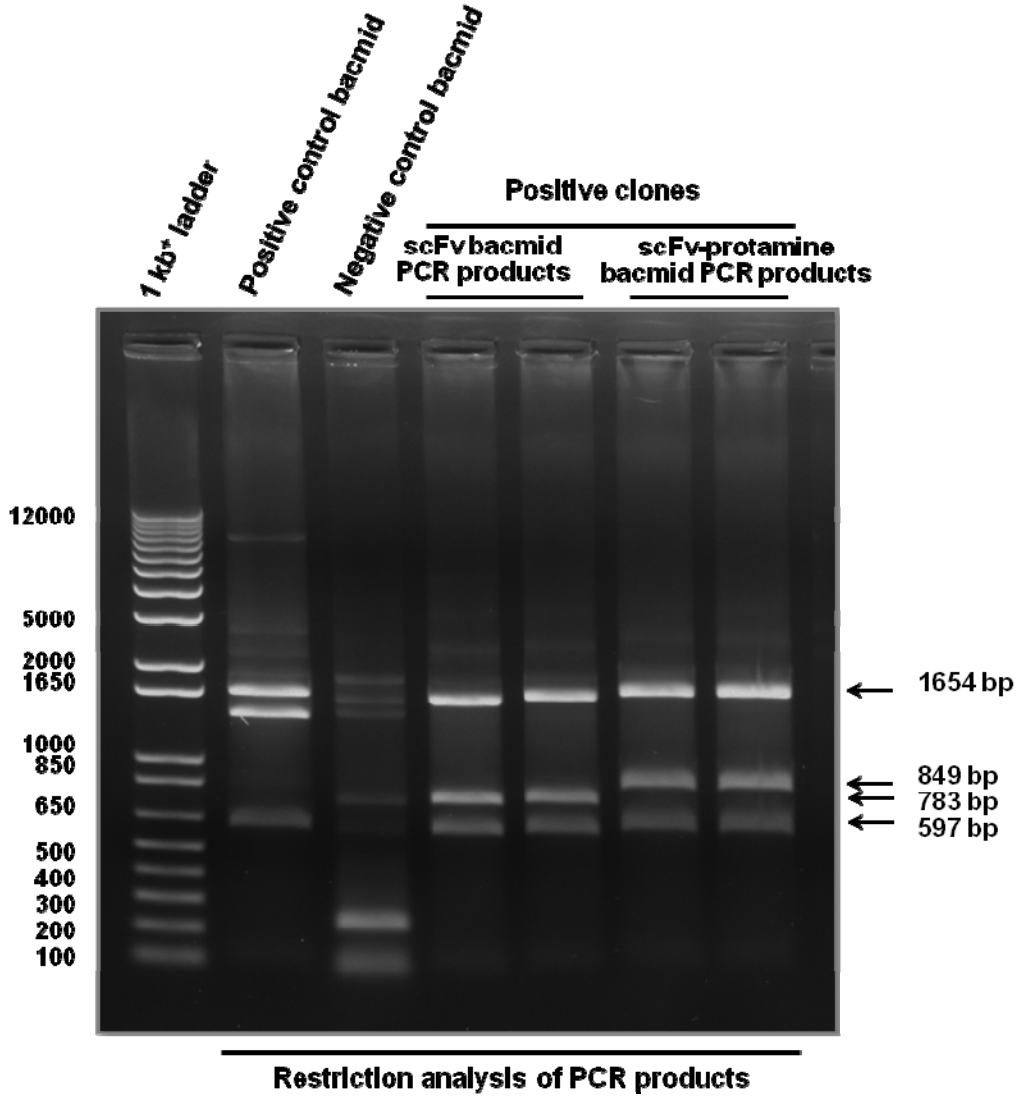

Figure 41: Restriction analysis of the PCR products amplified from the generated bacmids with M13 F and R primers to release the expression cassettes. The PCR products were restricted with *Hind*III and *Apa*I enzymes. Positive control is anti-hen egg lysozyme scFv-IL10-V5-His6 in bacmid.

3.18. Propagation of recombinant baculoviruses in SF9 cells and recombinant protein expression in HighFive cells:

The first step in the transfection procedure was to optimise the time course period for infecting the SF9 insect cells to propagate the baculoviruses (BV). To achieve this, SF9 cells were infected with the BV for 3-day and 5-day intervals independently when the first propagated BV stock was prepared (P1 BV). The second and third baculovirus stocks were similarly prepared 3-days and 5-days after transfection (P2 and P3 BV respectively). The results revealed that the 3-day transfection approach does not generate enough BV to successfully infect SF9 cells in the next two stages (P2 and P3) of BV propagation. Therefore, SF9 insect cells were routinely infected with the BV at each stage for 5 days and the P3 round of BV propagation used to infect the HighFive insect cells for expression of recombinant proteins. Different time points and titers of the P3 BV were used to optimise recombinant protein production in the HighFive insect cells. Although intracellular expression of the proteins was confirmed in the time course and titration experiments (Figures 42 and 43) but secretion of the proteins was inconclusive.

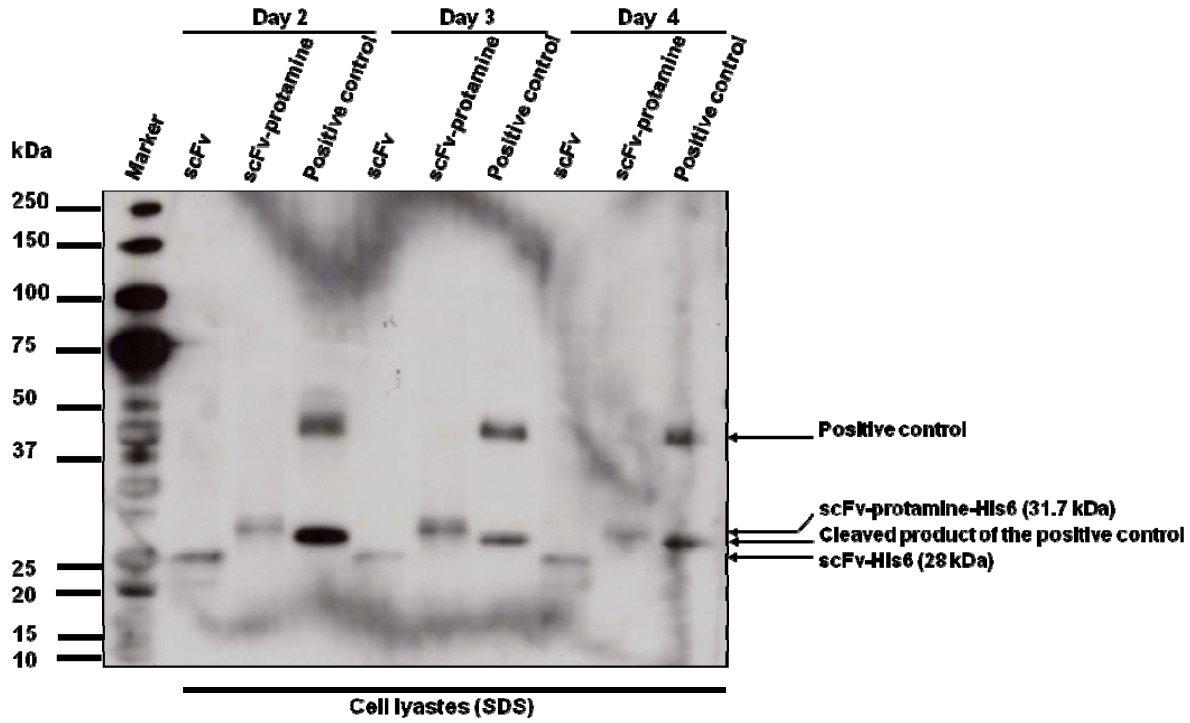

Figure 42: Expression of recombinant scFv-His6 and scFv-protamine-His6 proteins. Expression of recombinant proteins was studied by Western blotting using HRP-conjugated anti-His mAb. The figure shows a Western blot membrane for the result of studying the effect of different incubation times for infecting the insect cells with the baculovirus on the generation of recombinant proteins in the HighFive insect cells. Positive control included in the experiment was mIFNβ-MMP-1-11E scFv-His6. 1-11E scFv is recombinant protein with specificity for human modified collagen type II.

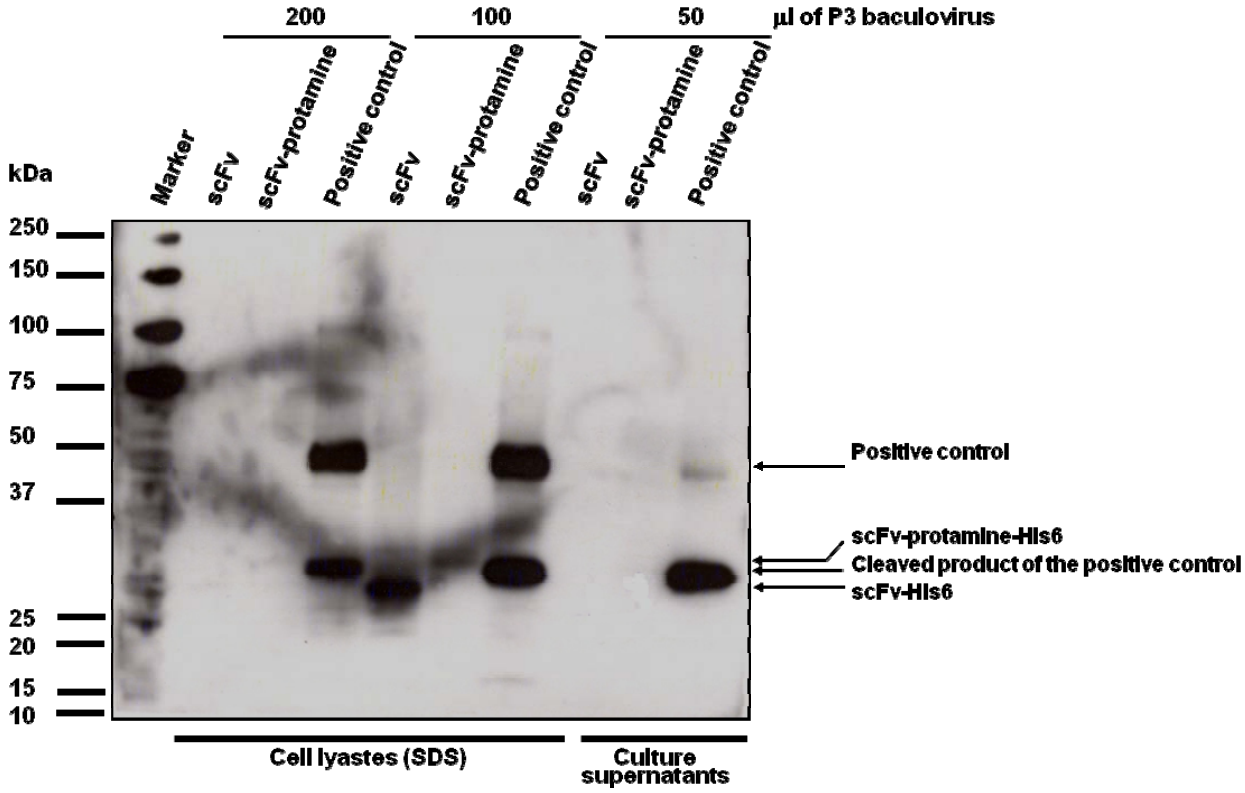

Figure 43: Western blot analysis showing the effect of P3 baculovirus levels on recombinant protein expression. The Western blot membrane depicts the level of scFv-His6 and scFv-protamine-His6 proteins at day 4 post-infection in the HighFive cells pellet**.** Positive control protein is mIFNβ-MMP-1-11E scFv-His6. 4-12% gradient pre-cast gel under non-reducing conditions.

Once the optimal time for BV stock generation and infection were determined, the next step was to determine whether the recombinant proteins are secreted or retained inside the insect cells. To test this, culture supernatants and pelleted cells obtained after harvesting the HighFive insect cells were analysed. The culture supernatant was concentrated 20 times through a specialised Immobilized Metal Affinity Chromatography (IMAC) purification device by centrifugation. Results from this experiment showed that the recombinant proteins are retained inside the cells and not secreted (Figure 44).

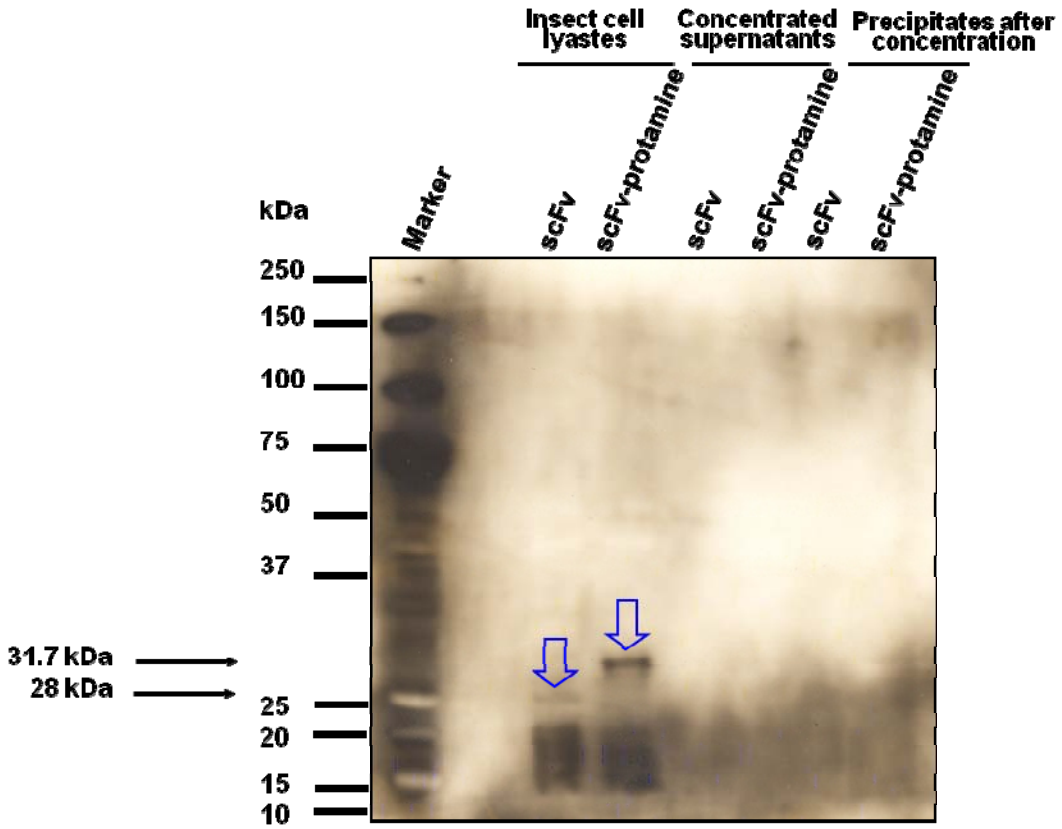

Figure 44: Western blot analysis for recombinant proteins scFv-His6 and scFv-protamine-His6 production in HighFive insect cells. The presence of recombinant proteins inside cells and in culture supernatants was analysed 3 days post-transfection. The HighFive insect cell supernatants were concentrated using an IMAC purification device. About 20 mL of the culture supernatants were concentrated to 1 mL through 10 kDa cut-off molecular weight spin column (Vivapure Metal Chelate Maxi spin columns). The concentrated sample was then analysed by Western blotting. Precipitates formed inside the column after concentration of protein samples were also analysed alongside the cell lysates and supernatants (right). 4-12% gradient pre-cast gel under reducing conditions. Western blot was exposed for 30 seconds.

3.19. Purification of recombinant proteins under native conditions:

Since the recombinant proteins were not secreted, protocols were designed to isolate the proteins from the HighFive cell lyastes. For this purpose, the Insect Cell Protein Extraction Reagent (I-PER®; Thermo Fisher Scientific) was used. This reagent contains a proprietary non-ionic detergent in 130 mM NaCl and 25 mM Tris-HCl; pH 7.5 and a microbial growth inhibitor (the exact composition of this extraction reagent was not provided by the manufacturer). According to the manufacturer, the I-PER® buffer is a non-denaturing reagent that retains the protein in native form. Cells were then lysed with the buffer and the expressed proteins were detected in the lysates (Figure 45).

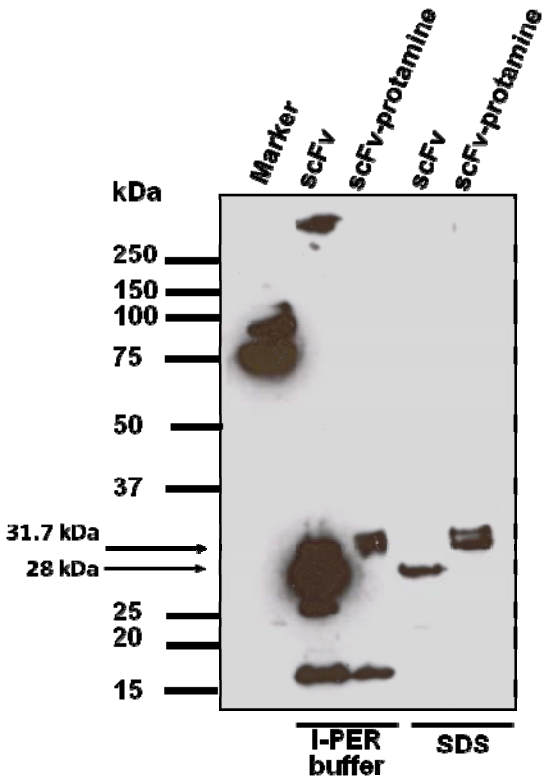

Figure 45: Comparative analysis of the recombinant proteins extracted using I-PER® lysis buffer or 10% SDS (Laemmli buffer). 10% gel was run under reducing conditions. The Western blot was revealed with HRP-conjugated anti-His(C-term) mAb were exposed for 1 minute.

The I-PER® lysates obtained from insect cells were then clarified by centrifugation and applied to nickel affinity columns prepared for purification under native conditions. The results showed that the proteins were not able to bind to nickel beads in the column and, hence, not obtained upon elution (Figure 46).

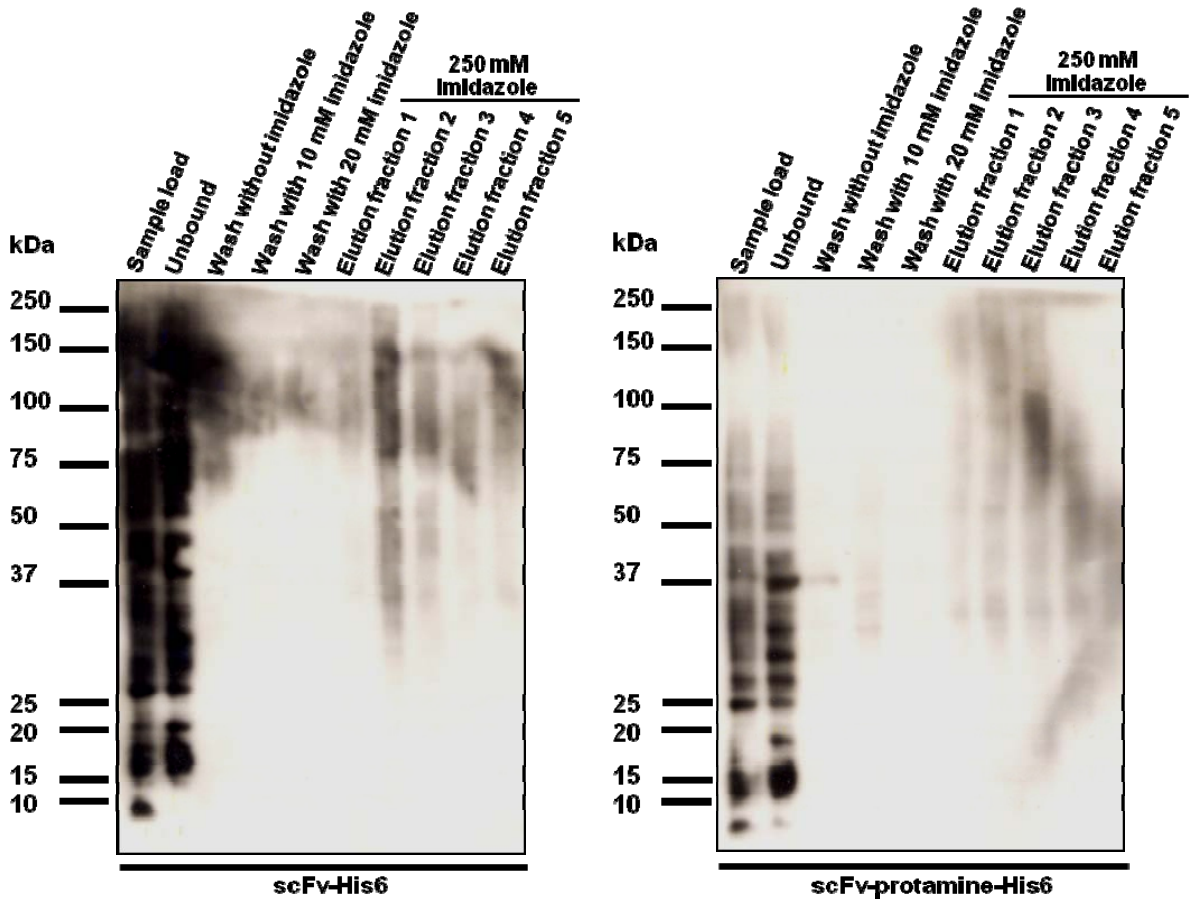

Figure 46: Detection of recombinant proteins scFv-His6 and scFv-protamine-His6 affinity purified under native conditions. Western blotting analysis of scFv-His6 (left) and scFv-protamine-His6 (right) proteins obtained from HighFive insect cell lysates using the I-PER® followed by protein purification using nickel columns. The salt concentration of the lysates was adjusted from 130 mM NaCl to 300 mM NaCl by adding an appropriate volume of 5 M NaCl for optimal purification using immobilized nickel-chelated resin. Samples were reduced and run on 4-12% pre-cast SDS gels. Western blots were detected with anti-His mAb. The film was exposed for 5 minutes.

3.20. Assessment of HRP-conjugated anti-His mAbs for optimisation of the Western blotting protocol:

One major obstacle to the identification of the recombinant proteins was a high background obtained with the Qiagen HRP-conjugated anti-His mAb. In order to reduce the background staining with the chemiluminescence reagents, different blocking buffers were assessed including 3% [w/v] BSA in TBS buffer and 1% [w/v] alkali-soluble casein in TBS. However, these blocking buffers did not reduce background nor improved the detection. Therefore, a different detection Ab for His-tag was tried in the Western blotting experiments. The results revealed that HRP-conjugated anti-His(C-term) mAb from Invitrogen improved detection of the recombinant protein (Figure 47).

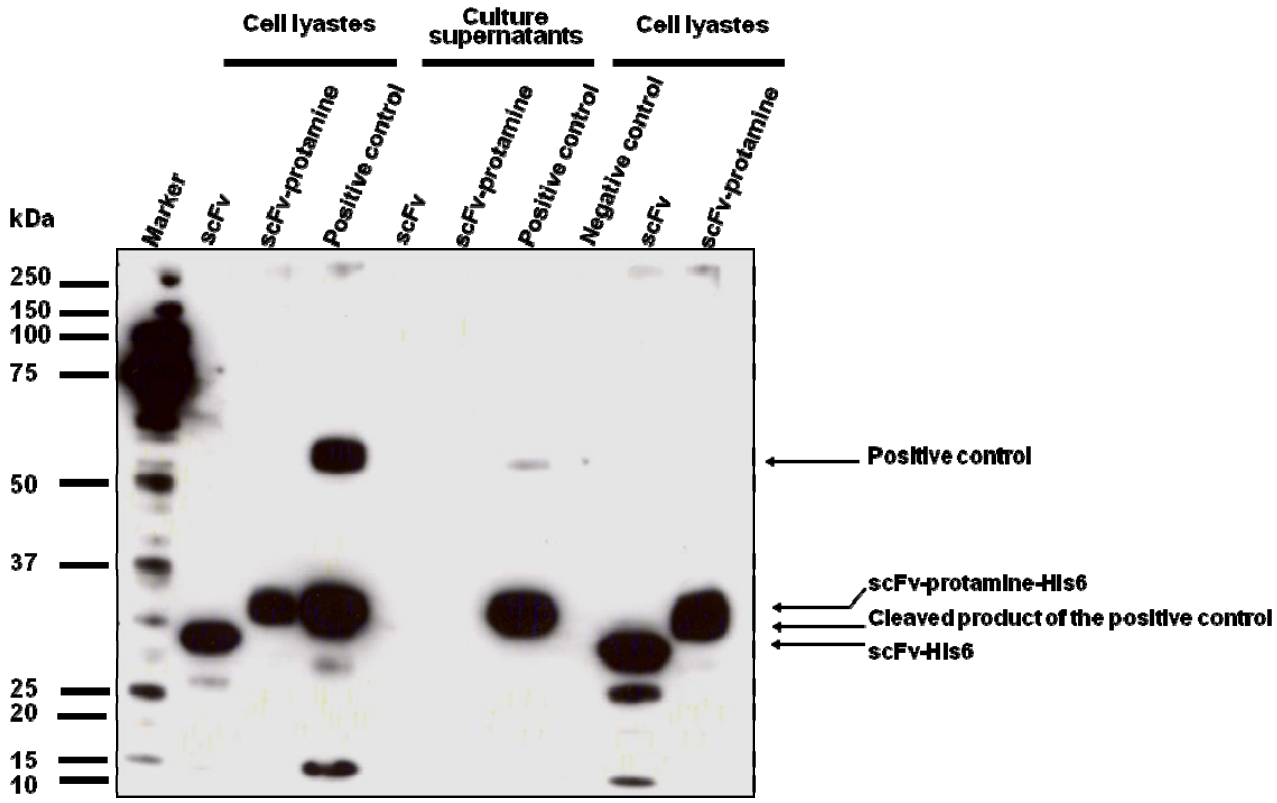

Figure 47: Optimisation of Western blotting for the detection of recombinant scFv-His6 and scFv-protamine-His6 proteins. The figure shows the analysis of recombinant protein expression using the new HRP-conjugated anti-His (C-term) mAb. All HighFive insect cell lysates were prepared by incubation with Laemmli buffer (10% SDS) for 5 minutes at 95°C. The positive control protein is mIFNβ-MMP-1-11E scFv-His6. The negative control is HighFive insect cell lysate which was used to exclude detection of any endogenous histidine-containing protein that could be present in cells and thereby interfere with the detection system. The presence of recombinant proteins was revealed with the HRP-conjugated anti-His (C-term) mAb (Invitrogen) and the film exposed for 1 minute.

3.21. Comparative assessment of different insect cells for the expression of recombinant scFv-His6 and scFv-protamine-His6 proteins:

The SF9 cell line is highly susceptible to infection with AcMNPV baculovirus and can be used with all baculovirus expression vectors. The SF9 cell line was used to isolate and propagate recombinant baculoviral stocks. Because the whole transfection procedure takes 18-days, which is a lengthy process, a question has arisen to whether or not the SF9 cells could possibly express and secrete the recombinant proteins. To investigate the possibility that SF9 insect cells can produce recombinant proteins in secretable forms, which would render the protocol less time-consuming, culture supernatants and lysates of infected SF9 cells were analysed by Western blotting. The results revealed that although the SF9 cells propagated the baculovirus, it was not ideal for the expression and secretion of the recombinant proteins of interest (Figure 48).

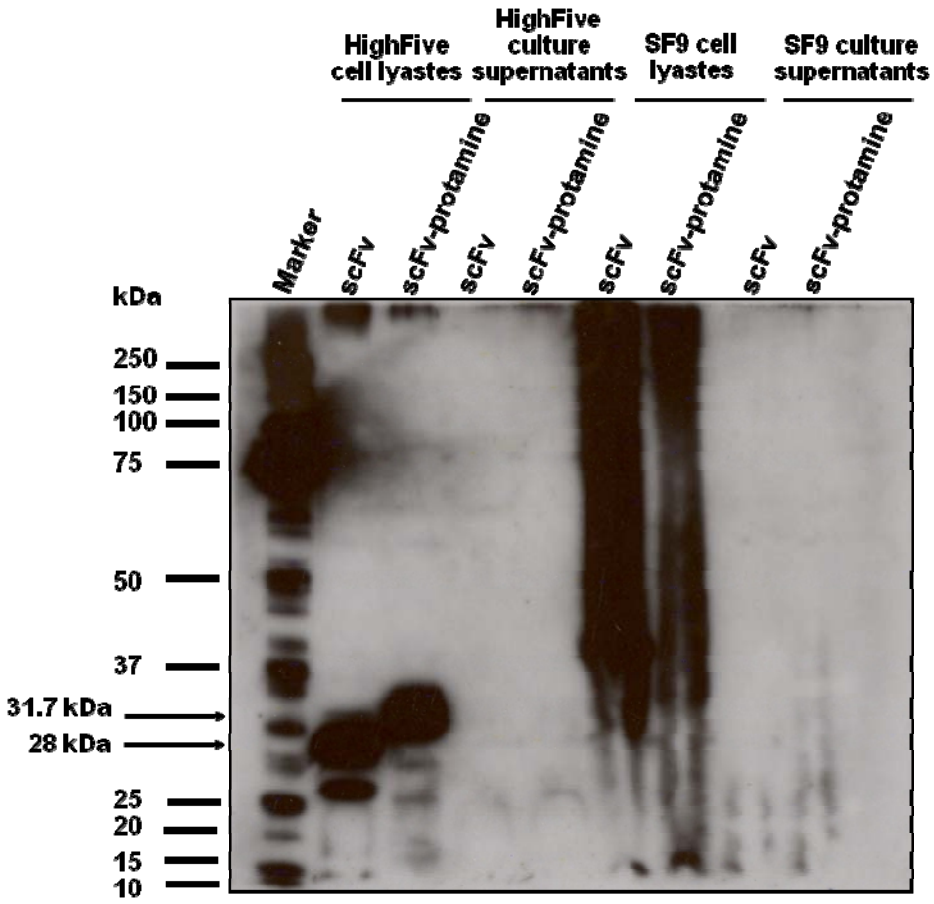

Figure 48: Comparative analysis of HighFive and SF9 insect cells for recombinant scFv-His6 and scFv-protamine-His6 protein production. Supernatants and cell lysates were analysed for recombinant proteins production on a 10% pre-cast gel under reducing conditions. Cell lysates were prepared by incubation with the Laemmli buffer (10% SDS). Recombinant proteins were detected with the HRP-conjugated anti-His(C-term) mAb and film exposed for 1 minute.

3.22. cDNAs of scFv-His6 and scFv-protamine-His6 were cloned into pcDNA3 for expression in a mammalian system:

Because the recombinant proteins were produced but not secreted by the insect cells, attempts were made to express the recombinant proteins in mammalian cells including HEK293T and CHO-S cells. Although genes of the baculovirus are expressed under the control of the polyhedrin gene promoter (*polh*), the baculoviral promoters that are generally used for insect cells are not active in mammalian cells. Thus, the *polh* promoter cannot drive expression of genes in mammalian cells (238, 239). Therefore, the pFastBac^{TM}1 plasmid donor vector which encodes the scFv-His6 or scFv-protamine-His6 could not be used for expression in mammalian cells. For this reason, scFv-His6 and scFv-protamine-His6 cDNAs from the plasmid pFastBac^{TM}1 were PCR amplified so they could be cloned into the pcDNA3 plasmid vector (Figure 49 top) which has the CMV promoter for expression in mammalian cells. The expression cassettes were cloned into pcDNA3 using the native signal sequence of the antibody for secretion from mammalian cells. A schematic illustration for the cloning strategy is shown in Figure 15, page 77. Positive clones from transformants were analysed by restriction digestion (Figure 49 bottom) and sequencing.

Full sequencing data showing the in-frame nucleotide sequences for the expression constructs is shown in Appendix 2, pages 345 and 346. The genetic maps with unique restriction sites of both constructs are shown in Appendix 3, pages 357 and 358 respectively.

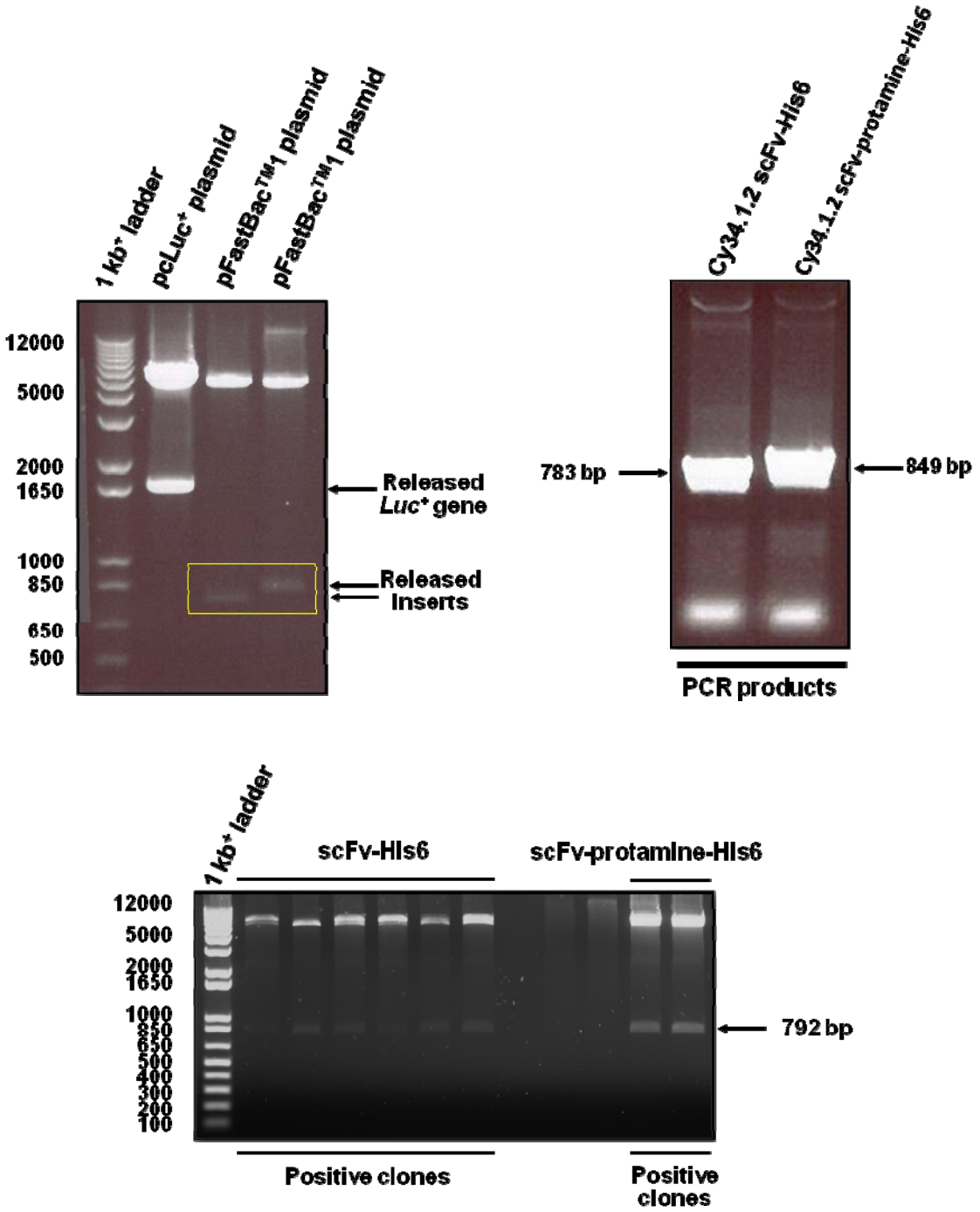

Figure 49: Cloning of scFv-His6 and scFv-protamine-His6 DNA into pcDNA3 for expression in mammalian cells. Restriction digestion of pcLuc^{+} and the pFastBac^{TM}1 vectors with *Hind*III and *Apa*I enzymes to release the luciferase gene (*Luc*$^{+}$) and scFv DNA inserts, respectively (top left). PCR amplification of scFv-His6 and scFv-protamine-His6 DNAs to incorporate *Hind*III and *Apa*I restriction sites (top right). The amplified products were digested with the corresponding enzymes, extracted by gel purification and used for ligation with the linearised pcLuc^{+} plasmid. The ligation reactions were carried out at 4°C overnight and DH5α *E. coli* transformed with the ligation reactions. Analysis of DNA minipreps by restriction digestion with *Hind*III and *Nde*I to check for the fidelity of the positive clones (bottom).

For expression of the recombinant proteins, HEK293T and CHO-S cells were transfected with scFv-His6 and scFv-protamine-His6 in pcDNA3 vector and three days post-transfection culture supernatants and cell lysates were analysed by Western blotting. Analysis of supernatants and lysates showed no protein production (results are not shown). The vectors were re-sequenced and checked for stop codons and the transfection experiments repeated three times for each cell system.

3.23. Cloning of cDNAs of scFv-His6 and scFv-protamine-His6 into pHEN1 phagemid for expression in bacteria:

The cloning strategy involved PCR amplification of the scFv-His6 and the scFv-protamine-His6 DNA expression cassettes with primers that enable cloning into the MCS of pHEN1 plasmid. The DNAs were cloned in-frame downstream of the pectate lyase B (pelB) signal sequence of the Gram-negative bacterium *Erwinia carotovora* in the pHEN1 vector. The PCR products of scFv-His6 and scFv-protamine-His6 and the vector were digested with *Nco*I and *Not*I enzymes (Figure 50). A schematic illustration for the cloning strategy is shown in Figure 16, page 79. Transformants that were positive clones (Figure 51) were further analysed by restriction digestion and sequencing.

Full sequencing data showing the in-frame nucleotide sequences for the anti-CD22.2 scFv-His6 pHEN1 expression construct is shown in Appendix 2, page 347. The genetic map of the construct with unique restriction sites is shown in Appendix 3, pages 359.

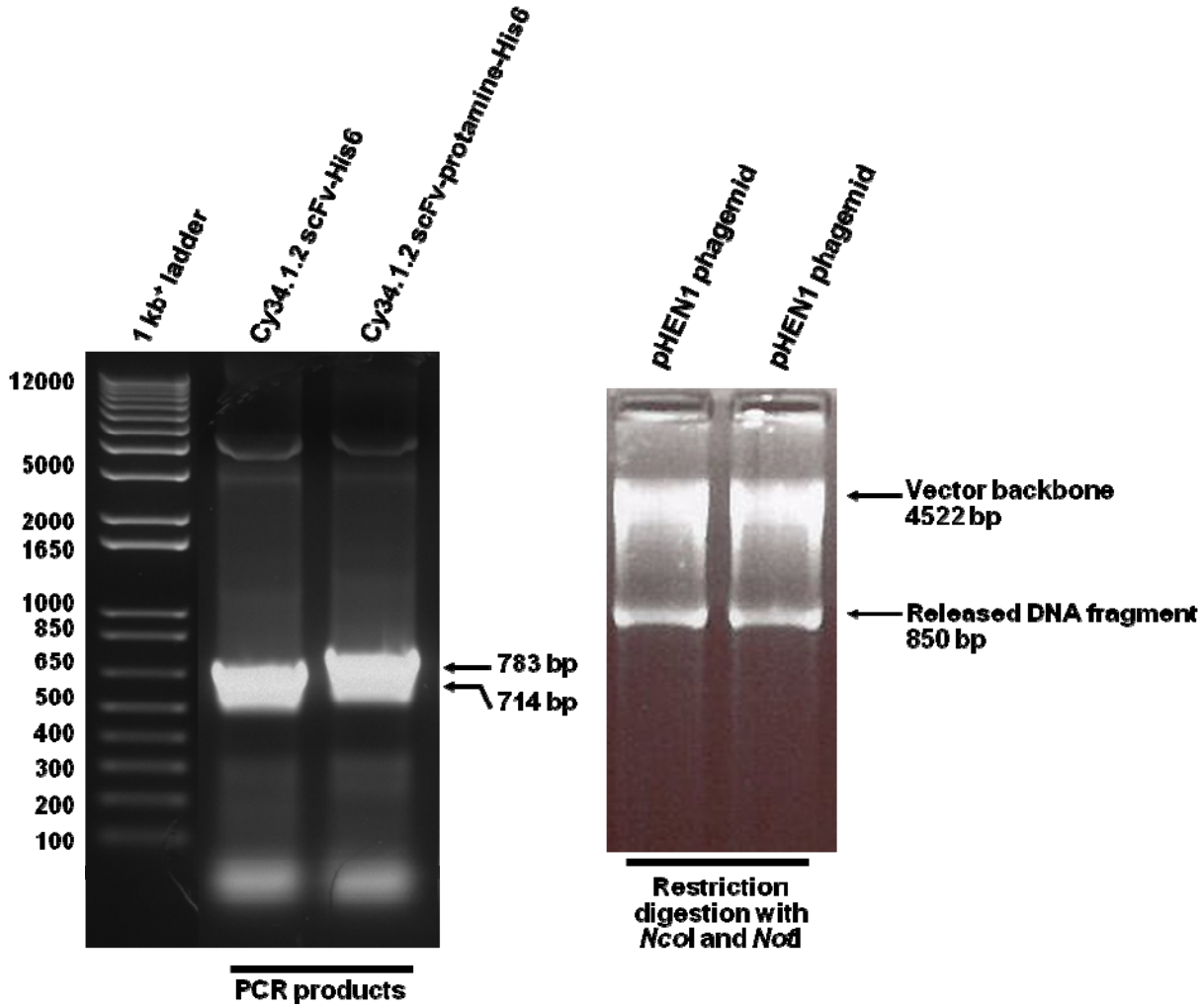

Figure 50: Cloning of scFv-His6 and scFv-protamine-His6 DNA into pHEN1 plasmid. PCR amplification of scFv-His6 and scFv-protamine-His6 DNAs to incorporate *Nco*I and *Not*I restriction sites (left). The amplified products were digested with *Nco*I and *Not*I enzymes, extracted by gel purification and used in the ligation reaction with the vector backbone. Restriction digestion of pHEN1 plasmid with *Nco*I and *Not*I restriction enzymes to prepare the vector for cloning (right).

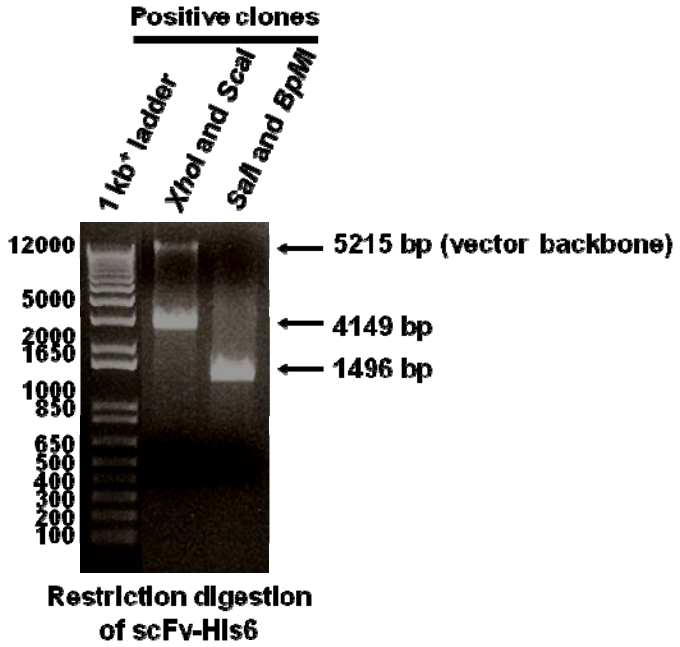

Figure 51: Restriction digestion analysis of plasmid DNA minipreps to determine positive clones. Positive clones were sequenced with LMB3 forward (5'CAGGAAACAGCTATGAC3') and pHEN1 reverse primers.

After induction with IPTG, expression of the recombinant proteins in the HB2151 *E. coli* culture was assessed by testing the bacterial culture supernatants, periplasmic extracts and the cell pellet by Western blotting. Results from the analysis showed that scFv-protamine-His6 was not produced (data not shown) while only the scFv-His6 was produced but not secreted to the periplasmic space which indicated inclusion body formation with insoluble proteins (Figure 52).

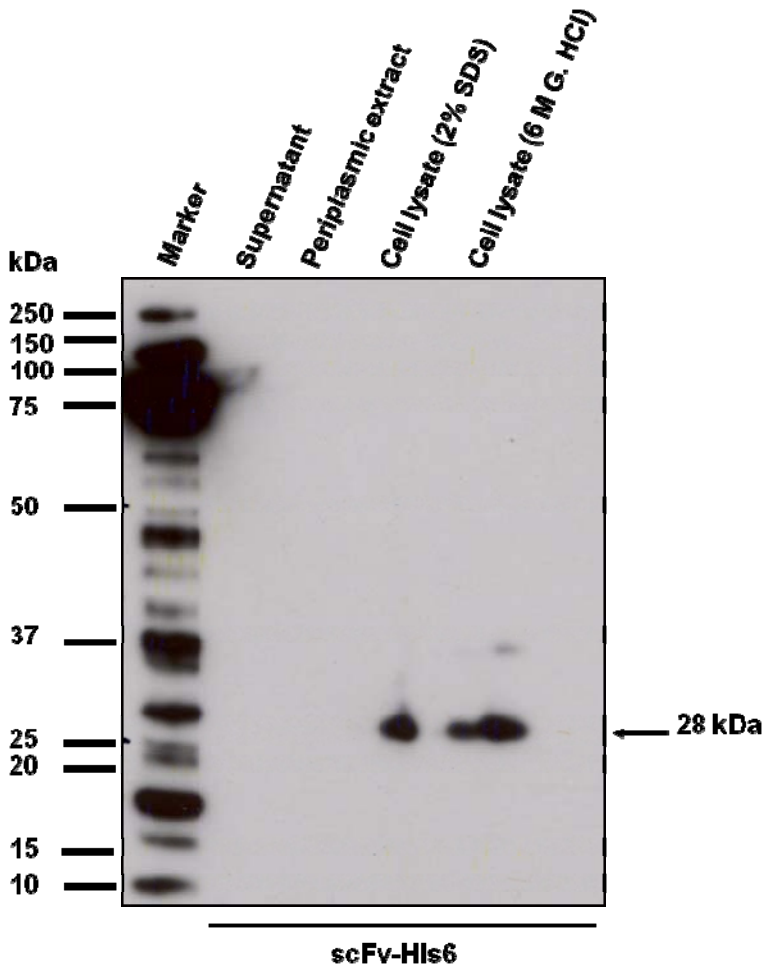

Figure 52: Western blotting analysis for the production of scFv-His6 recombinant protein in HB2151 strain of *Escherichia coli.* Supernatant, periplasmic extract and lysates of inclusion bodies isolated from bacterial cells were analysed on Western blotting for the production and secretion of the recombinant protein. Proteins were detected with HRP-conjugated anti-His(C-term) mAb.

3.24. Cloning of scFv-His6 and scFv-protamine-His6 at the C-terminus of human LAP with HRV3C protease cleavage site for expression in a mammalian system:

Because secretable proteins were not obtained from the eukaryotic insect cells and bacteria, a different expression system was assessed. This involved the use of latency associated peptide (LAP) of TGFβ protein to shield the recombinant proteins while they make their way through cellular secretory pathways. This assumption was partly based on the fact that there is a possibility for electrostatic interactions between the positive charges of protamine peptide and cell membrane though the scFv *per se* without protamine was also not secreted. Another reason for using LAP protein was to assess the human LAP signal peptide because the LAP of TGFβ is a secreted protein.

For this purpose, the constructs were PCR-amplified with specific primers to incorporate the human rhinovirus type 14 3C (HRV3C) cleavage site. HRV3C cleavage site has a recognition sequence Leu-Glu-Val-Leu-Phe-Gln-↓-Gly-Pro that can be cleaved with HRV3C protease. This was to help cleave the recombinant proteins for separation of the scFv proteins from the LAP shell. The human LAP with pcDNA3 vector backbone was prepared for cloning. Ligation reactions were then set up between the PCR-amplified products and the vector backbone (Figure 53) and the resulting transformants were further analysed for the validity of the constructs (Figure 54). Sequencing data is shown in Appendix 2, pages 348 and 349. The genetic maps are shown in Appendix 3, pages 360 and 361.

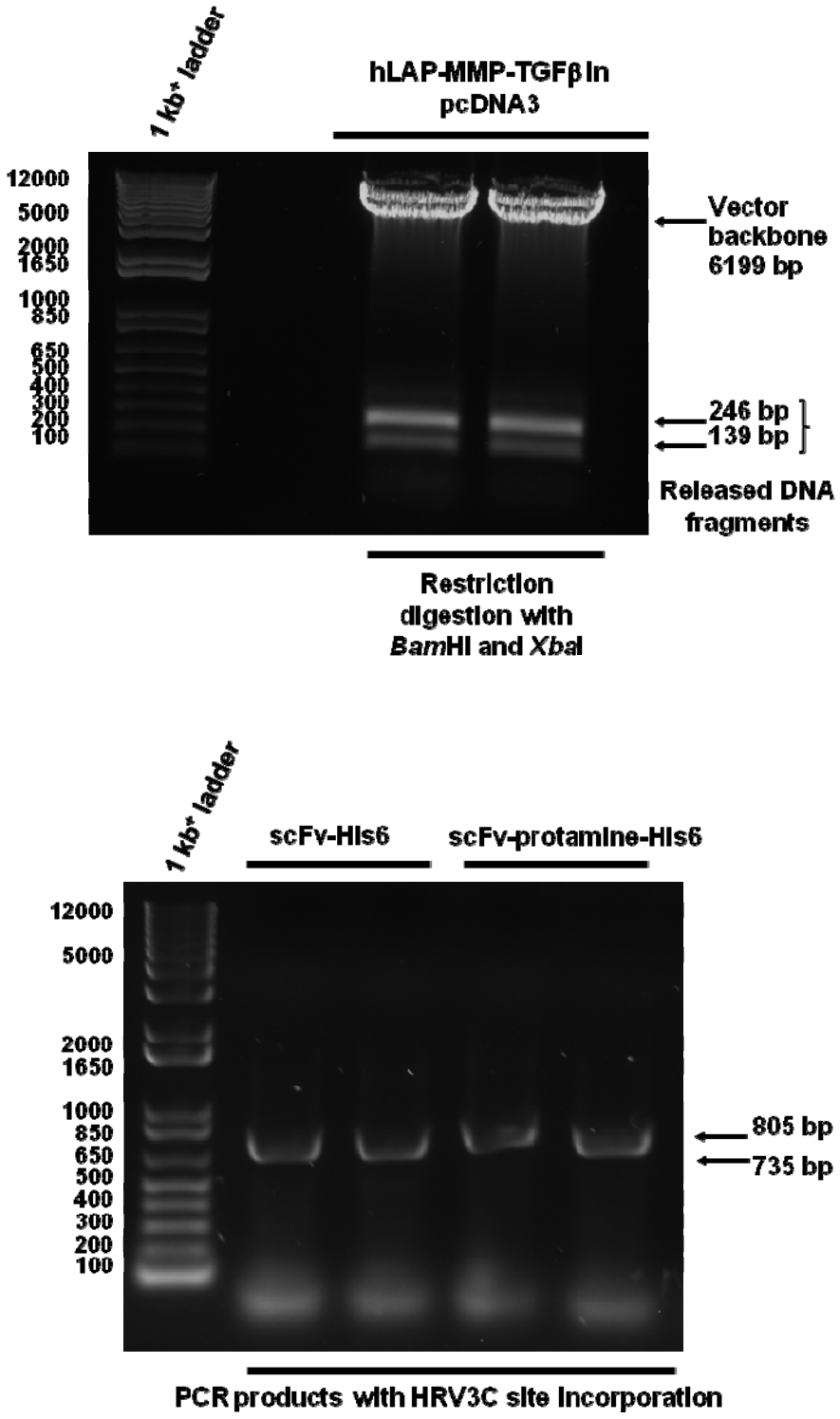

Figure 53: Cloning of scFv-His6 and scFv-protamine-His6 DNA at the C-terminal region of human LAP with the HRV3C cleavage site. Restriction digestion of hLAP-MMP-TGFβ in pcDNA3 with *Bam*HI and *Xba*I enzymes to remove MMP-TGFβ DNA fragment (top). PCR amplification of scFv-His6 and scFv-protamine-His6 DNAs to incorporate the HRV3C cleavage site (bottom).

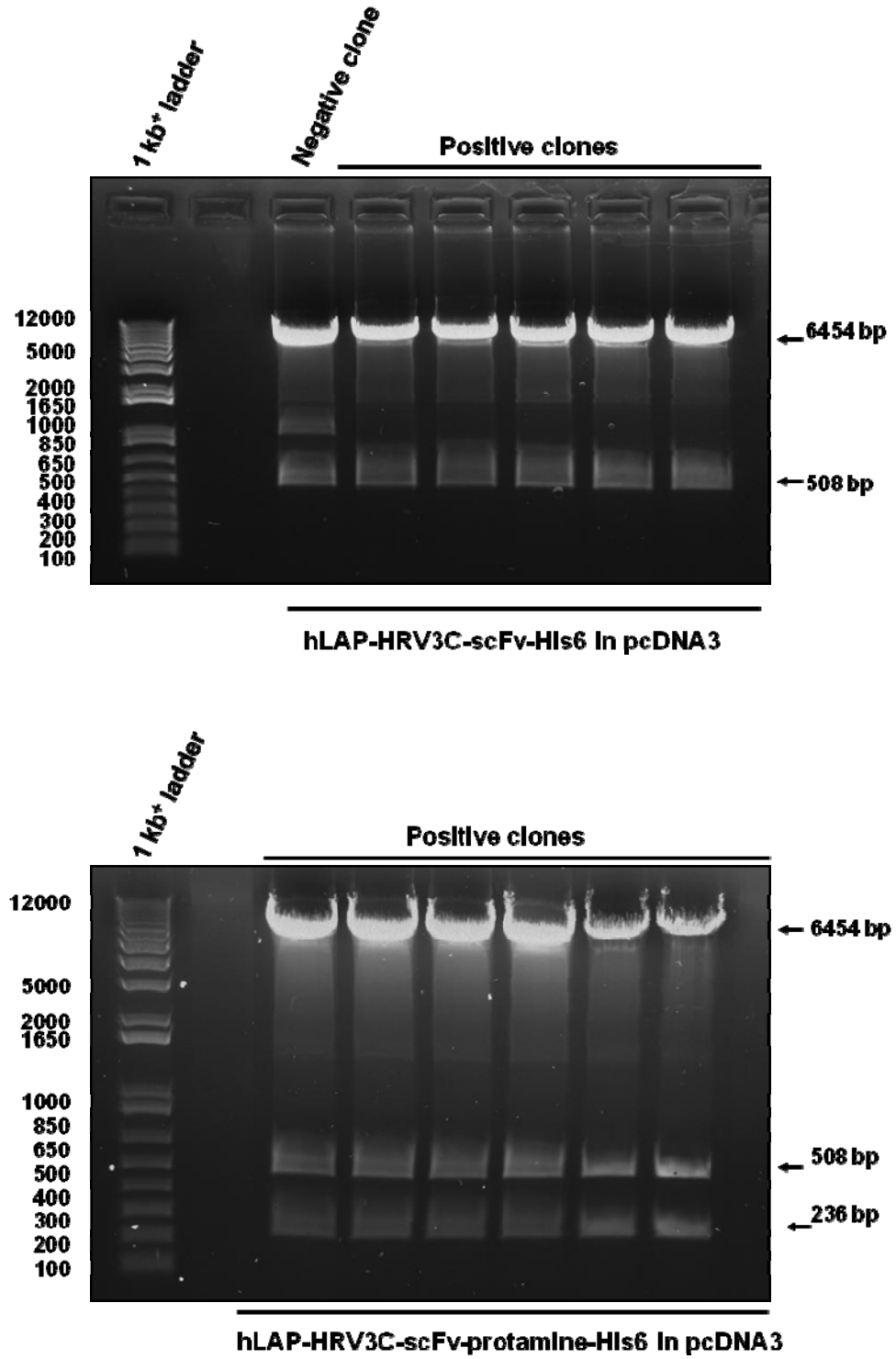

Figure 54: Restriction analysis of plasmid DNA minipreps with *Eco*RI and *Sbf*I to confirm fidelity of positive clones. Positive clones from restriction analysis of hLAP-HRV3C-scFv-His6 (top) and hLAP-HRV3C-scFv-protamine-His6 (bottom) were further analysed by sequencing with F-LAP forward and BGH reverse primers.

3. 25. Analysis of recombinant LAP proteins expression in mammalian cells:

CHO-S cells were transiently transfected with the expression constructs using PEI. An aliquot of supernatant was harvested at three different time points of the culture. The culture supernatants and clarified cell lysates were analysed by Western blotting. For detection of LAP-engineered proteins, goat anti-LAP antibody (goat IgG polyclonal antibody to human LAP TGFβ1 at 1:1000 (0.1 μg/μL) in blocking buffer) and HRP-conjugated secondary antibody (mouse anti-goat at 1:1000 in blocking buffer) were used to detect the proteins. The results showed endogenous LAP of TGFβ was produced and secreted by CHO-S cells and the positive control (hLAP-agg-IFNβ) but not the LAP-HRV3C-scFv-His6 or LAP-HRV3C-scFv-protamine-His6 constructs (Figure 55). The same samples were analysed by Western blotting with HRP-conjugated anti-His(C-term) mAb but the proteins were not detectable (data not shown).

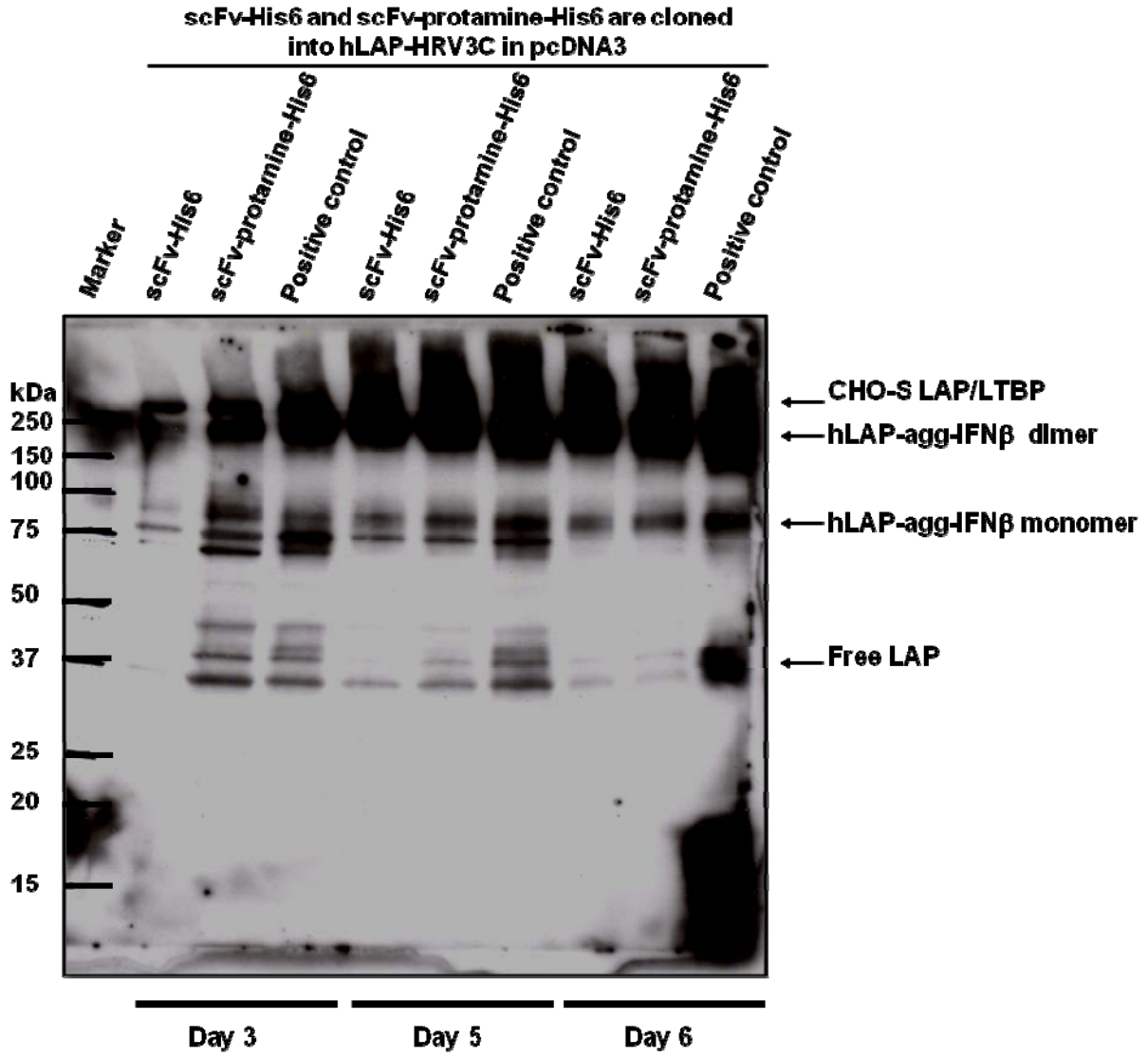

Figure 55: Expression of recombinant proteins cloned at the C-terminal region of LAP protein. CHO-S cells were transfected with the expression vectors using PEI. The positive control for the expression system is hLAP-agg-IFNβ. Aliquots of culture supernatants were collected at different time points (days 3, 5 and 6) to test for the peak of protein expression. Polyclonal goat IgG anti-human LAP antibody was used to probe the proteins using HRP-conjugated secondary mouse anti-goat IgG Ab. Expected Mw t. of recombinant proteins were 131.65 kDa for hLAP-HRV3C-scFv-His6 and 138.68 kDa for hLAP-HRV3C-scFv-protamine-His6. The positive control is hLAP-aggrecan-IFNβ in pcDNA3. SDS gel was run under non-reducing conditions to see monomer and dimer formation. Recombinant proteins were not detectable with HRP-conjugated anti-His(C-term) mAb for the same samples.

3.26. Cloning of anti-CD22.2 scFv-protamine-His6 into pDisplay vector with murine Ig kappa chain signal peptide for expression in a mammalian system:

Proteins expressed from pDisplay™ vector are fused at the N-terminus to the murine Ig kappa chain signal sequence, which is a well-known signal peptide that directs proteins to the extracellular space. The ability of Ig kappa chain signal peptide to impel secretion of the recombinant protein was tested following from the expression of the anti-human CD22.2 scFv-protamine-His6 protein (reasoning and outcome of this approach will be discussed in detail in chapter 4). To achieve this, the anti-CD22.2 scFv-protamine-His6 was cloned into pDisplay vector to investigate whether, or not, the choice of a different signal peptide can result in the secretion of the recombinant proteins.

The construct (Appendix 3, page 362) was successfully generated by inserting the PCR-amplified product of scFv-protamine-His6 into pDisplay vector (Figure 56) and confirmation of the validity of the construct by restriction analysis (Figure 57) and sequencing (Appendix 2, page 350).

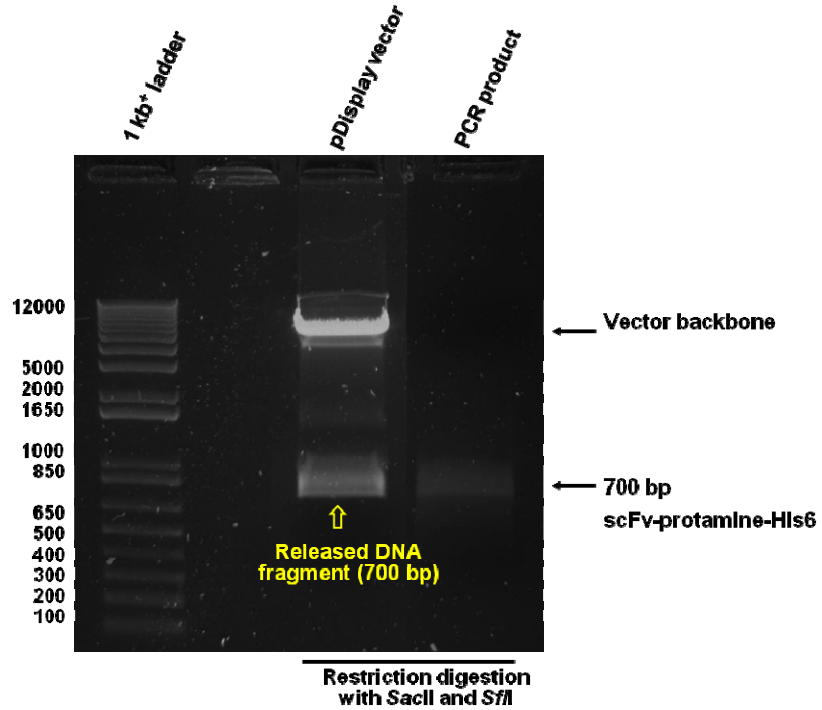

Figure 56: Cloning of scFv-protamine-His6 DNA into pDisplay vector. scFv-protamine-His6 DNA was amplified by PCR to incorporate *Sfi*I and *Sac*II sites, followed by digestion and gel extraction. pDisplay vector was digested with *Sfi*I and *Sac*II enzymes and after gel purification it was ligated with the processed PCR product.

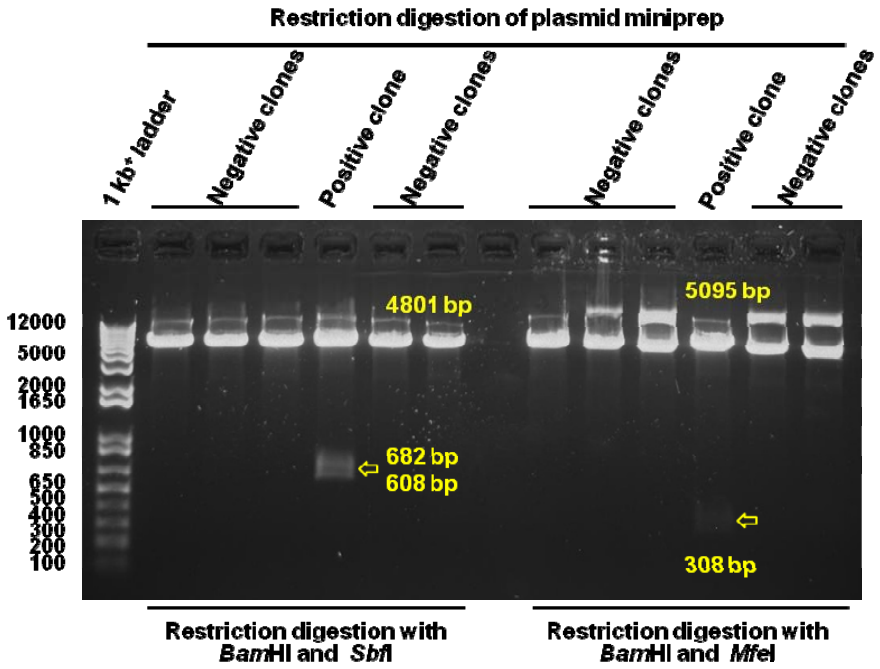

Figure 57: Restriction digestion analysis of plasmid DNA minipreps. All plasmid DNA minipreps were digested with *Bam*HI and either *Sbf*I or *Mfe*I enzymes. Positive clones were determined and sequenced with T7 forward and pMH R-113 reverse primers.

To investigate the impact of murine Ig kappa chain signal peptide on secretion of the recombinant protein, CHO-S, HEK293T and HEK293F cells were transiently transfected with plasmids from the positive clones. Results from Western blotting showed no secretion of the protein (data not shown).

3.27. Purification of recombinant proteins under denaturing conditions:

Having established that the recombinant proteins were not secreted using a mammalian cell system after trying different approaches, attempts were made to purify the recombinant proteins from the cell lysates of transfected HighFive insect cells under denaturing conditions using 6 M guanidinium lysis buffer. For small-scale purification, about 800 μL of clarified cell lysates were mixed with 200 μL of nickel agarose resuspended in denaturing binding buffer. At the time of lysing the cells on ice, a cocktail of six protease inhibitors with broad specificity for aspartic, cysteine, and serine proteases as well as aminopeptidases (1:200) was added to the cells. After preparation of the nickel affinity chromatography columns under denaturing conditions, most of the recombinant proteins that passed over the nickel column did not bind and were detected in the flow-through. There was also some degradation, or low molecular weight fragment generation, from the scFv-protamine-His6 flow through (Figure 58). Because of formation of precipitates and crystals in the 6 M guanidinium lysis buffer at 4°C, it was not possible to perform the protein purification at 4°C. This may partly explain the low molecular weight fragments detected in the Western blotting. A cocktail of EDTA-free protease inhibitors was, therefore, used during cell lysis to prevent degradation by proteolytic enzymes liberated during cell lysis.

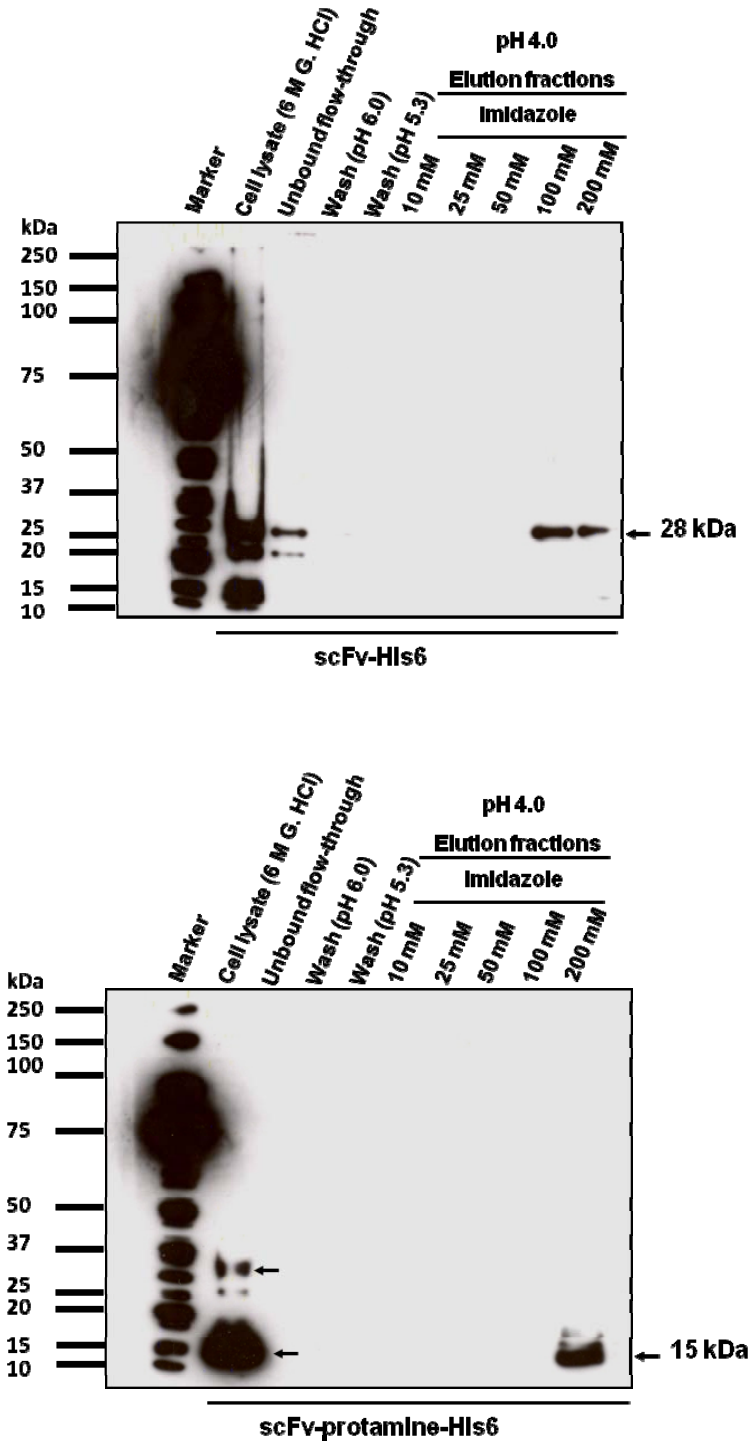

Figure 58: Western blotting analysis of recombinant proteins purified under denaturing conditions. HighFive insect cells were lysed on ice using 6 M guanidinium HCl for 15 minutes. Clarified lysates containing the recombinant proteins were added to the nickel column. Sample load, unbound flow-through, washes and elution fractions were collected and analysed on a 10% pre-cast gel under reducing conditions, transferred onto PVDF membrane and protein bands detected with HRP-conjugated anti-His(C-term) mAb.

3.28. Assessment of HRP-conjugated Staphylococcal protein A for the detection of recombinant proteins:

Staphylococcal protein A (SpA), a 56 kDa cell wall protein from *Staphylococcus aureus,* which interacts with the Fc region of most immunoglobulins and also the Fab fragments of a proportion of serum immunoglobulins that are encoded by the human V_H3 family of genes. The binding of SpA to the V_H regions is restricted to antibodies encoded by a subset of the V_H3 family (V3-23 and related genes in humans) and the S107 and J606 families in mice (240). Interaction of HRP-conjugated SpA with the expressed recombinant proteins was assessed to see if this reagent could be used both for detection and purification. For this purpose, the HRP-conjugated SpA was assessed for binding to the recombinant proteins by Western blotting. The experiments showed that the SpA-HRP did not bind to the recombinant proteins (data not shown).

3.29. Improvements in the purification of recombinant proteins:

Several attempts were made to purify the recombinant proteins under native and denaturing conditions. However, all were ineffective. Although the recombinant proteins were extracted with I-PER®, they did not bind to nickel columns under native conditions. Therefore, an alternative approach used was to denature the recombinant proteins and attempt binding them to the nickel column under denaturing conditions. The results from the latter approach showed that most of the protein did not bind as it was collected in the flow-through fraction. In order to address these problems and implement modifications that could increase binding of the denatured recombinant proteins to the nickel affinity column, a number of possibilities were considered. One approach was to add 50 mM L-arginine, or L-glutamine to all the buffers to improve purification. Thus, 50 mM L-glutamine was added to all the buffers used for purification under denaturing conditions. This enhanced binding of the recombinant proteins to the nickel column when the binding was carried out for 90 minutes at room temperature. After binding, washing and elution, the samples were analysed by Western blotting and a great improvement was noted (Figure 59).

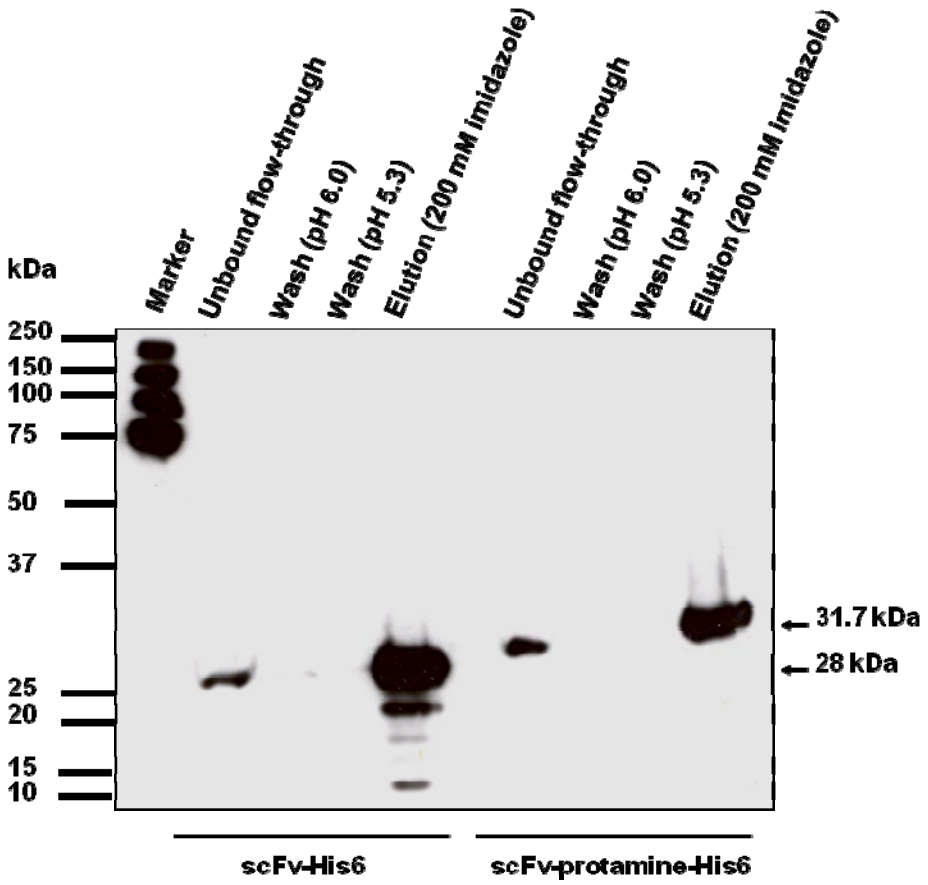

Figure 59: L-glutamine (Glu) improves purification of recombinant proteins using nickel affinity chromatography. Western blotting analysis of recombinant proteins expressed in HighFive insect cells following the addition of 50 mM L-glutamine to all buffers used in the purification of recombinant proteins. HighFive cells were lysed with 6 M guanidinium lysis buffer and clarified lysates purified using nickel-affinity chromatography under denaturing conditions. Addition of 50 mM L-glutamine to the binding, wash and elution buffers significantly improved binding and elution of the proteins. Unbound flow-through, washes and elution fractions were analysed on a 10% pre-cast SDS PAGE gel and transferred to PVDF membrane and probed with HRP-conjugated anti-His(C-term) mAb.

Having optimised the system for recombinant protein purification under denaturing conditions with the addition of 50 mM L-glutamine, the eluted protein fractions were dialysed to remove the urea and then further purified. For this purpose, ion exchange chromatography was used. The average isoelectric points [PI] were 7.268 and 9.665 for scFv-His6 and scFv-protamine-His6 proteins, respectively. Based on this, the Q Sepharose™ Fast Flow HiTrap™ anion exchanger column was used for scFv-His6 protein and an SP Sepharose™ Fast Flow HiTrap™ cation exchange column was used for scFv-protamine-His6 protein. After performing the purification at 4°C using FPLC, the elution fractions were analysed by Western blotting but the proteins were not detectable (data not shown). At this stage, more intracellularly trapped proteins were produced by insect cell transfection. These proteins were hereafter only purified through nickel affinity chromatography under the optimal conditions. The proteins were refolded and analysed by silver staining of SDS PAGE gels and Western blotting (Figure 60) and then tested for binding to CD22.2 receptor on BCL1-3B3 B cells.

3.30. Assessment of the refolded recombinant proteins by flow cytometry for binding to CD22.2 on mouse B cells:

Flow cytometry was carried out to verify binding of the recombinant proteins to CD22.2 on BCL1-3B3 B cells. Total protein concentration of the refolded protein was determined, scFv-His6 (330 μg/mL) and scFv-protamine-His6 (600 μg/mL). From each, about 100 μg/mL of protein was used for staining of 1 x 10^6 cells/mL. A dilution of 1:500 of anti-6X His tag® DyLight®650 antibody was used as a secondary detection antibody. Results of the FACS data showed no binding of the recombinant proteins to BCL1-3B3 B cells (Figure 61).

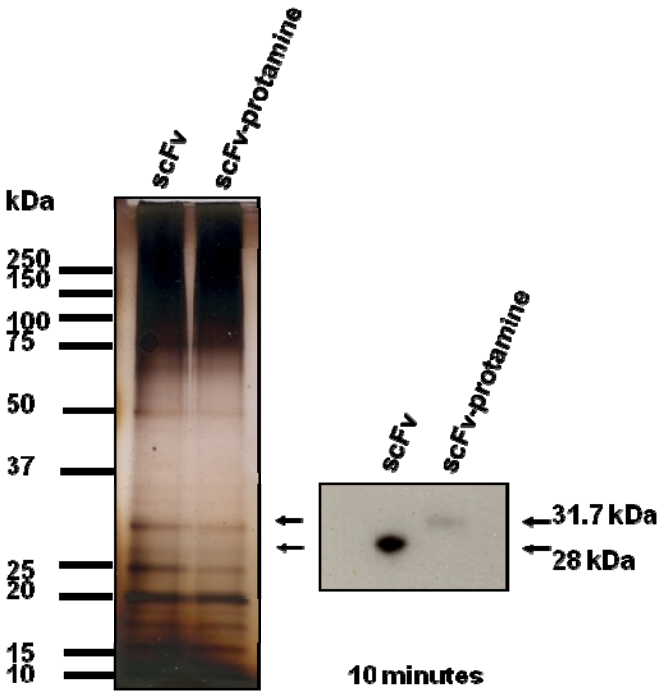

Figure 60: Analysis of refolded recombinant proteins by silver staining and Western blotting. The protein yields resulting from nickel affinity and cation exchange chromatography are not yet suitable for labeling with fluorescent dyes. Therefore, proteins were tested, indirectly using anti-6X His tag® DyLight®650 antibody, for binding to CD22.2 receptor on BCL1-3B3 B cells.

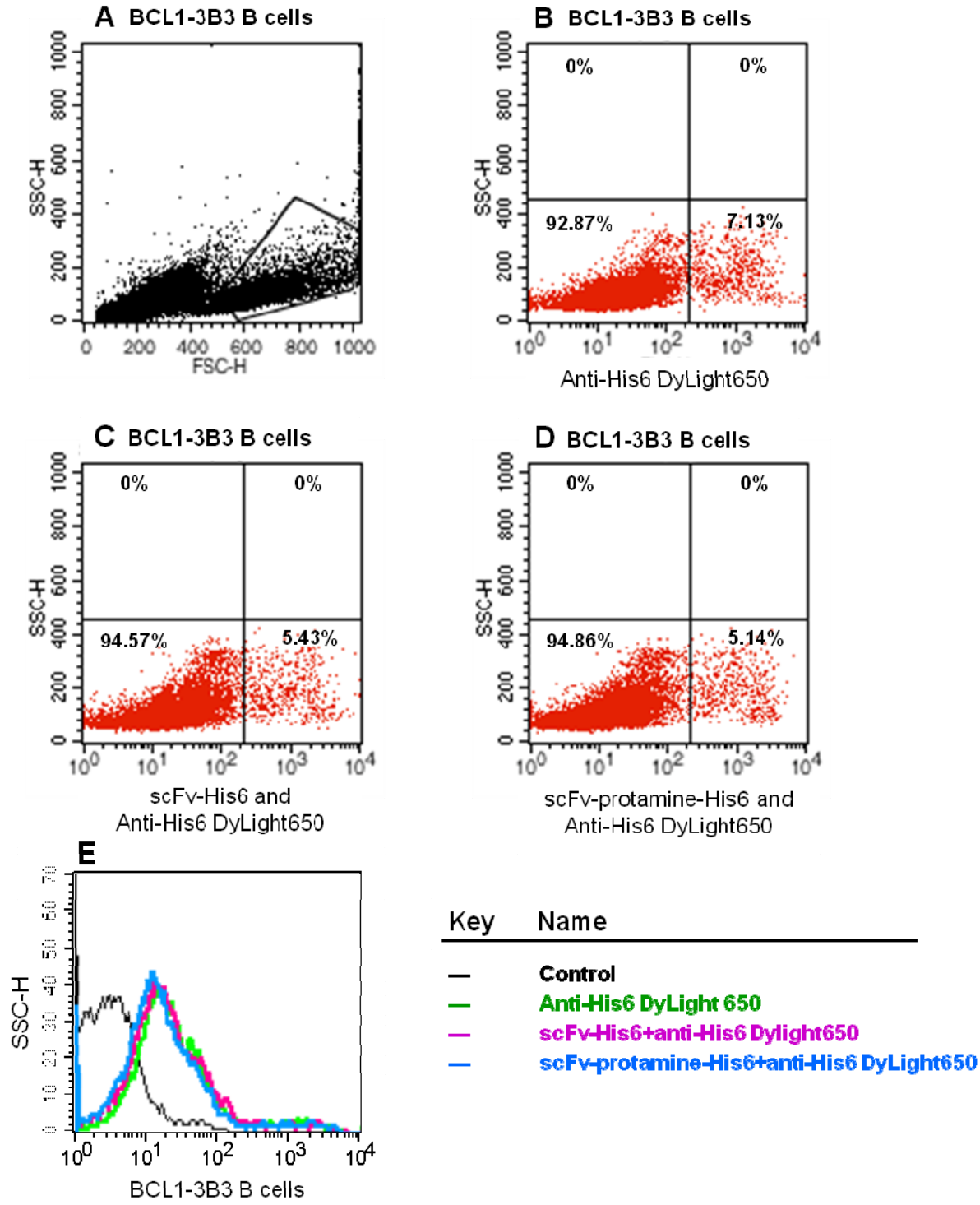

Figure 61: FACS analysis to assess binding of refolded recombinant proteins to the CD22.2 receptor on mouse BCL1-3B3 B cells. (A) Forward and side scatter of unstained B cells. The cells show high background staining from non-specific binding of the anti-6X His tag® DyLight®650 antibody (B). In (C) and (D), binding of scFv-His6 and scFv-protamine-His are tested respectively after staining with the secondary antibody. In (E) the histogram profile of binding is compared.

3.31. Discussion:

B cell targeted therapies have broad-spectrum applications for many diseases. This study describes a new approach for targeting pathogenic B cells in disease, including malignant B cells in leukaemias and lymphomas.

CD22 is a constitutively expressed receptor that is endocytosed and recycled and can be used to shuttle cargo between the cell surface and the endosomal compartments of B cells (93). CD22 is of considerable interest as a therapeutic target for B cell directed therapies. Its expression is restricted to the B cell lineage with nearly all mature B cells expressing membrane CD22, with the exception of plasma cells. To treat $CD22^+$ B cell leukaemias/lymphomas, several approaches including using anti-CD22 antibodies alone, or in conjugated forms, as well as combination immunotherapies have been developed (82, 89 and 90).

A promising treatment approach for B cell malignancies includes the use of new combinatorial therapies including biological agents such as mAbs and chemotherapeutics. For example, CMC-544, now called inotuzumab ozogamicin, a potent immunoconjugate of the chemotherapeutic agent calicheamicin combined with a humanised IgG4 anti-CD22 mAb (G5/44), has shown potent cytotoxicity against $CD22^+$ B cell lymphoma in cell lines and preclinical models (241). Recently, inotuzumab ozogamicin was assessed and shown significant activity in adults and paediatric patients with relapsed and refractory B cell acute lymphoblastic leukaemia (ALL) (242). However, toxicities from the chemotherapeutic drugs limit their potential applications. Therefore, there is an urgent need for the development of new therapeutics.

Over the past several years, generations of recombinant fusion proteins, including anti-CD22 scFv immunotoxin conjugates BL22 and HA22 were assessed in clinical trials for the treatment of $CD22^+$ B cell malignancies and proved to be effective with reduced toxicities (230).

The approach explored in this study is based on using scFv of mAbs with specificity for CD22 to deliver siRNA to modulate the biology and fate of malignant B lymphocytes. The potential of this approach was demonstrated by using purified anti-CD22 mAb and testing the kinetics of its binding to membrane CD22 and internalisation by B cells. For this purpose, the mouse mAb anti-CD22.2, specific for the CD22.2 allele, purified from the Cy34.1.2 hybridoma was examined. When the kinetics of internalisation was studied by CLSM using the AlexaFluor®488-conjugated anti-CD22.2 mAb, the surface-bound antibody/receptor complex on B cells was shown to traffic to the intracellular compartments soon after incubation of the cells at 37°C for 15 minutes. Most of the receptor-bound antibody was clustered inside the cytoplasm and more of the complex was located intracellularly after 60 minutes at 37°C. Slicing through various cell planes using Z-stacking in confocal microscopy confirmed the intracellular localisation of the receptor-antibody complex. Binding and internalisation, thus, confirmed the foundation and suitability of this approach. Several investigators have shown binding and internalisation of anti-CD22 mAb and constitutive endocytosis of CD22 receptor (83-94). Similarly, the current experiments have shown that binding of anti-CD22.2 mAb AlexaFluor®488 to CD22 resulted in internalisation after about 15 minutes of incubation with BCL1-3B3 B cells at 37°C which is consistent with the kinetics of internalisation ($t_{1/2}$) reported to be about < 1 hour from the cell surface (82).

In order to engineer the anti-CD22.2 scFv fusion protein with the truncated protamine domain and hexahistidine purification tag, the cDNAs for the V_H and the V_L genes were first generated and then a poly-G tail nucleotides sequence was added onto the 5'UTR sequence of the V_H and V_L cDNA using the TdT. TdT polymerase, belongs to the nucleotidyltransferase superfamily, catalyses repetitive addition of mononucleotides from dNTPs to the terminal 3´-OH of a DNA initiator in an untemplated fashion (243, 244). The V_H and V_L genes were then amplified using nested PCR amplification. A similar approach to PCR-amplify V_H and V_L genes of C2 hybridoma cells was used and shown in a previous study (245). The V_H and V_L poly-G tailed cDNA PCR products were then used in TA cloning. The viability of TA cloning has been shown previously in several studies to quickly clone a given gene in order to obtain sequence information or to simply amplify enough DNA for traditional cloning methods (246-249). Based on

alignments with related germ-line nucleotide sequences in the IgBLAST search, the V_H and V_L genes families for the mouse anti-CD22.2 IgG1 mAb were determined. To establish an expression system for scFvs that would allow easy cloning of the V_H and V_L domains and production of large amounts of correctly processed and secreted scFvs, baculoviruses were used to transfect insect cells. The baculovirus expression vector system exhibits many advantages including high expression level (250), capacity for large DNA fragment insertions (251) and proper protein refolding, disulfide bond formation and post-translational modifications (252). For this purpose, the constructs were generated in a donor plasmid vector (pFastBac^{TM}1) which was then transferred to baculovirus genome by site-specific transposition.

The baculovirus *Autographa californica* multinucleocapsid NPV (AcMNPV), which was used in the current study, has a genome of 134 kb. Thus, recombinant baculovirus particles can accommodate large amounts of foreign DNA (253).

The strategy for efficient generation of recombinant baculoviruses is based on site-specific transposition in DH10Bac^{TM} *E. coli* which contains the baculovirus shuttle vector (bacmid). Bacmid DNA contains a mini-F replicon, which allows autonomous replication and stable segregation of plasmids at low copy number, a selectable Kanamycin resistance marker and *att*Tn7, the target site for the bacterial transposon Tn7, all inserted into the polyhedrin (*polh*) locus of AcMNPV. The mini-Tn7 element on the donor plasmid pFastBac^{TM}1, contains the gene of interest, transposes to the target plasmid (bacmid) in DH10Bac^{TM} *E. coli* when Tn7 transposition function by the transposase is provided by a helper plasmid in the DH10Bac. The foreign gene is then expressed under the control of the baculovirus promoter *polh* when the resulting composite bacmid is introduced into insect cells (254, 255). In this case, the recombinant bacmid was engineered to carry the scFv-His6 or scFv-protamine-His6 constructs.

The ability to process and perform posttranslational modifications on secreted proteins is a major strength of the baculovirus expression vector system which has contributed to its increased use (250-252). However, yields of secreted proteins by

insect cells may suffer due to incomplete processing and aggregation (256-259). Intracellular retention of the recombinant anti-CD22.2 scFv-His6 and scFv-protamine-His6 proteins was an indication of difficulty with secretion of the protein. In support of the speculation of retention of the recombinant proteins, investigators have shown that in addition to mature length polypeptides, protein precursor polypeptides have been observed to accumulate in insect cells as well (260). In another study, a significant fraction of immunoglobulin light chain (Cκ) expressed in insect cells was also observed to accumulate as aggregates at a higher molecular weight than the processed polypeptide chains. These preprocessed immunoglobulin polypeptides are believed to include the unprocessed signal peptide sequence (261).

Signal peptides, needed to direct proteins to the various cellular compartments, must be cleaved to obtain a functional protein. Upon membrane translocation, the signal peptide is removed by a signal peptidase complex that is membrane-bound to the endoplasmic reticulum in eukaryotic cells or bound to the cellular membrane in prokaryotic cells (262).

The function of the signal peptide in the secretion process is to direct the newly synthesised polypeptide into the translocation machinery of the cellular membrane (263). Without removal of the signal peptide the protein may aggregate and remain within incorrect compartments such as endoplasmic reticulum and be prevented from further passage along the secretion pathway (264, 265). Consequently, the yields of secreted proteins can be drastically reduced. A previous study has shown that signal peptidase overexpression resulted in increase of the processing of antibody scFv fragments. Such results demonstrate that low signal peptidase activity can limit the production of recombinant proteins (265).

In a strategy to enhance recombinant protein secretion, a number of investigators used a novel secretion signal from bacterial endotoxin (proprietary sequence). This signal, engineered on constructs intended for the production of recombinant proteins in prokaryotes and eukaryotes, allowed the secretion of recombinant protein in all cases (266).

Previous studies have shown that DNA inserts cloned in-frame with the gp64 signal sequence can produce target proteins that may be secreted from the recombinant baculovirus-infected insect cells (267). In this regard, efforts were invested in the current study to swap the native signal sequence of the anti-CD22.2 scFv with the baculovirus gp64 signal sequence for enhanced expression and secretion of the recombinant proteins from insect cells. Therefore, the pBAC^{TM}-6 transfer plasmid (Merck Chemicals Ltd, Nottingham, UK) was first used to clone the anti-CD22.2 scFv-His6 and scFv-protamine-His6 cDNA expression cassettes. Then, these transfer plasmids were used for recombination by site-specific transposition to baculovirus genome (bacmid). pBAC^{TM}-6 is a baculovirus transfer plasmid that contains a 20 amino acid gp64 signal peptide sequence capable of directing high levels of proteins into the secretory pathway of infected insect cells. However, this cloning process was not pursued further because of obtaining the anti-human CD22 scFvs BL22 and HA22 from the National Cancer Institute. Henceforth, the new expression construct was made from anti-human CD22 (HA22) which is described in detail in chapter four. Nevertheless attempts were made to purify the mouse recombinant proteins produced by insect cells under both native and denaturing conditions although these proteins were retained intracellularly.

The findings reported in this chapter are in agreement with a previous study to produce anti-HER2 scFv-protamine in insect cells using baculovirus expression system (120). These investigators encountered difficulties to express and secrete recombinant protein. Additionally, they showed that the scFv fusion proteins could only be extracted from cell pellets by using strong denaturants such as 6 M guanidinium HCl. Further to the low protein yield they obtained, an extensive refolding process was required to recover binding activity of the scFv-protamine protein (120).

Various expression systems were used in the current study for the production of the recombinant proteins, including insect, mammalian and bacterial cells.

One possible explanation for lack of recombinant protein secretion from mammalian cells is an increase in the level of phosphorylation of eukaryotic translation initiation factor 2 (eIF2), which can inhibit polypeptide chain initiation completely. This

proposition is based on findings from previous studies which attempted to produce recombinant proteins in mammalian systems. According to these studies, a major mechanism that limits translational rates *in vivo* and *in vitro* is phosphorylation of eIF2 on the α-subunit at Ser51 (eIF2α) (268). During translation initiation, eIF2, guanosine triphosphate (GTP) and methionyl initiator transfer RNA (Met-$tRNA_i^{Met}$) form a ternary complex that interacts with the 40S ribosomal subunit and the translation initiation complex (269). When the anti-codon of the Met-$tRNA_i^{Met}$ in the ternary complex base pairs with the mRNA initiation codon, this triggers hydrolysis of the GTP and release of eIF2 in the guanosine diphosphate (GDP)-bound form. Release of GDP from eIF2 and regeneration of eIF2-GTP is facilitated by the guanine nucleotide exchange factor eIF2B. Phosphorylation of the α-subunit of eIF2 increases its affinity for GDP by 100-fold so that eIF2B cannot catalyse nucleotide exchange and remains bound to eIF2-GDP. Because the eIF2B is usually 10 times less abundant than eIF2, small increases in the level of eIF2α phosphorylation can completely inhibit polypeptide chain initiation because eIF2B becomes sequestered in an inactive form, which prevents eIF2 recycling (270). Furthermore, efficient *in vitro* protein synthesis in cell-free systems has been limited by phosphorylation of eIF2α factor (270). This phosphorylation has been explained by the activation of the eIF2α kinases in the cell-free systems. In an attempt to overcome this limitation, investigators have shown that protein synthesis in a hybridoma extract was increased by 3-4 folds after addition of growth arrest and DNA damage inducible protein (GADD34), which stimulated eIF2α dephosphorylation (270). Similar results were obtained by supplementation of cell extracts with the vaccinia virus K3L protein, which can also be phosphorylated by the eIF2 kinases due to its structural resemblance to eIF2α (271, 272). In addition, it has been shown that the mRNA 5′-m^7G-cap structure and 3′-poly(A) tail act synergistically to stimulate translation *in vivo* (273).

An alternative approach for the production of recombinant proteins would be the use of *in vitro* cell-free translation systems. Cell-free translation systems are increasingly used for the production of recombinant proteins that are either toxic, or difficult to produce in high yields in mammalian cells (274, 275). However, many mammalian cell-free systems have limited yield or do not reproduce the properties of translation *in vivo*. Thus, the cell-free system cannot perform these post-translational modifications.

Until writing this thesis, extensive efforts were made to express the recombinant proteins from mammalian cells backed up with auxiliary range of additional approaches. Hypothetically, it may be possible that electrostatic interactions of amino acid side chains on the protamine peptide to hamper secretion of the protein through the secretory pathway. It is a well-known fact that eukaryotic cell membranes from the cytoplasmic side usually confer a net negative charge because of the abundance of anionic phospholipid phosphatidylserine. This will facilitate trapping of the recombinant proteins due to the fact that protamines have a high content of positively charged amino acids, particularly arginine (276). The positive charge of the protamine peptide could, therefore, be a hurdle for the secretion, or exportation of the recombinant protein.

Because of similarities in the amino acid sequences between the truncated protamine peptide (RSQSRSRYYRQRQRSRRRRRR) and human immunodeficiency virus 1 (HIV-1) trans-activator of transcription protein transduction domain (TAT-PTD) peptide (YGRKKRRQRRR), there is a possibility of difficulty in secretion of the recombinant proteins rich in cationic amino acids. There are suggestions from previous studies addressing problems with secretion of TAT-fusion proteins. In a study that compared different TAT-fusion proteins (TAT-EGFP, TAT-srIκBα, TAT-RBD), the major fraction of fusion proteins was found in the cell lysate, and only a small amount of the fusion proteins was present in the supernatant (277). In another study, several variants of HIV1-TAT-PTD with different numbers of cationic amino acids, secretion levels decreased with an increase in cationic charge (278). Similar to HIV1-TAT-PTD, protamine is cationic in nature.

Because of the possibility of entrapment of anti-CD22.2 scFv-protamine-His6 recombinant protein within producing cells, a method was used to protect and shield the charges on the protein while making its way through the cellular secretory pathway. Although this approach could be questioned because the scFv-His6 was also not expressed in mammalian cells, nevertheless, both anti-CD22.2 scFv antibody fragments were cloned at the C-terminal region of the latency associated peptide (LAP) of TGFβ. The “LAP-cleavage site-cargo” protein technology, generated in our department (279), comprises the LAP shell of TGFβ engineered to harbor a therapeutic moiety that will be

released by proteolytic cleavage of a cleavable site between the cargo and the LAP. The technology provides latency to the delivery and specificity of the therapeutics to disease sites. By using LAP protein here it would then be possible to shield the positive charges of the protamine peptide on scFv-protamine-His6. An additional reason for using the LAP construct was to investigate whether or not the human LAP signal sequence could drive secretion. For this purpose, the constructs generated comprised human LAP followed by HRV3C cleavage site and C-terminus scFv-His6 or scFv-protsmine-His6. Human LAP signal sequence was retained in the vector backbone to drive expression and secretion of the proteins. Unexpectedly, however, the proteins were not produced when the supernatants and cell lysates were analysed by Western blotting. Only the positive control construct did allow production. In addition to the distinguishing characteristic of LAP in providing latency, it would have been advantageous also for purification process. LAP can bind heparin-agarose columns and this protein purification platform is well-established and optimised for purification of LAP-associated proteins.

Further possible explanation for lack of scFv-protamine-His6 production/secretion could be attributed to the presence of a furin cleavage site. Furin is a mammalian endoprotease which recognises and cleaves the amino acid sequences RXRR or RXKR, where X can be any amino acid. It is mainly localised in the trans-Golgi network but can translocate between the trans-Golgi network and the cell surface (280). Therefore, the presence of these furin sites in protamine peptide would possibly result in protamine peptide being cleaved from fusion proteins that are secreted via the secretory pathway. In support to this hypothesis, a study has introduced mutations to destroy the furin cleavage sites without affecting TAT protein transduction ability. Using this system with the modified TAT, appropriate protein processing, correct folding and secretion of TAT fusion protein was achieved (281).

Further investigation of the signal peptide was pursued in the present study by using the murine immunoglobulin kappa light chain secretory signal. This signal peptide is derived from the first 21 amino acids (METDTLLLWVLLLWVPGSTGDAA) of the secretory signal which has been described to drive good expression/secretion of recombinant proteins (282). In another study, investigators also showed that with the

murine Ig κ-chain secretory signal peptide, efficient secretion of recombinant human UDP-N-acetyl-α-D-galactosamine polypeptide N-acetylgalactosaminyl-transferase 2 (GalNAc-T2) protein was achieved in insect SF9 and mammalian HEK293T cells (283).

A mammalian expression vector, pDisplay^{TM}, which contains the murine Ig kappa chain signal peptide was, therefore, used for cloning and production of anti-CD22.2 scFv-protamine-His6 protein. Results from the transient transfection experiments using HEK293F and CHO-S cells showed no protein production using this approach. It is worth mentioning, however, that the use of pDisplay^{TM} vector resulted in production and secretion of recombinant anti-human CD22 scFv-protamine-His6 protein (discussed in detail in chapter four).

In view of the fact that previous studies (284, 285) have reported the successful expression of scFv molecules in prokaryotic expression systems, such as *Escherichia coli* (*E. coli*), the anti-CD22.2 scFv constructs were cloned into pHEN1 phagemid. Using pHEN1 plasmid, a bacterial expression vector used in phage display, expression and secretion of engineered proteins are known to be directed to periplasmic space under pelB signal peptide. The secretion of a recombinant protein to the bacterial periplasm or the extracellular medium is advantageous because secreted proteins are more easily accessible; less contaminated with cellular proteins and usually have authentic N-termini. In addition, periplasmic or extracellular protein folding is improved and proteolysis is less extensive compared with cytoplasmic productions. The secretion capacity is, therefore, an important trait of viable production hosts. In the absence of an N-terminal signal peptide for periplasmic secretion, recombinant polypeptides expressed in bacteria accumulate in the cytoplasm. The fusion to suitable leader peptides allows for the translocation of unfolded precursors into the periplasm. The pelB signal sequence has proven to be successful in periplasmic production and precise processing of recombinant scFv antibodies and shown to direct recombinant proteins to the periplasmic space of the bacteria (284, 285).

Transformants obtained from cloning into pHEN1 plasmid were only positive for anti-CD22.2 scFv-His6 and production, but not secretion, of the recombinant protein in HB2151 *E. coli* cells was detected. Failure of pelB signal peptide to direct recombinant proteins into the periplasmic space has been reported in a previous study in an attempt to produce secretable scFv protein from bacteria. According to this study, there can be a number of possible explanations such as overloading of the secretion apparatus, the sequence following the pelB leader sequence in the antibody scFv fragment might negatively influence transport and processing or give rise to the production of insoluble antibody. In addition, the exact cleavage position by signal peptidase I recognition motive could have been altered; therefore the newly synthesised polypeptide will not be directed to the periplasmic space (285).

Although there have been reports on high production levels of soluble recombinant antibody fragments in *E. coli*, it still remains a troublesome host for the production of many recombinant antibody fragments. Previous studies have shown that recombinant antibody fragments have a tendency to generate inclusion bodies in *E. coli* and, thus, requiring additional refolding steps in order to achieve sufficient amounts of functional antibodies (286, 287). Nevertheless, several refolding systems for recovery of soluble and active scFv and Fab fragments from non-native aggregates have been reported and were shown to be promising (24, 288 and 289).

Generally, the ease, timescale and throughput favour engineering of antibody fragments in a bacterial expression system. One caveat is that antibody fragments are multi-domain proteins with multiple disulfides, which may not be correctly produced during *E. coli* expression. The odd incidence of obtaining anti-CD22.2 scFv trapped in a misfolded state in bacterial inclusion bodies was cumbersome and the purification was, therefore, not pursued further.

Due to the fact that insect cells were the only eukaryotic host cells that could be used to produce recombinant proteins, extensive experiments were, therefore, invested in purifying and refolding the recombinant proteins.

To purify and retrieve the proteins from clarified cell pellets lysates under denaturing conditions using 6 M guanidinium lysis buffer, a major improvement in protein purification was achieved only after addition of 50 mM L-glutamine to all the buffers used for protein purification under denaturing conditions.

In a previous study, investigators have demonstrated that the addition of 50 mM L-arginine (Arg) and 50 mM L-glutamine (Glu) to protein sample solutions significantly increased achievable protein concentration and improved the protein stability (290). These amino acids function by prevention of protein aggregation and thus help protein solubilisation. L-arginine and L-glutamine, oppositely charged in the pH range 5–7, together form a highly-soluble arginine glutamate salt. The efficiency and anti-aggregational effects of arginine glutamate salt has been established in previous studies (291-297). Furthermore, it has been established that when Arg and Glu are added together, provide the most efficient inhibition of protein aggregation (298).

Nickel affinity purified recombinant proteins, after the addition of L-glutamine, were refolded and regardless of protein contaminants, scFv proteins were tested for binding to CD22.2 on B cells by flow cytometry. Results of these experiments showed that protein renaturation and refolding were ineffective as no binding could be demonstrated.

Although anti-CD22.2 recombinant proteins were expressed in insect cells and in bacteria, but not in mammalian systems, there are a number of explanations for lack of expression of the recombinant proteins in a mammalian system.

The biosynthesis of secretary and membrane proteins in the endoplasmic reticulum (ER) is strictly monitored by a mechanism called ER quality control to ensure that only properly folded and assembled proteins are allowed to reach their final destination (299). Generally, a higher recombinant protein production is achieved by targeting naturally secreted proteins to the secretory pathway, where post-translational modifications, like protein folding, assembly and gycosylation, take place, as compared with a cytoplasmic localisation (300, 301). Proteins reach their proper folding and

conformation by the action of the folding-refolding machinery assisted by a set of folding chaperones, which mainly reside in the ER lumen (302-305). When stress affects the protein-folding mechanism in the ER, or when too many secretory proteins are synthesised and transported into the ER lumen, the folding-refolding system becomes overloaded and the proteins cannot achieve their proper conformation anymore. In this way, unfolded or misfolded proteins can accumulate which may compromise ER activities, for example protein synthesis and folding needed for cellular housekeeping, due to a decrease in essential proteins (306).

Recombinant protein production is a demanding process for the host cell, as an additional foreign protein needs to be produced besides the endogenous proteins. In some cases, production of this foreign protein leads into the activation of the unfolded protein response (UPR) and this can both positively and negatively influence the recombinant protein yield. For example, investigators have found in yeast that the overexpression of anti-fluorescein 4-4-20 scFv variants activated the UPR response, which in turn led to a reduction of the scFv yield (307, 308). Further, others have shown that disrupting the endoplasmic reticulum-associated degradation (ERAD) pathway in filamentous fungi led to an enhanced protein expression by delaying protein degradation (309).

Misfolded or faulty proteins produced as a result of mutations or affected by stresses, are retrotranslocated from the ER into the cytosol for degradation by the 26S proteasome after modification with polyubiquitin chains, by the ERAD process (310). During the ERAD process, misfolded proteins are recognised by the ER-degradation enhancing α-mannosidase-like protein (EDEM) and then transferred from the ER to the cytosol (retrotranslocated) as unfolded polypeptide chains through the translocon channel for degradation (311). However, how other toxic species, such as severely aggregated proteins, are eliminated from the ER is largely unknown.

Although production of secretable and properly folded anti-CD22.2 scFv proteins was not achieved, there has been profound progress in knowledge acquisition while generating and constructing the expression vectors. An array of molecular approaches and protein expression and purification systems were used to optimise the systems for the best-case-scenario in the next step that follows. By the time these efforts were made to obtain functional recombinant mouse anti-CD22.2 scFv proteins, anti-human CD22 scFv cDNAs were obtained courtesy of Dr. Ira Pastan (National Cancer Institute, Center for Cancer Research, Bethesda, USA). Subsequently, recombinant fusion protein was generated in properly folded and secreted forms from serum-free cultures of mammalian cells.

Chapter Four

Generation of anti-Human CD22 scFv-protamine Fusion Protein for Targeted Delivery of siRNA to B lymphocytes

This chapter describes methods used for the generation, purification, preservation and functional analyses of a soluble engineered anti-human CD22 recombinant protein. HA22, an anti-human CD22 scFv-protamine-His6, was generated as a secreted protein in serum-free cultures of HEK293F cells. Extensive attempts were made to produce and isolate high purity HA22 fusion protein. The dual functional property of the protein is in its ability to bind to CD22 on B cells and also to electrostatically bind with siRNAs. It is for the first time that such studies have succeeded in the generation of proteins tagged with protamine in secretable and soluble forms from serum-free cultures of mammalian cells with high purity. Results of the specificity of binding, kinetics of internalisation and delivery of siRNA into B cells and the effects of gene downregulation are presented.

4.1. Assessment of CD22 receptor expression on human B cell lines by flow cytometry:

Expression of CD22 on human B cell lines HF28 RA and L3/Bcl-2 was assessed by flow cytometry. Anti-human CD22 AlexaFluor®647 (AbD serotec) and anti-human CD19 FITC (BD Biosciences) were used for this purpose. The B cell lines were stained with the anti-CD19 and anti-CD22 Abs as described in the Materials and Methods chapter (section 2.4). Both B cell lines were shown to be positive for CD19 and CD22. Positive cells in the forward scatter were analysed by gating on live cells and excluding dead, or dying cells by propidium iodide (PI) staining (Figures 62 and 63).

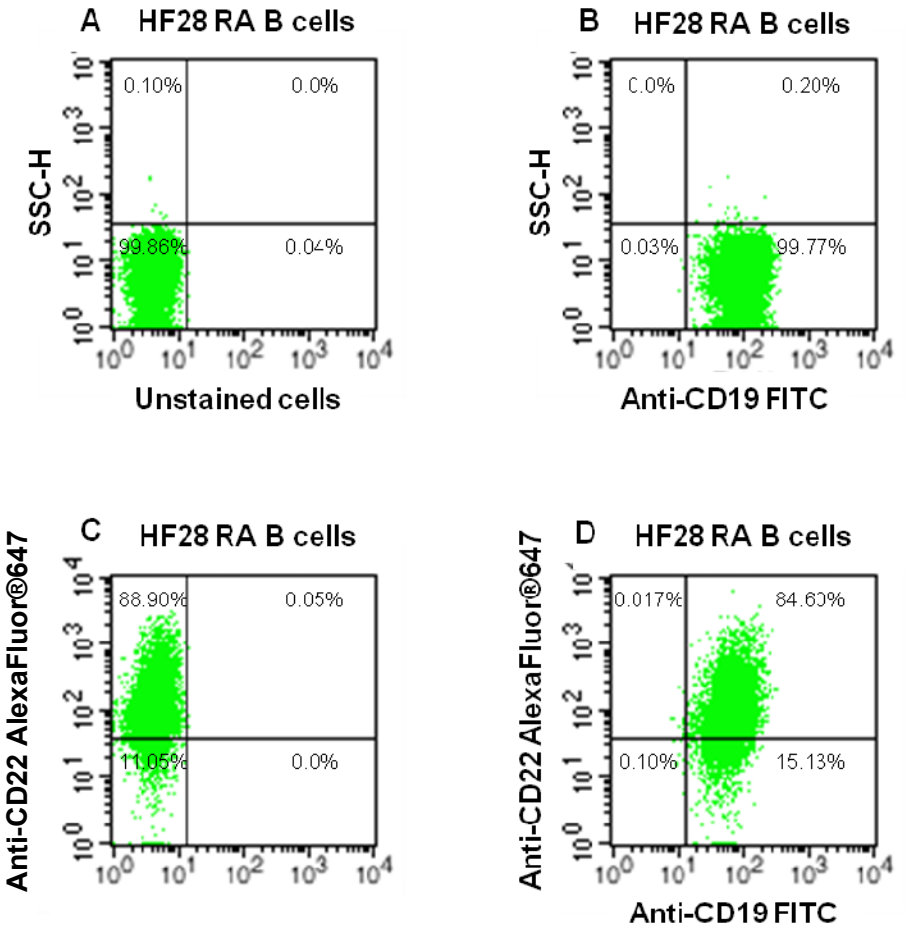

Figure 62: Analysis of human HF28 RA follicular lymphoma B cells by flow cytometry for CD19 and CD22 expression. The figure shows the dot plot profile of the forward and side scatter for the cells (A) and expression of CD19 (B) and CD22 expression (C). (D) Shows the B cell population which were double positive for both CD19 and CD22 expression.

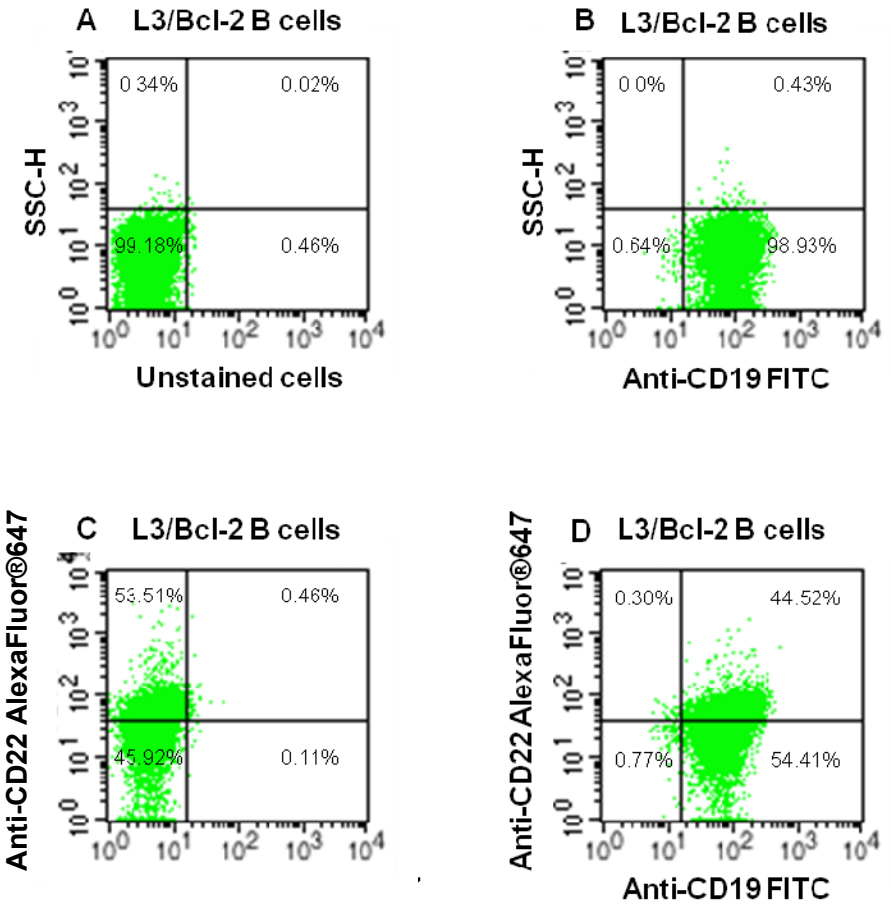

Figure 63: Analysis of human L3/Bcl-2 Burkitt's lymphoma B cells by flow cytometry for CD19 and CD22 expression. (A) Shows the dot plot profile of the forward and side scatter of the cells. Expression of CD19 and CD22 are shown in B and C, respectively. The B cell populations which were double positive for both CD19 and CD22 expression are shown in D.

4.2. The generation of the anti-human CD22 scFv-protamine-His6 construct:

For the construction and generation of the anti-human CD22 scFv-protamine-His6 cDNA, plasmid DNA pMH112 (BL22) and pMH113 (HA22) were obtained courtesy of Dr. Ira Pastan (National Cancer Institute, Center for Cancer Research, Bethesda, USA). Sequences of anti-human CD22 scFvs BL22 and HA22 were reported in previous studies (229, 312) and are shown in Figure 64. The dry format plasmids were retrieved and expanded in preparation for cloning as described earlier in the Materials and Methods (section 2.27). Subsequent to mini- and maxi-preparations, the plasmids were digested with *Bam*HI to confirm the presence of the inserts (Figure 65). To create the engineered antibody fragment, truncated protamine peptide and hexahistidine tag were attached to HA22 scFv from pMH113.

Schematic illustrations showing the genetic maps of pMH112 and pMH113 constructs containing anti-human HA22 (mutant) scFv with unique restriction sites are shown in Appendix 4, page 364 and Appendix 5, page 365 respectively.

RFB4 heavy chain (V_H):

```
Rearranged RFB4  ATG GAA GTG CAG CTG GTG GAG TCT GGG GGA GGC TTA GTG AAG CCT GGA GGG TCC CTG
a.a.              M   E   V   Q   L   V   E   S   G   G   G   L   V   K   P   G   G   S   L
IGHV5S21         ............AAG.....................GAA.....................................
a.a.             ............K.......................E.....................................
                                                                 |       CDR1      |
Rearranged RFB4  AAA CTC TCC TGT GCA GCC TCT GGA TTC GCT TTC AGT ATC TAT GAC ATG TCT TGG GTT
a.a.              K   L   S   C   A   A   S   G   F   A   F   S   I   Y   D   M   S   W   V
IGHV5S21         ..................................ACT.........AGC.....GCC.................
a.a.             ..................................T...........S.......A...................
                                                                 |       CDR2
Rearranged RFB4  CGC CAG ACT CCG GAG AAG AGG CTG GAG TGG GTC GCA TAC ATT AGT AGT GGT GGT GGT
a.a              R   Q   T   P   E   K   R   L   E   W   V   A   Y   I   S   S   G   G   G
IGHV5S21         ..................................................................GAT.
a.a.             ..................................................................D..
                                                    |
Rearranged RFB4  ACC ACC TAC TAT CCA GAC ACT GTG AAG GGC CGA TTC ACC ATC TCC AGA GAC AAT GCC
a.a.              T   T   Y   Y   P   D   T   V   K   G   R   F   T   I   S   R   D   N   A
IGHV5S21         TAC.ATC.........GCA.....................................................
a.a.             .Y...I...........A.....................................................

Rearranged RFB4  AAG AAC ACC CTG TAC CTG CAA ATG AGC AGT CTG AAG TCT GAG GAC ACA GCC ATG TAT
a.a.              K   N   T   L   Y   L   Q   M   S   S   L   K   S   E   D   T   A   M   Y
IGHV5S21         AGG.....................................................................
a.a.             R.......................................................................
                             |                                          CDR3          |
Rearranged RFB4  TAC TGT GCA AGA CAT AGT GGC TAC GGT AGT AGC TAC GGG GTT TTG TTT GCT TAC TGG
a.a.              Y   C   A   R   H   S   G   Y   G   S   S   Y   G   V   L   F   A   Y   W
IGHV5S21          ..............CGA.....................................................
a.a.              ..............R......................................................

Rearranged RFB4  GGC CAA GGG ACT CTG GTC ACT GTC TCT GCA
a.a.              G   Q   G   T   L   V   T   V   S   A
IGHV5S21         ..................................
a.a.             ..................................
```

RFB4 light chain (V_L):

```
Rearranged RFB4  GAT ATC CAG ATG ACC CAG ACT ACA TCC TCC CTG TCT GCC TCT CTG GGA GAC AGA GTC
a.a.              D   I   Q   M   T   Q   T   T   S   S   L   S   A   S   L   G   D   R   V
IGKV10-J1        ..............ACA.....................................................
a.a              .......................................................................

                             |                 CDR1                  |
Rearranged RFB4  ACC ATT AGT TGC AGG GCA AGT CAG GAC ATT AGC AAT TAT TTA AAC TGG TAT CAG CAG
a.a.              T   I   S   C   R   A   S   Q   D   I   S   N   Y   L   N   W   Y   Q   Q
IGKV10-J1        .......................................................................
a.a.             .......................................................................
                                                        |          CDR2          |
Rearranged RFB4  AAA CCA GAT GGA ACT GTT AAA CTC CTG ATC TAC TAC ACA TCA ATA TTA CAC TCA GGA
a.a.              K   P   D   G   T   V   K   L   L   I   Y   Y   T   S   I   L   H   S   G
IGKV10-J1        ..................................................AGA..................
a.a.             ..................................................R....................

Rearranged RFB4  GTC CCA TCA AGG TTC AGT GGC AGT GGG TCT GGA ACA GAT TAT TCT CTC ACC ATT AGC
a.a.              V   P   S   R   F   S   G   S   G   S   G   T   D   Y   S   L   T   I   S
IGKV10-J1        .......................................................................
a.a.             .......................................................................
                                                                |       CDR3
Rearranged RFB4  AAC CTG GAG CAA GAA GAT TTT GCC ACT TAC TTT TGC CAA CAG GGT AAT ACG CTT CCG
a.a.              N   L   E   Q   E   D   F   A   T   Y   F   C   Q   Q   G   N   T   L   P
IGKV10-J1        ........................ATT....................................................
a.a.             ........................I.....................................................
                       |
Rearranged RFB4  TGG ACG TTC GGT GGA GGC ACC AAG CTG GAA ATC AAA
a.a.              W   T   F   G   G   G   T   K   L   E   I   K
IGKV10-J1        ..........................................
a.a.             ..........................................
```

Figure 64: Nucleotide and amino acid sequences of the mouse anti-human CD22 scFv RFB4 (BL22) heavy (V_H) and light (V_L) chains. Arg45 in the V_H and Gly100 in the V_L (shown in red) are mutagenised to Cys44 and Cys100, respectively to create the high affinity disulfide-stabilised HA22 scFv.

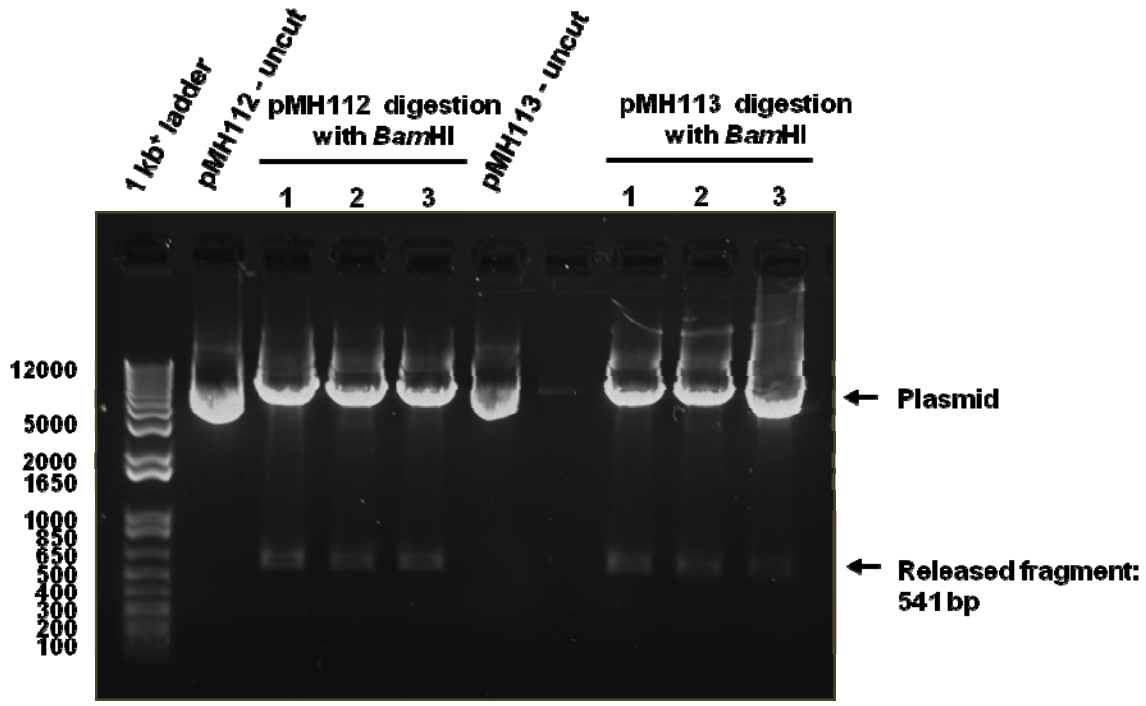

Figure 65: Agarose gel electrophoresis showing restriction analysis of plasmid vectors pMH112 and pMH113 with *Bam*HI enzyme. Expected size of DNA fragment to be released from the digestions is 541 bp. There are two *Bam*HI sites, therefore, a single digestion resulted in the release of the DNA fragment. The plasmid DNA was then sequenced with T7 forward and pMH R-113 primers and fidelity of the inserts confirmed.

4.3. Construction of the anti-human CD22 scFv-protamine-His6 in pcDNA6|IL2ss for expression in mammalian systems:

pcDNA6|IL2ss expression vector, routinely used in our department, drives expression and secretion of recombinant proteins. For this purpose, the protamine peptide and hexahistidine DNA fragment, generated earlier in this study for the mouse antibody constructs, was PCR-amplified using specific primers (*Bgl*II F forward and *Nhe*I R reverse primers with the corresponding restriction sites) compatible with the scFv and pcDNA6|IL2ss backbone. HA22 scFv was also PCR-amplified with specific primers (*Eco*RI F forward and *Bgl*II R reverse primers with the corresponding restriction sites) for insertion into the plasmid backbone together with protamine-His6 (section 2.28, page 85 and Figure 19, page 86). Only one construct of the engineered anti-human CD22 was generated from HA22 scFv by ligation of PCR products with pcDNA6|IL2ss vector backbone which was then digested with *Eco*RI and *Xba*I enzymes (Figure 66).

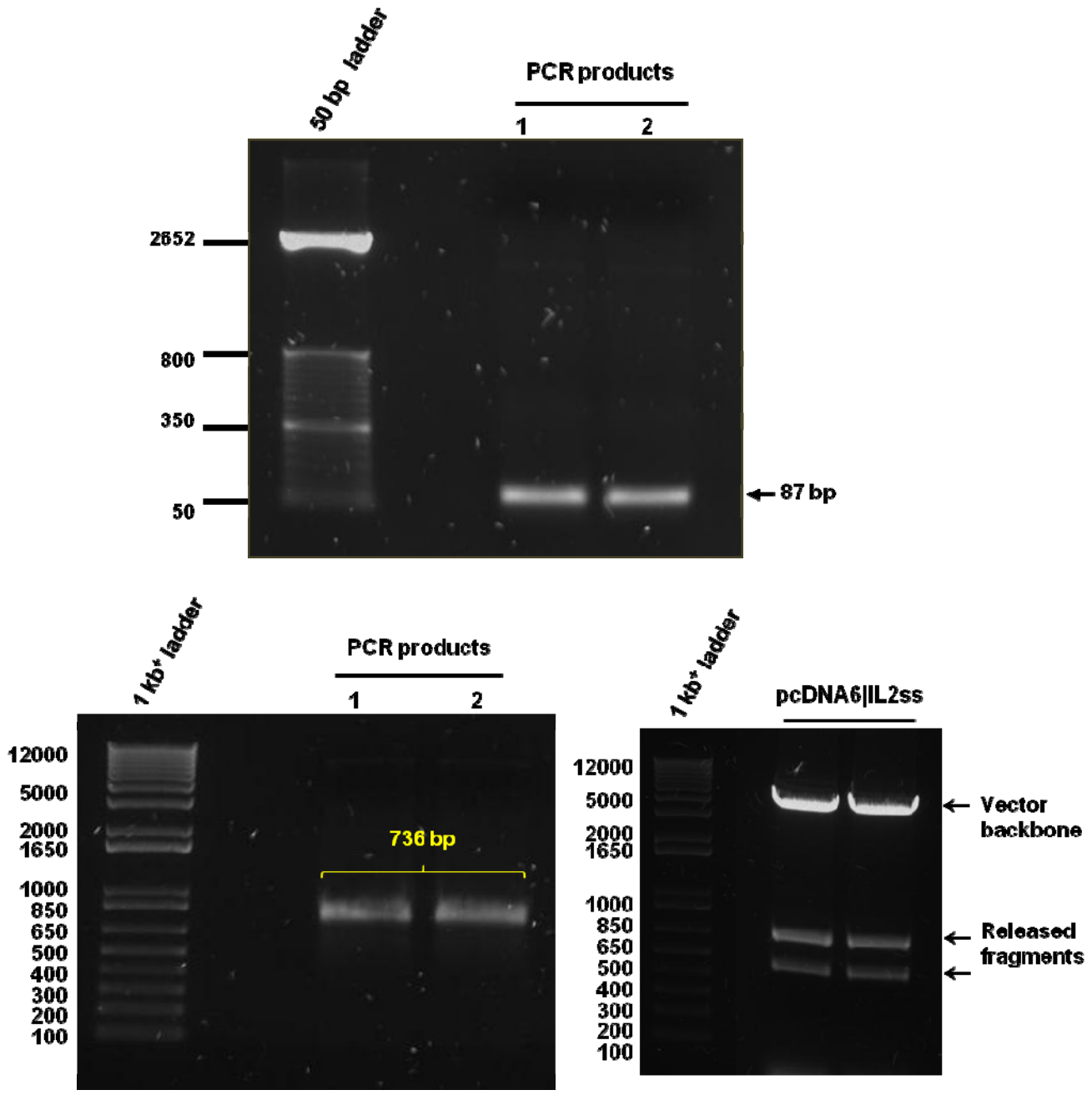

Figure 66: Agarose gel electrophoresis showing PCR amplification of the protamine-His6 and HA22 scFv and restriction digestion of pcDNA6|IL2ss vector. The protamine-His6 DNA fragment, 87 bp, was amplified from the mouse Cy34.1.2 pFastBac^{TM}1 scFv-protamine-His6 construct,digested with *Bgl*II and *Nhe*I enzymes and purified by gel extraction (top). HA22 scFv was also PCR-amplified with *Eco*RI forward and *Bgl*II reverse primers, digested using the corresponding enzymes for use in the ligation reaction (bottom left) with the vector backbone. pcDNA6|IL2ss vector was digested with *Eco*RI and *Xba*I, gel extracted and used in the ligation reaction (bottom right).

A schematic illustration depicting the construction of the in-frame DNA expression cassette of anti-human CD22 scFv-protamine-His6 is shown in Figure 67. This construct is consisted of the heavy chain (V_H) which is linked through a flexible glycine-serine linker at its C-terminus with a light chain (V_L) N-terminus followed by a truncated protamine and hexahistidine tag.

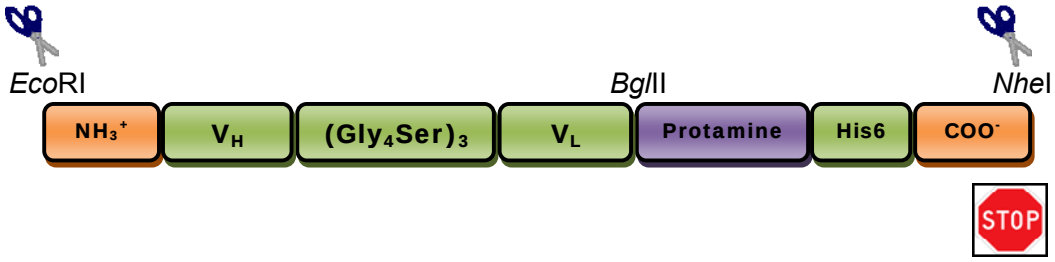

Figure 67: A schematic figure depicting HA22 scFv-protamine-His6 construct generated by the attachment of *Eco*RI-HA22-*Bgl*II DNA to *Bgl*II-truncated protamine-His6-*Nhe*I DNA fragment. The combined DNA fragment was ligated into pcDNA6|IL2ss backbone. The vector backbone was restricted with *Eco*RI and *Xba*I. Because the two *Nhe*I sites are present in the vector backbone, the vector was digested with *Xba*I enzyme instead of *Nhe*I so that *Xba*I and *Nhe*I sites could then ligate together as these two sites have compatible cohesive ends.

PCR products of HA22 scFv and protamine-His6 amplification were ligated with pcDNA6|IL2ss backbone DNA after purification of the DNA fragments by gel extraction. The ligation reaction was used for bacterial transformation and plasmid minipreps from the transformants were analysed by restriction digestion (Figure 68). Positive clones were further analysed by sequencing (Appendix 2, page 351). Plasmids from positive clones were expanded by maxipreparations and used for protein expression by transient transfection of mammalian cells.

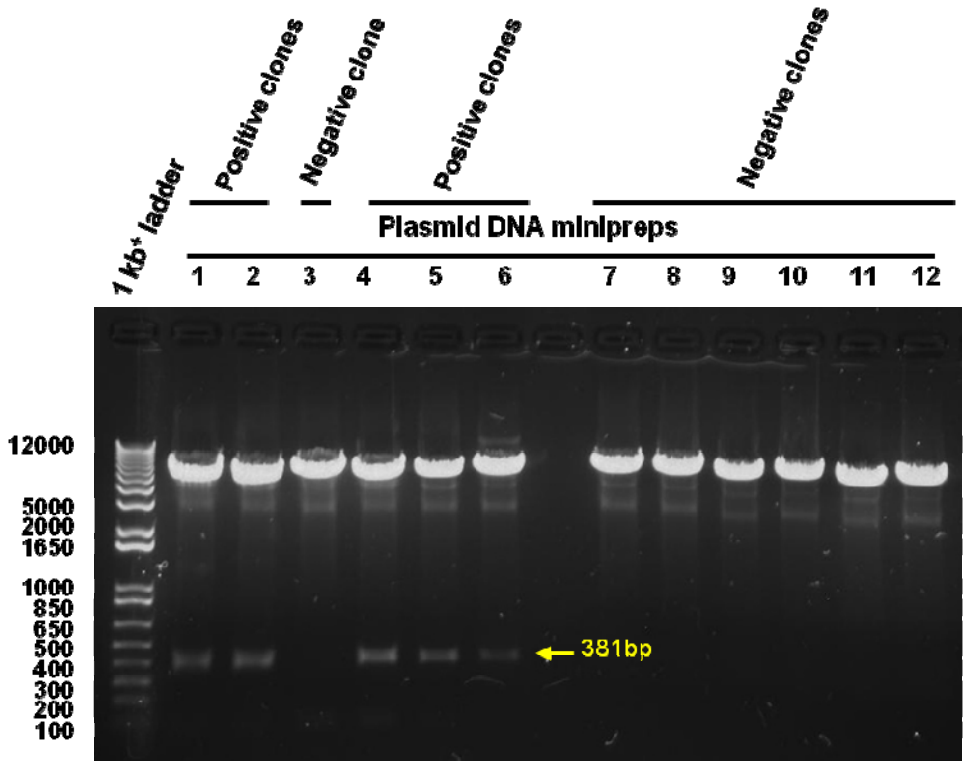

Figure 68: Restriction digestion of pcDNA6|IL2ss plasmid DNA minipreps with *Eco*RI and *Bam*HI to identify positive clones. Positive clones were identified by the release of a 381 bp fragment. These were further analysed by sequencing using T7 forward and BGH reverse primers.

4.4. Transient transfection of HEK293T and CHO-S cells for the expression of recombinant HA22 protein:

The pcDNA6|IL2ss-HA22 scFv-protamine-His6 construct was used for the expression of the protein in CHO-S and HEK293T cells. Results from the analysis of culture supernatants and cell lysates did not confirm expression of the protein (data not shown). The validity of the correct insertion of the in-frame construct was confirmed for a second time by re-sequencing the plasmid DNA. Transfection experiments were repeated in HEK293T cells including the original pMH113 vector which has HA22 scFv alone. pMH113 is HA22 scFv fused with haemagglutinin A, c-myc and PDGFR transmembrane domain as has been reported in a previous study (313). Analysis of culture supernatants and cell lysates of transfected cells showed expression from the original pMH113 vector but not pcDNA6|IL2ss (Figures 69 and 70).

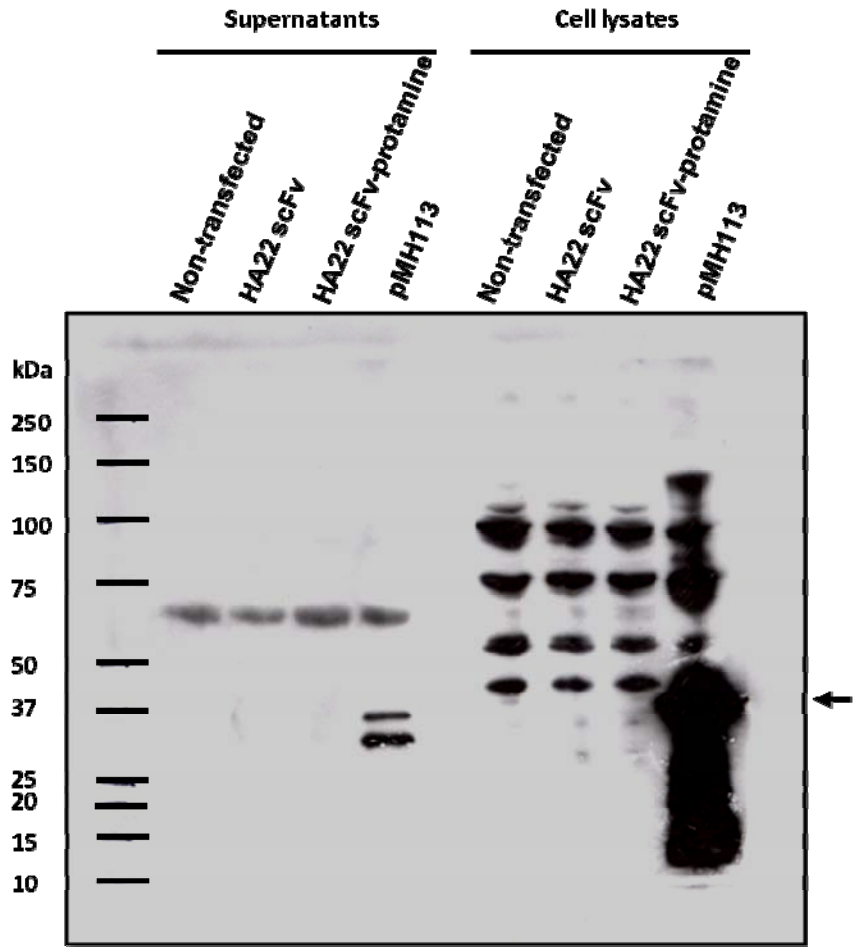

Figure 69: Western blot analysis for expression of anti-human CD22 (HA22) from the un-modified vector pMH113 and the pcDNA6|IL2ss by transient transfection of HEK293T cells. HA22 in pMH113 vector was tagged with c-Myc and PDGFR transmembrane domain. Following expression and secretion, HA22 protein from pMH113 will remain bound extracellularly to HEK293T cells via the PDGFR transmembrane domain. Rabbit anti-myc antibody (1:1000) and secondary HRP-conjugated anti-rabbit antibody (1:1000) were used for the detection of the protein on a reducing SDS PAGE gel. The blot was exposed for 1 minute.

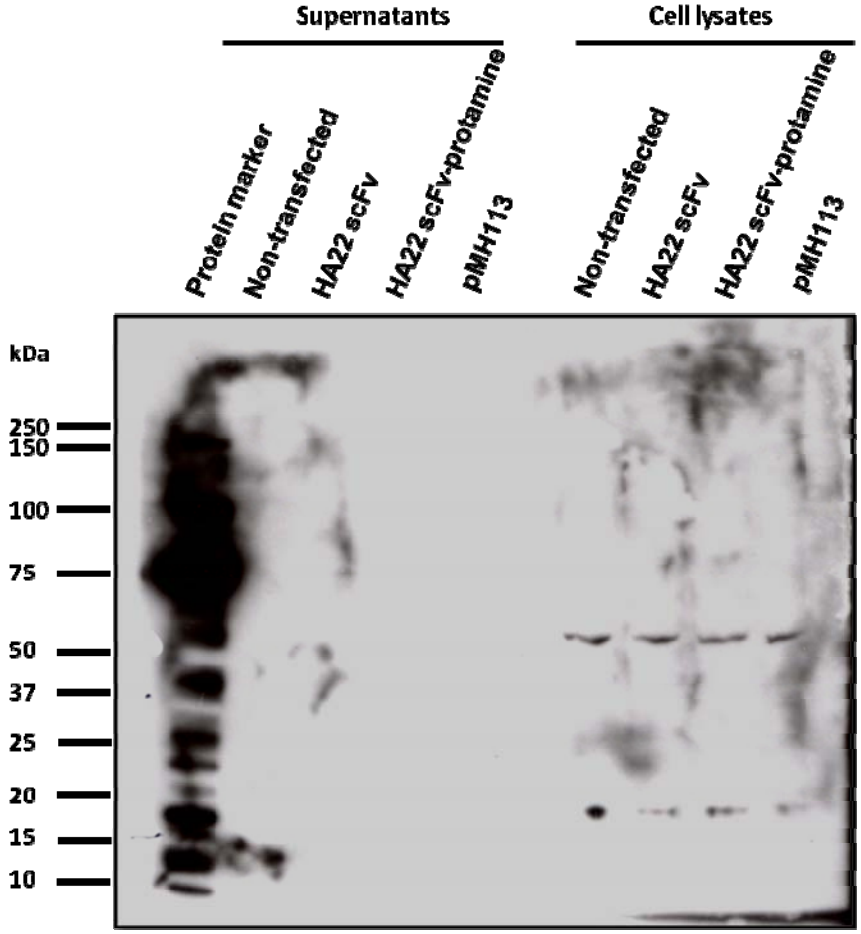

Figure 70: Western blot analysis of anti-human CD22 (HA22) production using the original vector pMH113 or with pcDNA6|IL2ss by transient transfection of HEK293T cells. The figure depicts sample duplicates from Figure 69 probed with HRP-conjugated anti-His(C-term) mAb. No proteins were expressed from the pcDNA6 construct.

4.5. Cloning of HA22 scFv-protamine-His6 into pDisplay vector for expression in mammalian systems:

pMH113 vector has a murine Ig kappa chain signal peptide which drives expression/secretion of the recombinant protein. Attempts were made to determine whether changing the signal peptide could decipher the hurdle of protein expression and secretion. Therefore, HA22 scFv-protamine-His6 DNA fragment was PCR-amplified and cloned into the pDisplay vector. HA22 scFv-protamine-His6 DNA fragment was cloned into the pDisplay vector to investigate the effect of the IL2 and murine Ig kappa chain signal peptides on secretion of HA22 recombinant protein. The DNA fragment that codes for scFv-protamine-His6 was PCR-amplified from pcDNA6|IL2ss with *Sfi*I forward and *Sac*II reverse primers. PCR products and the pDisplay vector were digested with *Sfi*I and *Sac*II enzymes, purified by gel extraction and ligated (Figure 71). In order to generate the construct in the pDisplay vector, the ligation reaction was set up between the PCR product and the vector backbone (section 2.29, page 87; a schematic illustration of the cloning strategy is shown in Figure 20, page 87). The ligation reaction was used to transform bacteria and colonies from the transformants were expanded for DNA mini-preparations and plasmid DNA minipreps analysed by restriction digestion (Figure 72) and sequencing.

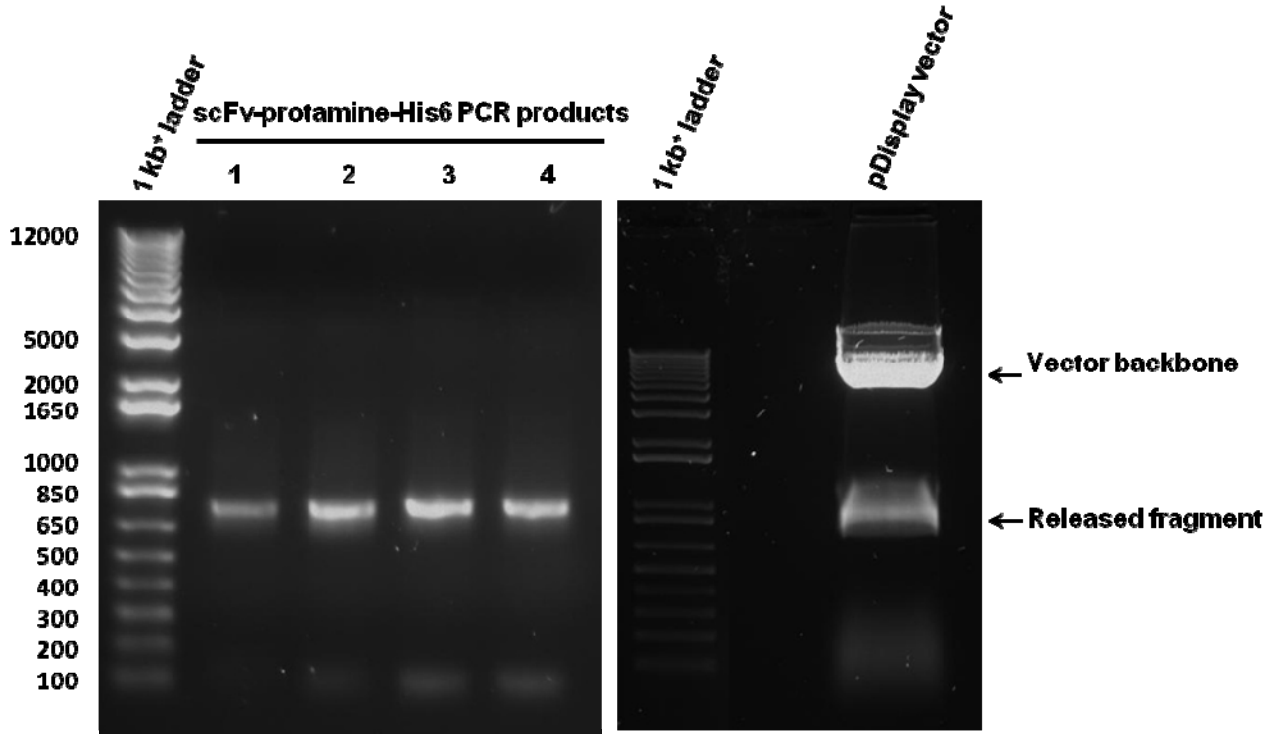

Figure 71: Agarose gel electrophoresis of PCR-amplified HA22 scFv-protamine-His6 and restrction digestion of pDisplay vector with *Sfi*I and *Sac*II enzymes. PCR products of HA22 scFv-protamine-His6, right, (823 bp) and pDisplay (left) were digested with *Sfi*I and *Sac*II enzymes, extracted by gel purification and ligated together.

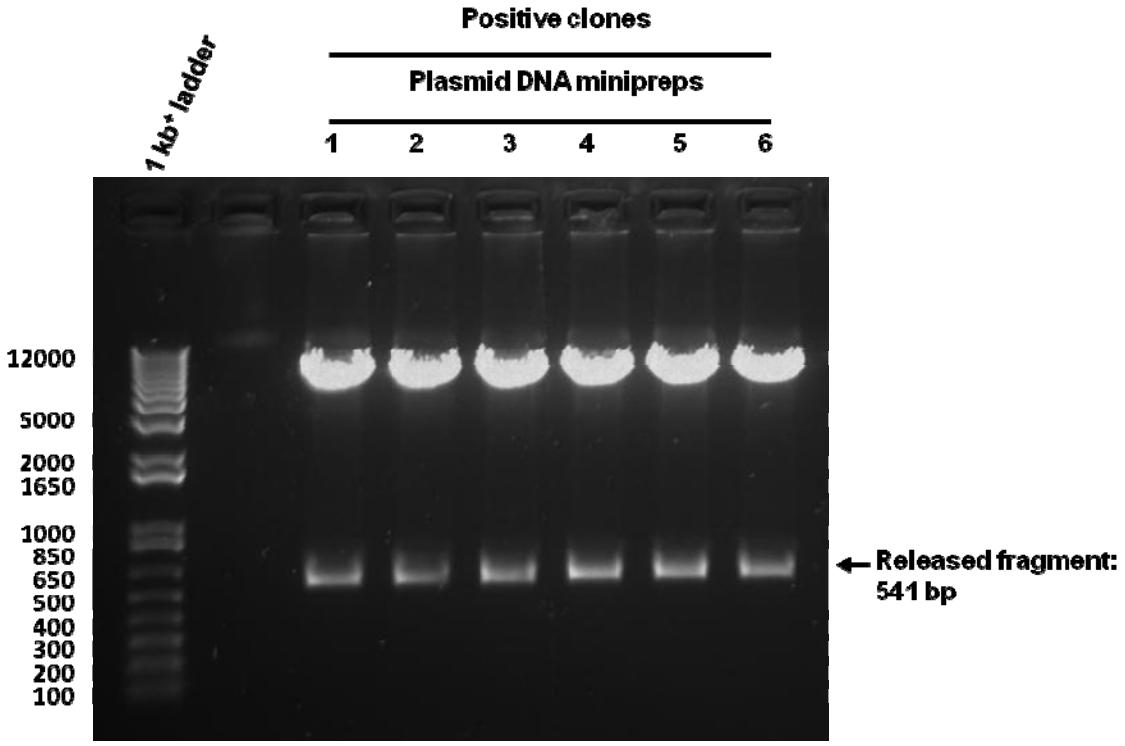

Figure 72: Analysis of plasmid DNA minipreps on agarose gel electrophoresis. Positive clones for HA22 scFv-protamine-His6 inserts were confirmed by visual observation of the released DNA fragment by restriction digestion with *Bam*HI enzyme. Positive clones were also confirmed by sequencing.

4.6. Expression and secretion of recombinant HA22 protein from HEK293T cells:

HA22 scFv-protamine-His6 in pcDNA6|IL2ss, or in pDisplay vectors was used for transient transfection of HEK293T cells. After 3 days of transfection, the cultures were harvested and centrifuged at 5000 rpm for 5 minutes at 4°C. Culture supernatnats and cell lysates were resolved on SDS PAGE gel and the protein detected with HRP-conjugated anti-His(C-term) mAb. Protein expression and secretion was only seen from pDisplay vector (Figure 73). Interestingly, the recombinant protein was not detected in the cell lysates. This might be explained by the fact that the majority of the recombinant protein is directed through the secretory pathway to extracellular space after being produced.

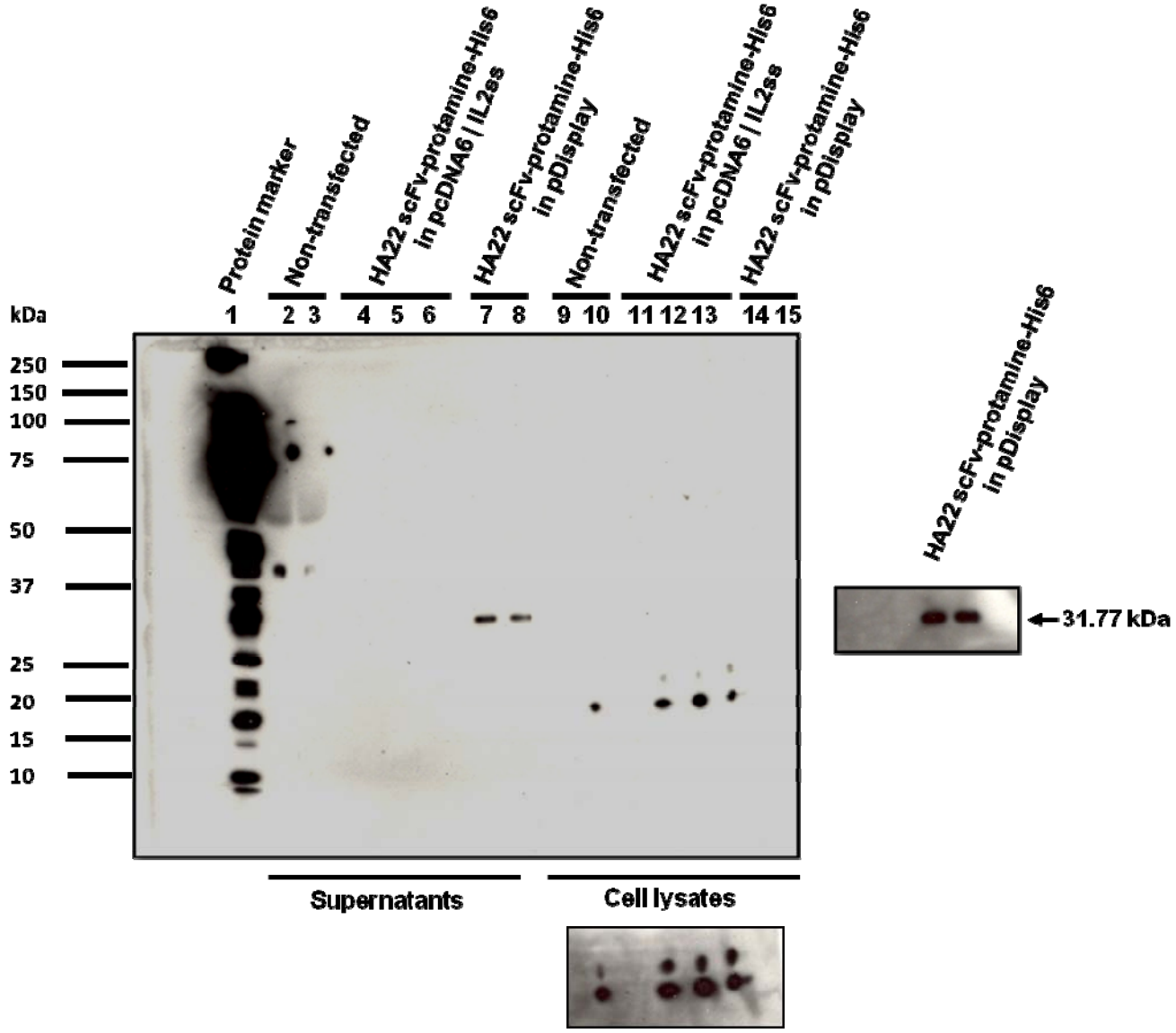

Figure 73: Western blot analysis of recombinant protein HA22 scFv-protamine-His6 production and secretion by HEK293T cells. HA22 protein was detected in clarified culture supernatants of pDisplay-transfected cells (lanes 7 and 8) but not in pcDNA6|IL2ss transfected cells (lanes 4, 5 and 6). Cells were lysed in lysis buffer (50 mM HEPES, 420 mM KCl, 0.1% NP-40, 1 mM EDTA, pH8.3) and resolved on a 4-12% gradient SDS PAGE gel under reducing conditions. Recombinant protein was not detected in cell lysates of either pcDNA6|IL2ss or pDisplay vector transfected cells (lanes 11, 12, 13, 14 and 15).

4.7. Expression and secretion of recombinant HA22 protein in serum-free cultures of HEK293F cells:

HEK293T mammalian cells, widely used for recombinant protein production, are an established expression system as it endows proteins with relevant post-translational modifications. However, the use of HEK293T cells has limitations for mass production of recombinant proteins for experimental purposes. Since the cells are growing in adherent monolayers, large-scale cultures are usually not possible due to limited space of culture vessel surfaces. Furthermore, the cells are growing in complete medium with 10% HI-FBS which is then replaced 24 hours after transfection with serum-free medium. Growing the cells in serum-free medium is essential so that pure recombinant protein devoid of contamination with proteins of animal origin be obtained which is required for most experimental purposes. This problem was previously dealt with by using HEK293F cells adapted for growing in serum-free media. More important is the adaptation of the cells to grow in suspension cultures which helps to grow bulk cultures in large cell culture flasks. The floating HEK293F cells were grown to a density of ~2 x 10^6 cells/mL in serum-free FreeStyle growth medium at the time of transfection. The cells were transiently transfected with the pDisplay plasmid expression vector using PEI as described earlier in the Materials and Methods chapter (section 2.33).

In order to investigate the transfectability of linear polyethylenimine (PEI, 25 kDa) and also determine the optimal ratio of DNA:PEI complex formation for maximal yield of the protein, initially two different ratios of PEI was used to form the complex before addition to cells. Results from the titration of PEI ratios showed that DNA:PEI at 1:3 ratio has a superior transfectability and yields more protein compared with the 1:1 ratio (Figure 74). Therefore for subsequent expression experiments the 1:3 ratio was used.

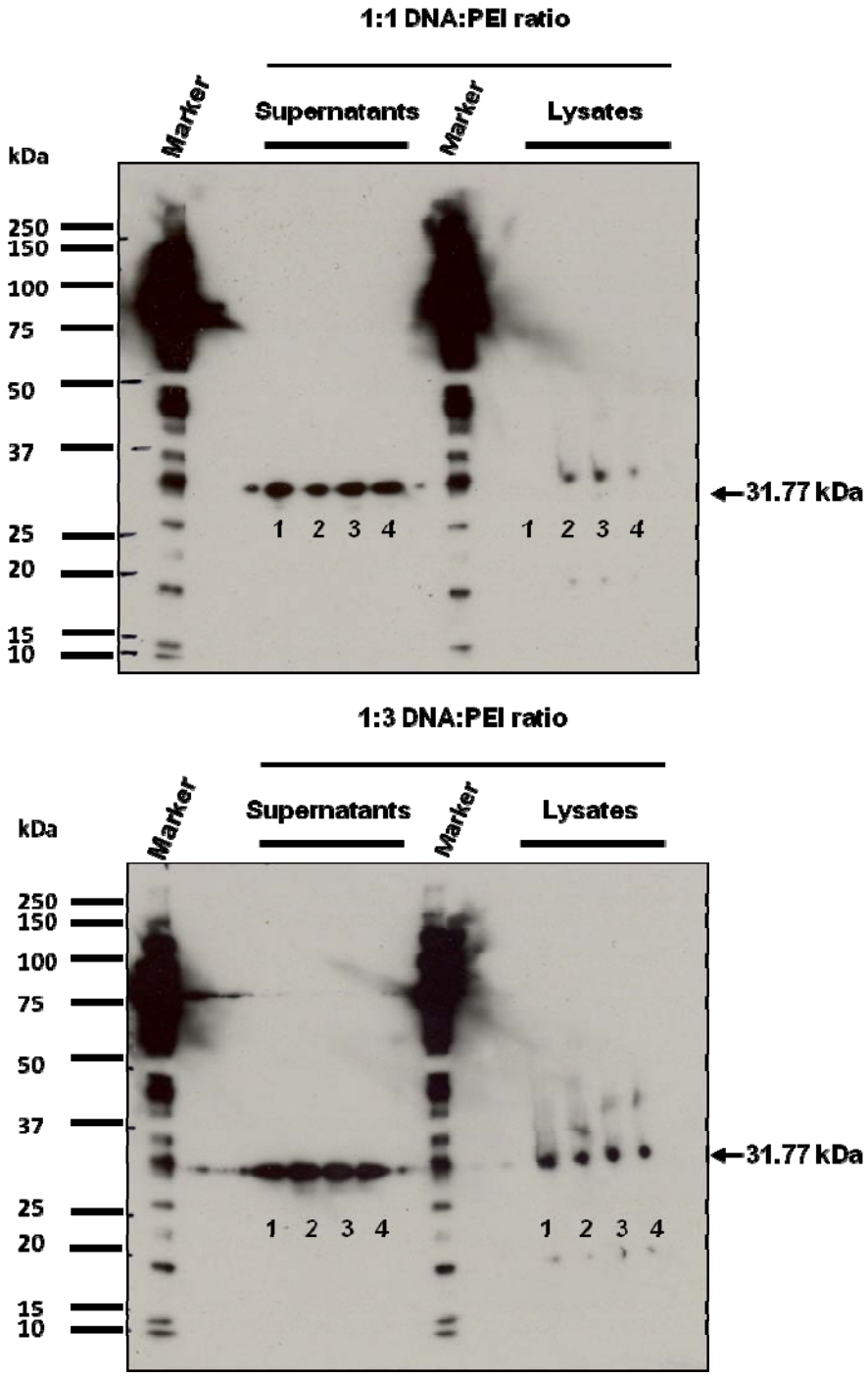

Figure 74: Comparative analysis by Western blotting of expression/secretion of the recombinant protein from HEK293F cells. The figure represents the outcome of experiments to identify the optimal DNA:PEI ratio for the expression efficiency. Culture supernatants and clarified cell lysates were subjected to reducing 10% SDS PAGE electrophoresis and the proteins were detected with HRP-conjugated anti-His(C-term) mAb and films were exposed for 1 minute. Lanes 1, 2, 3 and 4 refer to the same sample load from HEK293F cultures (30 mL) transfected with pDisplay vector for production of recombinant proteins.

The first choice for HA22 protein purification was nickel affinity chromatography due to the presence of a C-terminal hexahistidine tag. Prior to purification, proteins were analysed on a non-reducing gel.

The results obtained from non-reducing gels may possibly indicate that the hexahistidine tag was not inhibited functionally by the conformation of the recombinant protein intramolecular moieties. This has assured possible binding of an exposed hexahistidine tag to the nickel column (Figure 75). Additionally, no protein dimers were seen on the Western blots. Furthermore, density of the protein bands on the Western blot was measured to determine the difference between the relative amount of protein ratio due to the effect of 1:1 and 1:3 DNA:PEI. Consequently, ~2.03 fold more protein was obtained using DNA:PEI ratio at 1:3 than DAN:PEI ratio at 1:1. This was calculated from the densitometry TotalLab 1D Quant software based on images of Figure 75.

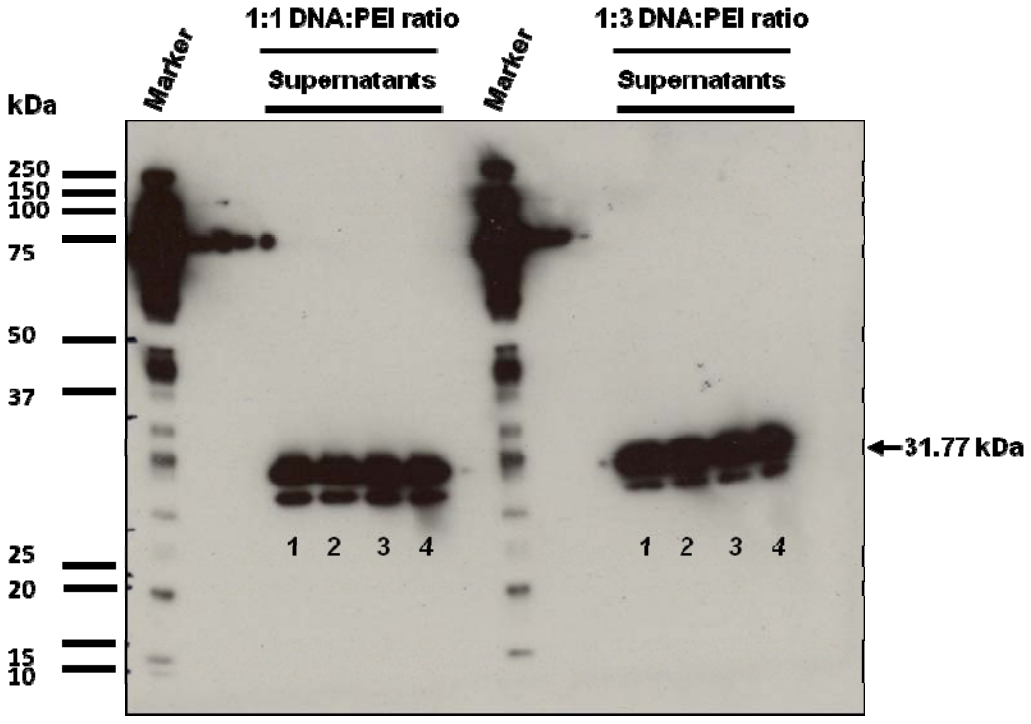

Figure 75: Western blot analysis of HA22 recombinant protein from culture supernatants under non-reducing conditions. No dimer formation or protein aggregates could be detected on the blot. The poly-histidine tag was not concealed in protein intramolecular structure instead it was exposed and bound to nickel column. The protein was detected with HRP-conjugated anti-His(C-term) mAb after 1 minute exposure of the films. Lanes 1, 2, 3 and 4 refer to the same sample load from HEK293F cultures (30 mL) transfected with pDisplay vector for production of recombinant proteins.

4.8. Optimisation of recombinant protein purification:

Following on from the previous experiments of expression/secretion of HA22 protein, optimal DNA:PEI ratios for high transfectability and detection under non-reducing and reducing conditions were determined. The next set of experiments were to study whether dialysis of the culture supernatant would be necessary and whether the hexahistidine tagged protein can bind to the nickel column and be retrieved in the elution fractions. For this purpose, culture supernatants harvested from the transfection experiments were tested to confirm HA22 protein expression and secretion by Western blotting. Culture supernatants were divided into two fractions, one was kept undialysed at 4°C and the other dialysed for 24 hours against native binding buffer for nickel affinity purification (50 mM NaH_2PO_4 and 0.5 M NaCl; pH 8.0). The dialysis was carried out using a Slide-A-Lyzer 10,000 MW cut-off cassette at 4°C. Protein samples from undialysed and dialysed culture supernatants were bound to the nickel column for 90 minutes at 4°C.

Unbound proteins were washed away with native binding buffer, the column was then washed with 6 column volumes of native wash buffer (50 mM NaH_2PO_4 and 0.5 M NaCl with 20 mM imidazole; pH 8.0) and bound proteins eluted with the native elution buffer (50 mM NaH_2PO_4 and 0.5 M NaCl with 250 mM imidazole; pH 8.0). Loaded samples, unbound flow-through, wash and elution fractions from undialysed and dialysed supernatants were analysed on SDS PAGE gel and by Western blotting. Results from these experiments showed that the hexahistidine tagged protein bound to the nickel column and was obtained in the elution fractions, but dialysis resulted in significant loss of the protein (Figure 76).

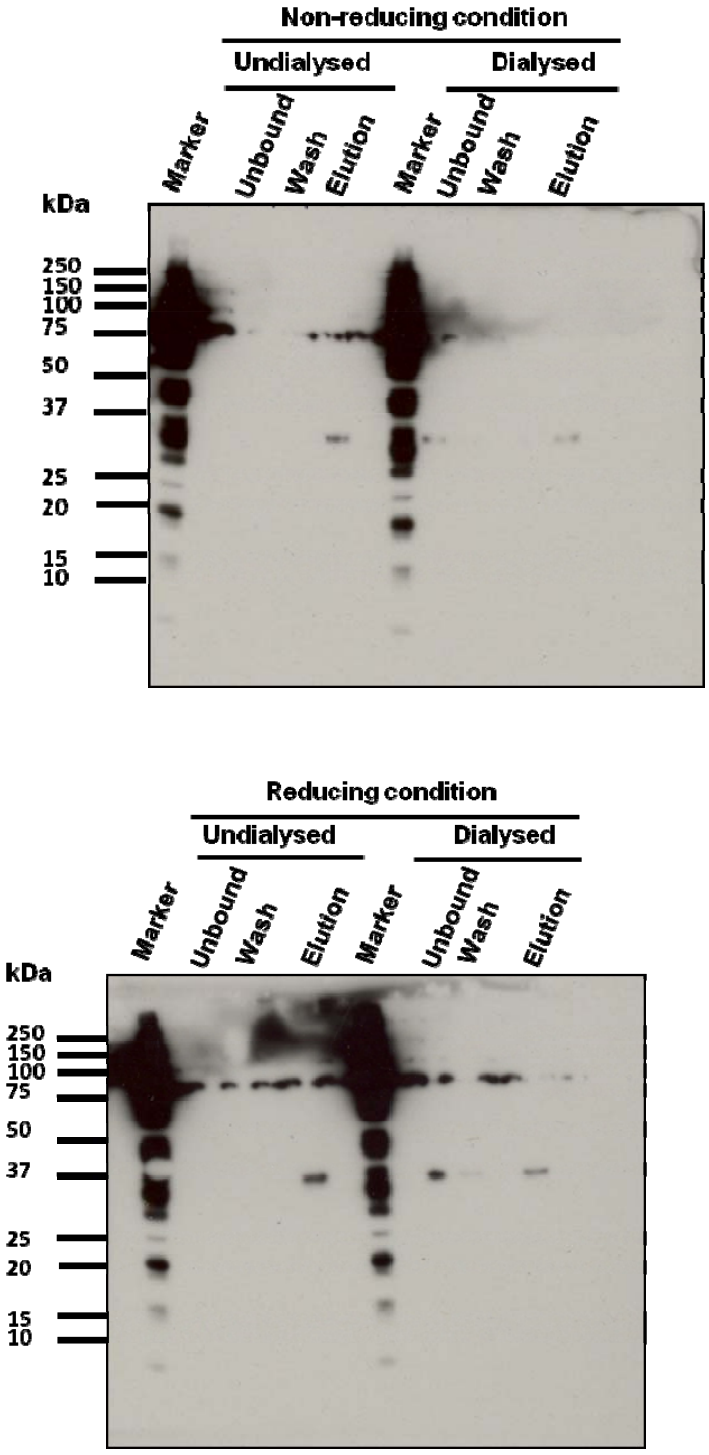

Figure 76: Small-scale protein purification using nickel affinity chromatography. The effect of dialysis on the purification of recombinant HA22 was studied by Western blotting. The results provide evidence for significant loss upon the dialysis of culture supernatants. Recombinant protein in the supernatants and different fractions were analysed on 10% precast SDS PAGE gel under non-reducing (top) and reducing (bottom) conditions. The protein was detected with HRP-conjugated anti-His(C-term) mAb. The X-ray films were exposed for 1 minute.

4.9. Large-scale production and purification of recombinant HA22 protein under native conditions using nickel affinity chromatography and FPLC:

Having optimised key aspects of the production and purification systems, large-scale production and purification of the fusion protein was initiated. For this purpose, early-passages of HEK293F cells were grown in fresh medium in large flasks on an orbital shaker at a rate of 95 rpm at 37°C with 8% CO_2 in air. The cultures were then transfected at a density of 2 x 10^6 cells/mL using a 1:3 DNA:PEI ratio. Culture supernatants were collected 3 days post transfection by centrifugation at 5000 rpm at 4°C for 5 minutes and frozen at -80°C until used. Before application to the column, culture supernatants were defrosted gradually at 4°C and filtered using a sterile vacuum low protein-binding filter unit with a polyethersulfone (PES) membrane (0.22 µm). The HiTrap 5 mL chelating HP nickel column was installed on the FPLC system (Amersham Pharmacia, GE Healthcare) and pre-equilibrated with cold filter-sterilised binding buffer (20 mM NaH_2PO_4 and 0.5 M NaCl; pH 7.4). Based on the data obtained from the available variables of small-scale protein purification, the FPLC system was adjusted for the large-scale purification scenario. Details of the set-up are described in the Materials and Methods chapter (section 2.42, page 103).

The process of protein purification on nickel affinity chromatography beginning with column equilibration, sample loading, washes and elution fraction collection was monitored and recorded by the FPLC system on a chromatogram recorder (Figure 77). The sample load, unbound flow-through, wash and elution fractions were analysed for purity on a Coomassie blue-stained SDS PAGE gel and Western blotting (Figure 78).

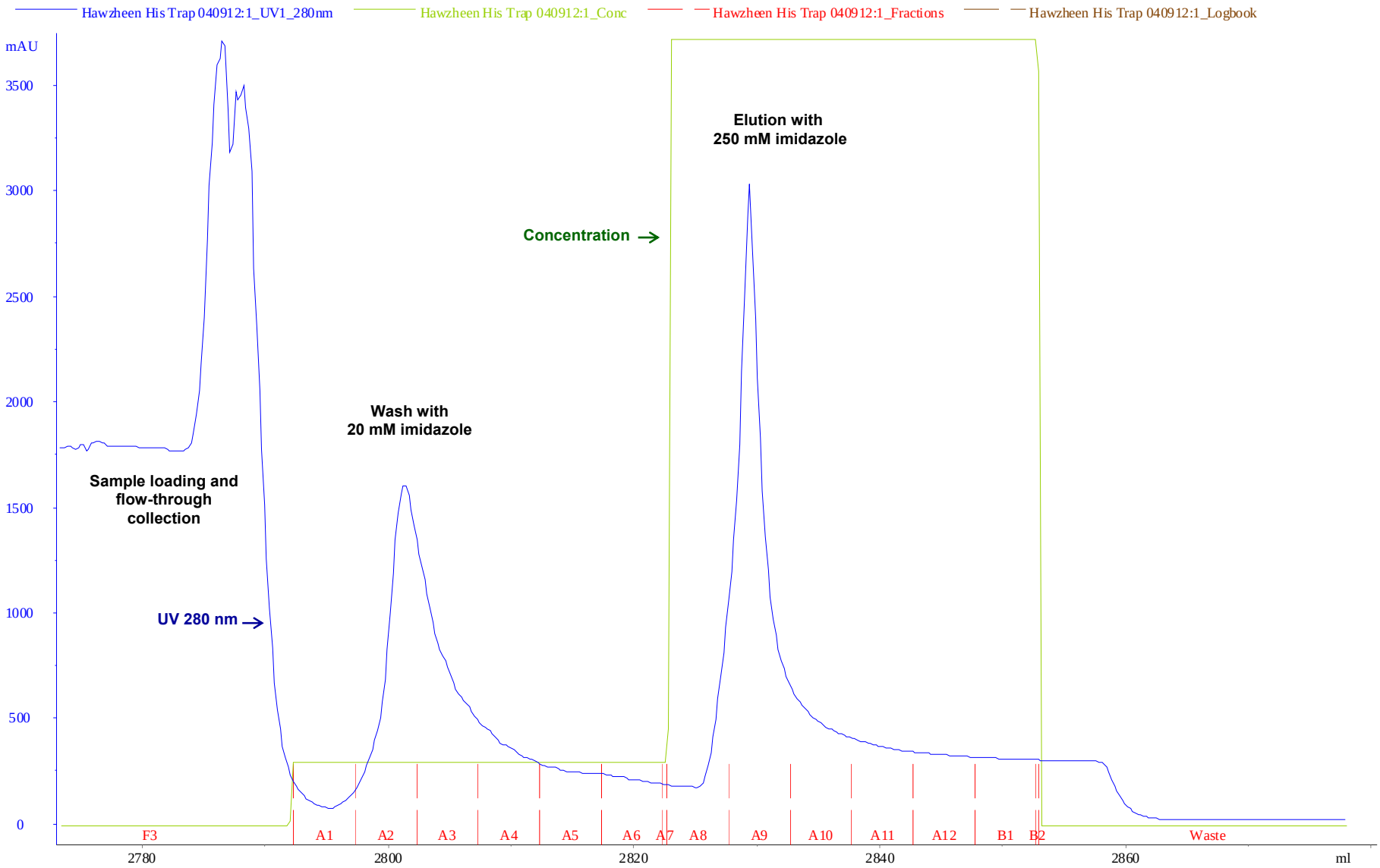

Figure 77: Nickel affinity chromatogram showing protein purification process under native conditions using FPLC. F3 indicates loading of culture supernatants containing HA22 protein onto the nickel column and collection of unbound flow-through. Fractions A1 to A7 represent protein impurities removed from the column by washing. Elution fractions A8 to A11 were collected and analysed on a Coomassie blue-stained gel and by Western blotting. X-axis: volume (mL); Y-axis: optical density (OD) at 280 nm.

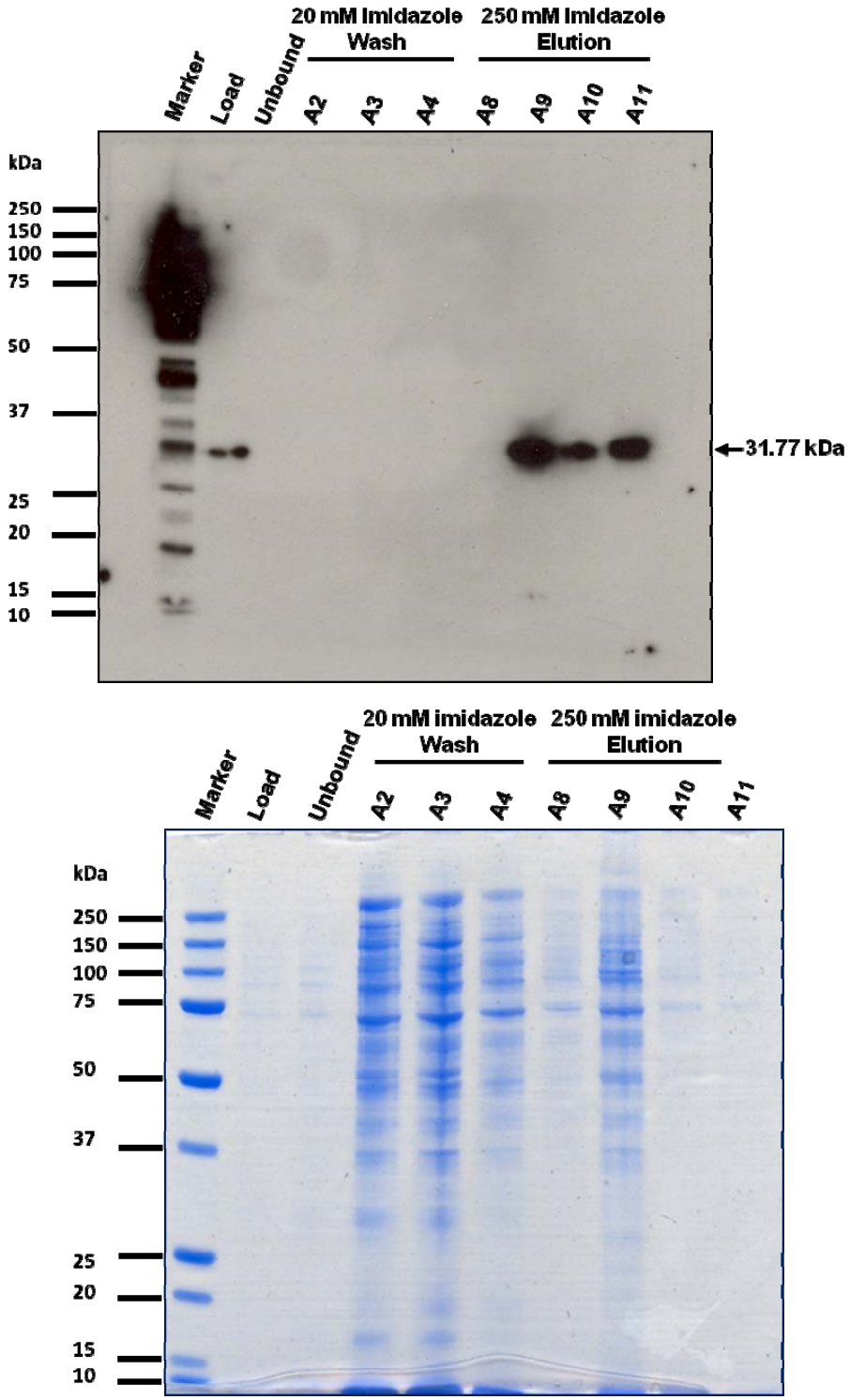

Figure 78: Analysis of the efficiency of recombinant HA22 protein purification on nickel affinity columns. The figure depicts Western blot (top) and Comassie blue-stained (bottom) analyses of loaded culture supernatants, unbound flow-through, wash and elution fractions following purification of the recombinant protein by nickel affinity chromatography. The analyses reveal no loss in the unbound, flow-through or wash fractions (A2-A4). The protein of the expected size can be seen in the elution fractions (A8-A11). The Coomassie blue-stained gel (bottom) shows the level of contaminants and impurities. The protein was detected with HRP-conjugated anti-His(C-term) mAb.

4.10. Purification of recombinant HA22 protein using ion exchange chromatography:

Elution fractions of nickel affinity purified protein were subjected to further purification by ion exchange chromatography. The isoelectric point (pI) of the HA22 fusion protein was estimated using a bioinformatics tools to be ~4.5. Accordingly, the net positive charge of the protein favours the use of cation exchange chromatography. For this purpose, the buffer was first exchanged by dialysis into a buffer that is compatible with cation exchange (20 mM Tris-HCl; pH 7.5). Based on the Coomassie blue-stained gel and the Western blotting data, the A9 fraction (His-A9) had significant protein content. Therefore, this fraction was processed for the cation exchange chromatography. It was noted that during the first few hours of buffer exchange, the protein started to form white precipitates within the dialysis membrane. The dialysis was stopped and protein sample retrieved from the dialysis cassette. The protein sample was gently resuspended and centrifuged at 1400 rpm for 2 minutes at 4°C. The supernatant was transferred to a fresh tube and 50 mM L-glutamine added to help protein solubilisation as carried out previously for the mouse recombinant proteins. This helped to clarify the protein sample. In parallel, the protein precipitate in the pellet was resuspended in the binding buffer (20 mM NaH_2PO_4 and 0.5 M NaCl; pH 7.4) with the addition of 50 mM L-glutamine. Only the clarified supernatant was added to the cation exchange HiTrap SP FF column. This was due to the fact that the tubing system of the FPLC system is thin and any impurity or precipitate would clog and damage the system. Therefore, it was not possible to use the resuspended protein precipitate of the A9 fraction (His-A9) through the FPLC system capillaries. Similar to nickel affinity chromatography, protein purification through cation exchange chromatography was monitored and recorded by the FPLC system chromatogram recorder (Figure 79). The sample load, wash and elution fractions were analysed by Western blotting but inexplicably most proteins were detected at low molecular weights (Figure 80).

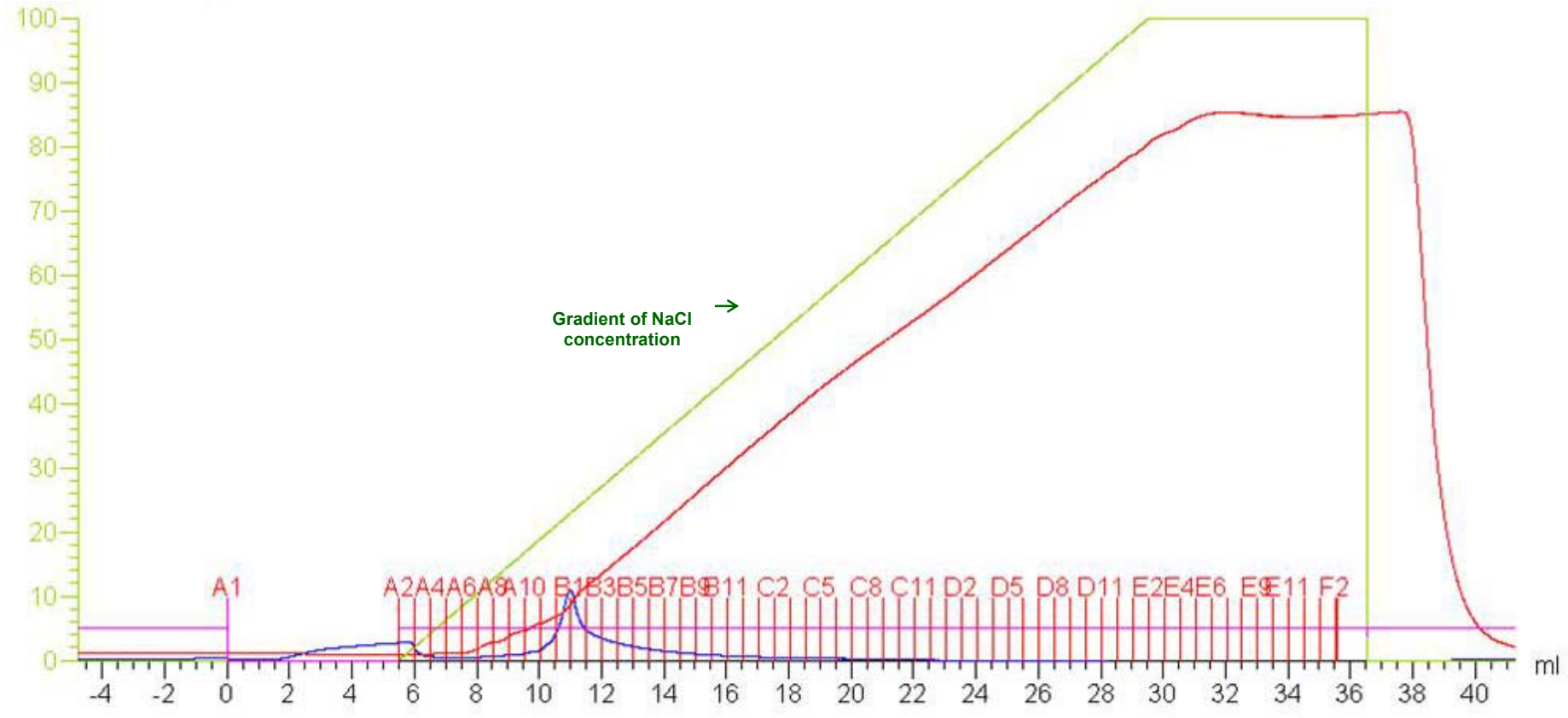

Figure 79: Cation exchange chromatogram showing the profile of protein purification under native conditions on FPLC. The elution fraction A9 (His-A9) of HA22 protein from the nickel affinity purification step was applied onto a cation exchange column. From cation exchange chromatography purification, the fractions A1 to A9 indicate sample loading and the fractions A10 to B5 indicate elution fractions which were analysed by Western blotting.

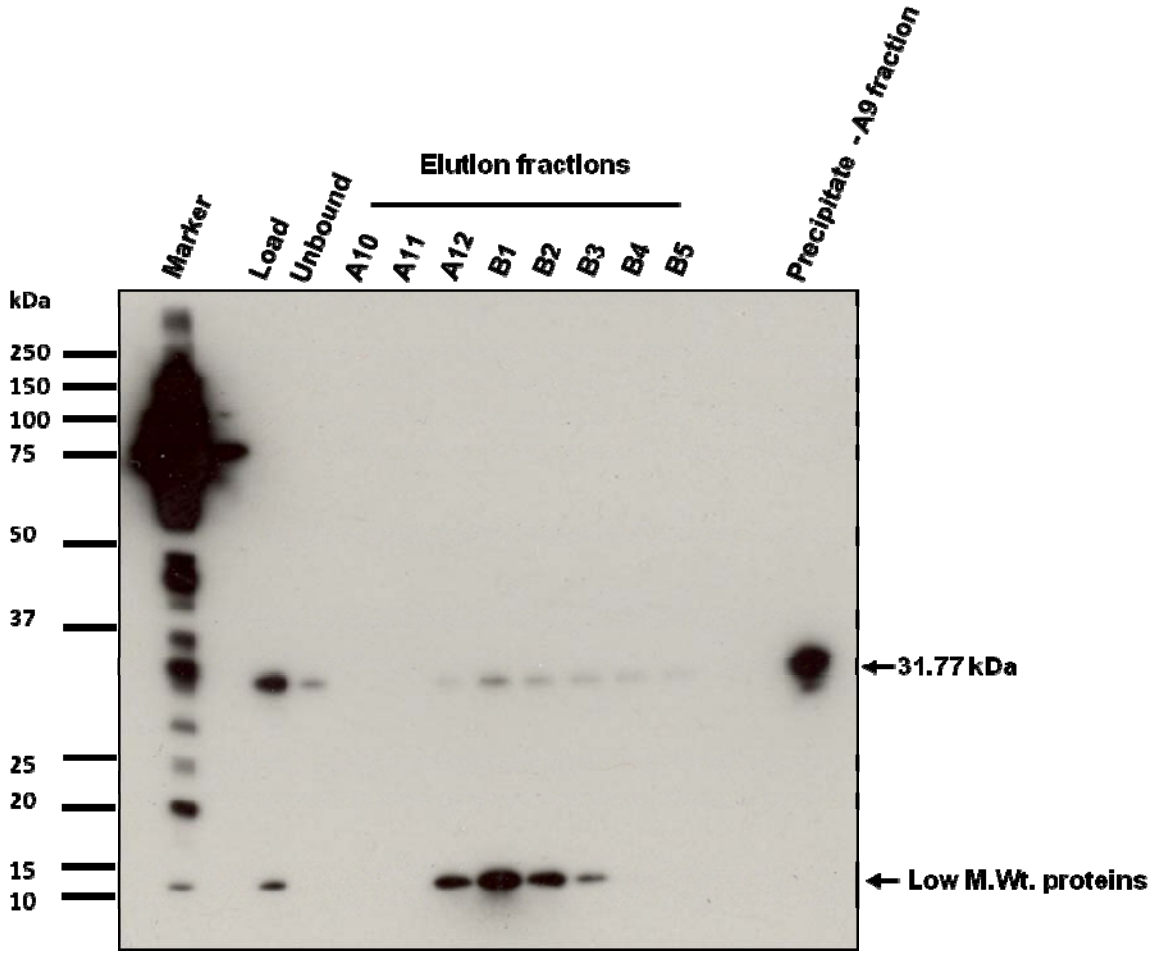

Figure 80: Western blot analysis of purified protein A9 fraction (His-A9) from cation exchange chromatography. Fraction A9 (His-A9) was dialysed against Tris-HCl, pH 7.5,which resulted in the formation of precipitates, some of which were dissolved back into solution by gentle resuspension. The sample was loaded onto HiTrap SP cation exchanger column and eluted with a gradient of elution buffer (20 mM Tris-HCl, 2 M NaCl, pH 7.5). The blot shows analysis of the sample load, wash and elution fractions. Degradation was observed for all the fractions analysed except for the precipitate from the A9 fraction (His-A9) which contains a high amount of the recombinant protein.

The various steps in the purification process of proteins (sample load, unbound flow-through, wash and elution fractions) were analysed by Western blotting and on a Coomasie blue-stained gel. However, for HA22 fusion protein which is a unique protein, the spectrum of analysis has revealed that a significant amount of non-specific protein contaminants can be removed on the nickle column by using 250 mM imidazole in the wash buffer. Thus, high purity fusion protein was isolated by using 500 mM imidazole in the elution buffer.

High proportions of pure recombinant HA22 fusion proteins were detected in the elution fractions using 500 mM imidazole. The elution fractions with highly pure protein isolated using 500 mM imidazole were analysed by Western blotting and on a Coomassie blue-stained gel (Figure 81).

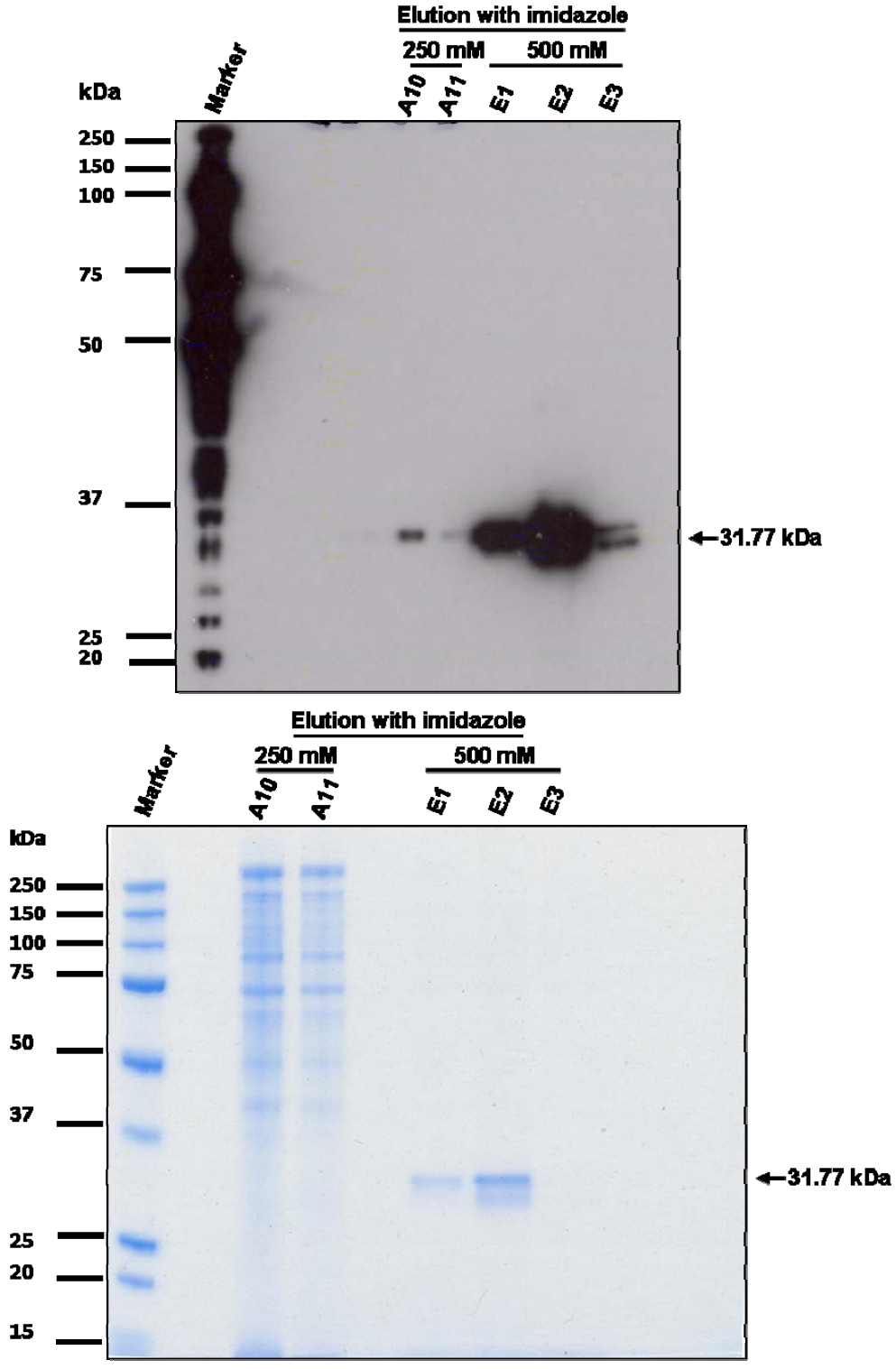

Figure 81: Comparative analysis of HA22 fusion protein obtained by elution with different concentrations of imidazole. After loading the column with culture supernatant containing recombinant protein, bound HA22 was eluted with buffer containing either 250 mM imidazole (fractions A10 and A11) or 500 mM imidazole (fractions E1 - E3) on the nickel affinity column. Elution with 500 mM imidazole yielded more protein as shown by Western blotting (top) and Coomassie blue-stained gel (bottom).

4.11. Removal of imidazole from the purified recombinant HA22 protein by dialysis and desalting:

The effect of dialysis on protein loss was established previously (section 4.8). Therefore, although it was deemed not the best option for removal of imidazole from all of the purified protein but a small volume was dialysed against the binding buffer (20 mM NaH_2PO_4 and 0.5 M NaCl; pH 7.4) to remove imidazole. The protein sample was then analysed by Western blotting before and after dialysis. Results from the Western blot analysis confirmed that a significant amount of the protein would be lost during dialysis (Figure 82). Changes of volumes before and after dialysis were not observed.

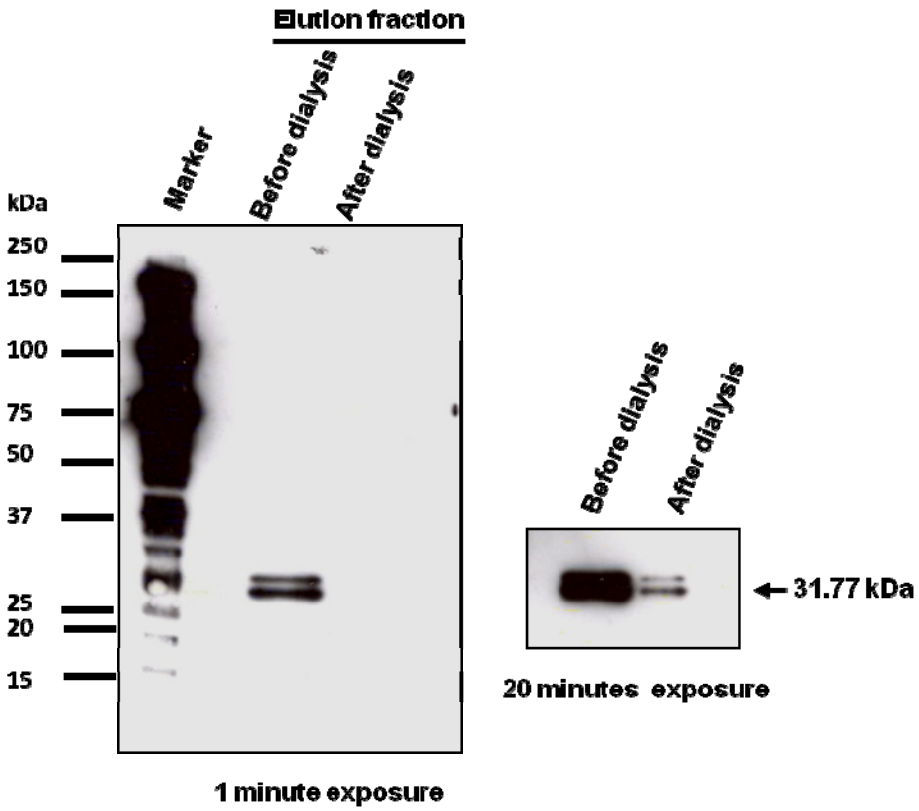

Figure 82: Effect of imidazole dialysis on HA22 fusion protein content. The protein sample was analysed before and after dialysis by Western blotting. The analysis shows a significant loss of the protein during the dialysis process. The analysis was carried out using a 10% SDS PAGE gel under reducing conditions.

As an alternative step to dialysis, imidazole was removed from the protein sample by buffer exchange on PD-10 Sephadex G-25 desalting column. The result from the PD-10 desalting was encouraging and almost the same amount of protein was retrieved after the desalting process (Figure 83).

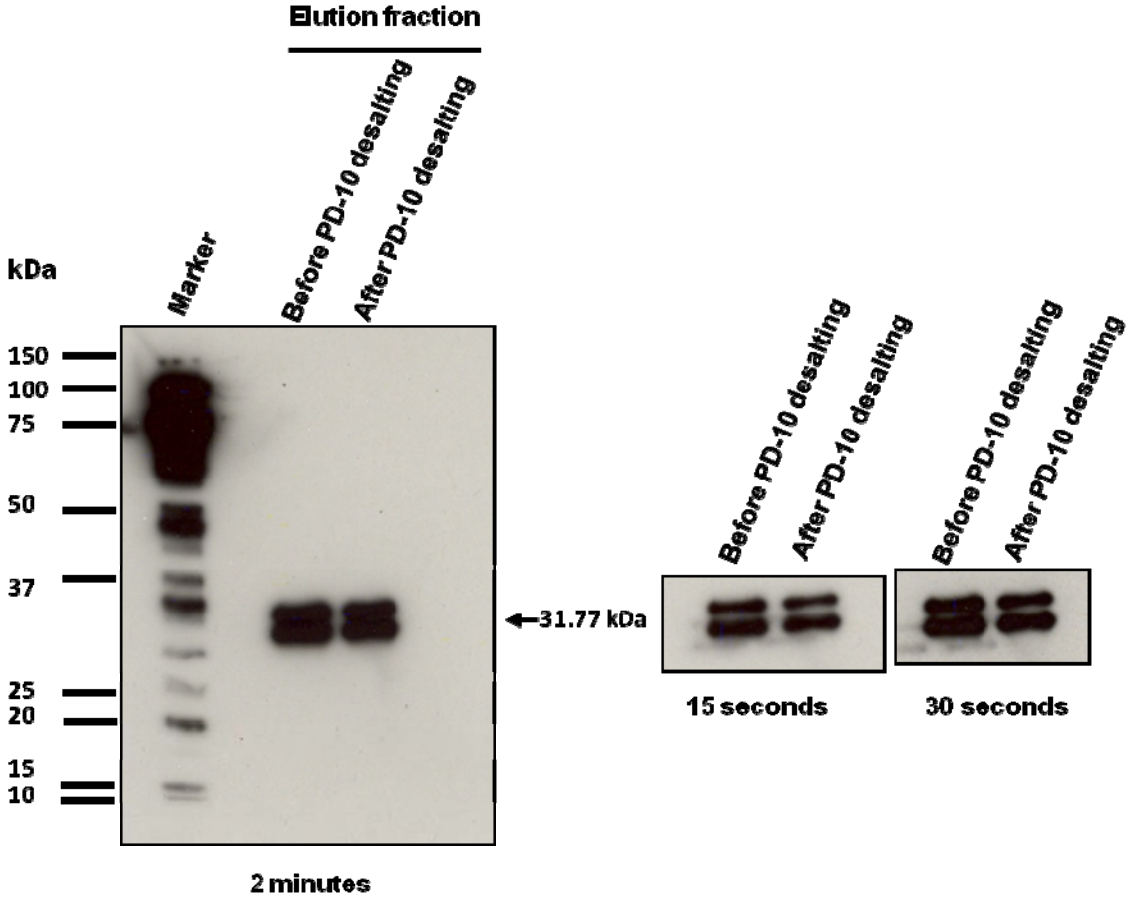

Figure 83: Western blot analysis of HA22 fusion protein samples before and after removal of imidazole by desalting. The yield of protein after PD-10 desalting is the same as before PD-10 desalting. The dilution factor of the protein from the variation of elution buffer volume was compensated for before and after PD-10 desalting by loading 15 μl and 21 μl of the protein sample respectively on 10% SDS PAGE gel under reducing conditoins.

4.12. Removal of haemagglutinin A epitope (HA tag) from the recombinant HA22 fusion protein:

In the original pDisplay vector, the nucleotide sequence which encodes haemagglutinin A epitope (YPYDVPDYA) precedes the MCS in-frame with the signal peptide. The murine Ig kappa chain signal peptide is fused at the C-terminus with the HA tag. Initially, removal of the HA tag was not possible for the cloning. After construction of the expression vector with HA22 scFv-protamine-His6, a fragment of DNA that overlaps the signal peptide upstream of the HA tag was PCR-amplified in a way that is compatible with the start site of HA22 scFv (*Sfi*I site). Therefore, the construct was restricted with *Hind*III and *Sfi*I enzymes to release a DNA fragment upstream of the signal peptide which includes the haemagglutinin A epitope. Then, a DNA fragment for the region between *Hind*III and end of the leader signal sequence was amplified by PCR using specific primers to restore the *Sfi*I site (Figure 84). The construct (vector backbone) which was digested with *Hind*III and *Sfi*I enzymes was ligated with the PCR product (digested with the same enzymes) and the ligation reaction was used to transform bacteria. Transformants were expanded from positive colonies and plasmid minipreps analysed by restriction digestion and sequencing (Appendix 2, page 352). The genetic map for the construct is shown in Appendix 3, page 363.

A schematic illustration emphasising the process of removal of HA tag from pDisplay expression vector is shown in Appendix 6, page 366.

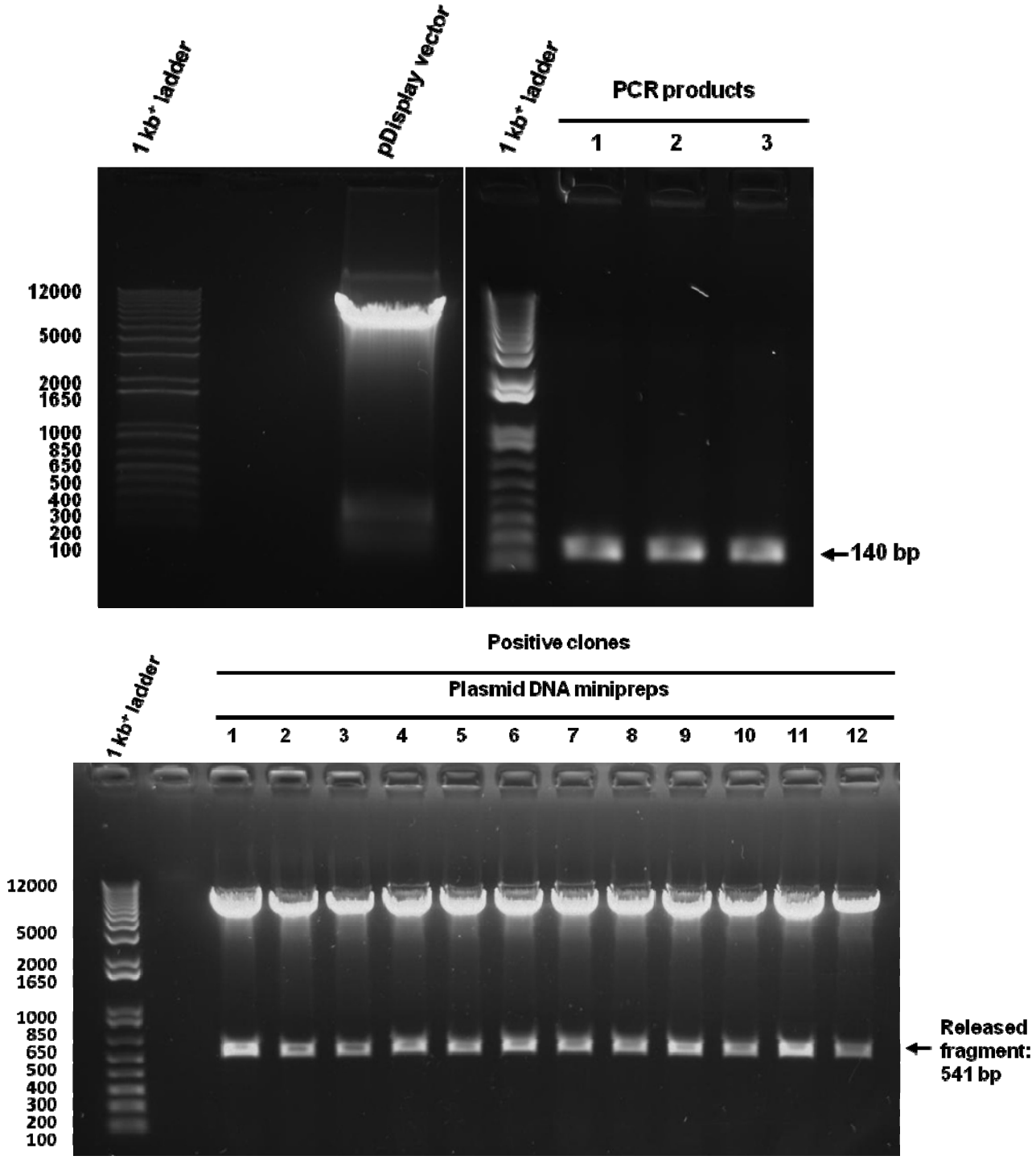

Figure 84: Agarose gel electrophoresis of the cloning process for removal of HA tag. pDisplay vector was digested at the unique *Hind*III site upstream to and the start site of MCS including signal peptide and HA tag with *Hind*III and *Sfi*I enzymes (upper left). The DNA fragment between *Hind*III site and end of signal peptide was PCR-amplified (upper right). Positive clones from ligation reaction were analysed by restriction digestion (bottom) and sequencing.

New batches of the protein were produced on a large scale using the modified pDisplay vector without the HA tag. Modifications in the purification process on nickel affinity chromatography consisted of using 50 and 250 mM imidazole concentrations in the wash buffers to wash and remove the protein impurities on the nickel column. Then additionally pure protein was eluted with 500 mM imidazole. These modifications, documented in the legend to the chromatogram in Figure 85, were incorporated into the FPLC program. Isolation of pure protein was made feasible because of these modifications. The content of the fractions obtained from the protein purification process was analysed by Western blotting and on a Coomassie blue-stained gel (Figures 86 and 87). Cation exchange chromatography was avoided for additional purification because of precipitation of the protein, as shown earlier and also because only purification through nickel affinity chromatography has yielded a highly pure protein which was used to test for biological activity.

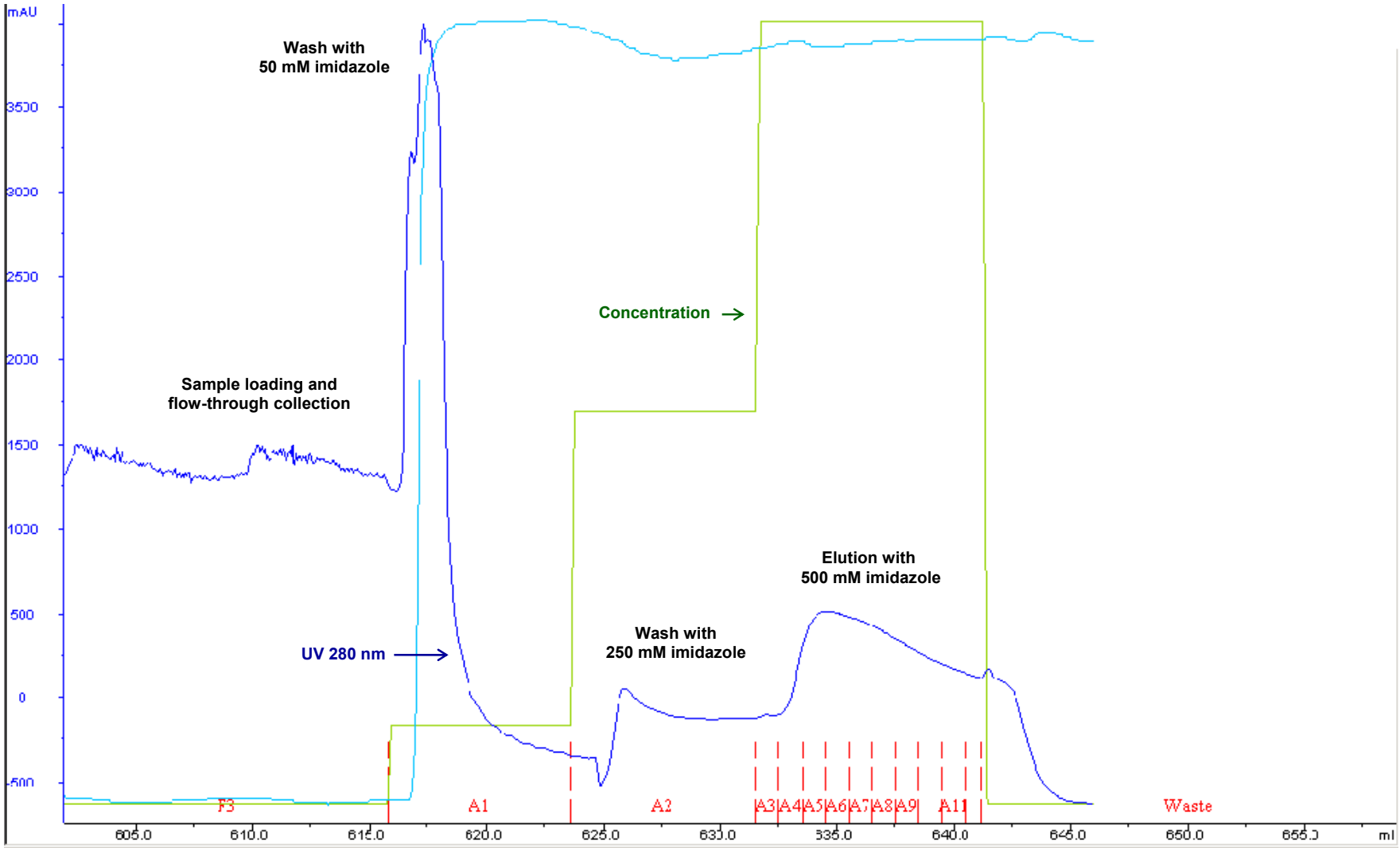

Figure 85: Nickel affinity chromatogram of HA22 protein purification using FPLC under optimal conditions. F3 indicates loading of culture supernatants containing HA22 fusion protein onto the nickel column and collection of unbound flow-through. Fraction A1 represents wash of the column with 50 mM imidazole in the washing buffer. Fraction A2 represents wash of the column with 250 mM imidazole in the washing buffer to remove protein impurities. HA22 fusion protein was collected in elution fractions A3 to A11 using 500 mM imidazole in the elution buffer. Sample load, unbound flow-through, 50 mM and 250 mM imidazole washes and all elution fractions were analysed on Coomassie blue-stained gel and by Western blotting. X-axis: volume (mL); Y-axis: optical density (OD) at 280 nm.

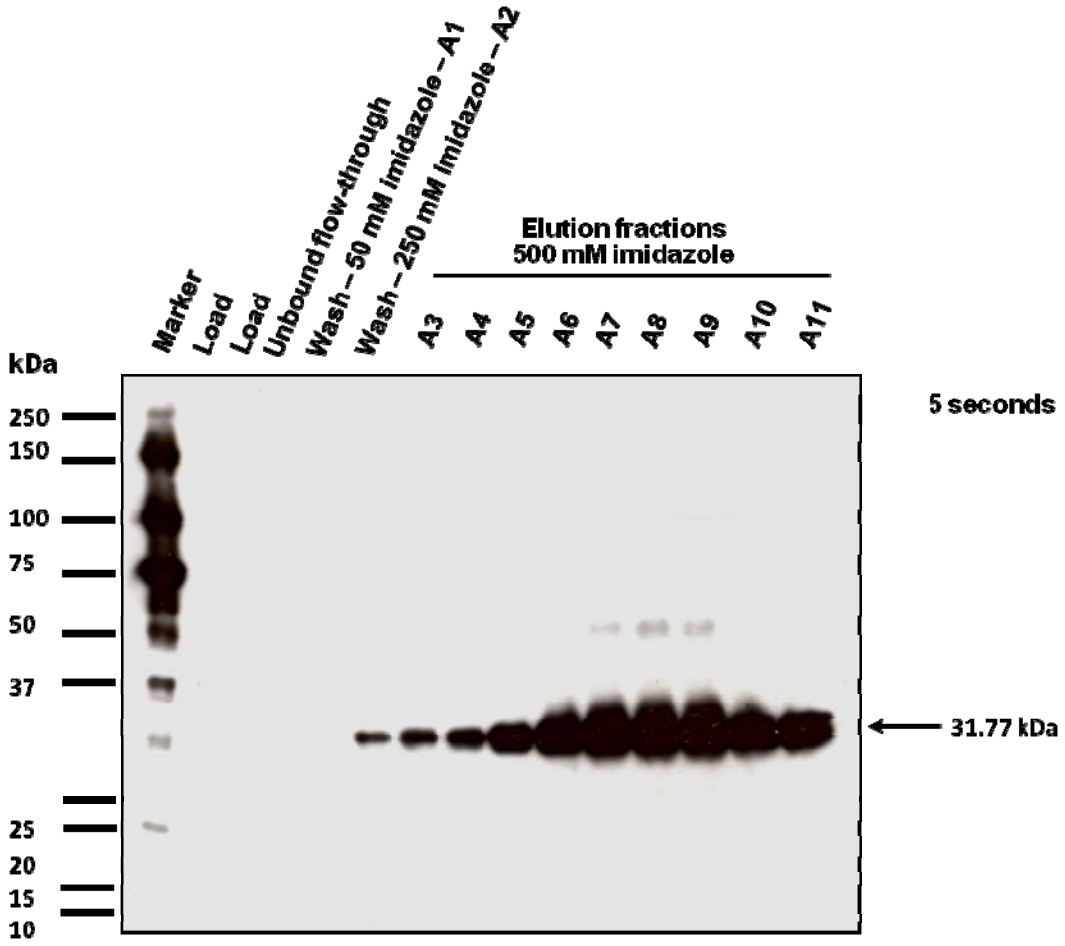

Figure 86: Analysis of recombinant HA22 fusion protein after purification on nickel affinity columns using different concentration of imidazole. The figure show the analysis of the loaded sample, unbound flow-through, wash and elution fractions by Western blotting. The figure shows that most of the proetin bound to the column with no protein loss detected in the unbound flow-through.

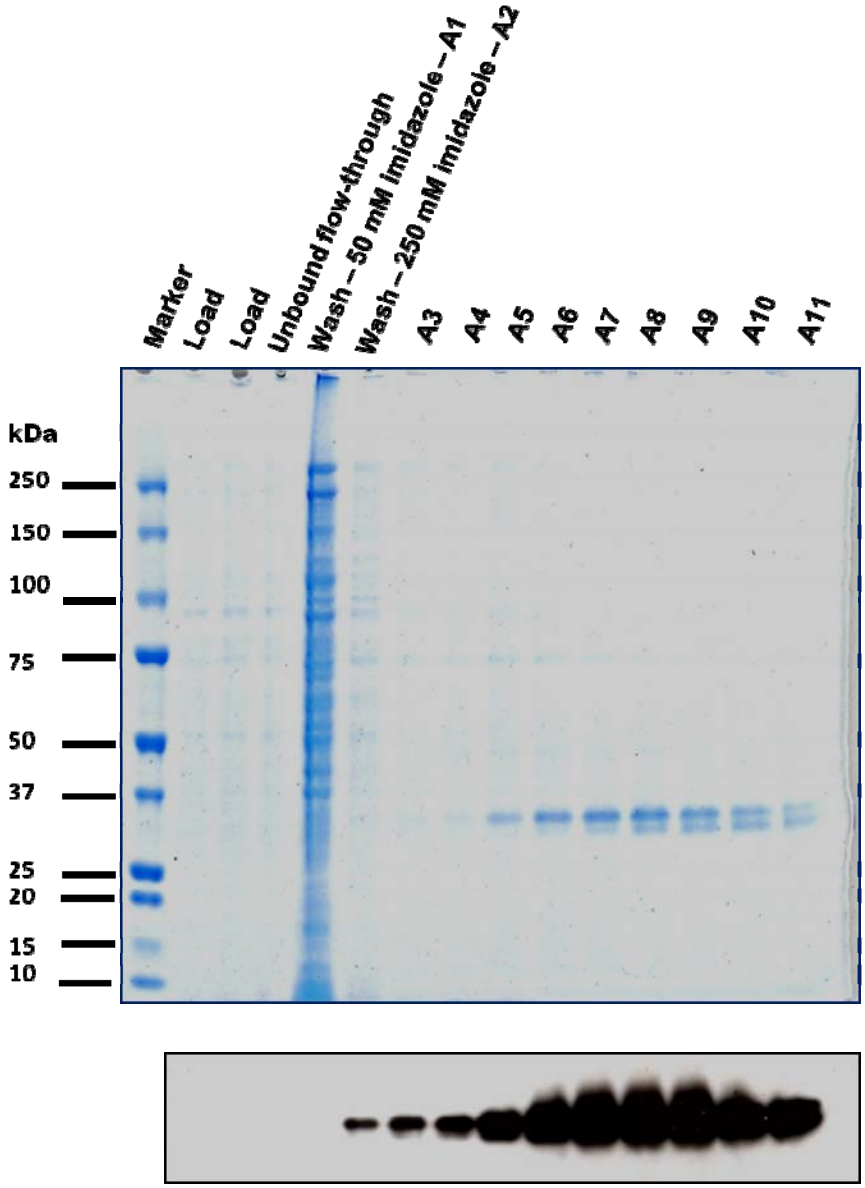

Figure 87: Analysis of recombinant HA22 fusion protein after purification on nickel affinity columns with different concentration of imidazole. The figure shows the analysis of the loaded sample, unbound flow-through, wash and elution fractions on a Coomassie blue-stained gel (top) for isolation of highly pure protein using nickel affinity chromatography and Western blotting (bottom).

4.13. Concentration of purified recombinant HA22 protein for assessing optimal storage and usage:

For convenience of use, the purified recombinant protein was concentrated by centrifugation using 10 kDa MW cut-off spin columns. The elution fractions of (90 mL) were pooled (fractions A3 to A11) and concentrated 18 times through an Immobilized Metal Affinity Chromatography (IMAC) spin column. Pooled fractions were loaded onto the column and centrifuged at 5000 rpm for 5 hours to reduce the volume to 5 mL of concentrated protein. Subsequent to pooling and concentration using IMAC spin column, HA22 fusion protein was then subjected to PD-10 desalting to remove the imidazole from the fusion protein. The pooled fraction was divided to two equal volumes and each was eluted from the PD-10 column with either buffer A (20 mM NaH_2PO_4 and 0.5 M NaCl; pH 7.4) or buffer B (20 mM Tris-HCl and 0.5 M NaCl; pH 7.4). Aliquots of the protein samples were then compared before and after PD-10 desalting by Western blotting (Figure 88).

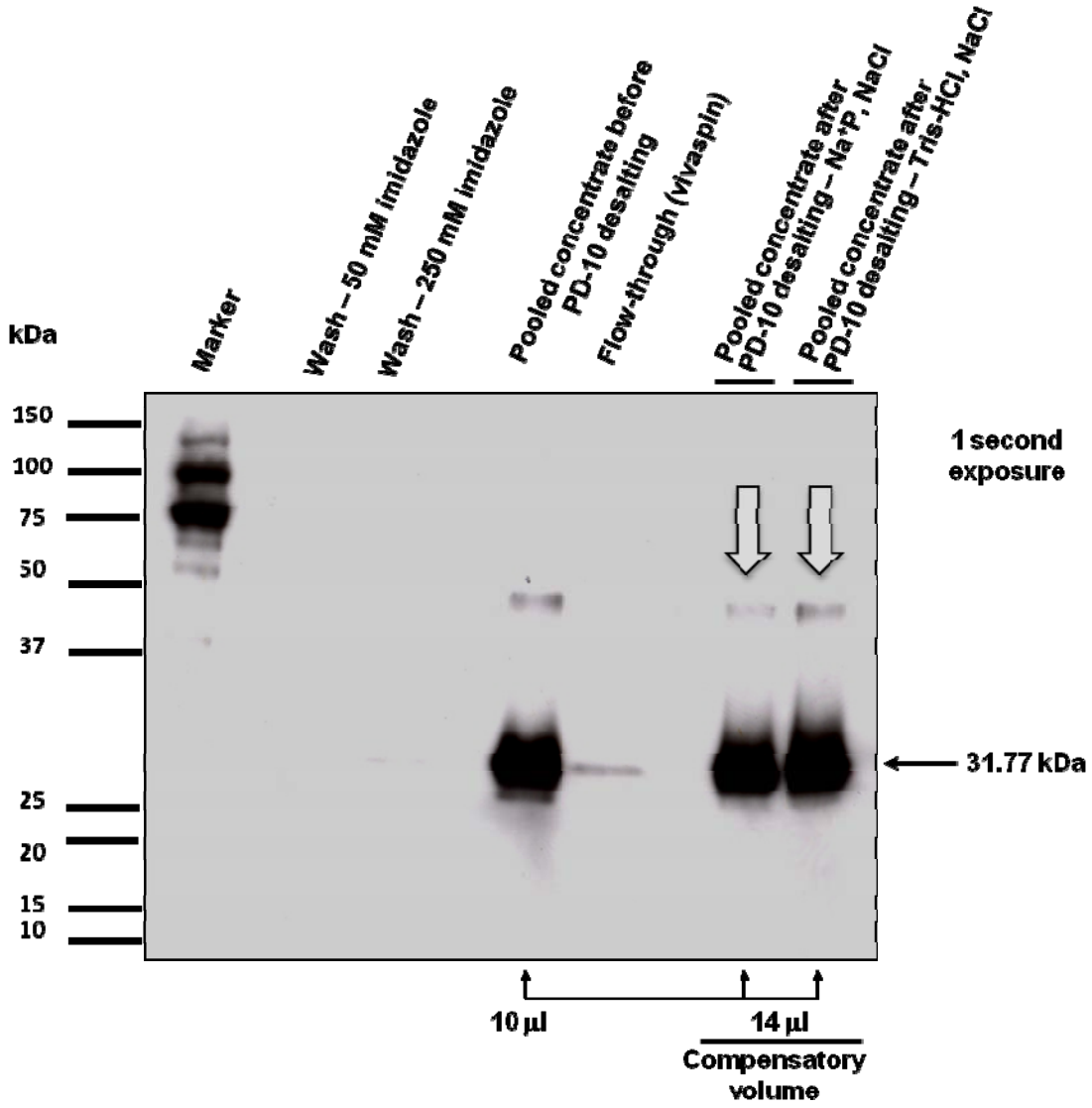

Figure 88: Western blot analysis of concentrated recombinant HA22 fusion protein. Aliquots of concentrated recombinant HA22 protein were compared before and after PD-10 desalting. Pooled concentrated protein fractions were desalted using PD-10 desalting columns to remove imidazole. The pooled fraction was divided to two equal volumes and each eluted from the PD-10 column with either buffer A (20 mM NaH_2PO_4 and 0.5 M NaCl; pH 7.4) or buffer B (20 mM Tris-HCl and 0.5 M NaCl; pH 7.4). Because the volume of protein sample added to the equilibrated columns was 2.5 mL and the volume of elution buffer A or B was 3.5 mL the difference in volume before and after elution is accounted for by using more of the protein on the Western blot. Protein samples were analysed on 10% precast SDS PAGE gel under reducing conditions and the X-ray film was exposed for 1 second.

4.14. Quantification of HA22 fusion protein using BCA assay:

Bicinchoninic acid (BCA) protein quantification assay was used to determine protein concentration. This was measured from the linear regression equation of the standard curve by plotting known concentrations of BSA (µg/mL) against optical density at 562 nm (Figure 89).

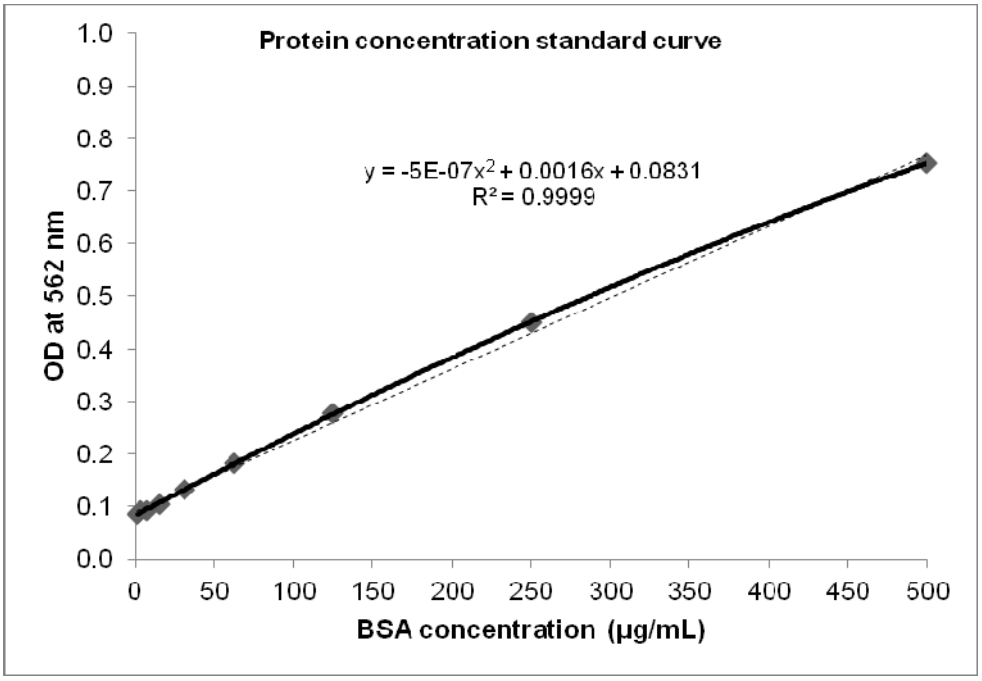

Figure 89: Quantification of purified recombinant HA22 fusion protein. The BCA assay is based on using a standard curve plot of absorbance (OD) at 562 nm versus known concentrations of BSA (µg/mL). The solid line is a point-to-point graph through the plotted standards. The dashed line is linear regression for the entire set of standard points. Accordingly, concentration of the recombinant HA22 protein was determined from the straight line equation. The concentrations were 228.5 µg/mL in elution buffer A (20 mM sodium phosphate, 0.5 M NaCl) buffer and 272.2 µg/mL in elution buffer B (20 mM Tris-HCl, 0.5 NaCl) buffer.

4.15. Optimisation of protein preservation:

Following protein quantification, methods for optimal protein preservation were investigated. For this purpose, aliquots of the protein were either stored at 4°C, frozen at -80°C without glycerol or at -195°C in liquid N_2 in 10% glycerol. For each storage condition, three aliquots were preserved in (20 mM NaH_2PO_4 and 0.5 M NaCl; pH 7.4), (20 mM NaH_2PO_4 and 0.15 M NaCl; pH 7.4) or (20 mM Tris-HCl and 0.5 M NaCl; pH 7.4). All aliquots were retrieved after 10 days of storage, defrosted on ice and analysed by Western blotting and on a Coomassie blue-stained SDS PAGE gel.

Results from these experiments revealed that storage of the purified protein at -80°C was better at conserving the protein than the other methods (Figures 90 and 91).

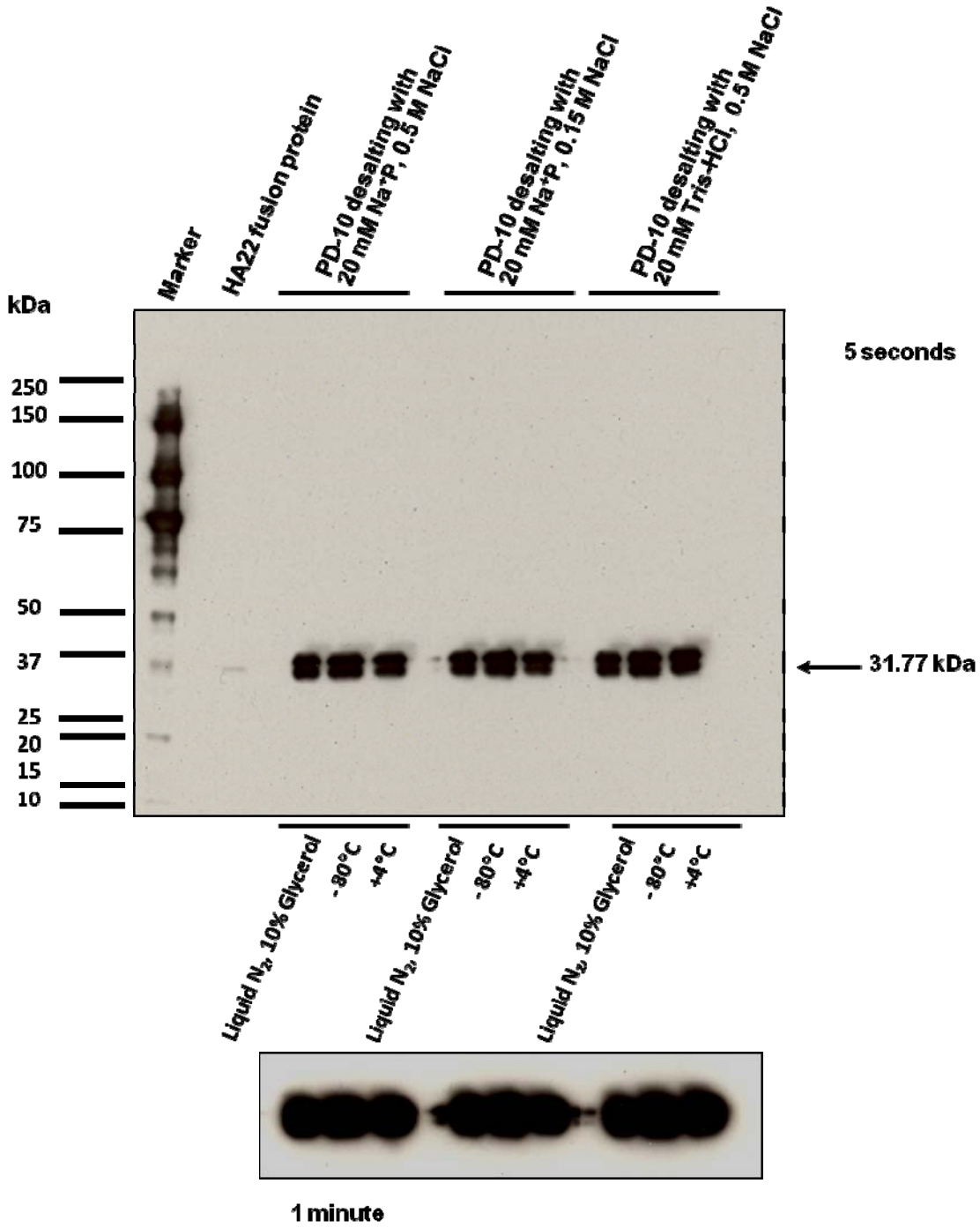

Figure 90: Western blot analysis of stored the HA22 fusion protein stored under different storage conditions. The experiments were carried out to determine optimal storage conditions for the recombinant protein. The analyses showed that freezing of the protein at -80°C was best at conserving protein entity during long-term storage.

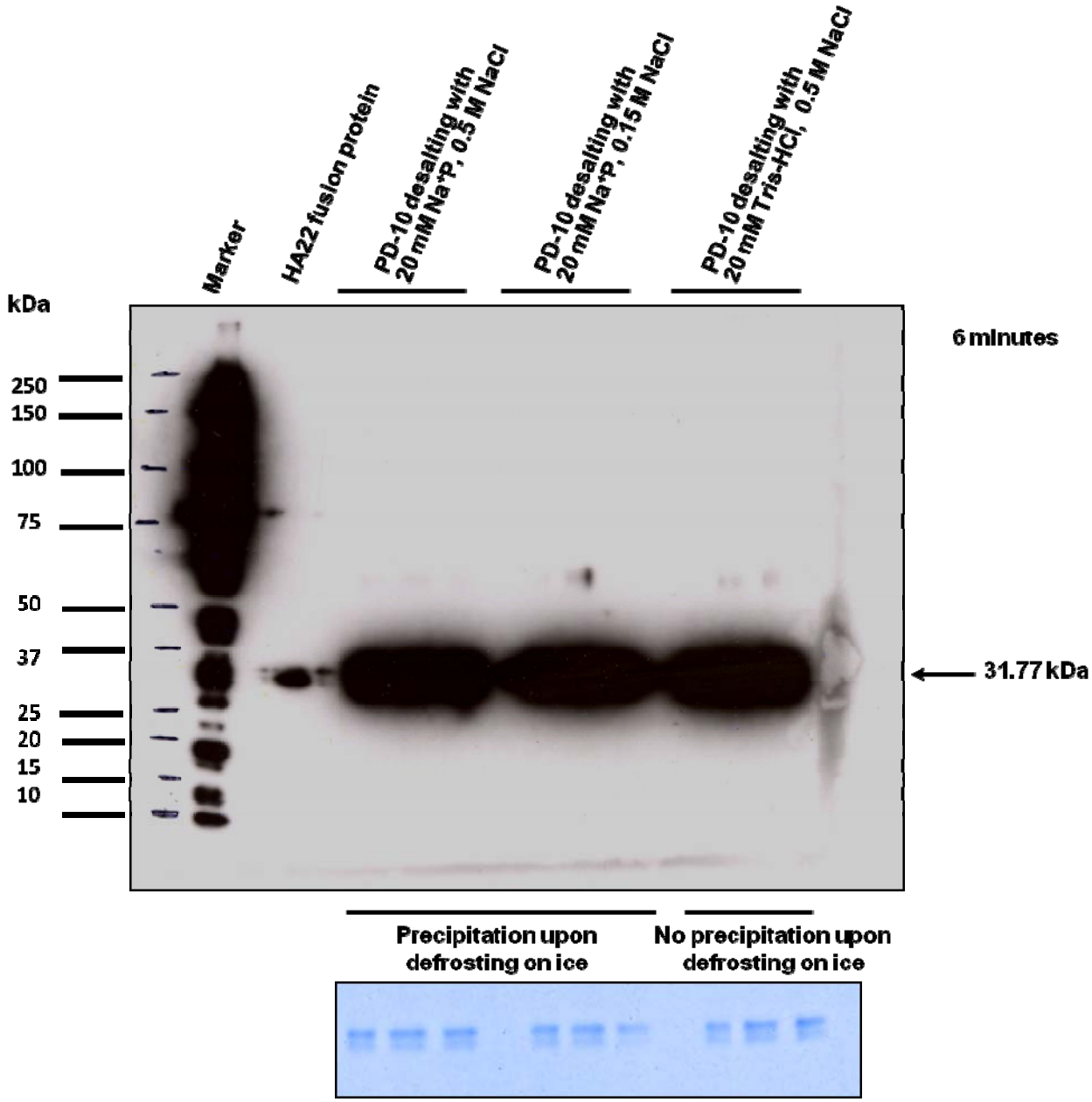

Figure 91: Analysis of HA22 fusion protein after storage under conditions described in Figure 90. The protein bands shown on the Western blot (top) and a Coomassie blue-stained SDS PAGE gel (bottom) are run under reducing conditions. The results show no sign of protein degradation. The Western blot was exposed for 6 minutes.

4.16. HA22 fusion protein binds specifically to CD22 on human mature B cells:

To assess whether the purified recombinant HA22 protein retains its binding and specificity to CD22 on positive B cell lines (HF28 RA and L3/Bcl-2) while not reacting with CD22-negative cells (Jurkat and U937) flow cytometry analyses were carried out. The cells were incubated with the purified HA22 protein (2.7 μg) for 45 minutes on ice, then overlaid with a fluorescently-labeled anti-His Ab (anti-6X His tag® antibody [DyLight® 650] (1.56 mg/mL) at a dilution of 1:500–1:800) as a secondary Ab for an additional 15 minutes on ice. The cells were washed, resuspended in staining buffer and analysed. In parallel, cells stained with anti-6X His tag® antibody [DyLight® 650] Ab were used as control for non-specific background staining. The results indicated that HA22 protein bound specifically to CD22 on B cells (Figure 92).

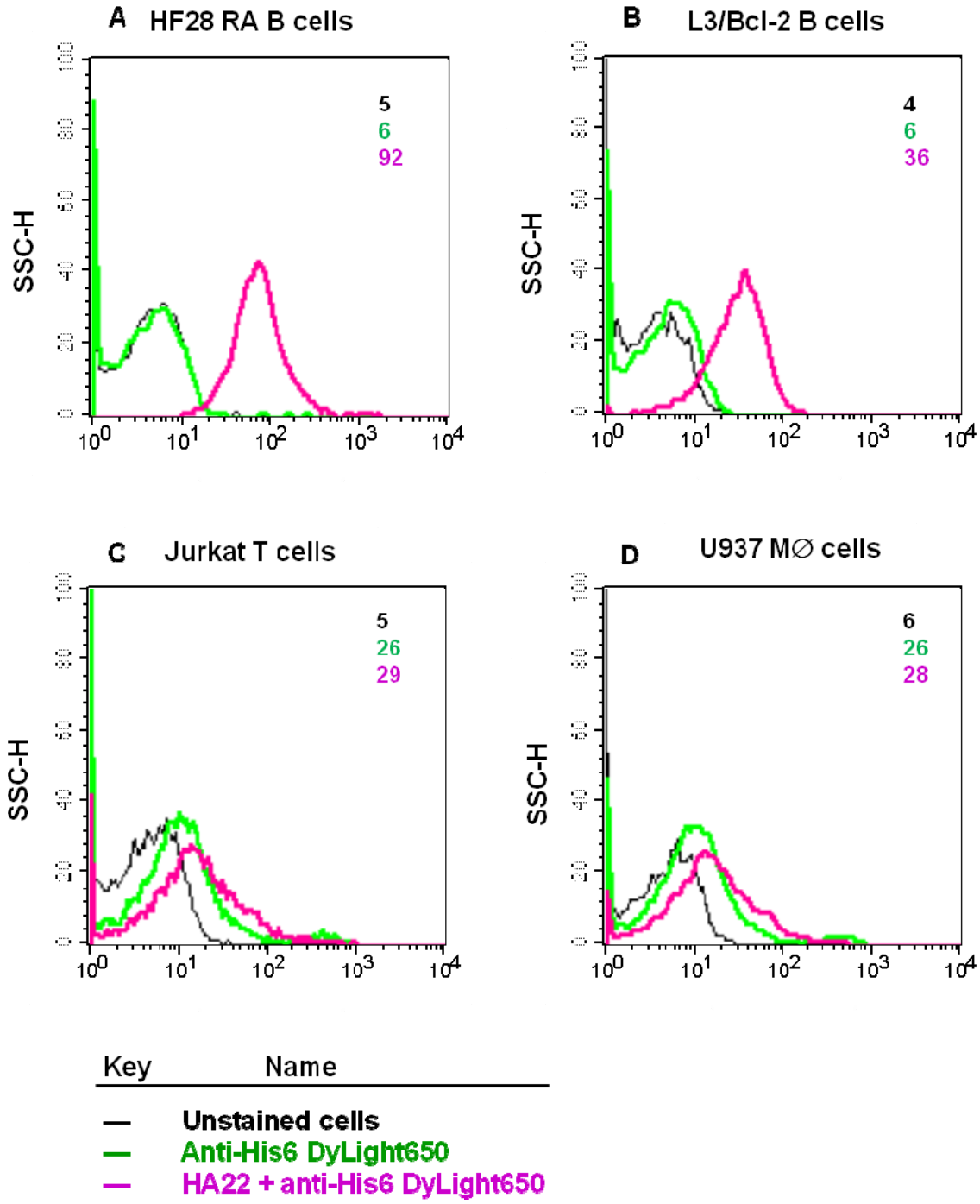

Figure 92: Flow cytometry analysis for the binding of purified recombinant HA22 protein to CD22. Cells were incubated with purified recombinant HA22 protein for 45 minutes on ice and then overlaid with anti-His6 DyLight650 to show binding to $CD22^{+}$ B cells (A and B) but not Jurkat T or U937 histiocytic cells (C and D respectively). Mean fluorescence intensity (MFI) is shown on the histograms.

4.17. Binding and internalisation kinetics of the recombinant HA22 protein and the delivery of siRNA into B cells:

In addition to specificity to CD22, purified recombinant HA22 protein was assessed by confocal microscopy for binding to membrane CD22, internalisation and the delivery of a red fluorescently-labeled scrambled siRNA (siGLO Red) into B cells. To study the kinetics of internalisation and delivery of siRNA, AlexaFluor®488-labeled HA22 fusion protein (10 μg) was mixed with siGLO Red siRNA (100 nM) and incubated on ice for 20 minutes. The complex was then incubated with the HF28 RA B cells or with Jurkat T cells for 45 minutes on ice. Excess protein/siRNA was washed off and the cells incubated at 37°C for 30 or 60 minutes. After washing the cells and treatment with proteinase K on ice, the cells were counterstained with DAPI and mounted for examination. The confocal microscopy data showed that HA22-AlexaFluor®488 bound specifically to B cells. Internalisation was observed after 30 minutes and extended to 60 minutes. Significantly, HA22 fusion protein did not bind Jurkat cells (Figure 93). In addition to these, Z-stacking imaging has also confirmed intracellular localisation of the protein/siGLO Red complex (Figure 94).

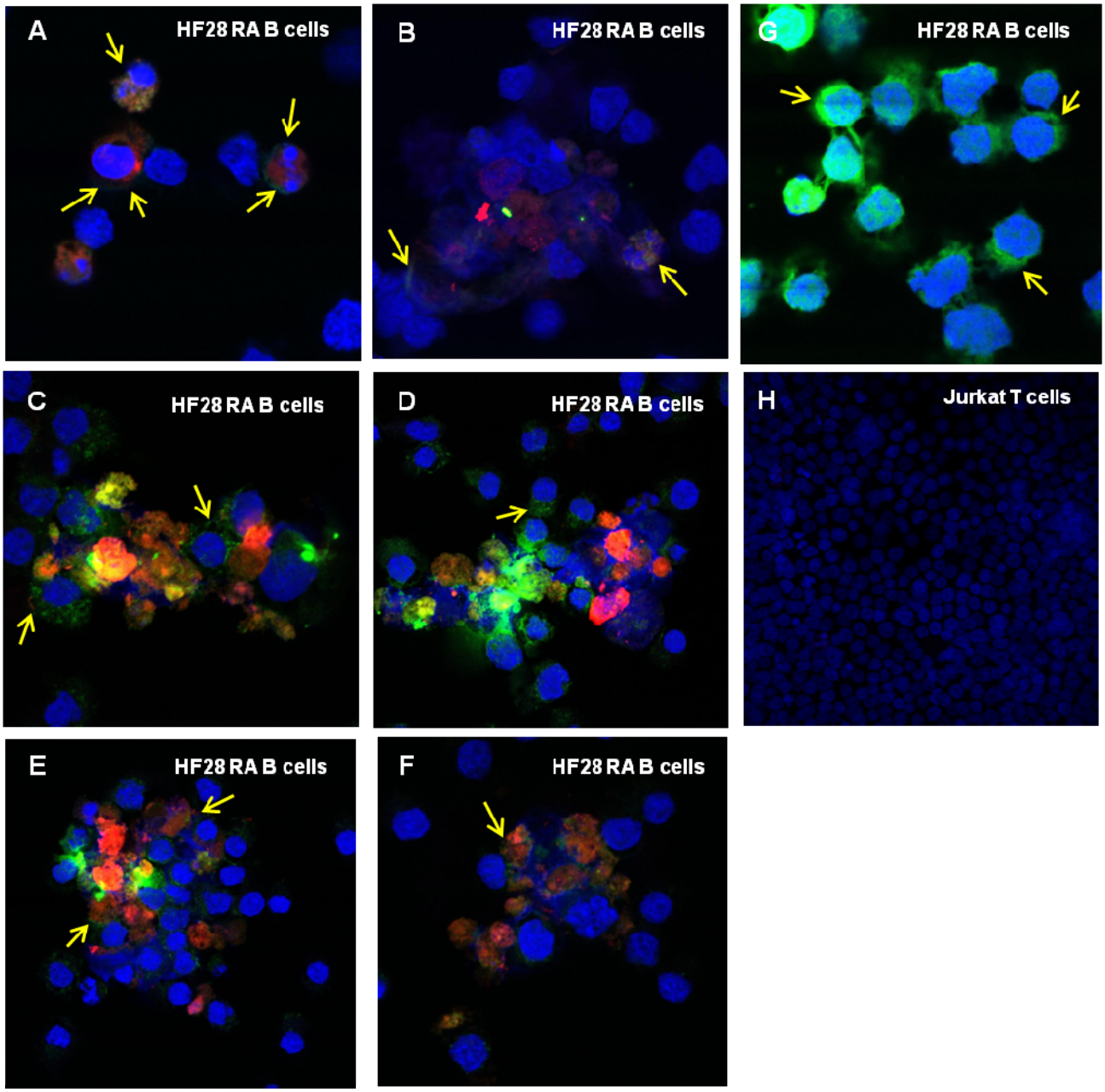

Figure 93: Confocal microscopic analysis for the binding and internalisation of purified recombinant HA22 protein and the delivery of siRNA into B cells. Membrane binding of HA22-AlexaFluor®488/siGLO Red (siRNA) to CD22 receptor on HF28 RA B cells at 0' time point (A and B) at 4°C followed by internalisation into the cells after 30 minutes of incubation at 37°C (C and D). E and F depict cytoplasmic localisations of siGLO Red siRNA (red) following 60 minutes incubation at 37°C. (G) Shows membrane binding of HA22AlexaFluor®488 (green) to CD22 on HF28 RA B cells stained on ice and (H) shows the lack of HA22AlexaFluor®488/siGLO Red binding to Jurkat T cells which are CD22 negative (on ice).

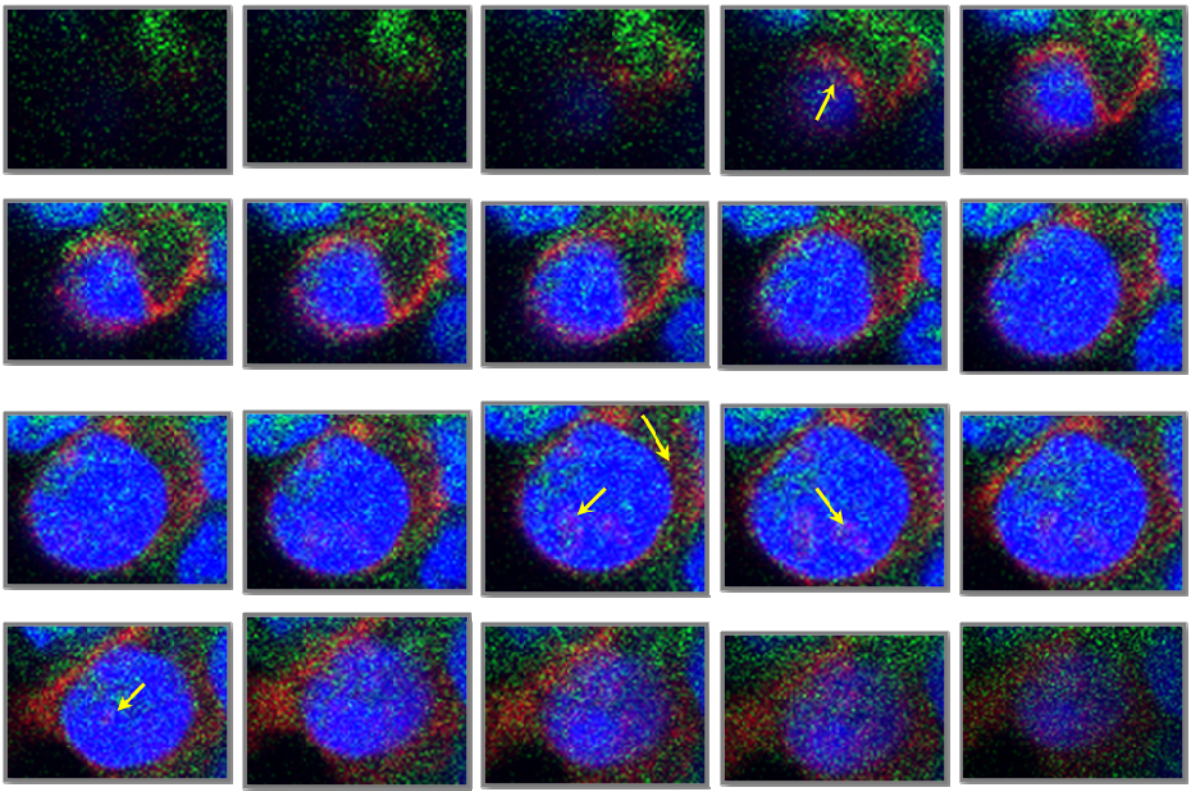

Figure 94: Z-stacking confocal microscopy images for intracellular localisation of HA22 fusion protein/siGLO Red complex in HF28 RA B cells. The Z-stacking slices are based on the images shown in Figure 93 (C and D) after incubation of HF28 RA B cells for 30 minutes at 37°C. The yellow arrow indicates peptide/siRNA complex inside the cells.

4.18. Confirmation of protein/DNA interaction by gel retardation assay:

The gel mobility retardation assay confirmed electrostatic interactions between HA22 fusion protein and pcLuc+ plasmid DNA. To demonstrate retardation of migration of the plasmid DNA through the gel, a constant amount of plasmid DNA (2 μg) was mixed with increasing concentrations of HA22 protein (1–6 μg) and incubated on ice for 30 minutes. The mixture was then resolved on a 1% agarose gel containing 1 μg SYBER safe dye and visualised under UV light. This assay demonstrated hindrance of movement of the plasmid DNA through the gel as an indication of DNA/protein interaction (Figure 95).

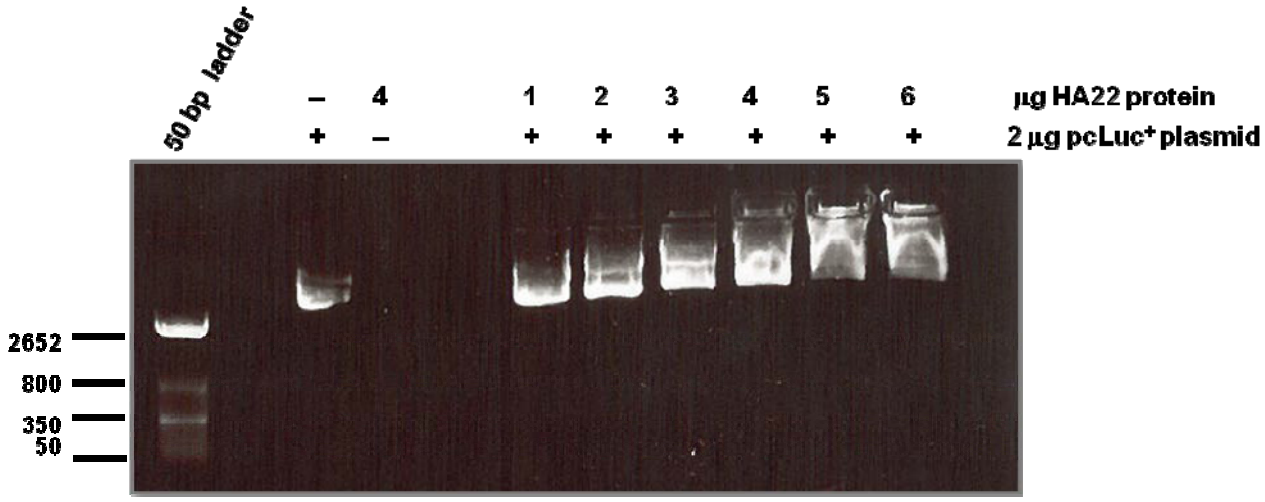

Figure 95: Agarose gel electrophoretic mobility shift assay. The experiment illustrates retardation of plasmid DNA migration due to complex formation by electrostatic interaction between the positively charged protamine domain of HA22 fusion protein and the negatively charged pcLuc+ plasmid.

4.19. Delivery of siRNA to mRNA of the anti-apoptotic protein *MCL1* and cell cycle kinase *PLK1* with the HA22 fusion protein:

Evasion of apoptosis is one of the characteristic hallmarks of cancer cells including malignant B cells. Therefore, reversal of this defect has been widely considered to be an efficacious strategy for cancer therapy (3, 163).

Induction of apoptosis in cancer cells can be achieved by several means, downregulation of specific genes with a role in survival of malignant cells is one approach. In order to accomplish this, I studied whether downregulation of anti-apoptotic or cell cycle kinase genes with a role in cell survival and proliferation is sufficient to instruct B cells to die by apoptosis. For this purpose, the anti-apoptotic myeloid cell leukaemia sequence 1 (*MCL1*) gene (isoform 1 splice variant) and the cell cycle kinase polo-like kinase 1 (*PLK1*) gene were targeted using a SMARTpool of siRNA to mRNA of these genes (siMCL1 and siPLK1 respectively). To carry out these experiments, HA22 fusion protein was mixed with siMCL1 or siPLK1, incubated on ice for 20 minutes and then added to HF28 RA B cells. The INTERFERin or NeoFX transfection reagents were used as positive controls for siRNA delivery. After the indicated time points, the cells were harvested and analysed for viability using CellTiter-Glo® assay. Results from kinetic experiments to downregulate the *MCL1* gene have shown a significant reduction in B cell viability up to 96 hours (Figure 96).

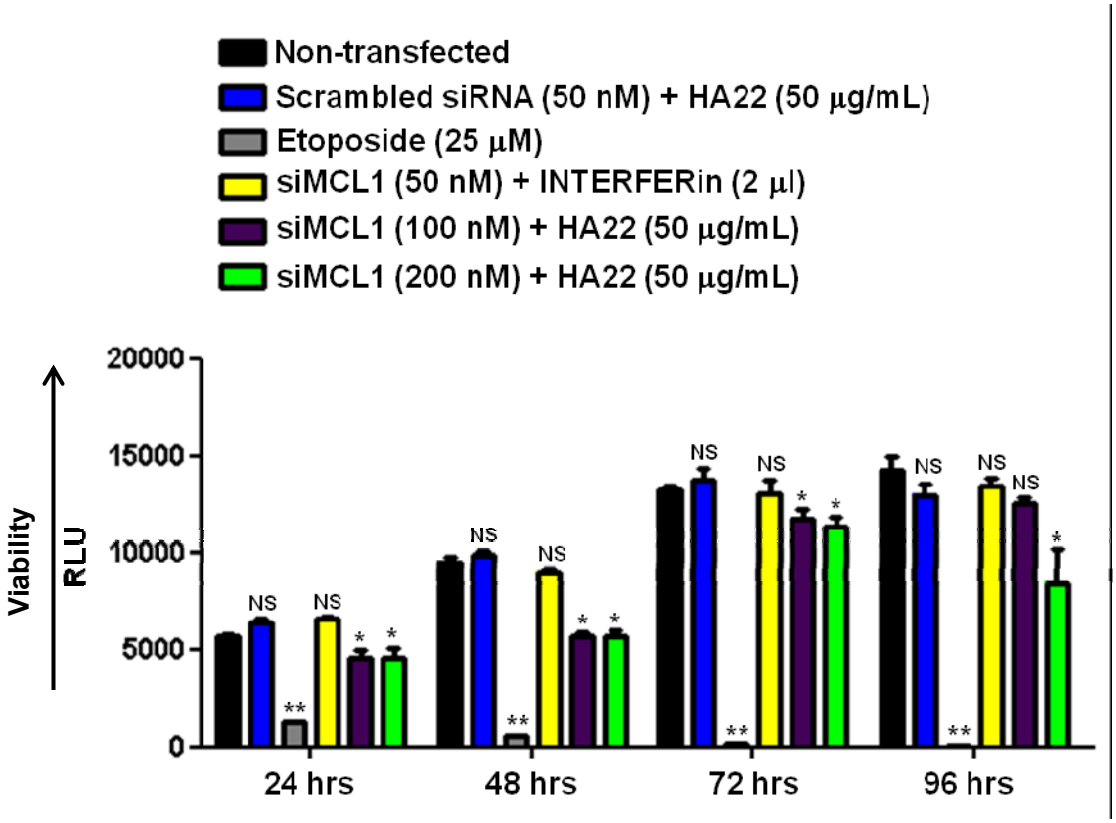

Figure 96: Cell viability assay for B cells following *MCL1* gene downregulation. SMARTpool of siRNAs to mRNA of the anti-apoptotic *MCL1* gene (siMCL1) delivered with HA22 fusion protein caused significant B cell death which was obvious up to 96 hours in the kinetic study despite the high turnover rate of MCL1 decay (~30 minutes). HF28 RA B cells (200 x 10^3 cells/well in 500 μL of medium) were grown in quadruplets. HA22 fusion protein (50 μg)/siMCL1 (100 nM) at the molar ratio of 9.44/8 protein/siRNA molecules was used. Each experimental unit was compared individually with non-transfected cells at the indicated time points. Etoposide was used as a positive inducer of cell death. Luminescence detection is based on using the luciferase reaction to measure the amount of ATP in viable cells which correlates with cell viability. Measurement of cell viability indirectly reflects amount of cell death under investigation. Luminescence was measured as relative light units (RLU). Data analysed by GraphPad Prism and Microsoft Excel using unpaired student *t*-test; n=4; NS: non significant; *: p≤0.05; **: p≤0.01. Error bars are for the standard error of the mean (SEM).

Further cell viability experiments were conducted to test the hypothesis that HA22 fusion protein is non-cytotoxic when added to cells alone. To investigate this possibility, recombinant HA22 protein at a concentration of 25 µg/mL was added to cells with, or without siRNA concomitantly. In these experiments HF28 RA B cells were grown to ~60% confluence at a density of 2 x 10^6 cells/mL in complete growth medium without antibiotics. The kinetics of MCL1 downregulation was studied at two different time points. HA22 protein at 12.5 or 25 µg/mL was mixed with either scrambled siRNA or siMCL1 and added to the cells. The protein alone showed no cytotoxicity. Further, the scrambled siRNA did not interfere with viability of the cells. In contrast, siMCL1 delivered with the protein resulted in significant reduction of cell survival. Moreover, high protein concentration was shown to deliver more siMCL1 into B cells (Figure 97).

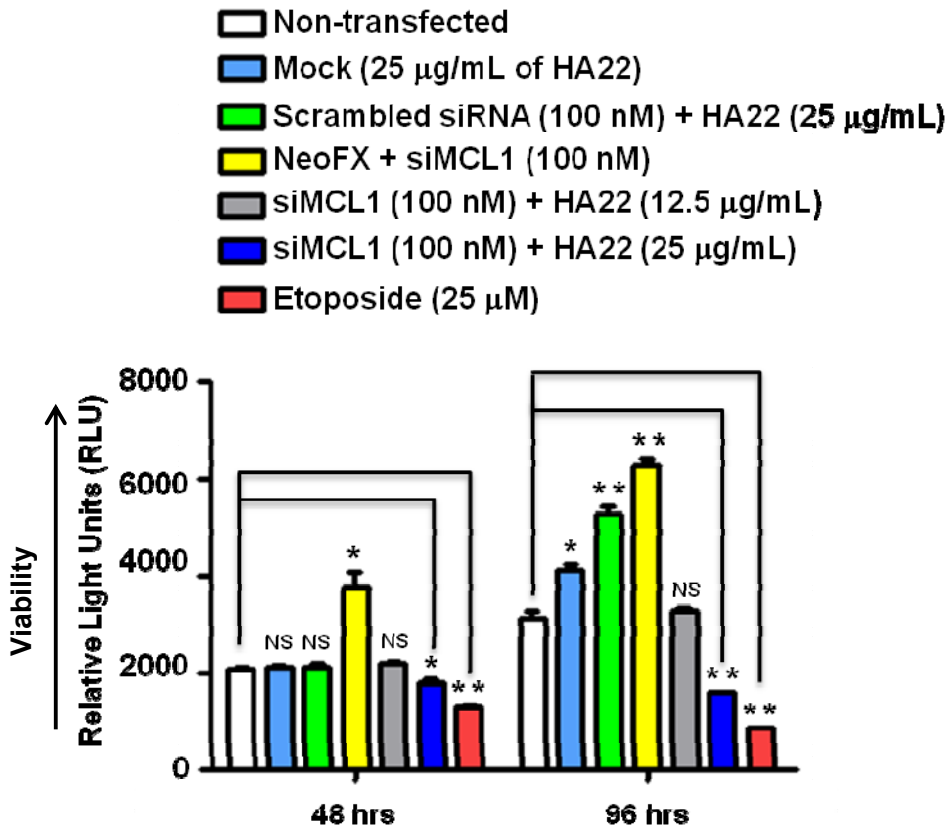

Figure 97: Cell viability assay for B cells following *MCL1* gene downregulation. Each experimental unit was compared individually with non-transfected cells at the indicated time points. HA22 fusion protein at a concentration of 25 µg mixed with 100 nM of siMCL1 significantly reduced cell viability after 48 and 96 hours. However, no reduction in cell viability was seen using scrambled siRNA at both time points or with siMCL1 at 12.5 µg for 48 or 96 hours. In contrast, the rate of B cell proliferation continued as expected when the cells were incubated with scrambled siRNA delivered with HA22 protein. Unpaired student *t*-test; n=3; NS: non significant; *: p≤0.05. **: p≤0.01. The data are presented as the mean ± SEM.

To provide further proof for the specific delivery of siRNAs into RNA-inducing silencing complex (RISC) using HA22 fusion protein, the cell cycle kinase gene *PLK1* was targeted. Similar to the delivery of siRNA for MCL1 in the previous section, siRNA to mRNA of *PLK1* gene (siPLK1) was mixed with two different concentrations of HA22 fusion protein. The mixture was added to HF28 RA B cells as described for the previous experiments. Results from this experiment have shown significant reduction in the survival of B cells (Figure 98).

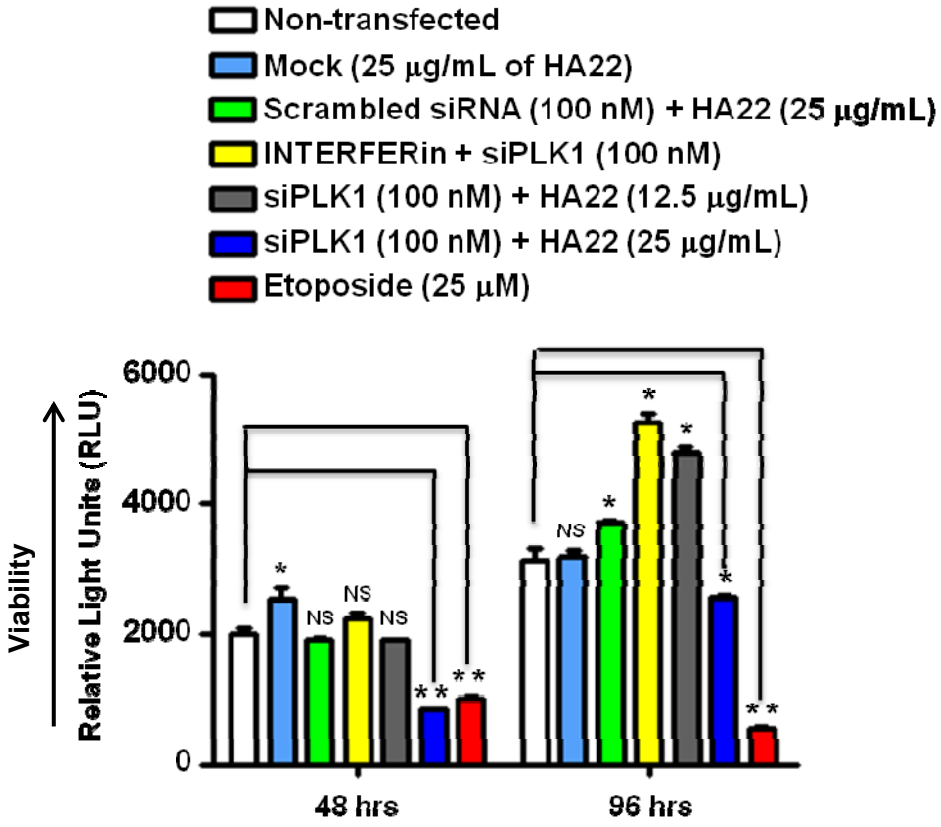

Figure 98: Downregulation of *PLK1* gene in B cells with HA22/siPLK1 promotes cell death. Each experimental unit was compared individually with non-transfected cells at the indicated time points. HA22 fusion protein at a concentration of 25 µg mixed with 100 nM of SMARTpool siRNA to PLK1 (siPLK1) reduced B cell survival and caused significant cell death at both time points (48 and 96 hours). In contrast, neither scrambled siRNA/HA22 (25 µg) nor siPLK1 delivered with 12.5 µg HA22 caused reduction in cell viability. Turnover rate of PLK1 gene is ~7.66 seconds. Unpaired student *t*-test; n=3; NS= non-significant; *: $p<0.05$. Data are presented as the mean ± SEM.

To confirm type of cell death because of downregulation of *MCL1* gene, activation of caspase-3 and -7 were measured using Caspase-Glo®3/7 assay. For this purpose, HF28 RA B cells were transfected either with HA22 fusion protein alone, transfection reagent with siMCL1 or HA22 fusion protein and siMCL1 at two different concentrations. Results from these experiments showed increases in activated caspase-3 and -7 with decreases in the number of viable B cells in the siMCL1 treated cells but not the non-transfected, mock or scrambled siRNA transfected cells (Figures 99 and 100). In addition to reduction in the number of viable B cells and activation of caspase-3 and -7, the mRNA level of *MCL1* gene was shown by real-time PCR (qRT-PCR) to be reduced by ~2.5 fold when the cells were treated with HA22 fusion protein/siMCL1 complex for 48 hours (Figure 101).

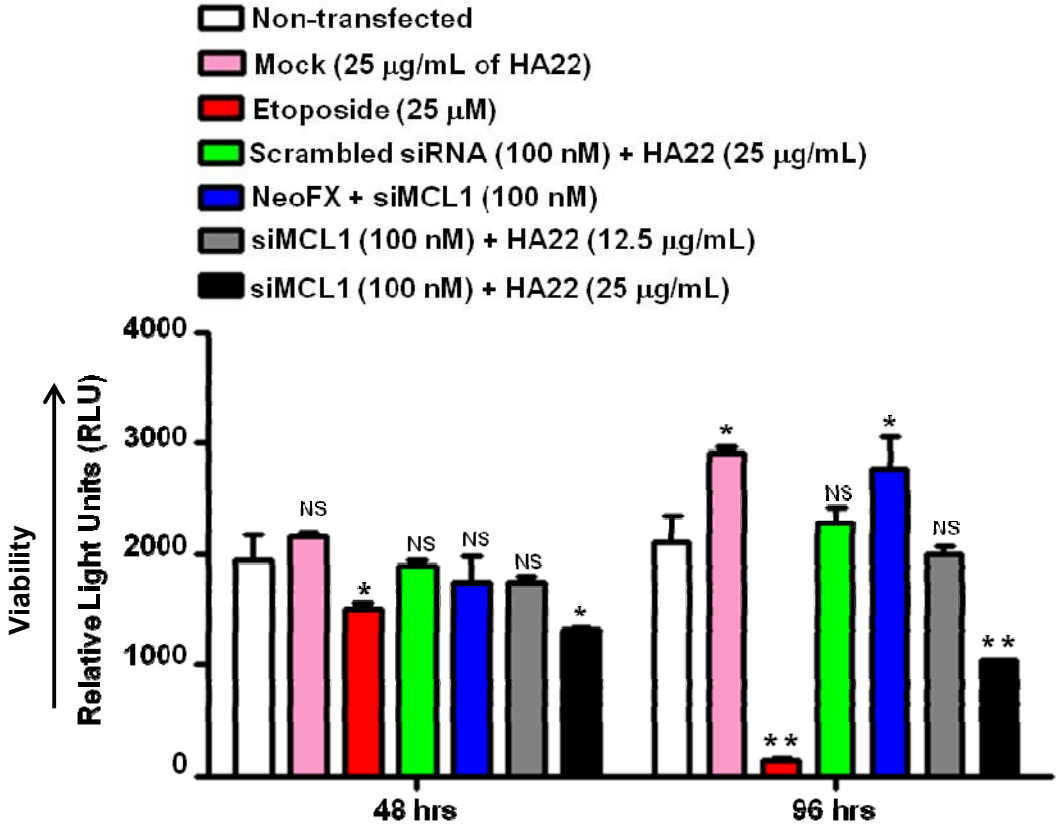

Figure 99: Cell viability assay for B cells following *MCL1* gene downregulation. Each experimental system was compared individually with non-transfected cells at the indicated time points. HA22 fusion protein at a concentration of 25 μg was mixed with 100 nM of siMCL1 and this mixture significantly reduced cell viability after 48 and 96 hours. However, no reduction in cell viability was seen using scrambled siRNA at both time points or with siMCL1 at 12.5 μg for 48 or 96 hours. In contrast, the rate of cell proliferation continued as expected when the cells were incubated with scrambled siRNA delivered with HA22 fusion protein. Unpaired student *t*-test; n=3; NS: non significant; *: $p \leq 0.05$. **: $p \leq 0.01$. The data are presented as the mean ± SEM.

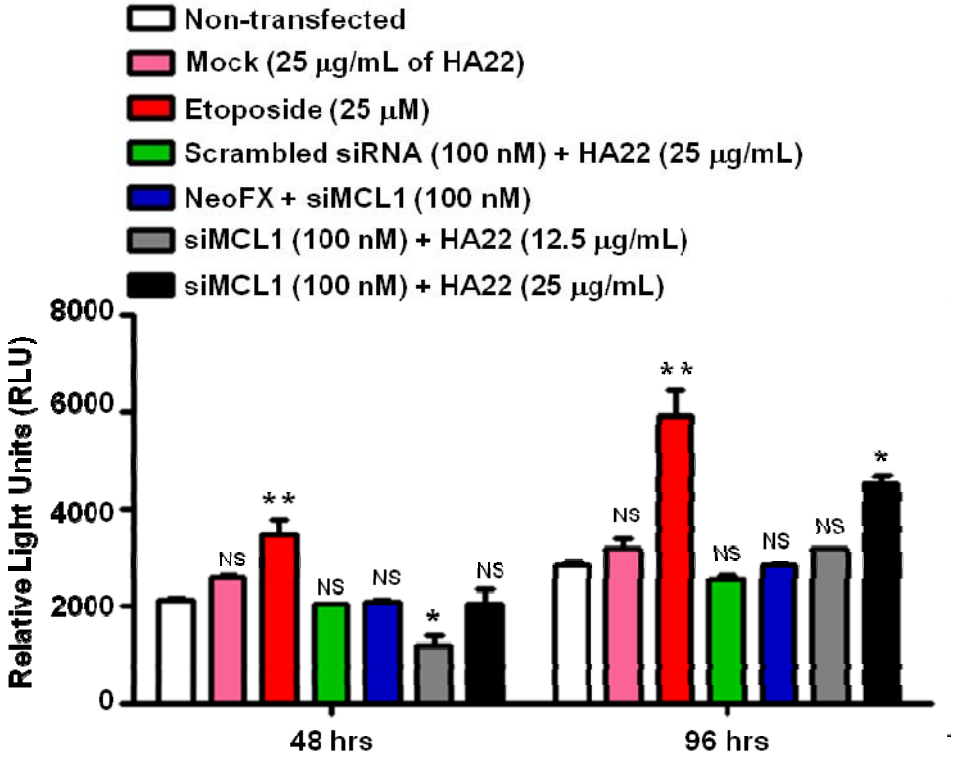

Figure 100: Caspase-3 and -7 activation in B cells following *MCL1* gene downregulation. The Caspase-Glo®3/7 assay was carried out on the same samples that were tested for B cell viability and analysed as shown in Figure 99. With a decrease in the number of viable B cells there was simultaneous increase in luminescence which was proportional to caspase-3 and -7 activation. HA22 fusion protein at a concentration of 12.5 or 25 μg/siMCL1 (100nM) at 2.36/8 or 4.72/8 protein/siRNA molar ratios were mixed and added to cells. However, no significant caspase-3 and -7 activation was seen in non-transfected, mock, scrambled or when using transfection reagent. Each experimental system was compared individually with non-transfected cells at the indicated time points. Unpaired student *t*-test; n=3; NS: non significant; *: p≤0.05. **: p≤0.01. The data are presented as the mean ± SEM.

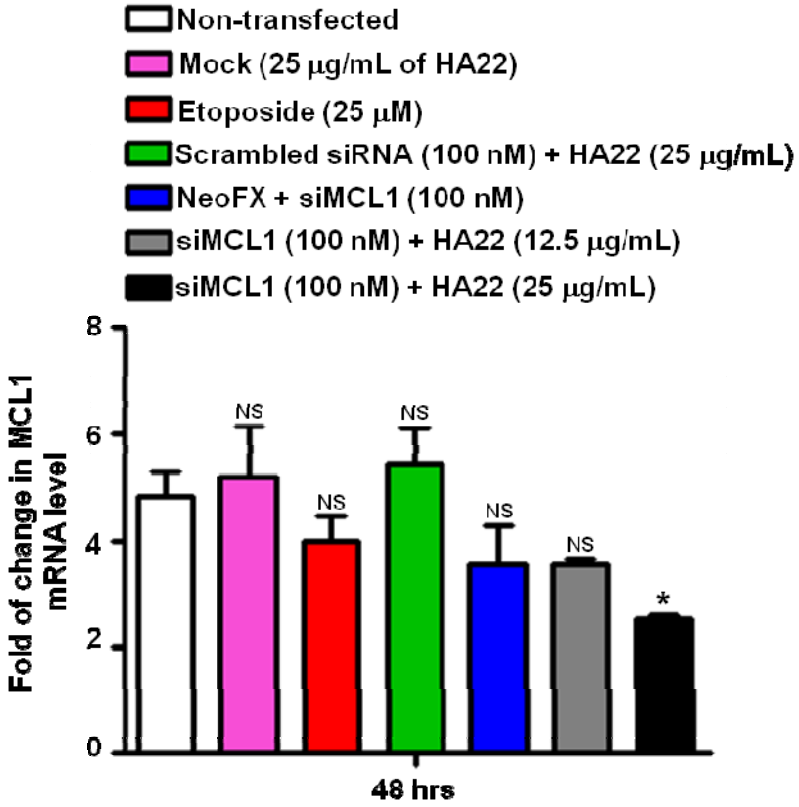

Figure 101: Quantitative real-time PCR for *MCL1* mRNA in B cells following gene downregulation. The experiment was carried out in tandem with the CellTiter-Glo® and Caspase-Glo®3/7 assays shown in Figures 99 and 100. mRNA levels of *MCL1* gene were determined by real-time PCR. Fold changes in *MCL1* expression were normalised to the expression of β-actin (*ACTB*), β-2 microglobulin (*B2M*), glyceraldehyde-3-phosphate dehydrogenase (*GAPDH*), phosphoglycerate kinase (*PGK1*) and transferrin receptor (*TFRC*) housekeeping genes using ABI 7900HT software version 2.4.1. After 48 hours treatment of the cells, no significant reduction in mRNA levels was observed the experiments except for cells treated with HA22 fusion protein (25 μg)/siMCL1 (100nM) at 4.72/8 protein/siRNA molar ratio. The level of *MCL1* mRNA was not significantly reduced with etoposide. Etoposide kills eukaryotic cells by inhibition of topoisomersae II enzyme activity rather than degradation of MCL1 protein. Experimental units were compared using unpaired student *t*-test. n=3; NS: non significant; *: $p \leq 0.05$. The data are presented as the mean ± SEM.

4.20. Discussion:

Therapeutics based on RNAi hold promise for the treatment of numerous diseases including cancer. In recent years, both viral and non-viral methods for the delivery and expression of siRNA molecules have been used (314). Examples of non-viral delivery systems include using peptides, proteins, aptamers, cationic polymers and liposomes (315-320). Some of these agents are not suitable for systemic *in vivo* delivery due to factors such as instability in serum, undesirable pharmacokinetics, costs or feasibility of scaling-up to obtain therapeutic quantities. In addition to meeting these criteria, effective intracellular delivery of therapeutic genes is important and requires targeting to disease relevant tissues to minimise potentially toxic side effects of either the agent or associated siRNA. For example, viral vectors have been shown to be extremely efficient in gene transfer, but alteration in target specificity can result in a decrease in infectivity of the recombinant virus. In addition to concerns about safety and immunogenicity of viral vectors, these findings have spurred the development of non-viral vectors with targeting capacities for selective gene delivery (314).

One approach used for delivering siRNA to specific cells is by small proteins, or polypeptides that contain a receptor-binding, or cell-homing domain to direct the complex to the surface of the desired cell population. These approaches require RNA binding capability, a property sometimes conferred using cationic peptide sequences that electrostatically interact with negatively charged siRNA backbones (321). Thus, a highly effective targeting gene delivery can be achieved by using engineered recombinant scFv antibody fragments (322-324).

The results presented in this chapter describe the construction and generation of a biologically functional recombinant anti-CD22 scFv antibody fragment with specificity to human CD22.

The increasing demand for recombinant proteins to be used for treatment and structural studies justifies the need for a rapid and scalable expression system. In this regard various expression systems have been used for the production of recombinant scFv proteins, including bacterial, yeast, insect and mammalian cells (325).

Currently, about 60–70% of all recombinant pharmaceutical proteins are produced in mammalian cells because their proper polypeptide folding, secretion and post-translational apparatus are better suited to produce antibodies indistinguishable from those produced in the human body. Many of these recombinant proteins are expressed in immortalised cell lines such as Chinese Hamster Ovary cells (CHO), mouse myeloma cells (NS0), baby hamster kidney cells (BHK), human embryonic kidney cells (HEK293) and human retinal cells. For instance, it has been shown that industrial levels of IgG production in CHO cells achieved about 5-12 g/L as result of an improved high producer cell line, optimised serum-free production media as well as optimised and prolonged production processes at very high cell densities (326).

Stable expression technologies, based on integration of transgenes into the host genome are currently the most important systems to produce recombinant proteins in mammalian cells. The development of these technologies is costly because it involves considerable investments of time, labour, materials and equipment. More efficient methods for generating proteins are needed for faster evaluation of therapeutic proteins and for the analysis and screening in high-throughput formats such as proteomics. Transient gene expression in mammalian cells such as CHO and HEK293 cells is considered well-suited to fill these needs, with the capabilities to generate large quantities of products within a relatively short timeframe (327, 328). In this respect, successful production of recombinant antibodies in mammalian cells has been reported in previous studies (329-331).

To address the first aim of the work described in this thesis, extensive experiments were carried out to generate and test recombinant anti-human anti-CD22 scFv-protamine-His6 protein (henceforth called HA22 fusion protein). This scFv was shown to have retained specificity for binding to CD22 receptor on human B cells and able to be internalised by $CD22^+$ B cells.

Production of HA22 scFv by incorporating its cDNA into pMH113 vector has been described previously (228). The RFB4 IgG-producing hybridoma produces and secretes a mAb with specificity for human CD22 (59). Generation and use of the recombinant scFv immunotoxin BL22 as a therapeutic agent in clinical studies for treatment of patients with $CD22^+$ B cell malignancies has been described (229). BL22, for B cell leukaemia/lymphoma/CD22, is the immuntotoxin generated by attaching RFB4 IgG scFv with *Pseudomonas* exotoxin A (PE38) to create RFB4(scFv)-PE38. BL22 was then cloned into pDisplay vector (named pMH112). A mutated version of anti-CD22, called HA22 was generated by creating mutations in 3 amino acid residues in CDR3 region of the heavy chain from SSY to THW which increased affinity to human CD22 receptor by ~15 fold (230).

The HA22 scFv cDNA was used in the current study to construct a vector for expression in mammalian systems. To create this, the truncated protamine peptide and a hexahistidine tag were cloned at the C-terminus of HA22 scFv and the entire DNA fragment was then cloned into pcDNA6|IL2ss. This construct was used for expression of the recombinant protein in mammalian cells. The results showed that the protein was not expressed by CHO-S or HEK293T cells using pcDNA6|IL2ss. This was predicted to be due to inability of the IL2 signal sequence (IL2ss) to drive expression/secretion of the recombinant HA22 fusion protein. The finding that HA22 fusion was not expressed/secreted using IL2ss is in disagreement with a previous study which has shown secretion of recombinant proteins using the IL2 signal sequence (332). Thus, these investigators showed that the native coding sequence of IL2 was sufficient to cause secretion of recombinant murine cytokines, IL2 and gamma-interferon (γ-IFN) by transfected *Trypanosoma cruzi* protozoan parasite. Furthermore, they showed that the γ-IFN was produced and secreted only when the γ-IFN signal sequence was replaced by the IL2ss (332).

In order to investigate the effect of a different signal sequence, expression/secretion of the original HA22 scFv in pMH113 vector was studied. Protein expression and secretion was confirmed in HEK293T cells using pMH113 vector (pDisplay). Therefore, the DNA expression cassette was cloned back from pcDNA6|IL2ss into the original pDisplay vector which has the murine Ig kappa chain signal peptide. Protein expression and secretion was confirmed in the HEK293T culture and in the serum-free culture of HEK293F cells. The HEK293F cells were then used for large-scale transient transfection for its advantages such as higher transfectability, suspension cultivation in serum-free conditions and cost-effective scalability. Previous studies have also shown the successful expression/secretion of recombinant proteins using the murine Ig kappa chain signal peptide (282, 283).

Analyses of protein expression in HEK293F cells by Western blotting showed that ~2.03 fold more protein yield was obtained using DNA:PEI at 1:3 ratio compared with 1:1 ratio. It has been reported that the DNA:PEI ratio is considered important to the optimisation of DNA compaction during transfection of human umbilical vein endothelial cells (HUVEC) and A549 human lung carcinoma cells (333). These observations are also consistent with a previous study which demonstrated that the transfection efficiency of DNA:PEI at 1:4 and 1:6 ratio work better than 1:1 ratio in CHO-S cells to produce recombinant proteins because the amount of PEI can affect the particle size of DNA:PEI complexes (334). PEI transfection vehicle, a cationic polymer, combines and condenses DNA into positively charged particles, which bind to anionic cell surface residues and are transported into cells via endocytosis. Inside the cell, PEI inhibits acidification of endosomes which will then lower the osmotic potential, hence swelling and eventual rupture of the organelle (‘‘proton sponge effect’’) and, thus, release of the complex into the cytoplasm (335-338). The emphasis of this mechanism is important because by extrapolation from those studies it could be presumed that HA22 fusion protein which contains the cationic protamine peptide causes a “proton sponge effect” for the liberation of the siRNA cargo from the endosome/lysosomes compartment. In addition, due to factors such as low cost of materials, simplicity in handling and facility in large-scale operations, transfection with calcium phosphate and PEI have been the most widely used technique among numerous commercially available transfection agents (339).

The effect of dialysis on the recombinant protein was also studied and proved to be troublesome because of significant loss of the recombinant protein. Although HA22 fusion protein was obtained in secretable form from transfected HEK293F cell cultures, presumably with a properly folded and disulfide-stabilised structure, but the possibilities of improper folding, dimer formation or concealed hexahistidine tag were examined. For this purpose, the protein was analysed under non-reducing conditions as well as reducing conditions. No dimer formation, protein aggregates or notably concealed hexahistidine tag was noticed under non-reducing conditions. In a previous study, it has been reported that difficulty of binding of histidine tagged recombinant proteins to nickel column or inability to retrieve the protein by elution is possibly because of a change in the conformation of recombinant proteins concealing the histidine tag (340).

The next issue to address was to determine the optimal concentration of imidazole. Unexpectedly, large amounts of impurities were removed from the nickel column with washes using 50 and 250 mM imidazole. Consequently, pure yields of HA22 fusion protein of the correct molecular size were obtained by using 500 mM imidazole in the elution buffer. In agreement with the present study, investigators have shown that CB515 scFv generated from a complement-independent bactericidal monomeric IgM mAb (26 kDa) against a relapsing fever caused by *Borrelia* species was obtained to high purity when the histidine tagged scFv was eluted from nickel column using 500 mM imidazole. The CB515 scFv was produced as soluble protein extracted from the periplasmic space of *E. coli* (341). In another study, investigators produced recombinant scFvPOM1 and scFvPOM2 from anti-PrP^c mAbs directed against the epitopes of mouse prion protein PrP^c. scFvPOM1 and scFvPOM2 proteins were expressed as soluble proteins and isolated from periplasmic extracts of *E. coli* cultures. After binding to nickel column and washing off the impurities, pure proteins were eluted with elution buffer containing 500 mM imidazole pH7.0 (342). HA22 fusion protein is a positively charged protein and hence its binding to nickel-coated beads was expected to be strong; thereby a higher competitive concentration of imidazole (500 mM) was needed to elute the protein. A recent report about significance of supercharged proteins has also shown that 500 mM imidazole was needed to obtain pure recombinant proteins (343).

Previous studies have shown that scFvs typically have low thermal stability and tend to denature or aggregate under conditions of practical uses, thus, limiting their biomedical and biotechnological applications (344, 345). For this reason, optimal conditions of storage for protein preservation was determined by investigating the effect of storage and freezing at 4°C, -80°C without glycerol or at -195°C in liquid N_2 in 10% glycerol respectively. These conditions were assessed based on a technical resource obtained from a biotechnology company (Thermo Scientific, http://www.thermoscientific.com/). Analyses of the protein by Western blotting and on a Coomassie blue-stained SDS PAGE gel of protein retrieved after preservation confirmed that storage at -80°C was the best for long-term preservation of the protein.

Final modification in the protein structure involved removal of the haemagglutinin A epitope (HA) tag at the N-terminus of HA22 protein. The HA tag was removed by modifying the pDisplay vector backbone so that the signal peptide is unaffected because this HA tag was preceded by Ig kappa-chain signal peptide. Elimination of HA epitope was carried out to minimise the possibility of non-specific binding of the HA tag to cell surface receptors on T cells. In support of this notion, a previous study revealed that $CD4^+$ T cells can recognise epitopes within the influenza HA protein and that naive T cells specific for HA epitopes undergo significant expansion (346).

The immediate issue to address, subsequent to obtaining the protein, was whether HA22 fusion protein has retained its binding to CD22. Data form the flow cytometry analyses showed that the HA22 fusion protein bound specifically and only to $CD22^+$ B cells HF28 RA and L3/Bcl-2.

This new delivery system, fusion protein, for siRNA that utilises CD22-mediated endocytosis relies on the specificity of the recombinant protein and ability to form electrostatic interactions with siRNA. siRNA is a negatively charged molecule because of the phosphate group in the nucleotides backbone. Therefore, it will be possible for siRNA to form electrostatic interactions with positively charged protamine. Despite the fact that HA22 fusion protein was shown by confocal microscopy to deliver a red-labeled siRNA (siGLO red) intracellularly, the robustness of this interaction was validated by gel

mobility retardation assay. Thus, binding of a plasmid DNA (pcLuc^{+}) to cationic HA22 fusion protein was confirmed by observation of resistance of DNA migration using electrophoretic mobility gel shift assay (EMSA). In support of this, a previous report has shown retardation of DNA movement due to DNA/protein interaction (347). Similarly, siRNA/protein interaction was observed in another study using EMSA (348).

A number of studies have used engineered scFv-protamine fusion proteins for directed delivery of siRNA into cancer cells via receptor-mediated endocytosis. For antibody-mediated targeted delivery of siRNA *in vivo*, anti-HIV1 envelope scFv-protamine was complexed with siRNA and used to deliver siRNAs to cells transfected to express HIV envelope glycoprotein gp160 as a proof of concept (120). Similarly, an anti-ErbB2 scFv-protamine fusion protein was shown to deliver siRNAs specifically to ErbB2-expressing (ErbB2^{+}) breast cancer cells (160). In another study it was shown that a scFv-protamine fusion protein targeting the human integrin lymphocyte function-associated antigen-1 (LFA-1) allowed efficient delivery of siRNAs and cell type-specific gene silencing in primary lymphocytes, monocytes and dendritic cells (161). Recently, it has been shown that targeted delivery of PLK1 siRNA with the fusion protein anti-HER2 scFv-protamine *in vivo* using Her2^{+} breast cancer models in mice significantly suppressed Her2^{+} breast cancer growth and metastasis (162).

The induction of apoptosis in aberrant B cells including cancer cells is one of the objectives of targeted therapies in cancer. The results shown in this chapter confirmed that this objective could be accomplished. In order to achieve this, siRNA was used to downregulate a specific gene involved in B cell survival. The question asked was whether downregulation of the anti-apoptotic *MCL1* gene, or the cell cycle kinase *PLK1* gene using siRNA could be sufficient to induce apoptosis.

Most conventional cytotoxic agents indirectly induce apoptosis through DNA damage and cell cycle arrest. However, malignant cells frequently acquire defects, including oncogene activation and downregulation of apoptotic signaling pathways, thereby, allowing the cells to evade apoptosis (3, 163). For these reasons and the high levels of toxicity frequently observed with standard chemotherapeutic drugs, recent

approaches to cancer therapy have focused on targeting key components of pathways shown to be fundamental to tumour survival and disease progression (349). This approach is intended to circumvent acquired drug resistance pathways and re-sensitise the malignant cell to apoptosis.

Previous studies have shown that the anti-apoptotic BCL-2 family member, *MCL1* is highly expressed in haematopoietic stem cells (HSCs) and it is essential for promoting their survival (350, 351). Furthermore, it has been shown that deletion of *MCL1* during early lymphocyte differentiation increases apoptosis and arrests development at the pro-B cell stage (352). In addition, overexpression of *MCL1* has been reported in various forms of leukaemia (353, 354).

Therefore, *MCL1* gene was selected for targeted downregulation using siRNA. For this purpose, siRNA to *MCL1* (siMCL1) was either delivered with 12.5 or 25 µg of HA22 fusion protein or delivered with NeoFX or INTERFERin transfection reagent to B cells. The results revealed significant reduction in B cell viability after 48 and 96 hours using siMCL1/HA22 complexes. However, no reduction in cell viability was seen using scrambled siRNA, HA22 fusion protein alone or siMCL1 delivered with transfection reagent.

Whilst reduction in B cell viability was observed using HA22 fusion protein/siMCL1 complex, an intriguing finding was that no reduction in B cell viability was seen using the lipid based NeoFX or INTERFERin transfection reagents. There is, however, a possible explanation for this phenomenon. Lipid nanoparticles (LNPs) are the most advanced siRNA delivery system to date, having recently shown therapeutic efficacy in clinical trials (355). Although efforts to understand the physicochemical properties of nanoparticles that contribute to efficient cellular delivery are ongoing, the cellular processes that determine the efficiency of nanoparticle-mediated siRNA delivery remain largely unclear (356, 357). In this regard, investigators have recently examined the cellular uptake of AlexaFluor®647–labeled siRNA to green fluorescent protein (GFP) complexed with LNPs using cellular trafficking probes in combination with automated high-throughput confocal microscopy. HeLa cells, NPC1 fibroblasts and stably-GFP-

transfected LLC-PK1 epithelial cells were used for this purpose. These experiments showed that siRNA delivery was substantially reduced as ~70% of the internalised siRNA underwent exocytosis through escape of LNPs/siRNA complexes from late endosomes/lysosomes and the genes under investigation were unaffected. Furthermore, these studies showed that Niemann-Pick type C1 (NPC1), a protein that resides in the limiting membrane of endosomes and lysosomes and mediates intracellular cholesterol trafficking, is an important regulator of the major recycling pathways of LNP-delivered siRNAs. Thus, NPC1-deficient cells showed enhanced cellular retention of LNPs inside late endosomes and lysosomes and increased gene silencing of the target gene (358).

In the current experiments, HA22 fusion protein alone did no show any cytotoxic effect on HF28 RA treated B cells as B cell viability was not reduced. In agreement with this finding, a previous study has shown that HA22 scFv on its own is non-cytotoxic unless toxicity is attached to it using either a cytotoxic drug or a toxin for therapeutic purposes (359).

The scFv of mutated BL22, HA22 which has higher affinity for CD22 was shown to be resistant to proteolytic digestion and, therefore, with increased anti-tumour activity because of less intracellular degradation (360, 361). HA22 immunotoxin, called Moxetumomab pasudotox, is currently in development by the biologics division of AstraZeneca and MedImmune and is in Phase III trial for the treatment of patients with mature B cell malignancies: (http://www.astrazeneca.com/, http://www.medimmune.com/).

Treatment with Moxetumomab pasudotox led to complete remission in patients with relapsed/refractory hairy cell leukaemia (HCL) and improved outcome in patients with chronic lymphocytic leukaemia (CLL) and paediatric acute lymphoblastic leukaemia (ALL) (230). In addition, results from a recent single-cycle pharmacokinetic and pharmacodynamic study in cynomolgus monkeys supported the clinical benefits of Moxetumomab pasudotox immunotoxin in patients with $CD22^{+}$ B cell malignancies (362).

BL22 recombinant immunotoxin is composed of the scFv of anti-CD22 RFB4 mAb fused with a 38 kDa truncated *Pseudomonas aeruginosa* exotoxin derivative (PE38) (228, 230). Following internalisation of BL22, the C-terminus translocation domain of the PE38 toxin, which contains a REDL sequence (KDEL ER-targeting motif sequence for ER retrieval), binds intracellularly to the Lys-Asp-Glu-Leu endoplasmic reticulum protein retention receptor 1 (KDEL receptor) that carries it to the endoplasmic reticulum. The toxin is then translocated to the cytosol where its adenosine diphosphate (ADP)-ribosylating enzyme domain inactivates translation elongation factor 2 (EF2), thereby inhibiting protein synthesis and apoptotic cell death (363). The mechanism of leukaemic cell killing was reported in a previous study to be through lowering MCL1 protein level and unleashing the pro-apoptotic Bak protein, thereby, inducing caspase-3-mediated apoptosis (364).

With regards to downregulation of *MCL1* gene, several studies have reported that downregulation of *MCL1* leads to sensitisation of tumour cells to different treatment regimens *in vitro*, as has been shown for cholangiocarcinoma, chronic myelogenous leukaemia, sarcoma and malignant melanoma (365-368). It has also been reported that the anti-apoptotic protein MCL1 is a rapidly inducible protein with a short half life of ~20-40 minutes (369-372). Therefore, MCL1 differs from other members of the Bcl-2 family in having a short half-life and inhibition of its expression and/or neutralisation of its anti-apoptotic function could probably make MCL1-dependent cells more susceptible to induction of apoptosis (373). Consequently, interference with the synthesis of MCL1 could have an effect on protein levels and be of potential therapeutic use in many types of cancers. In this respect, investigators have shown that targeting of *MCL1* gene with siRNA renders hepatocellular carcinoma cells more sensitive to chemotherapy *in vitro*. Thus, it was reported that siRNA to *MCL1* gene mRNA efficiently downregulated MCL1 expression in the human hepatoma cell lines Hep3B and HepG2 treated with cisplatin, mitomycin C and 5-Fluorouracil, led to activation of caspase-3 and -9 and increased apoptosis rates from ~20% to ~60% (202).

Consistent with findings by other investigators, the present study of *MCL1* gene downregulation by HA22/siMCL1 resulted in reduced B cell viability and activation of caspase-3 and -7. However it remains to determine how exactly degradation of MCL1 protein by HA22/siMCL1 initiates apoptosis. In a previous study, investigators revealed that downregulation of MCL1 results in permeabilisation of the outer mitochondrial membrane and consequently release of the apoptogenic cytochrome *c* (cyt *c*) and apoptosis-inducing factor (AIF) into cytoplasm. These in turn activated caspase-9 and instructed the human leukaemia cells to die by apoptosis (374). In the current study, quantitative RT-PCR analysis has shown that HA22 fusion protein (25 μg)/siMCL1 (100 nM) complex added to HF28 RA B cells decreased MCL1 mRNA level by ~2.5 fold after 48 hours. In contrast, in a recent study investigators reported ~0.5 fold decrease in MCL1 mRNA level in association with the induction of apoptosis in $CD84^+$ B cells from patients with CLL treated with anti-CD84 antibody. Furthermore, these investigators reported downregulation of CD84 expression and its immune-mediated blockade induced cell death *in vitro* and *in vivo* which was associated with reduction of MCL1 expression (375).

In parallel to MLC1, downregulation of the cell cycle kinase *PLK1* gene has been shown to cause cell cycle arrest and apoptosis as it has been shown to be overexpressed in cancer (207). In the current study, cell viability assays showed that 100 nM siRNA to mRNA of *PLK1* gene delivered with HA22 fusion protein via CD22 reduced B cell viability. This is consistent with a study in which investigators tested the therapeutic potential of anti-HER2 scFv-protamine/siRNA delivery *in vivo* using mice models xenografted with human breast cancer biopsies. These investigators assessed whether PLK1 siRNAs complexed with anti-HER2 scFv-protamine fusion protein (F5-P) could suppress $Her2^+$ breast cancer cell lines and primary human cancers in orthotopic breast cancer models (162). PLK1-siRNAs at 30, 50 and 100 nM mixed with F5-P fusion protein inhibited target gene expression, reduced proliferation and induced apoptosis of $Her2^+$ breast cancer cell lines and primary human cancer cells *in vitro* without triggering an interferon response. Intravenous injection of F5-P/siPLK1 complexes concentrated in orthotopic $Her2^+$ breast cancer xenografts and persisted for at least 72 hours. The result was suppression of PLK1 gene expression and hence induction of tumour cell

apoptosis. Further, intravenous injection of F5-P/siPLK1complexes (20 μg of F5-P/40 μg siPLK1 in 1:6 F5-P/siPLK1 molar ratio) retarded $Her2^+$ breast tumour growth, reduced metastasis and prolonged survival without evident toxicity (162). In a previous study, delivery of 100 nM of siPLK1 to human prostate cancer cells *in vitro* using oligofectamine transfection reagent resulted in induction of apoptosis (376). In a further study, PLK1 was targeted using a vector-based siRNA to the gene in HeLa cells. Results of this study showed that after 24 hours of transfection, PLK1 depletion inhibited cell proliferation, decreased viability and resulted in cell-cycle arrest and apoptosis (377). Other investigators used ~56 nM siRNA to downregulate PLK1 gene in colon, breast, cervix and lung cancer cell lines and shown that siRNA targeted to PLK1 decreased cell proliferation by ~66-99% after 48 hours of transfection and apoptosis was increased from ~5% to ~ 50% (378).

One of the advantages that targeted therapy provides over standard chemotherapies is less toxic side effects because of less damage to normal cells (1, 379). However, some of the adverse effects associated with chemotherapy can be improved upon, for instance by using liposome-based drugs. Liposome-based nanoparticle delivery systems have improved anti-cancer effects because they can improve the pharmacokinetics and pharmacodynamics of their associated drugs (380). It is expected that sustained release of anti-cancer drugs from the liposomes (approximate diameter ~60-150 nm) and passive diffusion of the released drugs throughout the tumour interstitial fluid results in uptake by tumour cells (381). However, because tumour vessels lack tight junctions between adjacent vasculature endothelial cells, the size of the gaps between the cells that line tumour blood vessels, ~100-600 nm (382, 383), is large enough to allow the extravasation of most liposomes from the vessel into the tumour interstitial space. This in turn can have detrimental effects on the healthy surrounding tissues. As a consequence, targeted anti-cancer drug delivery has more advantages because first, the high drug ratio relative to liposome-drug conjugates can be obtained and, second, specificity to target the desired cells can be increased for example through the multivalent presentation of univalent ligands such as scFv fragments (380).

With regards to therapeutic siRNAs, an advantage would be the potential for the development of co-delivery systems of various anti-cancer drugs and therapeutic siRNAs for synergistic effect. For example, in a previous study it was demonstrated that siRNA to *MCL1* gene could be formulated in cationic solid lipid nanoparticles (cSLN) for co-delivery with paclitaxel to cancer cells concomitantly. These nanoparticles were composed of 1,2-dioleoyl-sn-glycero-3-ethylphosphocholine and were prepared by emulsification solidification technique. For co-delivery of therapeutic siRNA, 20 nM of human MCL1 specific siRNA was complexed with paclitaxel/cSLN. The results showed that the *MCL1* mRNA levels were significantly reduced in human epithelial carcinoma KB cells treated with siMCL1/paclitaxel/cSLN complexes. Furthermore, in mice xenografted with KB cells, intra-tumoural injection of siMCL1/paclitaxel/cSLN complexes significantly reduced the growth of tumours (384).

In addition to the cited advantages, the use of siRNA can be advantageous in cancer patients who are resistant to chemotherapeutic drugs or small molecule inhibitors. For example, a chemical library for screening several compounds identified ABT-737 small molecule, a pan Bcl-2 inhibitor that binds Bcl-2/Bcl-xL (but not MCL1) with high affinity to disrupt their interaction with Bax/Bak and enhance the apoptotic signals, especially when combined with chemotherapeutic drugs (385). Upon binding of ABT-737, pro-apoptotic proteins such as Bid and Bim are prevented from heterodimer formation with anti-apoptotic Bcl-2 family proteins, thereby promoting Bax and Bak activation through oligomer formation (385). ABT-737 has been shown in preclinical studies, as a single agent or in combination with other chemotherapeutic drugs, to be effective against acute myeloid leukaemia (AML) (386), multiple myeloma (387), lymphoma (388), CLL (389), small cell lung cancer (390) and ALL (391). Although ABT-737 is a promising agent in development for cancer therapy, high level of MCL1 expression in small cell lung cancer cells (390) and other types of cancer cells (389, 392) has been associated with resistance to ABT-737. Therefore, because MCL1 overexpression is associated with resistance to ABT-737, inhibition of MCL1 expression may potentiate the cytotoxicity of ABT-737.

In conclusion, results presented in this chapter provide evidence of proof of principle for the approach and that this siRNA delivery approach can fulfill and establish the foundation for the next step. As the focus and interest of future studies, these involve the ability to induce apoptosis as a means for therapy. Therefore, future plans will focus on validation and reliability of the approach on how to specifically and selectively target aberrant cells, for example cancer cells *in vivo* using models of B cell leukaemias and lymphomas. The above mentioned *in vitro* experiments have clearly shown that the fate of mature B cells can be changed following controlled post-transcriptional downregulation of gene expression. In this study, this has been achieved by specific targeting of B cells using CD22 engineered mAb to deliver siRNA to downregulate genes with roles in B cell survival.

Chapter Five

Harnessing A20FMDV2-protamine Peptide for Targeted Delivery of siRNA to Tumour Cells expressing αvβ6 Integrin

My chosen study direction is based on, and leading to, development of innovative targeted therapies for cancer, essentially with the aim of inducing apoptosis in cancer cells through gene silencing. Thus, the approach embarked on exploiting siRNA delivery to B cells using engineered scFv-protamine proteins to achieve this objective. While carrying out these studies, a number of investigators reported a specific protein derived from foot-and-mouth-disease virus that binds specifically and with high affinity (~3-6 nmol/L) to αvβ6 integrin which is highly expressed on cancer cells (113, 393). This interesting finding was highly relevant to my studies and prompted experiments to address two possibilities. First, whether the protamine peptide can override the specificity of targeting using a synthetic peptide containing A20FMDV2 and the arginine-rich protamine peptide used to deliver siRNA directly to solid tumour cells; second, to verify the fidelity of siRNA delivery with A20FMDV2-protamine peptide to αvβ6-positive tumour cells. This was important because of the positive charge of the peptide which raises the possibility of non-specific interaction with cells irrespective of scFv specificity. For this purpose, I carried out experiments to specifically deliver siRNA with the protamine peptide attached to A20FMDV2 to tumour cells through receptor-mediated endocytosis.

This chapter describes the analysis of A20FMDV2-protamine peptide for the specificity of its binding and internalisation into cancer cells expressing αvβ6 integrin.

5.1. Generation of αvβ6 integrin-specific A20FMDV2-protamine peptide:

A 42-mer A20FMDV2-protamine peptide was synthesised by fusing the αvβ6 integrin-binding domain of A20FMDV2 (NAVPNLRGDLQVLAQKVART) with the truncated protamine domain (RSQSRS RYYRQRQRSRRRRRR) (PeptideSynthetics, Hampshire, UK). According to the manufacturer, the FITC labeled peptide was produced on an automatic synthesiser, purified and provided in a lyophilised format. For the purpose of imaging studies, the peptide was labeled with FITC at the N-terminus. Because FITC can not be directly attached to the N-terminus of an alpha amino acid as the thiourea bond is not stable. Alternatively, aminohexanoic acid (Ahx), a derivative and analogue of lysine, was used as a spacer as the FITC is stable on Ahx. In addition, the Ahx will provide a certain degree of protection against attack of the peptide by proteases (394). According to PeptideSynthetics, the FITC-Ahx-A20FMDV2-protamine peptide was first separated on a High Performance Liquid Chromatography (HPLC) column before being introduced to mass spectrometer. The peptides were eluted from the HPLC column using a linear increasing gradient of 0-80% organic solvent acetonitrile over 20 minutes, so that the peptides elute in order of their hydrophobicity (Figure 102). This separation step was crucial, since it is often assumed during the analysis that only a single peptide species enters the mass spectrometer during each cycle. The peptides were ionized before entering the mass spectrometer for the detailed analysis of the amino acid composition (Figure 103). The product was purified in acetonitrile and water containing 0.1 % trifluoroacetic acid prior to lyophilisation. The product would therefore be present as its trifluoroacetic acid salt. Lyophilised FITC-Ahx-A20FMDV2-protamine peptide was resuspended in 192 μL of 100% DMSO (1.1 g/mL) to give a final stock concentration of 10 mM. Aliquots of the peptide were frozen at -20°C and further diluted with the growth medium before use.

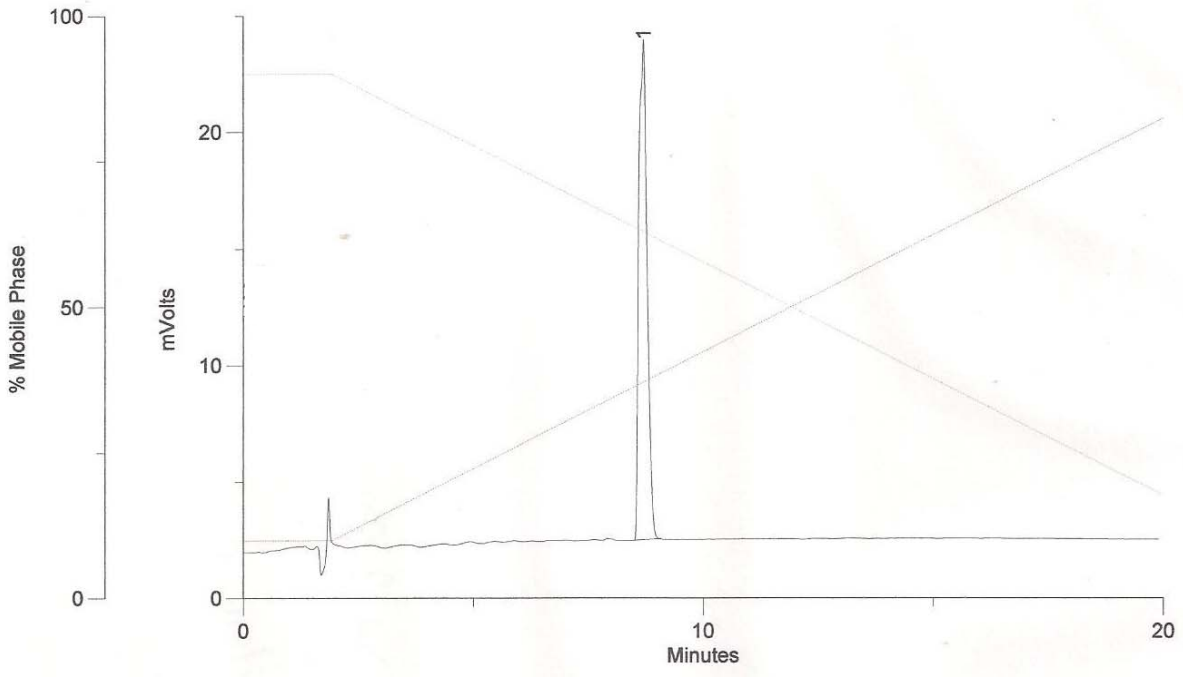

Figure 102: HPLC chromatogram depicting the purity of FITC-Ahx-A20FMDV2-protamine peptide according to the manufacturer, PeptideSynthetics. Signals generated from the peptide are detected by the instrument in the detector over time. This implies that, the signal increases and the chromatogram displays a "peak." Each peak in the chromatogram, labeled with retention time, indicates the presence of a chemical in the sample. Retention time indicates how long it takes for a compound to come out of the HPLC column. The first few small peaks in the chromatogram (around 2-3 minutes) are "noise" from the sample injection and those are ignored. The large peak represents the purified peptide in the sample. HPLC parameters include run conditions using 0-80% acetonitrile linear gradient over 20 minutes. Solvents are (water and 0.1% TFA) and (acetonitrile and 0.1%TFA). Flow rate is 1 mL/minute. Column is C18 5u 100A.

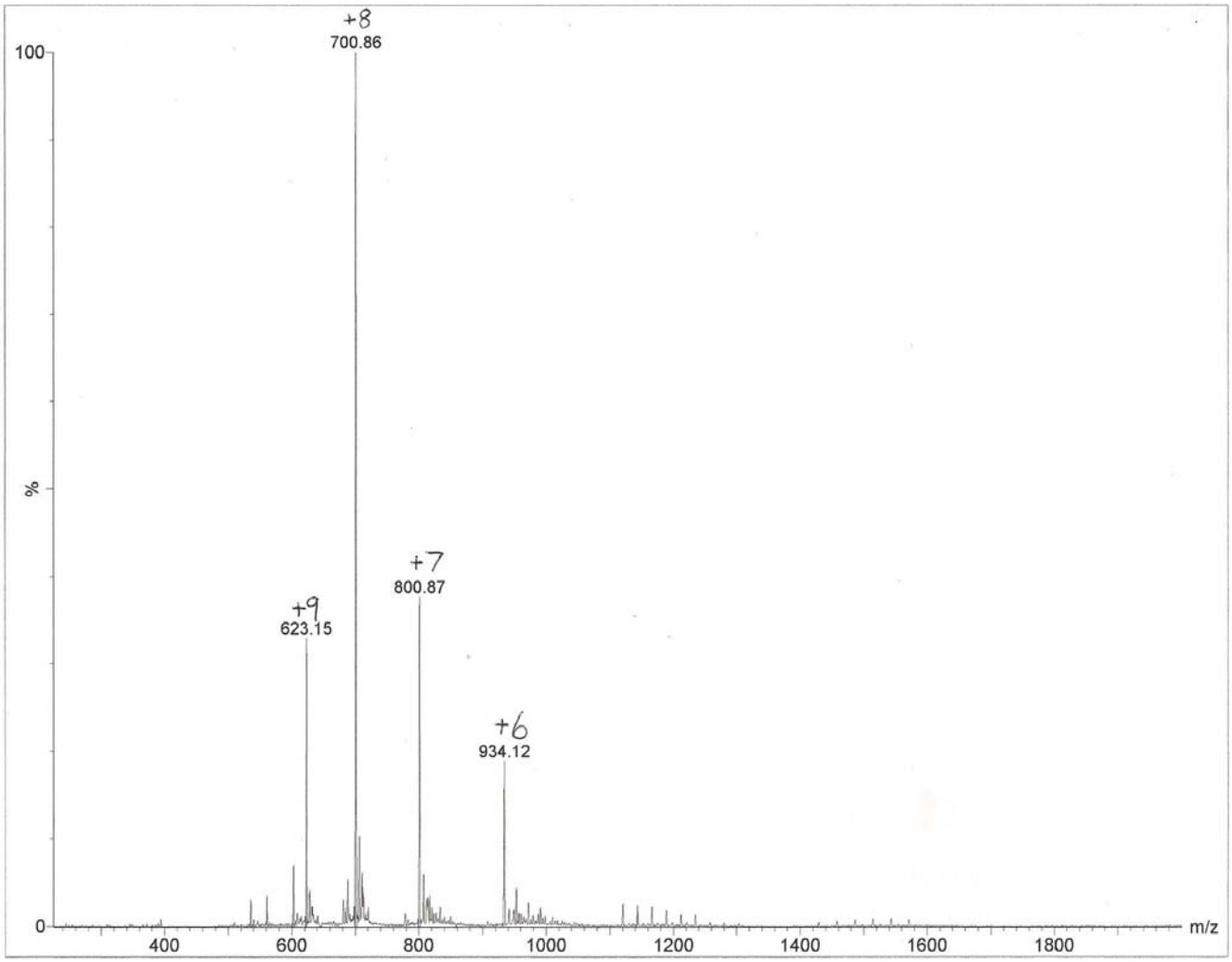

Figure 103: Mass spectrometry analysis of FITC-Ahx-A20FMDV2-protamine peptide according to the manufacturer, PeptideSynthetics. Component structure of the peptide was determined based on positively-charged ions seen on the spectrum. Electrospray ionization (ESI) was used in producing ions from the peptide because it overcomes the propensity of these molecules to fragment when ionized. Mass spectrometry parameters are ESI: +VE ion; molecular weight: 5599.3 Daltons; ions shown are (+9) 623.1, (+8) 700.9, (+7) 800.9 and (+6) 934.1. A 1 mass unit variance was considered within the range of the equipment used; in this case the mass spectrometer used was a micro mass ZMD 4000 ESI.

5.2. Analysis of the specificity and kinetics of internalisation of FITC-Ahx-A20FMDV2-protamine peptide by αvβ6-positive cells:

In order to assess the feasibility that using a truncated protamine peptide to deliver siRNA into cells will not compromise targeted delivery of A20FMDV2-protamine peptide to tumour cells expressing αvβ6 integrin was carried out.

For assessment of internalisation by confocal microscopy, adherent monolayers of αvβ6-negative A375Ppuro and αvβ6-positive A375Pβ6 cells were grown on 13 mm diameter coverslips placed in 4-well plates. Binding and internalisation assays revealed that the peptide retained its ability to specifically bind αvβ6 integrin on the cell membrane when cells were stained with the FITC labeled peptide on ice. In parallel, cells that did not express the integrin were also stained with the peptide but these did not show membrane staining. Furthermore, following incubation of the cells at 37°C, clustering of the peptide was observed in the cytoplasm of the αvβ6-positive cells. The kinetic data confirmed that the peptide bound specifically to and was internalised only by αvβ6-positive cells (Figure 104).

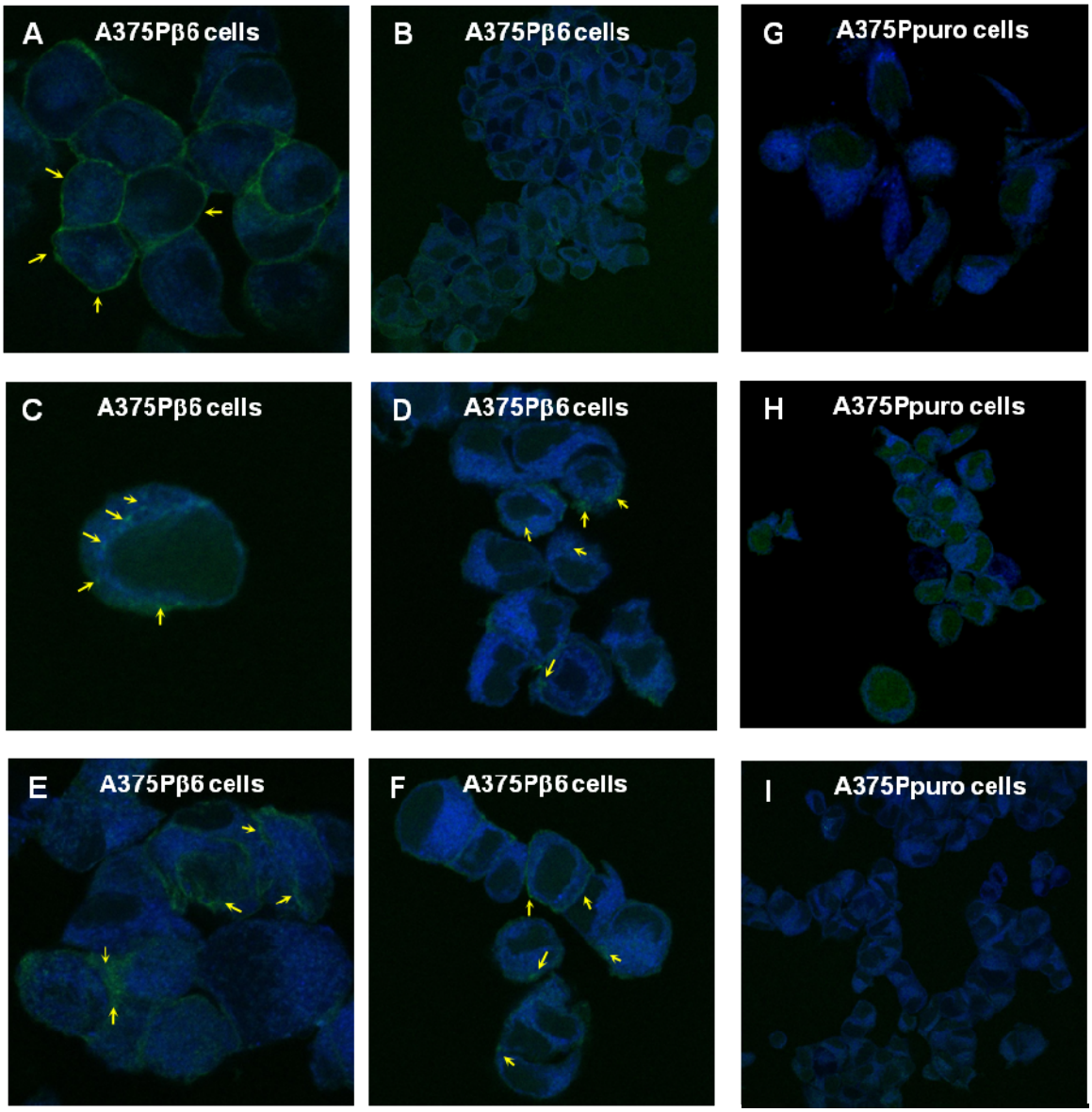

Figure 104: Confocal microscopy analysis of the binding to and kinetics of internalisation of FITC-Ahx-A20FMDV2-protamine peptide to αvβ6 integrin expressing cells. Cells at ~2 x 10^4 per well are plated onto 13 mm diameter coverslips in a 4-well plate overnight. Next day, cells are washed and replaced with ice-cold FITC-Ahx-A20FMDV2-protamine peptide (100 nM peptide/500 μL serum-free DMEM) and incubated for 15 minutes on ice. Cells are then incubated at 37°C for 15 and 30 minutes, fixed in 4% formaldehyde, stained with DRAQ5™ (far red) nuclear counter stain and mounted on slides. A and B represent A375Pβ6 cells stained with the peptide on ice at the start of the kinetics study (0 time point on ice) and then at 37°C for 15 (C and D) and 30 minutes (E and F), respectively. The figures show a clear marginal staining in A375Pβ6 cells, followed by clustering and internalisation of the peptide at different time points (indicated by yellow arrows). G, H and I represent A375Ppuro cells stained on ice and then incubated for 15 and 30 minutes at 37°C, respectively. Some of the green staining seen in β6-negative cells (H) could be due to non-specific entrance of truncated forms of the peptide. Slides are analysed using a Zeiss LSM710 confocal microscope using oil immersion 63x objective lens.

5.3. Peptide/DNA and peptide/siRNA complex formation were confirmed by gel retardation assay:

A constant amount of siRNA (100 nM) or plasmid DNA (200 ng/μL) was mixed with increasing concentrations of FITC-Ahx-A20FMDV2-protamine peptide and the mixture then resolved by 1% agarose gel electrophoresis. Gel retardation assays confirmed the formation of stable peptide/DNA and peptide/siRNA complexes (Figures 105 and 106).

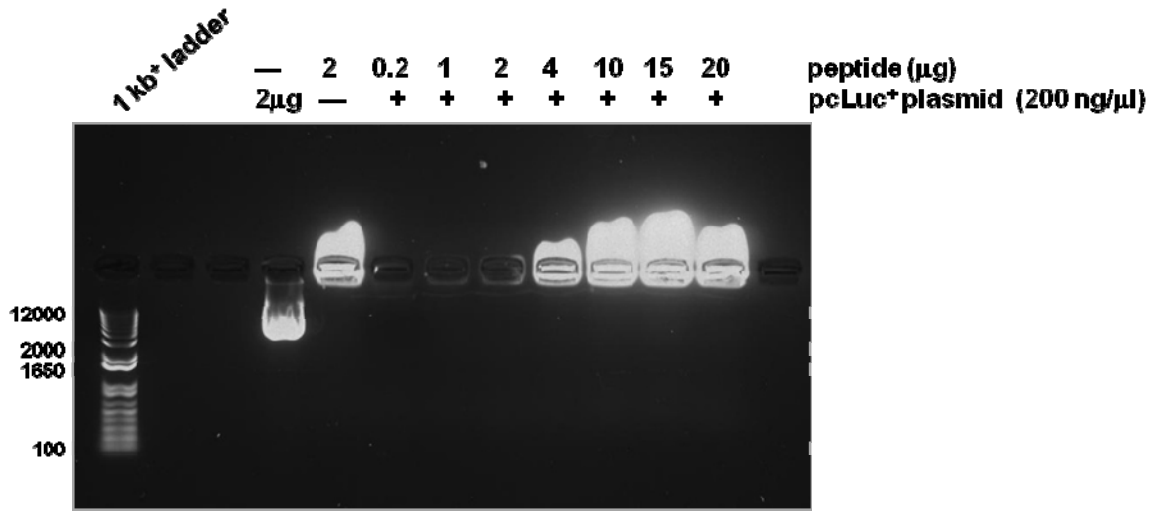

Figure 105: Agarose gel electrophoretic mobility shift assay indicating peptide/DNA complex formation. The gel shows retarded migration of DNA due to complex formation by electrostatic interaction between the positively charged protamine and the negatively charged pcLuc+ plasmid.

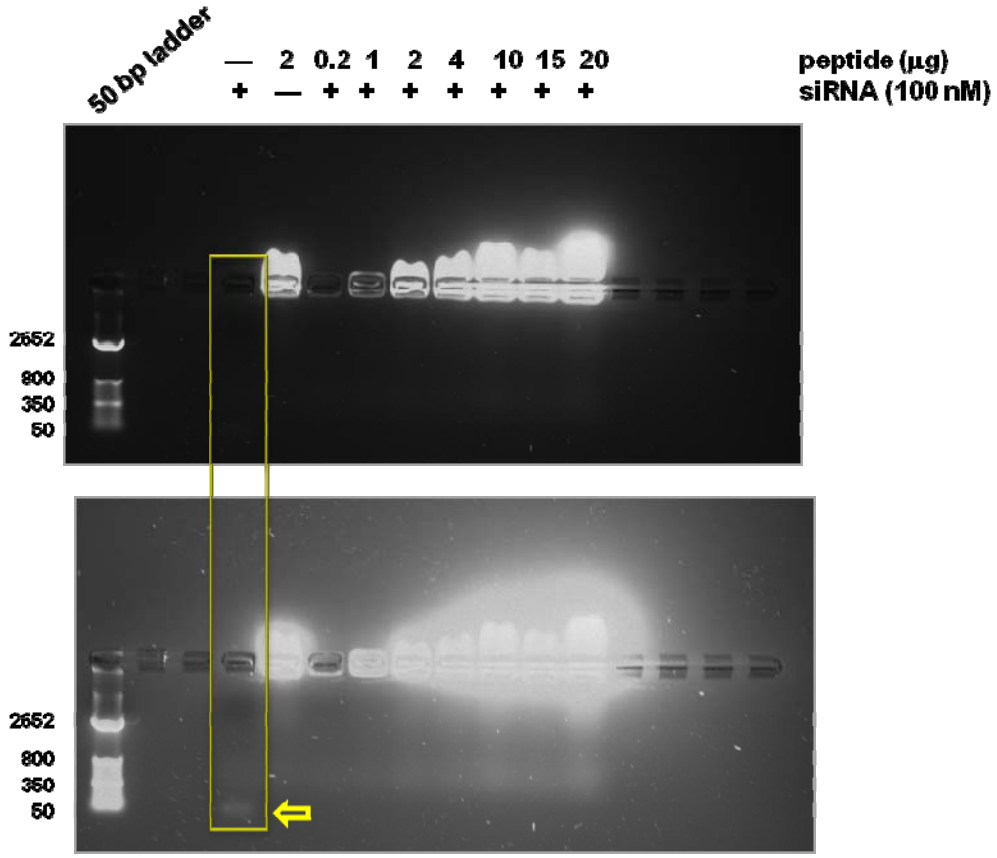

Figure 106: Agarose gel electrophoretic mobility shift assay indicating peptide/siRNA complex formation. The image shows retardation of migration of siRNA due to complex formation by electrostatic interaction between the positively charged protamine and the negatively charged siRNA (scrambled siRNA). The peptide/siRNA complexes in the agarose gel were exposed for 5 seconds (top) or 15 seconds (bottom) to UV light. The yellow arrow indicates siRNA.

5.4. FITC-Ahx-A20FMDV2-protamine peptide specifically delivers siGLO Red siRNA into αvβ6-positive cells:

Binding and kinetics of internalisation for FITC-Ahx-A20FMDV2-protamine peptide showed selectivity of peptide delivery. Experiments on the delivery of siGLO Red with the peptide were then performed to verify the ability of the A20FMDV2-protamine peptide to form a stable complex with siRNA and to selectively deliver into cells was carried out using αvβ6-negative (A375Ppuro or DX3Ppuro) and αvβ6-positive (A375Pβ6 or DX3Pβ6) cells. To achieve this, the peptide was diluted in growth medium to 10 μM and bound with siGLO Red siRNA (10 nM) for 15 minutes on ice. Adherent cells grown overnight on coverslips in 4-well plates were washed and the mixture added to cells. The results from these experiments showed that the peptide formed a stable complex with, and delivered siGLO Red siRNA specifically to αvβ6-positve A375Pβ6 cells only (Figures 107 and 108).

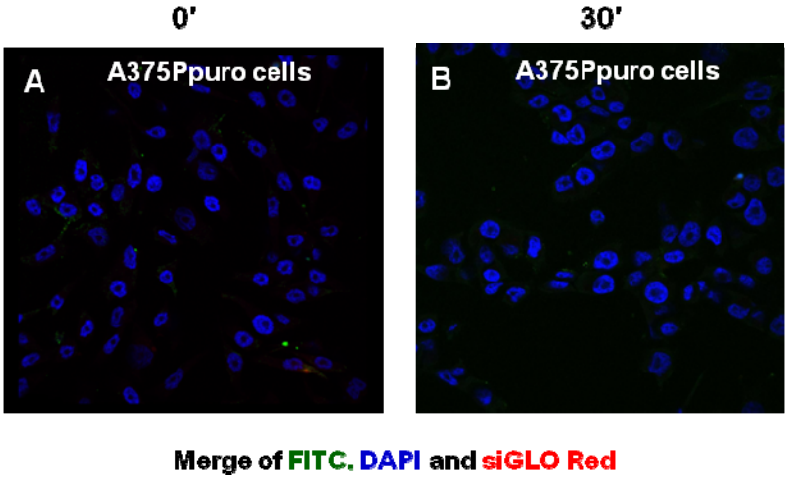

Figure 107: Confocal microscopy images confirming the lack of A20FMDV2-protamine peptide/siGLO Red complex binding to and internalisation by αvβ6-negative A375Ppuro cells. The complex did not bind to cells incubated on ice (A) nor was it internalised when the cells were incubated at 37°C for 30 minutes (B). Cells (~2 x 10^4 per well) are plated overnight, then incubated with FITC-Ahx-A20FMDV2-protamine peptide (10 μM)/siGLO Red (10 nM) in serum-free DMEM for 15 minutes on ice then incubated at 37°C for 30 minutes. Cells are then fixed in 4% formaldehyde, stained with DAPI and mounted on slides. The figures represent merging of FITC, DAPI and siGLO Red.

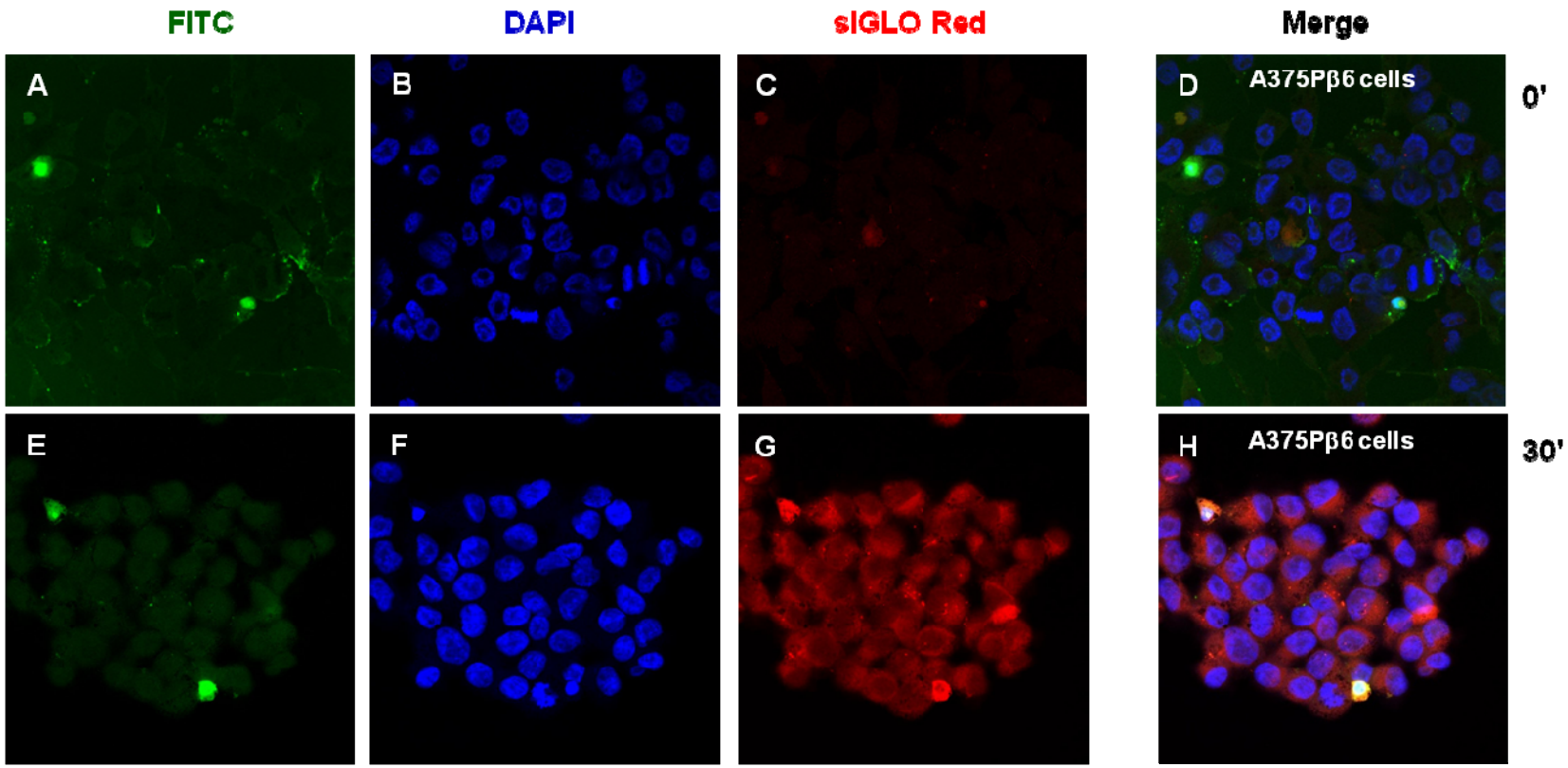

Figure 108: Confocal microscopy images demonstrating specific binding and delivery of siGLO Red siRNA combined with FITC-Ahx-A20FMDV2-protamine peptide to αvβ6-positive cells. Cells at ~2 x 10^4 per well are plated onto 13 mm diameter coverslips in a 4-well plate overnight. The peptide was mixed with the siGLO Red on ice for 15 minutes and then added to cells. The figures depict membrane binding of the peptide (10 μM)/siGLO Red (10 nM) complex to αvβ6-positve A375Pβ6 cells when the cells were kept on ice for 15 minutes (at 0 time point) (A to D) followed by intracellular localisation of the complex when cells were incubated at 37°C for 30 minutes (E to H).

Selective delivery of siGLO Red siRNA with the peptide was further confirmed using another matched pair of cell lines, DX3Ppuro and DX3Ppuroβ6. DX3 is a human melanoma cell line which is infected with pBabe retroviruses encoding the Puromycin resistance gene or, in addition, cDNA for human integrin β6 as described in a previous study (113). Accordingly, DX3Ppuro and DX3Ppuroβ6 cell lines were stably transfected either with a Puromycin resistance gene or Puromycin resistance gene and human integrin β6 respectively (113). Following membrane binding of the peptide/siGLO Red complex to cells on ice and subsequent to incubation at 37°C, obvious internalisation was observed in DX3Pβ6 cells. Intracellular focal clustering of peptide/siGLO Red complexes was clearly seen in the cytoplasm of these cells (Figure 109). Furthermore, intracellular localisation of the peptide/siGLO Red was confirmed by taking slices of Z-stacking images through different planes of DX3Ppuroβ6 cells incubated for 45 minutes at 37°C (Figure 110).

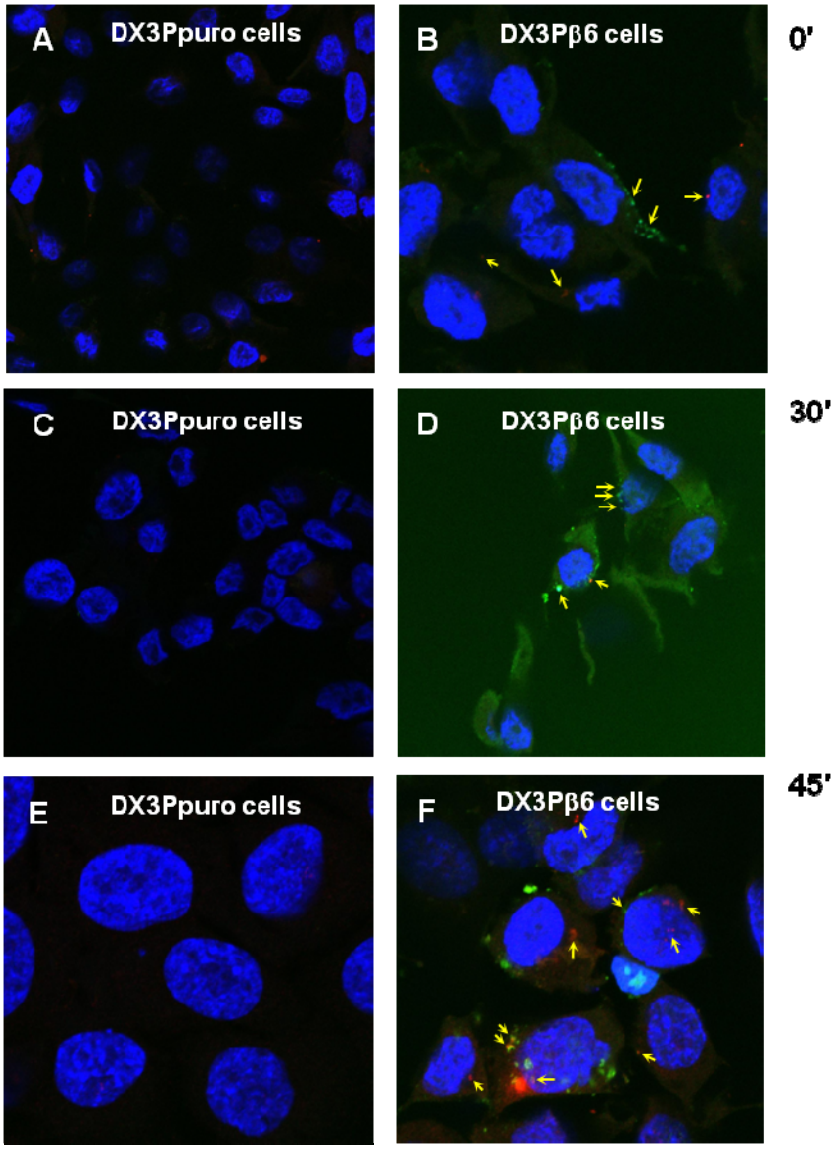

Figure 109: Kinetic study by confocal microscopy for the specific delivery of siGLO Red siRNA with FITC-Ahx-A20FMDV2-protamine peptide to αvβ6-positive cells. Cells at ~2 x 10^4 per well are plated onto 13 mm diameter coverslips in a 4-well plate overnight. The A20FMDV2-protamine peptide (10 μM)/siGLO Red (10 nM) complex was added to DX3Ppuro cells to which they neither bound to the membrane nor internalised (A, C and E). In contrast, membrane binding of the peptide/siGLO Red complex to DX3Pβ6 cells on ice (0 time point) (B) followed by intracellular localisation of the complex after incubation of the cells at 37°C for 30 and 45 minutes (D and F) respectively, can be clearly seen (yellow arrows). DAPI nuclear staining: blue.

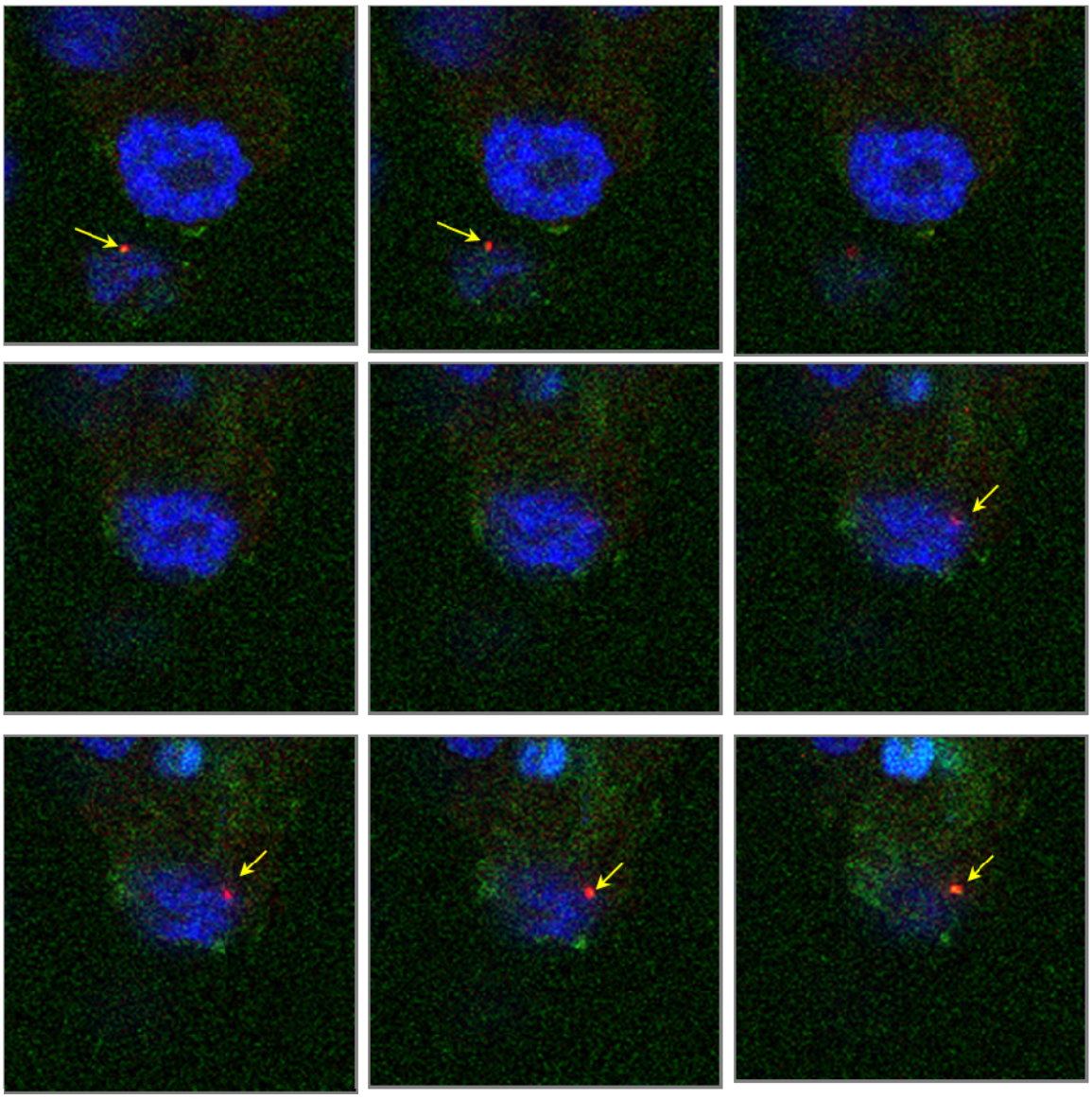

Figure 110: Z-stacking confocal microscopy images demonstrating intracellular localisation of FITC-Ahx-A20FMDV2-protamine/siGLO Red complex in DX3Pβ6 cells. The Z-stacking slices are based on the image F shown in Figure 109 after incubation of DX3Ppuroβ6 cells for 45 minutes at 37°C. The yellow arrow indicates peptide/siRNA complex inside the cells. The figures represent merging of FITC (green), DAPI (blue) and siGLO Red (red).

5.5. Delivery of siRNA to *ITGB6* gene by FITC-Ahx-A20FMDV2-protamine peptide via αvβ6 integrin:

In addition to the objective of testing for specificity of delivery of the truncated protamine peptide, FITC-Ahx-A20FMDV2-protamine was further investigated for its ability to modulate the biology of invasive carcinoma cells. The specific aim was to alter survival, or invasion that enables tumour cells to spread via αvβ6 integrin and, thereby, hinder tumour growth and invasion. For this purpose, siRNA to integrin β6 mRNA was delivered via the αvβ6 receptor. To investigate this, adherent monolayers of αvβ6-positive VB6 cells were used. FITC-Ahx-A20FMDV2-protamine peptide was diluted in the growth medium to 100 nM and bound with varying concentrations of siITGB6 (50, 100 and 150 nM) for 15 minutes on ice. The mixtures were then added to cells and incubated at 37°C for 5 days. The effect of *ITGB6* downregulation was studied at the protein level by Western blotting. Results from these experiments showed a reduction in *ITGB6* expression at the protein level. The peptide alone at 1000 nM resulted in the reduction of ITGB6 protein level. This could be explained by the fact that engagement of the integrin receptor with the peptide might result in receptor-mediated endocytosis of the complex and, ultimately, degradation of the receptor without being recycled back to cell surface. Additionally, siITGB6 delivered with the peptide reduced expression of ITGB6 protein (Figure 111). However, the result from transfection of cells with 100 nM of siITGB6 using NeoFX transfection reagent did not show reduction of the ITGB6 protein.

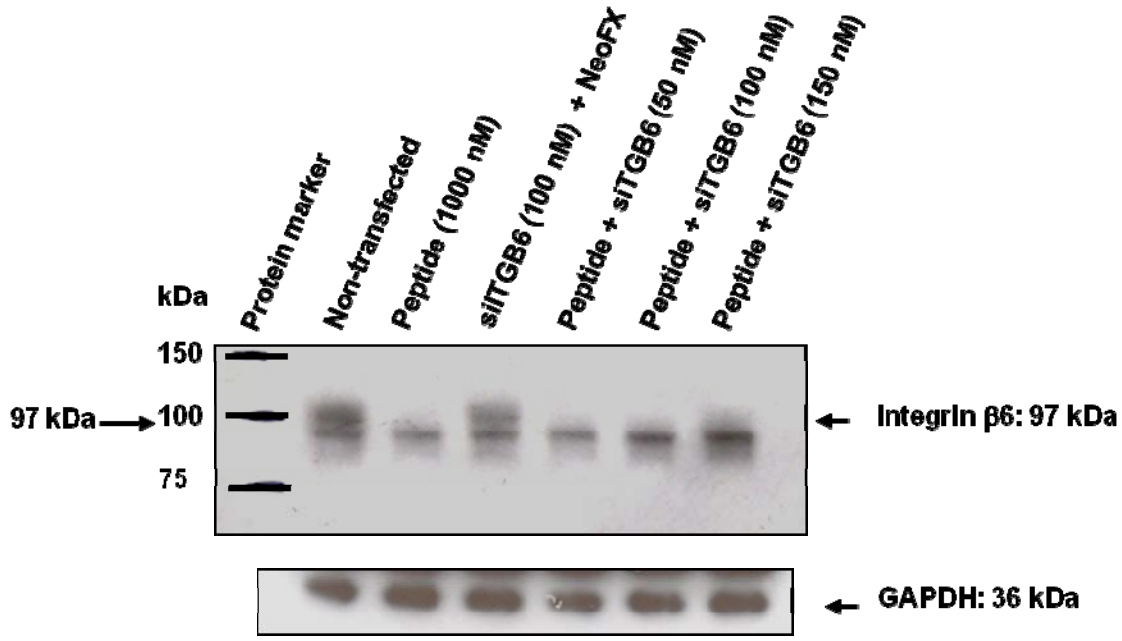

Figure 111: Western blot analysis of integrin β6 protein downregulation. The peptide without siRNA at 1000 nM reduced ITGB6 expression and also 100 nM of the peptide with siRNA to ITGB6 resulted in the reduction of ITGB6 protein level. The cells were also analysed for the level of expression of GAPDH housekeeping gene to exclude any toxicity due to the peptide or off-target effect from the siRNA. Integrin β6 was detected with goat polyclonal anti-integrin β6 antibody (1:200) and revealed with secondary HRP-conjugated anti-goat IgG antibody (1:2000). αv integrin subunit is 150 kDa.

5.6. Discussion:

Targeted therapies have a number of advantages over standard therapies including the delivery of the therapeutic specifically to the desired cells so achieving maximal therapeutic effects and minimising the adverse effects associated with the treatment (2). However, several challenges for all targeted therapeutic approaches remain. For example, in the case of the targeted therapy I have been developing it is possible that the protamine peptide could override the targeting molecule to which it is attached in order to directly mediate uptake into cells.

Protamines are a group of arginine-rich cationic proteins that function to package spermatids DNA in vertebrate species (46, 47). Because of condensation of large amounts of DNA, ~50 kb DNA in each protamine/DNA particle (48), therefore, one major advantage of using the protamine peptide is the nucleic acid-binding property which allows condensation of siRNA or DNA and hence facilitation of intracellular delivery. In recent years, protamine has attracted growing interest as a cell penetrating peptide, as it possesses potency in mediating cellular translocation of its payloads such as siRNA (395-397). Furthermore, studies have shown that truncated protamine exhibits low toxicity (398, 399).

Protamine salts have been used in combination with liposomal preparations as a non-specific cell delivery mechanism of nucleic acids such as plasmid DNA into cells because of their characteristic arginine-rich and strongly basic aliphatic nature (400). The first attempts to deliver oligonucleotides with nanoparticles consisting only of protamine and oligonucleotide were described previously (401, 402). In these studies, investigators have complexed phosphodiester antisense oligonucleotides (ODNs) against the c-*myc* proto-oncogene with protamine peptide and showed increased cellular uptake into human histiocytic lymphoma U937 cells (401). Furthermore, complex formation between ODN and protamine particles was confirmed by gel mobility shift assay (402). Other investigators also showed that protamine can be used in the delivery of ODNs into cells such as albumin/protamine/oligonucleotide nanoparticles (403, 404).

In the experiments described in this chapter, selectivity in targeting was examined in a well-defined cell system based on delivery through αvβ6 integrin receptor by fusing protamine peptide to αvβ6 integrin-specific A20FMDV2 peptide. The FITC-A20FMDV2-protamine peptide was synthesised commercially to examine (a) non-specific delivery of unconjugated peptide into αvβ6-positive and -negative cells and (b) to explore targeted delivery and activity of the peptide conjugated with siRNA.

αvβ6 integrin belongs to a large family of heterodimeric transmembrane receptors that mediate cell-substratum adhesion. It is an epithelial specific integrin that is not expressed in healthy adult epithelia but is upregulated during wound healing and in cancer (101, 102). αvβ6 integrin has been shown to inhibit apoptosis, modulate invasion and promote carcinoma progression (405).

In a previous study it has been shown that a 35 kDa HS1-associated protein X-1 (HAX-1), a binding partner protein of the β6 cytoplasmic tail, regulates cancer cell motility and invasion via αvβ6 internalisation by clathrin-mediated endocytosis. Hence, the kinetics of αvβ6 internalisation was shown to be 15-30 minutes and reached a steady-state level inside the cells as studied by relative decrease of band intensity of both αv and β6 subunits on a Western blot after downregulation of the *HAX-1* gene using siRNA (406). Thus αvβ6 integrin can be efficiently targeted with A20FMDV2 peptide. A20FMDV2, which shows specificity and forms stable binding to αvβ6 integrin, is a 20-mer peptide derived from the VP1 coat protein of the foot-and-mouth-disease virus (407).

For the first aim, initial confocal microscopy experiments confirmed that the FITC-A20FMDV2-protamine peptide did not mediate non-specific uptake into αvβ6-negative cells. Thus, specific binding and internalsiation of the FITC-A20FMDV2-protamine peptide was confirmed in αvβ6-positive cells after 15 minutes. This was an important experiment because it both confirmed previous observations of A20FMDV2 binding characteristics such as internalisation by αvβ6-expressing cells using both fluorescently-labeled and radio-labeled A20FMDV2 peptides with similar kinetics (408). In the same study, they have also tested specificity of binding of A20FMDV2 peptide to αvβ6 integrin

by flow cytometry using either biotinylated diethylene triamine penta-acetic acid (DTPA)-A20FMDV2 or a scrambled peptide (A20FMDV2ran). A375Pβ6 or A375Ppuro cells incubated with either peptide at different concentrations (0.001–10 μM), showed specific binding of DTPA-A20FMDV2 peptide. The affinity of DTPA-A20FMDV2 peptide, shown to bind only to A375Pβ6 cells, was at 1 nM concentration (408).

The fact that the protamine domain did not directly mediate cell delivery is a good indication that it will not alter targeted delivery when fused with a scFv. Indeed in several previous studies investigators showed that protamine did not alter specificity of scFv delivery in these molecules and when the truncated human protamine was combined with scFv of mAbs it could deliver siRNA specifically to target cells (120, 160-162).

This initial experiment also ensured that protamine did not override A20FMDV2 peptide binding specificity which has been observed when another peptide was linked to A20FMDV2.

However, in a previous work investigators reported that a liposomal drug consisting of H2009.1 tetrameric peptide liposomal doxorubicin overrides peptide ligand targeting to αvβ6 irrespective of ligand affinity or density (409). The H2009.1 peptide was originally selected from a phage display library against the non-small cell lung cancer (NSCLC) cell line H2009 (410) and was discovered to bind the integrin αvβ6 (411). In contrast to the *in vitro* results, *in vivo* studies for αvβ6-specific H2009.1 peptide/liposomal doxorubicin have demonstrated no difference in *in vivo* targeting or efficacy for H2009.1 peptide/liposomal doxorubicin, compared to control peptide and no peptide liposomes. The results highlighted that using a high affinity and high specificity H2009.1 tetrameric peptide in the context of liposomal doxorubicin targeting αvβ6 overexpressed on tumour cells overrides the specificity of the peptide and does not guarantee enhanced efficacy of a liposomal drug *in vivo* (409).

The second aim was to examine targeted delivery with the FITC-A20FMDV2-protamine peptide when complexed with siRNA. In the complex state, the positive charges of protamine will be neutralised so it is even less likely to mediate direct cell delivery but it is important to confirm that targeted delivery is maintained. To validate the method, the ability of the FITC-A20FMDV2-protamine peptide to form complexes with DNA or siRNA was tested. Thus, peptide/DNA and peptide/siRNA complex formation by electrostatic interactions were confirmed by gel retardation assays. Previous reports, using EMSA, have confirmed retardation of movement of DNA or siRNA when combined with positively charged peptides because of electrostatic interactions between cationic proteins and nucleic acids (347, 348). Furthermore, cell uptake and intracellular delivery of siRNA with the peptide was confirmed in confocal microscopy experiments. This was done using siGLO Red siRNA where cell uptake was demonstrated with similar kinetics as the uncomplexed peptide.

Investigators have also explored the potential of A20FMDV2 to transport a therapeutic cargo intracellularly via αvβ6 internalisation (408). To do this, the peptide was conjugated with the radio-labeled indium-111 isotope (^{111}In-DTPA-A20FMDV2) and was tested for internalisation in a mouse xenograft model bearing A375Pβ6 breast tumour cells. Results of single-photon emission computed tomography (SPECT) imaging confirmed specific binding and internalisation of ^{111}In-DTPA-A20FMDV2 by A375Pβ6 tumour cells within 20 minutes. Similar results from internalisation experiments performed by confocal microscopy showed membrane staining at the start (on ice) followed by localisation of the peptide in cytoplasm of A375Pβ6 cells by 30 minutes at 37°C (408).

Additionally, in another study A20FMDV2 peptide was incorporated into a recombinant adenovirus type5 (Ad5) which resulted in increased cytotoxicity on a panel of αvβ6-positive human carcinoma cell lines *in vitro* and enhancement in tumour uptake and improved tumour transduction in an αvβ6-positive xenograft model *in vivo* over the Ad5 wild type (412).

With regard to the FITC-A20FMDV2-protamine peptide, the intracellular delivery of siGLO Red provides no indication of siRNA activity. Thus, activity was analysed using siRNA to β6 subunit of integrin (siITGB6) and expression of β6 subunit protein was monitored by Western blotting. These studies proved inconclusive because the FITC-A20FMDV2-protamine peptide alone resulted in the reduction of the β6 subunit protein. Retrospectively, downregulation of β6 subunit of integrin (ITGB6) was not the best target to study the effect of siRNA delivery with the FITC-A20FMDV2-protamine peptide. Thus, with further time it would be good to study and verify downregulation of genes with role in αvβ6-positive tumour survival and invasion using siRNA. There are no studies to report inhibition of αv or β6 subunits using peptides, however recently investigators showed that the αvβ6-blocking 264RAD human mAb inhibits αvβ6 integrin and reduces tumour growth and metastasis *in vivo* (413).

In conclusion, preliminary data from the results presented in this chapter provide experimental evidence for the objectives of using FITC-Ahx-A20FMDV2-protamine peptide in targeted therapeutic studies.

Chapter Six

General Discussion, Conclusions and Future Perspectives

6.1. General discussion:

Targeted therapies with mAbs have revolutionised medicine and are increasingly used for the treatment of a range of diseases, including chronic inflammatory diseases, solid tumours and haematological malignancies. However, there are still unmet needs for novel therapeutic approaches, especially for patients with relapsed/refractory diseases. Therapeutic agents with specificity for membrane proteins on malignant cells hold promise for improving the clinical outcome in cancer. CD22, a B cell-restricted membrane phosphoglycoprotein found on nearly all mature B lymphocytes including most B cell leukaemias and lymphomas, is potentially an ideal therapeutic target for B cell-directed therapies. CD22 is continually internalised and binding of anti-CD22 antibodies induces rapid receptor-mediated endocytosis, making CD22, potentially, an attractive vital gateway for intracellular delivery of drugs (414).

In B cell malignancies, CD22 expression has been reported in at least 60–80% of tumour samples (415). In this respect, anti-CD22 mAbs and antibody-drug conjugates have been investigated in B cell leukaemias and lymphomas. These malignancies include paediatric ALL, HCL, diffuse large B cell lymphoma (DLBCL), mantle cell lymphoma, marginal zone B cell lymphoma, Burkitt's lymphoma, follicular lymphoma (FL) and CLL (416-421).

RNAi is a powerful gene silencing process that holds promise in the field of cancer therapy. A major obstacle in the development of siRNA, as a cancer therapeutic, is the lack of a reliable mode of targeted delivery. Therefore, targeting delivery of siRNA via internalising cell surface receptors is an appealing strategy to improve tumour-specific uptake. Thus, a highly effective targeting gene delivery method could be achieved by using recombinant scFv-protamine fusion proteins (322).

Similar to the results presented in this thesis which provide proof of concept for the use of antibody scFv specific for CD22 to target genes of interest using siRNA therapeutics, investigators showed suitability of targeting the CD22 receptor with kinetics of internalisation of ~30-60 minutes followed by degradation in ~8 hours (82-92) or recycling of the intracellular CD22 to the surface of the B cells (93).

Therefore, gene constructs of the anti-CD22 scFv-protamine fusion protein were generated, expressed and purified. Similarly, in previous studies, investigators generated scFv-protamine fusion proteins for targeted delivery of siRNA to desired cells (120, 160 and 162).

Several criteria for siRNA delivery has been explored in these studies including the demonstration that siRNA complexes with the protamine domain of HA22; that the protamine domain alone in the context of the A20FMDV2 peptide does not mediate non-specific cell uptake and that CD22 specific intracellular delivery of fluorescently labelled siRNA was demonstrated through confocal microscopy.

Successful escape of siRNA carriers from endosomes and release of the payload into the cytoplasm is integral to the efficiency of gene silencing. Previous studies showed that due to the acid nature of endosomal/lysosomal vesicles, pH-buffering agents can be widely exploited to promote cargo release (215-217). Hence, under acidic conditions, various macromolecules with a cationic nature have been shown to exhibit a “proton sponge effect”, such as PEI and its derivates. Previous studies have shown that histidine oligomers add endosomal escape functionality to C-terminus of a dsRNA binding domain (dsRBD) (422, 423). At neutral pH such as in the blood, histidine molecules are mainly deprotonated or uncharged while in acidic compartments such as the endosome; they become protonated and facilitate osmotic swelling that leads to cargo release (424). Therefore, the hexahistidine tag in HA22 fusion protein may also buffer acidify and thereby facilitate the release of cargo siRNA from the endolysosomal compartment.

Preliminary experiments provide proof of concept that siRNA can be delivered with HA22 fusion protein resulting in reduction of target mRNA and achieving biological effects.

The HA22 fusion protein was shown to retain its ability to bind CD22 specifically and deliver siRNA into B cells. Studies were then carried out to verify that the capacity of the protamine peptide to bind to cell membranes did not override the specificity of the delivery system to solid tumour cells by targeting αvβ6 integrin. Selective expression of αvβ6 integrin on epithelial cells only during cancer has been well established (411). Since αvβ6 is internalised by a clathrin-mediated endocytosis mechanism (406), the potential of intracellular delivery of therapeutics has been explored using peptides such as A20FMDV2 peptide that can specifically bind to αvβ6 integrin (407).

Experiments were then carried out to assess the effect of siRNA delivery on gene expression in relevant tumour cells. For this purpose, genes with roles in survival of malignant B cells were targeted. Because the siRNA sequence seeks out and destroys its target without affecting other genes, the use of siRNA therapeutics is an appealing treatment strategy for viral infections, cancer and dominantly inherited genetic disorders (425-428). siRNA has the potential as a therapeutic agent to target genes in the anti-apoptosis pathway because it is now clear that many cancers overexpress anti-apoptotic proteins (429). Several anti-apoptotic proteins are expressed in cancer cells and can serve as targets for RNAi. These include FLIP, Bcl-2, Bcl-xL, Bcl-w, Mcl-1, survivin and XIAP (430). For example, in the current study siRNA was delivered with HA22 fusion protein to knockdown mRNA of the *MCL1* gene, thereby activating the initiation of apoptosis in B cells. Preliminary experiments indicated that HA22 fusion protein was able to specifically deliver siRNA to downregulate the *MCL1* gene via CD22 into B cells and consequently cause cell death as demonstrated by the cell viability assay and activation of caspase-3 and -7 along with confirmation of MCL1 mRNA downregulation through real-time PCR.

Other molecules with anti-apoptotic properties, though not directly related to the apoptosis pathway, can also serve as targets for RNAi therapeutics. For example, the

mitotic serine/threonine protein kinase PLK1 is overexpressed in many types of human malignant tumours (431). PLK1 inhibitors are valuable anti-cancer drug candidates and, currently, they are being used in patients with several types of cancer to monitor efficacy and safety in clinical trials (432). siRNA to mRNA of *PLK1* gene delivered with the HA22 fusion protein via CD22 to B cells resulted in the downregulation of *PLK1* gene and reduced cell viability.

Although the HA22 fusion protein provides an approach to target delivery to CD22 expressing B lymphocytes it will be important for therapeutic effect that delivered siRNA differentiates between cancerous and healthy $CD22^{+}$ B cells, a concept that will be considered further in future perspectives.

6.2. Conclusions:

Compared to other strategies such as antisense DNA oligonucletides (ASO) and ribozymes, RNAi is much more potent for gene downregulation (433).

Important criteria for siRNA efficacy (measured as half-maximal inhibition levels or IC_{50} values) include thermodynamic end stability (434), target mRNA accessibility (435) and structural features (436).

A major challenge to develop siRNAs as novel therapeutics for the treatment of a range of diseases is to overcome barriers to their delivery to target cells. siRNAs do not readily cross the cellular membrane because of their negative charge and size. Cellular delivery of chemically synthesised or *in vitro* transcribed siRNAs is usually achieved by using cationic liposome-based strategies. The disadvantage of cationic liposome-based siRNA complexes delivery schemes *in vivo* is the rapid liver clearance and lack of target tissue specificity (437, 438).

Another barrier for using siRNA in therapies is their serum stability and protection against nucleases. In this regard, chemical modifications of siRNA such as 2'-methoxy (2'-OMe) and 2'-fluoro (2'-F) substitution in the siRNA backbone will improve serum stability and immunostimulatory properties but does not improve potency (439).

In addition, immunostimulatory effect of siRNA must also be taken into account when using siRNA *in vivo*. Thus, long dsRNA is known to rapidly induce interferon responses by binding to double-stranded-RNA-activated protein kinase (PKR), 2′,5′-oligoadenylate synthetase-RNase L system or several Toll-like receptors (TLRs). This is because the innate immune system recognises dsRNAs similar to invading RNA viruses (440). For example, it has been demonstrated that a particular sequence motif (5'GUCCUUCAA3') seems to be recognised by TLR7 in the endosomal compartment of plasmacytoid dendritic cells and activates immune responses (441).

There are also concerns about safe therapeutic use of siRNA because siRNA-mediated immune induction seems to rely on endosome located TLR receptors (TLR7 and TLR8) and hence compartmentalisation of the siRNA greatly influences cellular responses (442).

In addition to the liposome-based siRNA delivery approach, other delivery methods for siRNAs include conjugation of cholesterol to the siRNA sense strand (443), cyclodextrin nanoparticles (444) and aptamer-siRNA conjugates (445). However, these methods are not cell-type specific. Therefore, the concept of targeting and intracellular delivery of siRNAs with scFv-protamine fusion proteins is likely to increase efficacy and reduce side effects.

Generation of scFvs by engineering of therapeutic antibodies has a number of advantages. For example, scFvs are less likely to generate an immune response and the smaller size of fragments enables deeper penetration into tissues than the mAbs for tumour targeting (38, 39). Furthermore, antibody engineering allows increased affinity of the antibodies to their targets by mutagenesis of certain amino acids to increase polypeptide stability (42-44). In addition, the smaller size of scFvs makes them appropriate for diagnostic imaging (40, 41).

The potential of using scFvs in biomedical applications has also been shown in several reported studies. For example, scFv antibody fragments can be used in immunoassays including ELISA (446), immunoblotting assay (447), antigen and antibody microarray (448), immunohistochemistry (449), immunofluorescence (450, 451) and flow cytometry (452, 453). Moreover, scFv antibodies have been successfully used to neutralise viral, bacterial and fungal pathogens *in vitro* and *in vivo* (454-456) which illustrates their potential use in therapy.

The half-life of whole antibodies especially chimeric, humanised or fully human IgG molecules can reach ~27 days in the blood in the human body (457). While antibody fragments such as Fab fragments or recombinant scFvs are rapidly cleared from the blood due to their short half-life and renal clearance (458, 459). Thus, repeated injections or infusions are required to maintain a therapeutically effective dose in the body (460).

However, there are certain strategies to improve pharmacokinetic properties and thus dosing and therapeutic efficacy of recombinant antibodies. For example, PEGylation of proteins is a well-established strategy to improve pharmacokinetic properties by increasing the molecular mass and the hydrodynamic radius thus reducing renal clearance (461, 462). Furthermore, the introduction of N-glycosylation sites is another approach successfully applied to improve pharmacokinetic and pharmacodynamic properties of a few therapeutic proteins (463).

Regarding the protamine attached to the scFv, there are also concerns about immunogenicity of the protamine. Protamine sulfate, a 5 kDa cationic polypeptide derived from salmon sperm (464), has been used in the clinic for treatment of patients who develop significant bleeding complications while receiving heparin (465). Furthermore, protamine sulfate is administered post-operatively to reverse the high concentrations of heparin required for patients undergoing cardiac surgery and cardiopulmonary bypass (466). Clinical use of protamine is, however, associated with several important adverse side effects, including potentially life-threatening systemic arterial hypotension and pulmonary artery hypertension (465). In addition, salmon protamine is shown to be immunogenic as the protamine-heparin complex was found in a mouse model to cause generation of anti-protamine/heparin antibodies (467). Furthermore, a recent clinical study has shown the production of anti-protamine/heparin antibodies in patients undergoing cardiac surgery (468).

In contrast to these observations, harnessing the truncated protamine has attracted growing interest as it possesses potency in mediating cellular translocation of its payloads (395-397) as it has been shown to be non-toxic (398, 399). However, it is hardly optimal to apply protamine alone for systemic administration due to its lack of selectivity in cellular association and tissue biodistribution, which could increase the risk of drug-induced toxic effect on normal tissues (469).

However, the use of protamine for targeted delivery in the context of scFv antibody fragments should overcome the issue of non-specific targeting. It is important to note that in addition to the above observations regarding immunogenicity or side effects associated with use of protamine sulfate, it could be very different in case of delivery of siRNA where the truncated human protamine is covered and neutralised with bound siRNA. This could also be true for siRNA enabling it to evade TLR receptor recognition because of the masking effect of charge neutralisation by protamine.

A dilemma for the use of anti-CD22 scFv-protamine fusion protein as a therapeutic tool to deliver siRNA into aberrant B cells is the downstream application for different diseases. For example, the objective of targeting siRNA for gene therapy to aberrant B cells could be different for cancer or inflammatory diseases. In this regard, the goal of gene therapy in the treatment of autoimmune diseases is to restore immune homeostasis by modulation of cell physiology allowing basal activity required for cellular functions such as housekeeping and cell survival to avoid non-specific side effects. Therefore, there is the need for repeated and controlled administration of the siRNA to avoid off-target effects which could be difficult to achieve (470); whereas in cancer the objective of the gene downregulation is to kill the cancer cells (471). Furthermore, genome wide scanning in autoimmune diseases and clinical trials for biomarker identification has not yet revealed candidate genes that can be targeted in therapeutic designs (472).

6.3. Future perspectives:

The remarkable progress made towards understanding the molecular and genetic basis of diseases in general and cancer in particular has transformed the discipline of gene therapy from theoretic concepts to practical applications.

RNAi has evolved from a powerful laboratory tool utilised to reveal the function of novel genes to a potential therapeutic modality especially in viral infections, cancers and inherited genetic disorders.

In cancer, a number of important oncogenic targets within many critical cellular pathways have been identified and RNAi-mediated gene silencing of these targets has produced encouraging results *in vitro* and *in vivo*. Translation of such findings to more complex clinical applications has made great progress in recent years. Hence, RNAi-mediated silencing gene therapy can potentially be used in conjunction with chemotherapy, radiotherapy and/or immunotherapy.

As more selective targeted delivery methods for RNAi therapeutics begin to develop, many challenges that currently exist in this system can be overcome and, thereby, exploit this powerful tool as an adjunct in the multimodality therapy of malignancies.

However, several critical issues associated with this approach must be resolved to permit realisation of its promise in humans and to progress to clinical trials. The keys to this transition and to paving the way for RNAi from bench to bedside will be safety, stability and efficacy.

As with any novel therapy, a stringent test for gene silencing therapy strategies will be *in vivo* evaluation using relevant animal models of diseases. Importantly, *in vivo* trials will not only allow evaluation of the efficacy of the new therapeutic directly but also provides better clues on the physiological role of the putative cancer specific siRNA suppressors.

Further future studies, therefore, should focus on methods to investigate the use of anti-CD22 scFv-protamine fusion carrier protein with clinically relevant siRNA gene targets in $CD22^{+}$ leukaemias/lymphomas B cells and its efficacy *in vivo* using animal tumour models.

Over the past decade, mAbs targeting CD4, CD19, CD20, CD22, CD23, CD25, CD45, CD66 and CD122 have been studied and used in clinical trials for the treatment of leukaemias and significantly improved the treatment of haematological malignancies (473). For example, intracellular targeting of B cells through harnessing the internalisation of CD19 and CD22 receptors has been explored using anti-CD19 and anti-CD22 mAbs or their immunoconjugates (90). CD19 is a B cell restricted molecule expressed at all stages of B cell differentiation except for mature plasma cells (474). It constitutes an important component of the B cell receptor complex (BCR) involved in cell signaling and antigen processing (475) and is expressed in the majority of precursor B cell acute lymphoblastic leukaemias (ALL) and B cell non-Hodgkin's lymphomas (NHL) (476). CD19 has long been recognised as a possible target in these malignancies, for example anti-CD19 immunoconjugates with ricin toxin, pokeweed antiviral protein and genistein have been used in clinical trials for the treatment of these B cell malignancies (477, 478). However, there are disappointing outcomes from initial clinical trials with these agents due to massive suppression in the number of B cells and also the increased toxicities associated with these therapies (473, 479 and 480).

In comparison to CD19 targeting in B cells, CD22 makes a better target for intracellular delivery of therapeutics due to the fact that CD22 expression on B cells is restricted only to mature stages of B cell differentiation (59-64). Furthermore, rapid receptor-mediated endocytosis makes CD22 a better therapeutic target than CD19 for intracellular targeting (90).

Moreover, constitutive endocytosis makes CD22 receptor an ideal target for therapeutic intervention in a broad spectrum of applications not only for B cell malignancies and autoimmune diseases but perhaps also for tumour vaccine development. For example, recently BiovaxID^{TM} vaccine was developed which is

composed of the clonal immunoglobulin molecule idiotype (ID) expressed on the surface of B cells from patients with B cell non-Hodgkin's lymphoma (NHL). The isolated patient's ID that can function as a tumour-specific antigen conjugated to the carrier protein keyhole limpet haemocyanin (KLH) can be administered into patients together with granulocyte-macrophage colony-stimulating factor (GM CSF). Results from phase II clinical trials have shown induced tumour-specific cellular and humoral immunity in patients with follicular lymphoma and mantle cell lymphoma (481).

Similarly, it could be possible to target antigens to B cells via CD22 as a means for tumour vaccine development as B cells are capable of eliciting anti-tumour responses through the production of antibodies as well as serving as antigen-presenting cells (APCs) to induce T cell responses (482, 483).

It will, therefore, be possible to deliver tumour antigens with anti-CD22 scFv to B cells to elicit anti-tumour immunity by engineering these antigens in tandem with anti-CD22 scFv. This approach may offer a new avenue for vaccine development which may be of use not only for cancer therapy but also for infectious agents.

One paradigm for improving cancer treatment is the development of targeting therapies that selectively deliver drugs to cancer cells, thus increasing drug accumulation in the tumour and decreasing toxicities and adverse effects of drugs. In this regard, both mAbs and peptide targeting ligands have been used to increase the efficacy and decrease the toxicity by actively targeting tumour cells and cells of the tumour microenvironment and the vasculature (484-492).

Therefore, cancer treatment is evolving from systemic, non-specific, high-dose chemotherapies to a wide variety of specific targeted therapies. Yet better than specificity is a drug's ability to discriminate between the cancer and the normal healthy counterpart of a particular cell type. Therefore, not only specificity but also selectivity of targeting is more desirable to minimise adverse effects on normal healthy cells and tissues. Then a drug's ability to discriminate and affect only a particular gene, protein, signaling pathway or cell in preference to others in a cell population is selectivity (493).

Regarding selective targeting, for example, a number of haematological malignancies such as chronic myelogenous leukaemia (CML), ALL and AML is reported to be associated with a chromosomal translocation that produces the abnormal Philadelphia chromosome (494). This fusion between Ableson (Abl) tyrosine kinase gene at chromosome 9 and break point cluster (Bcr) gene at chromosome 22 encodes a chimeric oncogene protein, Bcr-Abl that is associated with uncontrolled activity of the Abl tyrosine kinase (495). This cancer-specific abnormality can then be selectively targeted using Bcr-Abl kinase inhibitors such as Imatinib and Dasatinib which can induce remission in patients with positive Philadelphia chromosome abnormality (496, 497).

Another example for selectively targeting malignant $CD22^+$ B cells while sparing the normal B cell counterparts is by targeting the zeta-chain associated protein kinase 70 (ZAP-70). This is a 70 kDa ζ-chain CD3-receptor-associated protein tyrosine kinase (PTK) that operates in the T lymphocyte signaling pathways triggered by the stimulation of the T cell receptor (TCR) (498).

In previous studies, investigators have reported that ZAP-70 is aberrantly expressed in a number of B cell malignancies including CLL, precursor B cell ALL, DLBL, MCL and very rare cases of classic Hodgkin's lymphoma (499, 500). It has been reported that ZAP-70-associated PTK in CLL cells undergoes tyrosine phosphorylation following BCR ligation, indicating that ZAP-70 expression was associated with increased signal transduction via BCR complex which may contribute to the more aggressive CLL disease (501). Recently, investigators have used the tyrosine kinase inhibitor Gefitinib to selectively induce apoptosis in $ZAP\text{-}70^+$ CLL cells through inhibition of BCR signaling (502).

Regarding specific targeting of the αvβ6-positive tumours, a large number of solid tumour malignancies were reported to express αvβ6 integrin including colon, gastric, non-small cell lung, skin, cervical, ovarian and head and neck cancers (104, 411, 503-506). Despite promising preliminary data from Cilengitide, an experimental drug for the treatment of patients with αvβ6-positive tumours, its use as anticancer therapeutic has been discontinued due to failure in phase III clinical trials (507).

Therefore, the development of novel targeted therapies remains urgently needed to improve overall survival in these cancers. A20FMDV2-protamine peptide holds the promise to justify its use for the targeted delivery of therapeutic siRNAs into these invasive cancers. Several genes with roles in invasion have been identified amongst which are hepatocyte growth factor receptor (*HGFR*), matrix metalloproteinase-9 (*MMP9*), transforming growth factor β1 (*TGFβ1*) and *αvβ6* integrin (508, 509). Future experiments should be carried out to provide proof of concept that targeting these genes with roles in invasion and spread of these tumour cells using the A20FMDV2-protamine peptide would prove to be useful.

In summary, the findings in this study demonstrated that anti-CD22 scFv-protamine fusion protein was produced in secretable forms from mammalian cells and can form complexes with siRNAs and deliver these specifically via CD22 to mature B cells. This provides “proof of concept” for a novel targeted gene delivery strategy into $CD22^+$ B cells in disease settings particularly malignant B cells from patients with leukaemias and lymphomas.

Bibliography

1. Gerber DE. Targeted therapies: a new generation of cancer treatments. Am. Fam. Physician. 2008; 1:77(3) 311-319.

2. Chernajovsky Y, Gould DJ and Podhajcer. Gene therapy for autoimmune diseases: quo vadis? Nat. Rev. Immunol. 2004; 4(10): 800-811.

3. Hanahan D and Weinberg RA. Hallmarks of cancer: the next generation. Cell. 2011; 4; 144(5):646-674.

4. Siegel R, Naishadham D and Jemal A. Cancer statistics, 2013. CA Cancer J. Clin. 2013; 63(1):11-30.

5. Ettinger DS, Agulnik M, Cates JM, Cristea M, Denlinger CS, Eaton KD, Fidias PM, Gierada D, Gockerman JP, Handorf CR, Iyer R, Lenzi R, Phay J, Rashid A, Saltz L, Shulman LN, Smerage JB, Varadhachary GR, Zager JS and Zhen WK. Occult primary. J. Natl. Compr. Canc. Netw. 2011; 9(12):1358-1395.

6. Morandi P, Ruffini PA, Benvenuto GM, Raimondi R and Fosser V. Cardiac toxicity of high-dose chemotherapy. Bone Marrow Transplant. 2005; 35(4):323-334.

7. Barnett GC, West CM, Dunning AM, Elliott RM, Coles CE, Pharoah PD and Burnet NG. Normal tissue reactions to radiotherapy: towards tailoring treatment dose by genotype. Nat. Rev. Cancer. 2009; 9(2):134-142.

8. Carlsson J, Forssell Aronsson E, Hietala SO, Stigbrand T and Tennvall J. Tumour therapy with radionuclides: assessment of progress and problems. Radiother. Oncol. 2003; 66(2):107-117.

9. Alexandrov LB, Nik-Zainal S, Wedge DC, Aparicio SA, Behjat S, Biankin AV, Bignell GR, Bolli N, Borg A, Borresen-Dale AL, Boyault S, Burkhardt B, Butler AP, Caldas C, Davies HR, Desmedt C, Eils R, Eyfjord JE, Foekens JA, Greaves M, Hosoda F, Hutter B, Ilicic T, Imbeaud S, Imielinski M, Jager N, Jones DT, Jones D, Knappskog S, Kool M, Lakhani SR, Lopez-Otin C, Martin S, Munshi NC, Nakamura H, Northcott PA, Pajic M, Papaemmanuil E, Paradiso A, Pearson JV, Puente XS, Raine K, Ramakrishna M, Richardson AL, Richter J, Rosenstiel P, Schlesner M, Schumacher TN, Span PN, Teague JW, Totoki Y, Tutt AN, Valdes-Mas R, van Buuren MM, van't Veer L, Vincent-Salomon A, Waddell N, Yates LR; Australian Pancreatic Cancer Genome Initiative; ICGC breast Cancer Consortium; ICGC MMML-Seg Consortium; ICGC PedBrain, Zucman-Rossi J, Futreal PA, McDermott U, Lichter P, Meyerson M, Grimmond SM, Siebert R, Campo E, Shibata T, Pfister SM, Campbell PJ and Stratton MR. Signatures of mutational processes in human cancer. Nature. 2013; 22; 500 (7463):415-421.

10. Mwenifumbo J C and Marra M A. Cancer genome-sequencing study design. Nat. Rev. Genet. 2013; 14(5):321-332.

11. Green MR. Targeting targeted therapy. N. Engl. J. Med. 2004; 350:2191–2193.

12. Hamilton A, Gallipoli P, Nicholson E and Holyoake TL. Targeted therapy in haematological malignancies. J. Pathol. 2010; 220(4):404-418.

13. Provan D, Singer CRJ, Baglin T and Lilleyman J. *Oxford Handbook of Clinical Haematology*. 2nd Ed. 2004. Oxford University Press, Inc., New York.

14. Ross JS, Schenkein DP, Pietrusko R, Rolfe M, Linette GP, Stec J, Stagliano NE, Ginsburg GS, Symmans WF, Pusztai L and Hortobagyi GN. Targeted therapies for cancer 2004. Am J Clin Pathol 2004; 122(4):598-609.

15. Strebhardt K and Ullrich A. Paul Ehrlich's magic bullet concept: 100 years of progress. Nat. Rev. Cancer. 2008; 8(6):473-480.

16. Virella G and Wang AC. Immunoglobulin Structure. In Virella G. *Introduction to Medical Immunology*. 4th Edition. 1998. Marcel Dekker, Inc., New York.

17. Glennie MJ and van de Winkel JG. Renaissance of cancer therapeutic antibodies. Drug Discov. Today. 2003; 1; 8(11):503-510.

18. Carter PJ. Potent antibody therapeutics by design. Nat. Rev. Immunol. 2006; 6(5):343-357.

19. Beck A, Wurch T, Bailly C and Corvaia N. Strategies and challenges for the next generation of therapeutic antibodies. Nat. Rev. Immunol. 2010; 10(5):345-352.

20. Scott AM, Wolchok JD and Old LJ. Antibody therapy of cancer. Nat. Rev. Cancer. 2012; 22; 12(4):278-287.

21. Chan AC and Carter PJ. Therapeutic antibodies for autoimmunity and inflammation. Nat. Rev. Immunol. 2010; 10(5):301-316.

22. Weiner LM, Surana R and Wang S. Monoclonal antibodies: versatile platforms for cancer immunotherapy. Nat Rev Immunol. 2010; 10(5):317-327.

23. Bird RE, Hardman KD, Jacobson JW, Johnson S, Kaufman BM, Lee SM, Lee T, Pope SH, Riordan GS and Whitlow M. Single-chain antigen-binding proteins. Science.1988; 242: 423–426.

24. Huston JS, Levinson D, Mudgett-Hunter M, Tai MS, Novotny J, Margolies MN, Ridge RJ, Bruccoleri RE, Haber E, Crea R and Oppermann H. Protein engineering of antibody binding sites: recovery of specific activity in an anti-digoxin single-chain Fv analogue produced in *Escherichia coli*. Proc. Natl. Acad. Sci. 1988; 85, 5879–5883.

25. Holliger P and Hudson PJ. Engineered antibody fragments and the rise of single domains. Nat. Biotechnol. 2005; 23: 1126–1136.

26. Weisser NE and Hall JC. Applications of single-chain variable fragment antibodies in therapeutics and diagnostics. Biotechnol. Adv. 2009; 27: 502–520.

27. Arndt KM, Muller KM and Pluckthun A. Factors influencing the dimer to monomer transition of an antibody single-chain Fv fragment. Biochemistry. 1998; 37, 12918–12926.

28. McCartney JE, Lederman L, Drier EA, Cabral-Denison NA, Wu GM, Batorsky RS, Huston JS and Oppermann H. Biosynthetic antibody binding sites: development of a single-chain Fv model based on anti-dinitrophenol IgA myeloma MOPC 315. J. Protein Chem. 1991; 6: 669-683.

29. Skerra A and Pluckthun A. Assembly of a functional immunoglobulin Fv fragment in *Escherichia coli*. Science. 1988; 240, 1038–1041.

30. Begent RH, Verhaar MJ, Chester KA, Casey JL, Green AJ, Napier MP, Hope-Stone LD, Cushen N, Keep PA, Johnson CJ, Hawkins RE, Hilson AJ and Robson L. Clinical evidence of efficient tumor targeting based on single-chain Fv antibody selected from a combinatorial library. Nat. Med. 1996; 2,979–984.

31. Glasgow JN, Mikheeva G, Krasnykh V and Curiel DT. A strategy for adenovirus vector targeting with a secreted single chain antibody. PLoS ONE. 2009; 4: 1-12.

32. Eisenstein M. Something new under the skin. Nat. Biotechnol. 2011; 29, 107–109.

33. Dammeyer T, Steinwand M, Kruger SC, Dubel S, Hust M and Timmis KN. Efficient production of soluble recombinant single chain Fv fragments by a *Pseudomonas putida* strain KT2440 cell factory. Microb. Cell Fact. 2011; 21; 10:2-8.

34. Pleckaityte M, Zvirbliene A, Sezaite I and Gedvilaite A. Production in yeast of pseudotype virus-like particles harboring functionally active antibody fragments neutralizing the cytolytic activity of vaginolysin. Microb. Cell Fact. 2011; 15; 10:2-13.

35. Tran M, Van C, Barrera DJ, Pettersson PL, Peinado CD, Bui J and Mayfield SP. Production of unique immunotoxin cancer therapeutics in algal chloroplasts. Proc. Natl. Acad. Sci. 2013; 2; 110(1):15-22.

36. Reavy B, Ziegler A, Diplexcito J, Macintosh SM, Torrance L and Mayo M. Expression of functional recombinant antibody molecules in insect cell expression systems. Protein Expr. Purif. 2000; 18(2):221-228.

37. Jager V, Bussow K, Wanger A, Weber S, Hust M, Frenzel A and Schirrmann T. High level transient production of recombinant antibodies and antibody fusion proteins in HEK293 cells. BMC Biotechnol. 2013; 26; 13(1):2-20.

38. Thirion S, Motmans K, Heyligen H, Janssens J, Raus J and Vandevyver C, Mono- and bispecific single-chain antibody fragments for cancer therapy. Eur. J. Cancer Prev. 1996; 65, 507-511.

39. Le Gall F, Reusch U, Moldenhauer G, Little M and Kipriyanov SM. Immunosuppressive properties of anti-CD3 single-chain Fv and diabody. J. Immunol. Methods. 2004; 285, 111-127.

40. Colcher D, Pavlinkova G, Beresford G, Booth BJ, Choudhury A and Batra SK. Pharmacokinetics and biodistribution of genetically-engineered antibodies. Q. J. Nucl. Med. 1998; 42, 225-241.

41. Adams GP and Schier R. Generating improved single-chain Fv molecules for tumor targeting. J. Immunol. Methods. 1999; 231, 249-260.

42. Adams GP, McCartney JE, Tai MS, Oppermann H, Huston JS, Stafford WF, Bookman MA, Fand I, Houston LL and Weiner LM. Highly specific in vivo tumor targeting by monovalent and divalent forms of 741F8 anti-c-erbB-2 single-chain Fv. Cancer Res. 1993; 53, 4026-4034.

43. Adams GP, Schier R, McCall AM, Crawford RS, Wolf EJ, Weiner LM and Marks JD. Prolonged in vivo tumour retention of a human diabody targeting the extracellular domain of human HER2/neu. Br. J. Cancer. 1998; 77, 1405-1412.

44. Pavlinkova G, Beresford GW, Booth BJ, Batra SK and Colcher D. Pharmacokinetics and biodistribution of engineered single-chain antibody constructs of MAb CC49 in colon carcinoma xenografts. J. Nucl. Med. 1999; 40, 1536-1546.

45. Glover DJ, Glouchkova L, Lipps HJ and Jans DA. Overcoming barriers to achieve safe, sustained and efficient non-viral gene therapy. Adv. in Gene Mol. and Cell Ther. 2007; 1(2): 126-140.

46. Balhorn R. The protamine family of sperm nuclear proteins, Genome Biology. 2007; 8,227:1-8.

47. Lewis JD, Song Y, de Jong ME, Bagha SM and Ausió J. A walk through vertebrate and invertebrate protamines, Chromosoma. 2003; 111, 473-482.

48. Hud NV, Allen MJ, Downing K, Lee JD and Balhorn R. Identification of the elemental packing unit of DNA in mammalian sperm cells by atomic force microscopy. Biochem. Biophys. Res. Commun. 1993; 193, 1347–1354.

49. Bohnhorst, J. O., Bjorgan, M. B., Thoen, J. E., Natvig, J. B. & Thompson, K. M. Bm1–Bm5 classification of peripheral blood B cells reveals circulating germinal center founder cells in healthy individuals and disturbance in the B cell subpopulations in patients with primary Sjogren's syndrome. J. Immunol. 2001; 167, 3610–3618.

50. Niiro H and Clark EA. Regulation of B-cell fate by antigen-receptor signals. Nat. Rev. Immunol. 2002; 2:945–956.

51. Meffre E, Casellas R and Nussenzweig MC. Antibody regulation of B cell development. Nat. Immunol. 2000; 1:379–385.

52. Monroe JG. ITAM-mediated tonic signalling through pre-BCR and BCR complexes. Nat. Rev. Immunol. 2006; 6:283–294.

53. Rajewsky, K. Clonal selection and learning in the antibody system. Nature. 1996; 381: 751–758.

54. Lund FE and Randall TD. Effector and regulatory B cells: modulators of CD4+ T cell immunity. Nat. Rev. Immunol. 2010; 10(4):236-247.

55. Shaffer AL, Rosenwald A and Staudt LM. Lymphoid malignancies: the dark side of B-cell differentiation. Nat. Rev. Immunol. 2002; 2(12):920-932.

56. Martin F and Chan AC. B cell immunobiology in disease: evolving concepts from the clinic. Annu. Rev. Immunol. 2006; 24: 467-496.

57. Tedder TF, Tuscano J, Sato S and Kehrl JH. CD22, a B lymphocyte–specific adhesion molecule that regulates antigen receptor signaling. Ann. Rev. Immunol. 1997; 15: 481–504.

58. Dorken B, Moldenhauer G, Pezzutto A, Schwartz R, Feller A, Kiesel S and Nadler LM. HD39 (B3), a B lineage restricted antigen whose cell surface expression is limited to resting and activated human B lymphocytes. J. Immunol. 1986; 136: 4470–4479.

59. Campana D, Janossy G, Bofill M, Trejdosiewicz LK, Ma D, Hoffbrand AV, Mason DY, Lebacq A and Forster HK. Human B cell development: I. Phenotypic differences of B lymphocytes in the bone marrow and peripheral lymphoid tissue. J. Immunol. 1985; 134: 1524–1530.

60. Bofill M, Janossy G, Janossa M, Burford GD, Seymour GJ, Wernet P and Kelemen E. Human B cell development. II. Subpopulations in the human fetus. J. Immunol. 1985; 134: 1531–1538.

61. Haso W, Lee DW, Shah NN, Stetler-Stevenson M, Yuan CM, Pastan IH, Dimitrov DS, Morgan RA, FitzGerald DJ, Barrett DM, Wayne AS, Mackall CL and Orentas RJ. Anti-CD22-chimeric antigen receptors targeting B-cell precursor acute lymphoblastic leukemia. Blood. 2013; 14; 121(7):1165-1174.

62. Janossy G, Coustan-Smith E and Campana D. The reliability of cytoplasmic CD3 and CD22 antigen expression in the immunodiagnosis of acute leukemia: a study of 500 cases. Leukemia. 1989; 3: 170–181.

63. Mason DY, Stein H, Gerdes J, Pulford KAF, Ralfkiaer E, Falini B, Erber WN, Micklum K and Gatter KC. Value of monoclonal anti-CD22 (p135) antibodies for the detection of normal and neoplastic B lymphoid cells. Blood. 1987; 69: 836–840.

64. Erickson LD, Tygrett LT, Bhatia SK, Grabstein KH and Waldschmidt TJ. Differential expression of CD22 (Lyb8) on murine B cells. Int. Immunol. 1996; 8: 1121–1129.

65. Torres RM, Law CL, Santos-Argumedo L, Kirkham PA, Grabstein K, Parkhouse RME and Clark EA. Identification and characterization of the murine homologue of CD22, a B lymphocyte-restricted adhesion molecule. J. Immunol. 1992; 149: 2641–2649.

66. Stamenkovic I, Sgroi D, Aruffo A, Sy MS and Anderson T. The B lymphocyte adhesion molecule CD22 interacts with leukocyte common antigen CD45RO on T cells and α-2,6 sialyltransferase, CD75, on B cells. Cell. 1991; 66: 1133–1144.

67. Wilson GL, Najfeld V, Kozlow E, Menniger J, Ward D and Kehrl JH. Genomic structure and chromosomal mapping of the human CD22 gene. J. Immunol. 1993; 150: 5013–5024.

68. Engel P, Wagner N, Miller A and Tedder TF. Identification of the ligand binding domains of CD22, a member of the immunoglobulin superfamily that uniquely binds a sialic acid-dependent ligand. J. Exp. Med. 1995; 181: 1581–1586.

69. Jellusova J and Nitschke L. Regulation of B cell functions by the sialic acid-binding receptors Siglec-G and CD22. Front. Immunol. 2012; 11;2: 96.1-14.

70. Engel P, Nojima Y, Rothstein D, Zhou LJ, Wilson GL, Kehrl JH and Tedder TF. The same epitope on CD22 of B lymphocytes mediates the adhesion of erythrocytes, T and B lymphocytes, neutrophils and monocytes. J. Immunol. 1993; 150, 4719–4732.

71. Stamenkovic I and Seed B. The B-cell antigen CD22 mediates monocyte and erythrocyte adhesion. Nature. 1990; 344, 74–77.

72. Kelm S, Pelz A, Schauer R, Filbin MT, Tang S, de Bellard ME, Schnaar RL, Mahoney JA, Hartnell A, Bradfield P and Crocker PR. Sialoadhesin, myelin-associated glycoprotein and CD22 define a new family of sialic acid-dependent adhesion molecules of the immunoglobulin superfamily. Curr. Biol. 1994; 4, 965–972.

73. Powell LD and Varki A. The oligosaccharide binding specificities of CD22 beta, a sialic acid-specific lectin of B cells. J. Biol. Chem. 1994; 269, 10628–10636.

74. Powell LD, Sgroi D, Sjoberg ER, Stamenkovic I and Varki A. Natural ligands of the B-cell adhesion molecule CD22b carry N-linked oligosaccharides with a-2,6-linked sialic acids that are required for recognition. J. Biol. Chem. 1993; 268, 7019–7027.

75. Sgroi D, Varki A, Braesch-Andersen S and Stamenkovic I. CD22, a B-cell-specific immunoglobulin superfamily member, is a sialic acid-binding lectin. J. Biol. Chem. 1993; 268, 7011–7018.

76. Hanasaki K, Powell LD and Varki A. Binding of human plasma sialoglycoproteins by the B-cell-specific lectin CD22: Selective recognition of immunoglobulin M and haptoglobin. J. Biol. Chem. 1995; 270, 7543–7550.

77. Pflugh DL, Maher SE and Bothwell ALM. Ly-6 superfamily members Ly-6A/E, Ly-6C, and Ly-6I recognize two potential ligands expressed by B lymphocytes. J. Immunol. 2002; 169, 5130–5136.

78. Schulte RJ, Campbell M-A, Fischer WH and Sefton BM. Tyrosine phosphorylation of CD22 during B cell activation. Science. 1992; 258: 1001–1004.

79. Leprince C, Draves KE, Geahlen RL, Ledbetter JA and Clark EA. CD22 associates with the human surface IgM-B cell antigen receptor complex. Proc. Natl. Acad. Sci. 1993; 90: 3236–3240.

80. Chaouchi N, Vazquez A, Galanaud P and Leprince C. B cell antigen receptor mediated apoptosis. Importance of accessory molecules CD19 and CD22, and of surface IgM cross-linking. J. Immunol. 1995; 154: 3096–3104.

81. Boue DR and LeBien TW. Expression and structure of CD22 in acute leukemia. Blood. 1988; 71: 1480–1486.

82. Shan D and Press OW. Constitutive endocytosis and degradation of CD22 by human B cells. J. Immunol. 1995; 154: 4466–4475.

83. O'Reilly MK, Tian H and Paulson JC. CD22 is a recycling receptor that can shuttle cargo between the cell surface and endosomal compartments of B cells. J. Immunol. 2011; 186: 1554-1563.

84. Chan CHT, Wang J, French RR and Glennie MJ. Internalization of the lymphocytic surface protein CD22 is controlled by a novel membrane proximal cytoplasmic motif. J. Biol. Chem. 1998; 273: 27809–27815.

85. Arndt MA, Krauss J, Schwarzenbacher R, Vu Bk, Greene S and Rybak SM. Generation of a highly stable, internalizing anti-CD22 single-chain Fv fragment for targeting non-Hodgkin's lymphoma. Int. J. Cancer. 2003; 107: 822–829.

86. Zhang M and Varki A. Cell surface sialic acids do not affect primary CD22 interactions with CD45 and surface IgM nor the rate of constitutive CD22 endocytosis. Glycobiology. 2004; 14: 939–949.

87. Collins BE, Blixt O, Han S, Duong B, Li H, Nathan JK, Bovin N and Paulson JC. High-affinity ligand probes of CD22 overcome the threshold set by cis ligands to allow for binding, endocytosis, and killing of B cells. J. Immunol. 2006; 177: 2994-3003.

88. Haas KM, Sen S, Sanford IG, Miller AS, Poe JC and Tedder TF. CD22 ligand binding regulates normal and malignant B lymphocyte survival in vivo. J. Immunol. 2006; 177; 3063-3073.

89. Tateno H, Li H, Schur MJ, Bovin N, Crocker PR, Wakarchuk WW and Paulson JC. Distinct endocytic mechanisms of CD22 (Siglec-2) and Siglec-F reflect roles in cell signaling and innate immunity. Mol. and Cellular Biol. 2007; 27: 5699–5710.

90. Du X, Beers R, FitzGerald DJ and Pastan I. Differential cellular internalization of anti-CD19 and -CD22 immunotoxins results in different cytotoxic activity. Cancer Res. 2008; 68: 6300-6305.

91. Tuscano JM, Martin SM, Ma Y, Zamboni W and O'Donnell RT. Efficacy, biodistribution and pharmacokinetics of CD22-targeted pegylated liposomal Doxorubicin in a B-cell non–Hodgkin's lymphoma xenograft mouse model. Clin. Cancer Res. 2010; 16: 2760-2768.

92. John BJ, Herrin BR, Raman C, Wang Y, Bobbitt KR, Brody BA and Justement LB. The B cell coreceptor CD22 associates with AP50, a clathrin-coated pit adapter protein, via tyrosine-dependent interaction. J. Immunol. 2003; 170: 3534-3543.

93. Sherbina NV, Linsley PS, Myrdal S, Crosmaire LS, Ledbetter JA and Schieven GL. Intracellular CD22 rapidly moves to the cell surface in a tyrosine kinase-dependent manner following antigen receptor stimulation. J. Immunol. 1996; 157: 4390-4398.

94. Tuscano JM, Kato J, Pearson D, Xiong C, Newell L, Ma Y, Gandara DR and O'Donnell RT. CD22 antigen is broadly expressed on lung cancer cells and is a target for antibody-based therapy. Cancer Res. 2012; 1; 72(21):5556-5565.

95. Dorner T and Goldenberg DM. Targeting CD22 as a strategy for treating systemic autoimmune diseases. Ther. Clin. Risk Manag. 2007; 3(5):953-959.

96. Hynes RO. Integrins: bidirectional, allosteric signaling machines. Cell. 2002; 110:673–687.

97. Giancotti FG and Ruoslahti E. Integrin signaling. Science. 1999; 285:1028–1032.

98. Lewis JM, Truong TN and Schwartz MA. Integrins regulate the apoptotic response to DNA damage through modulation of p53. Proc. Natl. Acad. Sci. 2002; 19; 99(6):3627-3632.

99. Brakebusch C, Bouvard D, Stanchi F, Sakai T and Fassler R. Integrins in invasive growth. J. Clin. Invest. 2002; 109:999–1006.

100. Guo W and Giancotti FG. Integrin signalling during tumour progression. Nat. Rev. 2004; 5:816–826.

101. Breuss JM, Gallo J, DeLisser HM, Klimanskaya IV, Folkesson HG, Pittet JF, Nishimura SL, Aldape K, Landers DV, Carpenter W, Gillett N, Sheppard D, Matthay MA, Albelda SM, Kramer RH and Pytela R. Expression of the beta 6 integrin subunit in

development, neoplasia and tissue repair suggests a role in epithelial remodeling. J. Cell Sci. 1995; 108 (Pt 6):2241–2251.

102. Breuss JM, Gillett N, Lu L, Sheppard D and Pytela R. Restricted distribution of integrin beta 6 mRNA in primate epithelial tissues. J. Histochem. Cytochem. 1993; 41:1521–1527.

103. Hakkinen L, Koivisto L, Gardner H, Saarialho-Kere U, Carroll JM, Lakso M, Rauvala H, Laato M, Heino J and Larjava H. Increased expression of beta6-integrin in skin leads to spontaneous development of chronic wounds. Am. J. Pathol. 2004; 164, 229–242.

104. Thomas GJ, Nystrom ML and Marshall JF. Alphavbeta6 integrin in wound healing and cancer of the oral cavity. J. Oral Pathol. Med. 2006; 35, 1–10.

105. Munger JS, Huang X, Kawakatsu H, Griffiths MJ, Dalton SL, Wu J, Pittet JF, Kaminski N, Garat C, Matthay MA, Rifkin DB and Sheppard D. The integrin alpha v beta 6 binds and activates latent TGFbeta 1: a mechanism for regulating pulmonary inflammation and fibrosis. Cell. 1999; 96, 319–328.

106. Annes JP, Rifkin D B and Munger JS. The integrin alphaVbeta6 binds and activates latent TGFbeta3. FEBS Lett. 2002; 511, 65–68.

107. Jackson T, Sheppard D, Denyer M, Blakemore W and King AM. The epithelial integrin alphavbeta6 is a receptor for foot-and-mouth disease virus. J. Virol. 2000; 74, 4949–4956.

108. Thomas GJ and Speight PM. Cell adhesion molecules and oral cancer. Crit. Rev. Oral Biol. Med. 2001; 12(6):479-498.

109. Weinreb PH, Simon KJ, Rayhorn P, Yang WJ, Leone DR, Dolinski BM, Pearse BR, Yokota Y, Kawakatsu H, Atakilit A, Sheppard D and Violette SM. Function blocking integrin αvβ6 monoclonal antibodies. J. Biol. Chem. 2004; 279:17875–87.

110. Ahmed N, Niu J, Dorahy DJ, Gu X, Andrews S, Meldrum CJ, Scott RJ, Baker MS, Macreadie IG and Agrez MV. Direct integrin alphavbeta6-ERK binding: implications for tumour growth. Oncogene. 2002; 21:1370–1380.

111. Zhao-Yang Z, Ke-Sen X, Qing-Si H, Wei-Bo N, Jia-Yong W, Yue-Tang M, Jin-Shen W, Guo-Qiang W, Guang-Yun Y and Jun N. Signaling and regulatory mechanisms of integrin alphavbeta6 on the apoptosis of colon cancer cells. Cancer Lett. 2008; 266:209–215.

112. Van Aarsen LA, Leone DR, Ho S, Dolinski BM, McCoon PE, LePage DJ, Kelly R, Heaney G, Rayhorn P, Reid C, Simon KJ, Horan GS, Tao N, Gardner HA, Skelly MM, Gown AM, Thomas GJ, Weinreb PH, Fawell SE and Violette SM. Antibody-mediated blockade of integrin alpha v beta 6 inhibits tumor progression in vivo by a transforming growth factor-beta-regulated mechanism. Cancer Res. 2008. 15; 68(2):561-570.

113. Hausner SH, DiCara D, Marik J, Marshall JF and Sutcliffe JL. Use of a peptide derived from foot-and mouth disease virus for the noninvasive imaging of human cancer: generation and evaluation of 4-[18F]fluorobenzoyl A20FMDV2 for in vivo imaging of integrin alphavbeta6 expression with positron emission tomography. Cancer Res. 2007; 67:7 833–840.

114. Kay MA. State-of-the-art gene-based therapies: the road ahead. Nat. Rev. Genet. 2011; 12(5):316-328.

115. McCormick F. Cancer gene therapy: fringe or cutting edge? Nat. Rev. Cancer. 2001; 1(2):130-141.

116. Wu GY and Wu CH. Receptor-mediated in vitro gene transformation by a soluble DNA carrier system. J. Biol. Chem. 1987; 262:4429–4432.

117. Wu GY and Wu CH. Evidence for targeted gene delivery to Hep G2 hepatoma cells in vitro. Biochemistry. 1988; 27:887–892.

118. Wagner E, Zenke M, Cotten M, Beug H and Birnstiel ML. Transferrin–polycation conjugates as carriers for DNA uptake into cells. Proc. Natl. Acad. Sci. 1990; 87:3410–3414.

119. Fajac I, Grosse S, Briand P and Monsigny M. Targeting of cell receptors and gene transfer efficiency: a balancing act. Gene Ther. 2002; 9:740–742.

120. Li X, Stuckert P, Bosch I, Marks JD and Marasco WA. Single-chain antibody-mediated gene delivery into ErbB2-positive human breast cancer cells. Cancer Gene Ther. 2001; 8(8):555-565.

121. Dangai D, Abbott KL, Mookerjee A, Zhao A, Kirby PS, Sandaltzopoulos R, Powell DJ Jr, Lamaziere A, Siegel DL, Wolf C and Scholler N. Mannose receptor (MR) engagement by mesothelin GPI anchor polarizes tumor-associated macrophages and is blocked by anti-MR human recombinant antibody. PLoS One. 2011; 6(12):1-13.

122. Buschle M, Cotten M, Kirlappos H, Mechtler K, Schaffner G, Zauner W, Birnstiel ML and Wagner E. Receptor-mediated gene transfer into human T lymphocytes via binding of DNA/CD3 antibody particles to the CD3 T cell receptor complex. Hum. Gene Ther. 1995; 6, 753-761.

123. Gupta S, Eastman J, Silski C, Ferkol T and Davis PB. Single chain Fv: a ligand in receptor-mediated gene delivery. Gene Ther. 2001; 8, 586-592.

124. O'Neill MM, Kennedy CA, Barton RW and Tatake RJ. Receptor-mediated gene delivery to human peripheral blood mononuclear cells using anti-CD3 antibody coupled to polyethylenimine. Gene Ther. 2001; 8, 362-368.

125. Tabernero J, Shapiro GI, LoRusso PM, Cervantes A, Schwartz GK, Weiss GJ, Paz-Ares L, Cho DC, Infante JR, Alsina M, Gounder MM, Falzone R, Harop J, White AC, Toudjarska I, Bumcrot D, Meyers RE, Hinkle G, Svrzikapa N, Hutabarat RM, Clausen VA, Cehelsky J, Nochur SV, Gamba-Vitalo C, Vaishnaw AK, Sah DW, Gollob JA and burris HA. First-in-humans trial of an RNA interference therapeutic targeting VEGF and KSP in cancer patients with liver involvement. Cancer Discov. 2013; 3(4):406-417.

126. Malek A, Gyorffy B, Catapano CV and Schafer R. Selection of optimal combinations of target genes for therapeutic multi-gene silencing based on miRNA co-regulation. Cancer Gene Ther. 2013; 20(5):326-329.

127. Sledz CA and Williams BR. RNA interference in biology and disease. Blood. 2005; 106: 787–794.

128. de Fougerolles A, Vornlocher HP, Maraganore J and Lieberman J. Interfering with disease: a progress report on siRNA-based therapeutics. Nat. Rev. Drug Discov. 2007; 6: 443–453.

129. Liu Z, Sall A and Yang D. MicroRNA: an emerging therapeutic target and intervention tool. Int. J. Mol. Sci. 2008; 9, 978–999.

130. Fire A, Xu S, Montgomery MK, Kostas SA, Driver SE and Mello CC. Potent and specific genetic interference by double-stranded RNA in *Caenorhabditis elegans*. Nature. 1998; 19; 391:806-811.

131. Bumcrot D, Manoharan M, Koteliansky V and Sah DW RNAi therapeutics: a potential new class of pharmaceutical drugs. Nat. Chem. Biol. 2006; 2:711–719.

132. Kuhn R, Streif S and Wurst W. RNA interference in mice. Handb. Exp. Pharmacol. 2007; 178:149–176.

133. Caplen NJ. Gene Therapy Progress and Prospects. Downregulating gene expression: the impact of RNA interference. Gene Ther. 2004; 11, 1241–1248.

134. Kim DH and Rossi JJ. Strategies for silencing human disease using RNA interference. Nat. Rev. Genet. 2007; 8:173–184.

135. Aigner A. Delivery systems for the direct application of siRNAs to induce RNA interference (RNAi) in vivo. J. Biomed. Biotechnol. 2006; 71659:1-15.

136. Leung RK and Whittaker PA. RNA interference: from gene silencing to gene-specific therapeutics. Pharmacol. Ther. 2005; 107:222–239.

137. Xie FY, Woodle MC and Lu PY. Harnessing in vivo siRNA delivery for drug discovery and therapeutic development. Drug Discov. Today. 2006; 11:67–73.

138. Aagaard L and Rossi JJ. RNAi therapeutics: principles, prospects and challenges. Adv. Drug Deliv. Rev. 2007; 59:75–86.

139. Martin SE and Caplen NJ. Applications of RNA interference in mammalian systems. Annu. Rev. Genomics Hum. Genet. 2007; 8:81–108.

140. Liu G, Wong-Staal F and Li QX. Development of new RNAi therapeutics. Histol. Histopathol. 2007; 22:211–217.

141. Brummelkamp TR, Bernards R and Agami R. Stable suppression of tumorigenicity by virus-mediated RNA interference. Cancer Cell. 2002; 2(3):243-247.

142. Wu H, Hait WN and Yang JM. Small interfering RNA-induced suppression of MDR1 (P-glycoprotein) restores sensitivity to multidrug-resistant cancer cells. Cancer Res. 2003; 1; 63(7):1515-1519.

143. Spizzo R, Rushworth D, Guerrero M and Calin GA. RNA inhibition, microRNAs, and new therapeutic agents for cancer treatment. Clin. Lymphoma Myeloma and Leukaemia Suppl. 2009; 9(3); S313-S318.

144. George GP and Mittal RD. MicroRNAs: Potential biomarkers in cancer. Indian J. of Clin. Biochem. 2010; 25: 4-14.

145. Esquela-Kerscher A and Slack FJ. Oncomirs-microRNAs with a role in cancer. Cancer Nat. Rev. 2006; 6: 259-269.

146. Martinez J, Patkaniowska A, Urlaub H, Luhrmann R and Tuschl T. Single-stranded antisense siRNAs guide target RNA cleavage in RNAi. Cell. 2002; 110:563–574.

147. Parker JS and Barford D. Argonaute: a scaffold for the function of short regulatory RNAs. Trends Biochem. Sci. 2006; 31:622–630.

148. Gilmore IR, Fox SP, Hollins AJ, Sohail M and Akhtar S. The design and exogenous delivery of siRNA for post-transcriptional gene silencing. J. Drug Target. 2004: 12:315–340.

149. Gilmore IR, Fox SP, Hollins AJ and Akhtar S. Delivery strategies for siRNA-mediated gene silencing. Current Drug Deliv. 2006; 3:147–155.

150. Akhtar S and Benter I. Toxicogenomics of non-viral drug delivery systems for RNAi: Potential impact on siRNA-mediated gene silencing activity and specificity. Adv. Drug Deliv. Rev. 2007; 59:164–182.

151. Kawakami S and Hashida M. Targeted delivery systems of small interfering RNA by systemic administration. Drug Metab. Pharmacokinet. 2007; 22:142–151.

152. Whitehead KA, Langer R and Anderson DG. Knocking Down Barriers: Advances in siRNA Delivery. Nat. Rev. Drug Disc. 2009; 8(2) 129-138.

153. McCaffrey AP, Meuse L, Pham TT, Conklin DS, Hannon GJ and Kay MA. RNA interference in adult mice. Nature. 2002; 4; 418(6893):38-39.

154. Song E, Lee SK, Wang J, Ince N, Ouyang N, Min J, Chen J, Shankar P and Lieberman J. RNA interference targeting Fas protects mice from fulminant hepatitis. Nat. Med. 2003; 9(3):347-351.

155. Bitko V, Musiyenko A, Shulyayeva O and Barik S. Inhibition of respiratory viruses by nasally administered siRNA. Nat. Med. 2005; 11(1):50–55.

156. Aouadi M, Tesz GJ, Nicoloro SM, Wang M, Chouinard M, Soto E, Ostroff GR and Czech MP. Orally delivered siRNA targeting macrophage Map4k4 suppresses systemic inflammation. Nature. 2009; 30:458(7242):1180–1184.

157. Castanotto D and Rossi JJ. The promises and pitfalls of RNA-interference-based therapeutics. Nature. 2009; 22; 457(7228):426-433.

158. Dalby B, Cates S, Harris A, Ohki EC, Tilkins ML, Price PJ and Ciccarone VC. Advanced transfection with Lipofectamine 2000 reagent: primary neurons, siRNA, and high-throughput applications. Methods. 2004; 33(2): 95-103.

159. Wang J, Lu Z, Wientjes MG and Au JL. Delivery of siRNA Therapeutics: Barriers and Carriers. The AAPS Journal. 2010; 12(4): 492-503.

160. Song E, Zhu P, Lee SK, Chowdhury D, Kussman S, Dykxhoom DM, Feng Y, Palliser D, Weiner DB, Shankar P, Marasco WA and Lieberman J. Antibody mediated in vivo delivery of small interfering RNAs via cell-surface receptors. Nat. Biotechnol. 2005; 23(6): 709-717.

161. Peer D, Zhu P, Carman CV, Lieberman J and Shimaoka M. Selective gene silencing in activated leukocytes by targeting siRNAs to the integrin lymphocyte function-associated antigen-1. Proc. Natl. Acad. Sci. 2007; 104: 4095–4100.

162. Yao YD, Sun TM, Huang SY, Dou S, Lin L, Chen JN, Ruan JB, Mao CQ, Yu FY, Zeng MS, Zang JY, Liu Q, Su FX, Zhang P, Lieberman J, Wang J and Song E. Targeted delivery of PLK1-siRNA by ScFv suppresses Her2+ breast cancer growth and metastasis. Sci. Transl. Med. 2012; 18;4(130):1-10.

163. Hanahan D and Weinberg RA. The hallmarks of cancer. Cell. 2000; 7; 100(1):57-70.

164. Kaufmann SH and Gores GJ. Apoptosis in cancer: cause and cure. Bioessays. 2000; 22(11):1007-1017.

165. Kerr JF, Wyllie AH and Currie AR. Apoptosis: a basic biological phenomenon with wide-ranging implications in tissue kinetics. Br. J. Cancer. 1972; 26(4):239-257.

166. Ferreira CG, Epping M, Kruyt FA and Giaccone G. Apoptosis: target of cancer therapy. Clin. Cancer Res. 2002; 8(7):2024-2034.

167. Ghobrial IM, Witzig TE and Adjei AA. Targeting apoptosis pathways in cancer therapy. CA Cancer J. Clin. 2005; 55(3):178-194.

168. Nicholson DW. From bench to clinic with apoptosis-based therapeutic agents. Nature. 2000; 12; 407(6805):810-816.

169. Fischer U and Schulze-Osthoff K. New approaches and therapeutics targeting apoptosis in disease. Pharmacol. Rev. 2005; 57(2):187-215.

170. Petak I, Houghton JA and Kopper L. Molecular targeting of cell death signal transduction pathways in cancer. Current Signal Transduction Ther. 2006; 1,113-131.

171. Philchenkov A, Zavelevich M, Kroczak TJ and Los M. Caspases and cancer: mechanisms of inactivation and new treatment modalities. Exp. Oncol. 2004; 26(2):82-97.

172. Reed JC and Pellecchia M. Apoptosis-based therapies for hematologic malignancies. Blood. 2005; 15; 106(2):408-418.

173. Bremer E, van Dam G, Kroesen BJ, de Leij L and Helfrich W. Targeted induction of apoptosis for cancer therapy: current progress and prospects. Trends Mol. Med. 2006; 12(8):382-393.

174. Potten C and Wilson J. *Apoptosis: The Life and death of Cells*. 1st Ed. 2004. Cambridge University Press.

175. Youle RJ and Strasser A. The BCL-2 protein family: opposing activities that mediate cell death. Nat. Rev. Mol. Cell Biol. 2008; 9(1):47-59.

176. Cory S and Adams JM. The Bcl2 family: regulators of the cellular life-or-death switch. Nat. Rev. Cancer. 2002; 2(9):647-656.

177. Yip KW and Reed JC. Bcl-2 family proteins and cancer. Oncogene. 2008; 27; 27(50):6398-6406.

178. Ferri KF and Kroemer G. Organelle-specific initiation of cell death pathways. Nat. Cell Biol. 2001; 3(11):255-263.

179. Lawen A. Apoptosis-an introduction. Bioessays. 2003; 25(9):888-896.

180. Danial NN and Korsmeyer SJ. Cell death: critical control points. Cell. 2004; 23; 116(2):205-219.

181. Wilson NS, Dixit V, Ashkenazi A. Death receptor signal transducers: nodes of coordination in immune signaling networks. Nat. Immunol. 2009; 10(4):348-355.

182. Lessene G, Czabotar PE and Colman PM. BCL-2 family antagonists for cancer therapy. Nat. Rev. Drug Discov. 2008; 7(12):989-1000.

183. Van Cruchten S and Van Den Broeck W. Morphological and biochemical aspects of apoptosis, oncosis and necrosis. Anat. Histol. Embryol. 2002; 31(4):214-223.

184. Kroemer G, Reed JC: Mitochondrial control of cell death. Nat. Med. 2000, 6(5):513-519.

185. Schulze-Bergkamen H, Krammer PH: Apoptosis in cancer-implications for therapy. Semin. Oncol. 2004, 31(1):90-119.

186. Kozopas KM, Yang T, Buchan HL, Zhou P and Craig RW. MCL1, a gene expressed in programmed myeloid cell differentiation, has sequence similarity to BCL2. Proc. Natl. Acad. Sci. 1993; 90:3516-3520.

187. Koss B, Morrison J, Perciavalle RM, Singh H, Rehg JE, Williams RT and Opferman JT. Requirement for antiapoptotic MCL1 in the survival of BCR-ABL B-lineage acute lymphoblastic leukemia. Blood. 2013; 29; 122(9):1587-1598.

188. Vikstrom I, Carotta S, Lüthje K, Peperzak V, Jost PJ, Glaser S, Busslinger M, Bouillet P, Strasser A, Nutt SL and Tarlinton DM. MCL1 is essential for germinal center formations and B cell memory. Science. 2010; 19; 330(6007):1095-1099.

189. Akgul C, Turner PC, White MR and Edwards SW. Functional analysis of the human MCL1 gene. Cell Mol. Life Sci. 2000; 57:684-691.

190. Thomas LW, Lam C, Edwards SW. MCL1; the molecular regulation of protein function. FEBS Lett. 2010; 584: 2981–2989.

191. Yang T, Kozopas KM, Craig RW: The intracellular distribution and pattern of expression of MCL1 overlap with, but are not identical to, those of Bcl-2. J. Cell Biol. 1995, 128(6):1173-1184.

192. Han J, Goldstein LA, Gastman BR, Rabinovitz A, Rabinowich H: Disruption of MCL1. Bim complex in granzyme B-mediated mitochondrial apoptosis. J. Biol. Chem. 2005, 280(16):16383-16392.

193. Leu JI, Dumont P, Hafey M, Murphy ME, George DL: Mitochondrial p53 activates Bak and causes disruption of a Bak-Mcl1 complex. Nat. Cell Biol. 2004, 6(5):443-450.

194. Willis SN, Chen L, Dewson G, Wei A, Naik E, Fletcher JI, Adams JM and Huang DC. Proapoptotic Bak is sequestered by Mcl1 and BclxL, but not Bcl-2, until displaced by BH3-only proteins. Genes Dev. 2005, 19(11):1294-1305.

195. Chen L, Willis SN, Wei A, Smith BJ, Fletcher JI, Hinds MG, Colman PM, Day CL, Adams JM and Huang DC. Differential targeting of prosurvival Bcl-2 proteins by their

BH3-only ligands allows complementary apoptotic function. Mol. Cell. 2005, 17(3):393-403.

196. Clohessy JG, Zhuang J, de Boer J, Gil-Gomez G and Brady HJ. MCL1 interacts with truncated Bid and inhibits its induction of cytochrome c release and its role in receptor-mediated apoptosis. J. Biol. Chem. 2006, 281(9):5750-5759.

197. Fleischer B, Schulze-Bergkamen H, Schuchmann M, Weber A, Biesterfeld S, Muller M, Krammer PH and Galle PR. MCL1 is an anti-apoptotic factor for human hepatocellular carcinoma. Int. J. Oncol. 2006; 28:25-32.

198. Pepper C, Lin TT, Pratt G, Hewamana S, Brennan P, Hiller L, Hills R, Ward R, Starczynski J, Austen B, Hooper L, Stankovic T and Fegan C. MCL1 expression has in vitro and in vivo significance in chronic lymphocytic leukemia and is associated with other poor prognostic markers. Blood. 2008; 112:3807-3817.

199. Schulze-Bergkamen H, Ehrenberg R, Hickmann L, Vick B, Urbanik T, Schimanski CC, Berger MR, Schad A, Weber A, Heeger S, Galle PR and Moeher M. Bcl-x(L) and Myeloid cell leukaemia-1 contribute to apoptosis resistance of colorectal cancer cells. World J. Gastroenterol. 2008; 14:3829-3840.

200. O'Driscoll L, Cronin D, Kennedy SM, Purcell R, Linehan R, Glynn S, Larkin A, Scanlon K, McDermott EW, Hill AD, O'Higgins NJ, Parkinson M and Clynes M. Expression and prognostic relevance of MCL1 in breast cancer. Anticancer Res. 2004; 24:473-482.

201. Cho-Vega JH, Rassidakis GZ, Admirand JH, Oyarzo M, Ramalingam P, Paraguya A, McDonnell TJ, Amin HM and Medeiros LJ. MCL1 expression in B-cell non-Hodgkin's lymphomas. Hum. Pathol. 2004; 35(9):1095-1100.

202. Schulze-Bergkamen H, Fleischer B, Schuchmann M, Weber A, Weinmann A, Krammer PH and Galle PR. Suppression of MCL1 via RNA interference sensitizes human hepatocellular carcinoma cells towards apoptosis induction. BMC Cancer. 2006; 6:232: 1-14.

203. Rinkenberger JL, Horning S, Klocke B, Roth KA and Korsmeyer SJ. MCL1 deficiency results in peri-implantation embryonic lethality. Genes Dev. 2000; 14, 23-27.

204. Fernald K and Kurokawa M. Evading apoptosis in cancer. Trends Cell Biol. 2013; 23(12):620-633.

205. Glover DM, Hagan IM and Tavares AA. Polo-like kinases: a team that plays throughout mitosis. Genes Dev. 1998; 12, 3777–3787.

206. Archambault V and Glover DM. Polo-like kinases: conservation and divergence in their functions and regulation. Nat. Rev. Mol. Cell Biol. 2009; 10:265-275.

207. Strebhardt K and Ullrich A. Targeting polo-like kinase 1 for cancer therapy. Nat. Rev. Cancer. 2006; 6:321-330.

208. Yim H and Erikson RL. Polo-like kinase 1 depletion induces DNA damage in early S prior to caspase activation. Mol. Cell Biol. 2009; 29:2609-2621.

209. Barr FA, Sillje HH and Nigg EA. Polo-like kinases and the orchestration of cell division. Nat. Rev. Mol. Cell Biol. 2004; 5(6):429-440.

210. Golsteyn RM, Schultz SJ, Bartek J, Ziemiecki A, Ried T and Nigg EA. Cell cycle analysis and chromosomal localization of human Plk1, a putative homologue of the mitotic kinases Drosophila polo and Saccharomyces cerevisiae Cdc5. J. Cell Sci. 1994; 107:1509-1517.

211. Hamanaka R, Smith MR, O'Connor PM, Maloid S, Mihalic K, Spivak JL, Longo DL and Ferris DK. Polo-like kinase is a cell cycle-regulated kinase activated during mitosis. J. Biol. Chem. 1995; 270:21086-21091.

212. Lee KS, Yuan YL, Kuriyama R and Erikson RL. Plk is an M-phase-specific protein kinase and interacts with a kinesin-like protein, CHO1/MKLP-1. Mol. Cell Biol. 1995; 15:7143-151.

213. Uchiumi T, Longo DL and Ferris DK. Cell cycle regulation of the human polo-like kinase (PLK) promoter. J. Biol. Chem. 1997; 272:9166-9174.

214. Smith MR, Wilson ML, Hamanaka R, Chase D, Kung H, Longo DL and Ferris DK. Malignant transformation of mammalian cells initiated by constitutive expression of the polo-like kinase. Biochem. Biophys. Res. Commun. 1997; 234:397-405.

215. Kim HJ, Ishii A, Miyata K, Lee Y, Wu S, Oba M, Nishiyama N and Kataoka K. Introduction of stearoyl moieties into a biocompatible cationic polyaspartamide derivative, PAsp(DET), with endosomal escaping function for enhanced siRNA-mediated gene knockdown. J. Control Release. 2010; 14; 145(2):141-148.

216. Miyata K, Oba M, Nakanishi M, Fukushima S, Yamasaki Y, Koyama H, Nishiyama N and Kataoka K. Polyplexes from poly(aspartamide) bearing 1,2-diaminoethane side chains induce pH-selective, endosomal membrane destabilization with amplified transfection and negligible cytotoxicity. J. Am. Chem. Soc. 2008; 130(48):16287-1694.

217. Kang HC, Kang HJ and Bae YH. A reducible polycationic gene vector derived from thiolated low molecular weight branched polyethyleneimine linked by 2-iminothiolane. Biomaterials. 2011; 32(4):1193-1203.

218. Thomas GJ, Lewis MP, Hart IR, Marshall JF and Speight PM. αvβ6 integrin promotes invasion of squamous carcinoma cells through up-regulation of matrix metalloproteinase-9. Int. J. Cancer. 2001; 92, 641–650.

219. Ojala PM, Sodeik B, Ebersold MW, Kutay U and Helenius A. Herpes simplex virus type 1 entry into host cells: reconstitution of capsid binding and uncoating at the nuclear pore complex in vitro. Mol. Cell Biol. 2000; 20(13):4922-4931.

220. Mead DA, Pey NK, Herrnstadt C, Marcil RA and Smith LM. A universal method for the direct cloning of PCR amplified nucleic acid. Nat. Biotech. 1991; 9: 657-663.

221. Kyte J and Doolittle R. A simple method for displaying the hydropathic character of a protein. J. Mol. Biol. 1982; 5; 157(1):105-132.

222. Gould DJ, Bright C and Chernajovsky Y. Inhibition of established collagen-induced arthritis with a tumour necrosis factor-α inhibitor expressed from a self-contained doxycycline regulated plasmid. Arthritis Res. Ther. 2004; 6(2):103-113.

223. Hoogenboom HR, Griffith AD, Johnson KS, Chiswell DJ, Hudson P and Winter G. Multi-subunit proteins on the surface of filamentous phage: methodologies for displaying antibody (Fab) heavy and light chains. Nuc. Acids Res. 1991; 11;19 (15):4133-4137.

224. Jost CR, Kurucz I, Jacobus CM, Titus JA, George AJ and Segal DM. Mammalian expression and secretion of functional single-chain Fv molecules. Biol. Chem. 1994; 21; 269(42):26267-26273.

225. Stocker M, Tur MK, Sasse S, Krussmann A, Barth S and Engert A. Secretion of functional anti-CD30-angiogenin immunotoxins into the supernatant of transfected 293T-cells. Protein Expr. Purif. 2003; 28(2):211-219.

226. de Graaf M, Pinedo HM, Oosterhoff D, van der meulen-Muileman IH, Gerritsen WR, Haisma HJ and Boven E. Pronounced antitumor efficacy by extracellular activation of a doxorubicin-glucuronide prodrug after adenoviral vector-mediated expression of a human antibody-enzyme fusion protein. Hum. Gene Ther. 2004; 15(3):229-238.

227. Peipp M, Saul D, Barbin K, Bruenke J, Zunino SJ, Niederweis M and Fey GH. Efficient eukaryotic expression of fluorescent scFv fusion proteins directed against CD antigens for FACS applications. J. Immunol. Methods. 2004; 15;285(2):265-280.

228. Ho M, Nagata S and Pastan I. Isolation of anti-CD22 Fv with high affinity by Fv display on human cells. Proc. Natl. Acad. Sci. 2006; 20; 103 (25):9637-9642.

229. Mansfield E, Amlot P, Pastan I and Fitzgerald DJ. Recombinant RFB4 immunotoxins exhibit potent cytotoxic activity for CD22-bearing cells and tumors.Blood. 1997; 90: 2020-2026.

230. Kreitman RJ and Pastan I. Antibody Fusion Proteins: Anti-CD22 Recombinant Immunotoxin Moxetumomab Pasudotox. Clin. Cancer Res. 2011; 15; 17(20):6398-6405.

231. Sambrook J and Russell D. *Molecular Cloning: A Laboratory Manual*. 3rd ed. 2001. Cold Spring Harbor Laboratory Press, Cold Spring Harbor, NY.

232. Harrison JL, Williams SC, Winter G and Nissim A. Screening of phage antibody libraries. Methods Enzymol. 1996; 267: 83-109.

233. Sedlmayr P, Leitner V, Pilz S, Wintersteiger R, Stewart CC and Dohr G. Species-Specific Blocking of Fc Receptors in Indirect Immunofluorescence Assays. Laboratory Hematology. 2001; 7:81-84.

234. Nolan T, Hands RE and Bustin SA. Quantification of mRNA using real-time RT-PCR. Nat. Protoc. 2006; 1(3):1559-1582.

235. Symington FW, Subbarao B, Mosier DE and Sprent J. Lyb-8.2: a new B cell antigen defined and characterized with a monoclonal antibody. Immunogenetics. 1982; 16: 381-391.

236. Ono M, Murakami T, Kudo A, Isshiki M, Sawada H and Segawa A. Quantitative comparison of anti-fading mounting media for confocal laser scanning microscopy. J. Histochem. Cytochem. 2001; 49(3): 305-312.

237. Hughes C, Faurholm B, Dell'Accio F, Manzo A, Seed M, Eltawi N, Marrelli A, Gould D, Suang C, Al-Kashi A, De Bari C, Winyard P, Chernajovsky Y and Nissim A. Human single-chain variable fragment that specifically targets arthritic cartilage. Arthritis Rheum. 2010; 62(4):1007-1016.

238. Fujita R, Matsuyama T, Yamagishi J, Sahara K, Asano S and Bando H. Expression of Autographa californica multiple nucleopolyhedrovirus genes in mammalian cells and upregulation of the host β-actin gene. J. Virol. 2006; 80, 2390–2395.

239. Kenoutis C, Efrose RC, Swevers L, Lavdas AA, Gaitanou M, Matsas R and Latrou K. Baculovirus-mediated gene delivery into mammalian cells does not alter their transcriptional and differentiating potential but is accompanied by early viral gene expression. J Virol. 2006; 80, 4135–4146.

240. Feijo GCS, Sabbaga J, Carneiro CRW and Brigido MM. Variable region structure and Staphylococcal protein A binding specificity of a mouse monoclonal IgM anti-laminin-receptor antibody. Immunology. 1997; 91:479-485.

241. DiJoseph JF, Armellino DC, Boghaert ER, Khandke K, Dougher MM, Sridharan L, Kunz A, Hamann PR, Gorovits B, Udata C, Moran JK, Popplewell AG, Stephens S, Frost P and Damle NK. Antibody-targeted chemotherapy with CMC-544: a CD22-targeted immunoconjugate of calicheamicin for the treatment of B-lymphoid malignancies. Blood. 2004; 103(5):1807-1814.

242. Rytting M, Triche L, Thomas D, O'Brien S and Kantarjian H. Initial experience with CMC-544 (inotuzumab ozogamicin) in pediatric patients with relapsed B-cell acute lymphoblastic leukemia. Pediatr. Blood Cancer. 2013: 61 (2): 369-372.

243. Kato KI, Goncalves JM, Houts GE and Bollum FJ. Deoxynucleotide polymerizing enzymes of calf thymus gland. II. Properties of terminal deoxynucleotidyl transferase. J. Biol. Chem. 1967; 242: 2780–2789.

244. Repasky JA, Corbett E, Boboila C and Schatz DG. Mutational analysis of terminal deoxynucleotidyltransferase-mediated N-nucleotide addition in V(D)J recombination. J. Immunol. 2004; 172(9): 5478-5488.

245. Annenkov AE, Moyes SP, Eshhar Z, Mageed RA and Chernajovsky Y. Loss of original antigenic specificity in T cell hybridomas transduced with a chimeric receptor containing single-chain Fv of an anti-collagen antibody and Fc epsilon RI-signaling gamma subunit. J. Immunol. 1998; 15;161(12):6604-6613.

246. Zhou MY and Gomez-Sanchez CE. Universal TA cloning. Curr. Issues Mol. Biol. 2000; 2(1):1–7.

247. Czudai-Matwich V, Schnare M and Pinkenburg O. A simple and fast system for cloning influenza A virus gene segments into pHW2000- and pCAGGS-based vectors. Arch. Virol. 2013; 158(10):2049-2058.

248. Holton TA and Graham MW. A simple and efficient method for direct cloning of PCR products using ddT-tailed vectors. Nuc. Acids Res. 1991; 19(5):1156.

249. Clark JM. Novel non-templated nucleotide addition reactions catalyzed by Procaryotic and Eucaryotic DNA polymerases. Nuc. Acids Res. 1988; 16: 9677-9686.

250. Wu TY, Chen HA, Li FY, Lin CT, Wu CM, Hsieh FC, Tzen JT, Hsieh SK, Ko JL and Jinn TR. High-level expression, purification and production of the fungal immunomodulatory protein-gts in baculovirus-infected insect larva. Appl. Biochem. Biotechnol. 2013; 169(3):976-989.

251. Cheshenko N, Krougliak N, Eisensmith RC and Krougliak VA. A novel system for the production of fully deleted adenovirus vectors that does not require helper adenovirus. Gene Ther. 2001; 8:846-854.

252. Frenzel A, Hust M and Schirmann T. Expression of recombinant antibodies. Front Immunol. 2013; 29; 4:217:1-20.

253. DePamphilis ML. DNA replication in eukaryotic cells. Pp. 461-507. In *Concepts in Eukaryotic DNA Replication*. 1996. Cold Spring Harbor Laboratory Press, Cold Spring Harbor, New York.

254. Luckow VA, Lee SC, Barry GF and Olins PO. Efficient Generation of infectious recombinant baculoviruses by site-sSpecific transposon-mediated insertion of foreign genes into a baculovirus genome propagated in *Escherichia coli*. J. Virology. 1993; 67(8):4566-4579.

255. Cleaver SH and Wickstrom E. Transposon Tn7 gene insertion into an evolutionarily conserved human homolog of *Escherichia coli* attTn7. Gene. 2000; 254: 37-44.

256. Nakhai B, Pal R, Sridhar P, Talwar GP and Hasnain SE. The α subunit of human chorionic gonadotropin hormone synthesized in insect cells using a baculovirus vector is biologically active. FEBS J. 1991; 283, 104–108.

257. Stern LJ and Wiley DC. The human class II MHC protein HLA-DRI assembles as empty αβ heterodimers in the absence of antigenic peptide. Cell. 1992; 68, 465–477.

258. Murphy CI, McIntire JR, Davis DR, Hodgdon H, Seals JR and Young E. Enhanced expression, secretion, and large-scale purification of recombinant HIV-1 gp120 in insect cells using the baculovirus egt and P67 signal peptides. Protein Expression Purif. 1993; 4, 349–357.

259. Hsu T-A, Eiden JJ, Bourgarel P, Meo T and Betenbaugh MJ. Effects of Co-expressing chaperone BiP on functional antibody production in the baculovirus system. Protein Expression Purif. 1994; 5, 595–603.

260. Gunne H, Hellers M and Steiner H. Structure of preproattacin and its processing in insect cells infected with a recombinant baculovirus. Eur. J. Biochem. 1990; 187, 699–703.

261. Ailor E and Betenbaugh MJ. Overexpression of a cytosolic chaperone to improve solubility and secretion of a recombinant IgG protein in insect cells. Biotech. and Bioeng. 1997; 58, 196–203.

262. Paetzel M, Karla A, Strynadka NCJ and Dalbey RE. Signal peptidases. Chem. Rev. 2002; 102, 4549–4579.

263. Gierasch LM. Signal sequences. Biochemistry. 1989; 28, 923–930.

264. Bohni PC, Deshaies RJ and Schekman W. SEC11 is required for signal peptide processing and yeast cell growth. J. Cell. Biol. 1988; 106, 1035–1042.

265. Ailor E, Pathmanathan J, Jongbloed JDH and Betenbaugh MJ. A bacterial signal peptidase enhances processing of a recombinant single chain antibody fragment in insect cells. Biochem. Biophys. Res. Comm. 1999; 255, 444–450.

266. Tan NS, Ho B and Ding JL. Engineering a novel secretion signal for cross host recombinant protein expression. Prot. Eng. 2002; 15, 337–345.

267. Lindley KM, Su JL, Hodges PK, Wisely GB, Bledsoe RK, Condreay JP, Winegar DA, Hutchins JT and Kost TA: Production of monoclonal antibodies using recombinant baculovirus displaying gp-64 fusion proteins. J. Immunol. Methods. 2000; 3; 234(1-2):123-135.

268. Kaufman RJ. Regulation of mRNA translation by protein folding in the endoplasmic reticulum. Trends Biochem. Sci. 2004; 29:152–158.

269. Sudhakar A, Ramachandran A, Ghosh S, Hasnain SE, Kaufman RJ and Ramaiah KV. Phosphorylation of serine 51 in initiation factor 2 α (eIF2 α) promotes complex formation between eIF2 α(P) and eIF2B and causes inhibition in the guanine nucleotide exchange activity of eIF2B. Biochemistry. 2000; 39:12929–12938.

270. Mikami S, Kobayashi T, Yokoyama S and Imataka H. A hybridoma-based in vitro translation system that efficiently synthesizes glycoproteins. J. Biotechnol. 2006; 127:65–78.

271. Nonato MC, Widom J and Clardy J. Crystal structure of the N-terminal segment of human eukaryotic translation initiation factor 2α. J. Biol. Chem. 2002; 277:17057–17061.

272. Ramelot TA, Cort JR, Yee AA, Liu F, Goshe MB, Edwards AM, Smith RD, Arrowsmith, CH, Dever TE and Kennedy MA. Myxoma virus immunomodulatory protein M156R is a structural mimic of eukaryotic translation initiation factor eIF2α J. Mol. Biol. 2002; 322:943–954.

273. Gallie DR. The cap and poly(A) tail function synergistically to regulate mRNA translational efficiency. Genes and Dev. 1991; 5:2108–2116.

274. Spirin AS. High-throughput cell-free systems for synthesis of functionally active proteins. Trends Biotechnol. 2004; 22:538–545.

275. Endo Y and Sawasaki T. Cell-free expression systems for eukaryotic protein production. Curr. Opin. Biotechnol. 2006; 17:373–380.

276. Oliva R. Protamines and male infertility. Human Reproduction Update. 2006; 12(4):417–435.

277. Koutsokeras A, Kabouridis PS. Secretion and uptake of TAT-fusion proteins produced by engineered mammalian cells. Biochim. Biophys. Acta. 2009; 1790:147-153.

278. Shaw PA, Catchpole IR, Goddard CA and Colledge WH. Comparison of protein transduction domains in mediating cell delivery of a secreted CRE protein. Biochemistry 2008; 47:1157-1166.

279. Adams G, Vessillier S, Dreja H and Chernajovsky Y. Targeting cytokines to inflammation sites. Nat. Biotechnol. 2003; 21(11):1314-1320.

280. Tian S, Huang Q, Fang Y and Wu J. Furin DB: A database of 20-residue furin cleavage site motifs, substrates and their associated drugs. Int. J. Mol. Sci. 2011; 8; 12(2):1060-1065.

281. Flinterman M, Farzaneh F, Habib N, Malik Gõken J and Tavassoli M. Delivery of therapeutic proteins as secretable TAT fusion products. Mol. Ther. 2009; 17(2): 334-342.

282. Coloma MJ, Hastings A, Wims LA and Morrison SL. Novel vectors for the expression of antibody molecules using variable regions generated by polymerase chain reaction. J. Imm. Methods. 1992; 152: 89-104.

283. Horynova M, Takahashi K, Hall S, Renfrow MB, Novak J and Raska M. Production of N-acetylgalactosaminyl-transferase 2 (GalNAc-T2) fused with secretory signal Igκ in insect cells. Protein Expr. Purif. 2012; 81(2):175-180.

284. Zhao M, Mu W, Jiang B, Hang H, Zhou L and Zhang T. Cloning and extracellular expression of inulin fructotransferase from *Arthrobacter aurescens* SK 8.001 in *E. coli*. J. Science of Food and Agr. 2011; 91: 2715–2721.

285. Dammeyer T: Biomedicals from a soil bug: expanding scFv production host range. Bioengineered bugs. 2012; 3:67–71.

286. Kipriyanov SM, Little M, Kropshofer H, Breitling F, Gotter S and Dubel S. Affinity enhancement of a recombinant antibody: formation of complexes with multiple valency by a single-chain Fv fragment-core streptavidin fusion. Protein Engin. 1996; 9(2):203-211.

287. Korn T, Nettelbeck DM, Volkel T, Muller R and Kontermann RE. Recombinant bispecific antibodies for the targeting of adenoviruses to CEA-expressing tumour cells: a comparative analysis of bacterially expressed single-chain diabody and tandem scFv. J. Gene Med. 2004; 6(6):642-651.

288. Glockshuber R, Schmidt T and Plu¨chthun A. The disulfide bonds in antibody variable domains: effects on stability, folding in vitro and functional expression in *Escherichia coli*. Biochemistry. 1992; 31, 1270-1279.

289. Pantoliano MW, Bird RE, Johnson S, Asel ED, Dodd SW, Wood JF and Hardman KD. Conformational stability, folding, and ligand-binding affinity of single-chain Fv immunoglobulin fragments expressed in *Escherichia coli*. Biochemistry. 1991; 30, 10117-10125.

290. Golovanov AP, Hautbergue GM, Wilson SA and Lian LY. A simple method for improving protein solubility and long-term stability. J. Am. Chem. Soc. 2004; 126: 8933–8939.

291. Valente JJ, Verma KS, Manning MC, Wilson WW and Henry CS. Second viral coefficient studies of cosolvent-induced protein self-interaction. Biophys. J. 2005; 89: 4211–4218.

292. Vedadi M, Niesen FH, Allali-Hassani A, Fedorov OY, Finerty Jr PJ, Wasney GA, Yeung R, Arrowsmith C, Ball LJ, Berglund H, Hui R, Marsden BD, Nordlund P, Sundstrom M, Weigelt J and Edwards AM. Chemical screening methods to identify

ligands that promote protein stability, protein crystallization and structure determination. Proc. Natl. Acad. Sci. 2006; 103: 15835–15840.

293. Blobel J, Schmidl S, Vidal D, Nisius L, Bernado P, Millet O, Brunner E and Pons M. Protein tyrosine phosphatase oligomerization studied by a combination of N-15 NMR relaxation and Xe-129 NMR. Effect of buffer containing arginine and glutamic acid. J. Am. Chem. Soc. 2007; 129: 5946–5953.

294. Placzek WJ, Almeida MS and Wuthrich K. NMR structure and functional characterization of a human cancer-related nucleoside triphosphatase. J. Mol. Biol. 2007: 367: 788–801.

295. Golovanov AP, Hautbergue GM, Tintaru AM, Lian LY and Wilson SA. The solution structure of REF2-I reveals interdomain interactions and regions involved in binding mRNA export factors and RNA. RNA. 2006; 12:1933–1948.

296. Song JK, Zhao KQ, Newman CLL, Vinarov DA and Markley JL. Solution structure of human sorting nexin 22. Protein Sci. 2007; 16: 807–814.

297. Tintaru AM, Hautbergue GM, Hounslow AM, Hung ML, Lian LY, Craven CJ and Wilson SA. Structural and functional analysis of RNA and TAP binding to SF2/ASF. EMBO Rep. 2007; 8: 756–762.

298. Hautbergue GM and Golovanov AP. Increasing the sensitivity of cryoprobe protein NMR experiments by using the sole low-conductivity arginine glutamate salt. J. Magnetic Resonance. 2008; 191:335–339.

299. Anelli T and Sitia R. Protein quality control in the early secretory pathway. EMBO J. 2008; 27, 315–327.

300. Benchabane M, Goulet C, Rivard D, Faye L, Gomord V and Michaud D. Preventing unintended proteolysis in plant protein biofactories. Plant Biotechnol. J. 2008; 6: 633–648.

301. Sharma AK and Sharma MK. Plants as bioreactors: recent developments and emerging opportunities. Biotechnol. Adv. 2009; 27: 811–832.

302. Ellgaard L and Helenius A. ER quality control: towards an understanding at the molecular level. Curr. Opin. Cell Biol. 2001; 13: 431–437.

303. Ellgaard L and Helenius A. Quality control in the endoplasmic reticulum. Nat. Rev. Mol. Cell Biol. 2003; 4: 181–191.

304. Ellgaard L, Molinari M and Helenius A. Setting the standards: quality control in the secretory pathway. Science. 1999; 286: 1882–1888.

305. van Anken E and Braakman I. Versatility of the endoplasmic reticulum protein folding factory. Crit. Rev. Biochem. Mol. Biol. 2005; 40: 191–228.

306. Lu DP and Christopher DA. Endoplasmic reticulum stress activates the expression of a sub-group of protein disulfide isomerase genes and AtbZIP60 modulates the response in *Arabidopsis thaliana*. Mol. Genet Genomics. 2008; 280: 199–210.

307. Xu P, Raden D, Doyle FJ III and Robinson AS. Analysis of unfolded protein response during single-chain antibody expression in *Saccharomyces cerevisiae* reveals different roles for BiP and PDI in folding. Metab. Eng. 2005; 7: 269–279.

308. Xu P and Robinson AS. Decreased secretion and unfolded protein response up-regulation are correlated with intracellular retention for single-chain antibody variants produced in yeast. Biotechnol. Bioeng. 2009; 104: 20–29.

309. Carvalho NDSP, Arentshorst M, Kooistra R, Stam H, Sagt CM, van den Hondel CAMJJ and Ram AFJ. Effects of a defective ERAD pathway on growth and heterologous protein production in *Aspergillus niger*. Appl. Microbiol. Biotechnol. 2011; 89: 357–373.

310. Ron D and Walter P. Signal integration in the endoplasmic reticulum unfolded protein response. Nat. Rev. Mol. Cell Biol. 2007; 8, 519–529.

311. Oda Y, Hosokawa N, Wada I and Nagata K. EDEM as an acceptor of terminally misfolded glycoproteins released from calnexin. Science. 2003; 299, 1394–1397.

312. Ho M, Kreitman RJ, Onda M and Pastan I. In vitro antibody evolution targeting germline hot spots to increase activity of an anti-CD22 immunotoxin. J. Biol. Chem. 2005; 7; 280(1):607-617.

313. Onda M, Beers R, Xiang L, Lee B, Weldon JE, Kreitman RJ and Pastan I. Recombinant immunotoxin against B-cell malignancies with no immunogenicity in mice by removal of B-cell epitopes. Proc. Natl. Acad. Sci. 2011; 5; 108(14):5742-5747.

314. Davidson BL and McCray PB Jr. Current prospects for RNA interference-based therapies. Nat. Rev. Genet. 2011; 12: 329–340.

315. Kumar P, Wu H, McBride JL, Jung KE, Kim MH, Davidson BL, Lee SK, Shankar P and Manjunath N. Transvascular delivery of small interfering RNA to the central nervous system. Nature. 2007; 448: 39–43.

316. Kuwahara H, Nishina K, Yoshida K, Nishina T, Yamamoto M, Saito Y, Piao W, Yoshida M, Mizusawa H and Yokota T. Efficient in vivo delivery of siRNA into brain capillary endothelial cells along with endogenous lipoprotein. Mol. Ther. 2011; 19: 2213–2221.

317. Davis ME, Zuckerman JE, Choi CH, Seligson D, Tolcher A, Alabi CA, Yen Y, Heidel JD and Ribas A. Evidence of RNAi in humans from systemically administered siRNA via targeted nanoparticles. Nature. 2010; 464: 1067–1070.

318. Ren Y, Hauert S, Lo JH and Bhatia SN. Identification and characterization of receptor-specific peptides for siRNA delivery. ACS Nano. 2012; 23; 6(10):8620-8631.

319. Santel A, Aleku M, Keil O, Endruschat J, Esche V, Durieux B, Loffler K, Fechtner M, Rohl T, Fisch G, Dames S, Arnold W, Giese K, Klippel A and Kaufmann J. RNA interference in the mouse vascular endothelium by systemic administration of siRNA-lipoplexes for cancer therapy. Gene Ther. 2006; 13: 1360–1370.

320. Yonenaga N, Kenjo E, Asai T, Tsuruta A, Shimizu K, Dewa T, Nango M and Oku N. RGD-based active targeting of novel polycation liposomes bearing siRNA for cancer treatment. J. Control Release. 2012; 160: 177–181.

321. Lundberg P, El-Andaloussi S, Sótló T, Johansson H and Langel U. Delivery of short interfering RNA using endosomolytic cell-penetrating peptides. FASEB J. 2007; 21: 2664–2671.

322. Sioud M. RNAi therapy: antibodies guide the way. Gene Ther. 2006; 13(3): 194-195.

323. Kircheis R, Wightman L, Kursa M, Ostermann E and Wagner E. Tumor-targeted gene delivery: an attractive strategy to use highly active effector molecules in cancer treatment. Gene Ther. 2002; 9, 11, 731-735.

324. Batra RK, Wang-Johanning F, Wanger E, Garver RI Jr and Curiel DT. Receptor-mediated gene delivery employing lectin-binding specificity. Gene Ther. 1994; 1(4):255-260.

325. Sodoyer R. Expression systems for the production of recombinant pharmaceuticals. BioDrugs. 2004; 18(1):51-62.

326. Wurm FM. Production of recombinant protein therapeutics in cultivated mammalian cells. Nat. Biotechnol. 2004; 22:1393–1398.

327. Pham PL, Kamen A and Durocher Y. Large-scale transfection of mammalian cells for the fast production of recombinant protein. Mol. Biotechnology. 2006; 34, 2:225-237.

328. Han X, Sun L, Fang Q, Li D, Gong X, Wu Y, Yang S and Shen BQ. Transient expression of osteopontin in HEK293 cells in serum-free culture. Enz. Micr. Technol. 2007; 41, 1-2: 133-140.

329. Barnes LM, Bentley CM and Dickson AJ. Advances in animal cell recombinant protein production: GS-NS0 expression system. Cytotechnology. 2000; 32,109-123.

330. Chu L and Robinson DK. Industrial choices for protein production by large-scale cell culture. Curr. Opin. Biotechnol. 2001; 12(2):180-187.

331. Liu HF, Ma J, Winter C and Bayer R. Recovery and purification process development for monoclonal antibody production. MAbs. 2010; 2(5):480-499.

332. La Flamme AC, Buckner FS, Swindle J, Ajioka J and Van Voorhs WC. Expression of mammalian cytokines by *Trypanosoma cruzi* indicates unique signal sequence requirements and processing. Mol. Biochem. Parasitol. 1995; 75(1):25-31.

333. Godbey WT, Wu KK and Mikos AG. Poly(ethylenimine)-mediated gene delivery affects endothelial cell function and viability. Biomaterials. 2001; 22:471–480.

334. Sang Y, Xie K, Mu Y, Lei Y, Zhang B, Xiong S, Chen Y and Qi N. Salt ions and related parameters affect PEI-DNA particle size and transfection efficiency in Chinese hamster ovary cells. Cytotechnology. 2013; 29:1-8.

335. Rudolph C, Lausier J, Naundorf S, Müller RH and Rosenecker J. In vivo gene delivery to the lung using polyethylenimine and fractured polyamidoamine dendrimers. J. Gene Med. 2000, 2 (4): 269–278.

336. Akinc A, Thomas M, Klibanov AM and Langer R. Exploring polyethylenimine-mediated DNA transfection and the proton sponge hypothesis. J. Gene Med. 2004; 7 (5): 657–663.

337. Boussif O, Lezoualc'h F, Zanta MA, Mergny MD, Scherman D, Demeneix B and Behr JP. A versatile vector for gene and oligonucleotide transfer into cells in culture and in vivo: polyethylenimine. Proc. Natl. Acad. Sci. 1995; 92:7297–7301.

338. Kichler A, Leborgne C, Coeytaux E and Danos O. Polyethylenimine-mediated gene delivery: a mechanistic study. J. Gene Med. 2001; 3:135–144.

339. Schlaeger EJ and Christensen K. Transient gene expression in mammalian cells grown in serum-free suspension culture. Cytotechnology. 1999; 30:1-3, 71-83.

340. Teule F, Cooper AR, Furin WA, Bittencourt D, Rech EL, Brooks A and Lewis RV. A protocol for the production of recombinant spider silk-like proteins for artificial fiber spinning. Nat. Protocols. 2009; 4(3):341-355.

341. LaRocca TJ, Katona LI, Thanassi DG and Benach JL. Bactericidal action of a complement-independent antibody against relapsing fever *Borrelia* resides in its variable region. J. Immunol. 2008; 1; 180(9):6222-6228.

342. Sonati T, Reimann RR, Falsig J, Baral PK, O'Connor T, Hornemann S, Yaganoglu S, Li B, Herrmann US, Wieland B, Swayampakula M, Rahman MH, Das D, Kav N, Riek R, Liberski PP, James MN and Aguzzi A. The toxicity of antiprion antibodies is mediated by the flexible tail of the prion protein. Nature. 2013; 5; 501(7465):102-106.

343. Thompson DB, Cronican JJ and Liu DR. Engineering and identifying supercharged proteins for macromolecule delivery into mammalian cells. Methods Enzymol. 2012; 503:293-319.

344. Willuda J, Honegger A, Waibel R, Schubiger PA, Stahel R, Zangemeister-Wittke U and Pluckthun A. High thermal stability is essential for tumor targeting of antibody fragments: engineering of a humanized anti-epithelial glycoprotein-2 (epithelial cell adhesion molecule) single-chain Fv fragment. Cancer Res. 1999; 59, 5758–5767.

345. Worn A and Pluckthun A. Stability engineering of antibody single-chain Fv fragments. J. Mol. Biol. 2001; 305, 989–1010.

346. Yang J, James E, Gates TJ, Delong JH, Lafond RE, Malhotra U and Kwok WW. CD4+ T cells recognize unique and conserved H1N1 influenza hemagglutinin epitopes after natural infection and vaccination. Int. Immunol. 2013; 25(8): 444-457.

347. Laniel MA, Beliveau A and Guerin SL. Electrophoretic mobility shift assays for the analysis of DNA-protein interactions. Methods Mol. Biol. 2001; 148:13-30.

348. Geoghegan JC, Gilmore BL and Davidson BL. Gene silencing mediated by siRNA-binding fusion proteins is attenuated by double-stranded RNA-binding domain structure. Mol. Ther. Nucleic Acids. 2012; 13; 1:1-9.

349. Dai Y and Grant S. Targeting multiple arms of the apoptotic regulatory machinery. Cancer Res. 2007; 67: 2908–2911.

350. Sorensen RB, Nielsen OJ, Straten P and Andersen MH. Functional capacity of MCL1-specific cytotoxic T-cells. Leukemia. 2006; 20:1457–1458.

351. Opferman JT, Iwasaki H, Ong CC, Suh H, Mizuno S, Akashi K and Korsmeyer SJ. Obligate role of anti-apoptotic MCL1 in the survival of hematopoietic stem cells. Science. 2005; 307:1101–1104.

352. Opferman JT, Letai A, Beard C, Sorcinelli MD, Ong CC and Korsmeyer SJ. Development and maintenance of B and T lymphocytes requires anti-apoptotic MCL1. Nature. 2003; 11; 426(6967):671-676.

353. Petlickovski A, Laurenti L, Li X, Marietti S, Chiusolo P, Sica S, Leone G and Efremov DG. Sustained signaling through the B-cell receptor induces MCL1 and promotes survival of chronic lymphocytic leukemia B cells. Blood. 2005; 105: 4820-4827.

354. Andersen MH, Becker JC and Straten P. The anti-apoptotic member of the Bcl-2 family MCL1 is a CTL target in cancer patients. Leukemia. 2005; 19: 484–485.

355. Sheridan C. Proof of concept for next-generation nanoparticle drugs in humans. Nat. Biotechnol. 2012; 30, 471–473.

356. Sahay G, Alakhova DY and Kabanov AV. Endocytosis of nanomedicines. J. Control. Release. 2010; 145, 182–195.

357. Wang J, Byrne JD, Napier ME and DeSimone JM. More effective nanomedicines through particle design. Small. 2011; 7, 1919–1931.

358. Sahay G, Querbes W, Alabi C, Eltoukhy A, Sarkar S, Zurenko C, Karagiannis E, Love K, Chen D, Zoncu R, Buganim Y, Schroeder A, Langer R and Anderson DG. Efficiency of siRNA delivery by lipid nanoparticles is limited by endocytic recycling. Nat. Biotechnol. 2013; 31(7): 653-658.

359. Krauss J, Arndt MA, Vu BK, Newton DL and Rybak SM. Targeting malignant B-cell lymphoma with a humanized anti-CD22 scFv-angiogenin immunoenzyme. Br. J. Haematol. 2005; 128(5): 602-609.

360. Bang S, Nagata S, Onda M, Kreitman RJ and Pastan I. HA22 (R490A) is a recombinant immunotoxin with increased antitumor activity without an increase in animal toxicity. Clin. Cancer Res. 2005; 15; 11(4):1545-1550.

361. Salvatore G, Beers R, Margulies I, Kreitman RJ and Pastan I. Improved cytotoxic activity toward cell lines and fresh leukemia cells of a mutant anti-CD22 immunotoxin obtained by antibody phage display. Clin. Cancer Res. 2002; 8(4): 995-1002.

362. Wang B, Liang M, Yao Z, Vainshtein I, Lee R, Schneider A, Zusmanovich M, Jin F, O'Connor K, Donato-Weinstein B, Iciek L, Lavallee T and Roskos L. Pharmacokinetic and pharmacodynamic comparability study of moxetumomab pasudotox, an immunotoxin targeting CD22, in cynomolgus monkeys. J. Pharm. Sci. 2013; 102(1):250-261.

363. Decker T, Oelsner M, Kreitman RJ, Salvatore G, Wang QC, Pastan I, Peschel C and Licht T. Induction of caspase-dependent programmed cell death in B-cell chronic lymphocytic leukemia by anti-CD22 immunotoxins. Blood. 2004; 1; 103(7): 2718-2726.

364. Du X, Youle RJ, Fitzgerald DJ and Pastan I. Pseudomonas exotoxin A-mediated apoptosis is Bak dependent and preceded by the degradation of MCL1. Mol. Cell Biol. 2010; 30:3444-3452.

365. Taniai M, Grambihler A, Higuchi H, Werneburg N, Bronk SF, Farrugia DJ, Kaufmann SH and Gores GJ. MCL1 mediates tumor necrosis factor-related apoptosis-inducing ligand resistance in human cholangiocarcinoma cells. Cancer Res. 2004; 64(10):3517-3524.

366. Aichberger KJ, Mayerhofer M, Krauth MT, Skvara H, Florian S, Sonneck K, Akgul C, Derdak S, Pickl WF, Wacheck V, Selzer E, Monia BP, Moriggl R, Valent P and Sillaber C. Identification of MCL1 as a BCR/ABL-dependent target in chronic myeloid leukemia (CML): evidence for cooperative antileukemic effects of imatinib and MCL1 antisense oligonucleotides. Blood. 2005; 105(8):3303-3311.

367. Thallinger C, Wolschek MF, Maierhofer H, Skvara H, Pehamberger H, Monia BP, Jansen B, Wacheck V and Selzer E. Mcl-1 is a novel therapeutic target for human sarcoma: synergistic inhibition of human sarcoma xenotransplants by a combination of

MCL1 antisense oligonucleotides with low-dose cyclophosphamide. Clin. Cancer Res. 2004; 10:4185-4191.

368. Thallinger C, Wolschek MF, Wacheck V, Maierhofer H, Gunsberg P, Polterauer P, Pehamberger H, Monia BP, Selzer E, Wolff K and Jansen B. MCL1 antisense therapy chemosensitizes human melanoma in a SCID mouse xenotransplantation model. J. Invest. Dermatol. 2003; 120(6):1081-1086.

369. Liu H, Peng HW, Cheng YS, Yuan HS and Yang-Yen HF. Stabilization and enhancement of the anti-apoptotic activity of MCL1 by TCTP. Mol. Cell Biol. 2005; 25(8):3117-3126.

370. Schubert KM and Duronio V. Distinct roles for extracellular-signal regulated protein kinase (ERK) mitogen-activated protein kinases and phosphatidylinositol 3-kinase in the regulation of MCL1 synthesis. Biochem. J. 2001; 356 (2):473-480.

371. Moulding DA, Akgul C, Derouet M, White MR and Edwards SW. BCL-2 family expression in human neutrophils during delayed and accelerated apoptosis. J. Leukoc. Biol. 2001; 70, 783–792.

372. Chao JR, Wang JM, Lee SF, Peng HW, Lin YH, Chou CH, Li JC, Huang HM, Chou CK, Kuo ML, Yen JJ and Yang-Yen HF. MCL1 is an immediate-early gene activated by the granulocyte-macrophage colony-stimulating factor (GM-CSF) signaling pathway and is one component of the GM-CSF viability response. Mol. Cell. Biol.1998; 18, 4883–4898.

373. Akgul C. MCL1 is a potential therapeutic target in multiple types of cancer. Cell Mol. Life Sci. 2009; 66(8):1326-1336.

374. Zhou T, Li G, Cao B, Liu L, Cheng Q, Kong H, Shan C, Huang X, Chen J and Gao N. Downregulation of MCL1 through inhibition of translation contributes to benzyl isothiocyanate-induced cell cycle arrest and apoptosis in human leukemia cells. Cell Death Dis. 2013; 28; 4:1-11.

375. Binsky-Ehrenreich I, Marom A, Sobotta MC, Shvidel L, Berrebi A, Hazan-Halevy I, Kay S, Aloshin A, Sagi I, Goldenberg DM, Leng L, Bucala R, Herishanu Y, Haran M and Shachar I. CD84 is a survival receptor for CLL cells. Oncogene. 2013; 25: 1-11.

376. Reagan-Shaw S and Ahmad N. Silencing of polo-like kinase (Plk) 1 via siRNA causes induction of apoptosis and impairment of mitosis machinery in human prostate cancer cells: implications for the treatment of prostate cancer. FASEB J. 2005; 19(6):611-623.

377. Liu X and Erikson RL. Polo-like kinase (Plk1) depletion induces apoptosis in cancer cells. Proc. Natl. Acad. Sci. 2003; 13; 100(10):5789-5794.

378. Spankuch-Schmitt B, Bereiter-Hahn J, Kaufmann M, Strebhardt K. Effect of RNA silencing of polo-like kinase-1 (PLK1) on apoptosis and spindle formation in human cancer cells. J. Natl. Cancer Inst. 2002; 18; 94(24):1863-1877.

379. Donnelly JG. Pharmacogenetics in cancer chemotherapy: balancing toxicity and response. Ther. Drug Monit. 2004; 26(2):231-235.

380. Allen TM. Ligand-targeted therapeutics in anticancer therapy. Nat. Rev. Cancer. 2002; 2: 750-763.

381. Yuan F, Leunig M, Huang SK, Berk DA, Papahadjopoulos D and Jain RK. Microvascular permeability and interstitial penetration of sterically stabilized (stealth) liposomes in a human tumor xenograft. Cancer Res. 1994; 54: 3352-3356.

382. Hashizume H, Baluk P, Morikawa S, McLean JW, Thurston G, Roberge S, Jain RK and McDonald DM. Openings between defective endothelial cells explain tumor vessel leakiness. Am. J. Pathol. 2000; 156: 1363-1380.

383. Ruoslahti E. Specialization of tumour vasculature.Nat. Rev. Cancer. 2002; 2:83-90.

384. Yu YH, Kim E, Park DE, Shim G, Lee S, Kim YB, Kim CW and Oh YK. Cationic solid lipid nanoparticles for co-delivery of paclitaxel and siRNA. Eur. J. Pharm. Biopharm. 2012; 80(2):268-273.

385. Oltersdorf T, Elmore SW, Shoemaker AR, Armstrong RC, Augeri DJ, Belli BA, Bruncko M, Deckwerth TL, Dinges J, Hajduk PJ, Joseph MK, Kitada S, Korsmeyer SJ, Kunzer AR, Letai A, Li C, Mitten MJ, Nettesheim DG, Ng S, Nimmer PM, O'Connor JM, Oleksijew A, Petros AM, Reed JC, Shen W, Tahir SK, Thompson CB, Tomaselli KJ, Wang B, Wendt MD, Zhang H, Fesik SW and Rosenberg SH. An inhibitor of Bcl-2 family proteins induces regression of solid tumours. Nature. 2005; 2; 435 (7042): 677-681.

386. Kojima K, Konopleva M, Samudio IJ, Schober WD, Bornmann WG and Andreeff M. Concomitant inhibition of MDM2 and Bcl-2 protein function synergistically induce mitochondrial apoptosis in AML. Cell Cycle. 2006; 5 (23): 2778–2786.

387. Chauhan D, Velankar M, Brahmandam M, Hideshima T, Podar K, Richardson P, Schlossman R, Ghobrial I, Raje N, Munshi N and Anderson KC. A novel Bcl-2/Bcl-X(L)/Bcl-w inhibitor ABT-737 as therapy in multiple myeloma. Oncogene. 2006; 26 (16): 2374–2380.

388. van Delft MF, Wei AH, Mason KD, Vandenberg CJ, Chen L, Czabotar PE, Willis SN, Scott CL, Day CL, Cory S, Adams JM, Roberts AW and Huang DC. The BH3 mimetic ABT-737 targets selective Bcl-2 proteins and efficiently induces apoptosis via Bak/Bax if Mcl-1 is neutralized. Cancer Cell. 2006; 10(5):389-399.

389. Del Gaizo Moore V, Brown JR, Certo M, Love TM, Novina CD and Letai A. Chronic lymphocytic leukemia requires BCL2 to sequester prodeath BIM, explaining sensitivity to BCL2 antagonist ABT-737. J. Clin. Invest. 2007; 117 (1): 112–121.

390. Tahir SK, Yang X, Anderson MG, Morgan-Lappe SE, Sarthy AV, Chen J, Warner RB, Ng SC, Fesik SW, Elmore SW, Rosenberg SH and Tse C. Influence of Bcl-2 family members on the cellular response of small-cell lung cancer cell lines to ABT-737. Cancer Res. 2007; 67(3):1176-1183.

391. Kang MH, Kang YH, Szymanska B, Wilczynska-Kalak U, Sheard MA, Harned TM, Lock RB and Reynolds CP. Activity of vincristine, L-ASP, and dexamethasone against acute lymphoblastic leukemia is enhanced by the BH3-mimetic ABT-737 in vitro and in vivo. Blood. 2007; 110(6):2057-2066.

392. Chen S, Dai Y, Harada H, Dent P and Grant S. MCL1 down-regulation potentiates ABT-737 lethality by cooperatively inducing Bak activation and Bax translocation. Cancer Res. 2007; 67 (2): 782–791.

393. Hausner SH, Abbey CK, Bold RJ, Gagnon MK, Marik J, Marshall JF, Stanecki CE and Sutcliffe JL. Targeted in vivo imaging of integrin alphavbeta6 with an improved radiotracer and its relevance in a pancreatic tumor model. Cancer Res. 2009; 15; 69(14):5843-5850.

394. Green BR, Catlin P, Zhang MM, Fiedler B, Bayudan W, Morrison A, Norton RS, Smith BJ, Yoshikami D, Olivera BM and Bulaj G. Conotoxins containing nonnatural backbone spacers: cladistic-based design, chemical synthesis, and improved analgesic activity. Chem. Biol. 2007; 14(4):399-407.

395. Choi YS, Lee JY, Suh JS, Kwon YM, Lee SJ, Chung JK, Lee DS, Yang VC, Chung CP and Park YJ. The systemic delivery of siRNAs by a cell penetrating peptide, low molecular weight protamine. Biomaterials. 2010; 31:1429-1443.

396. Lee LM, Chang LC, Wrobleski S, Wakefield TW and Yang VC. Low molecular weight protamine as nontoxic heparin/low molecular weight heparin antidote (III): preliminary in vivo evaluation of efficacy and toxicity using a canine model. Aaps Pharmsci. 2001; 3:1-8.

397. Xia HM, Gao XL, Gu GZ, Liu ZY, Zeng N, Hu Q, Song Q, Yao L, Pang Z, Jiang X, Chen J and Chen H. Low molecular weight protamine-functionalized nanoparticles for drug delivery to the brain after intranasal administration. Biomaterials. 2011; 32:9888-9898.

398. Liang JF, Zhen L, Chang LC and Yang VC. A less toxic heparin antagonist - low molecular weight protamine. Biochemistry (Moscow) 2003; 68:116-120.

399. Tsui B, Singh VK, Liang JF and Yang VC. Reduced reactivity towards antiprotamine antibodies of a low molecular weight protamine analogue. Thromb. Res. 2001; 101:417-420.

400. Sorgi FL, Bhattacharya S and Huang L. Protamine sulfate enhances lipid-mediated gene transfer. Gene Ther. 1997; 4(9): 961–968.

401. Junghans M, Kreuter J and Zimmer A. Antisense delivery using protamine-oligonucelotide particles. Nuc. Acids Res. 2000; 15; 28(10):1-8.

402. Junghans M, Kreuter J and Zimmer A. Phosphodiester and phosphorothioate condensation and preparation of antisense nanoparticles. Bioch. Biophys. Acta. 2001; 12; 1544(1-2):177-188.

403. Lochmann D, Wevermann J, Georgens C, Prassl R and Zimmer A. Albumin-protamine-oligonucleotide nanoparticles as a new antisense delivery system. Part 1: physicochemical characterization. Eur. J. Pharm. Bioparm. 2005; 59(3):419-429.

404. Wevermann J, Lochmann D, Georgens C and Zimmer A. Albumin-protamine-oligonucleotide-nanoparticles as a new antisense delivery system. Part 2: cellular uptake and effect. Eur. J. Pharm. Bioparm. 2005; 59(3):431-438.

405. Bandyopadhyay A and Raghavan S. Defining the role of integrin alpha v beta 6 in cancer. Curr. Drug Targets. 2009; 10(7):645-652.

406. Ramsay AG, Keppler MD, Jazayeri M, Thomas GJ, Parsons M, Violette S, Weinreb P, Hart IR and Marshall JF. HS1-associated protein X-1 regulates carcinoma cell migration and invasion via clathrin-mediated endocytosis of integrin alphavbeta6. Cancer Res. 2007; 1; 67(11):5275-5284.

407. DiCara D, Rapisarda C, Sutcliffe JL, Violette SM, Weinreb PH, Hart IR, Howard MJ and Marshall JF. Structure-function analysis of Arg-Gly-Asp helix motifs in alpha v beta 6 integrin ligands. J. Biol. Chem. 2007. 30; 282(13):9657-9665.

408. Saha A, Ellison D, Thomas GJ, Vallath S, Mather SJ, Hart IR and Marshall JF. High-resolution in vivo imaging of breast cancer by targeting the pro-invasive integrin alphavbeta6. J. Pathol. 2010; 222(1):52-63.

409. Gray BP, McGuire MJ and Brown KC. A liposomal drug platform overrides peptide ligand targeting to a cancer biomarker, irrespective of ligand affinity or density. PLoS One. 2013; 23; 8(8):1-19.

410. Oyama T, Sykes KF, Samli KN, Minna JD, Johnston SA and Brown KC. Isolation of lung tumor specific peptides from a random peptide library: generation of diagnostic and cell-targeting reagents. Cancer Lett. 2003; 30; 202(2):219-230.

411. Elayadi AN, Samli KN, Prudkin L, Liu YH, Bian A, Xie XJ, Wistuba II, Roth JA, McGuire MJ and Brown KC. A peptide selected by biopanning identifies the integrin αvβ6 as a prognostic biomarker for nonsmall cell lung cancer. Cancer Res. 2007; 67, 5889-5895.

412. Coughlan L, Vallath S, Saha A, Flak M, McNeish IA, Vassaux G, Marshall JF, Hart IR and Thomas GJ. In vivo retargeting of adenovirus type 5 to avb6 integrin results in

reduced hepatotoxicity and improved tumor uptake following systemic delivery. J Virol. 2009; 83: 6416–6428.

413. Eberlein C, Kendrew J, McDaid K, Alfred A, Kang JS, Jacobs VN, Ross SJ, Rooney C, Smith NR, Rinkenberger J, Cao A, Churchman A, Marshall JF, Weir HM, Bedian V, Blakey DC, Foltz IN and Barry ST. A human monoclonal antibody 264RAD targeting αvβ6 integrin reduces tumour growth and metastasis, and modulates key biomarkers in vivo. Oncogene. 2013; 12; 32(37):4406-4416.

414. Sato S, Tuscano JM, Inaoki M and Tedder TF. CD22 negatively and positively regulates signal transduction through the B lymphocyte antigen receptor. Semin. Immunol. 1998; 10(4), 287–297.

415. Vitetta ES, Stone M, Amlot P, Fay J, May R, Till M, Newman J, Clark P, Collins R, Cunningham D, Ghetie V, Uhr JW and Thorpe PE. Phase I immunotoxin trial in patients with B-cell lymphoma. Cancer Res. 1991; 51(15), 4052–4058.

416. de Vries JF, Zwaan CM, De Bie M, Voerman JS, den Boer ML, van Dongen JJ and van der Velden VH. The novel calicheamicin-conjugated CD22 antibody inotuzumab ozogamicin (CMC-544) effectively kills primary pediatric acute lymphoblastic leukemia cells. Leukemia. 2012; 26(2):255-264.

417. Kreitman RJ. Hairy cell leukemia-new genes, new targets. Curr. Hematol. Malig. Rep. 2013; 8(3):184-195.

418. Chen WC, Completo GC, Sigal DS, Crocker PR, Saven A and Paulson JC. In vivo targeting of B-cell lymphoma with glycan ligands of CD22. Blood. 2010; 10; 115(23):4778-4786.

419. Leonard JP, Coleman M, Ketas JC, Chadburn A, Furman R, Schuster MW, Feldman EJ, Ashe M, Schuster SJ, Wegener WA, Hansen HJ, Ziccardi H, Eschenberg M, Gayko U, Fields SZ, Cesano A and Goldenberg DM. Epratuzumab, a humanized anti-CD22 antibody, in aggressive non-Hodgkin's lymphoma: phase I/II clinical trial results. Clin. Cancer Res. 2004; 15; 10(16):5327-5334.

420. Biberacher V, Decker T, Oelsner M, Wagner M, Bogner C, Schmidt B, Kreitman RJ, Peschel C, Pastan I, Meyer Zum Büschenfelde C and Ringshausen I. The cytotoxicity of anti-CD22 immunotoxin is enhanced by bryostatin 1 in B-cell lymphomas through CD22 upregulation and PKC-βII depletion. Haematologica. 2012; 97(5):771-779.

421. French RR, Penney CA, Browning AC, Stirpe F, George AJ and Glennie MJ. Delivery of the ribosome-inactivating protein, gelonin, to lymphoma cells via CD22 and CD38 using bispecific antibodies. Br. J. Cancer. 1995; 71(5):986-994.

422. Pichon C, Goncalves C and Midoux P. Histidine-rich peptides and polymers for nucleic acids delivery. Adv. Drug. Del. Rev. 2001; 53, 75–94.

423. Midoux P, Pichon C, Yaouanc JJ and Jaffres PA. Chemical vectors for gene delivery: a current review on polymers, peptides and lipids containing histidine or imidazole as nucleic acids carriers. Br. J. Pharmacol. 2009; 157, 166–178.

424. Behr JP. The proton sponge: A trick to enter cells the viruses did not exploit. Chimia. 1997; 51, 34–36.

425. Cerutti H. RNA interference: traveling in the cell and gaining functions? Trends Genet. 2003; 19:39–46.

426. Lieberman J, Song E, Lee SK and Shankar P. Interfering with disease: opportunities and roadblocks to harnessing RNA interference. Trends Mol. Med. 2003; 9:397–403.

427. Shuey DJ, McMallus DE and Giordano T. RNAi: gene-silencing in therapeutic intervention. Drug Discov. Today. 2002; 7:1040–1046.

428. Jain KK. RNAi and siRNA in target validation. Drug Discov. Today. 2004; 9:307–309.

429. Mohammad R, Giri A and Goustin AS. Small-molecule inhibitors of Bcl-2 family proteins as therapeutic agents in cancer. Recent Pat. Anticancer Drug Discov. 2008; 3(1):20-30.

430. Pai SI, Lin YY, Macaes B, Meneshian A, Hung CF and Wu TC. Prospects of RNA interference therapy for cancer. Gene Ther. 2006; 13(6):464-477.

431. Cholewa BD, Liu X and Ahmad N. The role of polo-like kinase 1 in carcinogenesis: cause or consequence? Cancer Res. 2013; 73: 6848-6855.

432. Yim H. Current clinical trials with polo-like kinase 1 inhibitors in solid tumors. Anticancer Drugs. 2013; 14; 999-1006.

433. Bertrand JR, Pottier M, Vekris A, Opolon P, Maksimenko A and Malvy C. Comparison of antisense oligonucleotides and siRNAs in cell culture and in vivo. Biochem. Biophys. Res. Commun. 2002; 296: 1000–1004.

434. Schwarz DS, Hutvagner G, Du T, Xu Z, Aronin N and Zamore PD. Asymmetry in the assembly of the RNAi enzyme complex. Cell. 2003; 115: 199–208.

435. Heale BS, Soifer HS, Bowers C and Rossi JJ. siRNA target site secondary structure predictions using local stable substructures. Nuc. Acids Res. 2005; 33: 2-10.

436. Patzel V, Rutz S, Dietrich I, Koberle C, Scheffold A and Kaufmann SH. Design of siRNAs producing unstructured guide-RNAs results in improved RNA interference efficiency. Nat. Biotechnol. 2005; 23:1440–1444.

437. Sorensen DR, Leirdal M and Sioud M. Gene Silencing by systemic delivery of synthetic siRNAs in adult mice. J. Mol. Biol. 2003; 327: 761–766.

438. Sioud M and Sorensen DR. Cationic liposome-mediated delivery of siRNAs in adult mice. Biochem. Biophys .Res. Commun. 2003; 312: 1220–1225.

439. Behlke MA. Progress towards in vivo use of siRNAs. Mol. Ther. 2006; 13:644–670.

440. Budt M, Niederstadt L, Valchanova RS, Jonji S and Brune W. Specific inhibition of the PKR-mediated antiviral response by the murine cytomegalovirus proteins m142 and m143. J. Vitol. 2009; 83(3):1260-1270.

441. Hornung V, Guenthner-Biller M, Bourquin C, Ablasser A, Schlee M, Uematsu S, Noronha A, Manoharan M, Akira S, de Fougerolles A, Endres S and Hartmann G. Sequence-specific potent induction of IFN-alpha by short interfering RNA in plasmacytoid dendritic cells through TLR7. Nat. Med. 2005; 11: 263–270.

442. Marques JT and Williams BR. Activation of the mammalian immune system by siRNAs. Nat. Biotechnol. 2005; 23: 1399–1405.

443. Soutschek J, Akinc A, Bramlage B, Charisse K, Constien R, Donoghue M, Elbashir S, Geick A, Hadwiger P, Harborth J, John M, Kesavan V, Lavine G, Pandey RK, Racie T, Rajeev KG, Rohl I, Toudjarska I, Wang G, Wuschko S, Bumcrot D, Koteliansky V, Limmer S, Manoharan M and Vornlocher HP. Therapeutic silencing of an endogenous gene by systemic administration of modified siRNAs. Nature. 2004; 432: 173–178.

444. Hu-Lieskovan S, Heidel JD, Bartlett DW, Davis ME and Triche TJ. Sequence-specific knockdown of EWS-FLI1 by targeted, nonviral delivery of small interfering RNA inhibits tumor growth in a murine model of metastatic Ewing's sarcoma. Cancer Res. 2005; 65: 8984–8992.

445. McNamara JO 2nd, Andrechek ER, Wang Y, Viles KD, Rempel RE, Gilboa E, Sullenger BA and Giangrande PH. Cell type-specific delivery of siRNAs with aptamer-siRNA chimeras. Nat. Biotechnol. 2006; 24(8):1005-1015.

446. Thie H, Toleikis L, Li J, von Wasielewski R, Bastert G, Schirrmann T, Esteves IT, Behrens CK, Fournes B, Fournier N, de Romeuf C, Hust M and Dübel S. Rise and fall of an anti-MUC1 specific antibody. PLoS One. 2011; 6(1):1-19

447. Kirsch MI, Hülseweh B, Nacke C, Rülker T, Schirrmann T, Marschall H-J, Hust M and Dübel S. Development of human antibody fragments using antibody phage display for the detection and diagnosis of Venezuelan equine encephalitis virus (VEEV). BMC Biotechnol. 2008; 8:66: 1-15.

448. Colwill K and Gräslund S. A roadmap to generate renewable protein binders to the human proteome. Nat. Methods. 2011; 15; 8(7):551-558.

449. Girgis MD, Olafsen T, Kenanova V, McCabe KE, Wu AM and Tomlinson JS. Targeting CEA in pancreas cancer xenografts with a Mutated scFv-Fc antibody fragment. EJNMMI Res. 2011; 1(1); 24: 1-10.

450. Moutel S, El Marjou A, Vielemeyer O, Nizak C, Benaroch P, Dübel S and Perez F. A multi-Fc-species system for recombinant antibody production. BMC Biotechnol. 2009; 9(14):1-9.

451. Menzel C, Schirrmann T, Konthur Z, Jostock T and Dübel S. Human antibody RNase fusion protein targeting CD30+ lymphomas. Blood. 2008; 111:3830–3837.

452. Schirrmann T and Pecher G. Human natural killer cell line modified with a chimeric immunoglobulin T-cell receptor gene leads to tumor growth inhibition in vivo. Cancer Gene Ther. 2002; 9:390–398.

453. Schirrmann T and Pecher G. Specific targeting of CD33+ leukemia cells by a natural killer cell line modified with a chimeric receptor. Leuk. Res. 2005; 29:301–306.

454. Capodicasa C, Chiani P, Bromuro C, De Bernardis F, Catellani M, Palma AS, Liu Y, Feizi T, Cassone A, Benvenuto E and Torosantucci A. Plant production of anti-β-glucan antibodies for immunotherapy of fungal infections in humans. Plant Biotechnol. J. 2011; 9:776–787.

455. Rülker T, Voß L, Thullier P, O' Brien LM, Pelat T, Langermann C, Schirrmann T, Dübel S, Marschall H-J, Hust M and Hülseweh B. Isolation and characterisation of a human-like antibody fragment (scFv) that inactivates VEEV in vitro and in vivo. PLoS One. 2012; 7:1-12.

456. West AP Jr, Galimidi RP, Gnanapragasam PNP and Bjorkman PJ. Single-chain Fv based anti-HIV proteins: potential and limitations. J. Virol. 2012; 86:195–202.

457. Lobo ED, Hansen RJ and Balthasar JP. Antibody pharmacokinetics and pharmacodynamics. J. Pharmaceut. Sci. 2004; 93(11): 2645-2668.

458. Fitch JCK, Rollins S, Matis L, Alford B, Aranki S, Collard CD, Dewar M, Elefteriades J, Hines R, Kopf G, Kraker P, Li L, O'Hara R, Rinder C, Rinder H, Shaw R, Smith B, Stahl G and Shernan SK. Pharmacology and biological efficacy of a recombinant, humanized, single-chain antibody C5 complement inhibitor in patients undergoing coronary artery bypass graft surgery with cardiopulmonary bypass. Circulation. 1999; 100, 2499-2506.

459. Müller D, Karle A, Meissburger B, Höfig I, Stork R and Kontermann RE. Improved pharmacokinetics of recombinant bispecific antibody molecules by fusion to human serum albumin. J. Biol. Chem. 2007; 282, 12650-12660.

460. Schlereth B, Fichtner I, Lorenczewski G, Kleindienst P, Brischwein K, da Silva A, Kufer P, Lutterbuese R, Junghahn I, Kasimir-Bauer S, Wimberger P, Kimmig R and Baeuerle PA. Eradication of tumors from a human colon cancer cell line and from

ovarian cancer metastases in immunodeficient mice by a single-chain Ep-CAM-/CD3-bispecific antibody construct. Cancer Res. 2005; 65, 2882-2889.

461. Duncan R. Polymer conjugates as anticancer nanomedicines. Nat. Rev. Cancer. 2006; 6, 688-701.

462. Chapman AP. PEGylated antibodies and antibody fragments for improved therapy: a review. Adv. Drug Deliv. Rev. 2002; 54, 531-545.

463. Elliott S, Lorenzini T, Asher S, Aoki K, Brankow D, Buck L, Busse L, Chang D, Fuller J, Grant J, Hernday N, Hokum M, Hu S, Knudten A, Levin N, Komorowski R, Martin F, Navarro R, Osslund T, Rogers G, Rogers N, Trail G and Egrie J. Enhancement of therapeutic protein in vivo activities through glycoengineering. Nat. Biotechnol. 2003; 21, 414-421.

464. Horrow JC. Protamine: a review of its toxicity. Anesth. Analg. 1985; 64:348-361.

465. Baglin T, Barrowcliffe TW, Cohen A and Greaves M. Guidelines on the use and monitoring of heparin. Br. J. Haematol. 2006; 133:19-34.

466. Dunning J, Versteegh M, Fabbri A, Pavie A, Kolh P, Lockowandt U, Nashef SA and EACTS Audit and Guidelines Committee. Guideline on antiplatelet and anticoagulation management in cardiac surgery. Eur. J. Cardiothorac. Surg. 2008; 34:73-92.

467. Chudasama SL, Espinasse B, Hwang F, Qi R, Joglekar M, Afonina G, Wiesner MR, Welsby IJ, Ortel TL and Arepally GM. Heparin modifies the immunogenicity of positively charged proteins. Blood. 2010; 116(26): 6046-6053.

468. Bakchoul T, Zollner H, Amiral J, Panzer S, Selleng S, Kohlmann T, Brandt S, Delcea M, Warkentin TE, Sachs UJ and Greinacher A. Anti-protamine-heparin antibodies: incidence, clinical relevance and pathogenesis. Blood. 2013; 11; 121(15):2821-2827.

469. Koren E and Torchilin VP. Cell-penetrating peptides: breaking through to the other side. Trends Mol. Med. 2012; 18:385-393.

470. Seroogy CM and Fathman CG. The application of gene therapy in autoimmune diseases. Gene Ther. 2000; 7(1):9-13.

471. DeFatta RJ, Li Y and De Benedetti A. Selective killing of cancer cells based on translational control of a suicide gene. Cancer Gene Ther. 2002; 9(7):573-578.

472. Leung PS, Dhirapong A, Wu PY and Tao MH. Gene therapy in autoimmune diseases: challenges and opportunities. Autoimmun. Rev. 2010; 9(3):170-174.

473. Morris JC and Waldmann TA. Antibody-based therapy of leukaemia. Expert Rev. Mol. Med. 2009; 11:1-25.

474. Tedder TF and Isaacs CM. Isolation of cDNAs encoding the CD19 antigen of human and mouse B lymphocytes. A new member of the immunoglobulin superfamily. J. Immunol. 1989; 143 (2): 712–717.

475. Harwood NE and Batista FD. New insights into the early molecular events underlying B cell activation. Immunity. 2008; 28:609–619.

476. Uckun F, Jaszcz W, Ambrus J, Fauci AS, Gajl-Peczalska K, Song CW, Wick MR, Myers DE, Waddick K and Ledbetter JA. Detailed studies on expression and function of CD19 surface determinant by using B43 monoclonal antibody and the clinical potential of anti-CD19 immunotoxins. Blood. 1988; 71:13–29.

477. Shah SA, Halloran PM, Ferris CA, Levine BA, Bourret LA, Goldmacher VS and Blattler WA. Anti-B4-blocked ricin immunotoxin shows therapeutic efficacy in four different SCID mouse tumor models. Cancer Res. 1993; 53:1360–1367.

478. UckunFM, EvansWE, Forsyth CJ, Waddick KG, Ahlgren LT, Chelstrom LM, Burkhardt A, Bolen J and Myers DE. Biotherapy of B-cell precursor leukemia by targeting genistein to CD19-associated tyrosine kinases. Science. 1995; 267:886–891.

479. Multani PS, O'Day S, Nadler LM and Grossbard ML. Phase II clinical trial of bolus infusion anti-B4 blocked ricin immunoconjugate in patients with relapsed B-cell non-Hodgkin's lymphoma. Clin. Cancer Res. 1998; 4: 2599–2604.

480. Szatrowski TP, Dodge RK, Reynolds C, Westbrook CA, Frankel SR, Sklar J, Tewart CC, Hurd DD, Kolitz JE, Velez-Garcia E, Stone RM, Bloomfield CD, Schiffer CA and Larson RA. Lineage specific treatment of adult patients with acute lymphoblastic leukemia in first remission with anti-B4-blocked ricin or high-dose cytarabine: Cancer and Leukemia Group B Study 9311. Cancer. 2003; 97:1471–1480.

481. Lee ST, Jiang YF, Park KU, Woo AF and Neelapu SS. BiovaxID: a personalized therapeutic cancer vaccine for non-Hodgkin's lymphoma. Expert Opin. Biol. Ther. 2007; 7(1):113-122.

482. Constant SL. B lymphocytes as antigen-presenting cells for CD4+ T cell priming in vivo. J. Immunol. 1999; 162: 5695–5703.

483. Guo K, Li J, Tang JP, Tan CP, Hong CW, Al-Aidaroos AQ, Varghese L, Huang C and Zeng Q. Targeting intracellular oncoproteins with antibody therapy or vaccination. Sci. Transl. Med. 2011; 7; 3(99):1-10.

484. Lee TY, Lin CT, Kuo SY, Chang DK and Wu HC. Peptide-mediated targeting to tumor blood vessels of lung cancer for drug delivery. Cancer Res. 2007; 67: 10958-10965.

485. Lee TY, Wu HC, Tseng YL and Lin CT. A novel peptide specifically binding to nasopharyngeal carcinoma for targeted drug delivery. Cancer Res. 2004; 64: 8002-8008.

486. Lo A, Lin CT and Wu HC. Hepatocellular carcinoma cell-specific peptide ligand for targeted drug delivery. Mol. Cancer Ther. 2008; 7: 579-589.

487. Allen TM, Mumbengegwi DR and Charrois GJ. Anti-CD19-targeted liposomal doxorubicin improves the therapeutic efficacy in murine B-cell lymphoma and ameliorates the toxicity of liposomes with varying drug release rates. Clin. Cancer Res. 2005; 11: 3567-3573.

488. Pastorino F, Brignole C, Marimpietri D, Sapra P, Moase EH, Allen TM and Ponzoni M. Doxorubicin-loaded Fab' fragments of anti-disialoganglioside immunoliposomes selectively inhibit the growth and dissemination of human neuroblastoma in nude mice. Cancer Res. 2003; 63: 86-92.

489. Lopes de Menezes DE, Pilarski LM and Allen TM. In vitro and in vivo targeting of immunoliposomal doxorubicin to human B-cell lymphoma. Cancer Res. 1998; 58: 3320-3330.

490. Katanasaka Y, Ishii T, Asai T, Naitou H, Maeda N, Koizumi F, Miyagawa S, Ohashi N and Oku N. Cancer anti-neovascular therapy with liposome drug delivery systems targeted to BiP/GRP78. Int. J. Cancer. 2010; 127: 2685-2698.

491. Hussain S, Plückthun A, Allen TM and Zangemeister-Wittke U. Antitumor activity of an epithelial cell adhesion molecule–targeted nanovesicular drug delivery system. Mol. Cancer Ther. 2007; 6: 3019-3027.

492. Herringson TP and Altin JG. Effective tumor targeting and enhanced anti-tumor effect of liposomes engrafted with peptides specific for tumor lymphatics and vasculature. Int. J. Pharm. 2011; 411: 206-214.

493. Mencher SK and Wang LG. Promiscuous drugs compared to selective drugs (promiscuity by a virtue). BMC Clin. Pharmacol. 2005; 26; 5:3:1-7.

494. Talpaz M, Shah NP, Kantarjian H, Donato N, Nicoll J, Paquette R, Cortes J, O'Brien S, Nicaise C, Bleickardt E, Blackwood-Chirchir MA, iyer V, Chen TT, Huang F, Decillis AP and Sawyers CL. Dasatinib in imatinib-resistant Philadelphia chromosome-positive leukemias. N. Engl. J. Med. 2006; 15; 354(24):2531-2541.

495. Sawyers CL. Chronic myeloid leukemia. N. Engl. J. Med. 1999; 340:1330-1340.

496. An X, Tiwari AK, Sun Y, Ding PR, Ashby CR Jr and Chen ZS. BCR-ABL tyrosine kinase inhibitors in the treatment of Philadelphia chromosome positive chronic myeloid leukemia: a review. Leuk. Res. 2010; 34(10):1255-1268.

497. Shawver LK, Slamon D and Ullrich A. Smart drugs: Tyrosine kinase inhibitors in cancer therapy. Cancer Cell. 2002; 1(2):117-123.

498. Chan AC, Iwashima M, Turck CW and Weiss A. ZAP-70: a 70 kd protein-tyrosine kinase that associates with the TCR zeta chain. Cell. 1992; 71: 649–662.

499. Sup SJ, Domiati-Saad R, Kelley TW, Steinle R, Zhao X and His ED. ZAP-70 expression in B-cell hematologic malignancy is not limited to CLL/SLL. Am. J. Clin. Pathol. 2004; 122(4):582-587.

500. Butrym A, Mejewski M, Dzietczenia J, Kuliczkowski K and Mazur G. High CD74 expression correlates with ZAP70 expression in B cell chronic lymphocytic leukemia patients. Med. Oncol. 2013; 30(2):560:1-6.

501. Chen L, Widhopf G, Huynh L, Rassenti L, Rai KR, Weiss A and Kipps TJ. Expression of ZAP-70 is associated with increased B-cell receptor signaling in chronic lymphocytic leukemia. Blood. 2002; 15; 100(13):4609-4614.

502. Dielschneider R, Xiao W, Yoon JY, Noh E, Johnston JB and Gibson SB. Tyrosine kinase inhibitor Gefitinib selectivley induces apoptosis in Zap70+ CLL cells and inhibits B cell receptor signaling. Poster session presented at: American Association for Cancer Research. 104th Annual Meeting 2013; April 6-10; Washington, DC.

503. Zhuang Z, Zhou R, Xu X, Tian T, Liu Y, Liu Y, Lian P, Wang J and Xu K. Clinical significance of integrin αvβ6 expression effects on gastric carcinoma invasiveness and progression via cancer-associated fibroblasts. Med. Oncol. 2013; 30(3):1-8.

504. Cantor D, Slapetova I, Kan A, McQuade LR and Baker MS. Overexpression of αvβ6 integrin alters the colorectal cancer cell proteome in favor of elevated proliferation and a switching in cellular adhesion that increases invasion. J. Proteome Res. 2013; 7; 12(6):2477-2490.

505. Xue B, Wu W, Huang K, Xie T, Xu X, Zhang H, Qi C, Ge J and Yu Y. Stromal cell-derived factor-1 (SDF-1) enhances cells invasion by αvβ6 integrin-mediated signaling in ovarian cancer. Mol. Cell. Biochem. 2013; 380(1-2):177-184.

506. Hazelbag S, Kenter GG, Gorter A, Dreef EJ, Koopman LA, Violette SM, Weinreb PH and Fleuren GJ. Overexpression of the αvβ6 integrin in cervical squamous cell carcinoma is a prognostic factor for decreased survival. J. Pathol. 2007; 212(3):316-324.

507. Marelli UK, Rechenmacher F, Sobahi TR, Mas-Moruno C and Kessler H. Tumor targeting via integrin ligands. Front. Oncol. 2013; 30; 3:222:1-12.

508. Marsh D, Dickinson S, Neill GW, Marshall JF, Hart IR and Thomas GJ. Alphav beta6 integrin promotes the invasion of morphoeic basal cell carcinoma through stromal modulation. Cancer Res. 2008; 1; 68(9):3295-3303.

509. Al-Hazmi N, Thomas GJ, Speight PM and Whawell SA. The 120 kDa cell-binding fragment of fibronectin up-regulates migration of alphavbeta6-expressing cells by increasing matrix metalloproteinase-2 and -9 secretion. Eur. J. Oral. Sci. 2007; 115:454–458.

Appendices

Appendix 1: PCR and sequencing primers used in generation of Cy34.1.2 and HA22 scFv constructs (Table 11).

Table 11: Primer names, sequences, restriction sites and their purity.

Primer name	Primer sequence (5' to 3')	Primer purity
PCR primers		
Mouse Cγ1 γ1 for V_H cDNA	AGTTAGTTTGGGCAGCAGAT	Desalted
Mouse Cκ1 for V_L cDNA	GTAGAAGTTGTTCAAGAAGCACAC	Desalted
Poly-(G) tail anchor primer	ACGAATTCTAGAGTCGACCCCCCCCCCCCCC	Desalted
Nested Cγ2 primer	GCCAGTGGATAGACAGAT	Desalted
Nested Cκ2 primer	AG**ATG**TTAACTGCTCACTGGAT	Desalted
V_H *Hind*III forward primer	CAGAAGCTT**ATG**AGATGGAGCTGTATC	Desalted
V_H *Xho*I reverse primer	CGCTCGAGACAAAGTAGAATGAGTAAGT	Desalted
Common V_L *Sal*I forward primer	GGCGGGTCGACGGATATTGTGATGACGCAG	Desalted
V_L1 *EcoR*I reverse primer	TCGGAATTCCGGAAGTTCTAGATTTT	Desalted
V_L2 *Nhe*I reverse primer	TCGGCTAGCCGGAAGTTCTAGATTTT	Desalted
Protamine *Eco*RI forward oligo	AATTCCGATCACAATCACGATCACGATACTACCGAC AACGACAACGATCACGACGACGACGACGACGAT	HPLC-purified
Protamine *Xba*I reverse oligo	CTAGATCGTCGTCGTCGTCGTCGTGATCGTTGTCG TTGTCGGTAGTATCGTGATCGTGATTGTGATCGG	HPLC-purified
M13 forward primer	GTTTTCCCAGTCAGAC	Desalted
M13 reverse primer	CAGGAAACAGCTATGAC	Desalted
pHEN1 *Nco*I forward primer	GCC**ATG**GCCCAGGTCCAACTGCAGCAGCCT	Desalted
pHEN1 *Not*I reverse primer	GCGGCC GCGGGCCCTCAATGGTGGTGGTGATG	Desalted
HRV-3C *Bam*HI forward primer	AT**ATG**GATCCCTCGAGGTTCTCTTTCAGGGACCCC AGGTCCAACTGCAGCAGCCT	HPLC-purified
Poly-His *Nhe*I reverse primer	TGCAGCTAGCGGGCCCTCAATGGTGGTGGTGATG	Desalted
Cy34 *Sfi*I forward primer	ATAAGGCCCAGCCGGCCCAGGTCCAACTGCAGCA GC CT	Desalted
Cy34 *Sac*II reverse primer	ATATCCGCGGTTAATGGTGGTGGTGATGGTG	Desalted
pMH113 *Eco*RI forward primer	GCGGGAATTCATGGAAGTGCAGCTGGTGGAG	Desalted
pMH113 *Bgl*II reverse primer	AGCAGATCTGCTTTCCAGCTTGGTGCCTCCACC	Desalted
Protamine-His6 *Bgl*II forward primer	AGCAGATCTCGATCACAATCACGATGA	Desalted
Protamine-His6 *Nhe*I reverse primer	AGCGCTAGCTCAATGGTGGTGGTGATGGTG	Desalted
HA22 *Sfi*I forward primer	GGGGCCCAGCCGGCC**ATG**GAAGTGCAGCTGGTGG AGTCT	Desalted
HA22 *Sac*II reverse primer	ATATCCGCGGTTAATGGTGGTGGTGATGGTG	Desalted
pDisplay-F *Hind*III forward primer	GACCCAAGCTTGGTACCGAGCTCGGATCCA	Desalted
pDisplay-R *Sfi*I reverse primer	TGGATAGGCCGGCTGGGCCCCGTCACCAGTGGAA CCTGG	Desalted
Sequencing primers		
SV40 pA reverse primer	GAAATTTGTGATGCTATTGC	Desalted
T7 promoter forward primer	TAATACGACTCACTATAGGG	Desalted
F-LAP forward primer	ATTGAGGGCTTTCGCCTTAGC	Desalted
LMB3 forward primer	CAGGAAACAGCTATGAC	Desalted
pHEN1 reverse primer	GCGGCCGCGGGCCCTCAATGGTGGTGGTGATG	Desalted
BGH reverse primer	TAGAAGGCACAGTCGAGG	Desalted
pMH R-113 reverse primer	GGAGAGTTTCAGGGACCCTCCAGG CTTCACTAA	Desalted

Note: restriction sites are underlined; start codon is indicated in bold.

Appendix 2: Annotated sequences of the constructs used in this study.

Shown below are the whole sequences from the engineered constructs presented in this study. Only known unique restrictions sites are shown. One letter code translation is shown for one open reading frame where * indicates termination of transcription (stop codon). Only the forward 5' to 3' strand is shown for each construct. Sequencing data and restriction analysis of the constructs were performed by using the SerialCloner version 2.6.1 and the CLC Sequence Viewer version 4.6.2 softwares.

Annotated sequences for the following constructs are shown:

Cy34.1.2 V_H in pCR2.1 TA cloning vector
Cy34.1.2 V_L in pCR2.1 TA cloning vector
Cy34.1.2 scFv-His6 in pFastBac^{TM}1
Cy34.1.2 scFv-protamine-His6 in pFastBac^{TM}1
Cy34.1.2 scFv-His6 in pcDNA3 vector with V_H native signal sequence
Cy34.1.2 scFv-protamine-His6 in pcDNA3 vector with V_H native signal sequence
Cy34.1.2 scFv-His6 in pHEN1 vector with pelB signal sequence
Cy34.1.2 scFv-His6 in pcDNA3 with hLAP signal sequence-hLAP-HRV3C
Cy34.1.2 scFv-protamine-His6 in pcDNA3 with hLAP signal sequence-hLAP-HRV3C
Cy34.1.2 scFv-protamine-His6 in pDisplay vector with murine Ig κ chain signal sequence
HA22 scFv-protamine-His6 in pDisplay vector with murine Ig κ chain signal sequence
HA22 scFv-protamine-His6 in modified pDisplay vector with murine Ig κ chain signal sequence

Cy34.1.2 V_H (Cγ2) gene nucleotide and amino acid sequences in pCR2.1 TA cloning vector:

```
5'-- GCTCTCTATAGGGCGATTGGGCCCTCTAGATGCATGCTCGAGCGGCCGCCAGTGTGATGGAT
                     |EcoRI|      |poly-C sequence|
  ATCTGCAGAATTCGGCTTACGAATTCTGTCGACCCCCCCCCCCCCCGCTCACAGTTACTA
                |start codon| ……..       native signal sequence …….
  GGCACACAGGACCTCACC ATG AGA TGG AGC TGT ATC ATT CTC TTC TTG GTA GCA ACA GCT
                      M   R   W   S   C   I   I   L   F   L   V   A   T   A
   ……….     |
  ACA AGT GTC GAC TCC CAG GTC CAA CTG CAG CAG CCT GGG GCT GAA ATT GTG AGG CCT GGG
   T   S   V   D   S   Q   V   Q   L   Q   Q   P   G   A   E   I   V   R   P   G
  ACT TCA GTG AAG CTG TCC TGT AAG GCT TCA GGC TAC ACC TTT ACC GAC TAT TGG ATG AAC
   T   S   V   K   L   S   C   K   A   S   G   Y   T   F   T   D   Y   W   M   N
                                                       | MfeI |
  TGG GTG AAG CAA AGG CCT GGA CAA GGC CTT GAG TGG TTC GGA GCA ATT GAT CCT TCT GAT
   W   V   K   Q   R   P   G   Q   G   L   E   W   F   G   A   I   D   P   S   D
  AGT TAT ACT AGG TAC AAT CAA GAG TTC AAG GGC AAG GCC ACA TTG ACT GTA GAC ACA TCC
   S   Y   T   R   Y   N   Q   E   F   K   G   K   A   T   L   T   V   D   T   S
  TCC ACC ACA GCC TAC ATG CAG CTC AGC AGC CTG ACA TCC GAG GAC TCT GCG GTC TAT TTC
   S   T   T   A   Y   M   Q   L   S   S   L   T   S   E   D   S   A   V   Y   F
  TGT GCA AGA TCG GAC TAT ACT TAC TCA TTC TAC TTT GACTACTGGGGCCTAGGCACCACT
   C   A   R   S   D   Y   T   Y   S   F   Y   F
                                                       |EcoRI|
CTCACAGTCTCCTCAGCCAAAACGACACCCCCATCTGTCTATCCACTGGCAAGCCGAATTCCAGCACACTGGCGGCCGTTACTAGTGGATCC
GAGCTCGGTACCAAGCTTGGCGTAATCATGGTCATAGCTGTTTCCTGTGTGAAATTGTTATCCGCTCACAATTCCACACAACATACGAGCCG
GAAGCATAAAGTGTAAAGCCTGGGGTGCCTAATGAGTGAGCTAACTCACATTAATTGCGTTGCGCTCACTGCCCGCTTTCCAGTCGGGAAAC
CTGTCGTGCCAGCTGCATTAATGAATCGGCCAACGCGCGGGAGAGGCGGTTTTGCTATTGGGCGCTCTTCGCTTCCTCGCTCACTGACTCGG
CGCTCGGCGTCGGCTGCGGCGAGCGATCTCACT -- 3'
```

Cy34.1.2 V_L (Cκ2) gene nucleotide and amino acid sequences in pCR2.1 TA cloning vector:

```
5′ -- AGGGGATACAATTTCCACAGGAAACAGTATGACCATGATTACGCCAAGCTTGGTACCGAGC
                                                |EcoRI|    |poly-C sequence|
TCGGATCCACTAGTAACGGCCGCCAGTGTGCTGGAATTCGGCTTACGAATTCTAGAGTCCCCCCCCCCCCCCCACGAGGTTCTCTGCTCAGCT
TCTGGGGCTGCTTGTGCTCTGGATCCCTGGATCCACTGCA
                  GAT ATT GTG ATG ACG CAG GCT GCA TTC TCC AAT CCA GTC ACT CTT GGA
                   D   I   V   M   T   Q   A   A   F   S   N   P   V   T   L   G
                       |  SbfI  |
  ACA TCA GCT TCC ATC TCC TGC AGG TCT AGT AAG AGT CTC CTA CAT AGT AAT GGC ATC ACT
   T   S   A   S   I   S   C   R   S   S   K   S   L   L   H   S   N   G   I   T
  TAT TTG TAT TGG TAT CTG CAG AAG CCA GGC CAG TCT CCT CAG CTC CTG ATT TAT CAG ATG
   Y   L   Y   W   Y   L   Q   K   P   G   Q   S   P   Q   L   L   I   Y   Q   M
  TCC AAC CTT GCC TCA GGA GTC CCA GAC AGG TTC AGT AGC AGT GGG TCA GGA ACT GAT TTC
   S   N   L   A   S   G   V   P   D   R   F   S   S   S   G   S   G   T   D   F
  ACA CTG AGA ATC AGC AGA GTG GAG GCT GAG GAT GTG GGT GTT TAT TAC TGT GCT CAA
   T   L   R   I   S   R   V   E   A   E   D   V   G   V   Y   Y   C   A   Q
  | XbaI |
AAT CTA GAA CTT CCG TGGACGTTCGGTGGAGGCACCAAGCTGGAAATCAAACGGGCTGATGCT
 N   L   E   L   P                                  |EcoRI|
  GCACCAACTGTATCCATCTTCCCACCATCCAGTGAGCAGTTAACATCTAAGCGAATTCTGCAGATATCCATCACACTGGCGGCCGCT
CGAGCATGCATCTAGAGGGCCCAATCGCCCTGGAGATGGC  -- 3′
```

Cy34.1.2 scFv-His6 nucleotide and amino acid sequences in pFastBac™1 vector:

```
5’TCCTAGTGCGCGCTGCGGTGGTGCTGACCCCGGATGAAGTGGTTCGCATCCTCGGTTTTCTGGAAGGCGAGCATCGTTTGTTCGCCCAGG
ACTCTAGCTATAGTTCTAGTGGTTGGCTACGTATACTCCGGAATATTAATAGATCATGGAGATAATTAAAATGATAACCATCTCGCAAATAA
ATAAGTATTTTACTGTTTTCGTAACAGTTTTGTAATAAAAAAACCTATAAATATTCCGGATTATTCATACCGTCCCACCATCGGGCGCGGAT
CCAAGGTACCACCGCCA

 AAG CTT ATG
  K   L   M
 AGA TGG AGC TGT ATC ATT CTC TTC TTG GTA GCA ACA GCT ACA AGT GTC GAC TCC CAG GTC
  R   W   S   C   I   I   L   F   L   V   A   T   A   T   S   V   D   S   Q   V
 CAA CTG CAG CAG CCT GGG GCT GAA ATT GTG AGG CCT GGG ACT TCA GTG AAG CTG TCC TGT
  Q   L   Q   Q   P   G   A   E   I   V   R   P   G   T   S   V   K   L   S   C
 AAG GCT TCA GGC TAC ACC TTT ACC GAC TAT TGG ATG AAC TGG GTG AAG CAG AGG CCT GGA
  K   A   S   G   Y   T   F   T   D   Y   W   M   N   W   V   K   Q   R   P   G
                              | MfeI |
 CAA GGC CTT GAG TGG TTC GGA GCA ATT GAT CCT TCT GAT AGT TAT ACT AGG TAC AAT CAA
  Q   G   L   E   W   F   G   A   I   D   P   S   D   S   Y   T   R   Y   N   Q
 GAG TTC AAG GGC AAG GCC ACA TTG ACT GTA GAC ACA TCC TCC ACC ACA GCC TAC ATG CAG
  E   F   K   G   K   A   T   L   T   V   D   T   S   S   T   T   A   Y   M   Q
 CTC AGC AGC CTG ACA TCC GAG GAC TCT GCG GTC TAT TTC TGT GCA AGA TCG GAC TAT ACT
  L   S   S   L   T   S   E   D   S   A   V   Y   F   C   A   R   S   D   Y   T
 TAC TCA TTC TAC TTT GTC TCG AGC GGT GGA GGC GGT TCA GGC GGA GGT GGC AGC GGC GGT
  Y   S   F   Y   F   V   S   S   G   G   G   G   S   G   G   G   G   S   G   G
 GGC GGG TCG ACG GAT ATT GTG ATG ACG CAG GCT GCA TTC TCC AAT CCA GTC ACT CTT GGA
  G   G   S   T   D   I   V   M   T   Q   A   A   F   S   N   P   V   T   L   G
                      |  SbfI  |
 ACA TCA GCT TCC ATC TCC TGC AGG TCT AGT AAG AGT CTC CTA CAT AGT AAT GGC ATC ACT
  T   S   A   S   I   S   C   R   S   S   K   S   L   L   H   S   N   G   I   T
 TAT TTG TAT TGG TAT CTG CAG AAG CCA GGC CAG TCT CCT CAG CTC CTG ATT TAT CAG ATG
  Y   L   Y   W   Y   L   Q   K   P   G   Q   S   P   Q   L   L   I   Y   Q   M
 TCC AAC CTT GCC TCA GGA GTC CCA GAC AGG TTC AGT AGC AGT GGG TCA GGA ACT GAT TTC
  S   N   L   A   S   G   V   P   D   R   F   S   S   S   G   S   G   T   D   F
 ACA CTG AGA ATC AGC AGA GTG GAG GCT GAG GAT GTG GGT GTT TAT TAC TGT GCT CAA
  T   L   R   I   S   R   V   E   A   E   D   V   G   V   Y   Y   C   A   Q
  | XbaI |                 |  hexahistidine tag  |
AAT CTA GAA CTT CCG GCT AGA CAC CAT CAC CAC CAC CAT TGA GGGCCCGAGCTTGTCGAGAAG
 N   L   E   L   P   A   R   H   H   H   H   H   H   *

  TACTAGAGGATCATAATCAGCCATACCACATTTGTAGAGGTTTTACTTGCTTAAAAAACCTCCCACACTCCGC 3’
```

Cy34.1.2 scFv-protamine-His6 nucleotide and amino acid sequences in pFastBac™1 vector:

```
5’TCCTACCTCGCGCTGCGGTGGTGCTGACCCCGGATGAAGTGGTTCGCATCCTCGGTTTTCTGGAAGGCGAGCATCGTTTGTTCGCCCAGG
ACTCTAGCTATAGTTCTAGTGGTTGGCTACGTATACTCCGGAATATTAATAGATCATGGAGATAATTAAAATGATAACCATCTCGCAAATAA
ATAAGTATTTTACTGTTTTCGTAACAGTTTTGTAATAAAAAAACCTATAAATATTCCGGATTATTCATACCGTCCCACCATCGGGCGCGGA
TCCAAGGTACCACCGCCA AAG CTT ATG
                   K   L   M
  AGA TGG AGC TGT ATC ATT CTC TTC TTG GTA GCA ACA GCT ACA AGT GTC GAC TCC CAG GTC
   R   W   S   C   I   I   L   F   L   V   A   T   A   T   S   V   D   S   Q   V
  CAA CTG CAG CAG CCT GGG GCT GAA ATT GTG AGG CCT GGG ACT TCA GTG AAG CTG TCC TGT
   Q   L   Q   Q   P   G   A   E   I   V   R   P   G   T   S   V   K   L   S   C
  AAG GCT TCA GGC TAC ACC TTT ACC GAC TAT TGG ATG AAC TGG GTG AAG CAG AGG CCT GGA
   K   A   S   G   Y   T   F   T   D   Y   W   M   N   W   V   K   Q   R   P   G
                               | MfeI |
  CAA GGC CTT GAG TGG TTC GGA GCA ATT GAT CCT TCT GAT AGT TAT ACT AGG TAC AAT CAA
   Q   G   L   E   W   F   G   A   I   D   P   S   D   S   Y   T   R   Y   N   Q
  GAG TTC AAG GGC AAG GCC ACA TTG ACT GTA GAC ACA TCC TCC ACC ACA GCC TAC ATG CAG
   E   F   K   G   K   A   T   L   T   V   D   T   S   S   T   T   A   Y   M   Q
  CTC AGC AGC CTG ACA TCC GAG GAC TCT GCG GTC TAT TTC TGT GCA AGA TCG GAC CAT ACT
   L   S   S   L   T   S   E   D   S   A   V   Y   F   C   A   R   S   D   H   T
  TAC TCA TTC TAC TTT GTC TCG AGC GGT GGA GGC GGT TCA GGC GGA GGT GGC AGC GGC GGT
   Y   S   F   Y   F   V   S   S   G   G   G   G   S   G   G   G   G   S   G   G
  GGC GGG TCG ACG GAT ATT GTG ATG ACG CAG GCT GCA TTC TCC AAT CCA GTC ACT CTT GGA
   G   G   S   T   D   I   V   M   T   Q   A   A   F   S   N   P   V   T   L   G
                       |  SbfI  |
  ACA TCA GCT TCC ATC TCC TGC AGG TCT AGT AAG AGT CTC CTA CAT AGT AAT GGC ATC ACT
   T   S   A   S   I   S   C   R   S   S   K   S   L   L   H   S   N   G   I   T
  TAT TTG TAT TGG TAT CTG CAG AAG CCA GGC CAG TCT CCT CAG CTC CTG ATT TAT CAG ATG
   Y   L   Y   W   Y   L   Q   K   P   G   Q   S   P   Q   L   L   I   Y   Q   M
  TCC AAC CTT GCC TCA GGA GTC CCA GAC AGG TTC AGT AGC AGT GGG TCA GGA ACT GAT TTC
   S   N   L   A   S   G   V   P   D   R   F   S   S   S   G   S   G   T   D   F
  ACA CTG AGA ATC AGC AGA GTG GAG GCT GAG GAT GTG GGT GTT TAT TAC TGT GCT CAA AAT
   T   L   R   I   S   R   V   E   A   E   D   V   G   V   Y   Y   C   A   Q   N
                   |EcoRI|
  CTA GAA CTT CCG GAA TTC
   L   E   L   P   E   F
|                                truncated protamine                                  |
CGA TCA CAA TCA CGA TCA CGA TAC TAC CGA CAA CGA CAA CGA TCA CGA CGA CGA CGA CGA CGA TCT AGA
 R   S   Q   S   R   S   R   Y   Y   R   Q   R   Q   R   S   R   R   R   R   R   R   S   R
|   hexahistidine tag |
CAC CAT CAC CAC CAC CAT TGA GGGCCCGAGCTT
 H   H   H   H   H   H   *

  GTCGAGAAGTATGGGATCATAATCAGCCATACCACATTTGTAGAGGTTTTACTTGCTTAAAAAACCTCCCACACTCCTCACTCGG 3’
```

Cy34.1.2 scFv-His6 nucleotide and amino acid sequences including the V_H native signal sequence in pcDNA3 vector:

```
                                                                    5’end of hCMV
                                                                    |
5’ GAATCTGCTTAGGGTTAGGCGTTTTGCGCTGCTTCGCGATGTACGGGCCAGATATACGCGTTGACATTGATTATTGACTAGTTATT
                                                      CMV enhancer region (5’end)
                                                      |
   AATAGTAATCAATTACGGGGTCATTAGTTCATAGCCCATATATGGAGTTCCGCGTTACATAACTTACGGTAAATGGCCCGCCTGGC
   TGACCGCCCAACGACCCCCGCCCATTGACGTCAATAATGACGTATGTTCCCATAGTAACGCCAATAGGGACTTTCCATTGACGTCA
   ATGGGTGGAGTATTTACGGTAAACTGCCCACTTGGCAGTACATCAAGTGTATCATATGCCAAGTACGCCCCCTATTGACGTCAATG
   ACGGTAAATGGCCCGCCTGGCATTATGCCCAGTACATGACCTTATGGGACTTTCCTACTTGGCAGTACATCTACGTATTAGTCATC
   GCTATTACCATGGTGATGCGGTTTTGGCAGTACATCAATGGGCGTGGATAGCGGTTTGACTCACGGGGATTTCCAAGTCTCCACCC
      CMV enhancer region (3’end)
                                  |
   CATTGACGTCAATGGGAGTTTGTTTTGGCACCAAAATCAACGGGACTTTCCAAAATGTCGTAACAACTCCGCCCCATTGACGCAAA
                                    TATA box     3'end hCMV promoter
                                    ----         |
   TGGGCGGTAGGCGTGTACGGTGGGAGGTCTATATAAGCAGAGCTCTCTGGCT……..

            |VH
… TTCCTTAG ATG AGC TGT ATC ATT CTC TTC TTG GTA GCA ACA GCT ACA AGT GTC GAC TCC CAG
             M   S   C   I   I   L   F   L   V   A   T   A   T   S   V   D   S   Q
  GTC CAA CTG CAG CAG CCT GGG GCT GAA ATT GTG AGG CCT GGG ACT TCA GTG AAG CTG TCC
   V   Q   L   Q   Q   P   G   A   E   I   V   R   P   G   T   S   V   K   L   S
  TGT AAG GCT TCA GGC TAC ACC TTT ACC GAC TAT TGG ATG AAC TGG GTG AAG CAG AGG CCT
   C   K   A   S   G   Y   T   F   T   D   Y   W   M   N   W   V   K   Q   R   P
                                  | MfeI |
  GGA CAA GGC CTT GAG TGG TTC GGA GCA ATT GAT CCT TCT GAT AGT TAT ACT AGG TAC AAT
   G   Q   G   L   E   W   F   G   A   I   D   P   S   D   S   Y   T   R   Y   N
  CAA GAG TTC AAG GGC AAG GCC ACA TTG ACT GTA GAC ACA TCC TCC ACC ACA GCC TAC ATG
   Q   E   F   K   G   K   A   T   L   T   V   D   T   S   S   T   T   A   Y   M
  CAG CTC AGC AGC CTG ACA TCC GAG GAC TCT GCG GTC TAT TTC TGT GCA AGA TCG GAC TAT
   Q   L   S   S   L   T   S   E   D   S   A   V   Y   F   C   A   R   S   D   Y
  ACT TAC TCA TTC TAC TTT GTC TCG AGC GGT GGA GGC GGT TCA GGC GGA GGT GGC AGC GGC
   T   Y   S   F   Y   F   V   S   S   G   G   G   G   S   G   G   G   G   S   G
  GGT GGC GGG TCG ACG GAT ATT GTG ATG ACG CAG GCT GCA TTC TCC AAT CCA GTC ACT CTT
   G   G   G   S   T   D   I   V   M   T   Q   A   A   F   S   N   P   V   T   L
                          |  SbfI  |
  GGA ACA TCA GCT TCC ATC TCC TGC AGG TCT AGT AAG AGT CTC CTA CAT AGT AAT GGC ATC
   G   T   S   A   S   I   S   C   R   S   S   K   S   L   L   H   S   N   G   I
  ACT TAT TTG TAT TGG TAT CTG CAG AAG CCA GGC CAG TCT CCT CAG CTC CTG ATT TAT CAG
   T   Y   L   Y   W   Y   L   Q   K   P   G   Q   S   P   Q   L   L   I   Y   Q
  ATG TCC AAC CTT GCC TCA GGA GTC CCA GAC AGG TTC AGT AGC AGT GGG TCA GGA ACT GAT
   M   S   N   L   A   S   G   V   P   D   R   F   S   S   S   G   S   G   T   D
  TTC ACA CTG AGA ATC AGC AGA GTG GAG GCT GAG GAT GTG GGT GTT TAT TAC TGT GCT CAA
   F   T   L   R   I   S   R   V   E   A   E   D   V   G   V   Y   Y   C   A   Q
    | XbaI |                 |  hexahistidine tag  |
  AAT CTA GAA CTT CCG GCT AGA CAC CAT CAC CAC CAC CAT TGA GGGCCCTATTTCTATA
   N   L   E   L   P   A   R   H   H   H   H   H   H   *
  GTGTCACCTAAATGCTAGAGCTCGCTGATCAGCCTCGACTGTGCCTTCTAGTTGCCAGCCATCTGTTGTTTGCCCCTCCCCCGTGCCTT
CCTTGACCCTGGAAGGTGCCACTCCACTGTCCTTTCCTAATAAAATGAGGAAATTGCATCGCATTTGTCTGATAGGTGTCATTCTATTCTGG
GGGGGTGGGGGTGGGGCAGACAA 3’
```

Cy34.1.2 scFv-protamine-His6 nucleotide and amino acid sequences including the V_H native signal sequence in pcDNA3 vector:

```
                                                                        5’end of hCMV
                                                                        |
5’ GAATCTGCTTAGGGTTAGGCGTTTTGCGCTGCTTCGCGATGTACGGGCCAGATATACGCGTTGACATTGATTATTGACTAGTTATT
                                                      CMV enhancer region (5’end)
                                                      |
   AATAGTAATCAATTACGGGGTCATTAGTTCATAGCCCATATATGGAGTTCCGCGTTACATAACTTACGGTAAATGGCCCGCCTGGC
   TGACCGCCCAACGACCCCCGCCCATTGACGTCAATAATGACGTATGTTCCCATAGTAACGCCAATAGGGACTTTCCATTGACGTCA
   ATGGGTGGAGTATTTACGGTAAACTGCCCACTTGGCAGTACATCAAGTGTATCATATGCCAAGTACGCCCCCTATTGACGTCAATG
   ACGGTAAATGGCCCGCCTGGCATTATGCCCAGTACATGACCTTATGGGACTTTCCTACTTGGCAGTACATCTACGTATTAGTCATC
   GCTATTACCATGGTGATGCGGTTTTGGCAGTACATCAATGGGCGTGGATAGCGGTTTGACTCACGGGGATTTCCAAGTCTCCACCC
      CMV enhancer region (3’end)
                                  |
   CATTGACGTCAATGGGAGTTTGTTTTGGCACCAAAATCAACGGGACTTTCCAAAATGTCGTAACAACTCCGCCCCATTGACGCAAA
                                    TATA box     3'end hCMV promoter
                                    ----         |
   TGGGCGGTAGGCGTGTACGGTGGGAGGTCTATATAAGCAGAGCTCTCTGGCT……..
……ATAAGATGGAGCTGTATCATTCTCTTCTTGGTAGCAACAGCTACAAGTGTCGACTCCCAGGTCCAACTGCAGCACT

GGG GCT GAA ATT GTG AGG CCT GGG ACT TCA GTG AAG CTG TCC TGT
 G   A   E   I   V   R   P   G   T   S   V   K   L   S   C
AAG GCT TCA GGC TAC ACC TTT ACC GAC TAT TGG ATG AAC TGG GTG AAG CAG AGG CCT GGA
 K   A   S   G   Y   T   F   T   D   Y   W   M   N   W   V   K   Q   R   P   G
                                | MfeI |
CAA GGC CTT GAG TGG TTC GGA GCA ATT GAT CCT TCT GAT AGT TAT ACT AGG TAC AAT CAA
 Q   G   L   E   W   F   G   A   I   D   P   S   D   S   Y   T   R   Y   N   Q
GAG TTC AAG GGC AAG GCC ACA TTG ACT GTA GAC ACA TCC TCC ACC ACA GCC TAC ATG CAG
 E   F   K   G   K   A   T   L   T   V   D   T   S   S   T   T   A   Y   M   Q
CTC AGC AGC CTG ACA TCC GAG GAC TCT GCG GTC TAT TTC TGT GCA AGA TCG GAC CAT ACT
 L   S   S   L   T   S   E   D   S   A   V   Y   F   C   A   R   S   D   H   T
TAC TCA TTC TAC TTT GTC TCG AGC GGT GGA GGC GGT TCA GGC GGA GGT GGC AGC GGC GGT
 Y   S   F   Y   F   V   S   S   G   G   G   G   S   G   G   G   G   S   G   G
GGC GGG TCG ACG GAT ATT GTG ATG ACG CAG GCT GCA TTC TCC AAT CCA GTC ACT CTT GGA
 G   G   S   T   D   I   V   M   T   Q   A   A   F   S   N   P   V   T   L   G
                    |  SbfI  |
ACA TCA GCT TCC ATC TCC TGC AGG TCT AGT AAG AGT CTC CTA CAT AGT AAT GGC ATC ACT
 T   S   A   S   I   S   C   R   S   S   K   S   L   L   H   S   N   G   I   T
TAT TTG TAT TGG TAT CTG CAG AAG CCA GGC CAG TCT CCT CAG CTC CTG ATT TAT CAG ATG
 Y   L   Y   W   Y   L   Q   K   P   G   Q   S   P   Q   L   L   I   Y   Q   M
TCC AAC CTT GCC TCA GGA GTC CCA GAC AGG TTC AGT AGC AGT GGG TCA GGA ACT GAT TTC
 S   N   L   A   S   G   V   P   D   R   F   S   S   S   G   S   G   T   D   F
ACA CTG AGA ATC AGC AGA GTG GAG GCT GAG GAT GTG GGT GTT TAT TAC TGT GCT CAA AAT
 T   L   R   I   S   R   V   E   A   E   D   V   G   V   Y   Y   C   A   Q   N
               |EcoRI| |  ……   truncated protamine     ……..
CTA GAA CTT CCG GAA TTC CGA TCA CAA TCA CGA TCA CGA TAC TAC CGA CAA CGA CAA CGA
 L   E   L   P   E   F   R   S   Q   S   R   S   R   Y   Y   R   Q   R   Q   R
         ……..              | |  hexahistidine tag  |
TCA CGA CGA CGA CGA CGA CGA TCT AGA CAC CAT CAC CAC CAC CAT TGA GGGCCCTATTC
 S   R   R   R   R   R   R   S   R   H   H   H   H   H   H   *

TATAGTGTCACCTAAATGCTAGAGCTCGCTGATCAGCCTCGACTGTGCCTTCTAGTTGCCAGCCATCTGTTGTTTGCCCCTCCCCCGTGCC
TTCCTTGACCCTGGAAGGTGCCACTCCACTGTCCTTTCCTAATAAATGAGGAAATTGCATCGCATTGTCTGAGTAGGTGTCATTCTATTCTG
GGGGGTGGGGTGGGGCAGGACAGCAGGGGAGGATTGGGAAGCAATAGCAGCATGCTGGGATGCGCG 3’
```

Cy34.1.2 scFv-His6 nucleotide and amino acid sequences in pHEN1 vector containing pelB signal sequence:

```
5′ AGCGCCCAATACGCAAACCGCCTCTCCCCGCGCGTTGGCCGATTCATTAATGCAGCTGGCACGACAGGTTTCCCGACTGGAAAGCGGGC
AGTGAGCGCAACGCAATTAATGTGAGTTAGCTCACTCATTAGGCACCCCAGGCTTTACACTTTATGCTTCCGGCTCGTATGTTGTGTGGAAT
TGTGAGCGGATAACAATTTCACACAGGAAACAGCTATGACCATGATTACGCCAAGCTTGCATGCAAATTCTATTTCAAGGAGACAGTCATAA
TGAAATACCTATTGCCTACGGCAGCCGCTGGATTGTTA

     |Pel B signal peptide sequence|     |scFv
  TTA CTC GCG GCC CAG CCG GCC ATG GCC CAG GTC CAA CTG CAG CAG CCT CAG
   L   L   A   A   Q   P   A   M   A   Q   V   Q   L   Q   Q   P   Q
  GTC CAA CTG CAG CAG CCT GGG GCT GAA ATT GTG AGG CCT GGG ACT TCA GTG AAG CTG TCC
   V   Q   L   Q   Q   P   G   A   E   I   V   R   P   G   T   S   V   K   L   S
  TGT AAG GCT TCA GGC TAC ACC TTT ACC GAC TAT TGG ATG AAC TGG GTG AAG CAA AGG CCT
   C   K   A   S   G   Y   T   F   T   D   Y   W   M   N   W   V   K   Q   R   P
                                   | MfeI |
  GGA CAA GGC CTT GAG TGG TTC GGA GCA ATT GAT CCT TCT GAT AGT TAT ACT AGG TAC AAT
   G   Q   G   L   E   W   F   G   A   I   D   P   S   D   S   Y   T   R   Y   N
  CAA GAG TTC AAG GGC AAG GCC ACA TTG ACT GTA GAC ACA TCC TCC ACC ACA GCC TAC ATG
   Q   E   F   K   G   K   A   T   L   T   V   D   T   S   S   T   T   A   Y   M
  CAG CTC AGC AGC CTG ACA TCC GAG GAC TCT GCG GTC TAT TTC TGT GCA AGA TCG GAC TAT
   Q   L   S   S   L   T   S   E   D   S   A   V   Y   F   C   A   R   S   D   Y
  ACT TAC TCA TTC TAC TTT GTC TCG AGC GGT GGA GGC GGT TCA GGC GGA GGT GGC AGC GGC
   T   Y   S   F   Y   F   V   S   S   G   G   G   G   S   G   G   G   G   S   G
  GGT GGC GGG TCG ACG GAT ATT GTG ATG ACG CAG GCT GCA TTC TCC AAT CCA GTC ACT CTT
   G   G   G   S   T   D   I   V   M   T   Q   A   A   F   S   N   P   V   T   L
                       |  SbfI  |
  GGA ACA TCA GCT TCC ATC TCC TGC AGG TCT AGT AAG AGT CTC CTA CAT AGT AAT GGC ATC
   G   T   S   A   S   I   S   C   R   S   S   K   S   L   L   H   S   N   G   I
  ACT TAT TTG TAT TGG TAT CTG CAG AAG CCA GGC CAG TCT CCT CAG CTC CTG ATT TAT CAG
   T   Y   L   Y   W   Y   L   Q   K   P   G   Q   S   P   Q   L   L   I   Y   Q
  ATG TCC AAC CTT GCC TCA GGA GTC CCA GAC AGG TTC AGT AGC AGT GGG TCA GGA ACT GAT
   M   S   N   L   A   S   G   V   P   D   R   F   S   S   S   G   S   G   T   D
  TTC ACA CTG AGA ATC AGC AGA GTG GAG GCT GAG GAT GTG GGT GTT TAT TAC TGT GCT CAA
   F   T   L   R   I   S   R   V   E   A   E   D   V   G   V   Y   Y   C   A   Q
    | XbaI |                 |  hexahistidine tag  |
  AAT CTA GAA CTT CCG GCT AGA CAC CAT CAC CAC CAC CAT TGA
   N   L   E   L   P   A   R   H   H   H   H   H   H   *

GGCGGCCGCAGAACAAAAACTCATCTCAGAAGAGGATCTGAATGGGGCCGCATAGACTGTTGAAAGTTGTTTAGCAAAACCTCATACA 3′
```

Cy34.1.2 scFv-His6 nucleotide and amino acid sequences in pcDNA3 with hLAP signal sequence, hLAP and HRV3C sequences:

```
                                                                    5’end of hCMV
                                                                    |
5’ GAATCTGCTTAGGGTTAGGCGTTTTGCGCTGCTTCGCGATGTACGGGCCAGATATACGCGTTGACATTGATTATTGACTAGTTATT
                                                    CMV enhancer region (5’end)
                                                    |
   AATAGTAATCAATTACGGGGTCATTAGTTCATAGCCCATATATGGAGTTCCGCGTTACATAACTTACGGTAAATGGCCCGCCTGGC
   TGACCGCCCAACGACCCCCGCCCATTGACGTCAATAATGACGTATGTTCCCATAGTAACGCCAATAGGGACTTTCCATTGACGTCA
   ATGGGTGGAGTATTTACGGTAAACTGCCCACTTGGCAGTACATCAAGTGTATCATATGCCAAGTACGCCCCCTATTGACGTCAATG
   ACGGTAAATGGCCCGCCTGGCATTATGCCCAGTACATGACCTTATGGGACTTTCCTACTTGGCAGTACATCTACGTATTAGTCATC
   GCTATTACCATGGTGATGCGGTTTTGGCAGTACATCAATGGGCGTGGATAGCGGTTTGACTCACGGGGATTTCCAAGTCTCCACCC
      CMV enhancer region (3’end)
                                  |
   CATTGACGTCAATGGGAGTTTGTTTTGGCACCAAAATCAACGGGACTTTCCAAAATGTCGTAACAACTCCGCCCCATTGACGCAAA
                                    TATA box     3'end hCMV promoter
                                    ----         |
   TGGGCGGTAGGCGTGTACGGTGGGAGGTCTATATAAGCAGAGCTCTCTGGCT……..

                                                ……..Human LAP……
G GGG GAT TCT TGT GCG CAG GTA TAC ACA CTG CAA GTG GAC ATC AAC GGG TTC ACT ACC GGC
   G   D   S   C   A   Q   V   Y   T   L   Q   V   D   I   N   G   F   T   T   G
  CGC CGA GGT GAC CTG GCC ACC ATT CAT GGC ATG AAC CGG CCT TTC CTG CTT CTC ATG GCC
   R   R   G   D   L   A   T   I   H   G   M   N   R   P   F   L   L   L   M   A
  ACC CCG CTG GAG AGG GCC CAT CAT CTG CAA AGC GAA TTC CGG GGA GGC GGA TCC
   T   P   L   E   R   A   H   H   L   Q   S   E   F   R   G   G   G   S
  |      HRV3C cleavage site    |
  CTC GAG GTT CTC TTT CAG GGA CCC
   L   E   V   L   F   Q   G   P
  |……Cy34.1.2 scFv…….
  CAG GTC CAA CTG CAG CAG CCT CAG GTC CAA CTG CAG CAG CCT
   Q   V   Q   L   Q   Q   P   Q   V   Q   L   Q   Q   P
  GGG GCT GAA ATT GTG AGG CCT GGG ACT TCA GTG AAG CTG TCC TGT AAG GCT TCA GGC TAC
   G   A   E   I   V   R   P   G   T   S   V   K   L   S   C   K   A   S   G   Y
  ACC TTT ACC GAC TAT TGG ATG AAC TGG GTG AAG CAA AGG CCT GGA CAA GGC CTT GAG TGG
   T   F   T   D   Y   W   M   N   W   V   K   Q   R   P   G   Q   G   L   E   W
           | MfeI |
  TTC GGA GCA ATT GAT CCT TCT GAT AGT TAT ACT AGG TAC AAT CAA GAG TTC AAG GGC AAG
   F   G   A   I   D   P   S   D   S   Y   T   R   Y   N   Q   E   F   K   G   K
  GCC ACA TTG ACT GTA GAC ACA TCC TCC ACC ACA GCC TAC ATG CAG CTC AGC AGC CTG ACA
   A   T   L   T   V   D   T   S   S   T   T   A   Y   M   Q   L   S   S   L   T
  TCC GAG GAC TCT GCG GTC TAT TTC TGT GCA AGA TCG GAC TAT ACT TAC TCA TTC TAC TTT
   S   E   D   S   A   V   Y   F   C   A   R   S   D   Y   T   Y   S   F   Y   F
  GTC TCG AGC GGT GGA GGC GGT TCA GGC GGA GGT GGC AGC GGC GGT GGC GGG TCG ACG GAT
   V   S   S   G   G   G   G   S   G   G   G   G   S   G   G   G   G   S   T   D
  ATT GTG ATG ACG CAG GCT GCA TTC TCC AAT CCA GTC ACT CTT GGA ACA TCA GCT TCC ATC
   I   V   M   T   Q   A   A   F   S   N   P   V   T   L   G   T   S   A   S   I
   |  SbfI  |
  TCC TGC AGG TCT AGT AAG AGT CTC CTA CAT AGT AAT GGC ATC ACT TAT TTG TAT TGG TAT
   S   C   R   S   S   K   S   L   L   H   S   N   G   I   T   Y   L   Y   W   Y
  CTG CAG AAG CCA GGC CAG TCT CCT CAG CTC CTG ATT TAT CAG ATG TCC AAC CTT GCC TCA
   L   Q   K   P   G   Q   S   P   Q   L   L   I   Y   Q   M   S   N   L   A   S
  GGA GTC CCA GAC AGG TTC AGT AGC AGT GGG TCA GGA ACT GAT TTC ACA CTG AGA ATC AGC
   G   V   P   D   R   F   S   S   S   G   S   G   T   D   F   T   L   R   I   S
                                                                | XbaI |
  AGA GTG GAG GCT GAG GAT GTG GGT GTT TAT TAC TGT GCT CAA AAT CTA GAA CTT CCG GCT
   R   V   E   A   E   D   V   G   V   Y   Y   C   A   Q   N   L   E   L   P   A
      |  hexahistidine tag  |
  AGA CAC CAT CAC CAC CAC CAT TGA
   R   H   H   H   H   H   H   *

  GGGCCCGCTAGAGGGCCCTATTCTATAGGTCACTAAAGGCAGAATTTGT  3’
```

Cy34.1.2 scFv-protamine-His6 nucleotide and amino acid sequences in pcDNA3 with hLAP signal sequence, hLAP and HRV3C sequences:

```
                                                                    5’end of hCMV
                                                                    |
5’ GAATCTGCTTAGGGTTAGGCGTTTTGCGCTGCTTCGCGATGTACGGGCCAGATATACGCGTTGACATTGATTATTGACTAGTTATT
                                                    CMV enhancer region (5’end)
                                                    |
   AATAGTAATCAATTACGGGGTCATTAGTTCATAGCCCATATATGGAGTTCCGCGTTACATAACTTACGGTAAATGGCCCGCCTGGC
   TGACCGCCCAACGACCCCCGCCCATTGACGTCAATAATGACGTATGTTCCCATAGTAACGCCAATAGGGACTTTCCATTGACGTCA
   ATGGGTGGAGTATTTACGGTAAACTGCCCACTTGGCAGTACATCAAGTGTATCATATGCCAAGTACGCCCCCTATTGACGTCAATG
   ACGGTAAATGGCCCGCCTGGCATTATGCCCAGTACATGACCTTATGGGACTTTCCTACTTGGCAGTACATCTACGTATTAGTCATC
   GCTATTACCATGGTGATGCGGTTTTGGCAGTACATCAATGGGCGTGGATAGCGGTTTGACTCACGGGGATTTCCAAGTCTCCACCC
      CMV enhancer region (3’end)
                                  |
   CATTGACGTCAATGGGAGTTTGTTTTGGCACCAAAATCAACGGGACTTTCCAAAATGTCGTAACAACTCCGCCCCATTGACGCAAA
                                    TATA box     3'end hCMV promoter
                                    ----         |
   TGGGCGGTAGGCGTGTACGGTGGGAGGTCTATATAAGCAGAGCTCTCTGGCT……..

…… hLAP …….
GG GGC GTT TTT TGC GCA GCA TAC ACA CTG CAA GTG GAC ATC AAC GGG TTC ACT ACC GGC CGC
    G   V   F   C   A   A   Y   T   L   Q   V   D   I   N   G   F   T   T   G   R
  CGA GGT GAC CTG GCC ACC ATT CAT GGC ATG AAC CGG CCT TTC CTG CTT CTC ATG GCC ACC
   R   G   D   L   A   T   I   H   G   M   N   R   P   F   L   L   L   M   A   T

  CCG CTG GAG AGG GCC CAG CAT CTG CAA AGC GAA TTC GGG GGA GGC GGA TCC
   P   L   E   R   A   Q   H   L   Q   S   E   F   G   G   G   G   S
|…… HRV3C cleavage site …….|
CTC GAG GTT CTC TTT CAG GGA CCC
 L   E   V   L   F   Q   G   P
  |……Cy34.1.2 scFv…….
  CAG GTC CAA CTG CAG CAG CCT CAG GTC CAA CTG CAG CAG CCT GGG
   Q   V   Q   L   Q   Q   P   Q   V   Q   L   Q   Q   P   G
  GCT GAA ATT GTG AGG CCT GGG ACT TCA GTG AAG CTG TCC TGT AAG GCT TCA GGC TAC ACC
   A   E   I   V   R   P   G   T   S   V   K   L   S   C   K   A   S   G   Y   T
  TTT ACC GAC TAT TGG ATG AAC TGG GTG AAG CAA AGG CCT GGA CAA GGC CTT GAG TGG TTC
   F   T   D   Y   W   M   N   W   V   K   Q   R   P   G   Q   G   L   E   W   F
       | MfeI |
  GGA GCA ATT GAT CCT TCT GAT AGT TAT ACT AGG TAC AAT CAA GAG TTC AAG GGC AAG GCC
   G   A   I   D   P   S   D   S   Y   T   R   Y   N   Q   E   F   K   G   K   A
  ACA TTG ACT GTA GAC ACA TCC TCC ACC ACA GCC TAC ATG CAG CTC AGC AGC CTG ACA TCC
   T   L   T   V   D   T   S   S   T   T   A   Y   M   Q   L   S   S   L   T   S
  GAG GAC TCT GCG GTC TAT TTC TGT GCA AGA TCG GAC TAT ACT TAC TCA TTC TAC TTT GTC
   E   D   S   A   V   Y   F   C   A   R   S   D   Y   T   Y   S   F   Y   F   V
  TCG AGC GGT GGA GGC GGT TCA GGC GGA GGT GGC AGC GGC GGT GGC GGG TCG ACG GAT ATT
   S   S   G   G   G   G   S   G   G   G   G   S   G   G   G   G   S   T   D   I
  GTG ATG ACG CAG GCT GCA TTC TCC AAT CCA GTC ACT CTT GGA ACA TCA GCT TCC ATC
   V   M   T   Q   A   A   F   S   N   P   V   T   L   G   T   S   A   S   I
  |  SbfI  |
 TCC TGC AGG TCT AGT AAG AGT CTC CTA CAT AGT AAT GGC ATC ACT TAT TTG TAT TGG TAT CTG
  S   C   R   S   S   K   S   L   L   H   S   N   G   I   T   Y   L   Y   W   Y   L
  CAG AAG CCA GGC CAG TCT CCT CAG CTC CTG ATT TAT CAG ATG TCC AAC CTT GCC TCA GGA
   Q   K   P   G   Q   S   P   Q   L   L   I   Y   Q   M   S   N   L   A   S   G
  GTC CCA GAC AGG TTC AGT AGC AGT GGG TCA GGA ACT GAT TTC ACA CTG AGA ATC AGC AGA
   V   P   D   R   F   S   S   S   G   S   G   T   D   F   T   L   R   I   S   R
                                                                          |EcoRI|
  GTG GAG GCT GAG GAT GTG GGT GTT TAT TAC TGT GCT CAA AAT CTA GAA CTT CCG GAA TTC
   V   E   A   E   D   V   G   V   Y   Y   C   A   Q   N   L   E   L   P   E   F
  | truncated protamine ……..
  CGA TCA CAA TCA CGA TCA CGA TAC TAC CGA CAA CGA CAA CGA TCA CGA CGA CGA CGA CGA
   R   S   Q   S   R   S   R   Y   Y   R   Q   R   Q   R   S   R   R   R   R   R
             | |  hexahistidine tag  |
  CGA TCT AGA CAC CAT CAC CAC CAC CAT TGA
   R   S   R   H   H   H   H   H   H   *

  GGGCCCGCTAGAGGGCCCTATTCTATAGTGTCACCTAAATGCTAGAGCTCGCTGATCAGCCTCGACTGTGCCTTCTAGTTGCCAGCCATC
TGTTGTTTGCCCCTCCCCCGTGCCTTCCTTGACCCTGGAAGGTGCCACTCCCACTGTCCTTCCTAATAAATAGATGCC  3’
```

Cy34.1.2 scFv-protamine-His6 nucelotdie and amino acid sequences in modified pDisplay vector with murine Ig kappa chain signal sequence:

```
5’CC TGG TCG AGC TCG GAT CCA CTA GTA ACG GCC GCC AGT GTG CTG GAA TTC GGC TTG GGG ATA
      W   S   S   S   D   P   L   V   T   A   A   S   V   L   E   F   G   L   G   I
          | ……..   Ig kappa chain signal sequence
  TCC ACC ATG GAG ACA GAC ACA CTC CTG CTA TGG GTA CTG CTG CTC TGG GTT CCA GGT TCC
   S   T   M   E   T   D   T   L   L   L   W   V   L   L   L   W   V   P   G   S
  …… |   |……..SfiI…….| | Cy34.1.2 scFv …….
  ACT GGT GAC GGG GCC CAG CCG GCC CAG GTC CAA CTG CAG CAG CCT GGG GCT GAA ATT GTG
   T   G   D   G   A   Q   P   A   Q   V   Q   L   Q   Q   P   G   A   E   I   V
  AGG CCT GGG ACT TCA GTG AAG CTG TCC TGT AAG GCT TCA GGC TAC ACC TTT ACC GAC TAT
   R   P   G   T   S   V   K   L   S   C   K   A   S   G   Y   T   F   T   D   Y
                                                                   | MfeI |
  TGG ATG AAC TGG GTG AAG CAG AGG CCT GGA CAA GGC CTT GAG TGG TTC GGA GCA ATT GAT
   W   M   N   W   V   K   Q   R   P   G   Q   G   L   E   W   F   G   A   I   D
  CCT TCT GAT AGT TAT ACT AGG TAC AAT CAA GAG TTC AAG GGC AAG GCC ACA TTG ACT GTA
   P   S   D   S   Y   T   R   Y   N   Q   E   F   K   G   K   A   T   L   T   V
  GAC ACA TCC TCC ACC ACA GCC TAC ATG CAG CTC AGC AGC CTG ACA TCC GAG GAC TCT GCG
   D   T   S   S   T   T   A   Y   M   Q   L   S   S   L   T   S   E   D   S   A
  GTC TAT TTC TGT GCA AGA TCG GAC CAT ACT TAC TCA TTC TAC TTT GTC TCG AGC GGT GGA
   V   Y   F   C   A   R   S   D   H   T   Y   S   F   Y   F   V   S   S   G   G
  GGC GGT TCA GGC GGA GGT GGC AGC GGC GGT GGC GGG TCG ACG GAT ATT GTG ATG ACG CAG
   G   G   S   G   G   G   G   S   G   G   G   G   S   T   D   I   V   M   T   Q
  GCT GCA TTC TCC AAT CCA GTC ACT CTT GGA ACA TCA GCT TCC ATC TCC TGC AGG TCT ……
   A   A   F   S   N   P   V   T   L   G   T   S   A   S   I   S   C   R   S

……..ATAAGAGTCTCCTACATAGTAATGGCATCACTTATTTGTATTGGTATCTGCAAAGCCAGCCAGTCTCCTCACTCCTGAATTATCAGAT
GCCAACCTTGCTCAGGATTCCC 3’
```

HA22 scFv-protamine-His6 nucleotide and amino acid sequences in pDisplay vector with murine Ig kappa chain signal sequence:

```
                                                                        5’end of hCMV
                                                                        |
5’ GAATCTGCTTAGGGTTAGGCGTTTTGCGCTGCTTCGCGATGTACGGGCCAGATATACGCGTTGACATTGATTATTGACTAGTTATT
                                                        CMV enhancer region (5’end)
                                                        |
   AATAGTAATCAATTACGGGGTCATTAGTTCATAGCCCATATATGGAGTTCCGCGTTACATAACTTACGGTAAATGGCCCGCCTGGC
   TGACCGCCCAACGACCCCCGCCCATTGACGTCAATAATGACGTATGTTCCCATAGTAACGCCAATAGGGACTTTCCATTGACGTCA
   ATGGGTGGAGTATTTACGGTAAACTGCCCACTTGGCAGTACATCAAGTGTATCATATGCCAAGTACGCCCCCTATTGACGTCAATG
   ACGGTAAATGGCCCGCCTGGCATTATGCCCAGTACATGACCTTATGGGACTTTCCTACTTGGCAGTACATCTACGTATTAGTCATC
   GCTATTACCATGGTGATGCGGTTTTGGCAGTACATCAATGGGCGTGGATAGCGGTTTGACTCACGGGGATTTCCAAGTCTCCACCC
      CMV enhancer region (3’end)
                                  |
   CATTGACGTCAATGGGAGTTTGTTTTGGCACCAAAATCAACGGGACTTTCCAAAATGTCGTAACAACTCCGCCCCATTGACGCAAA
                                    TATA box     3'end hCMV promoter
                                    ----         |
   TGGGCGGTAGGCGTGTACGGTGGGAGGTCTATATAAGCAGAGCTCTCTGGCT……..

CCA GCA TGC TCG AGC TCG GAT CCA CTA GTA ACG GCC GCC AGT GTG CTG GAA TTC GGC TTG
 P   A   C   S   S   S   D   P   L   V   T   A   A   S   V   L   E   F   G   L
               |   murine Ig kappa chain signal peptide sequence ……..
GGG ATA TCC ACC ATG GAG ACA GAC ACA CTC CTG CTA TGG GTA CTG CTG CTC TGG GTT CCA
 G   I   S   T   M   E   T   D   T   L   L   L   W   V   L   L   L   W   V   P

       ……..   | |haemaaglutinin A epitope sequence|   |…….SfiI……..|
GGT TCC ACT GGT GAC TAT CCA TAT GAT GTT CCA GAT TAT GCT GGG GCC CAG CCG GCC ATG
 G   S   T   G   D   Y   P   Y   D   V   P   D   Y   A   G   A   Q   P   A   M
|HA22 scFv…….
GAA GTG CAG CTG GTG GAG TCT GGG GGA GGC TTA GTG AAG CCT GGA GGG TCC CTG AAA CTC
 E   V   Q   L   V   E   S   G   G   G   L   V   K   P   G   G   S   L   K   L
TCC TGT GCA GCC TCT GGA TTC GCT TTC AGT ATC TAT GAC ATG TCT TGG GTT CGC CAG ACT
 S   C   A   A   S   G   F   A   F   S   I   Y   D   M   S   W   V   R   Q   T
CCG GAG AAG AGG CTG GAG TGG GTC GCA TAC ATT AGT AGT GGT GGT GGT ACC ACC TAC TAT
 P   E   K   R   L   E   W   V   A   Y   I   S   S   G   G   G   T   T   Y   Y
CCA GAC ACT GTG AAG GGC CGA TTC ACC ATC TCC AGA GAC AAT GCC AAG AAC ACC CTG TAC
 P   D   T   V   K   G   R   F   T   I   S   R   D   N   A   K   N   T   L   Y
CTG CAA ATG AGC AGT CTG AAG TCT GAG GAC ACA GCC ATG TAT TAC TGT GCA AGA CAT AGT
 L   Q   M   S   S   L   K   S   E   D   T   A   M   Y   Y   C   A   R   H   S
GGC TAC GGC ACG CAC TGG GGG GTT TTG TTT GCT TAC TGG GGC CAA GGG ACT CTG GTC ACT
 G   Y   G   T   H   W   G   V   L   F   A   Y   W   G   Q   G   T   L   V   T
                    |BamHI|
GTC TCT GCA GGC GGA GGC GGA TCC GGT GGT GGC GGA TCT GGA GGT GGC GGA AGC GAT ATC
 V   S   A   G   G   G   G   S   G   G   G   G   S   G   G   G   G   S   D   I
CAG ATG ACC CAG ACT ACT TCC TCC CTG TCT GCC TCT CTG GGA GAC AGA GTC ACC ATT AGT
 Q   M   T   Q   T   T   S   S   L   S   A   S   L   G   D   R   V   T   I   S
TGC AGG GCA AGT CAG GAC ATT AGC AAT TAT TTA AAC TGG TAT CAG CAG AAA CCA GAT GGA
 C   R   A   S   Q   D   I   S   N   Y   L   N   W   Y   Q   Q   K   P   D   G
ACT GTT AAA CTC CTG ATC TAC TAC ACA TCA ATA TTA CAC TCA GGA GTC CCA TCA AGG TTC
 T   V   K   L   L   I   Y   Y   T   S   I   L   H   S   G   V   P   S   R   F
AGT GGC AGT GGG TCT GGA ACA GAT TAT TCT CTC ACC ATT AGC AAC CTG GAG CAA GAA GAT
 S   G   S   G   S   G   T   D   Y   S   L   T   I   S   N   L   E   Q   E   D
TTT GCC ACT TAC TTT TGC CAA CAG GGT AAT ACG CTT CCG TGG ACG TTC GGT GGA GGC ACC
 F   A   T   Y   F   C   Q   Q   G   N   T   L   P   W   T   F   G   G   G   T
                    | truncated protamine …….
AAG CTG GAA AGC AGA TCT CGA TCA CAA TCA CGA TCA CGA TAC TAC CGA CAA CGA CAA CGA
 K   L   E   S   R   S   R   S   Q   S   R   S   R   Y   Y   R   Q   R   Q   R
      …….                  | |  hexahistidine tag  |
TCA CGA CGA CGA CGA CGA CGA TCT AGA CAC CAT CAC CAC CAC CAT TAA
 S   R   R   R   R   R   R   S   R   H   H   H   H   H   H   *    …….

…….CCGCGGCTGCAGGTCGACGAACAAAAACTCATCTCAGAAGAGGATCTGAATGCTGTGGGCCAGGACACGCAGGAGGTCATCGTGGT
GCCACACTCCTTGCCCTTTAAGGTGGTGGTGATCTCAGCCATCCTGGCCCTGGTGGTGCTCACCATCATCTCCCTTATCATCCTCATCATGC
TT GGCAGAAGAAGCCACGTAGCCCCGCCA  3’
```

HA22 scFv-protamine-His6 nucleotide and amino acid sequences in modified pDisplay vector with murine Ig kappa chain signal sequence:

```
                                                                      5’end of hCMV
                                                                      |
5’ GAATCTGCTTAGGGTTAGGCGTTTTGCGCTGCTTCGCGATGTACGGGCCAGATATACGCGTTGACATTGATTATTGACTAGTTATT
                                                        CMV enhancer region (5’end)
                                                        |
   AATAGTAATCAATTACGGGGTCATTAGTTCATAGCCCATATATGGAGTTCCGCGTTACATAACTTACGGTAAATGGCCCGCCTGGC
   TGACCGCCCAACGACCCCCGCCCATTGACGTCAATAATGACGTATGTTCCCATAGTAACGCCAATAGGGACTTTCCATTGACGTCA
   ATGGGTGGAGTATTTACGGTAAACTGCCCACTTGGCAGTACATCAAGTGTATCATATGCCAAGTACGCCCCCTATTGACGTCAATG
   ACGGTAAATGGCCCGCCTGGCATTATGCCCAGTACATGACCTTATGGGACTTTCCTACTTGGCAGTACATCTACGTATTAGTCATC
   GCTATTACCATGGTGATGCGGTTTTGGCAGTACATCAATGGGCGTGGATAGCGGTTTGACTCACGGGGATTTCCAAGTCTCCACCC
      CMV enhancer region (3’end)
                                  |
   CATTGACGTCAATGGGAGTTTGTTTTGGCACCAAAATCAACGGGACTTTCCAAAATGTCGTAACAACTCCGCCCCATTGACGCAAA
                                    TATA box     3'end hCMV promoter
                                    ----         |
   TGGGCGGTAGGCGTGTACGGTGGGAGGTCTATATAAGCAGAGCTCTCTGGCT……..

CGG CAG GCT TGG AAG GAG CTC GGA TCA CTA GTA ACG GCC GCC AGT GTG CTG GAA TTC GGC
 R   Q   A   W   K   E   L   G   S   L   V   T   A   A   S   V   L   E   F   G
                    | murine Ig kappa chain signal peptide sequence ……..
TTG GGG ATA TCC ACC ATG GAG ACA GAC ACA CTC CTG CTA TGG GTA CTG CTG CTC TGG GTT
 L   G   I   S   T   M   E   T   D   T   L   L   L   W   V   L   L   L   W   V
  signal sequence ends|   |     SfiI      | | HA22 scFv ……
CCA GGT TCC ACT GGT GAC GGG GCC CAG CCG GCC ATG GAA GTG CAG CTG GTG GAG TCT GGG
 P   G   S   T   G   D   G   A   Q   P   A   M   E   V   Q   L   V   E   S   G
GGA GGC TTA GTG AAG CCT GGA GGG TCC CTG AAA CTC TCC TGT GCA GCC TCT GGA TTC GCT
 G   G   L   V   K   P   G   G   S   L   K   L   S   C   A   A   S   G   F   A
TTC AGT ATC TAT GAC ATG TCT TGG GTT CGC CAG ACT CCG GAG AAG AGG CTG GAG TGG GTC
 F   S   I   Y   D   M   S   W   V   R   Q   T   P   E   K   R   L   E   W   V
GCA TAC ATT AGT AGT GGT GGT GGT ACC ACC TAC TAT CCA GAC ACT GTG AAG GGC CGA TTC
 A   Y   I   S   S   G   G   G   T   T   Y   Y   P   D   T   V   K   G   R   F
ACC ATC TCC AGA GAC AAT GCC AAG AAC ACC CTG TAC CTG CAA ATG AGC AGT CTG AAG TCT
 T   I   S   R   D   N   A   K   N   T   L   Y   L   Q   M   S   S   L   K   S
GAG GAC ACA GCC ATG TAT TAC TGT GCA AGA CAT AGT GGC TAC GGC ACG CAC TGG GGG GTT
 E   D   T   A   M   Y   Y   C   A   R   H   S   G   Y   G   T   H   W   G   V
                                                                    |BamHI|
TTG TTT GCT TAC TGG GGC CAA GGG ACT CTG GTC ACT GTC TCT GCA GGC GGA GGC GGA TCC
 L   F   A   Y   W   G   Q   G   T   L   V   T   V   S   A   G   G   G   G   S
GGT GGT GGC GGA TCT GGA GGT GGC GGA AGC GAT ATC CAG ATG ACC CAG ACT ACT TCC TCC
 G   G   G   G   S   G   G   G   G   S   D   I   Q   M   T   Q   T   T   S   S
CTG TCT GCC TCT CTG GGA GAC AGA GTC ACC ATT AGT TGC AGG GCA AGT CAG GAC ATT AGC
 L   S   A   S   L   G   D   R   V   T   I   S   C   R   A   S   Q   D   I   S
AAT TAT TTA AAC TGG TAT CAG CAG AAA CCA GAT GGA ACT GTT AAA CTC CTG ATC TAC TAC
 N   Y   L   N   W   Y   Q   Q   K   P   D   G   T   V   K   L   L   I   Y   Y
ACA TCA ATA TTA CAC TCA GGA GTC CCA TCA AGG TTC AGT GGC AGT GGG TCT GGA ACA GAT
 T   S   I   L   H   S   G   V   P   S   R   F   S   G   S   G   S   G   T   D
TAT TCT CTC ACC ATT AGC AAC CTG GAG CAA GAA GAT TTT GCC ACT TAC TTT TGC CAA CAG
 Y   S   L   T   I   S   N   L   E   Q   E   D   F   A   T   Y   F   C   Q   Q
                                                                        | ……..
GGT AAT ACG CTT CCG TGG ACG TTC GGT GGA GGC ACC AAG CTG GAA AGC AGA TCT CGA TCA
 G   N   T   L   P   W   T   F   G   G   G   T   K   L   E   S   R   S   R   S
         ……                    truncated protamine …….
CAA TCA CGA TCA CGA TAC TAC CGA CAA CGA CAA CGA TCA CGA CGA CGA CGA CGA CGA TCT
 Q   S   R   S   R   Y   Y   R   Q   R   Q   R   S   R   R   R   R   R   R   S
    |  hexahistidine tag  |
AGA CAC CAT CAC CAC CAC CAT TAA  …… CCGCGGCT 3’
 R   H   H   H   H   H   H   *
```

Appendix 3: Schematic illustrations of the constructs genetic maps with unique restriction sites.

IFNβ-MMP-1-11E scFv in pFastBac^{TM}1
Cy34.1.2 scFv-His6 in pFastBac^{TM}1
Cy34.1.2 scFv-protamine-His6 in pFastBac^{TM}1
Cy34.1.2 scFv-His6 in pcDNA3 vector with V_H native signal sequence
Cy34.1.2 scFv-protamine-His6 in pcDNA3 vector with V_H native signal sequence
Cy34.1.2 scFv-His6 in pHEN1 vector with pelB signal sequence
Cy34.1.2 scFv-His6 in pcDNA3 with hLAP signal sequence-hLAP-HRV3C
Cy34.1.2 scFv-protamine-His6 in pcDNA3 with hLAP signal sequence-hLAP-HRV3C
Cy34.1.2 scFv-protamine-His6 in pDisplay vector with murine Ig κ chain signal sequence
HA22 scFv-protamine-His6 in modified pDisplay vector with murine Ig κ chain signal sequence

Genetic map for IFNβ-MMP-1-11E scFv in pFastBac™1 vector showing unique restriction sites:

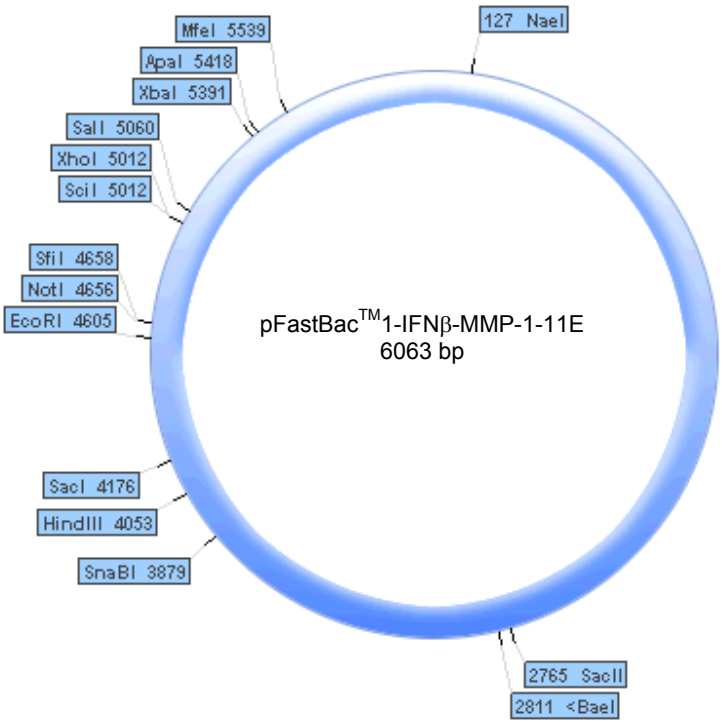

Genetic map for Cy34.1.2 scFv-His6 in pFastBac™1 vector showing unique restriction sites:

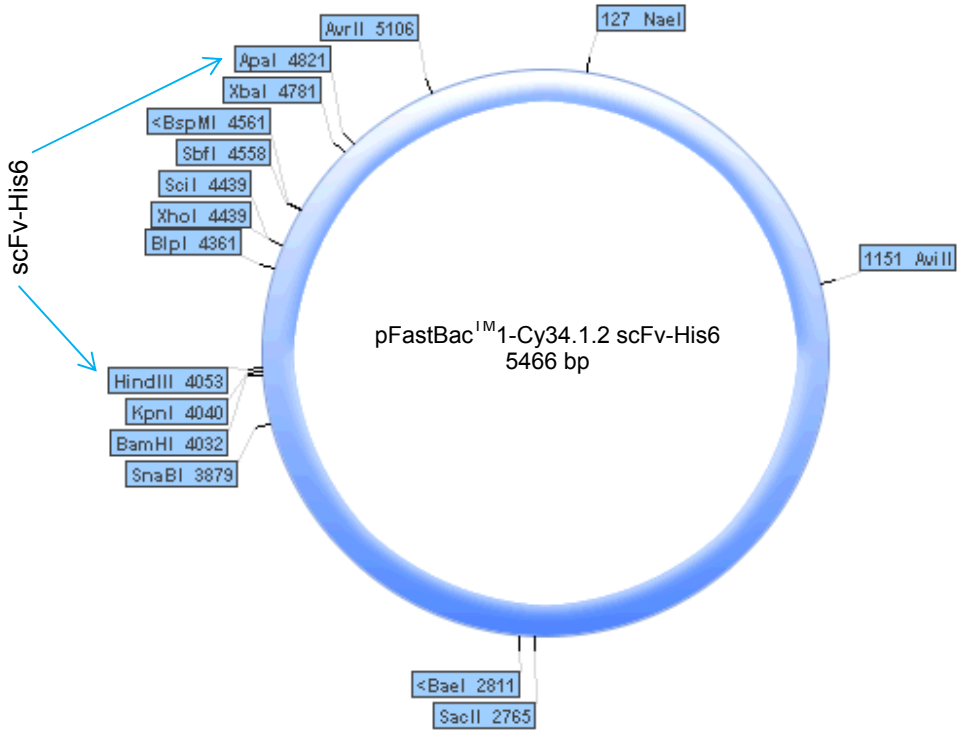

Genetic map for Cy34.1.2 scFv-protamine-His6 in pFastBac™1 vector showing unique restriction sites:

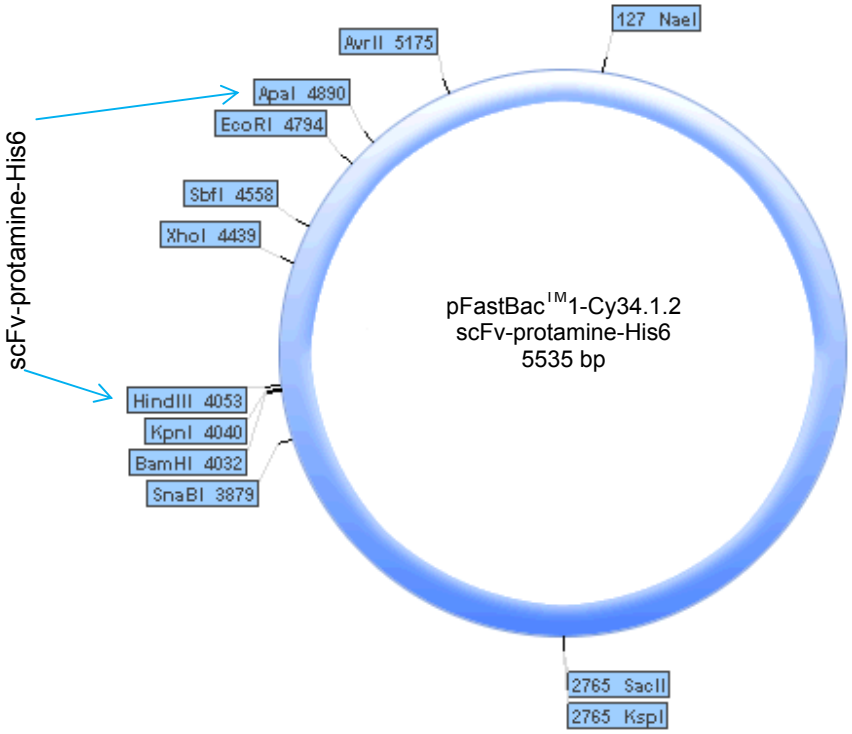

Cy34.1.2 scFv-His6 in pcDNA3 vector with V_H native signal sequence genetic map with unique restriction sites:

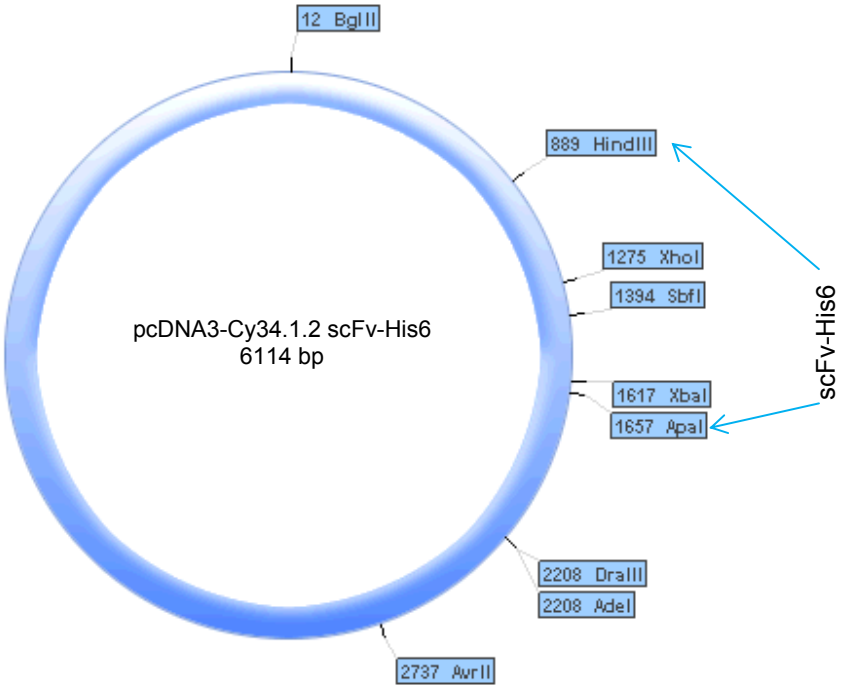

Cy34.1.2 scFv-protamine-His6 in pcDNA3 vector with V_H native signal sequence genetic map with unique restriction sites:

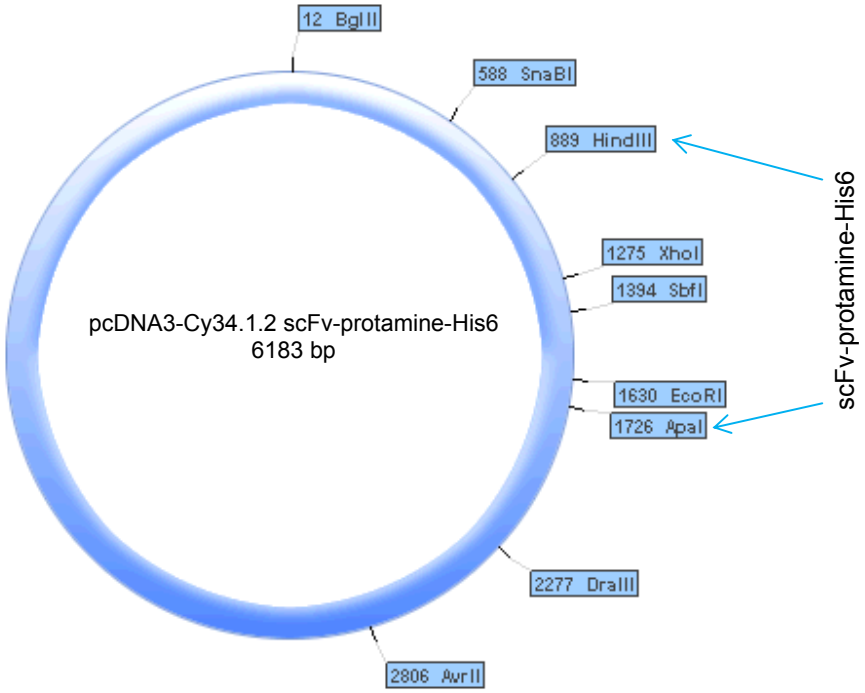

Genetic map for Cy34.1.2 scFv-His6 in pHEN1 vector with pelB signal sequence showing unique restriction sites:

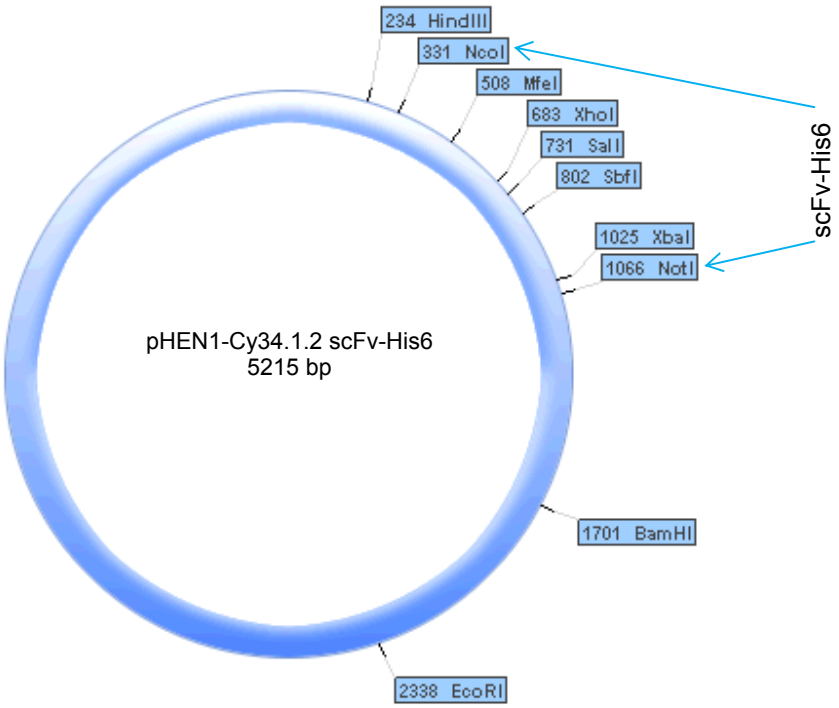

Genetic map for Cy34.1.2 scFv-His6 in pcDNA3 with hLAP and hLAP signal sequence showing unique restriction sites:

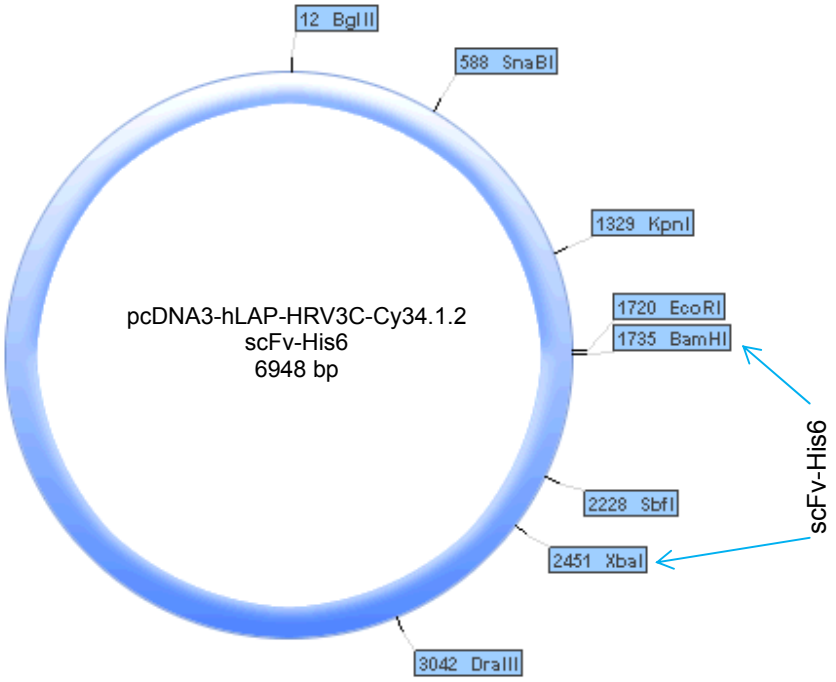

Genetic map for Cy34.1.2 scFv-protamine-His6 in pcDNA3 with hLAP and hLAP signal sequence showing unique restriction sites:

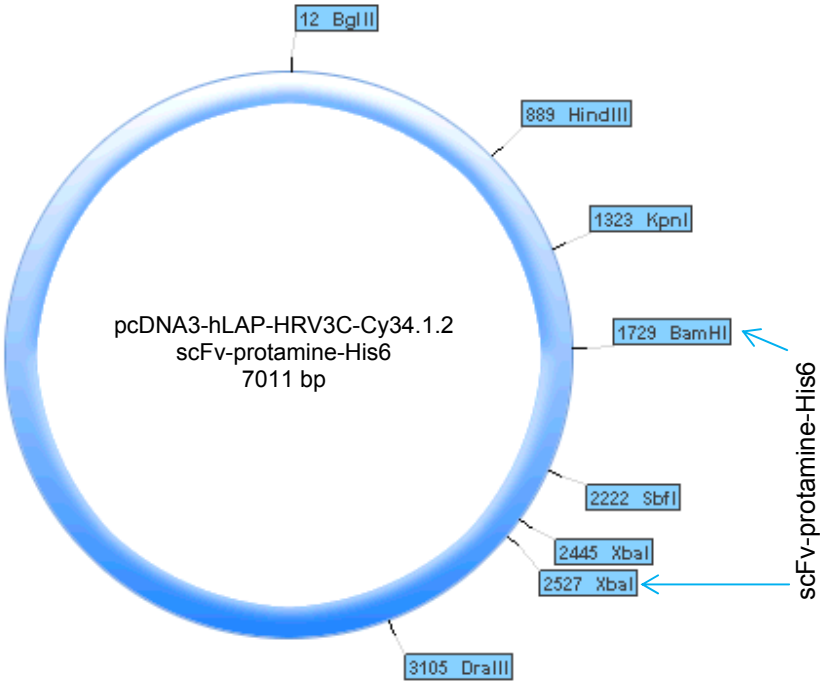

Genetic map for Cy34.1.2 scFv-protamine-His6 in modified pDisplay vector with murine Ig kappa-chain signal sequence showing unique restriction sites:

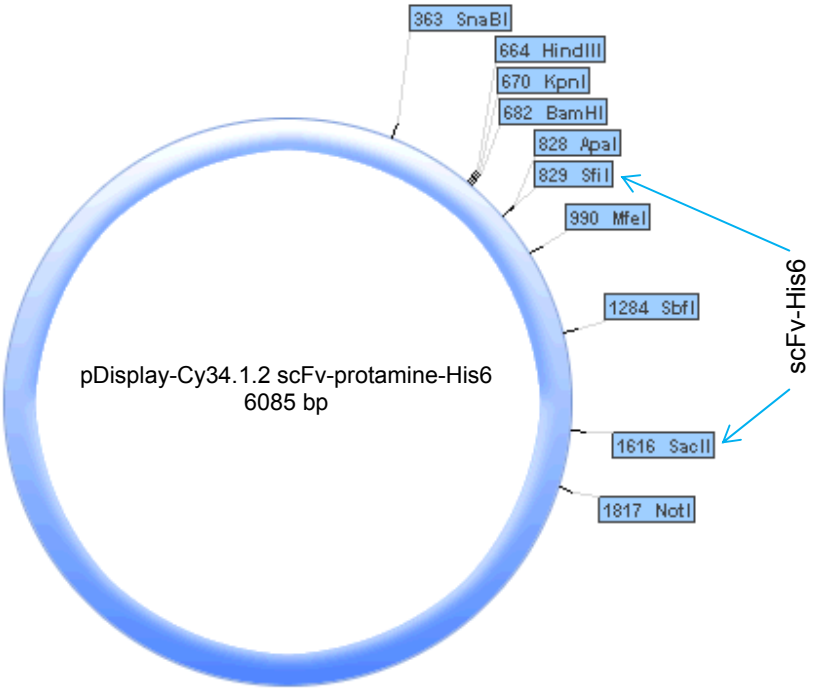

Genetic map for HA22 scFv-protamine-His6 in modified pDisplay vector with murine Ig kappa-chain signal sequence showing unique restriction sites:

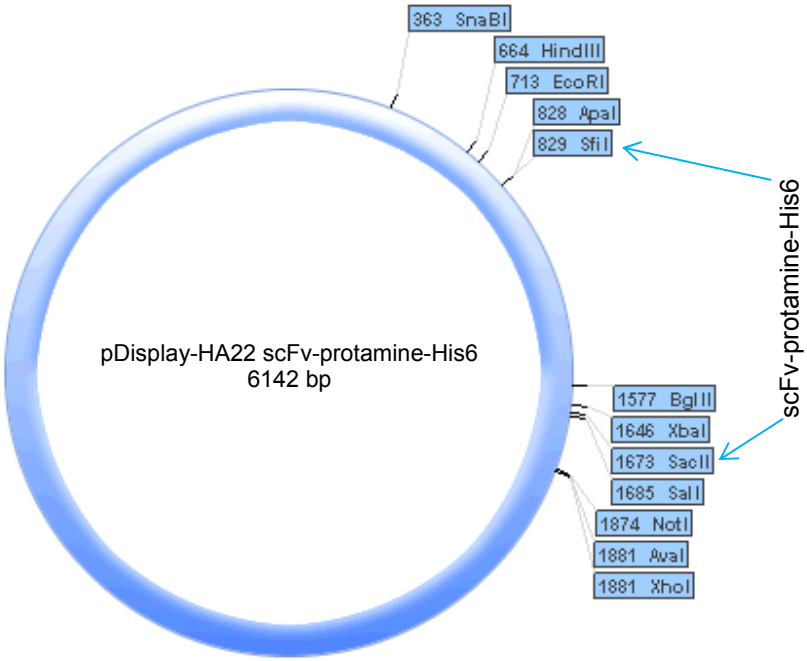

Appendix 4: schematic illustration showing the genetic map of pMH112 construct containing anti-human BL22 (wild type) scFv with unique restriction sites

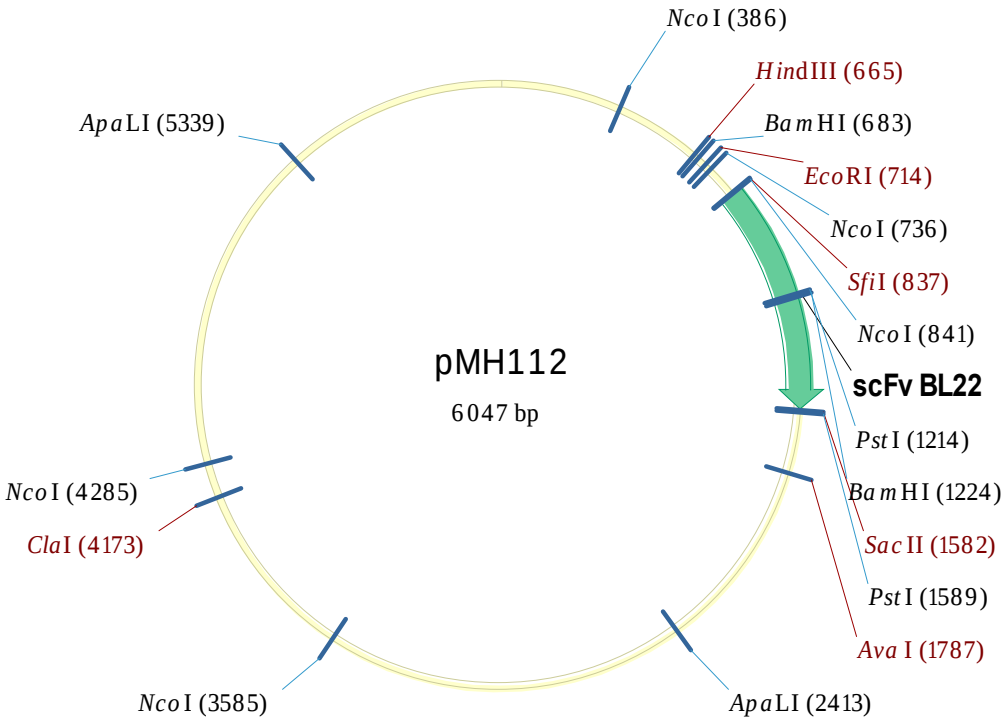

Appendix 5: schematic illustration showing the genetic map of pMH113 construct containing anti-human HA22 (mutant) scFv with unique restriction sites

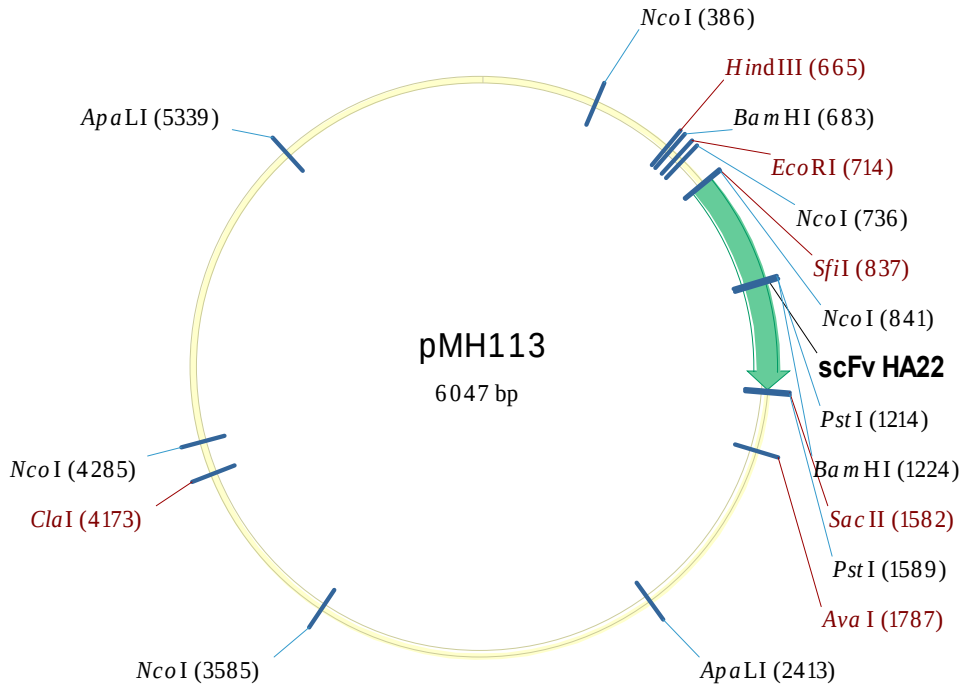

Appendix 6: strategy for removal of haemagglutinin A epitope (HA tag) from the pDisplay vector:

In the pDisplay mammalian expression vector, the nucleotide sequence which encodes haemagglutinin A epitope (YPYDVPDYA) precedes the multiple cloning site (MCS) in-frame with the signal peptide (Ig κ-chain signal sequence). In order to remove the HA tag (green), first a fragment of DNA that overlaps the signal peptide upstream of the HA tag between *Hind*III restriction site (red) and end of the leader signal sequence (blue) was PCR-amplified using pDisplay F *Hind*III forward primer: 5'GACCCAAGCTTGGTACCGAGCTCGGATCCA3' pDisplay R *Sfi*I reverse primer: 5'TGGATAGGCCGGCTGGGCCCCGTCACCAGTGGAACCTGG3' to incorporate *Sfi*I site at the start of MCS. Then the pDisplay vector backbone was digested with *Hind*III and *Sfi*I enzymes and ligated with the PCR product that was digested with *Hind*III and *Sfi*I enzymes. The ligation reaction was used to transform bacteria. Positive clones were identified and expanded by minipreparation.

```
                                                        HindIII -----------------
……..pDisplay backbone……..                              |       |
CT TAT CGA AAT TAA TAC GAC TCA CTA TAG GGA GAC CCA AGC TTG GTA CCG AGC TCG
    Y   R   N   *   Y   D   S   L   *   G   D   P   S   L   V   P   S   S
GA ATA GCT TTA ATT ATG CTG AGT GAT ATC CCT CTG GGT TCG AAC CAT GGC TCG AGC

----------------------------------------EcoRI---------------
                                         |     |
GAT CCA CTA GTA ACG GCC GCC AGT GTG CTG GAA TTC GGC TTG GGG
 D   P   L   V   T   A   A   S   V   L   E   F   G   L   G
CTA GGT GAT CAT TGC CGG CGG TCA CAC GAC CTT AAG CCG AAC CCC

----------------|----------Ig kappa chain leader sequence
ATA TCC ACC ATG GAG ACA GAC ACA CTC CTG CTA TGG GTA CTG CTG
 I   S   T   M   E   T   D   T   L   L   L   W   V   L   L
TAT AGG TGG TAC CTC TGT CTG TGT GAG GAC GAT ACC CAT GAC GAC

---------------------------------→| |    Haemagglutinin A epitope     |
CTC TGG GTT CCA GGT TCC ACT GGT GAC TAT CCA TAT GAT GTT CCA GAT TAT GCT
 L   W   V   P   G   S   T   G   D   Y   P   Y   D   V   P   D   Y   A
GAG ACC CAA GGT CCA AGG TGA CCA CTG ATA GGT ATA CTA CAA GGT CTA ATA CGA

   ……SfiI……
  |                ||Anti-CD22 scFv HA22 ……
GGG GCC CAG CCG GCC ATG GAA GTG CAG CTG GTG GAG TCT GGG AGG CTT G
 G   A   Q   P   A   M   E   V   Q   L   V   E   S   G   R   L
CCC CGG GTC GGC CGG TAC CTT CAC GTC GAC CAC CTC AGA CCC TCC GAA C
```

Scientific Communications

Conference abstracts for poster presentations:

Hawzheen A Muhammad, Yuti Chernajovsky, Taher E Taher, David J Gould and Rizgar A Mageed. “Therapeutic targeting of leukaemic B-lymphocytes using antibody-delivered siRNA”. Poster Presentation: 6th Meeting of Gene Therapy of Arthritis and Related Disorders, Queen Mary University of London, London, UK, 2011.

HA Muhammad, TE Taher, L Mullen, JF Marshal, Y Chernajovsky, DJ Gould and RA Mageed. “Therapeutic targeting of pathogenic B-lymphocytes using antibody-delivered siRNA”. Poster Presentation: William Harvey Day, Queen Mary University of London, London, UK, 2012

Hawzheen A Muhammad, Taher E Taher, Lisa Mullen, Ira H Pastan, Yuti Chernajovsky, David J Gould and Rizgar A Mageed. “Generation of a secreted anti-CD22 scFv for specific delivery of siRNA to B-lymphocytes”. Poster Presentation: BSGCT Conference, Royal Holloway, University of London, Egham, UK, April 2013.

Oral presentation:

Hawzheen A Muhammad, Taher E Taher, Lisa Mullen, Ira H Pastan, Yuti Chernajovsky, David J Gould and Rizgar A Mageed. “Generation of a secreted anti-CD22 scFv for specific delivery of siRNA to B-lymphocytes in leukaemias and lymphomas”. Oral Presentation: Annual Research Reviews, Queen Mary University of London, London, UK, 2013.

Publications:

Taher TE, Muhammad HA, Bariller E, Flores-Borja F, Renaudineau Y, Isenberg DA and Mageed RA. B-lymphocyte signaling abnormalities and lupus immunopathology. Int. Rev. Immunol. 2013; 32(4):428-444.

Taher TE, Muhammad HA, Rahim A, Flores-Borja F, Renaudineau Y, Isenberg DA, Mageed RA. Aberrant B-lymphocyte responses in lupus: inherent or induced and potential therapeutic targets. Eur. J. Clin. Invest. 2013; 43(8):866-880.